Title: The secret within

Date: Apr 26, 2011 01:30 PM

URL: http://pirsa.org/11040090

Abstract: Direct visualization of the electronic structure within each crystalline unit cell of a solid is a new frontier in condensed matter physics (M.J.
Lawler et al, Nature 466, 347 (2010)). In this talk, I will introduce the
techniques of spectroscopic imaging scanning tunneling microscopy (SI-ÃÂ,ÂÃ¢ÂÂ€ÂÂ•STM) and then explain how our new application of this technique allows
visualization of the intra-ÃÂ,ÂÃ¢ÂÂ€ÂÂ•unit-ÃÂ,ÂÃ¢ÂÂ€ÂÂ•cell electronic structure. We use this
approach to study the pseudogap phase of cuprate high temperature superconductors. Recent experiments provide evidence that this phase may be associated with spontaneously broken electronic symmetries. By studying
the Bragg peaks in Fourier transforms of SI-ÃÂ,Â-STM images, and in particular
by resolving both the real and imaginary components of these Bragg amplitudes (as opposed to the Bragg intensities without phase information which are the observables in scattering experiments), we reveal the intra-ÃÂ,ÂÃ¢ÂÂ€ÂÂ•unit-ÃÂ,ÂÃ¢ÂÂ€ÂÂ•cell broken electronic symmetries of the cuprate pseudogap phase
(J.P.Hinton et al, Science (2011)).

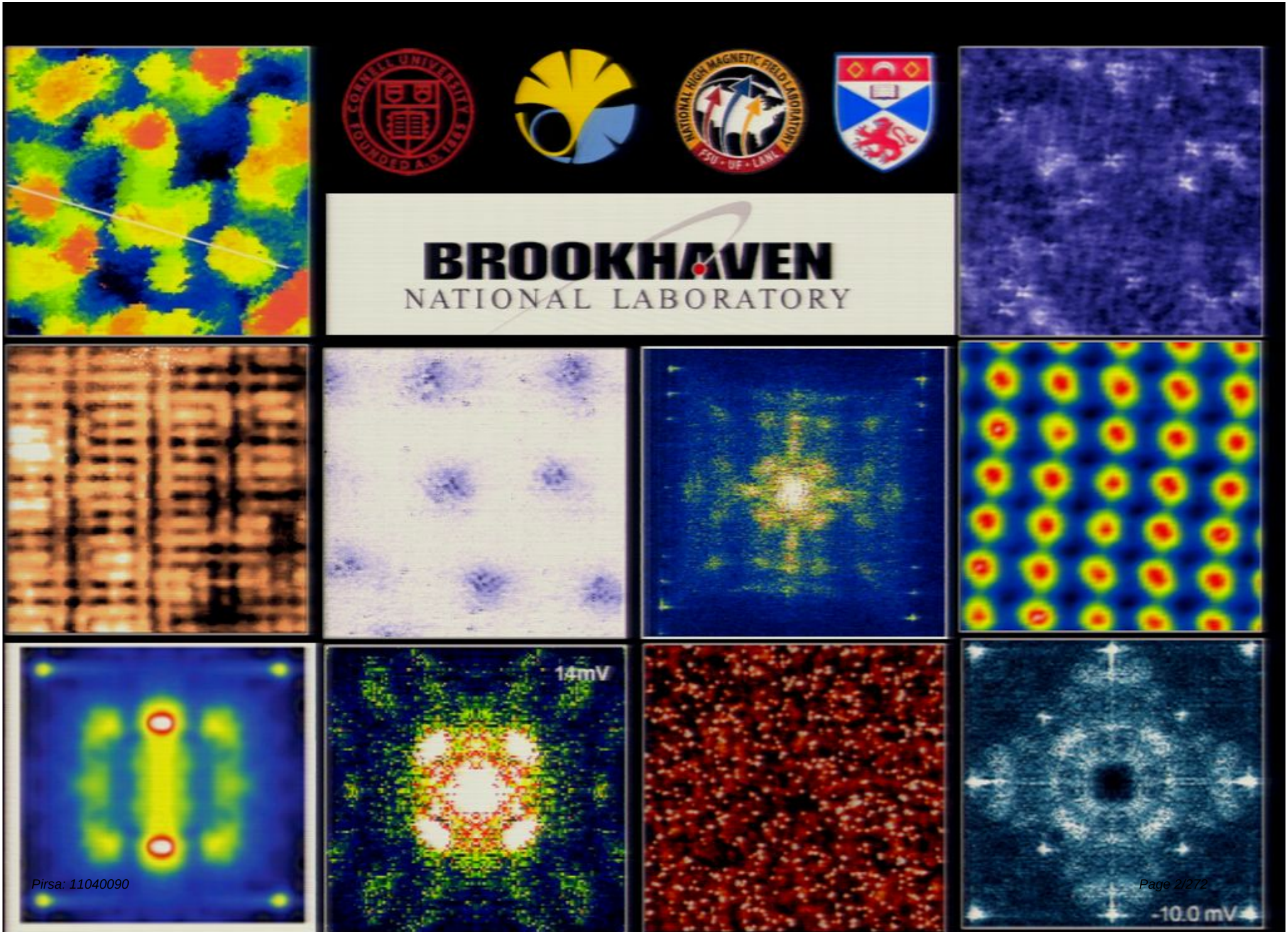
BROOKHAVEN
NATIONAL LABORATORY
14mV
-10.0 mV

STOP ME AND ASK QUESTIONS!

Standard Scanning Tunneling Microscopy (STM)

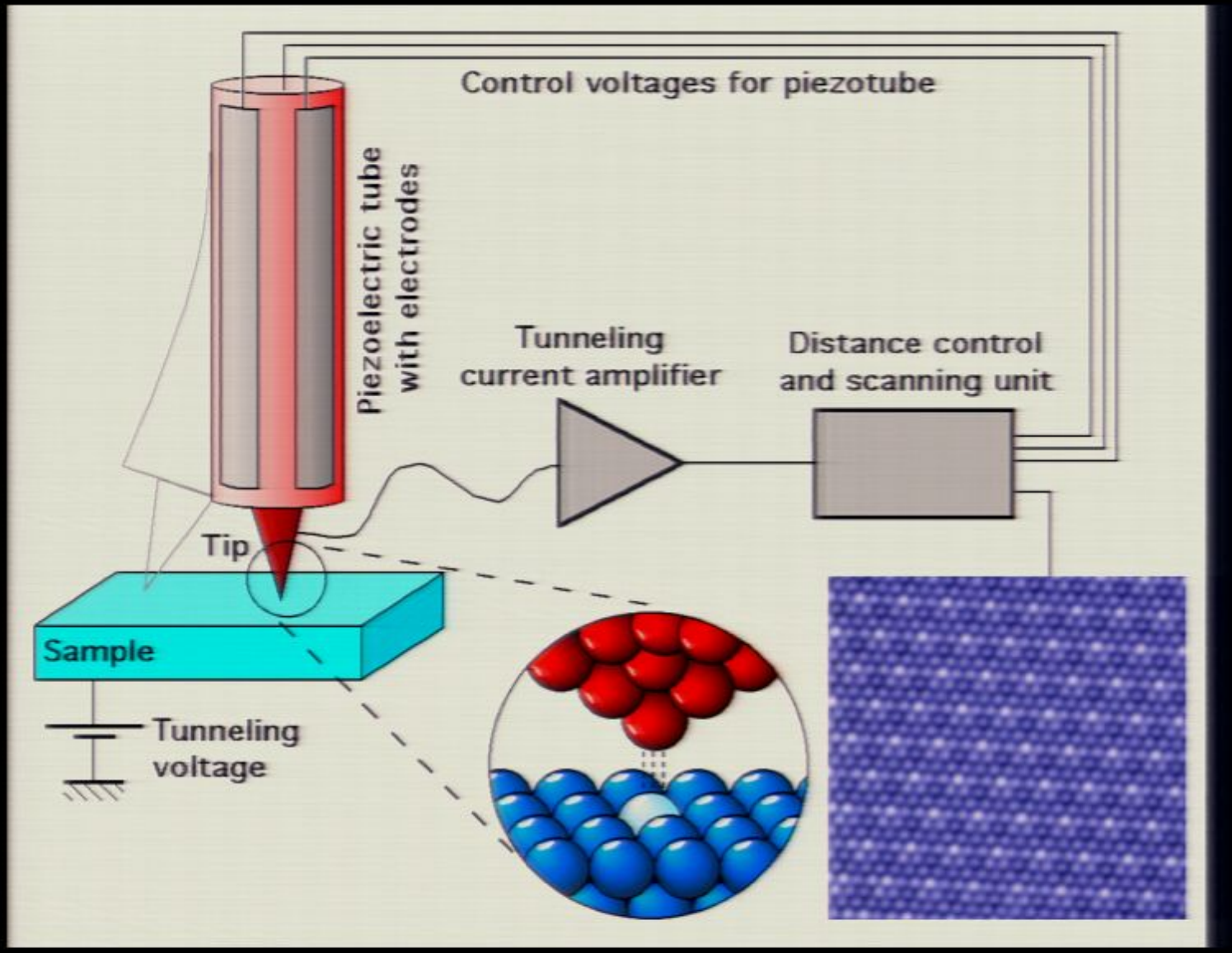

Images atomic locations – not electronic wavefunctions

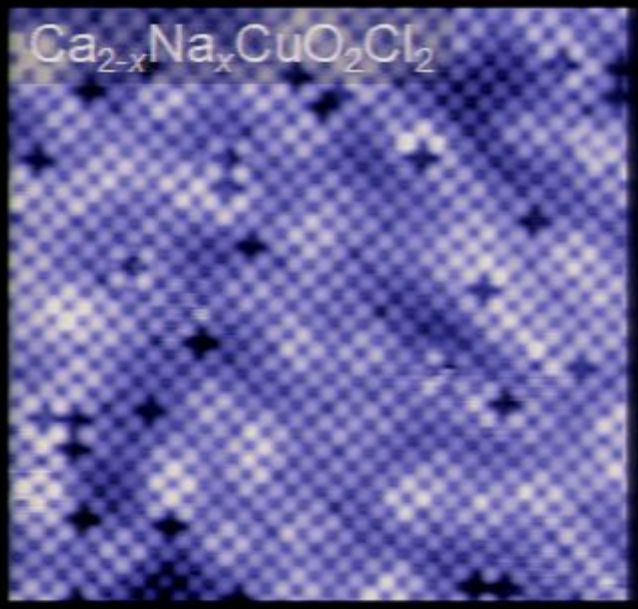

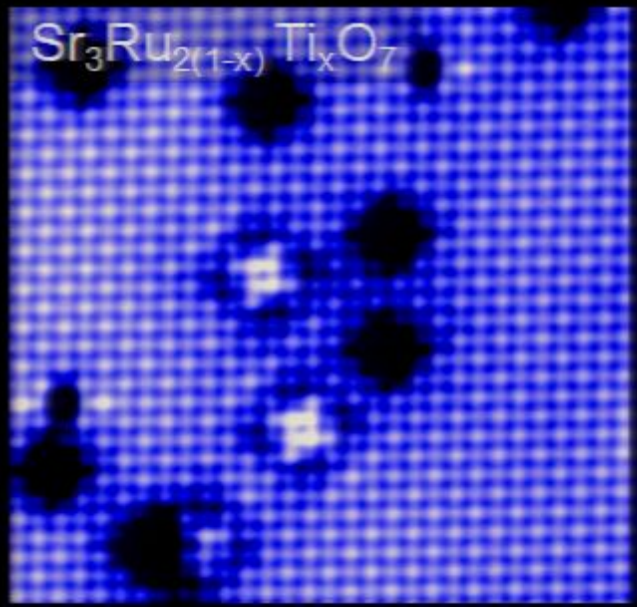

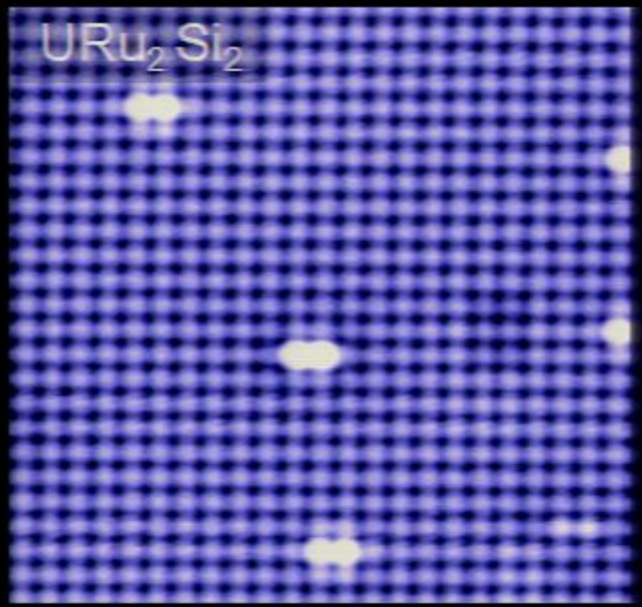

Tip-Sample Tunneling Current

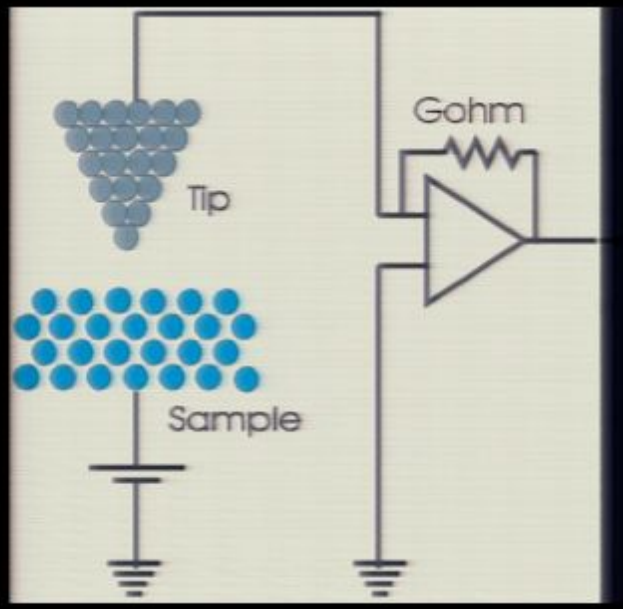

Bias voltage V=0 =>
no current flows.

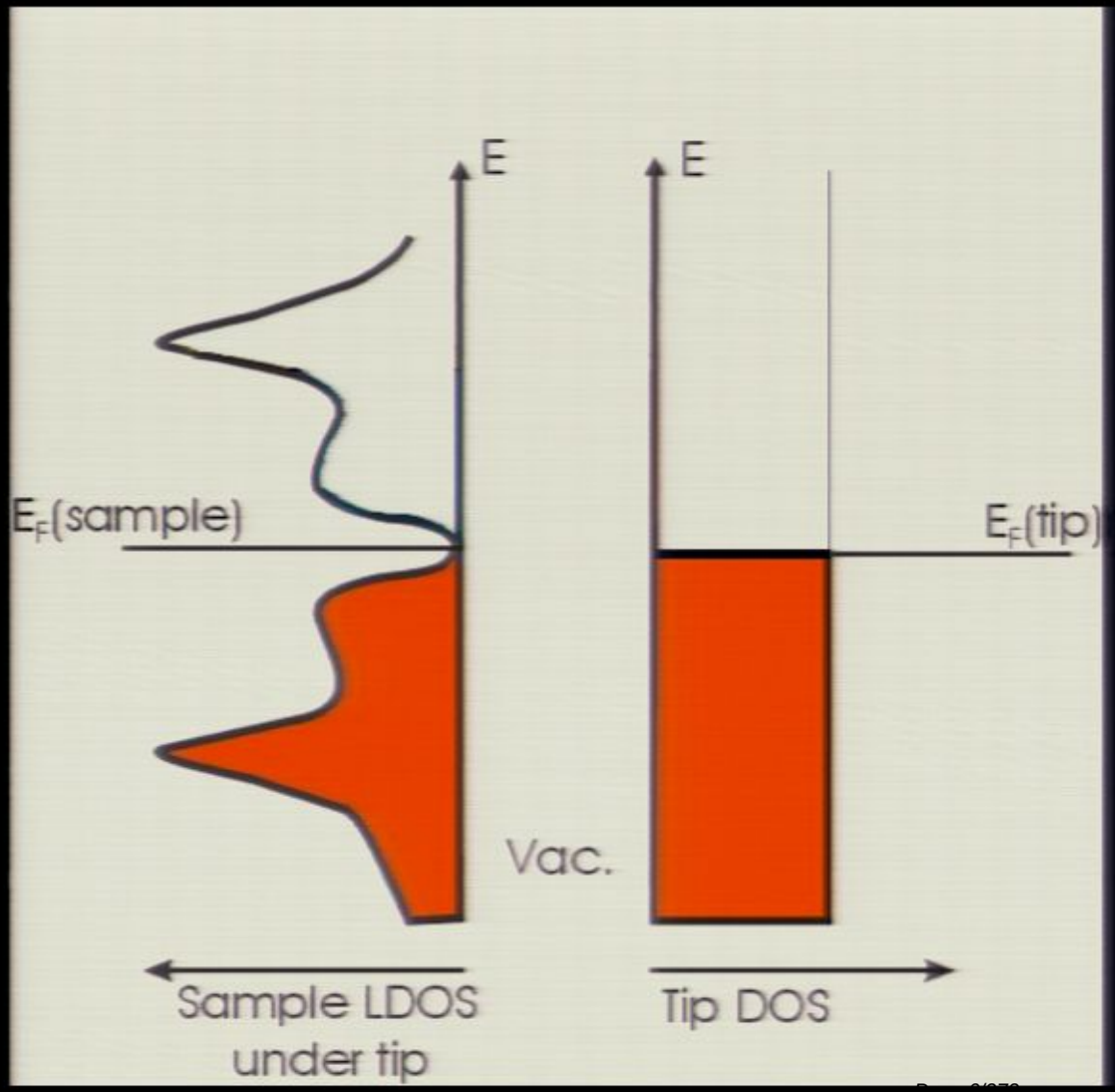

Tip-Sample Tunneling Current

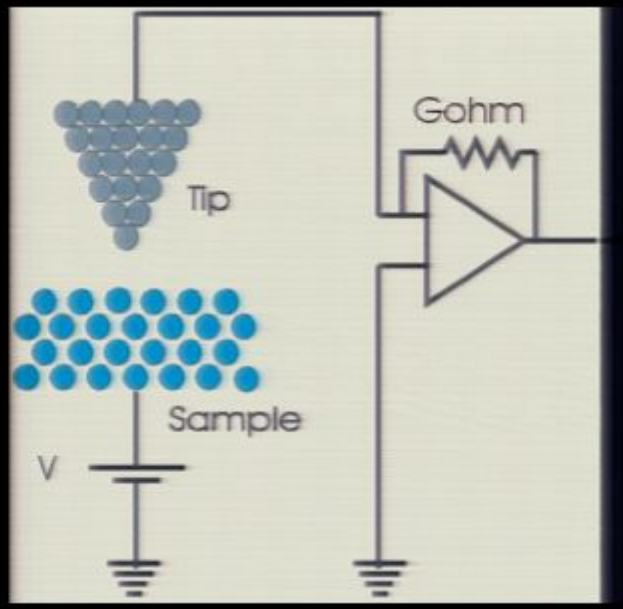

Bias voltage V>0 lowers sample Fermi-level compared to that of tip, electron tunneling occurs.

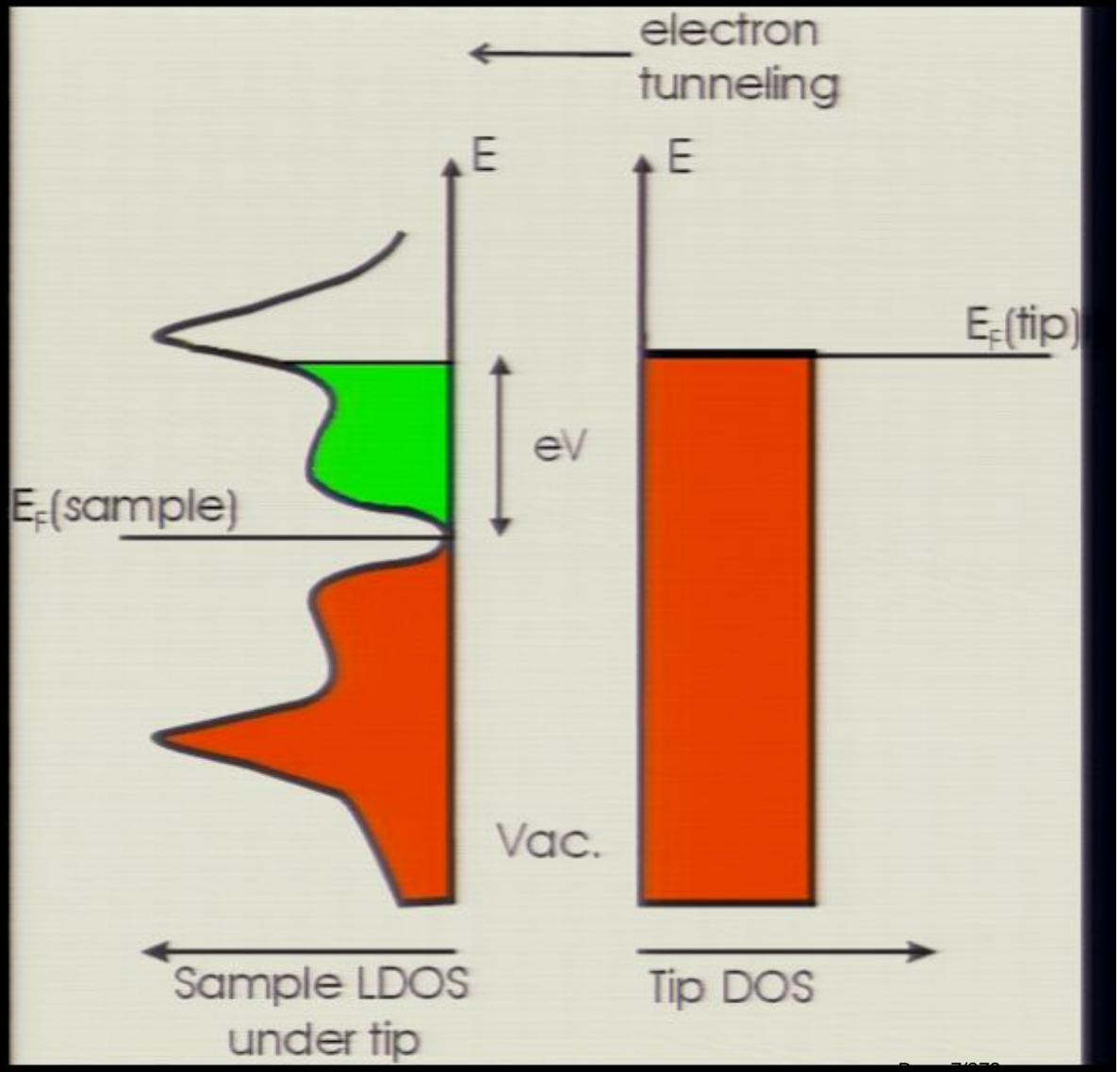

Tip-Sample Tunneling Current

$$I = Ce^{-\frac{z(V)}{z_0}} \int_0^{eV} LDOS(\mathbf{r}, E)\,dE$$

$$LDOS(\mathbf{r}, E) \propto |\Psi(r, E)|^2$$

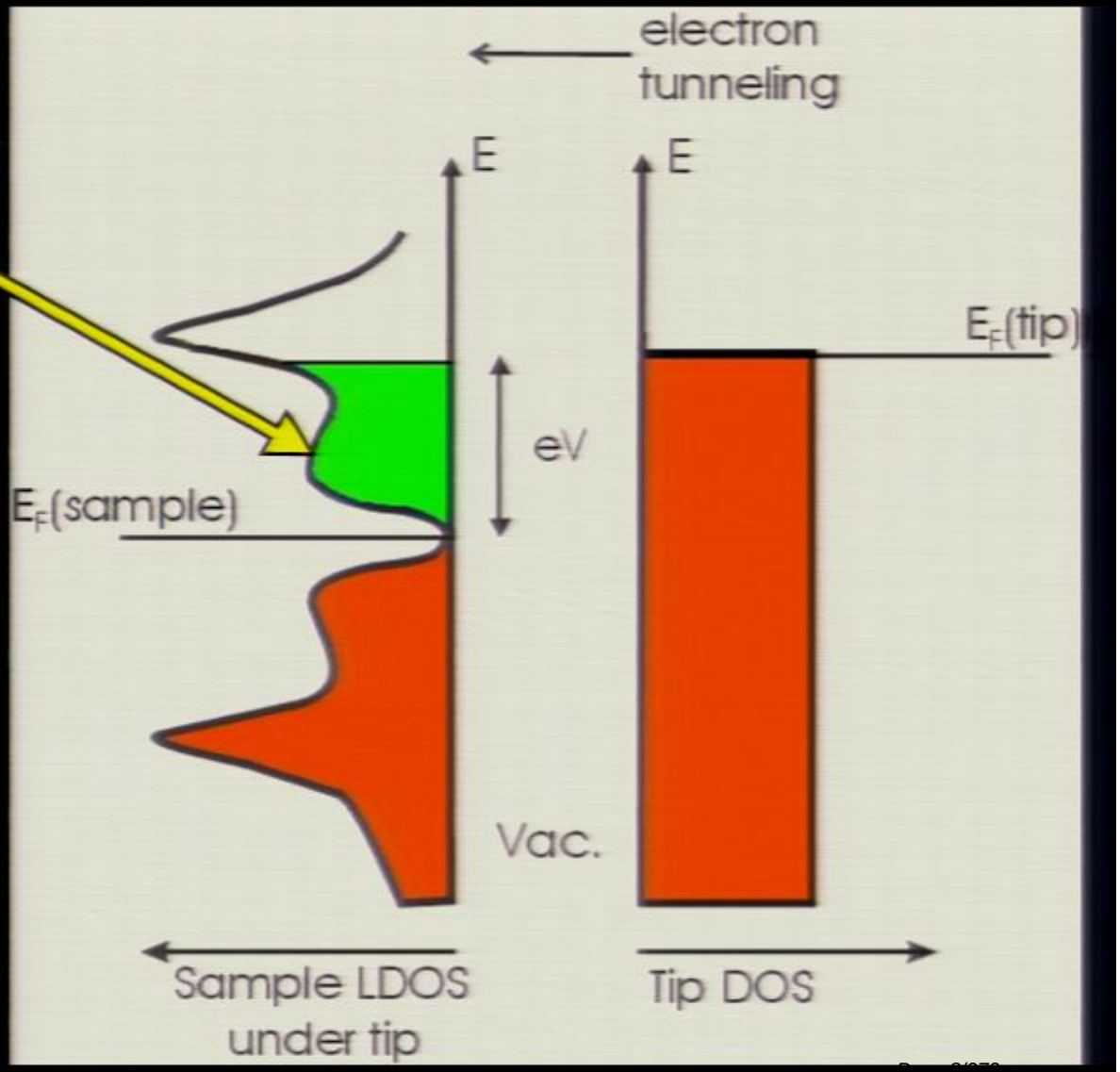

Differential Tunneling Conductance

$$dI \propto LDOS(E = eV)dV$$

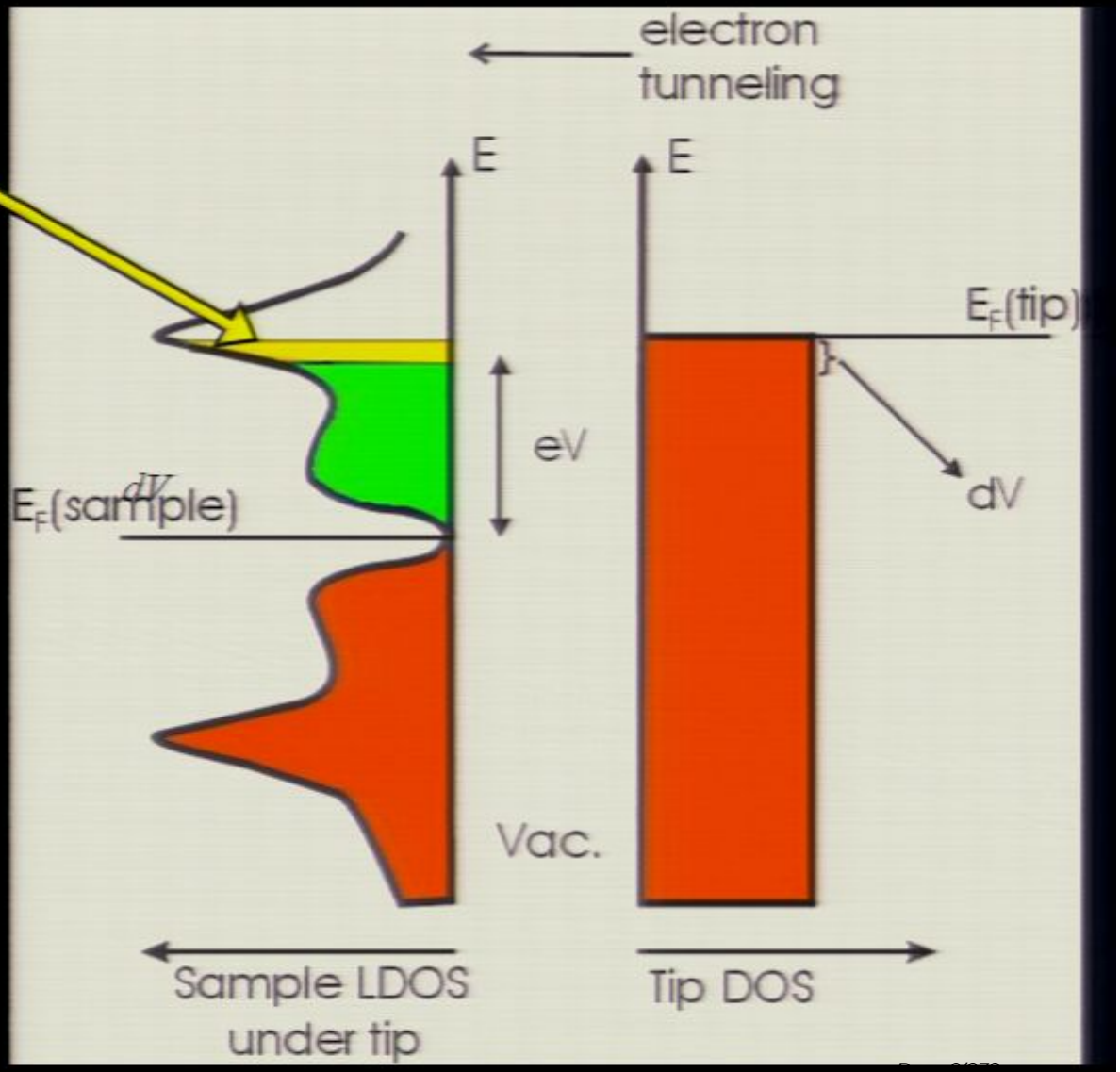

Tip-Sample Tunneling Current

$$I = Ce^{-\frac{z(V)}{z_0}} \int_0^{eV} LDOS(\mathbf{r}, E)\,dE$$

$$LDOS(\mathbf{r}, E) \propto |\Psi(r, E)|^2$$

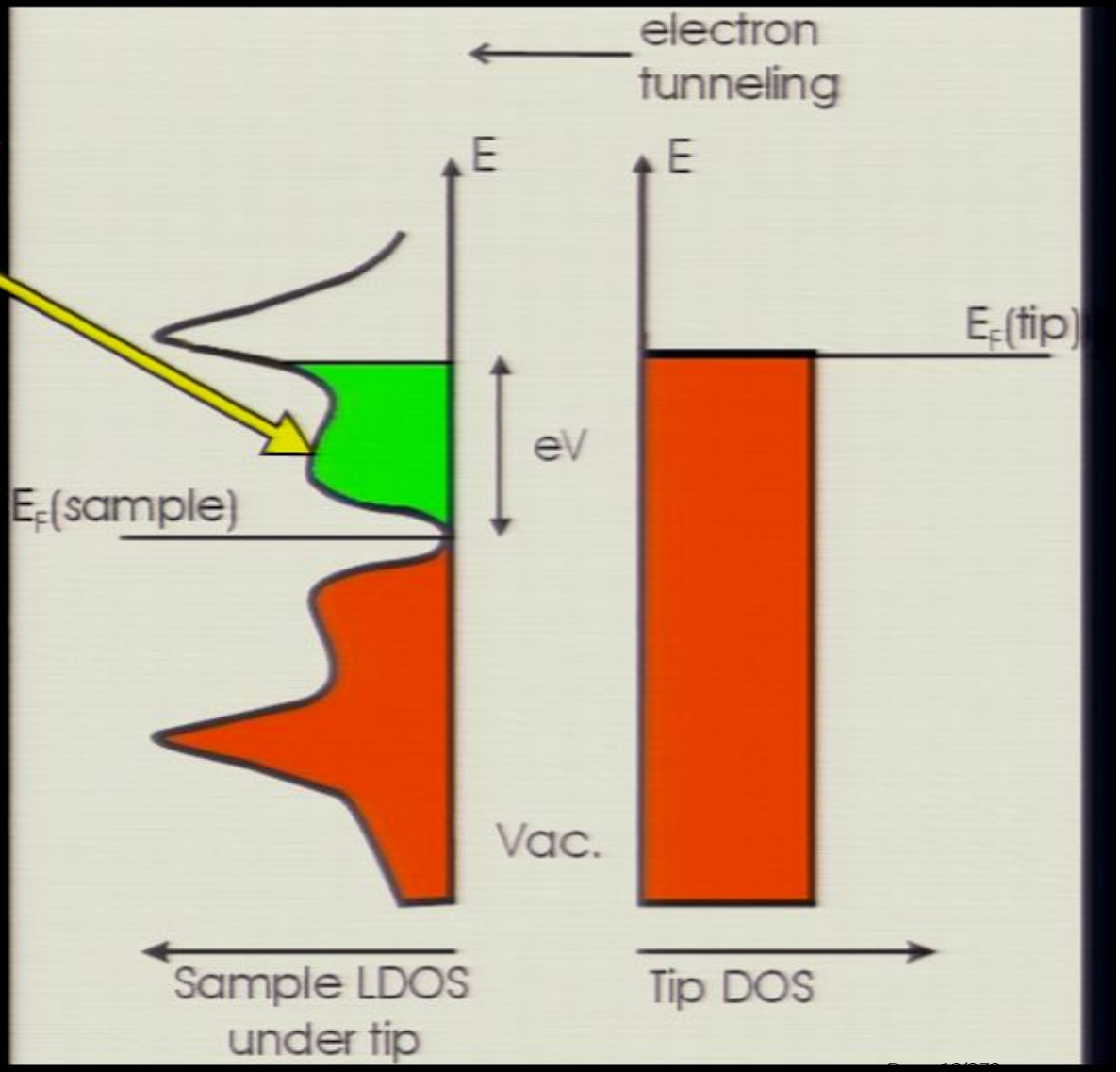

Differential Tunneling Conductance

$$dI \propto LDOS(E = eV)dV$$

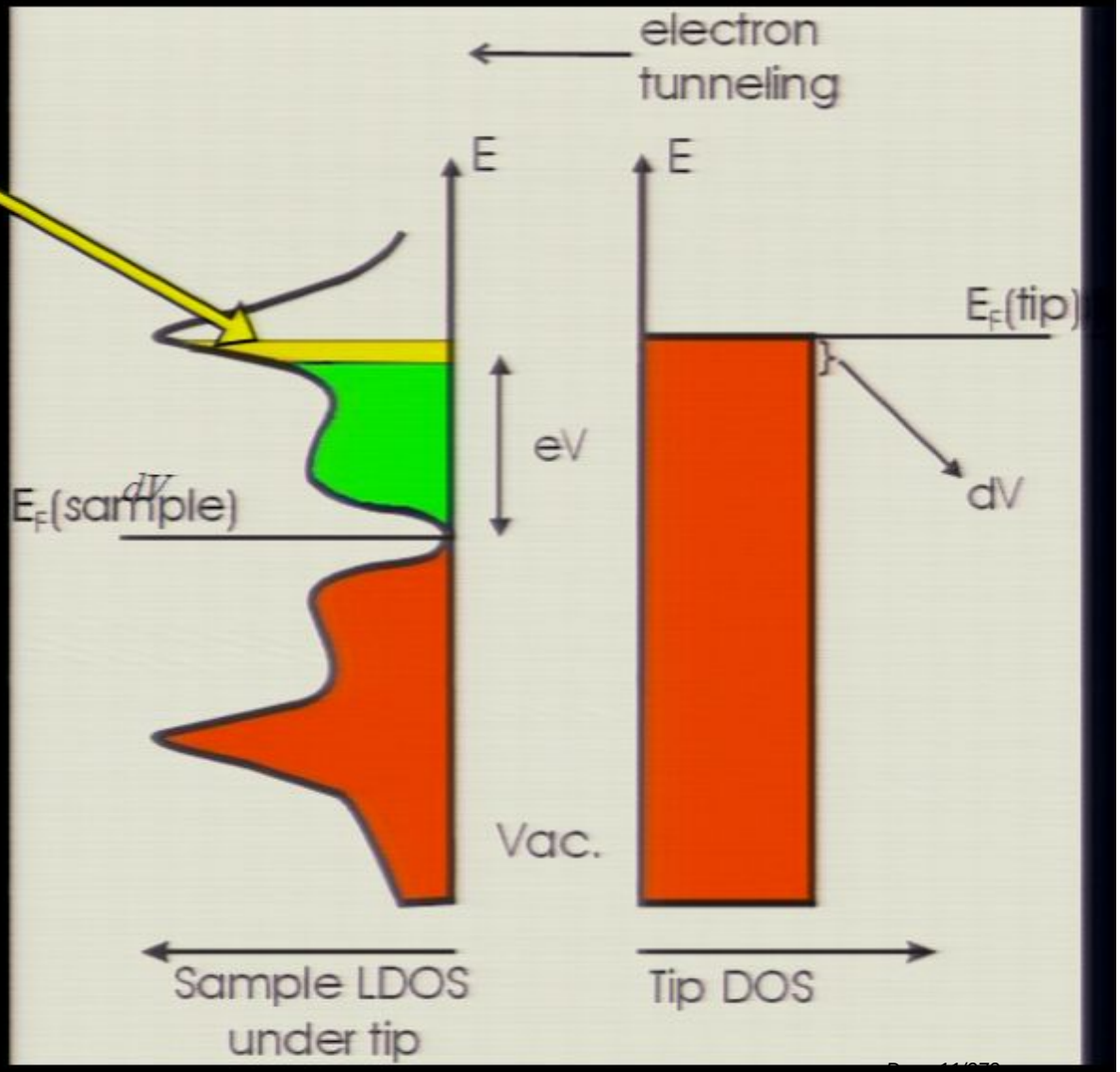

Local-Density-of-States $LDOS(E)$ Spectroscopy

$$dI \propto LDOS(E = eV)dV$$

$$\Rightarrow \frac{dI}{dV} \propto LDOS(E = eV)$$

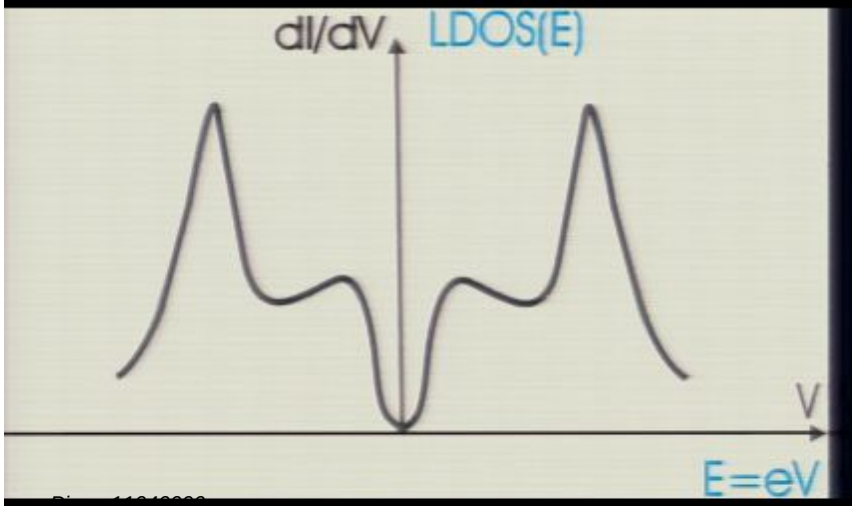

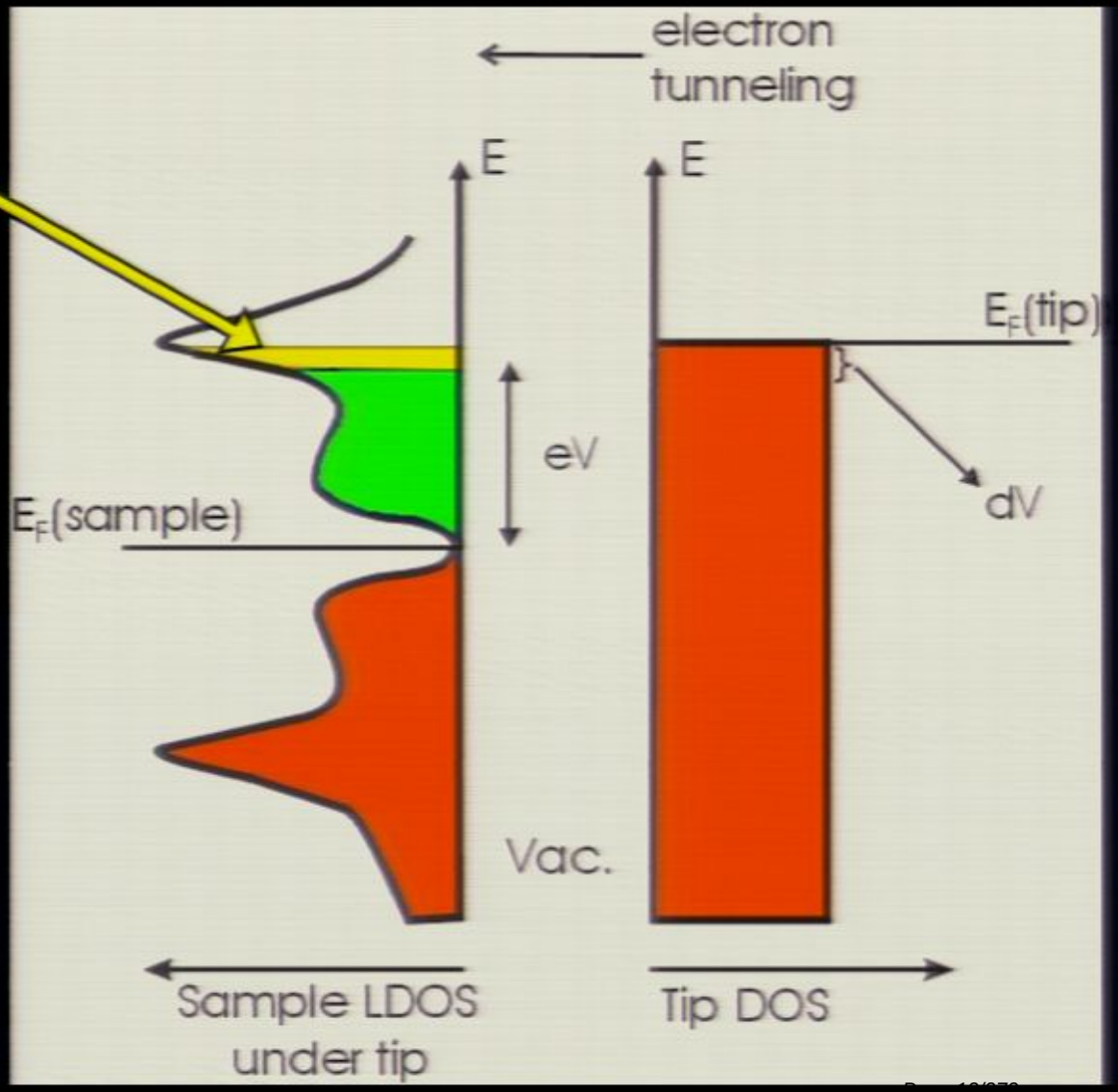

Spectroscopic Imaging STM (SI-STM)

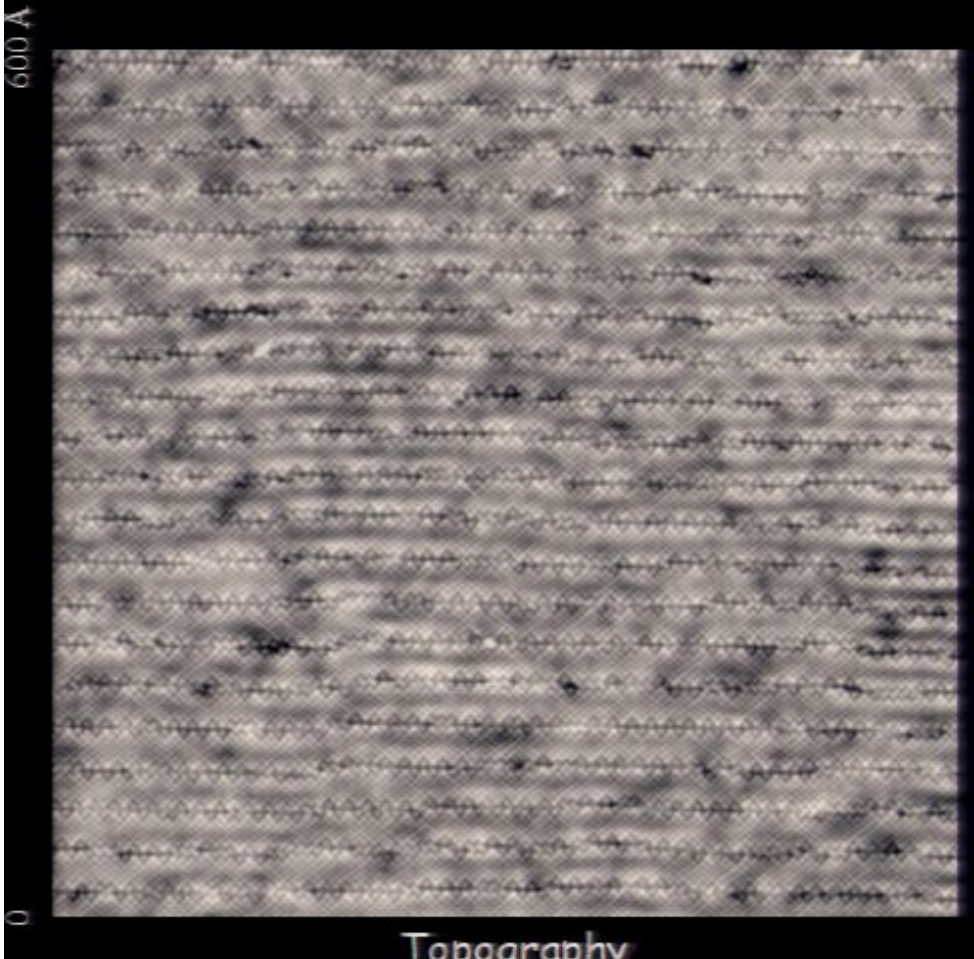

Spectroscopic Imaging STM (SI-STM)

Inset shows $LDOS(E)$ spectrum at single atom

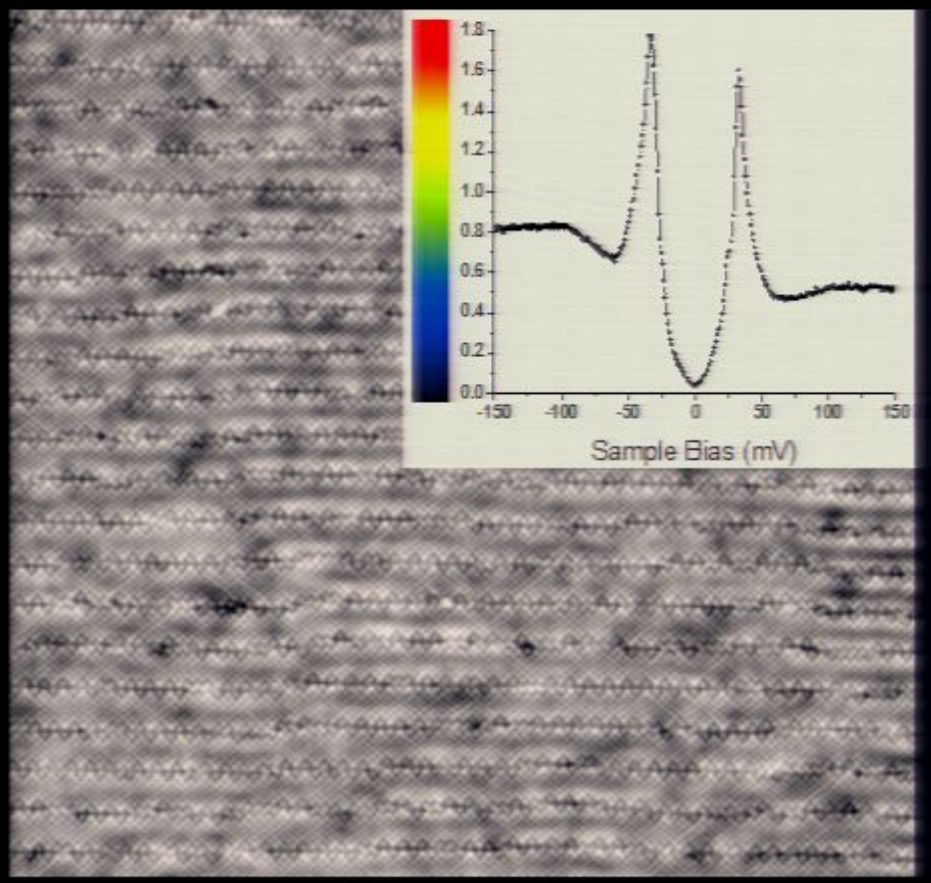

Topography

Spectroscopic Imaging STM (SI-STM)

Inset shows $LDOS(E)$ spectrum at single atom

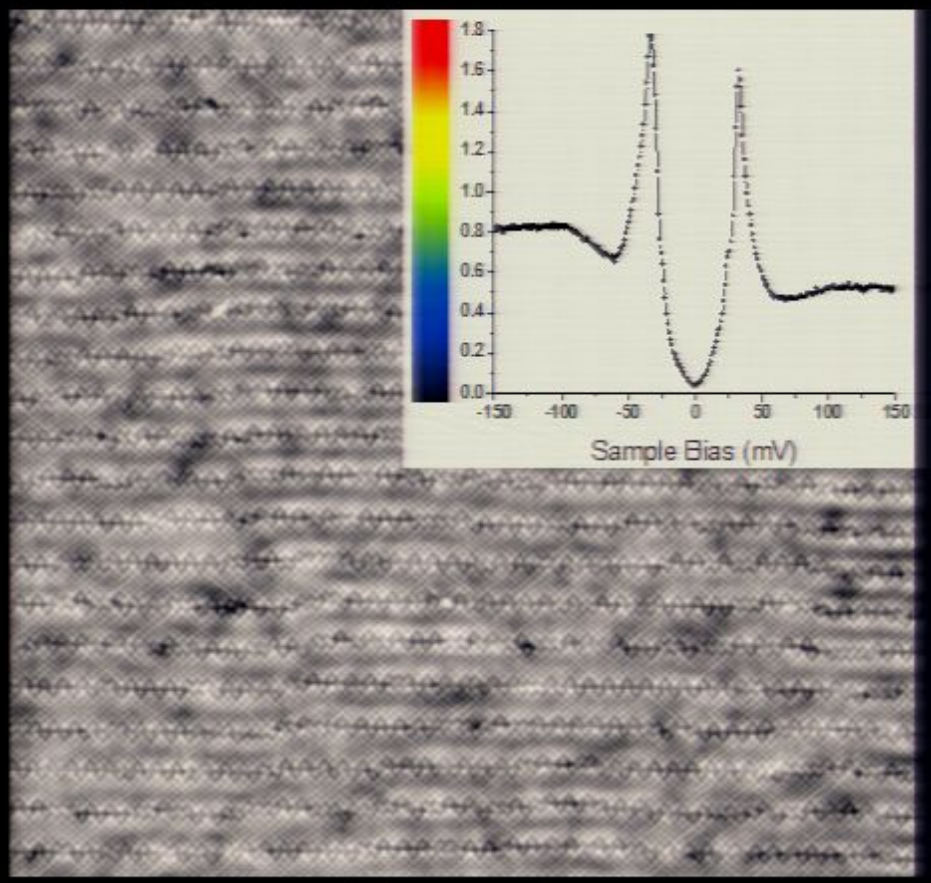

Topography

Measure $dI/dV \propto LDOS(E)$ at every atom

Spectroscopic Imaging STM (SI-STM)

Inset shows $LDOS(E)$ spectrum at single atom

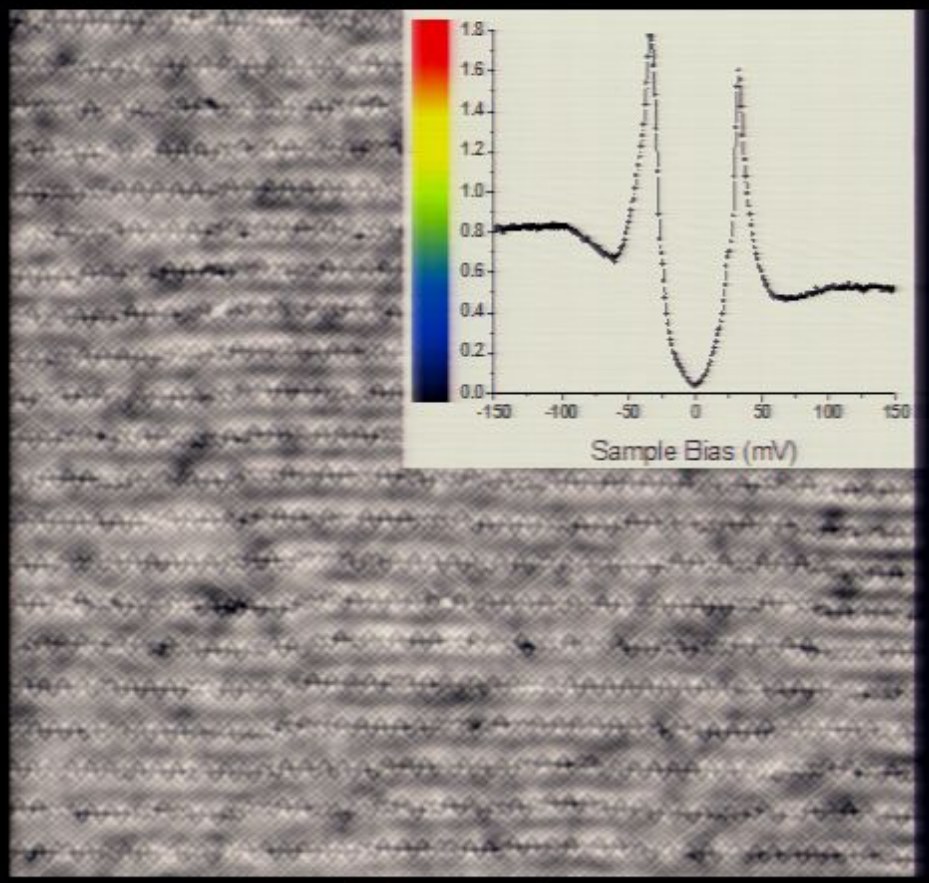

Topography

Atomic-resolution energy resolved

$$LDOS(\vec{r},E) \propto |\Psi(\vec{r},E)|^2$$

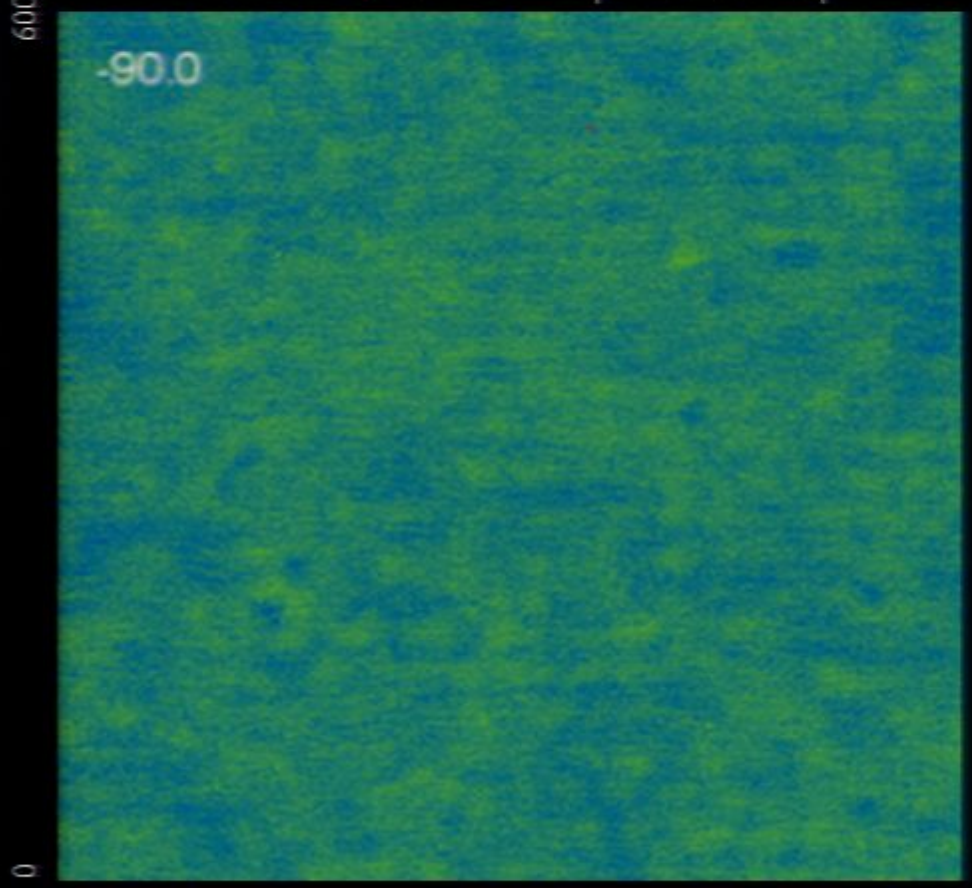

Measure $dI/dV \propto LDOS(E)$ at every atom

Spectroscopic Imaging STM (SI-STM)

Inset shows $LDOS(E)$ spectrum at single atom

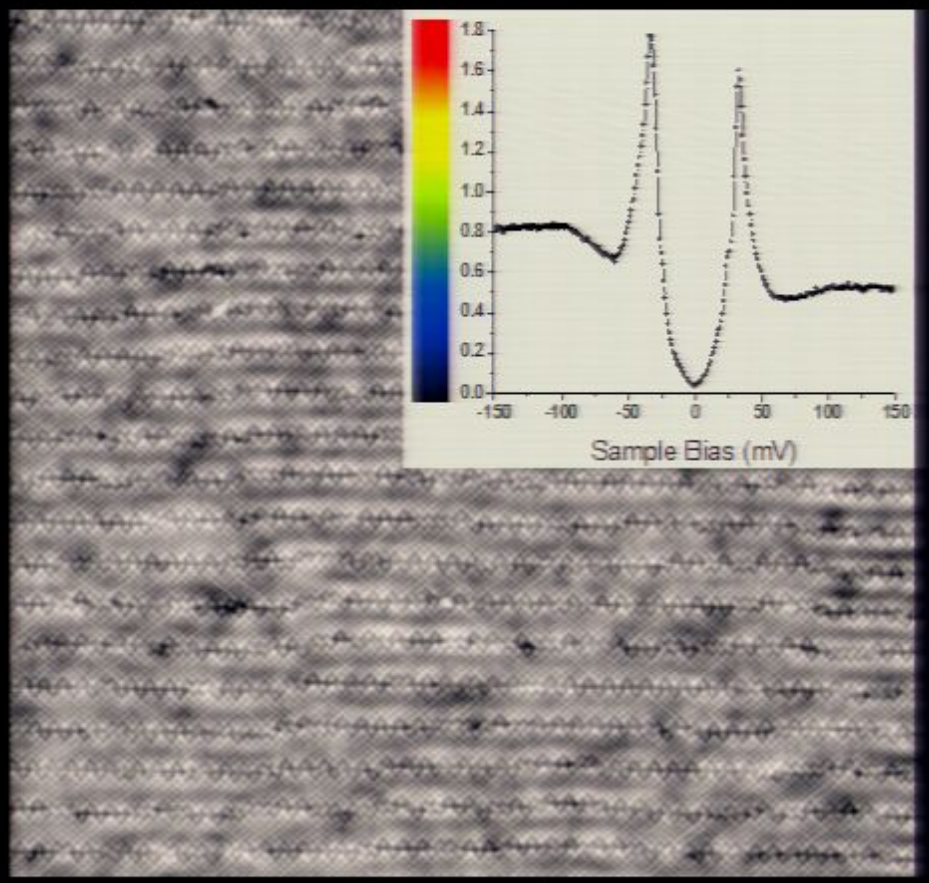

Topography

Atomic-resolution energy resolved

$$LDOS(\vec{r},E) \propto |\Psi(\vec{r},E)|^2$$

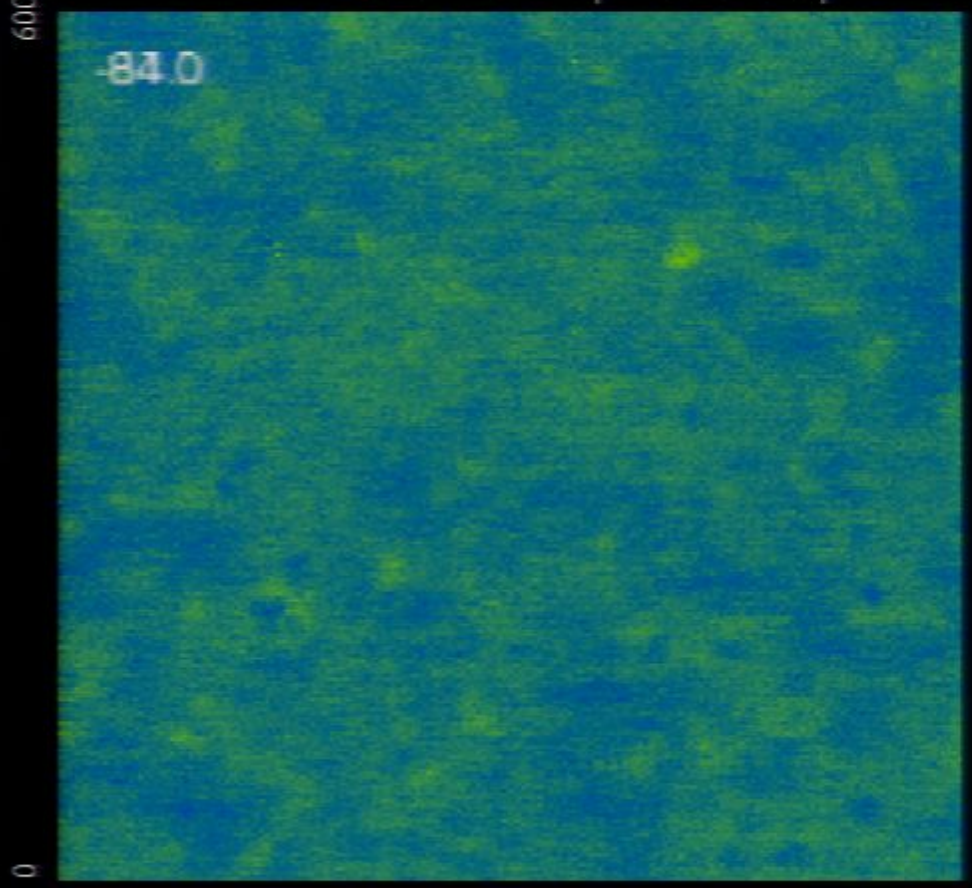

Measure $dI/dV \propto LDOS(E)$ at every atom

Spectroscopic Imaging STM (SI-STM)

Inset shows $LDOS(E)$ spectrum at single atom

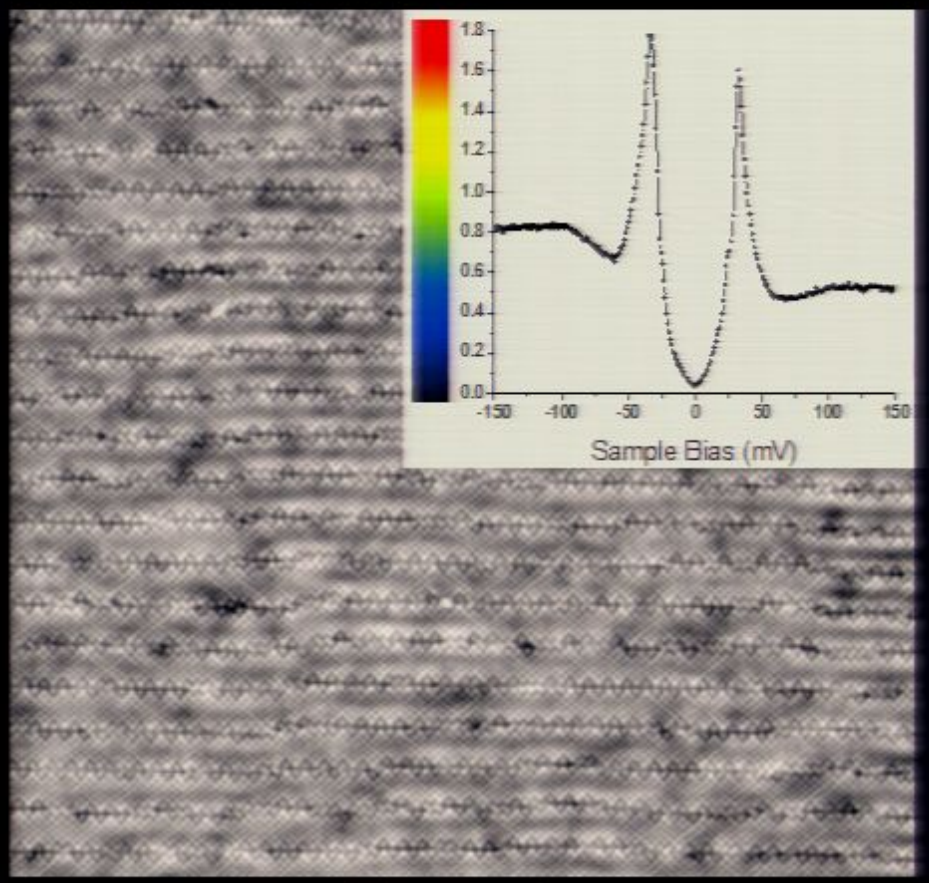

Topography

Atomic-resolution energy resolved

$$LDOS(\vec{r},E) \propto |\Psi(\vec{r},E)|^2$$

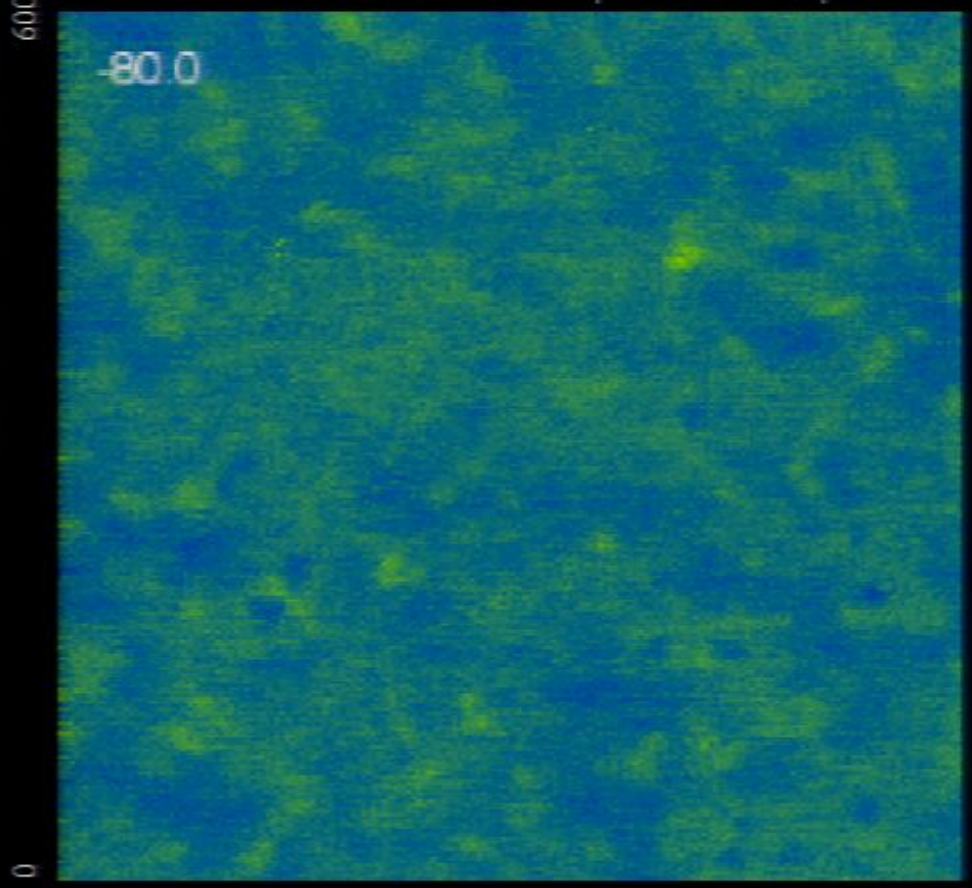

Measure $dI/dV \propto LDOS(E)$ at every atom

Spectroscopic Imaging STM (SI-STM)

Inset shows $LDOS(E)$ spectrum at single atom

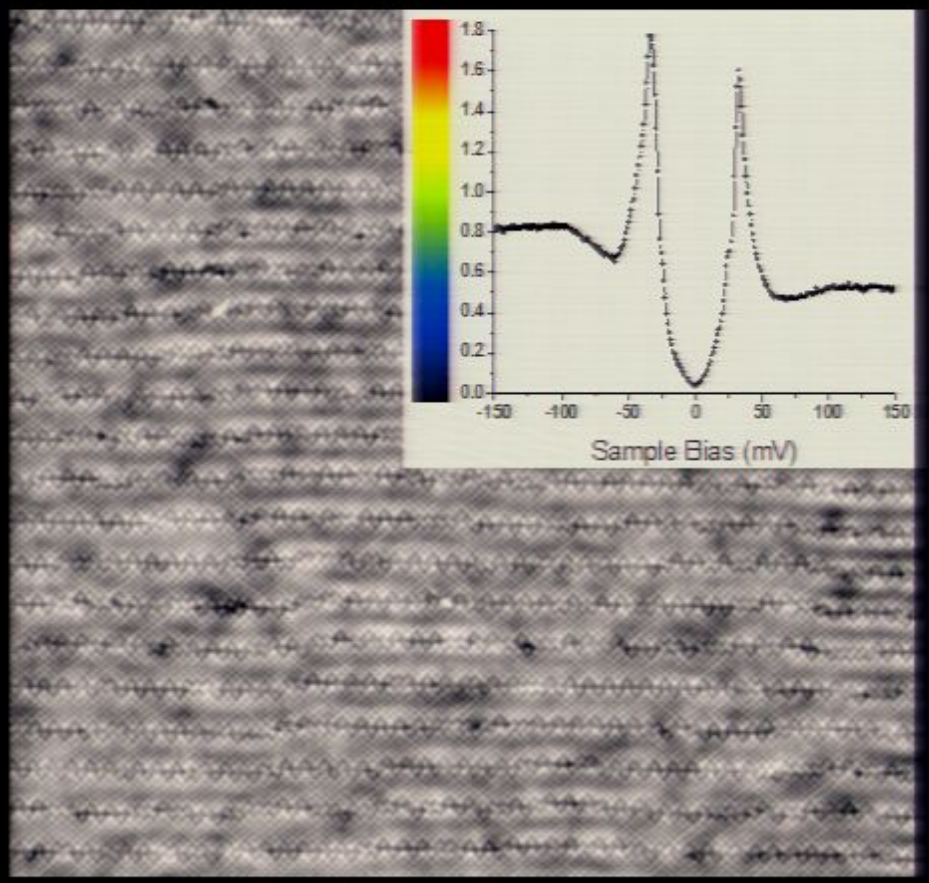

Topography

Atomic-resolution energy resolved

$$LDOS(\vec{r},E) \propto |\Psi(\vec{r},E)|^2$$

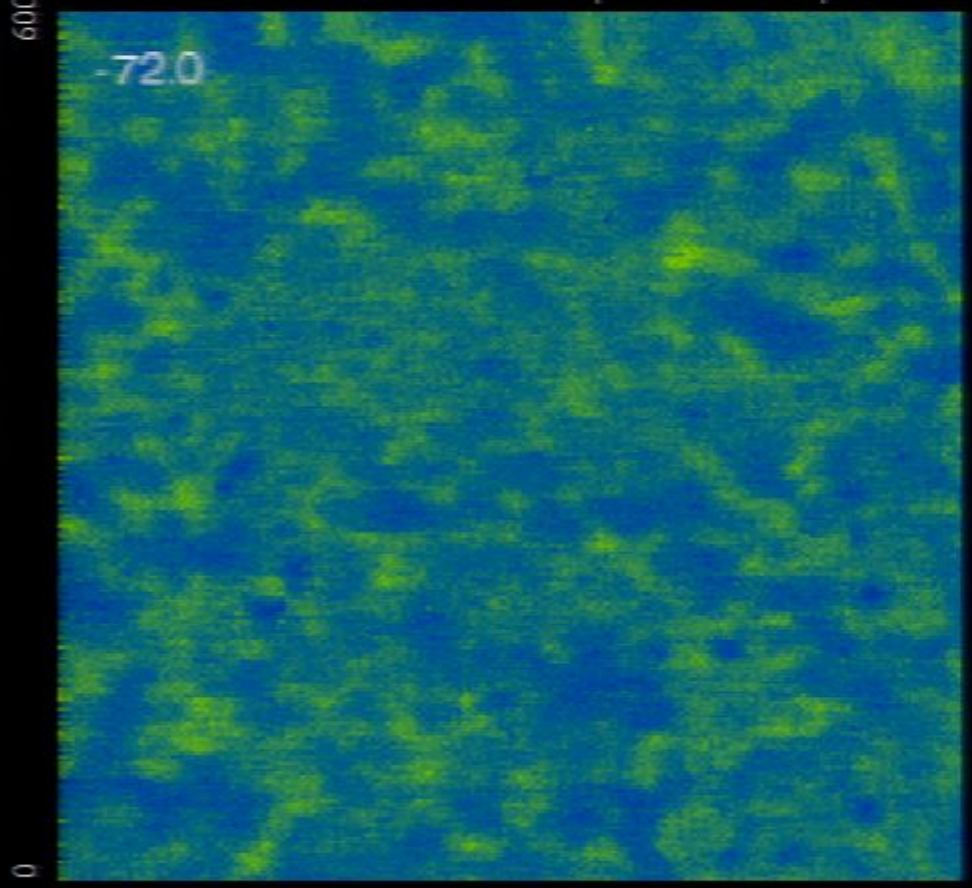

Measure $dI/dV \propto LDOS(E)$ at every atom

Spectroscopic Imaging STM (SI-STM)

Inset shows $LDOS(E)$ spectrum at single atom

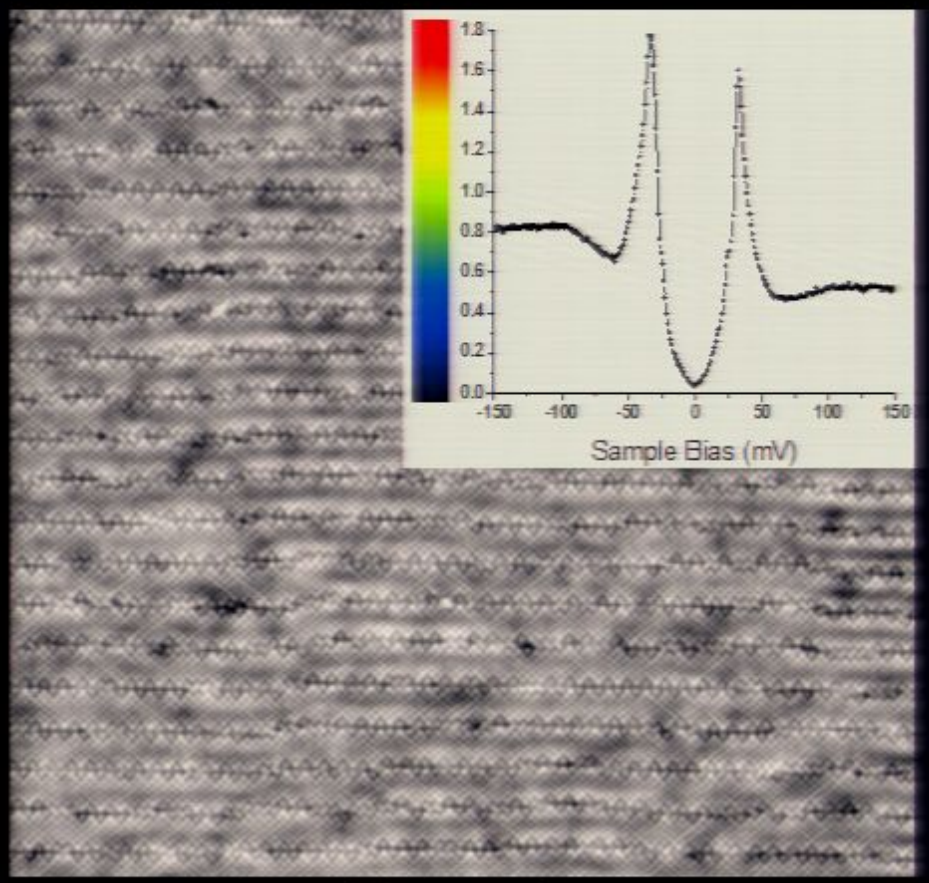

Topography

Atomic-resolution energy resolved

$$LDOS(\vec{r},E) \propto |\Psi(\vec{r},E)|^2$$

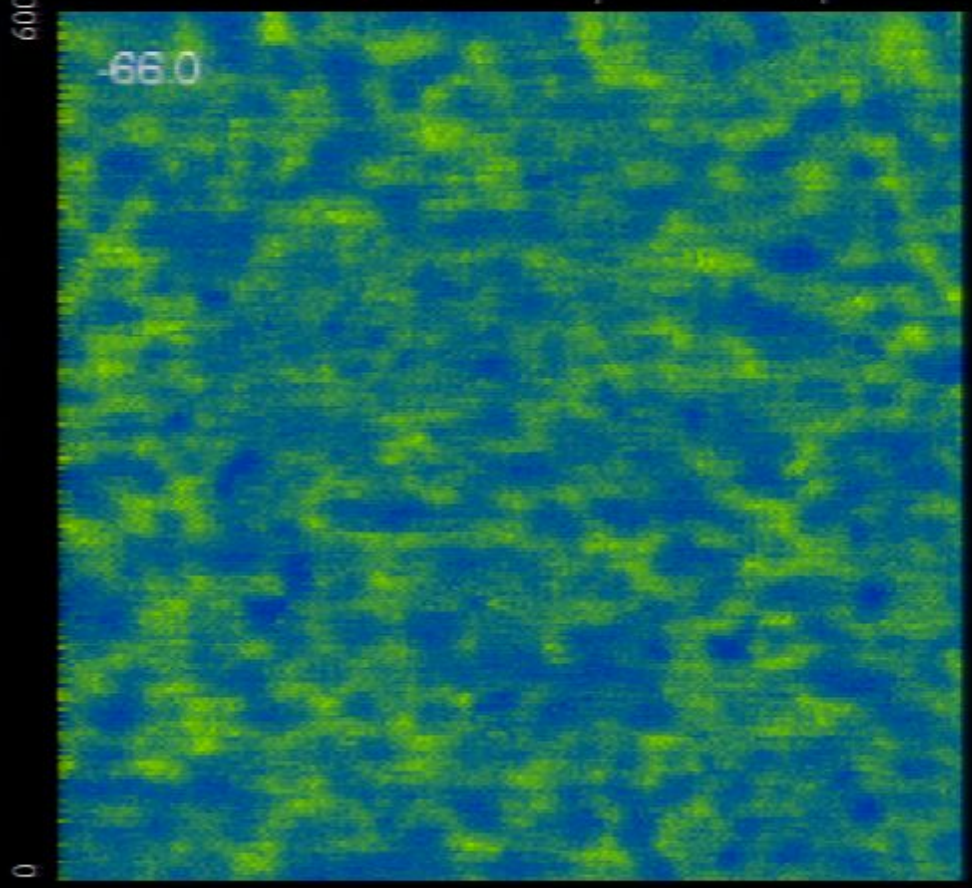

Measure $dI/dV \propto LDOS(E)$ at every atom

Spectroscopic Imaging STM (SI-STM)

Inset shows $LDOS(E)$ spectrum at single atom

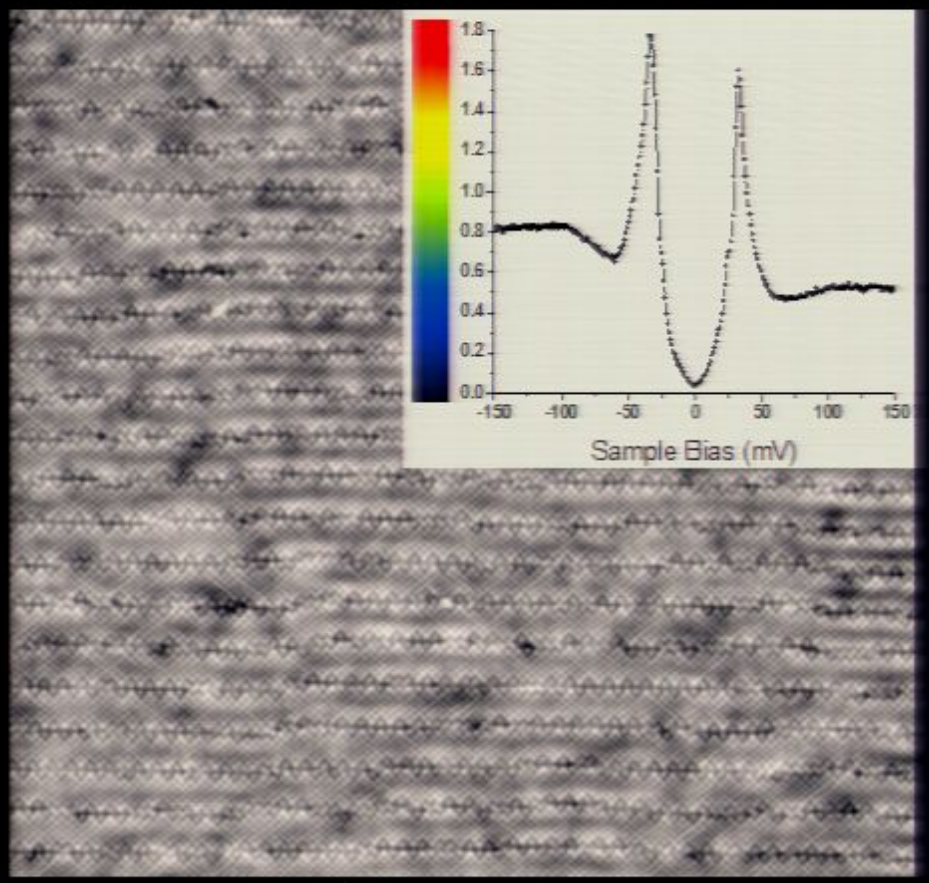

Topography

Atomic-resolution energy resolved

$$LDOS(\vec{r},E) \propto |\Psi(\vec{r},E)|^2$$

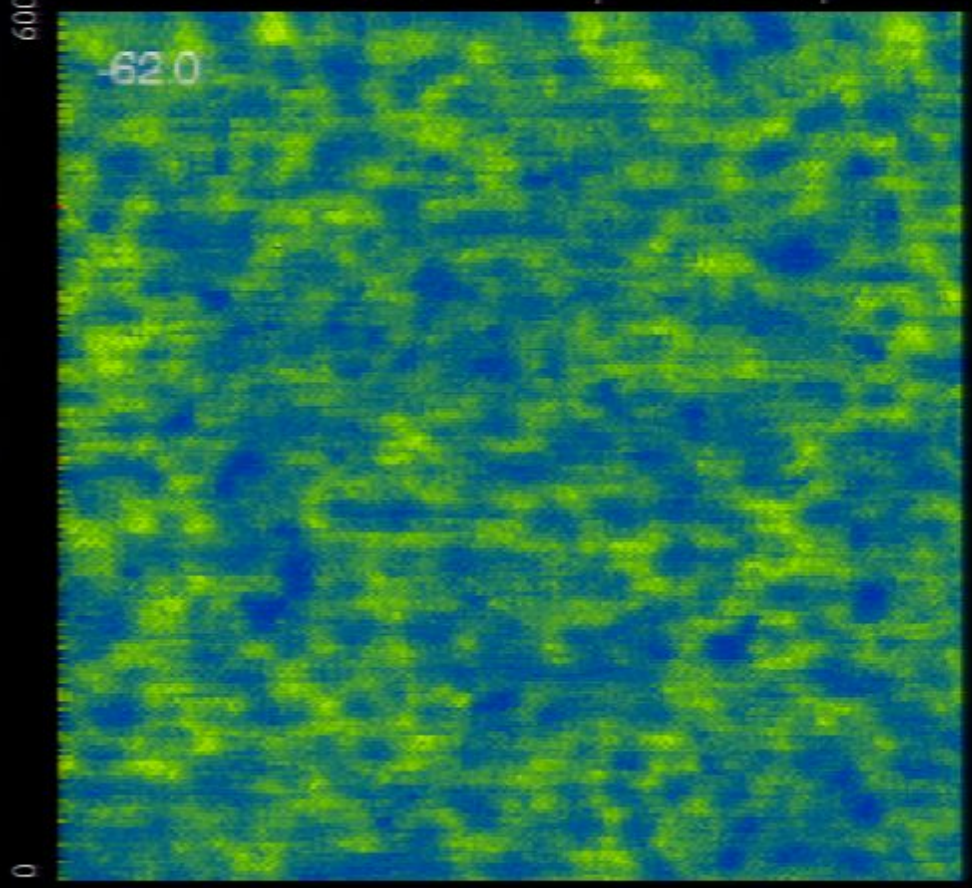

Measure $dI/dV \propto LDOS(E)$ at every atom

Spectroscopic Imaging STM (SI-STM)

Inset shows $LDOS(E)$ spectrum at single atom

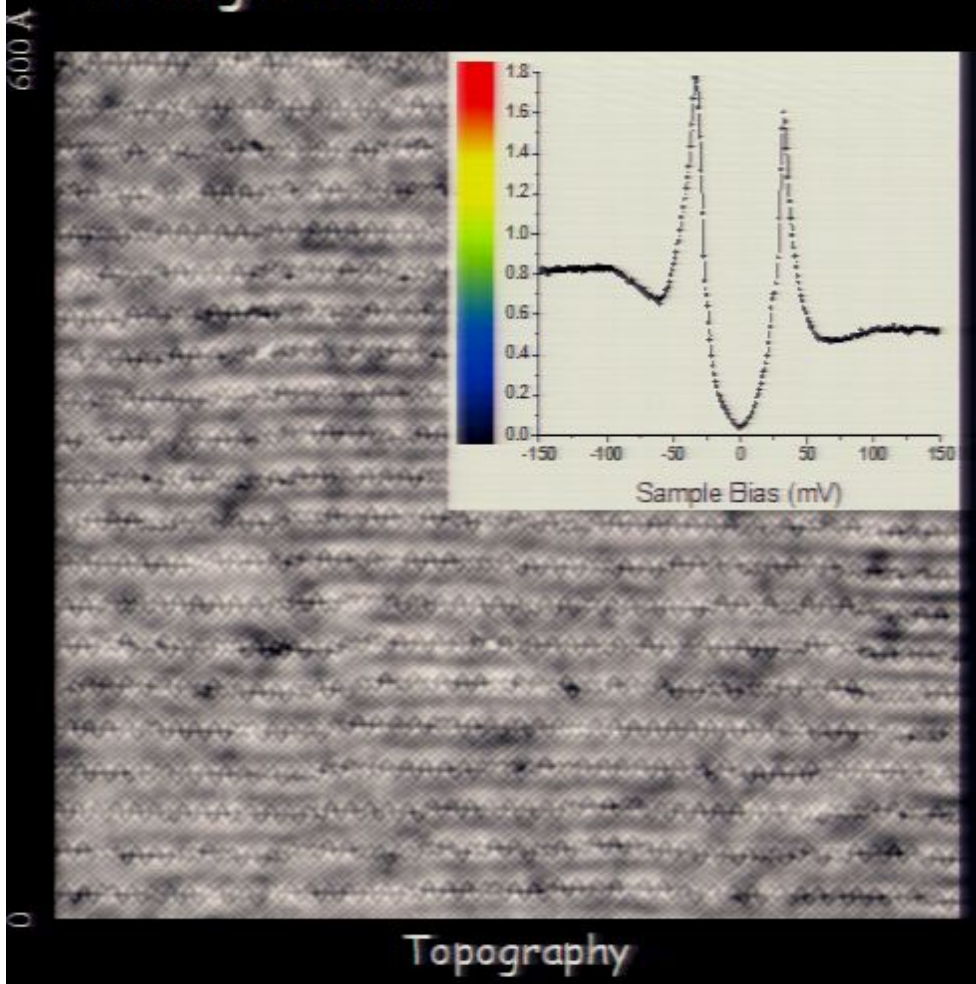

Topography

Atomic-resolution energy resolved

$$LDOS(\vec{r},E) \propto |\Psi(\vec{r},E)|^2$$

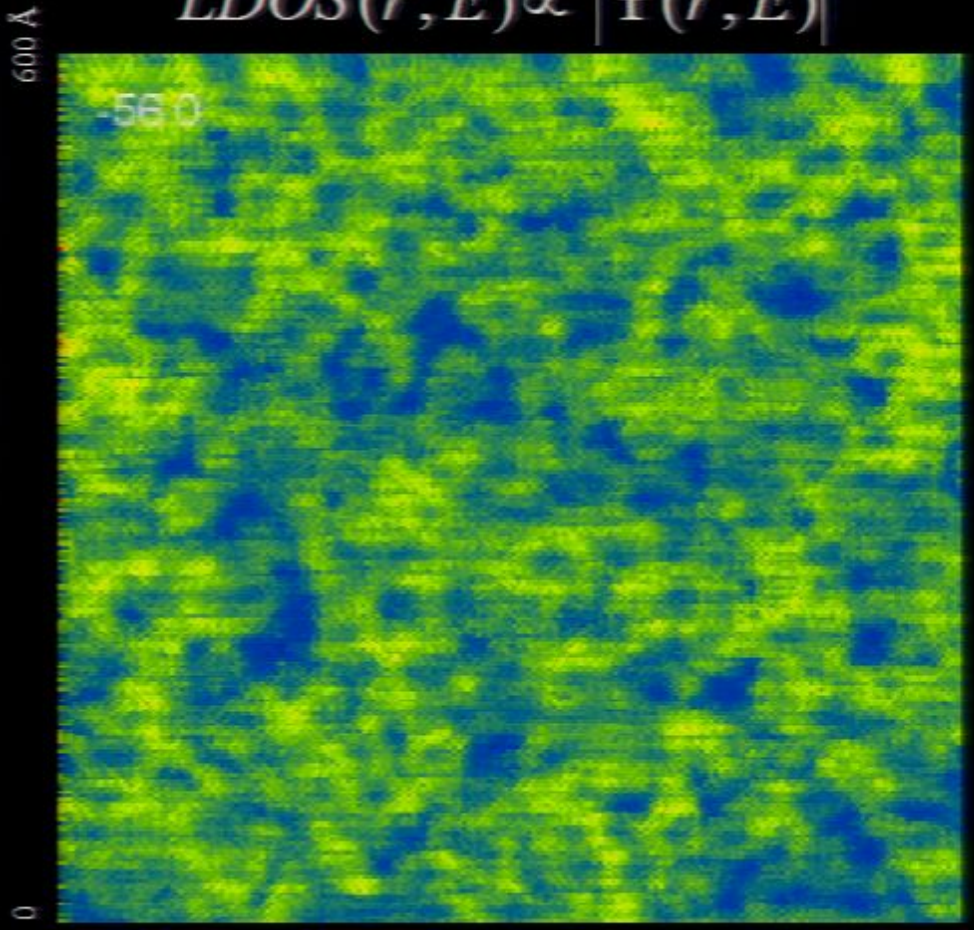

Measure $dI/dV \propto LDOS(E)$ at every atom

Spectroscopic Imaging STM (SI-STM)

Inset shows $LDOS(E)$ spectrum at single atom

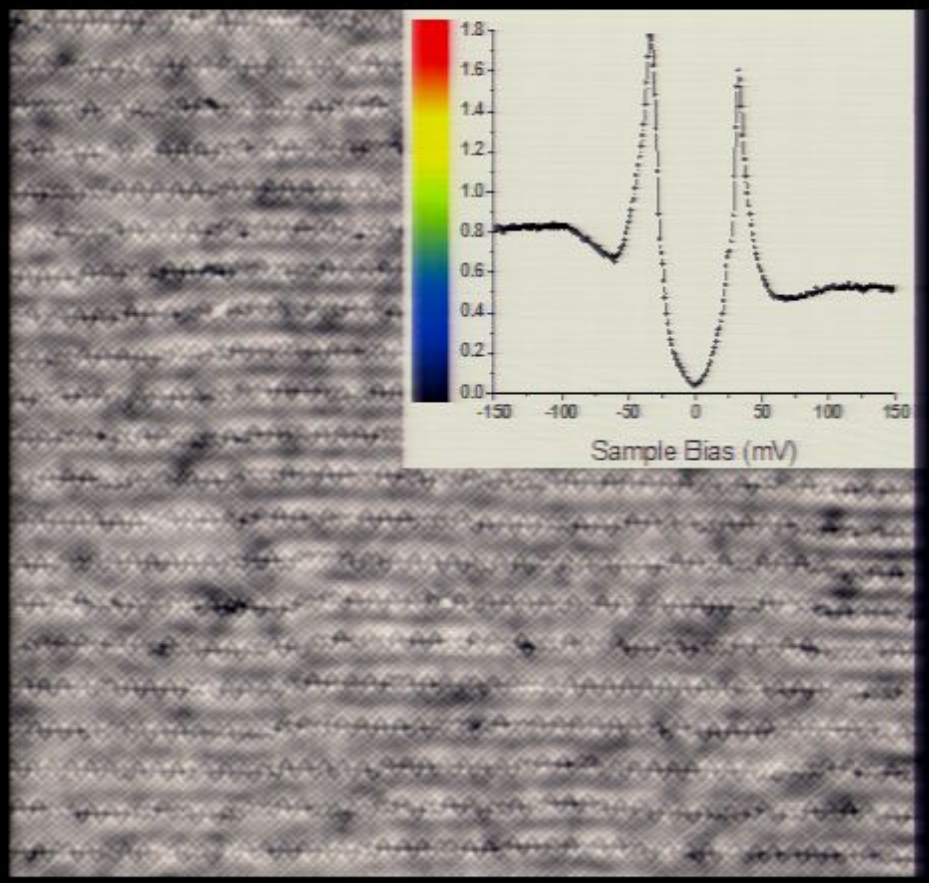

Topography

Atomic-resolution energy resolved

$$LDOS(\vec{r},E) \propto |\Psi(\vec{r},E)|^2$$

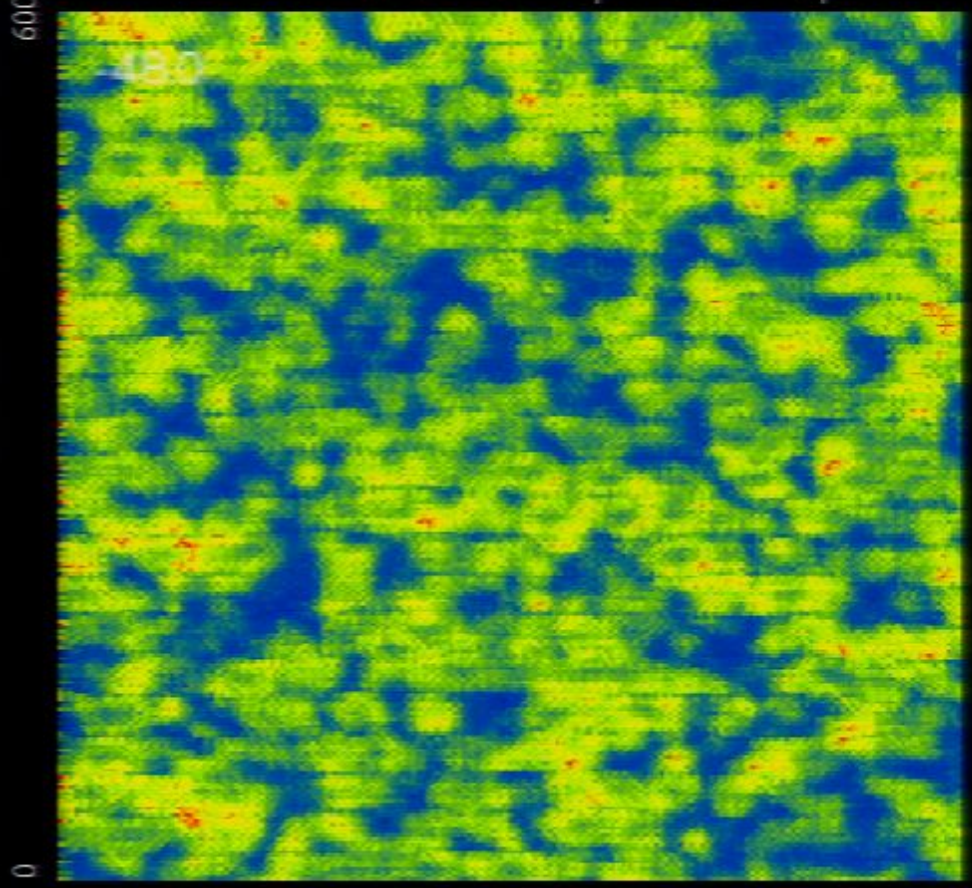

Measure $dI/dV \propto LDOS(E)$ at every atom

Spectroscopic Imaging STM (SI-STM)

Inset shows $LDOS(E)$ spectrum at single atom

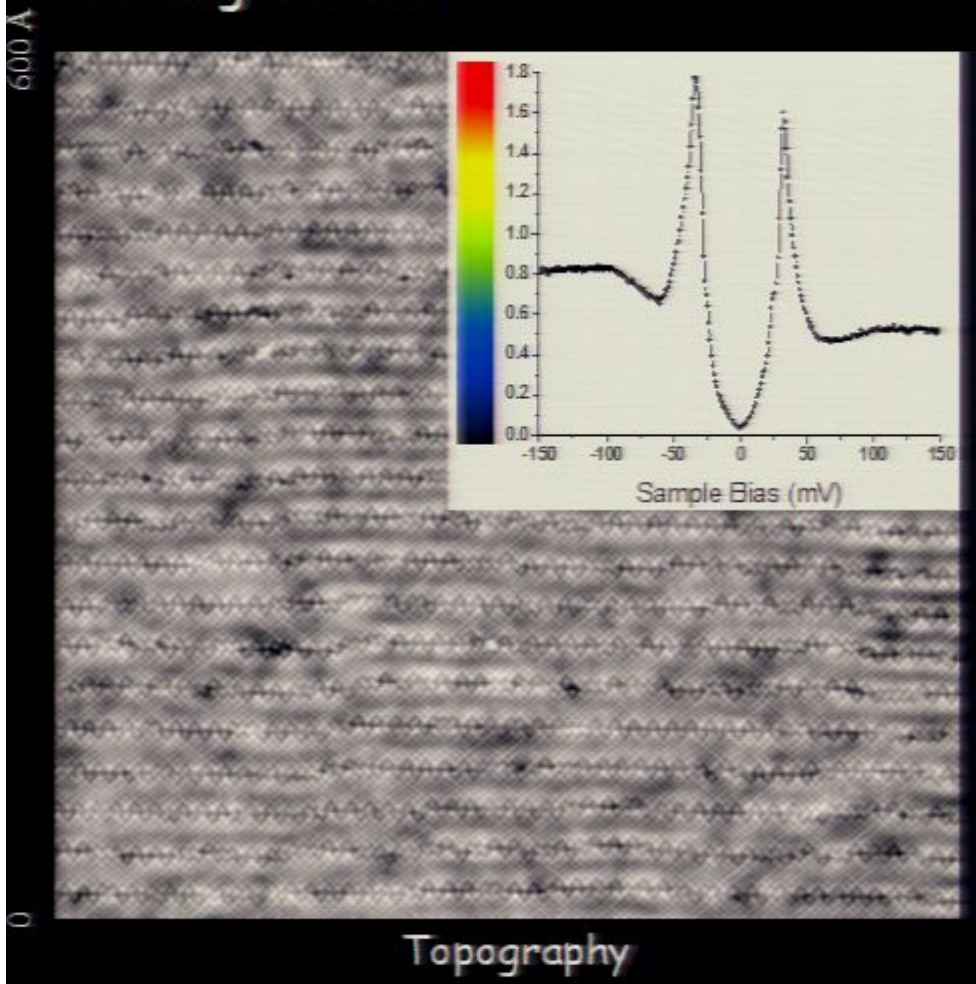

Topography

Atomic-resolution energy resolved

$$LDOS(\vec{r},E) \propto |\Psi(\vec{r},E)|^2$$

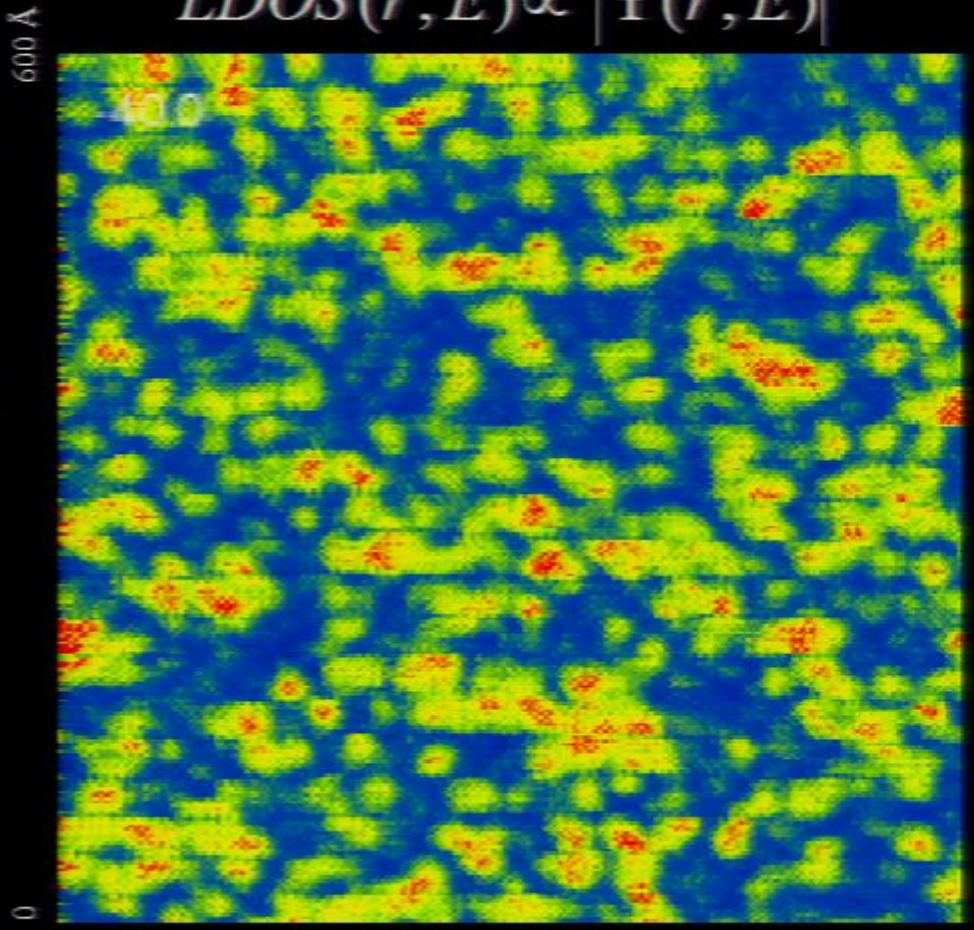

Measure $dI/dV \propto LDOS(E)$ at every atom

Spectroscopic Imaging STM (SI-STM)

Inset shows $LDOS(E)$ spectrum at single atom

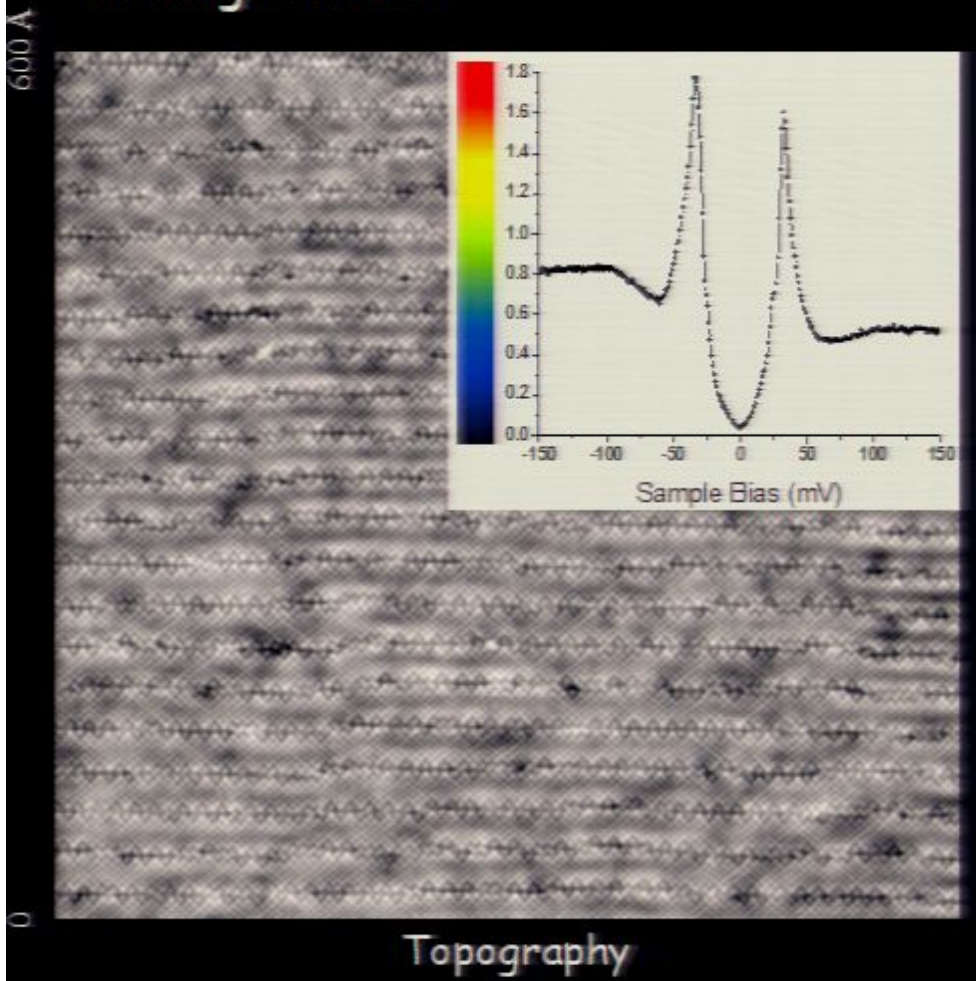

Topography

Atomic-resolution energy resolved

$$LDOS(\vec{r},E) \propto |\Psi(\vec{r},E)|^2$$

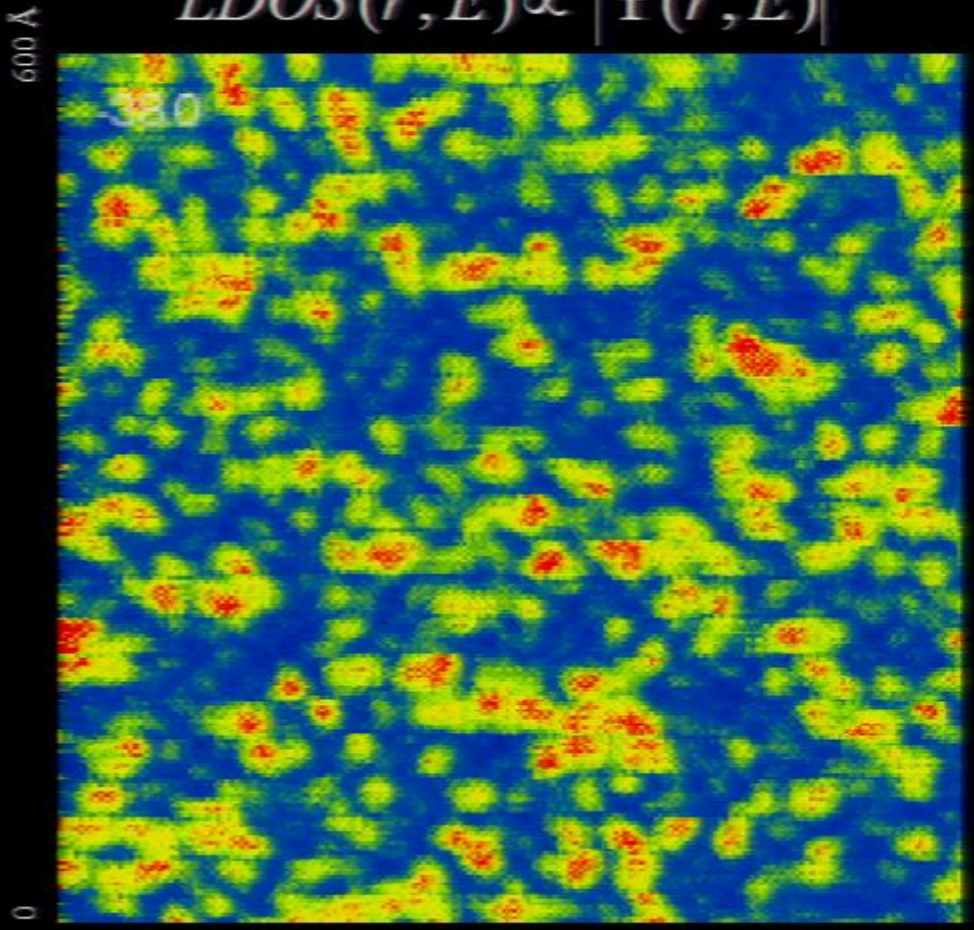

Measure $dI/dV \propto LDOS(E)$ at every atom

Spectroscopic Imaging STM (SI-STM)

Inset shows $LDOS(E)$ spectrum at single atom

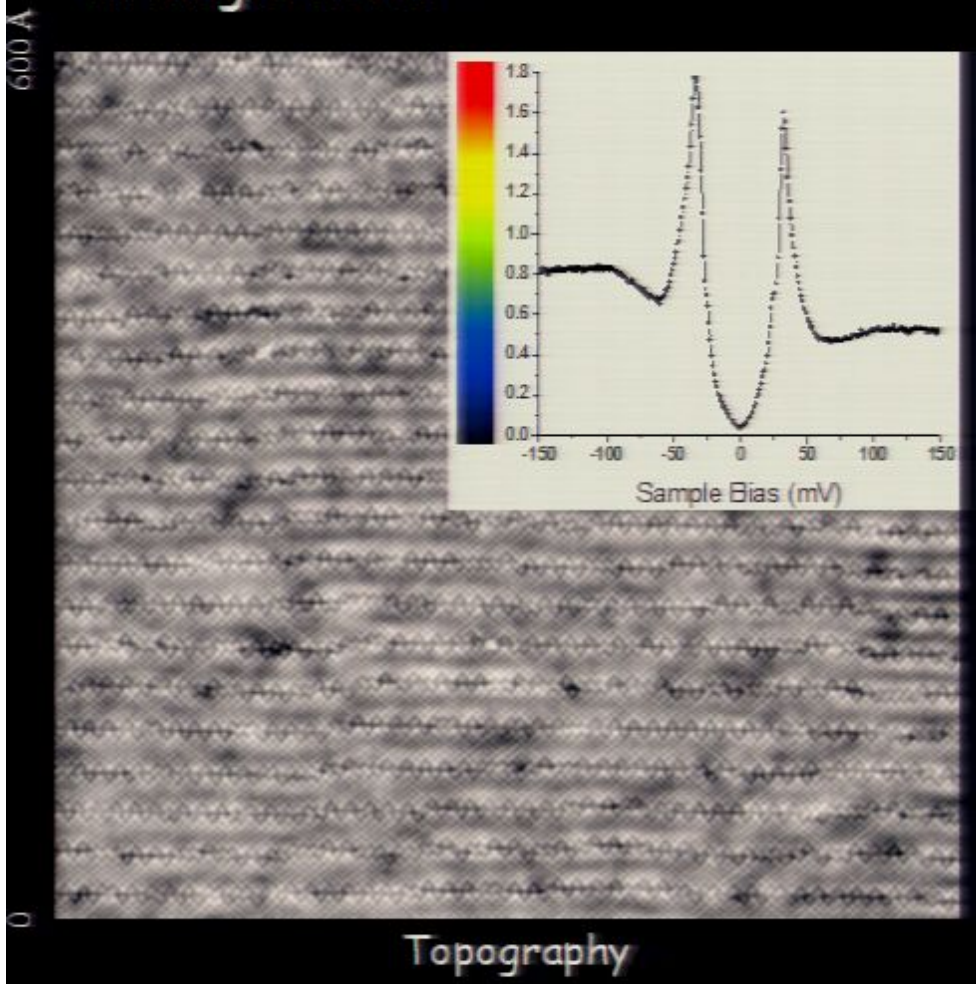

Topography

Atomic-resolution energy resolved

$$LDOS(\vec{r},E) \propto |\Psi(\vec{r},E)|^2$$

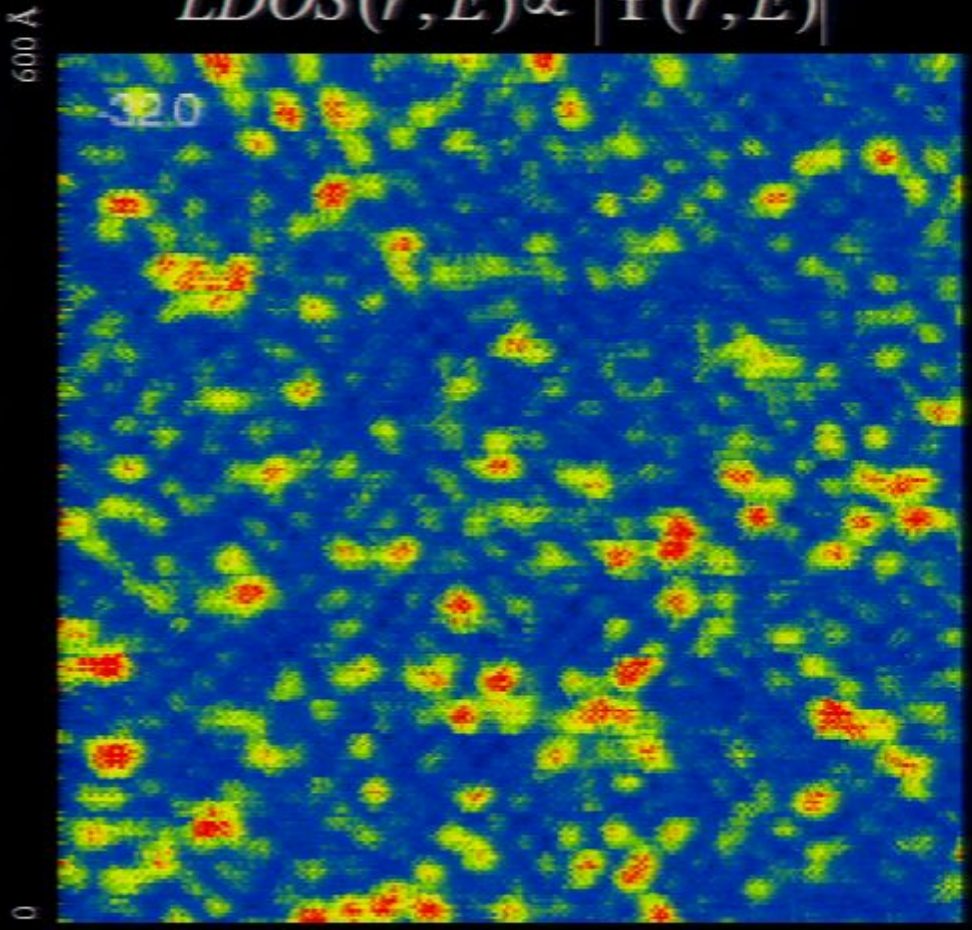

Measure $dI/dV \propto LDOS(E)$ at every atom

Spectroscopic Imaging STM (SI-STM)

Inset shows $LDOS(E)$ spectrum at single atom

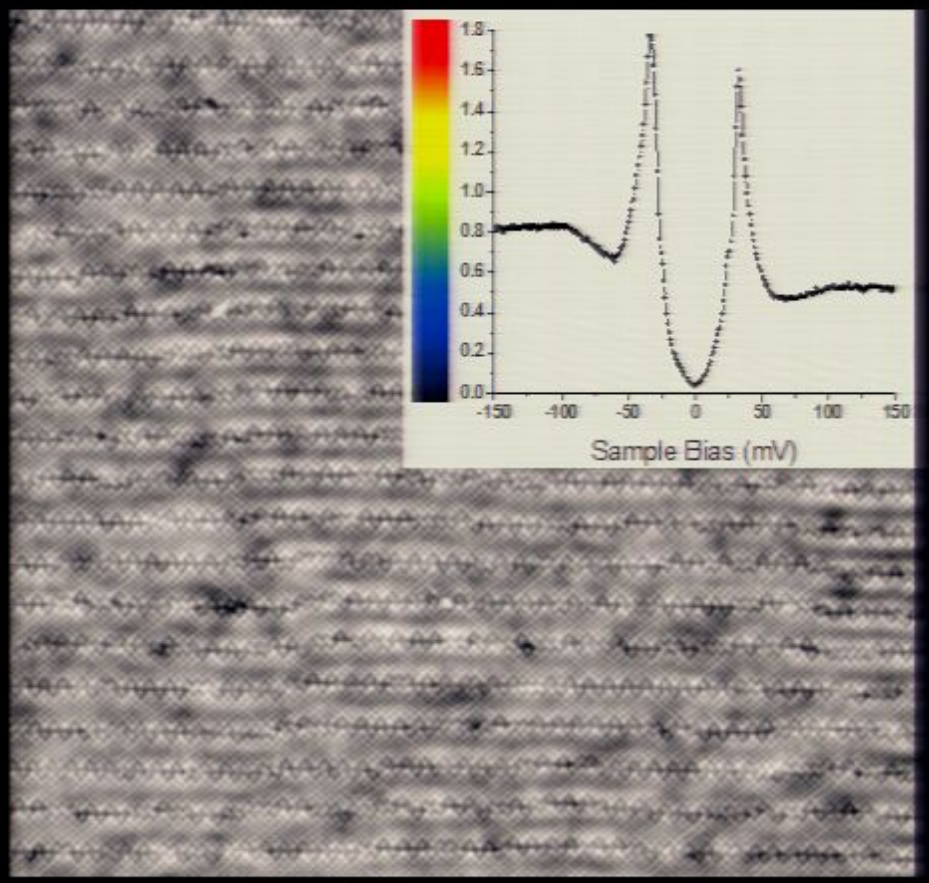

Topography

Atomic-resolution energy resolved

$$LDOS(\vec{r},E) \propto |\Psi(\vec{r},E)|^2$$

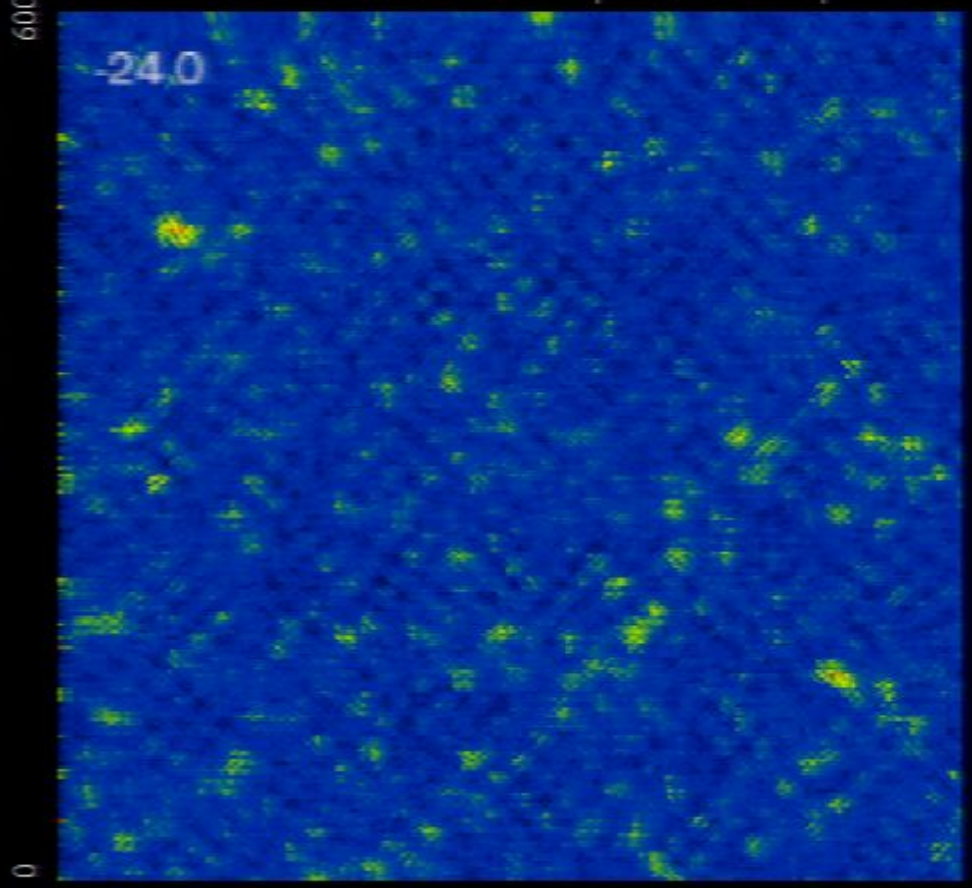

Measure $dI/dV \propto LDOS(E)$ at every atom

Spectroscopic Imaging STM (SI-STM)

Inset shows $LDOS(E)$ spectrum at single atom

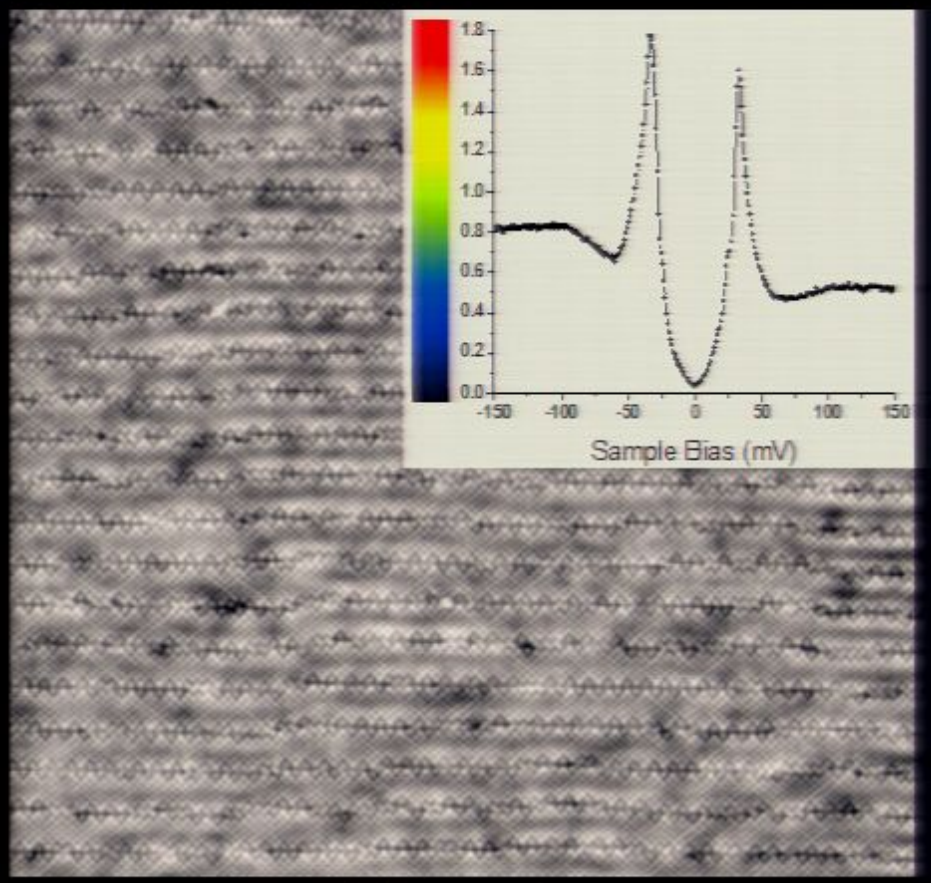

Topography

Atomic-resolution energy resolved

$$LDOS(\vec{r},E) \propto |\Psi(\vec{r},E)|^2$$

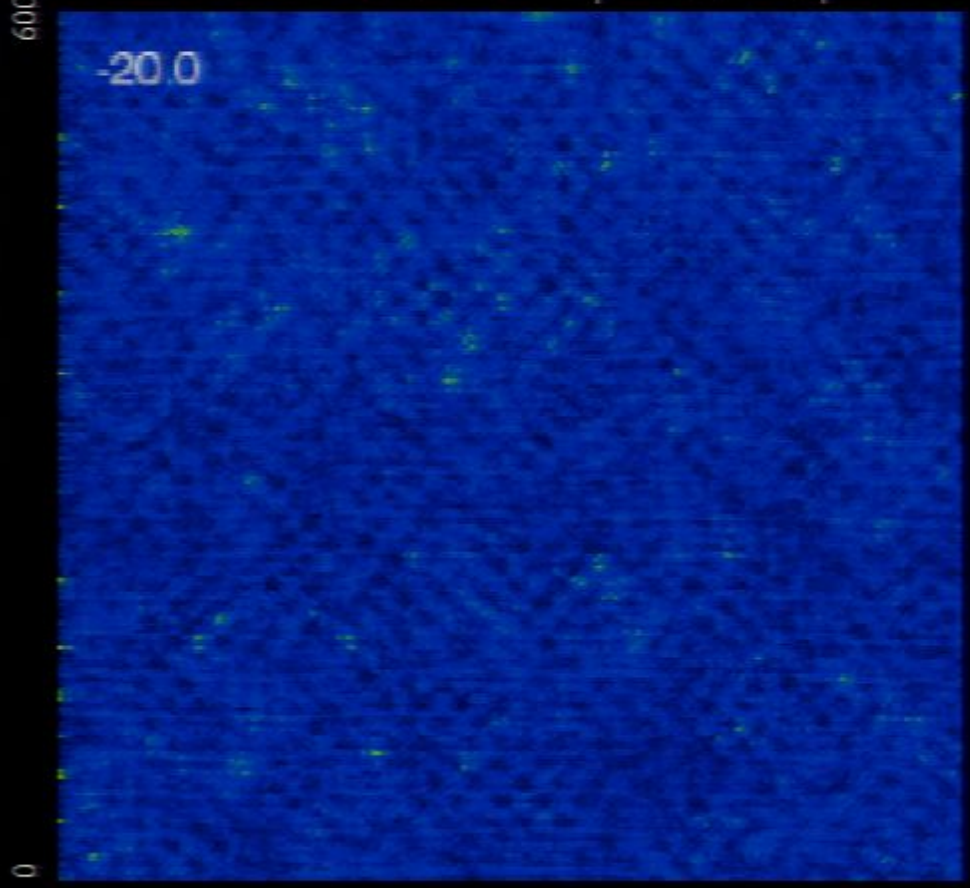

Measure $dI/dV \propto LDOS(E)$ at every atom

Spectroscopic Imaging STM (SI-STM)

Inset shows $LDOS(E)$ spectrum at single atom

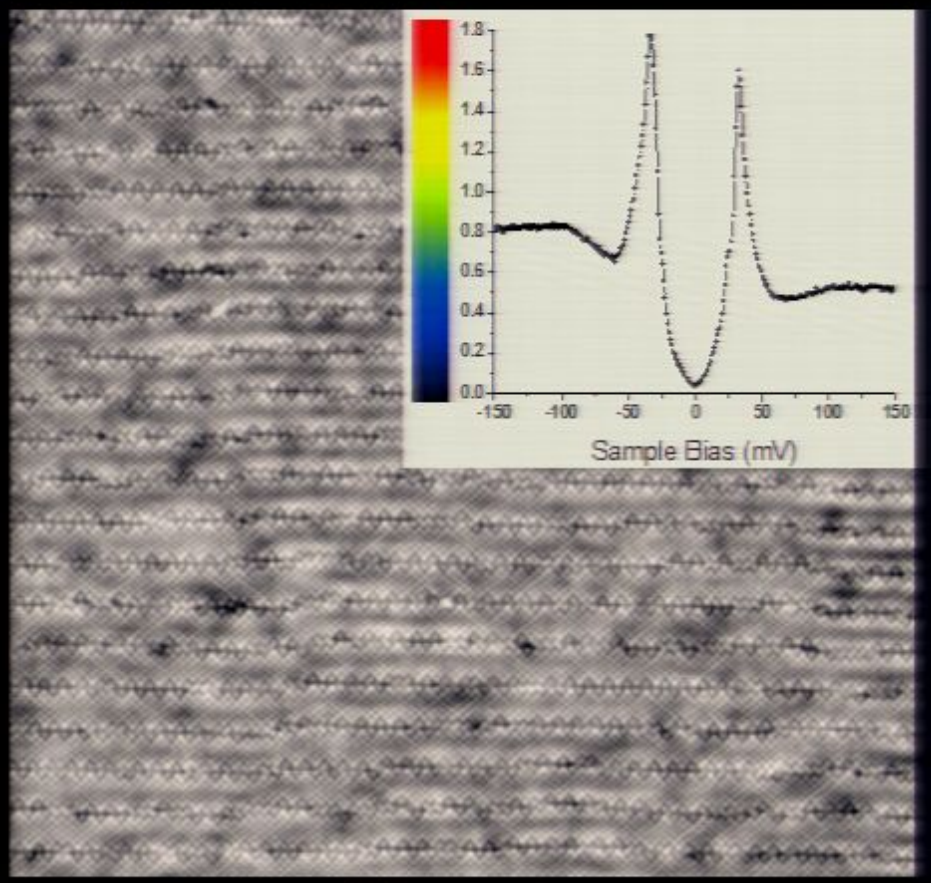

Topography

Atomic-resolution energy resolved

$$LDOS(\vec{r},E) \propto |\Psi(\vec{r},E)|^2$$

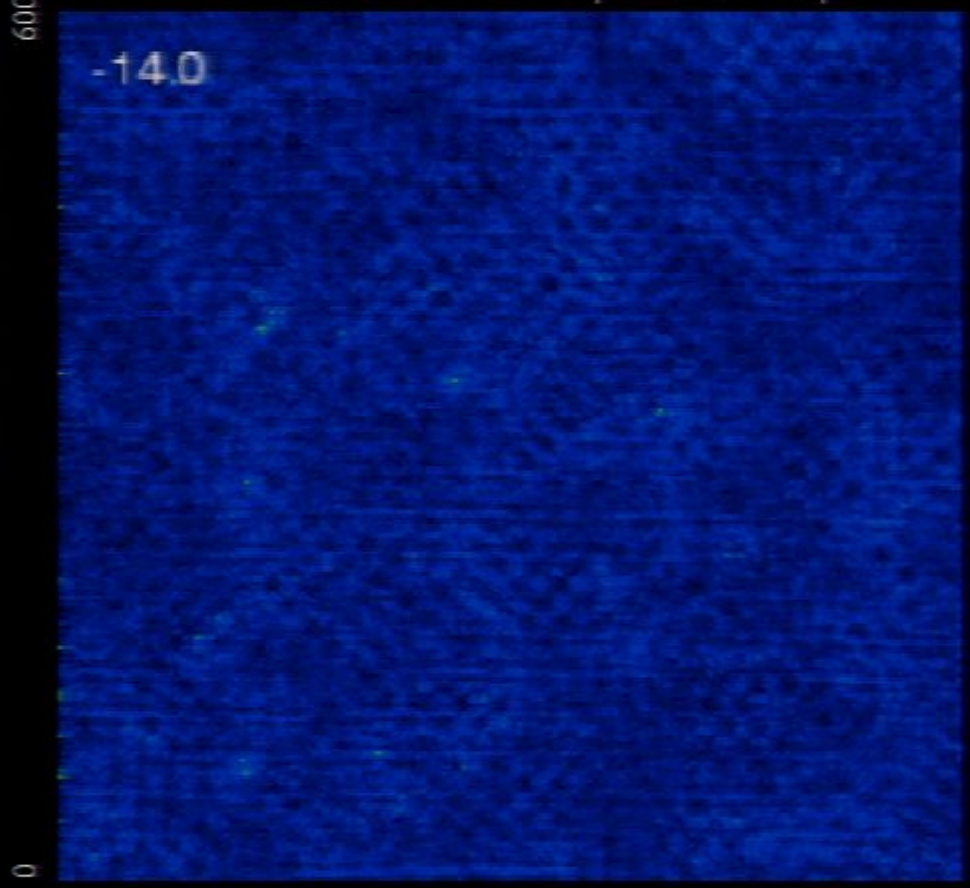

Measure $dI/dV \propto LDOS(E)$ at every atom

Spectroscopic Imaging STM (SI-STM)

Inset shows $LDOS(E)$ spectrum at single atom

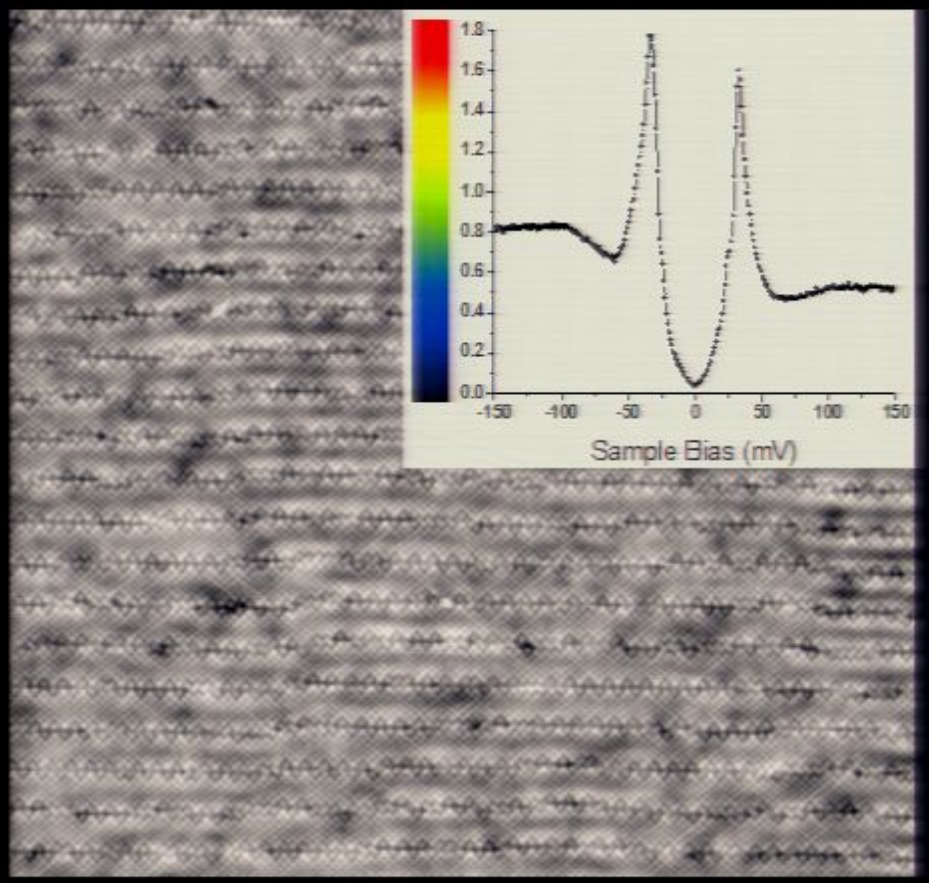

Topography

Atomic-resolution energy resolved

$$LDOS(\vec{r},E) \propto |\Psi(\vec{r},E)|^2$$

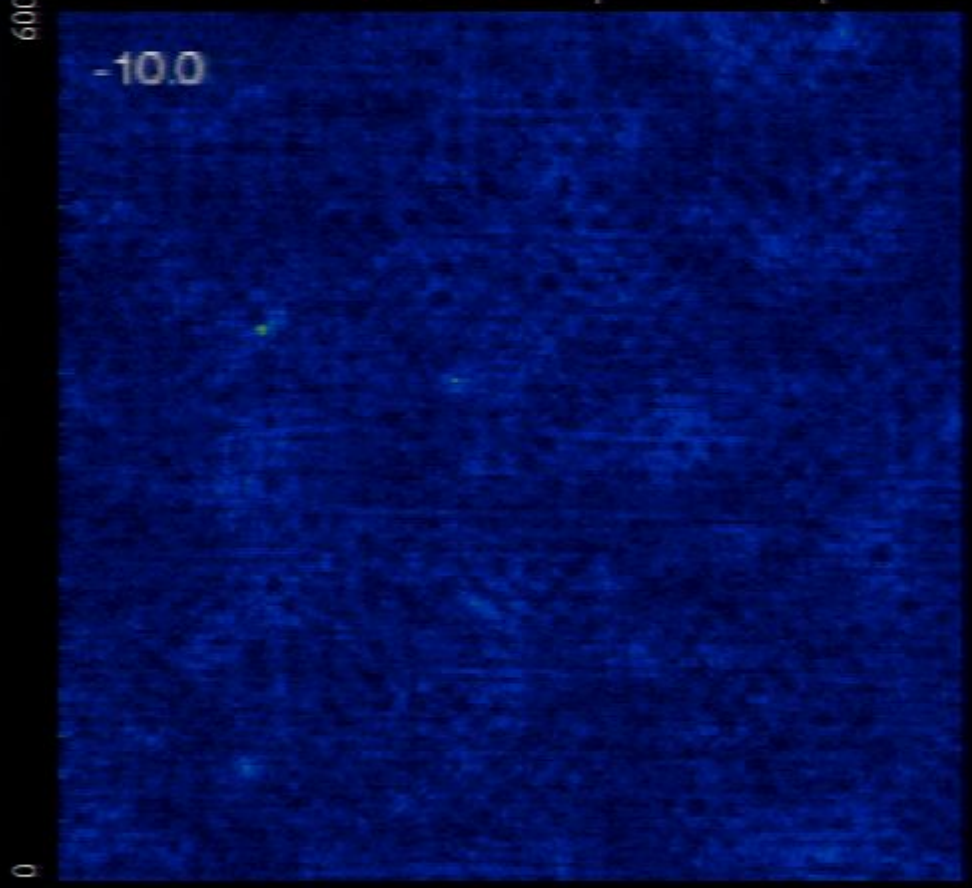

Measure $dI/dV \propto LDOS(E)$ at every atom

Spectroscopic Imaging STM (SI-STM)

Inset shows $LDOS(E)$ spectrum at single atom

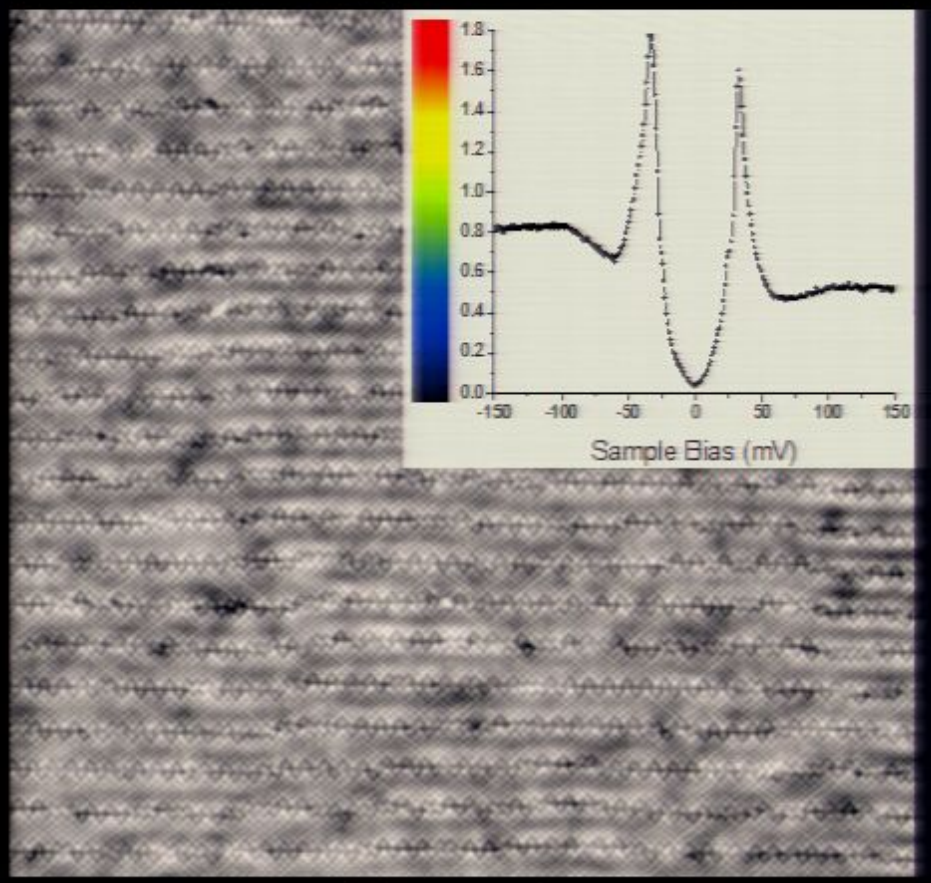

Topography

Atomic-resolution energy resolved

$$LDOS(\vec{r},E) \propto |\Psi(\vec{r},E)|^2$$

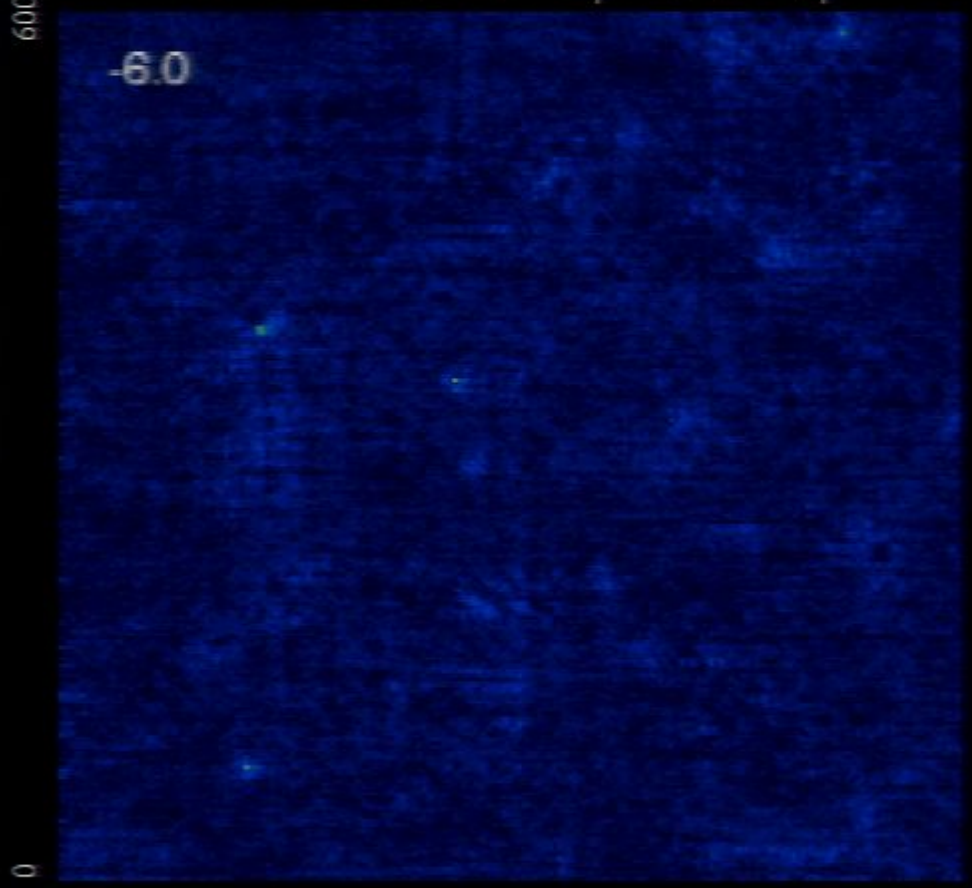

Measure $dI/dV \propto LDOS(E)$ at every atom

Spectroscopic Imaging STM (SI-STM)

Inset shows $LDOS(E)$ spectrum at single atom

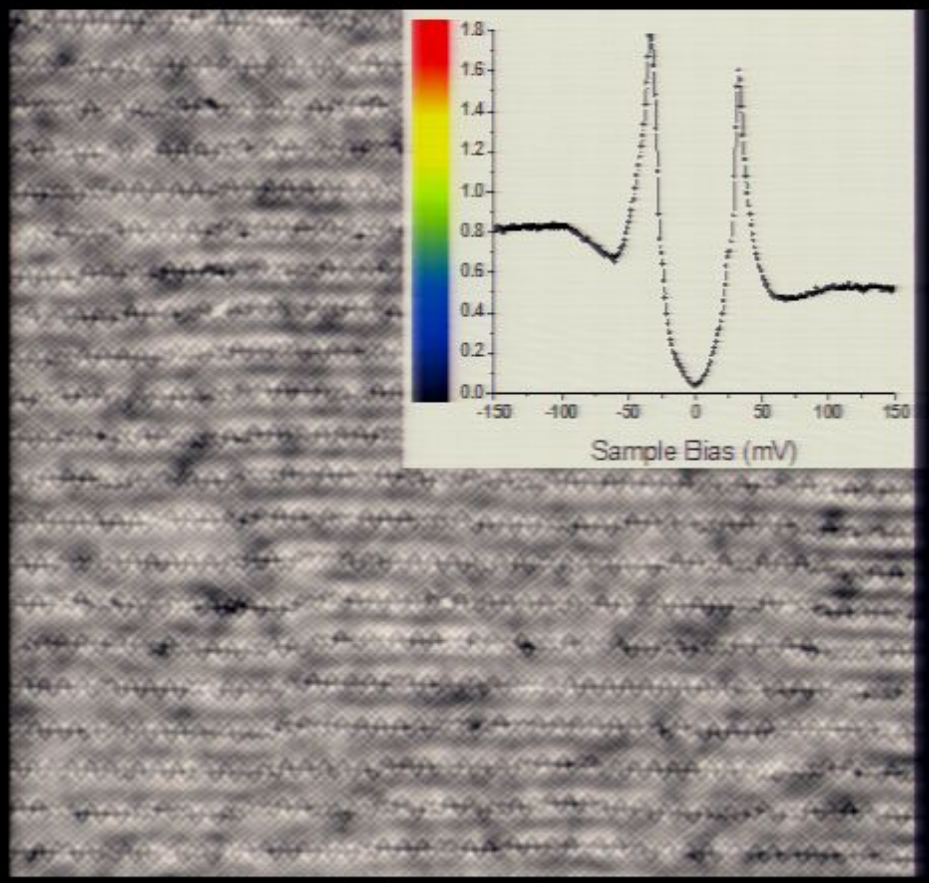

Topography

Atomic-resolution energy resolved

$$LDOS(\vec{r},E) \propto |\Psi(\vec{r},E)|^2$$

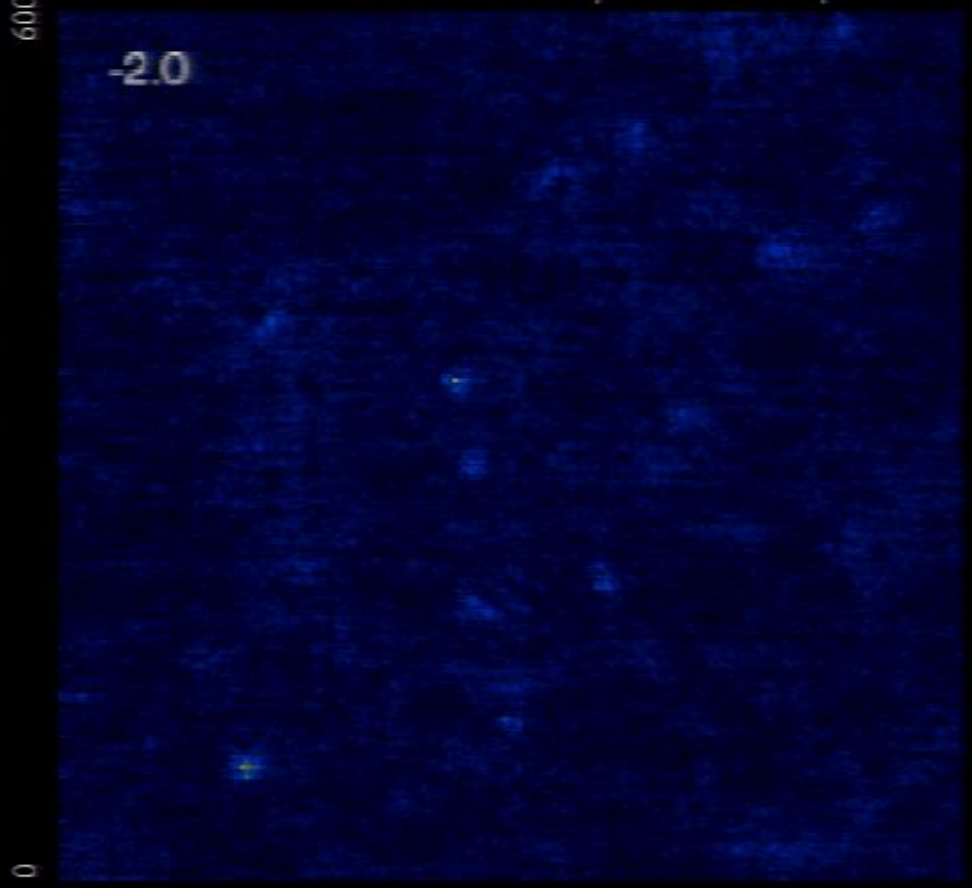

Measure $dI/dV \propto LDOS(E)$ at every atom

Spectroscopic Imaging STM (SI-STM)

Inset shows $LDOS(E)$ spectrum at single atom

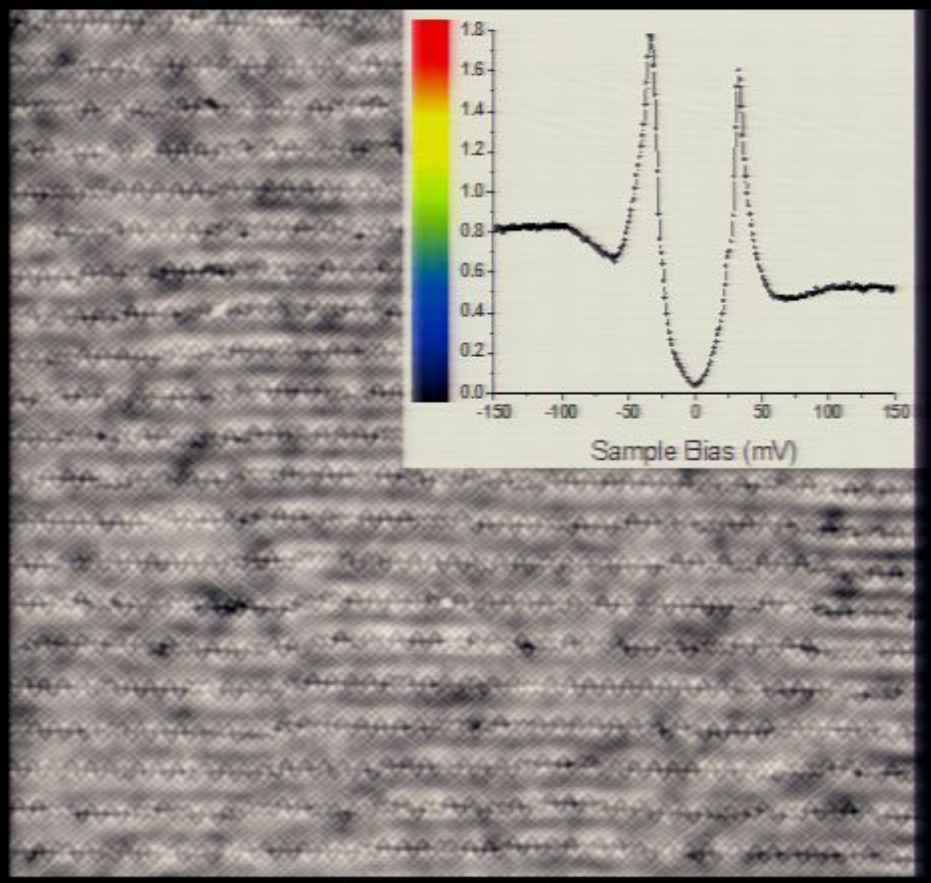

Topography

Atomic-resolution energy resolved

$$LDOS(\vec{r},E) \propto |\Psi(\vec{r},E)|^2$$

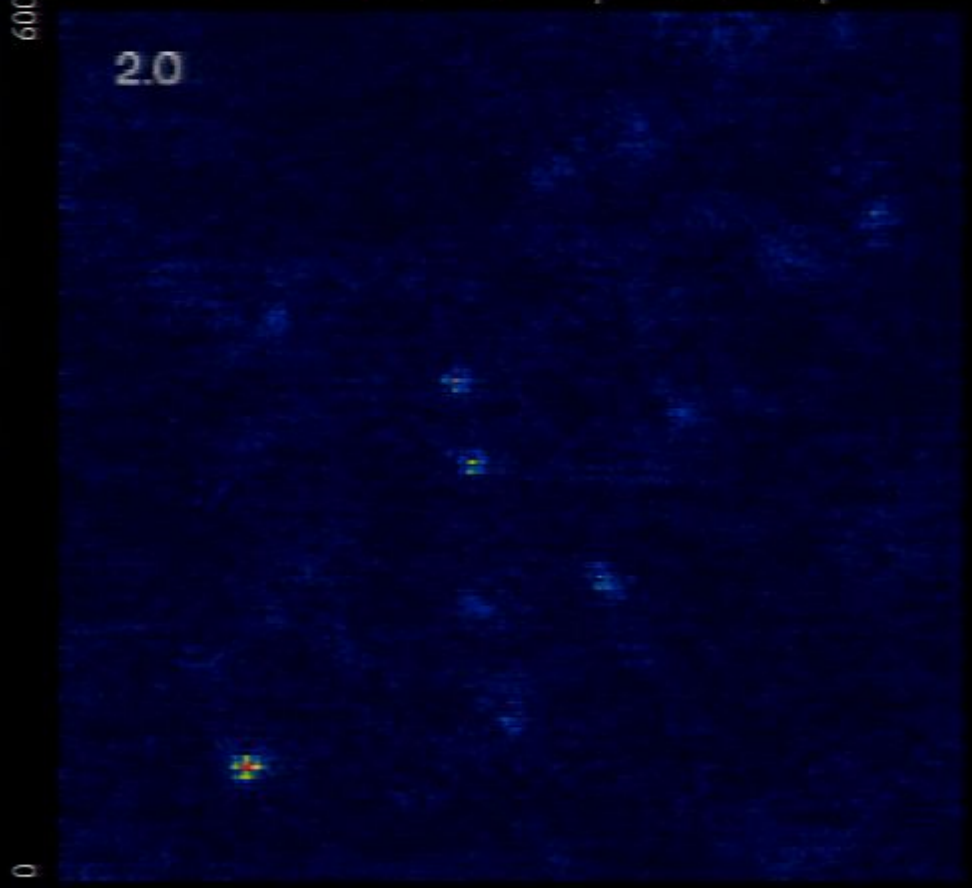

Measure $dI/dV \propto LDOS(E)$ at every atom

Spectroscopic Imaging STM (SI-STM)

Inset shows $LDOS(E)$ spectrum at single atom

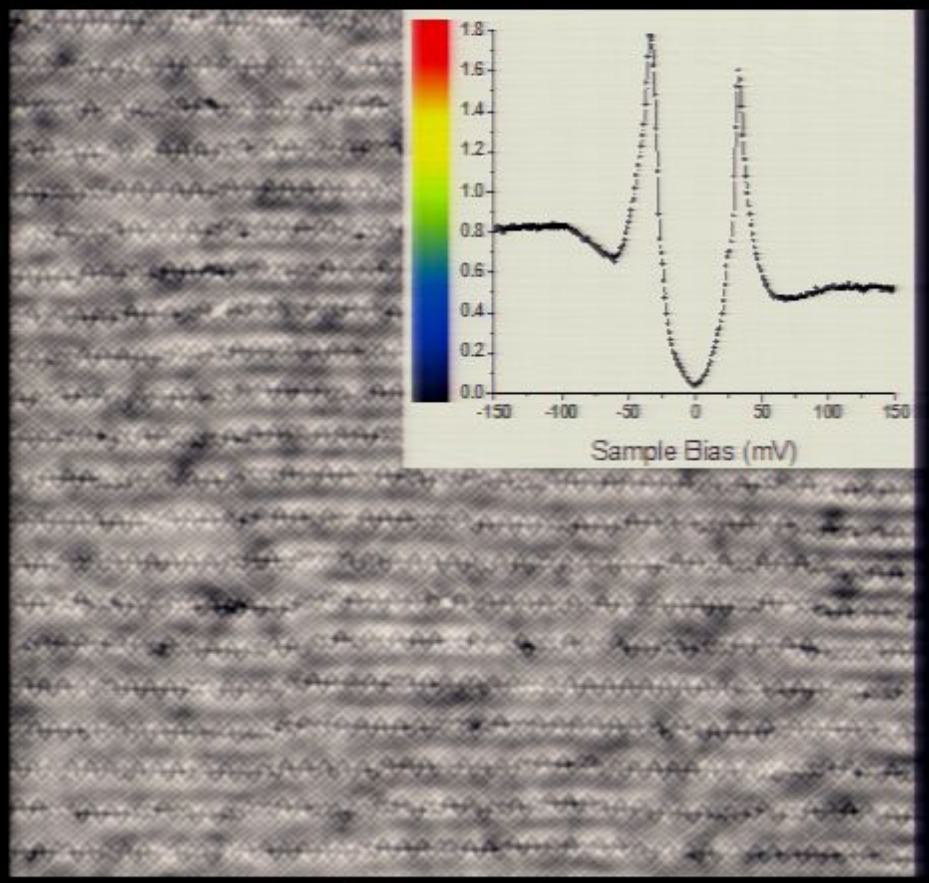

Topography

Atomic-resolution energy resolved

$$LDOS(\vec{r},E) \propto \left|\Psi(\vec{r},E)\right|^2$$

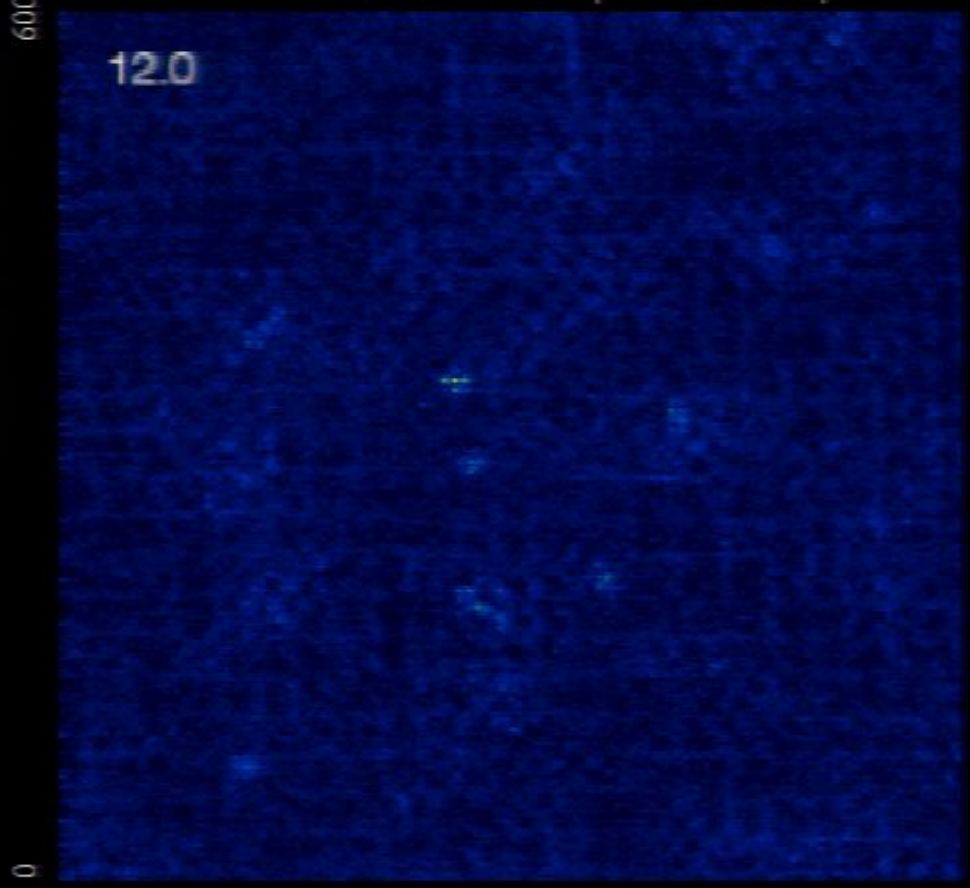

Measure $dI/dV \propto LDOS(E)$ at every atom

Spectroscopic Imaging STM (SI-STM)

Inset shows $LDOS(E)$ spectrum at single atom

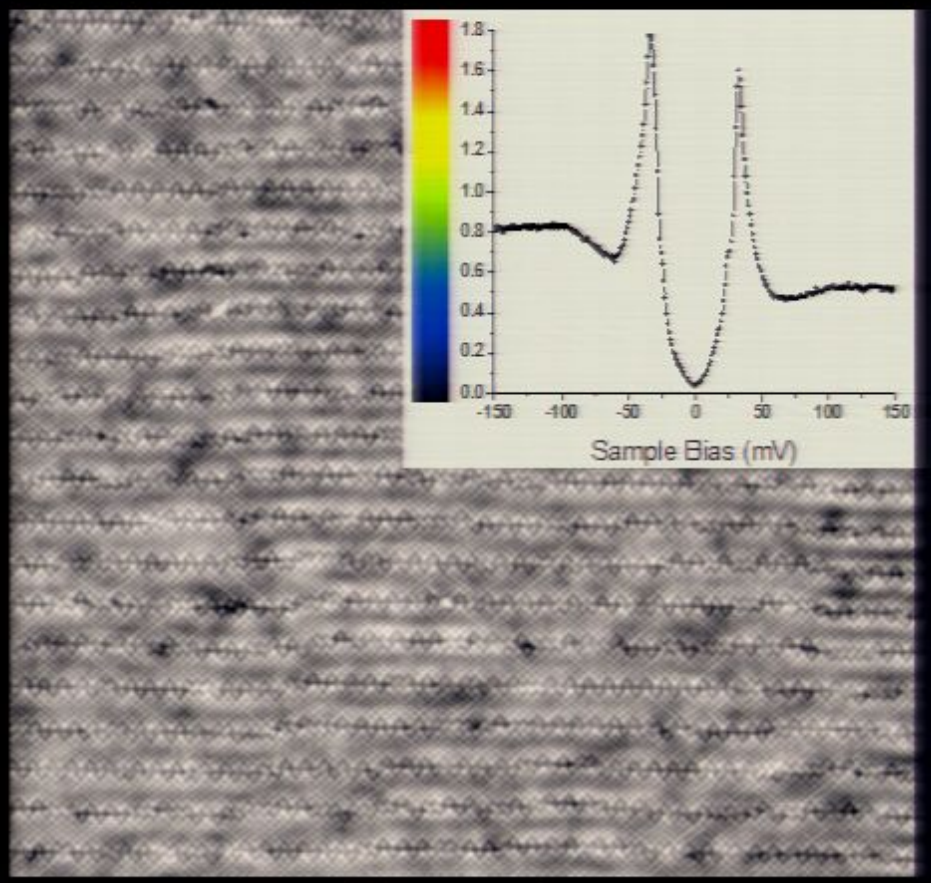

Topography

Atomic-resolution energy resolved

$$LDOS(\vec{r},E) \propto \left|\Psi(\vec{r},E)\right|^2$$

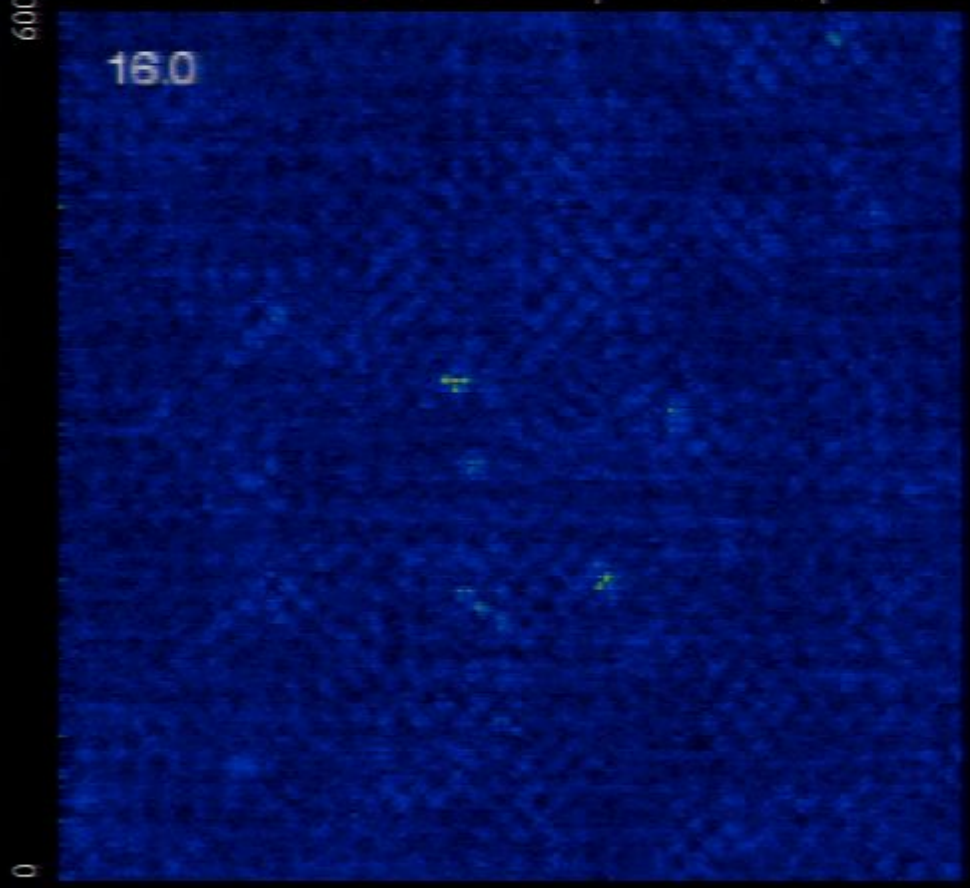

Measure $dI/dV \propto LDOS(E)$ at every atom

Spectroscopic Imaging STM (SI-STM)

Inset shows $LDOS(E)$ spectrum at single atom

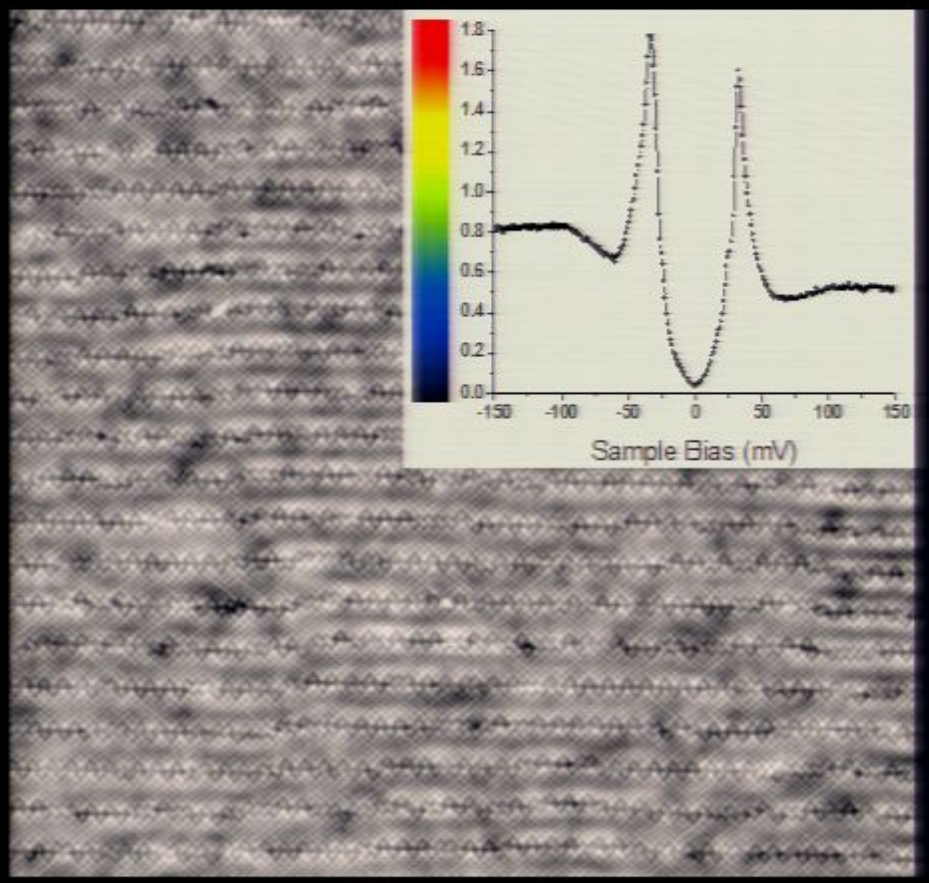

Topography

Atomic-resolution energy resolved

$$LDOS(\vec{r},E) \propto |\Psi(\vec{r},E)|^2$$

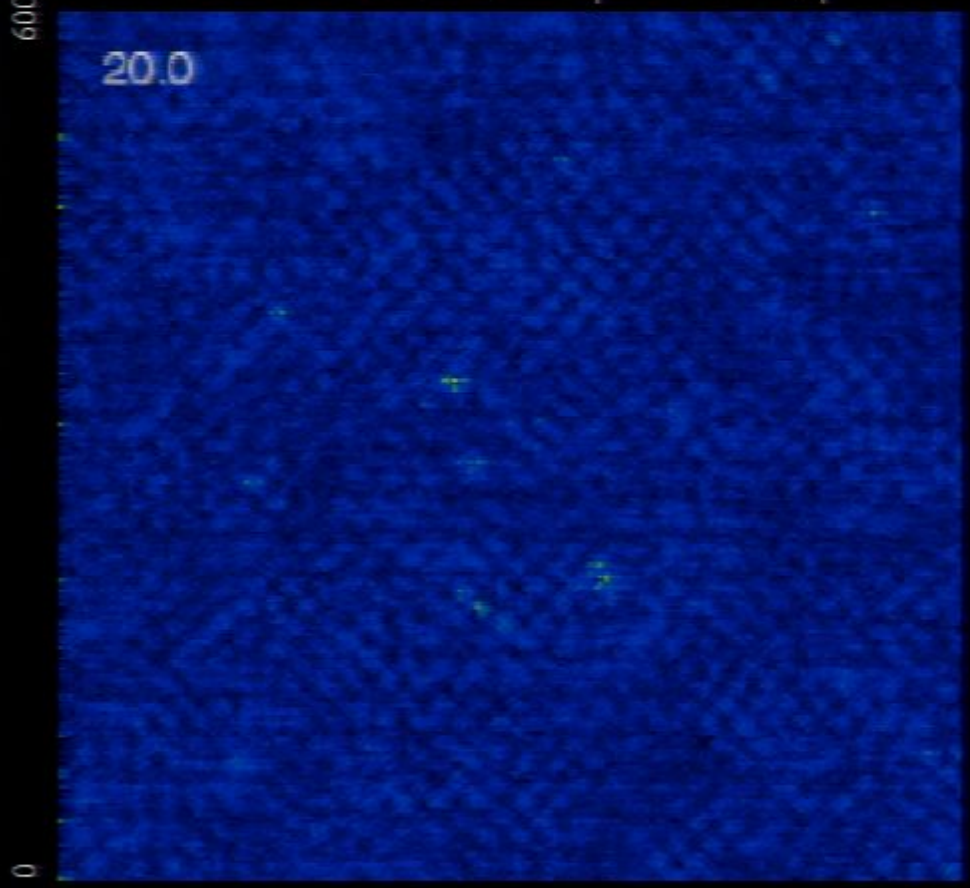

Measure $dI/dV \propto LDOS(E)$ at every atom

Spectroscopic Imaging STM (SI-STM)

Inset shows $LDOS(E)$ spectrum at single atom

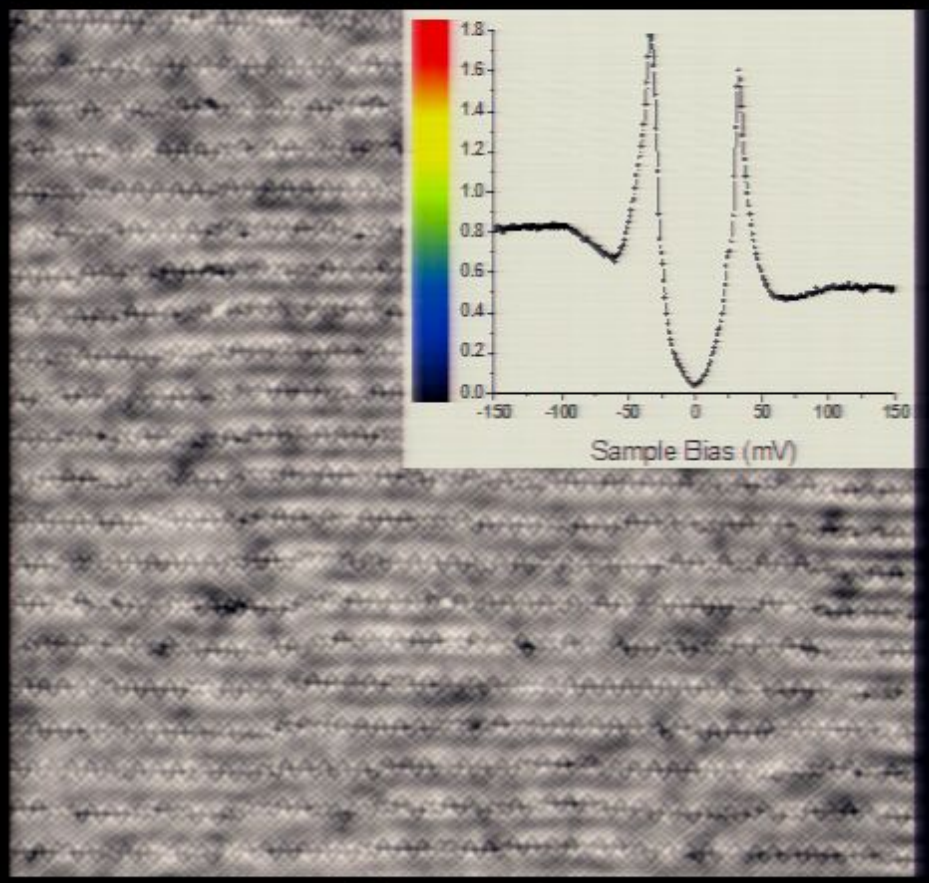

Topography

Atomic-resolution energy resolved

$$LDOS(\vec{r},E) \propto |\Psi(\vec{r},E)|^2$$

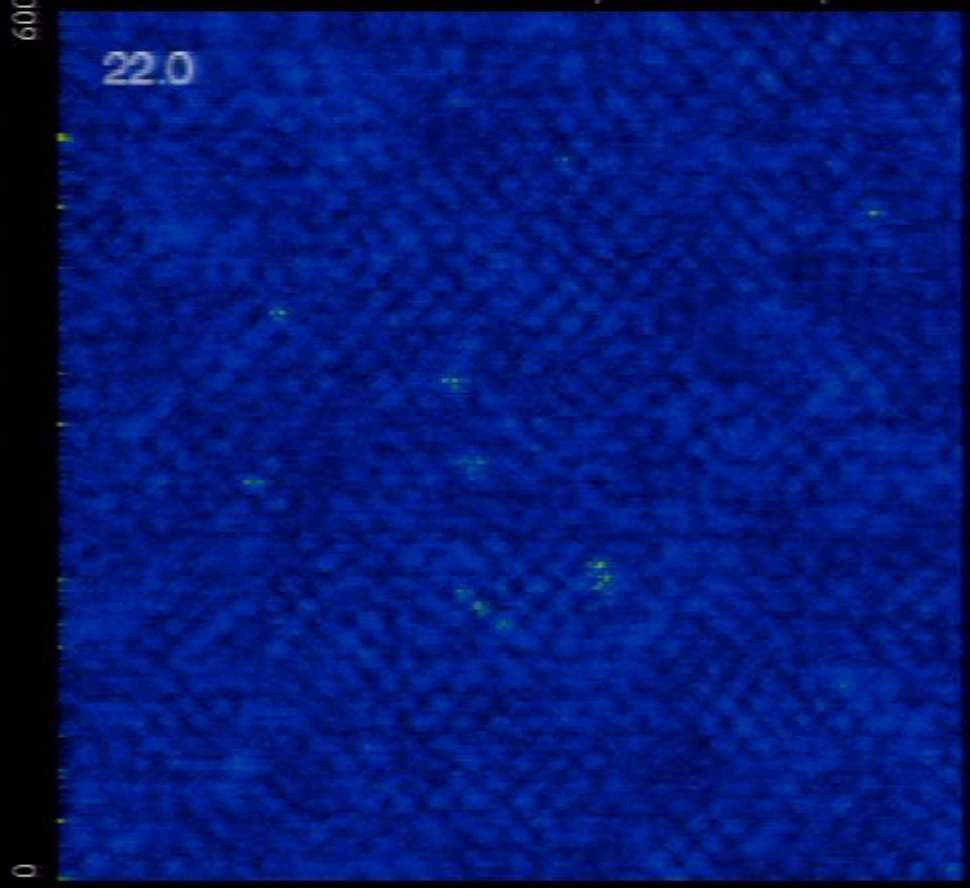

Measure $dI/dV \propto LDOS(E)$ at every atom

Spectroscopic Imaging STM (SI-STM)

Inset shows $LDOS(E)$ spectrum at single atom

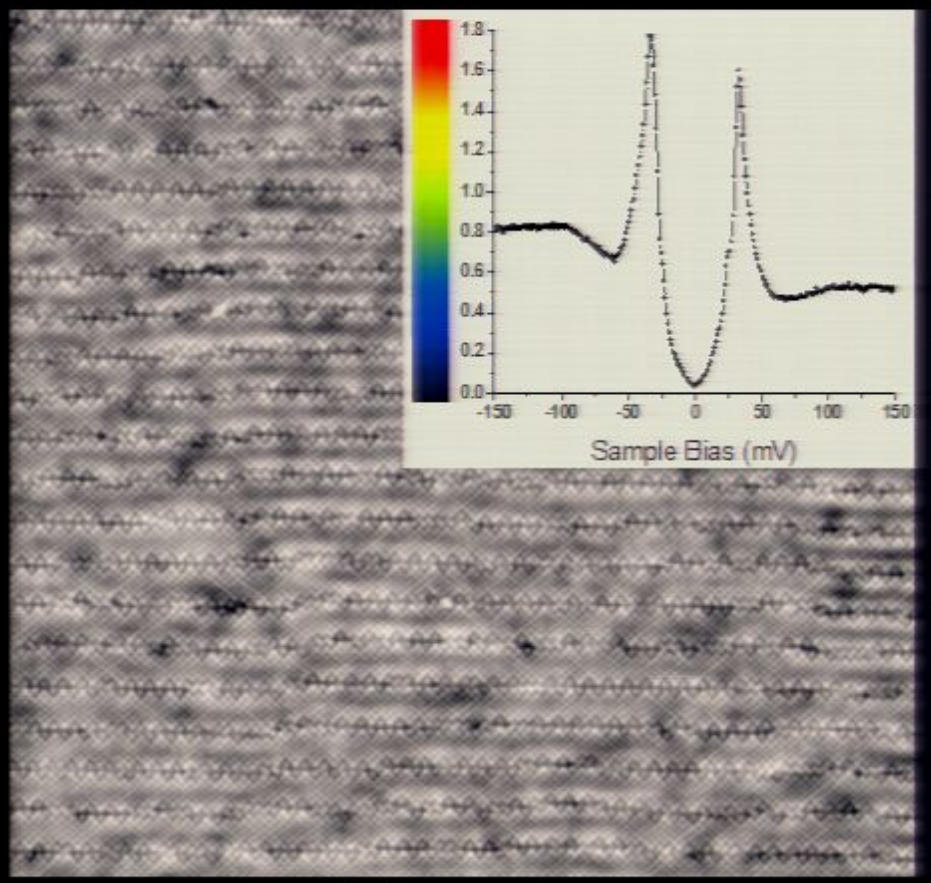

Topography

Atomic-resolution energy resolved

$$LDOS(\vec{r},E) \propto |\Psi(\vec{r},E)|^2$$

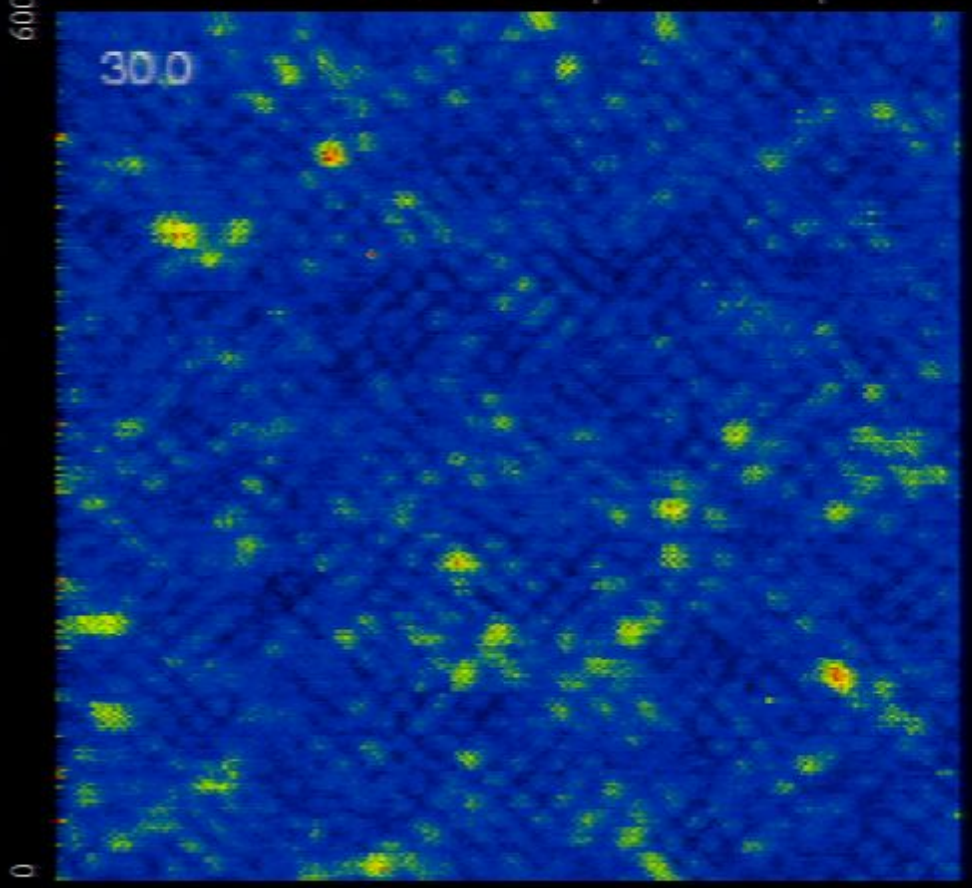

Measure $dI/dV \propto LDOS(E)$ at every atom

Spectroscopic Imaging STM (SI-STM)

Inset shows $LDOS(E)$ spectrum at single atom

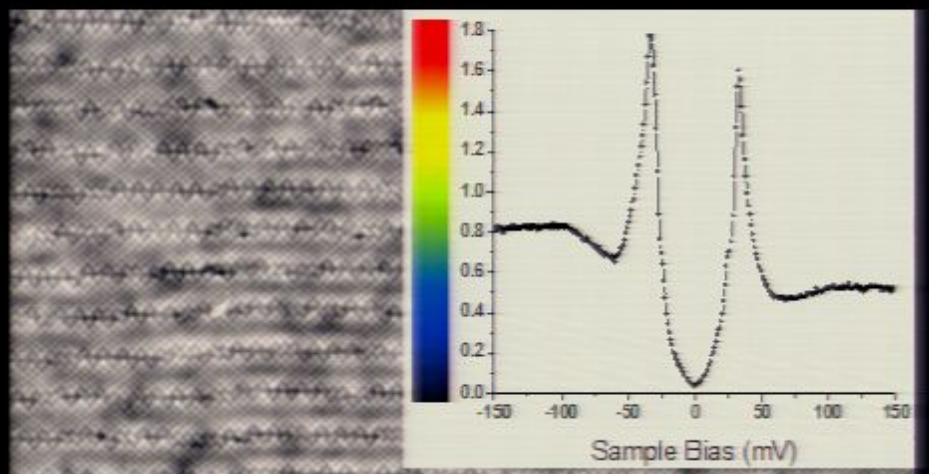

Topography

Atomic-resolution energy resolved

$$LDOS(\vec{r},E) \propto |\Psi(\vec{r},E)|^2$$

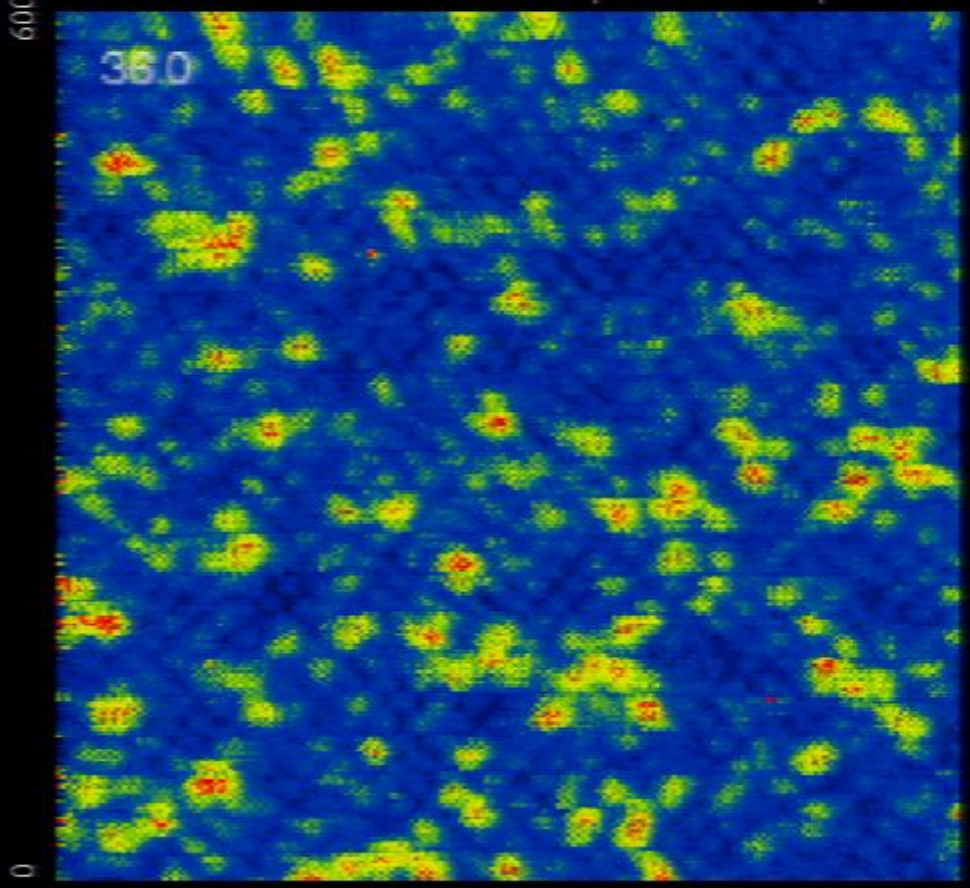

Measure $dI/dV \propto LDOS(E)$ at every atom

Spectroscopic Imaging STM (SI-STM)

Inset shows $LDOS(E)$ spectrum at single atom

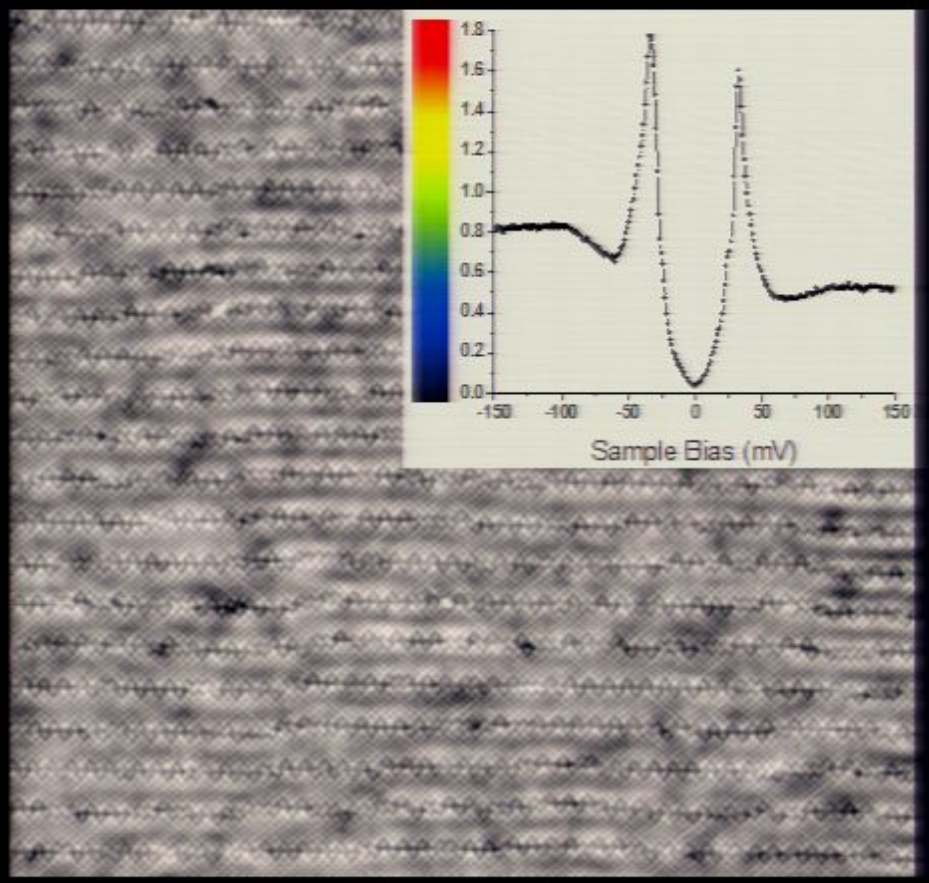

Topography

Atomic-resolution energy resolved

$$LDOS(\vec{r},E) \propto |\Psi(\vec{r},E)|^2$$

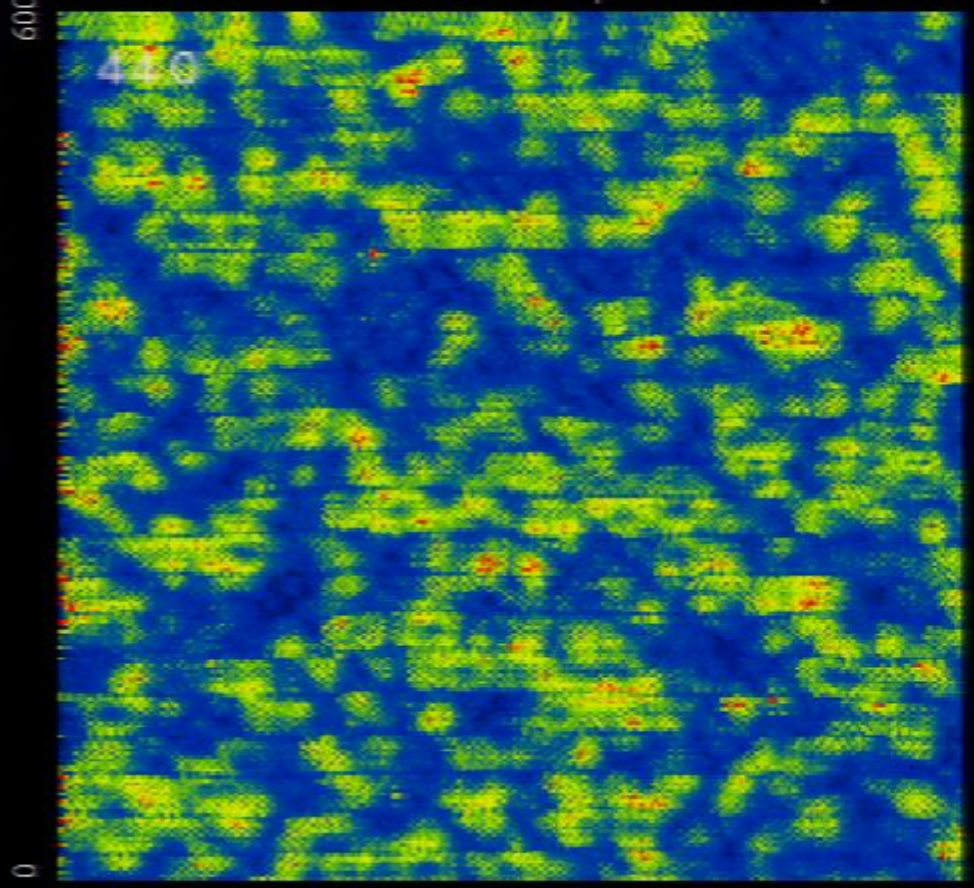

Measure $dI/dV \propto LDOS(E)$ at every atom

Spectroscopic Imaging STM (SI-STM)

Inset shows $LDOS(E)$ spectrum at single atom

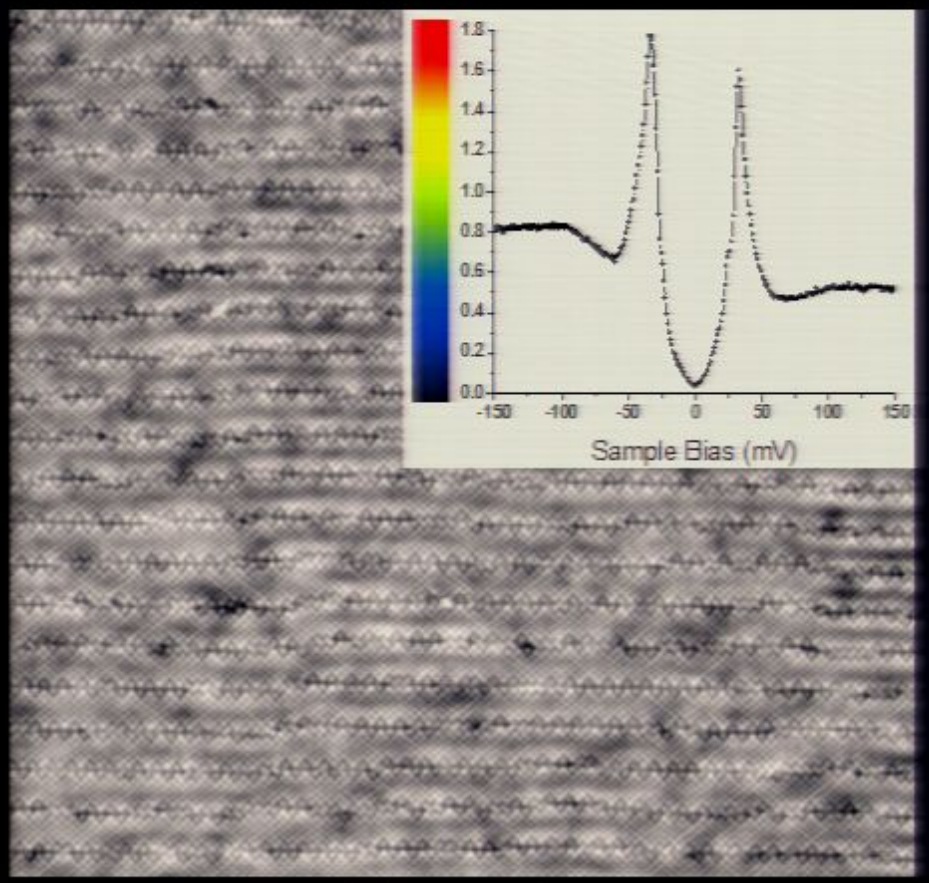

Atomic-resolution energy resolved $LDOS(\vec{r},E) \propto |\Psi(\vec{r},E)|^2$

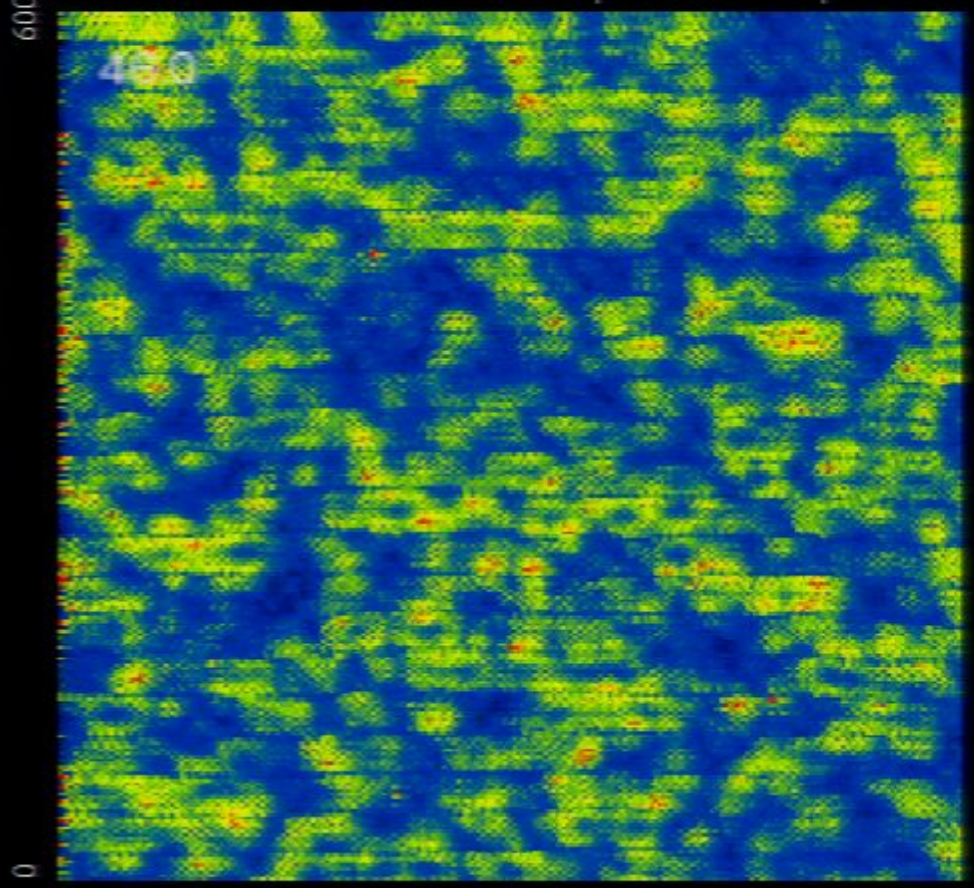

Measure $dI/dV \propto LDOS(E)$ at every atom

Spectroscopic Imaging STM (SI-STM)

Inset shows $LDOS(E)$ spectrum at single atom

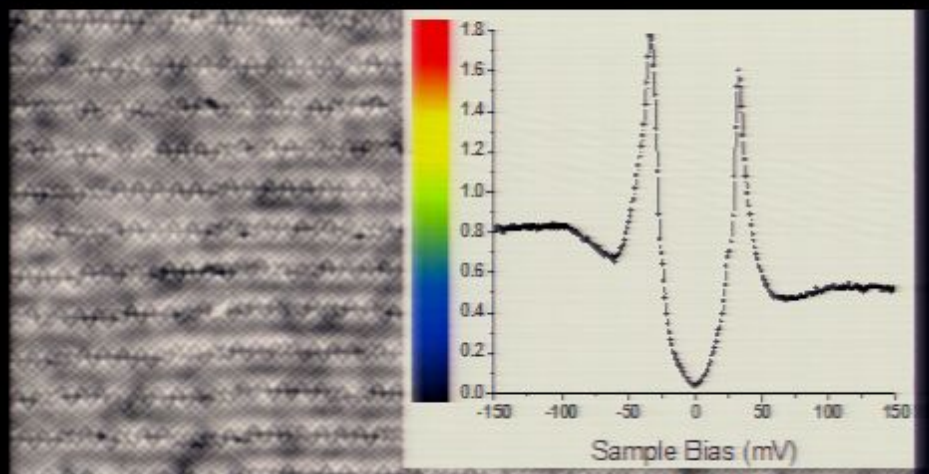

Topography

Atomic-resolution energy resolved

$$LDOS(\vec{r},E) \propto |\Psi(\vec{r},E)|^2$$

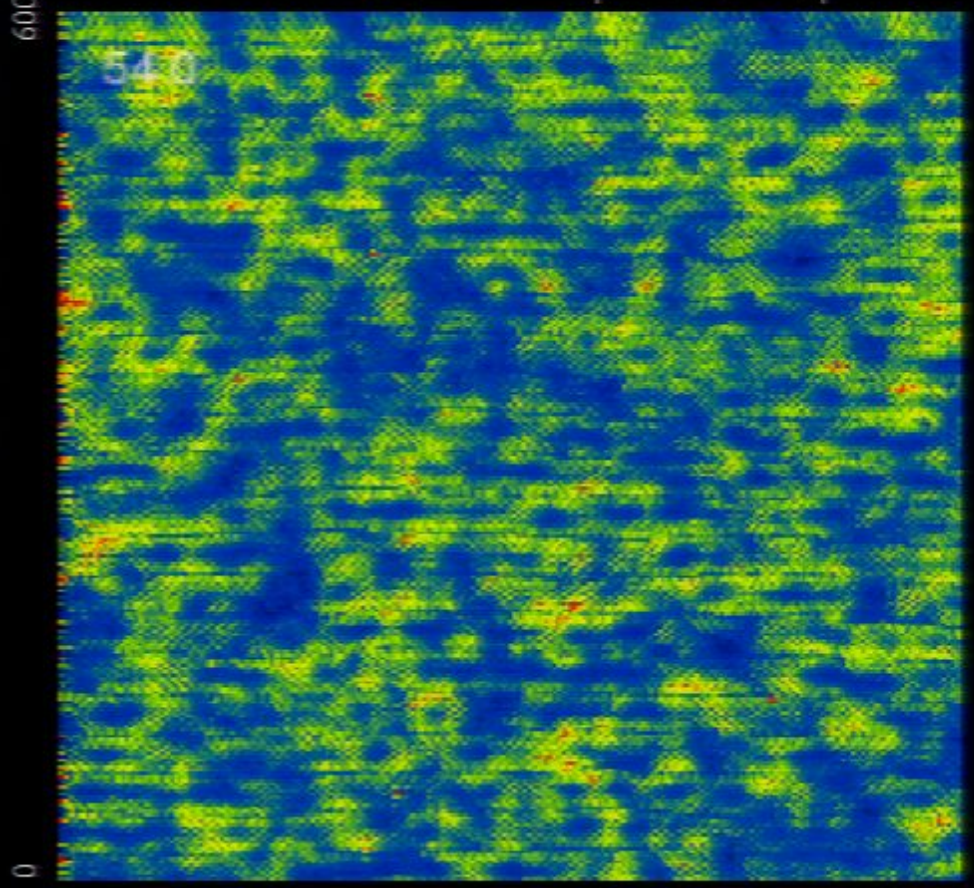

Measure $dI/dV \propto LDOS(E)$ at every atom

Spectroscopic Imaging STM (SI-STM)

Inset shows $LDOS(E)$ spectrum at single atom

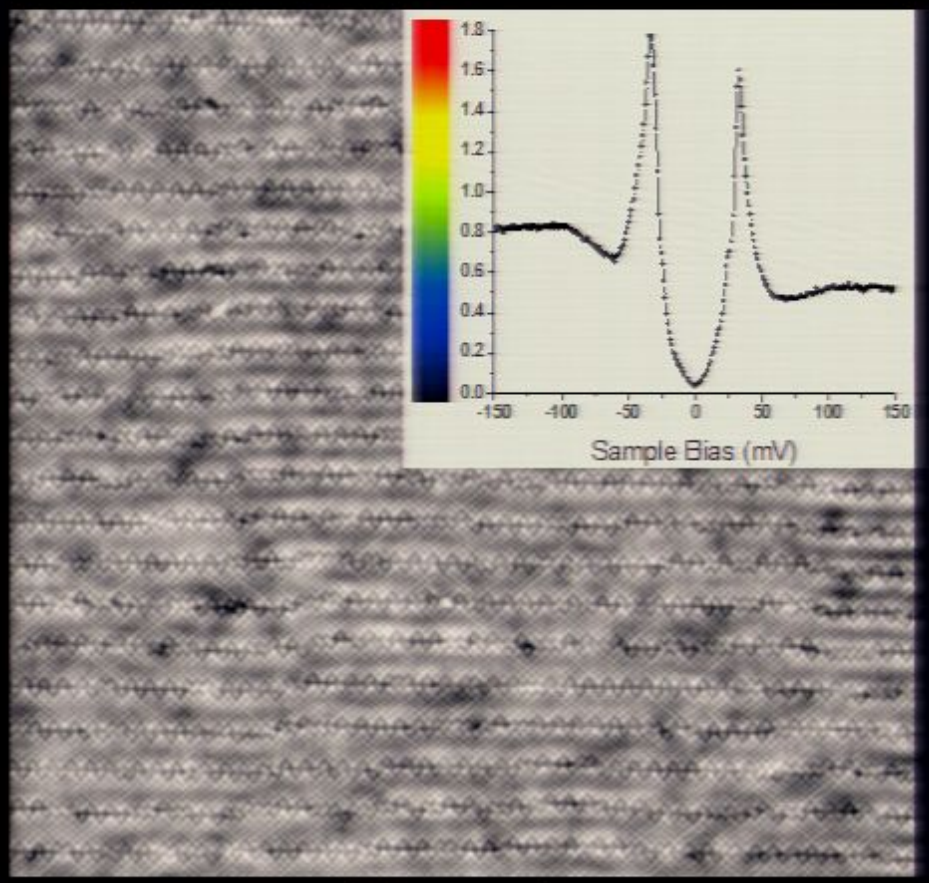

Topography

Atomic-resolution energy resolved

$$LDOS(\vec{r},E) \propto |\Psi(\vec{r},E)|^2$$

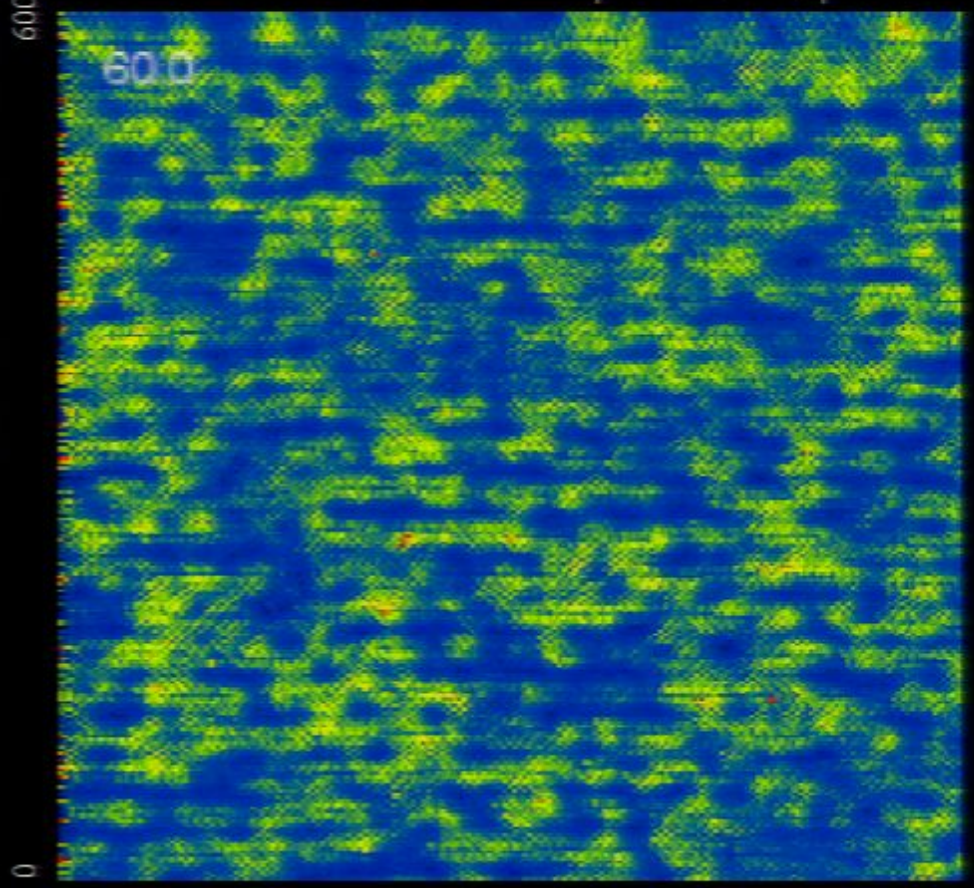

Measure $dI/dV \propto LDOS(E)$ at every atom

Spectroscopic Imaging STM (SI-STM)

Inset shows $LDOS(E)$ spectrum at single atom

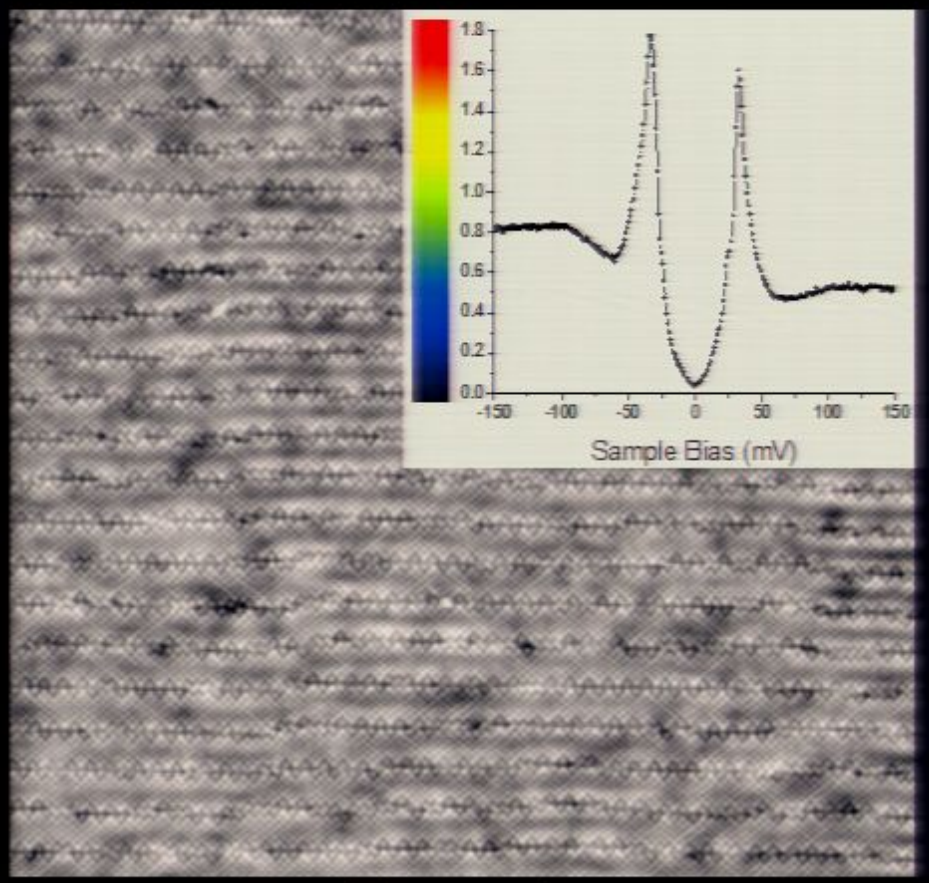

Topography

Atomic-resolution energy resolved

$$LDOS(\vec{r},E) \propto |\Psi(\vec{r},E)|^2$$

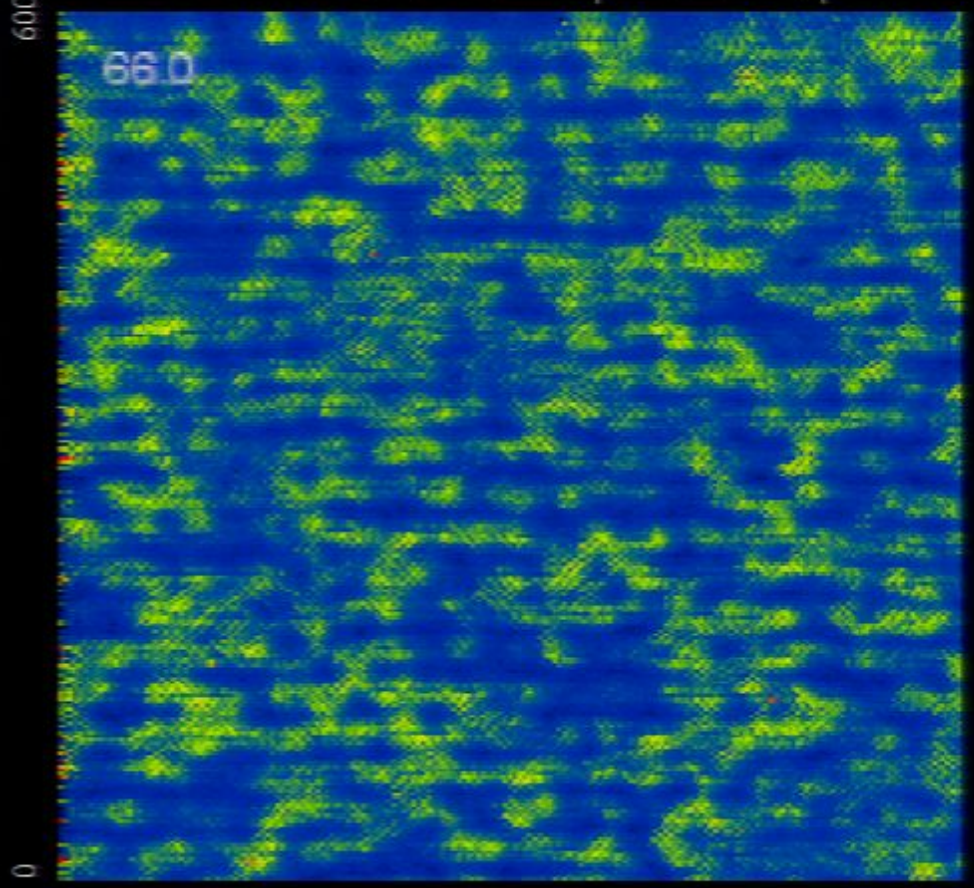

Measure $dI/dV \propto LDOS(E)$ at every atom

Spectroscopic Imaging STM (SI-STM)

Inset shows $LDOS(E)$ spectrum at single atom

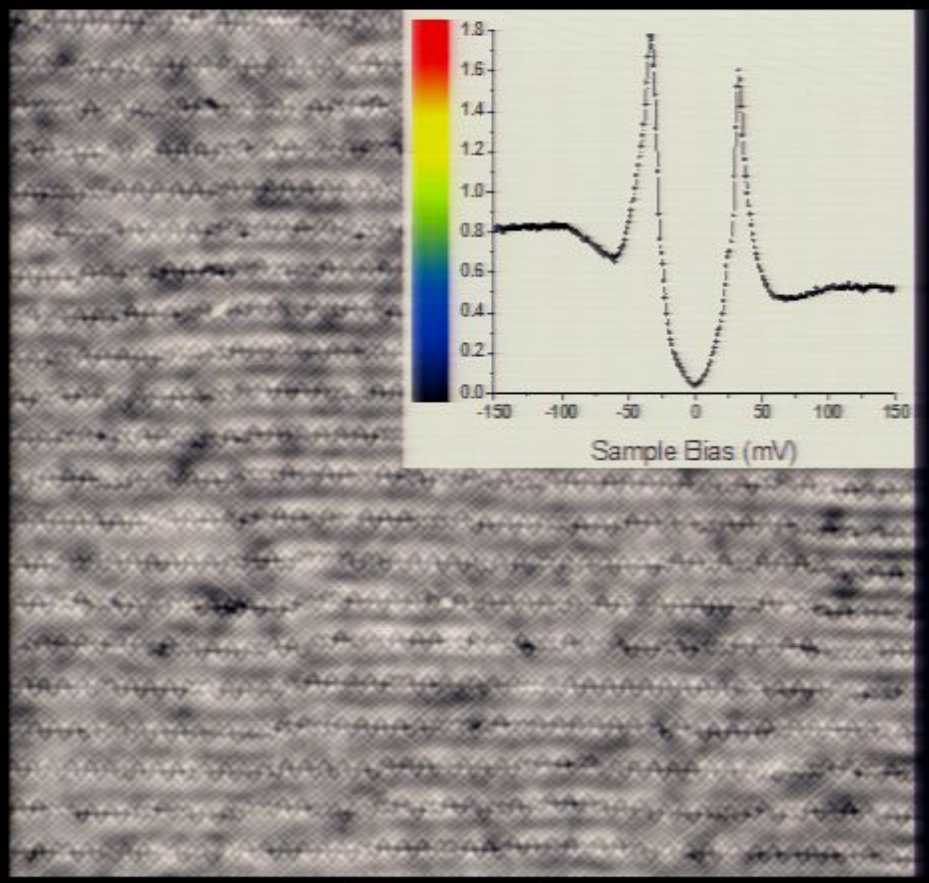

Topography

Atomic-resolution energy resolved

$$LDOS(\vec{r},E) \propto |\Psi(\vec{r},E)|^2$$

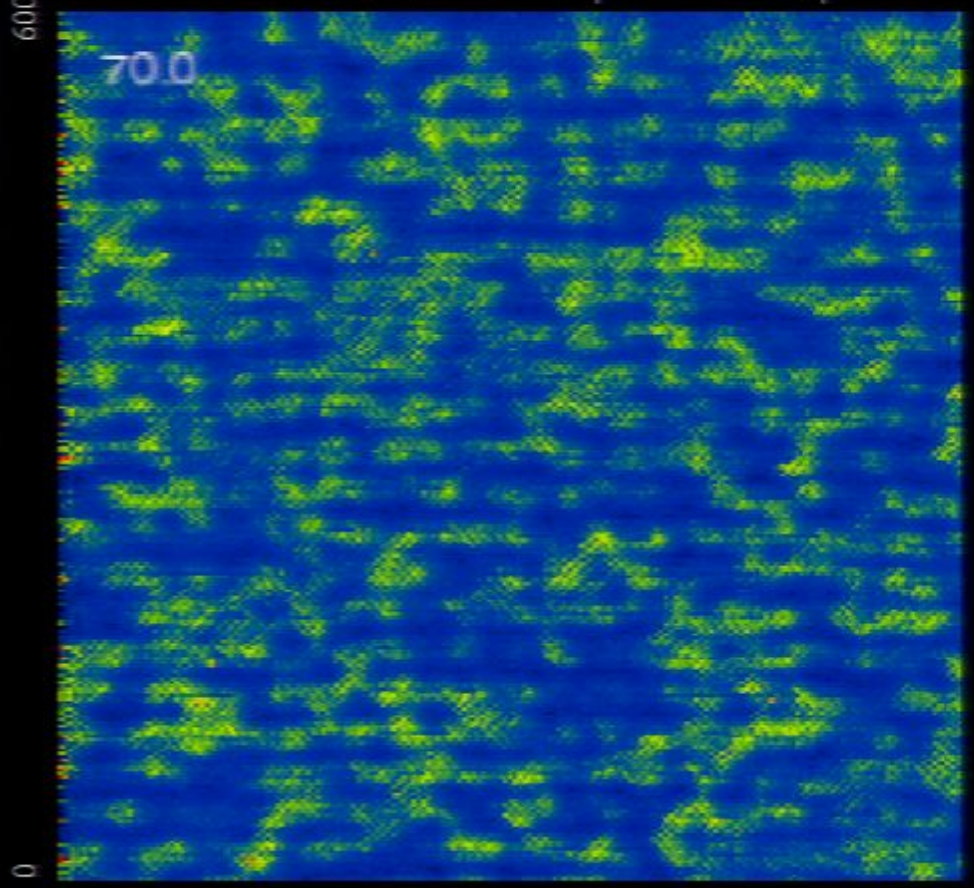

Measure $dI/dV \propto LDOS(E)$ at every atom

Spectroscopic Imaging STM (SI-STM)

Inset shows $LDOS(E)$ spectrum at single atom

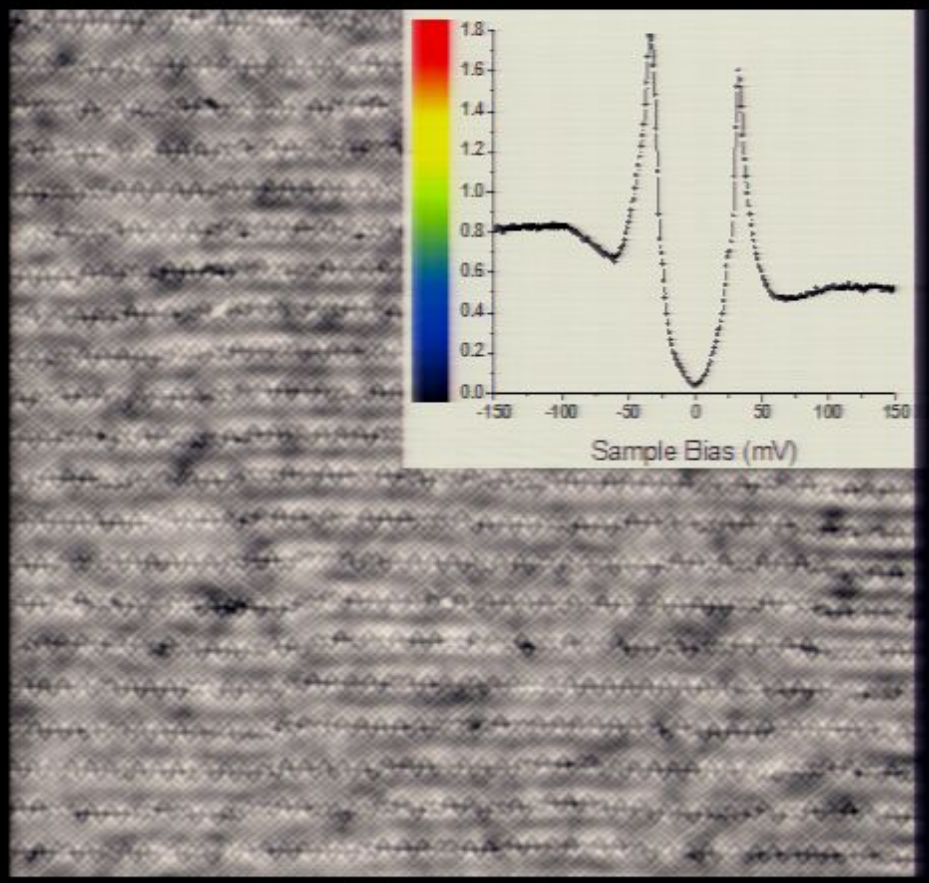

Topography

Atomic-resolution energy resolved

$$LDOS(\vec{r},E) \propto |\Psi(\vec{r},E)|^2$$

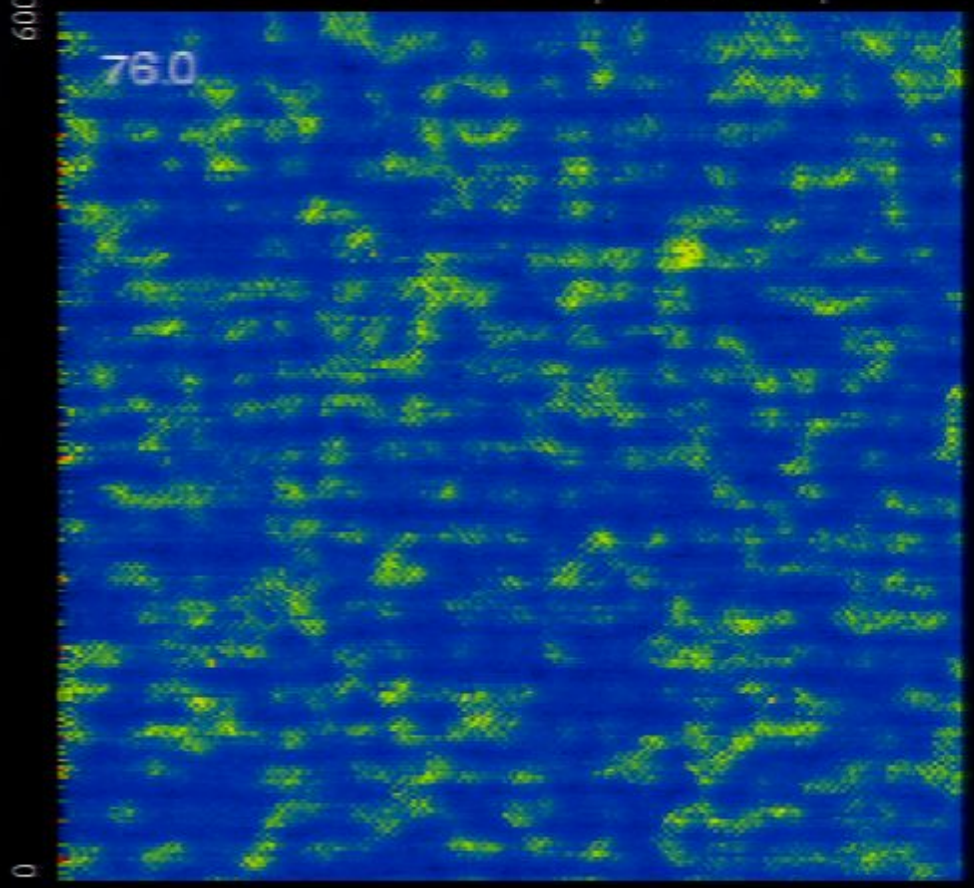

Measure $dI/dV \propto LDOS(E)$ at every atom

Spectroscopic Imaging STM (SI-STM)

Inset shows $LDOS(E)$ spectrum at single atom

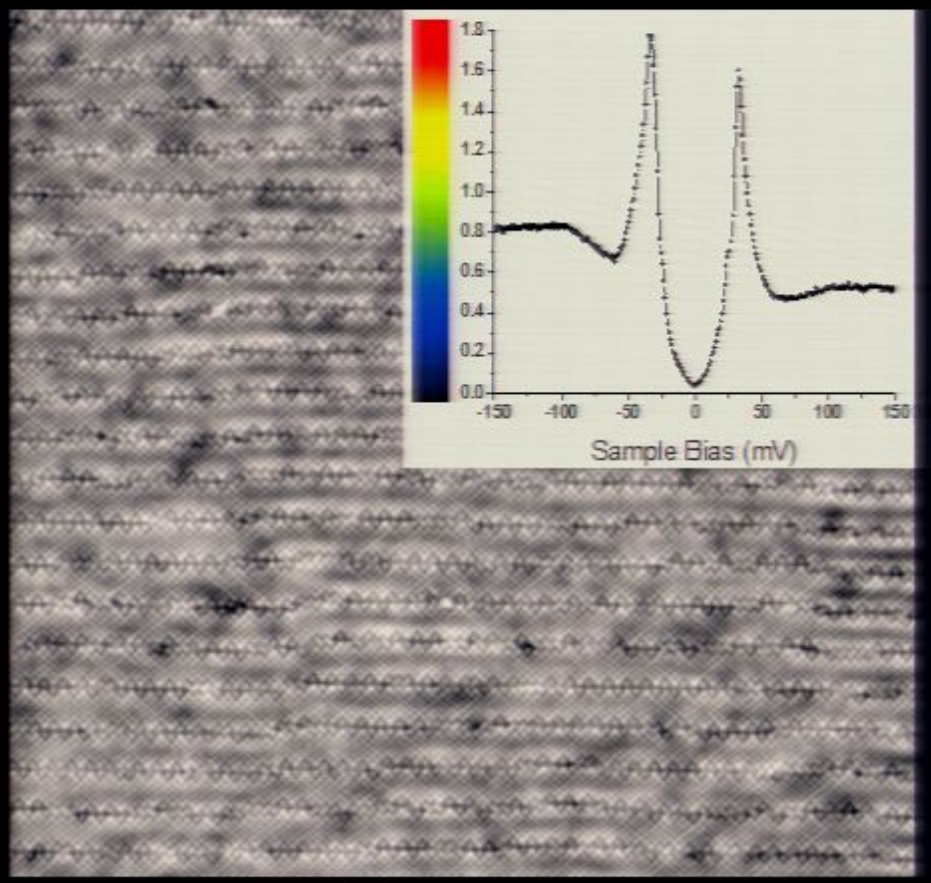

Topography

Atomic-resolution energy resolved

$$LDOS(\vec{r},E) \propto |\Psi(\vec{r},E)|^2$$

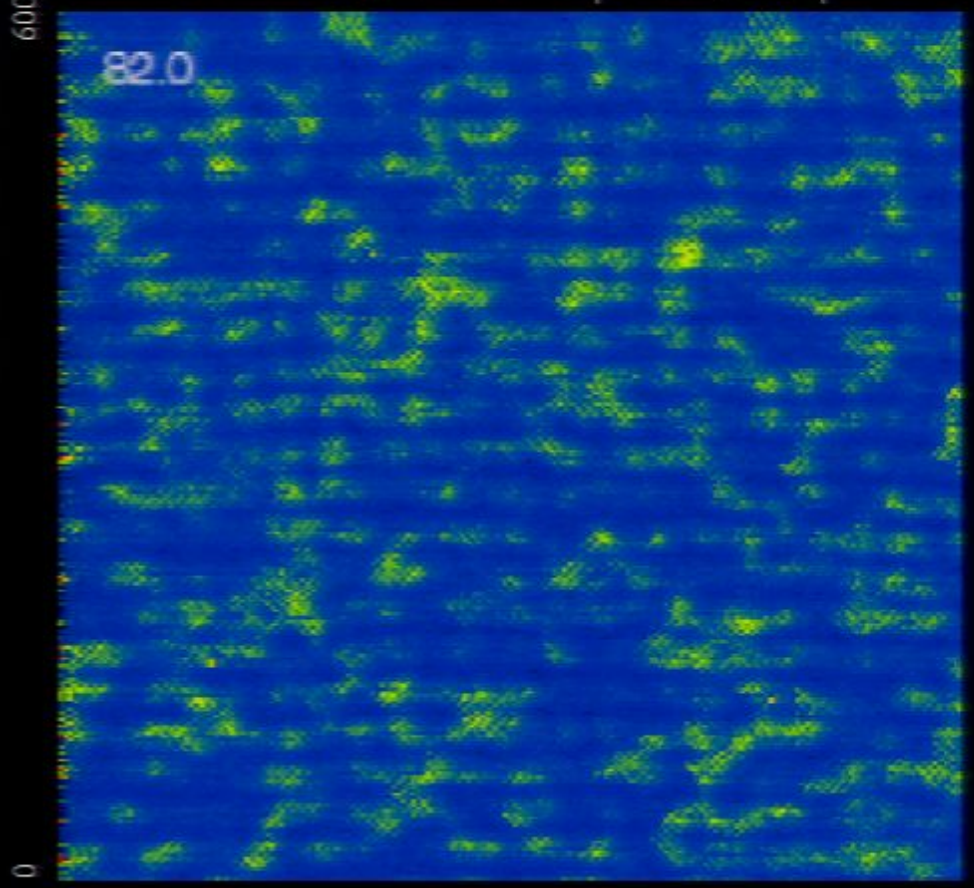

Measure $dI/dV \propto LDOS(E)$ at every atom

Spectroscopic Imaging STM (SI-STM)

Inset shows $LDOS(E)$ spectrum at single atom

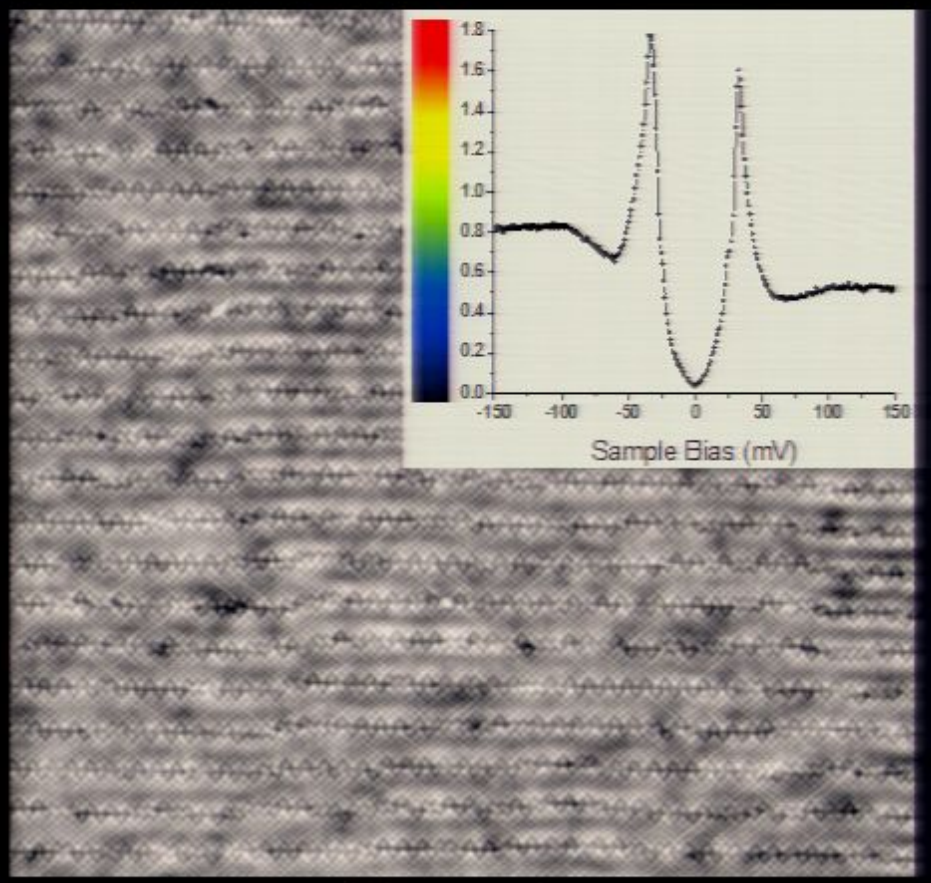

Topography

Atomic-resolution energy resolved

$$LDOS(\vec{r},E) \propto |\Psi(\vec{r},E)|^2$$

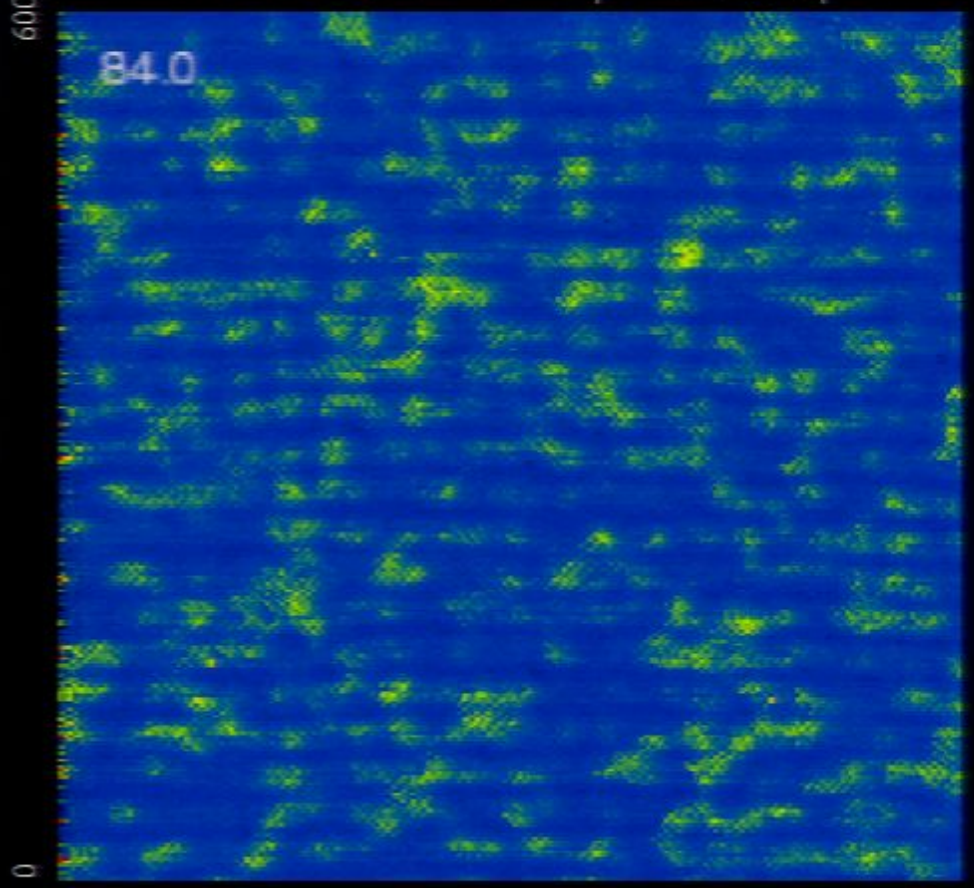

Measure $dI/dV \propto LDOS(E)$ at every atom

Spectroscopic Imaging STM (SI-STM)

Inset shows $LDOS(E)$ spectrum at single atom

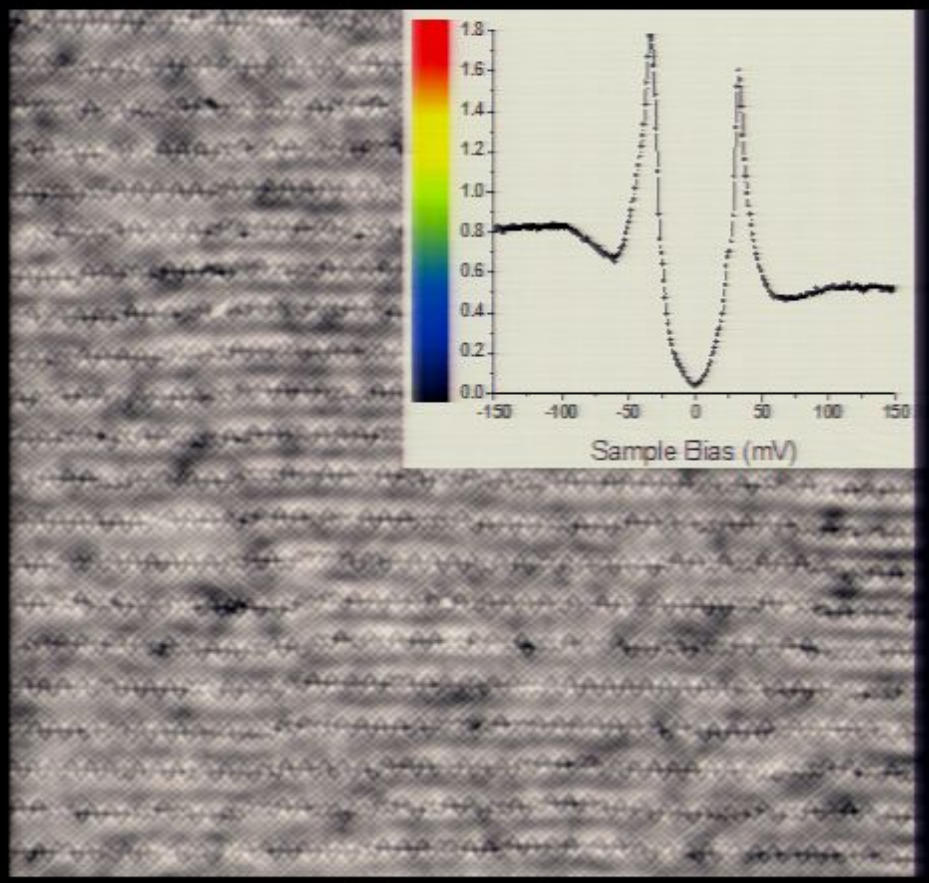

Topography

Atomic-resolution energy resolved

$$LDOS(\vec{r},E) \propto |\Psi(\vec{r},E)|^2$$

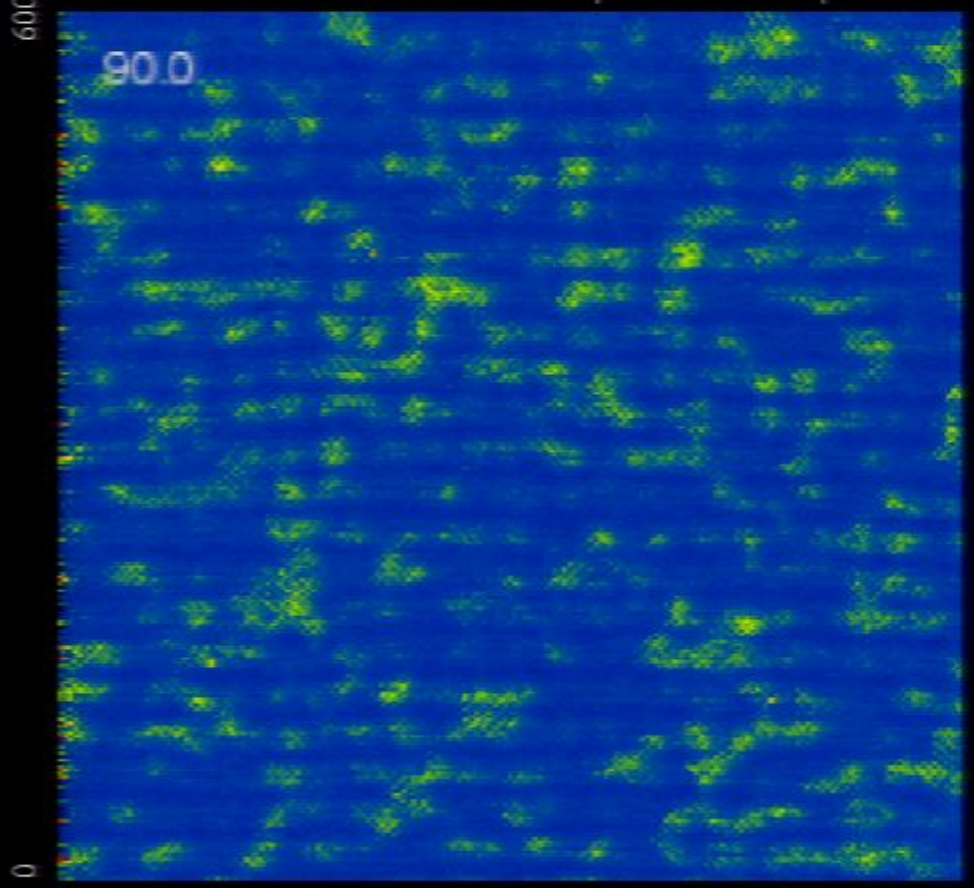

Measure $dI/dV \propto LDOS(E)$ at every atom

Davis Group Spectroscopic Imaging STM Systems

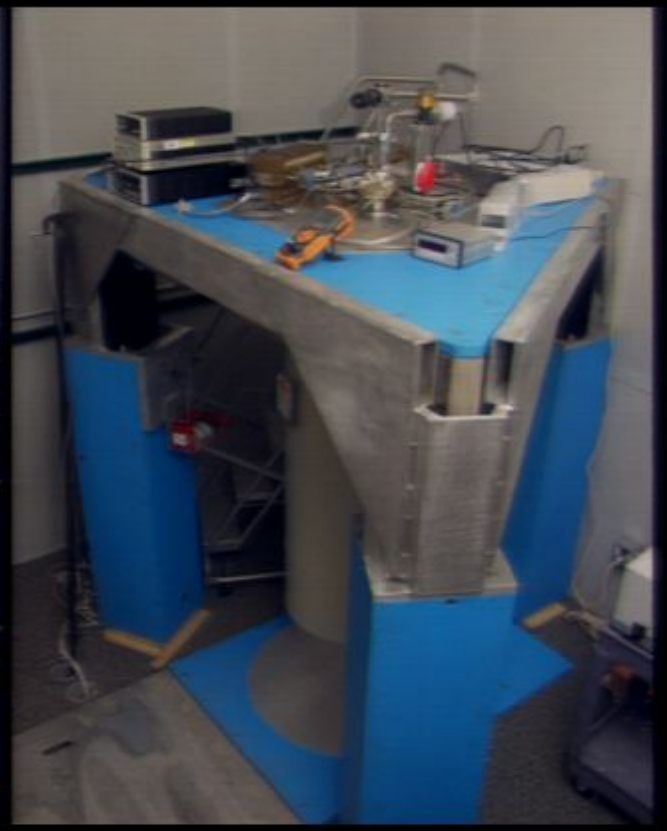

STM1 (9T/250mK)
Cornell

BNL STM1 (4K->100K
Bldg 480, BNL

STM2(9T/10mK)
Cornell

Iron-based HTS

Copper-based HTS

Heavy Fermion SC

Direct Visualization of Complex Electronic Matter

Nanoscale e-disorder

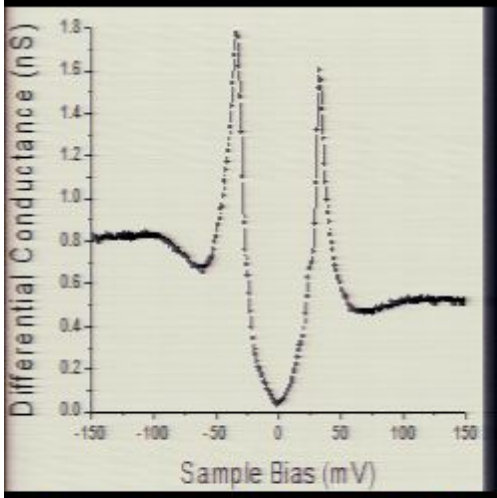

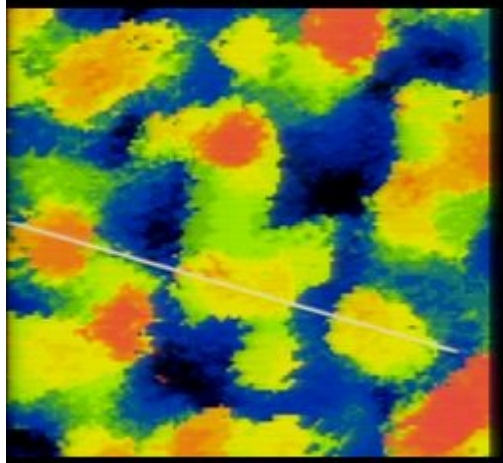

15 nm
Gapmap, B=0

Nature 414 282 (2001)

Q. Interference

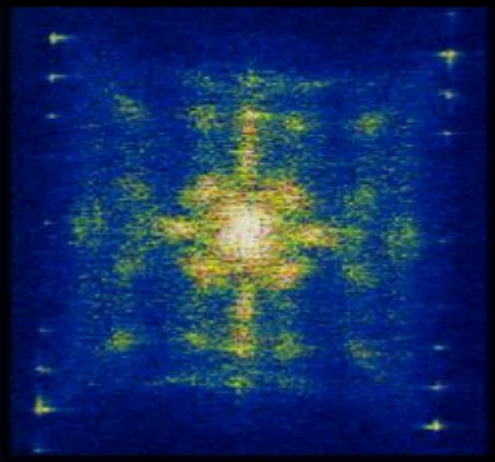

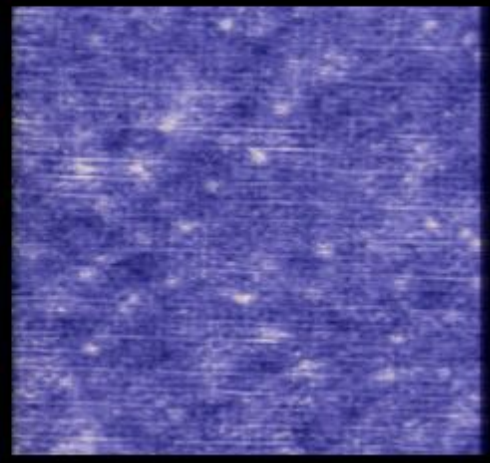

56 nm
0-12mV LDOS,B=5T

Science 297, 1148 (2002)

Impurity Atoms

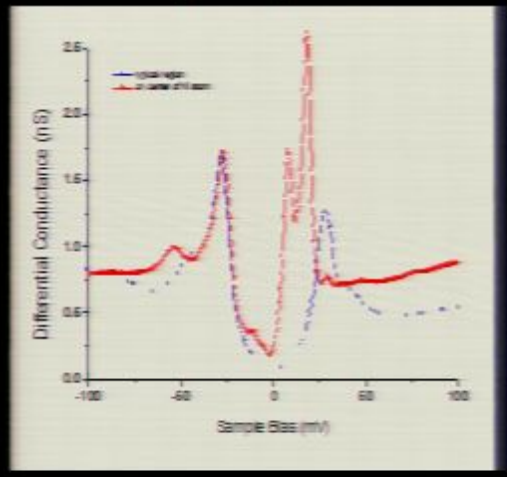

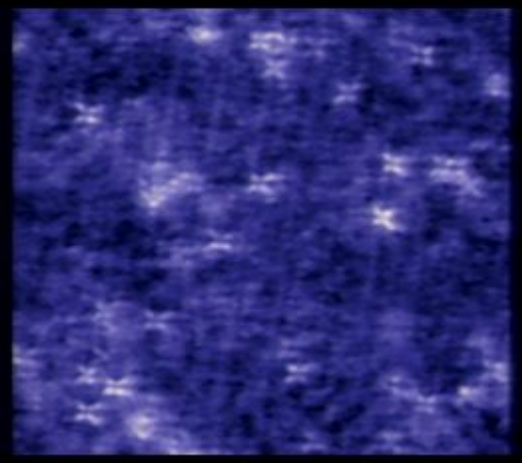

64 nm
12 mV LDOS, B=0

Nature 411, 920 (2001)

Heavy Fermions

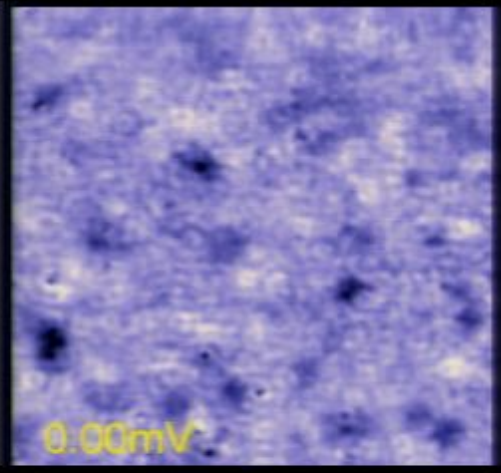

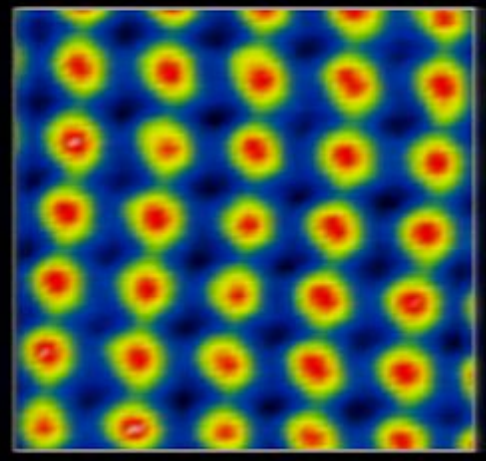

26 nm
Fano

Nature 465, 570 (2010)

Direct Visualization of Complex Electronic Matter

Phase Fluctuations | Electronic Nematic | Dopant Atoms | FeAs SC

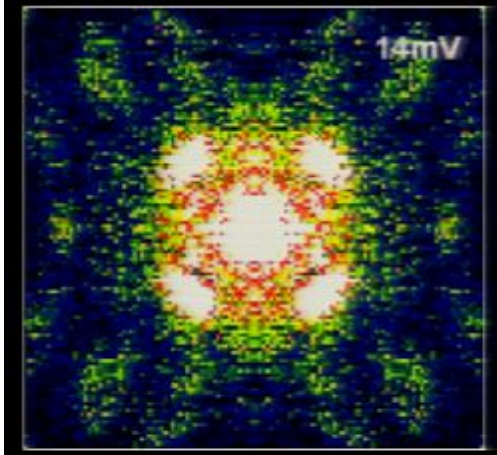

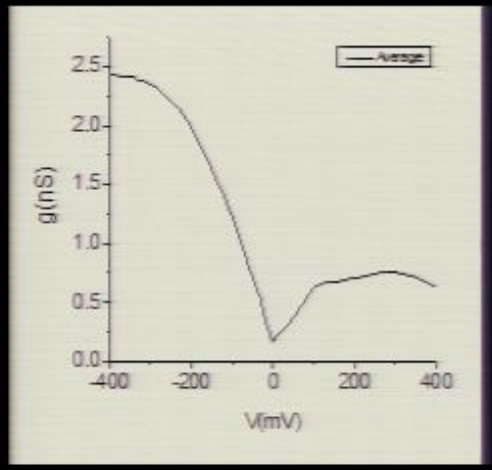

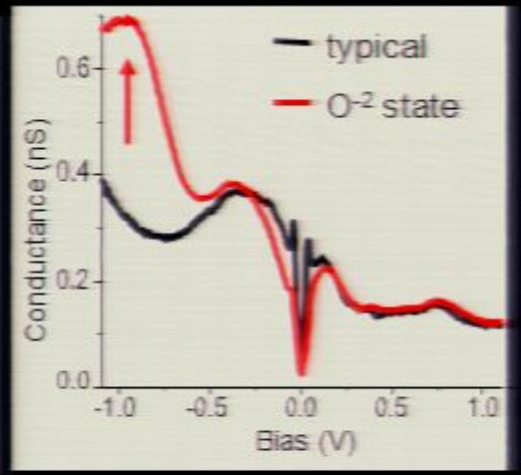

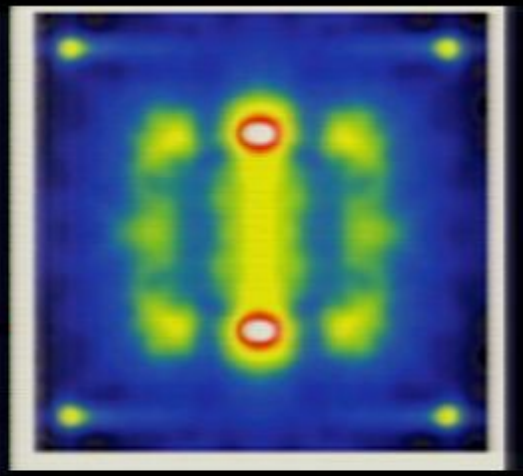

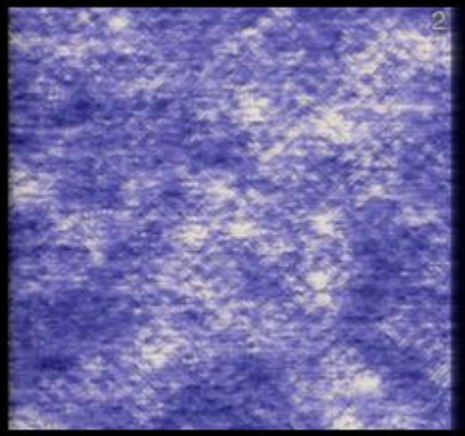

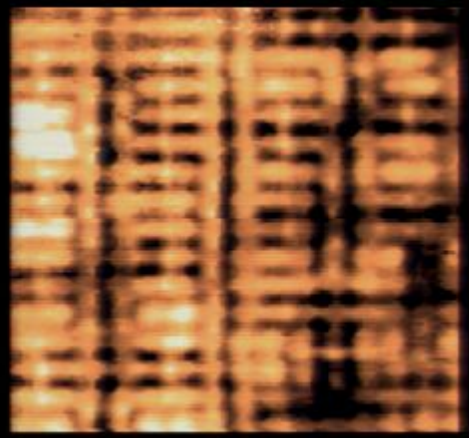

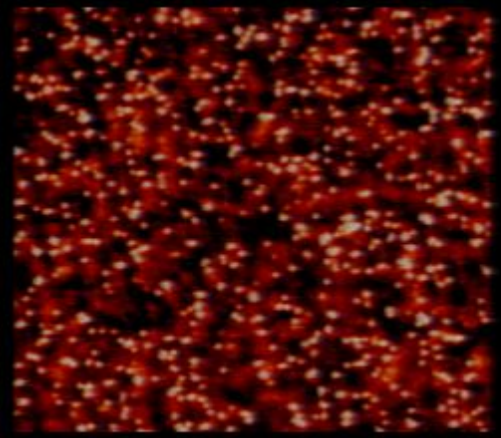

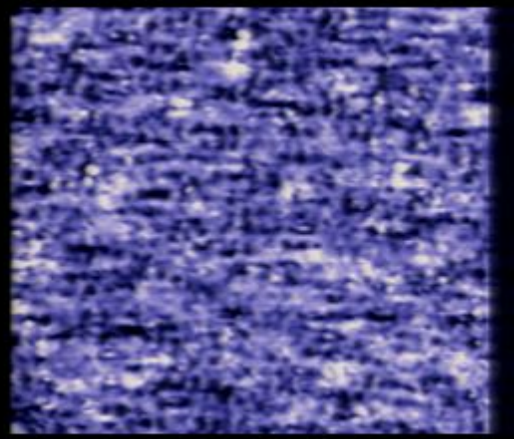

45 nm
dI/dV

Science 325, 1099 (2009)

6.4 nm
R=I+/I-

Science 315, 1380 (2007)

40nm
-1V LDOS, B=0

Science 309, 1048 (2005)

26 nm
-9mV LDOS, B=0

Science 327, 181 (2010)

Combined geometrical and electronic info.

Topographic Image

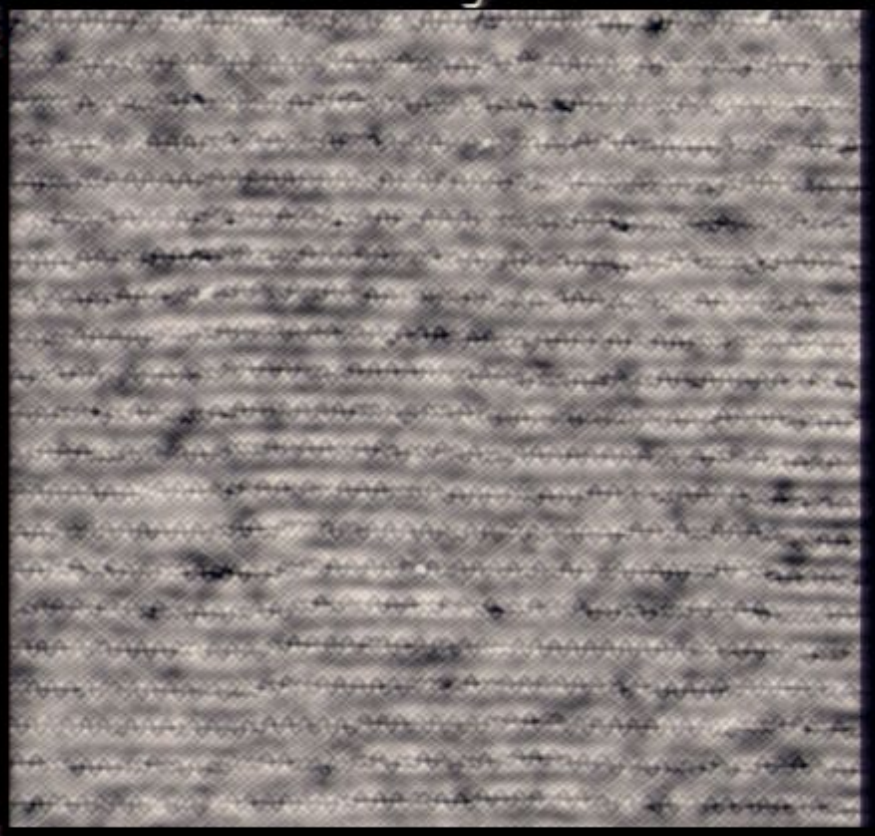

$T(\vec{r})$

Spectroscopic Image

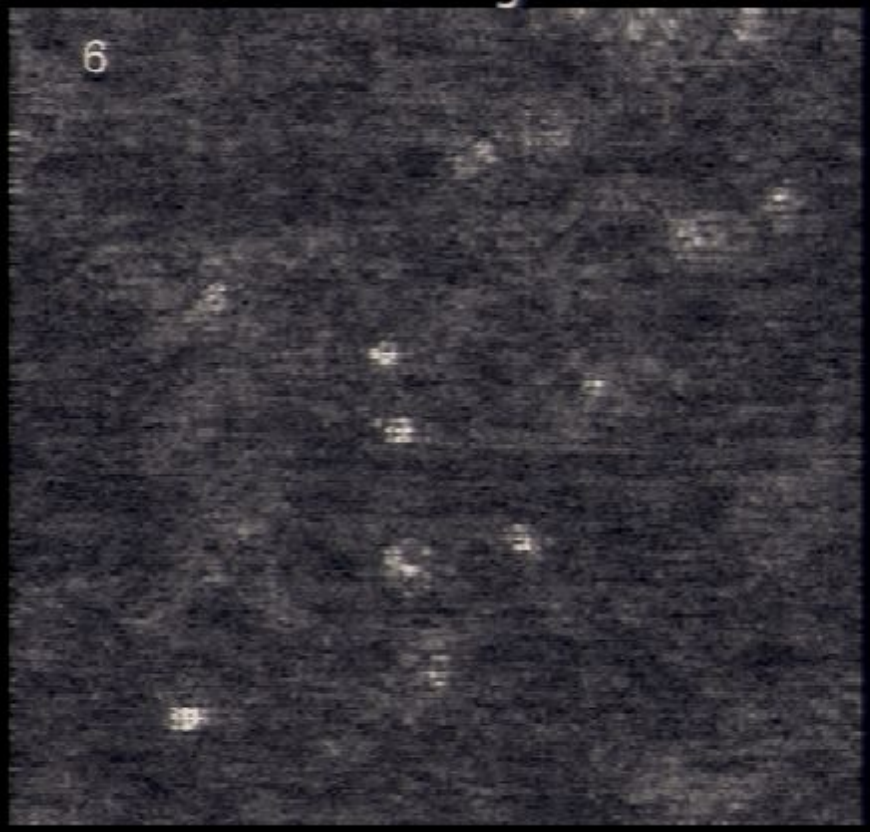

$g(\vec{r},E)$

Combined geometrical and electronic info.

Topographic Image

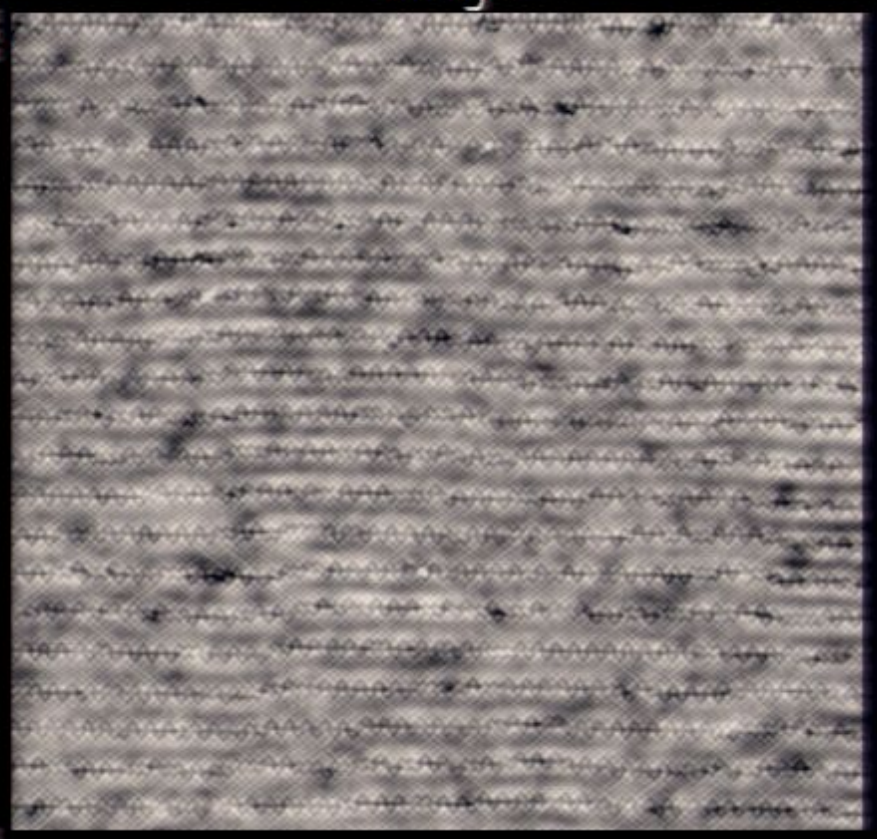

$T(\vec{r})$

Spectroscopic Image

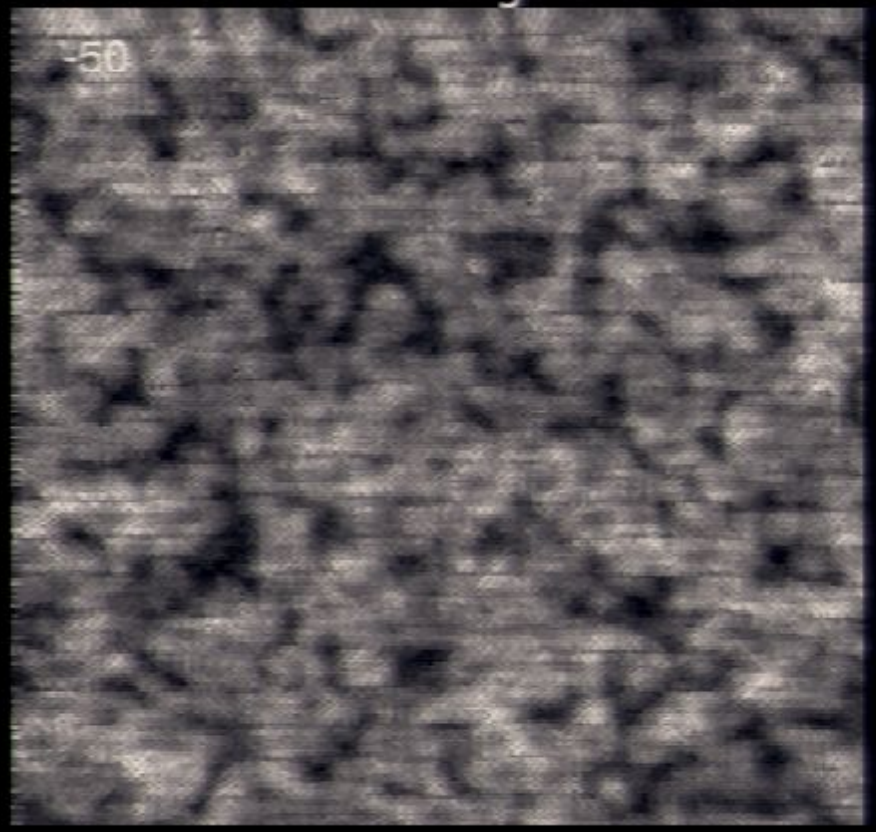

$g(\vec{r},E)$

Combined geometrical and electronic info.

Topographic Image

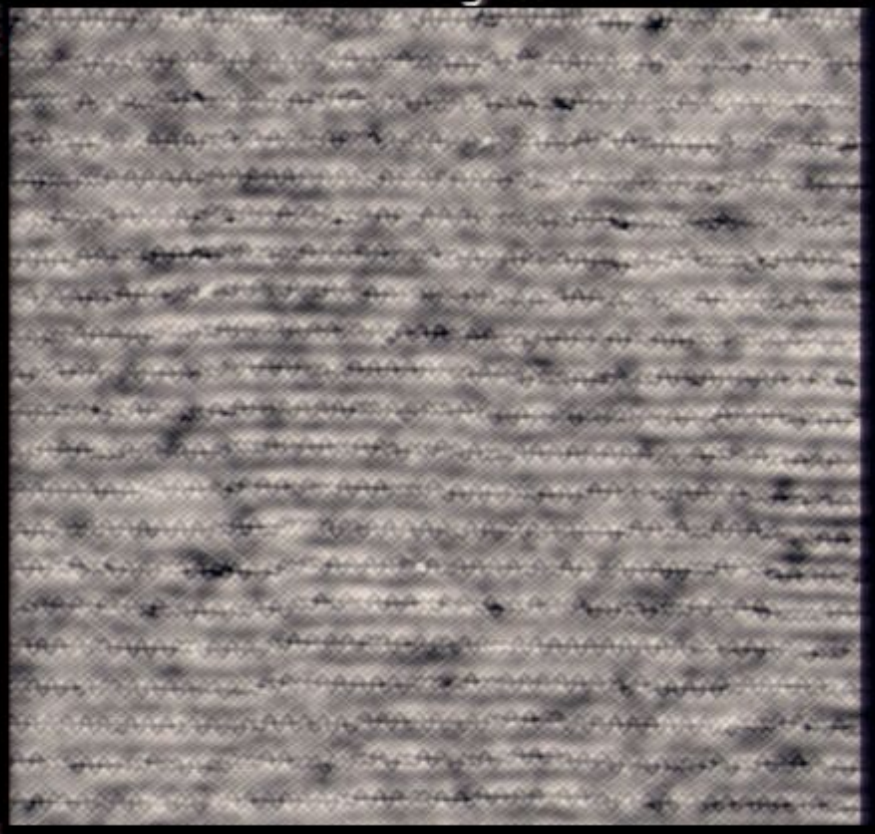

$T(\vec{r})$

Spectroscopic Image

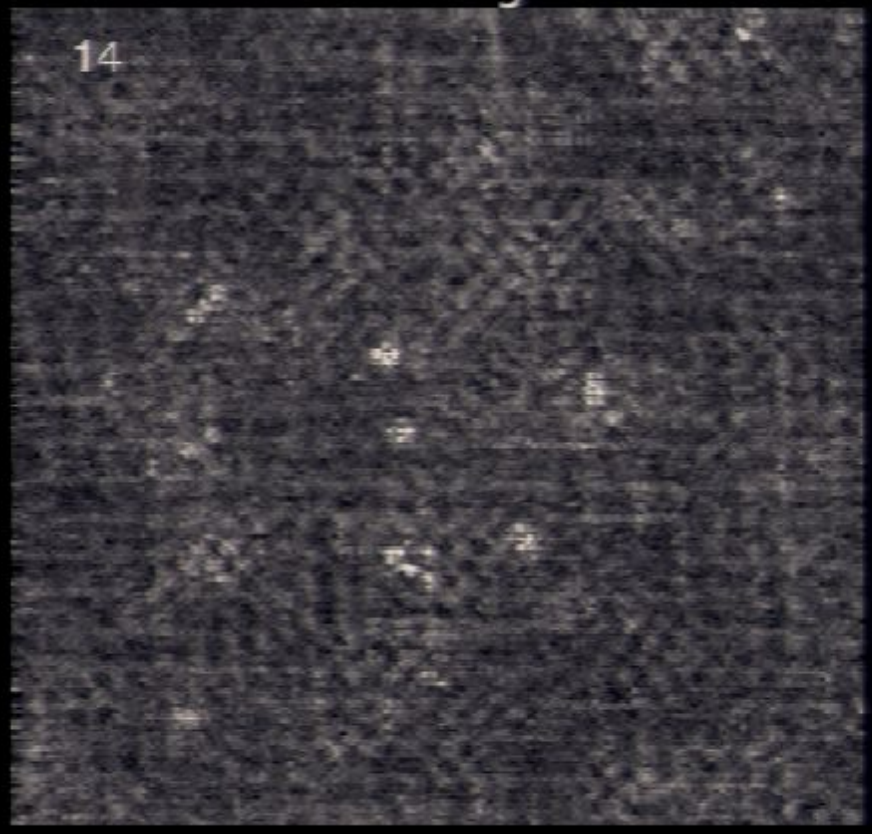

$g(\vec{r},E)$

Combined geometrical and electronic info.

Topographic Image

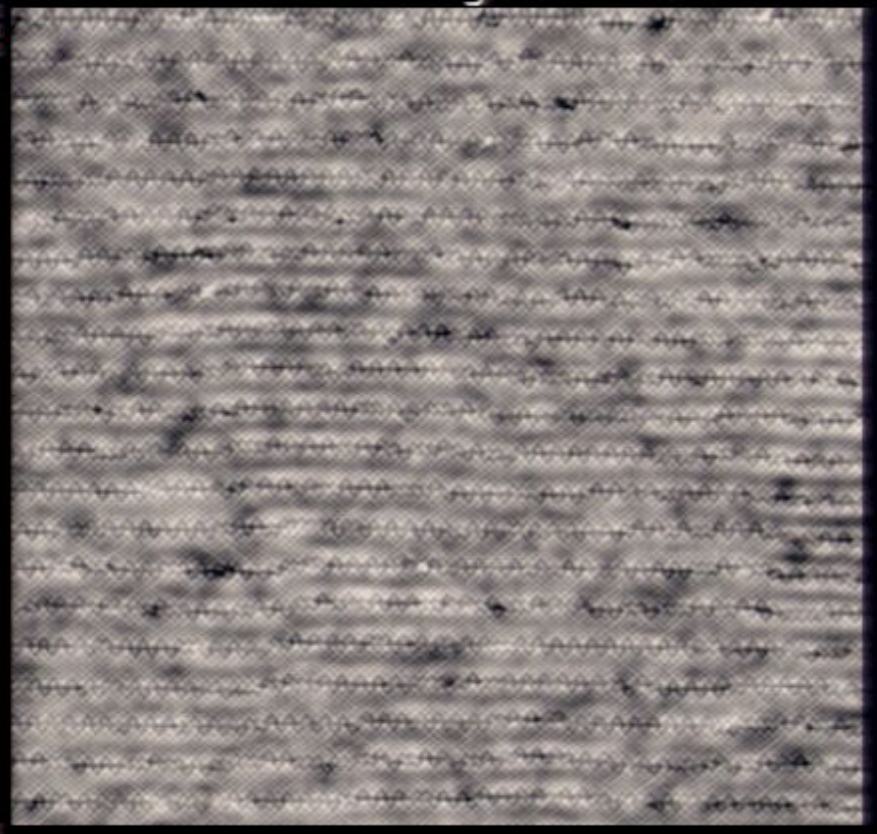

$T(\vec{r})$

Spectroscopic Image

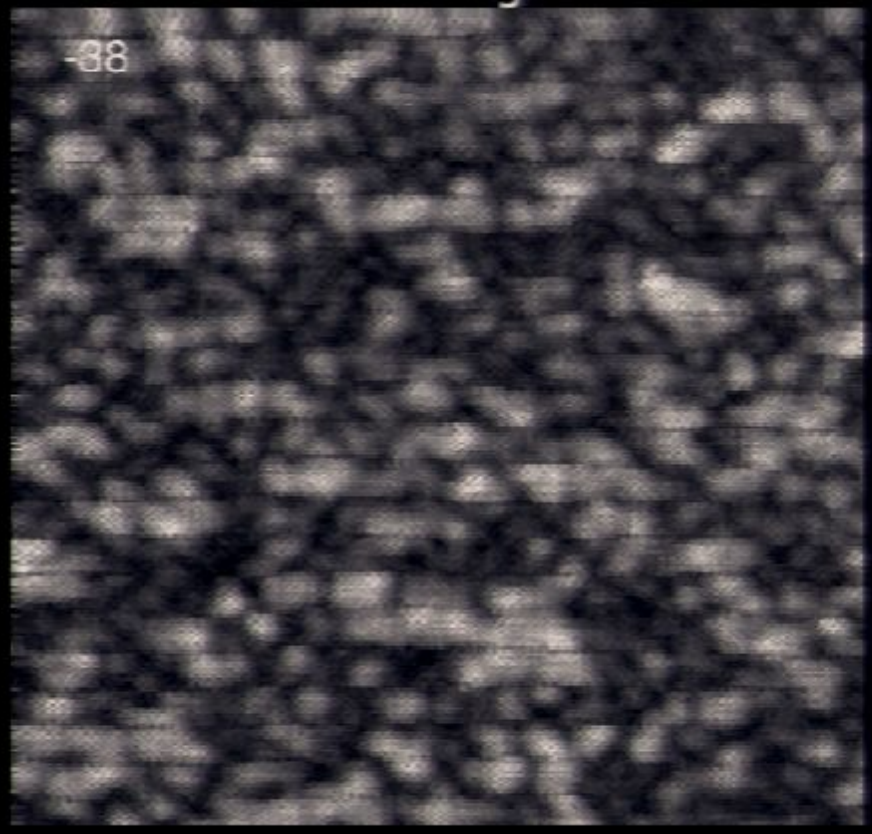

$g(\vec{r},E)$

Combined geometrical and electronic info.

Topographic Image

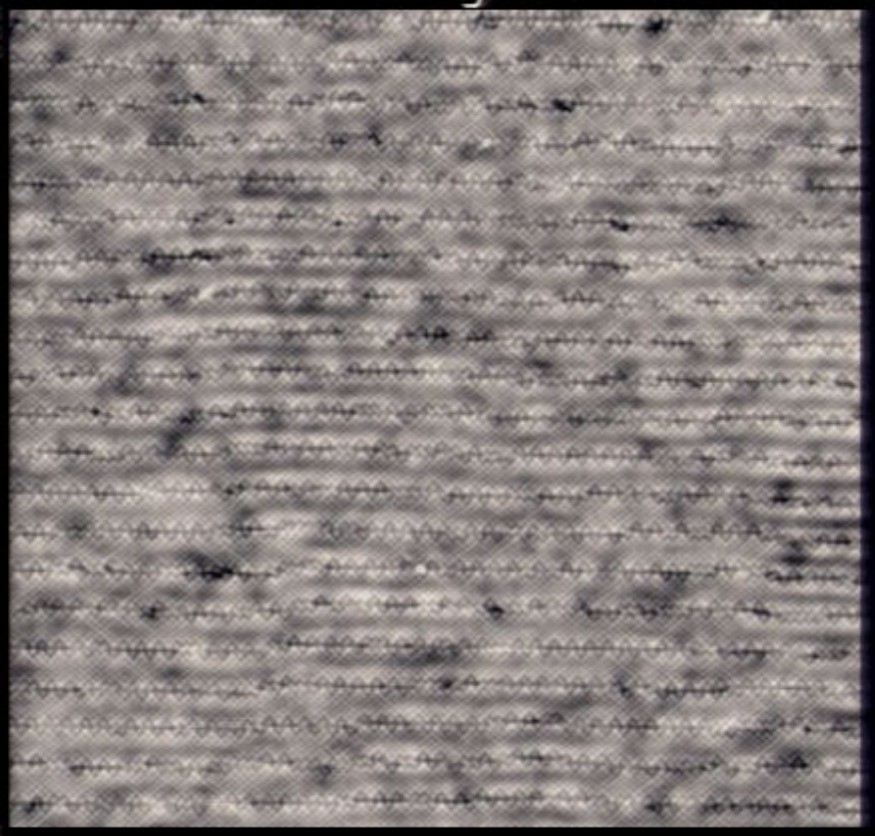

$T(\vec{r})$

Spectroscopic Image

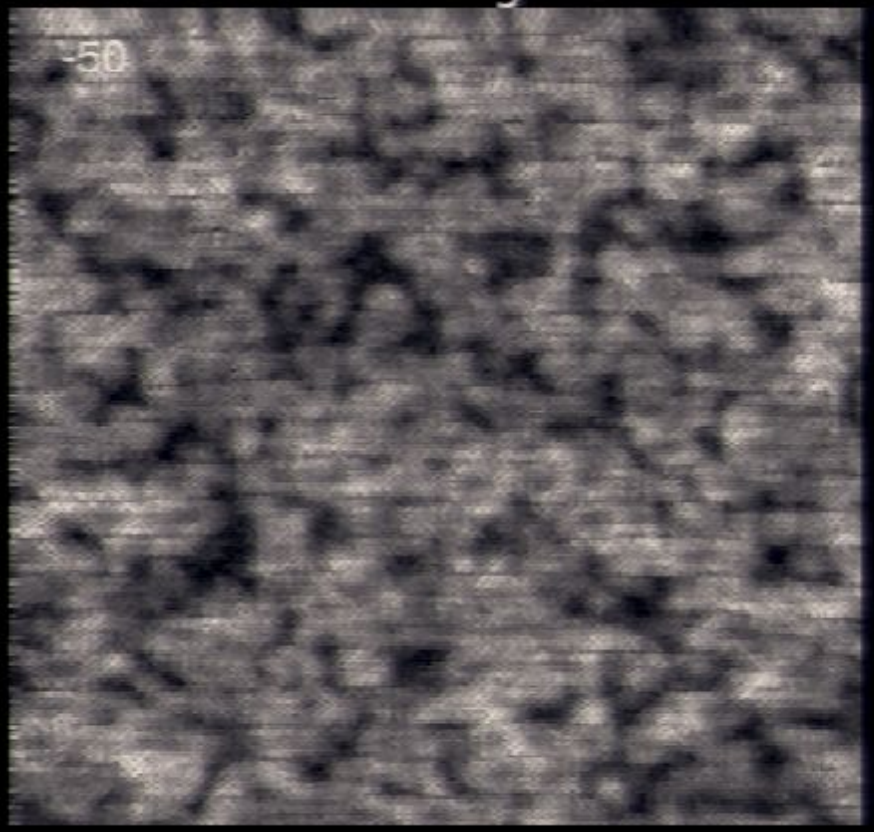

$g(\vec{r},E)$

High-T_c Superconductivity

Copper-based / Iron-based High-T_c Superconductors

Strongly correlated

Modestly correlated

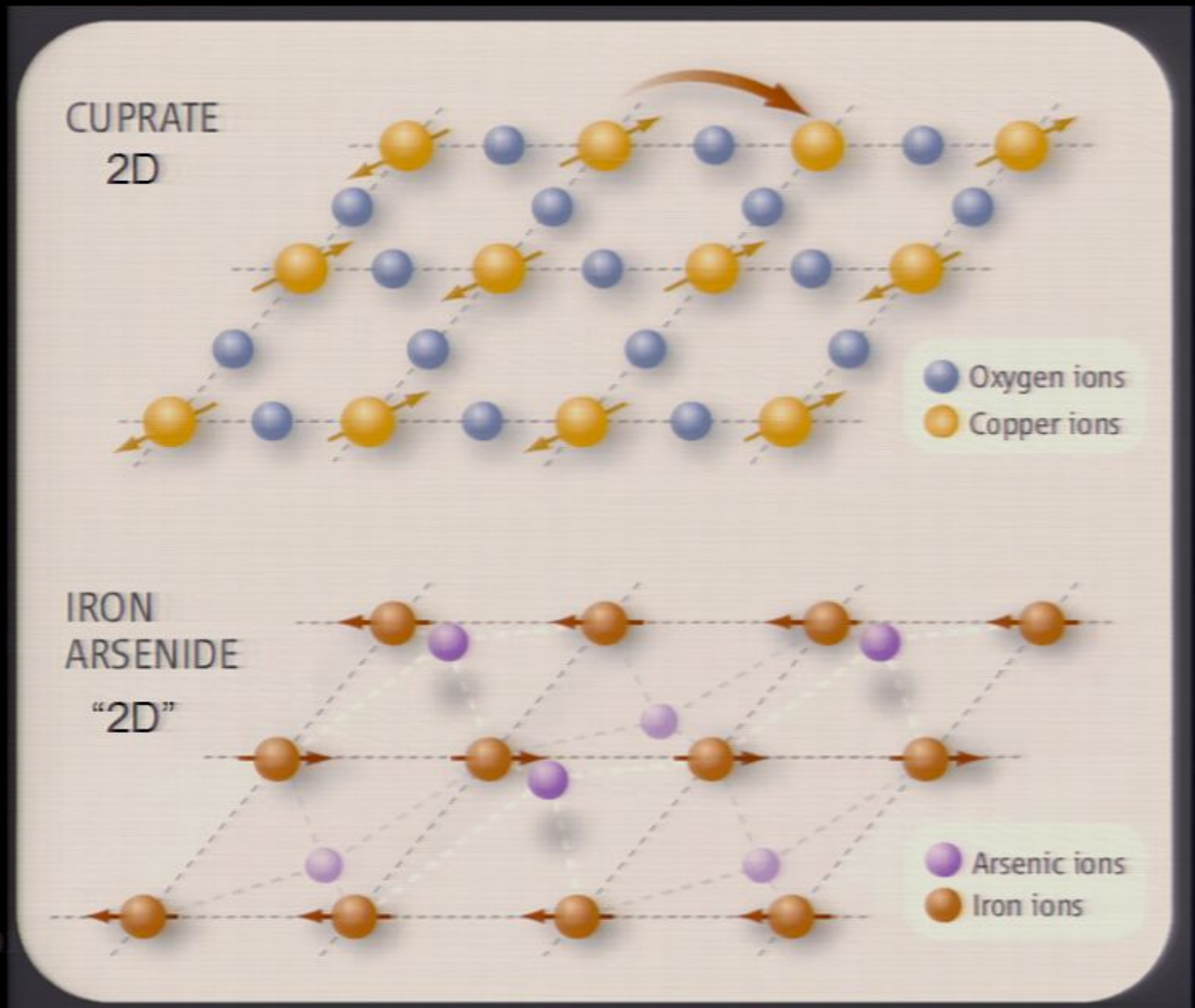

1 d-orbital

5 d-orbitals

Copper-based / Iron-based High-T_c Superconductors

Copper-based

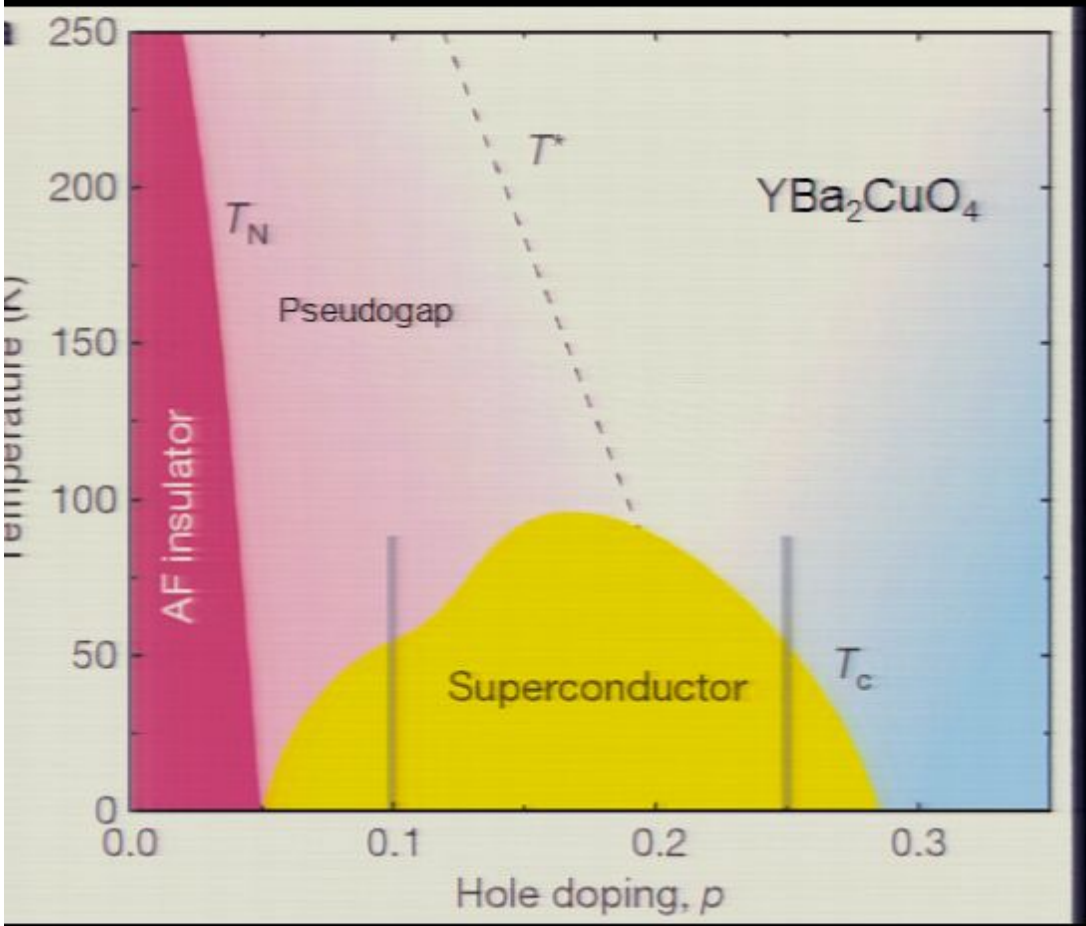

Iron-based

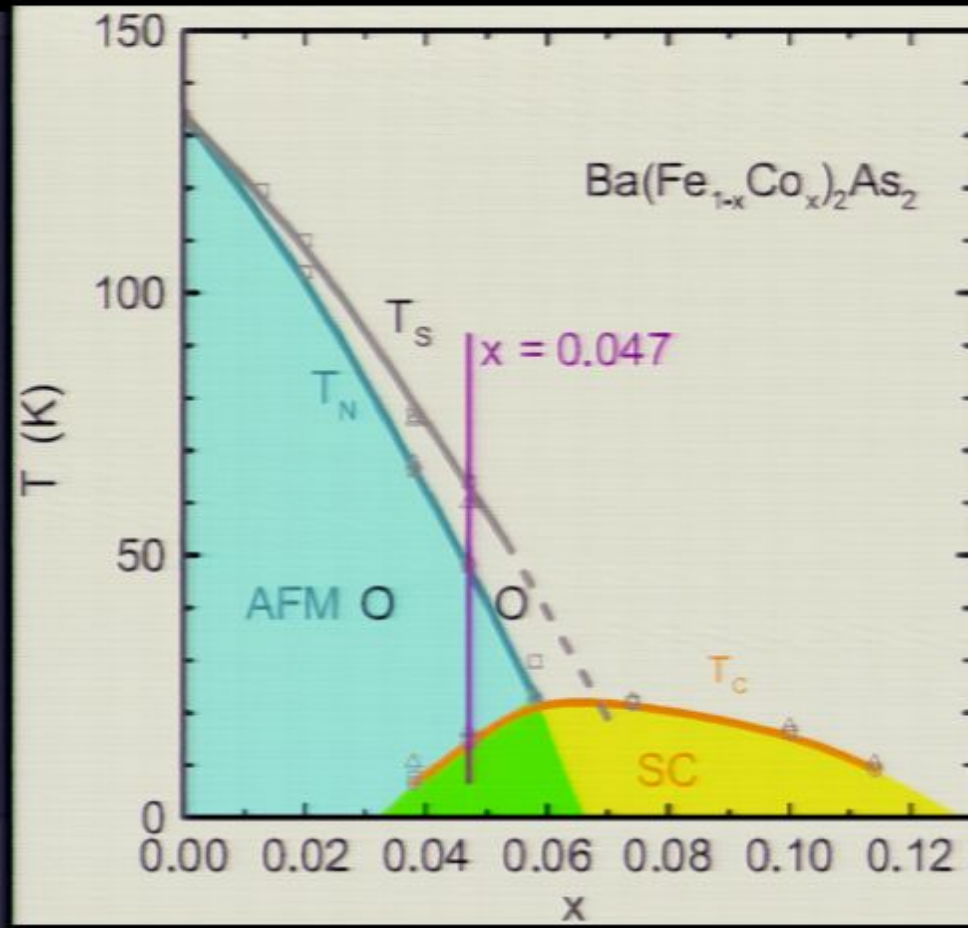

Phase diagrams as a function of hole/electron doping have many similarities – broken symmetry state penetrates center of SC dome

Underdoped CuO_2 Electronic Structure from SI-STM

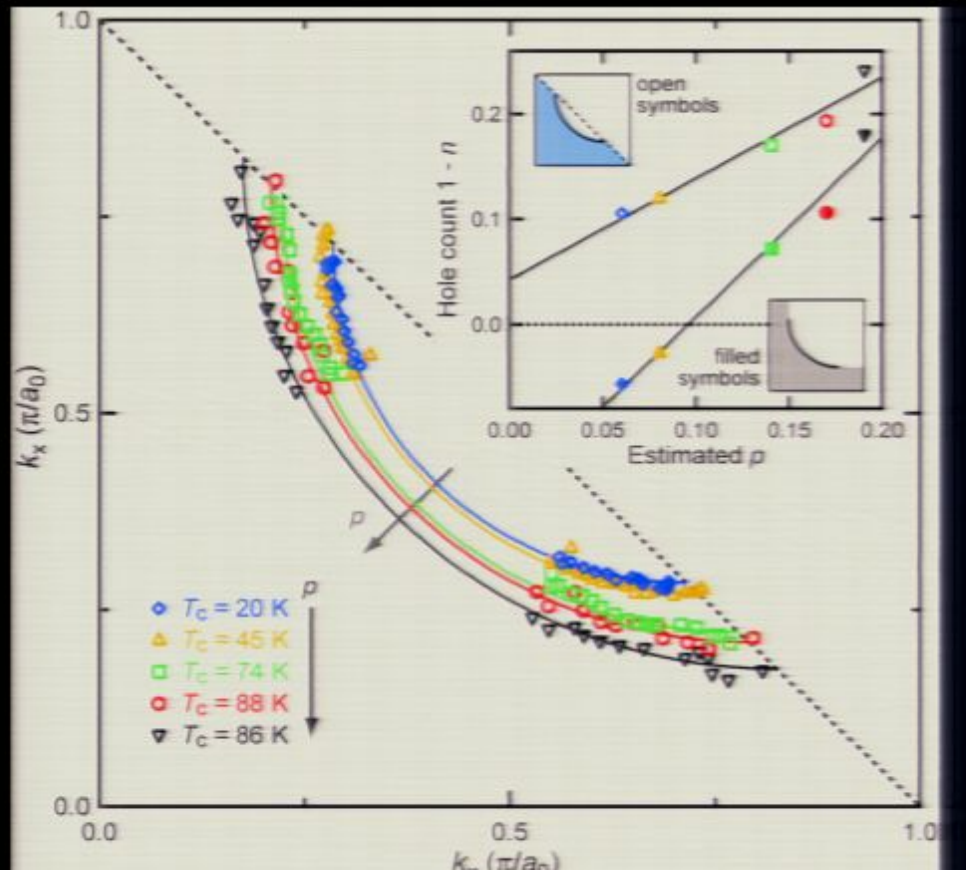

Dr. Y. Kohsaka
Cornell
RIKEN

Dr. A. R. Schmidt
Cornell
UC Berkeley

Chung Koo Kim
Cornell
BNL

Dr. K. Fujita
Cornell
BNL

Prof. D-H Lee
UC Berkeley./ LBNL

Dr. H. Eisaki
AIST

Prof. S. Uchida
U. Of Tokyo

Cuprate electronic structure: two characteristic energy scales

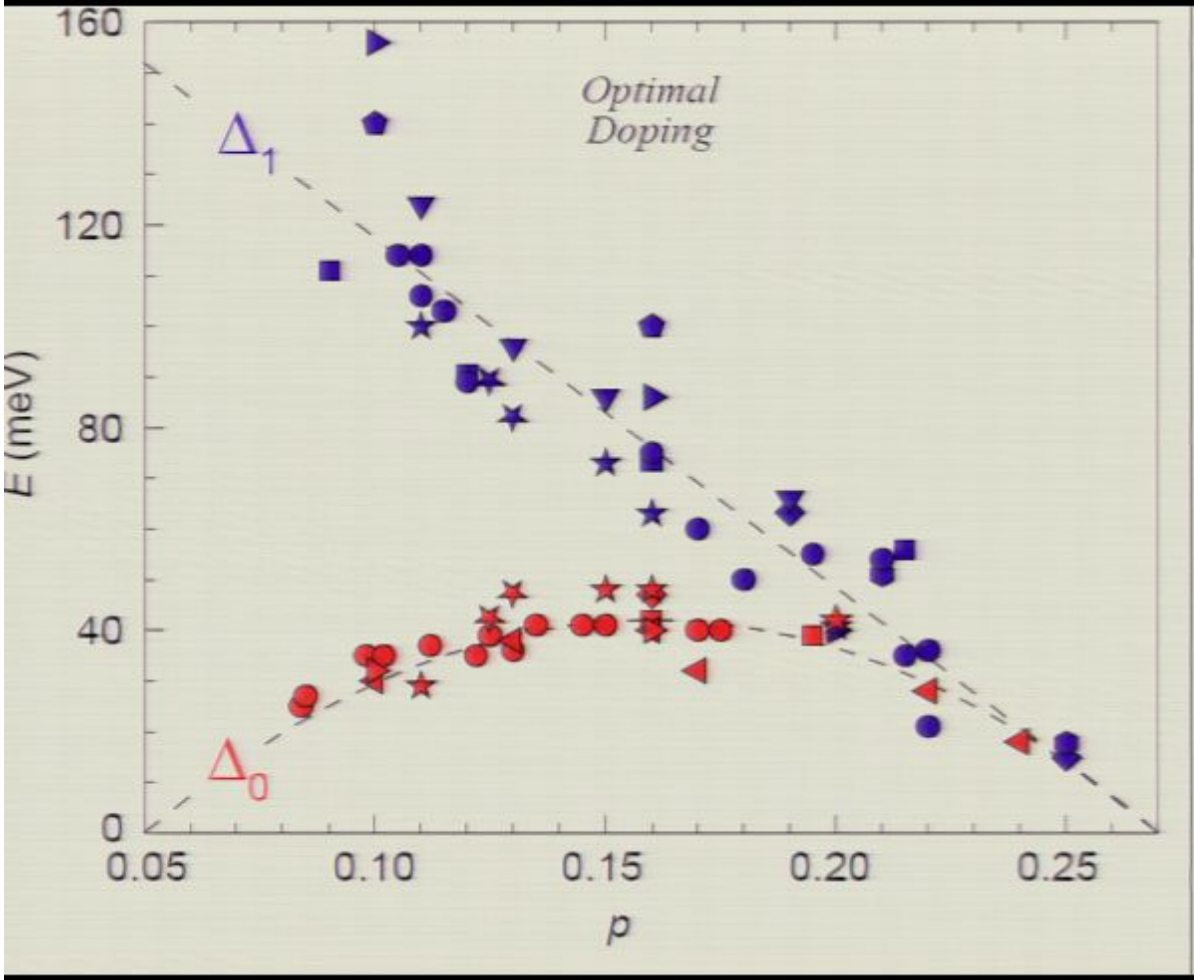

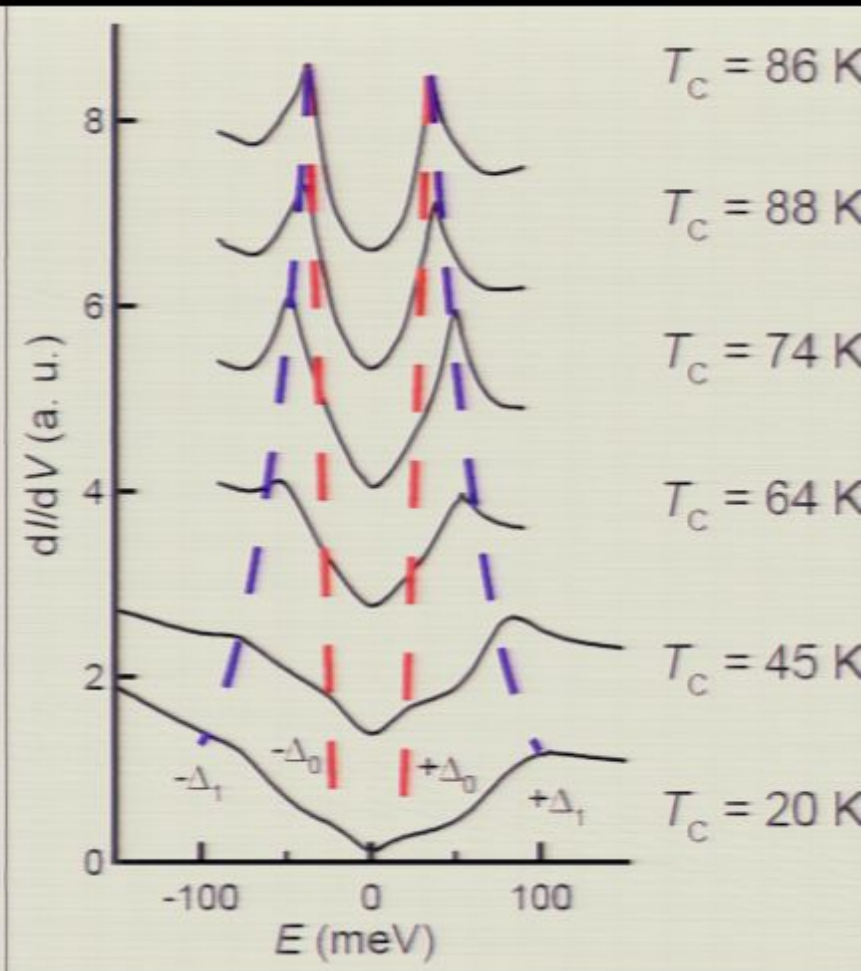

S. Hüfner *et al.*, *Rep. Prog. Phys.* **71** 062501 (2008)

PRL **94**, 197005, (2005)
Science **309**, 1048 (2005)
Nat. Phys. **4**, 319 (2008)

Cuprate electronic structure: two characteristic energy scales

Science 313, 1380 (2007); Nature 454, 1072, (2008), Nature 466, 374 (2010)

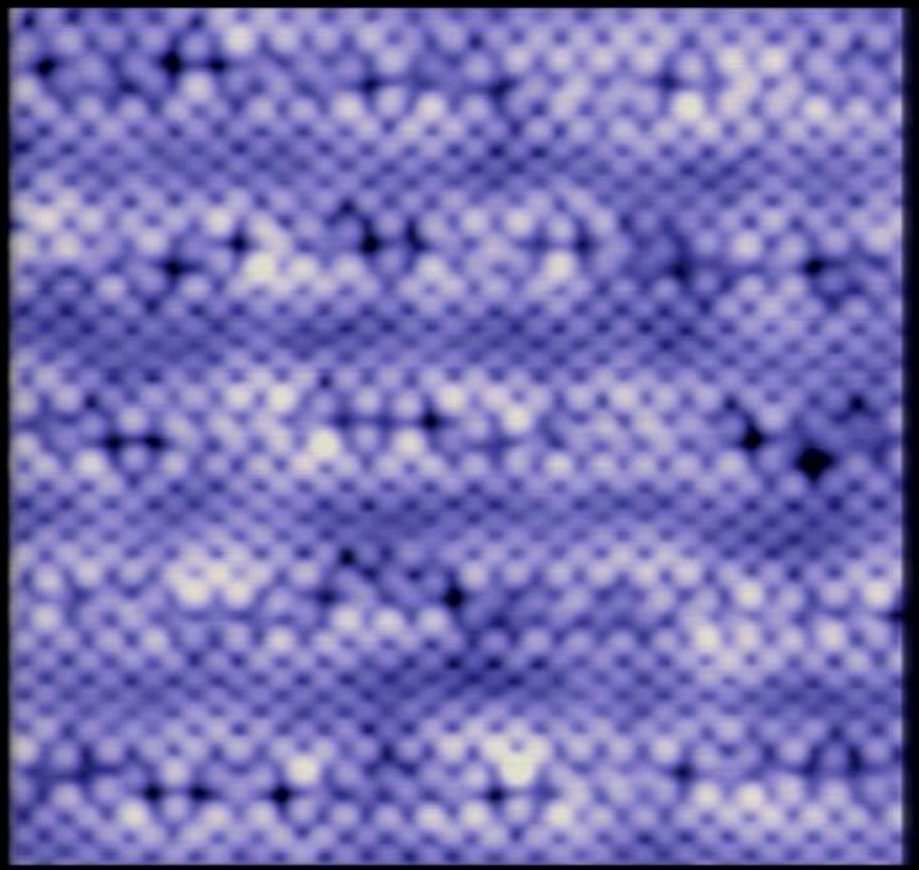

$Bi_{2.2}Sr_{1.8}(Ca,Dy)Cu_2O_y$

Cuprate electronic structure: two characteristic energy scales

Science 313, 1380 (2007); Nature 454, 1072, (2008), Nature 466, 374 (2010)

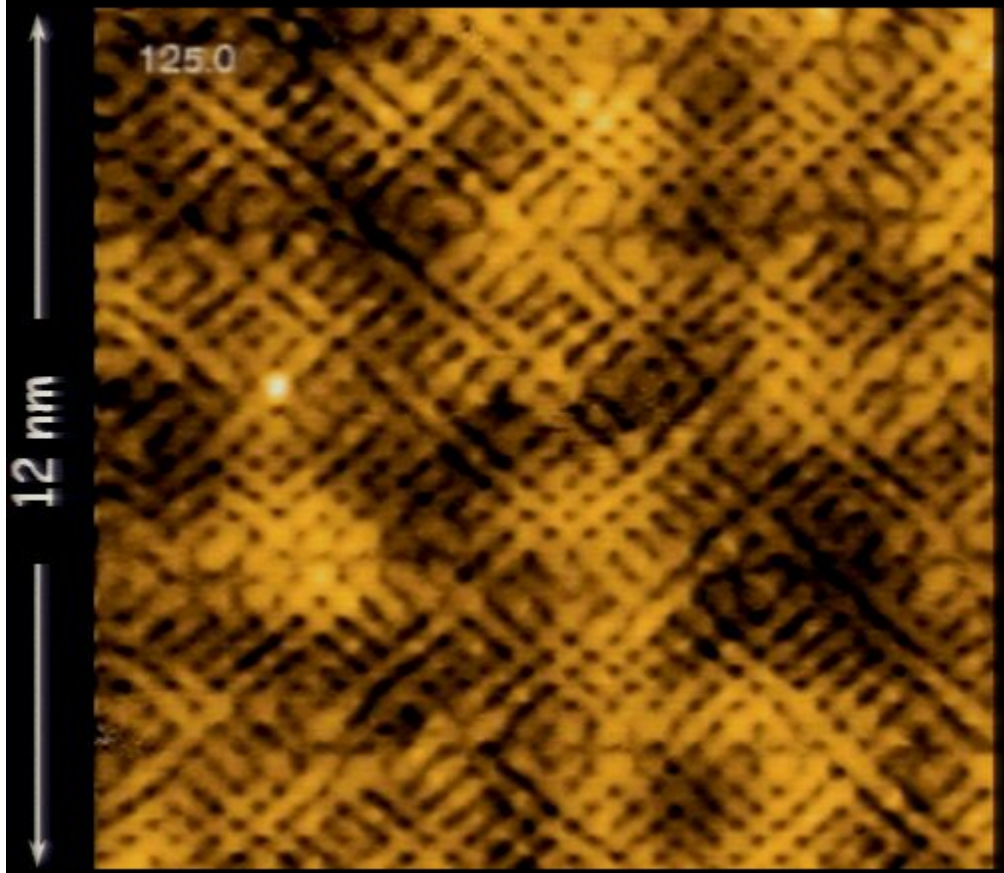

$Z(\vec{r},V)$

0.5 — 1.9

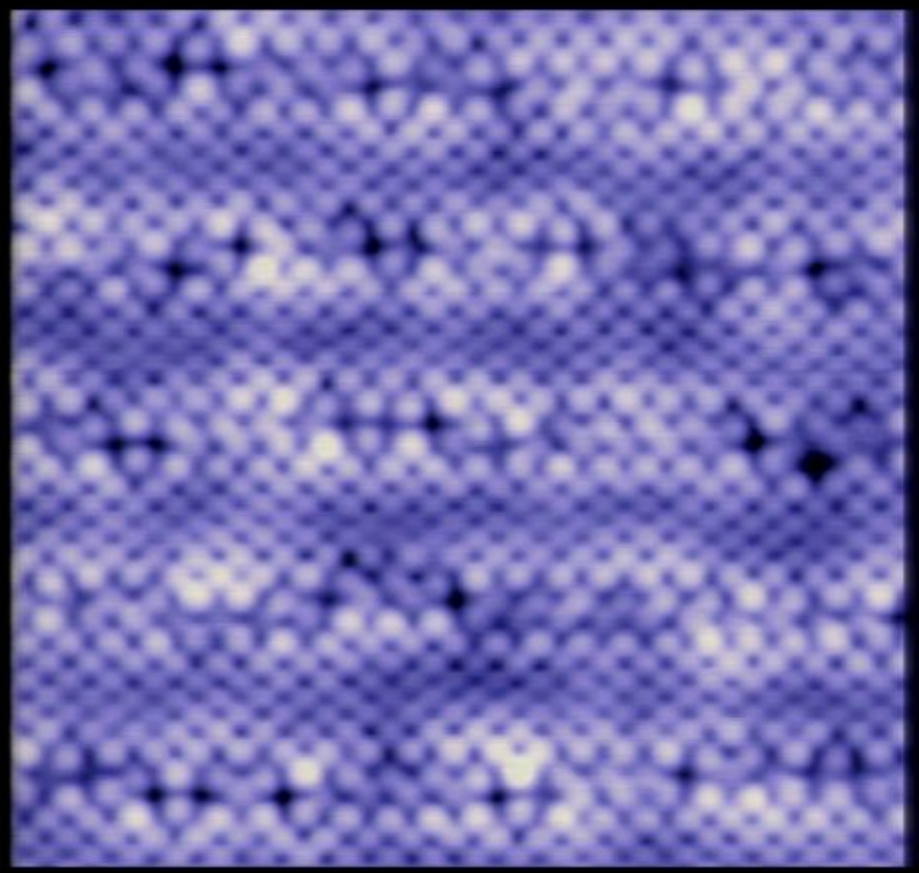

$Bi_{2.2}Sr_{1.8}(Ca,Dy)Cu_2O_y$

Cuprate electronic structure: two characteristic energy scales

Science 313, 1380 (2007); Nature 454, 1072, (2008), Nature 466, 374 (2010)

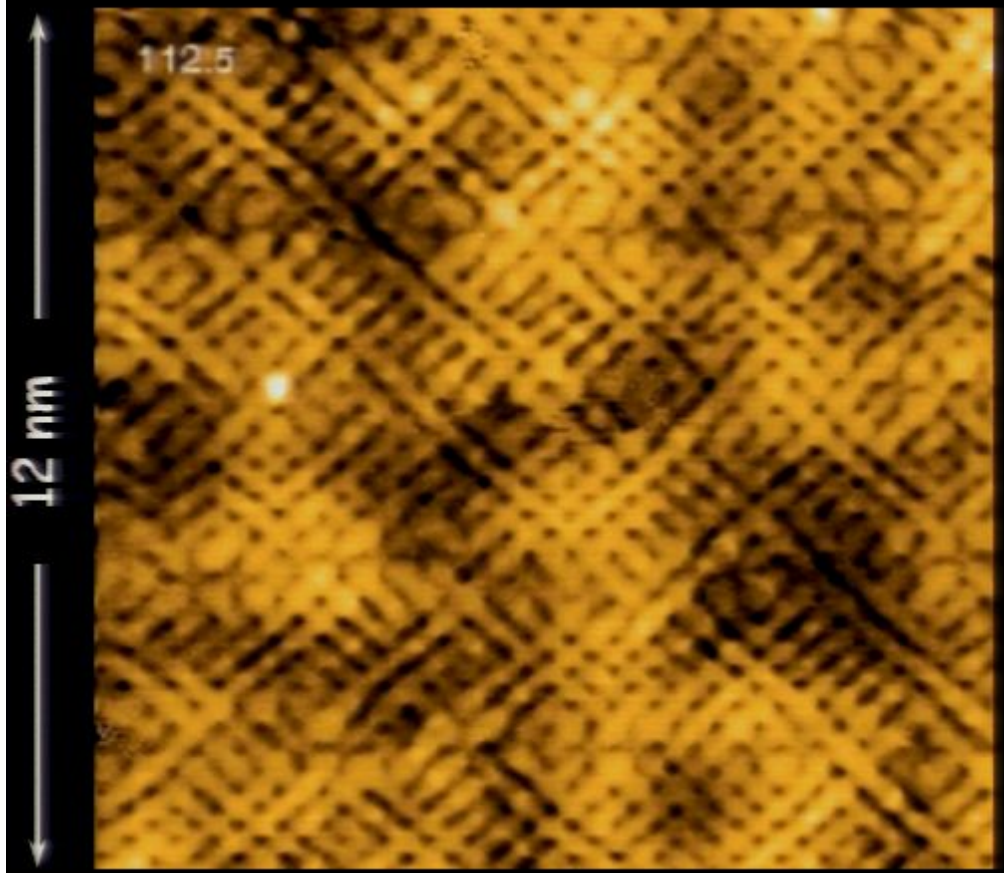

$Z(\vec{r},V)$

0.5 — 1.9

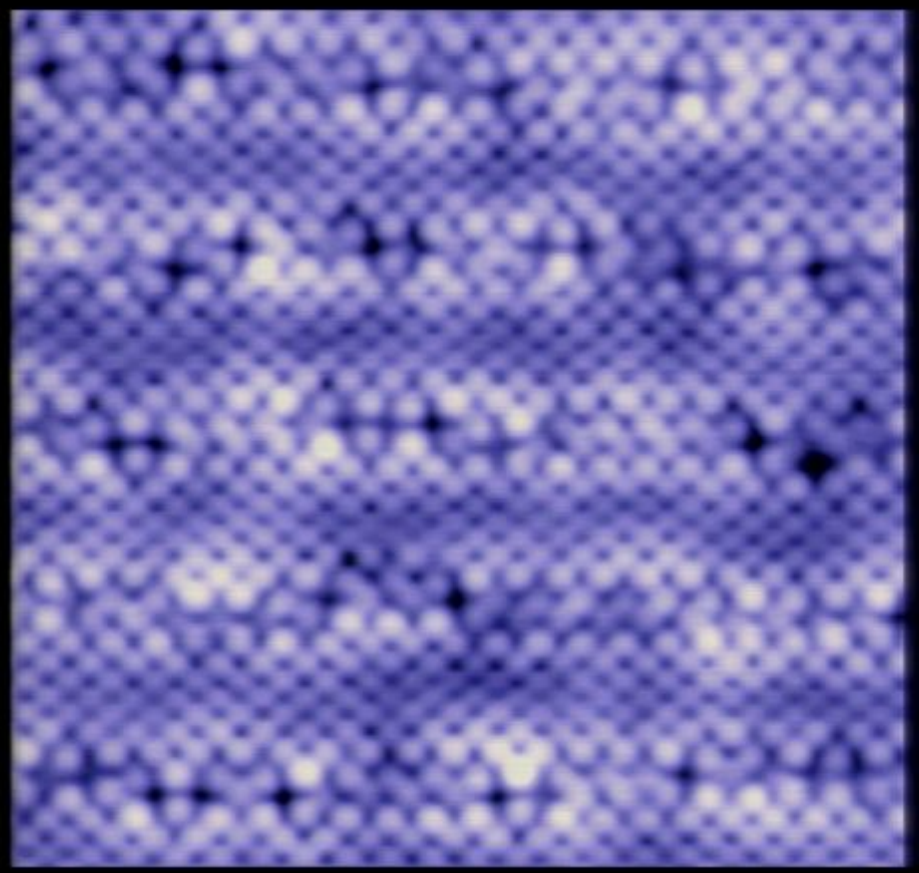

$Bi_{2.2}Sr_{1.8}(Ca,Dy)Cu_2O_y$

Cuprate electronic structure: two characteristic energy scales

Science 313, 1380 (2007); Nature 454, 1072, (2008), Nature 466, 374 (2010)

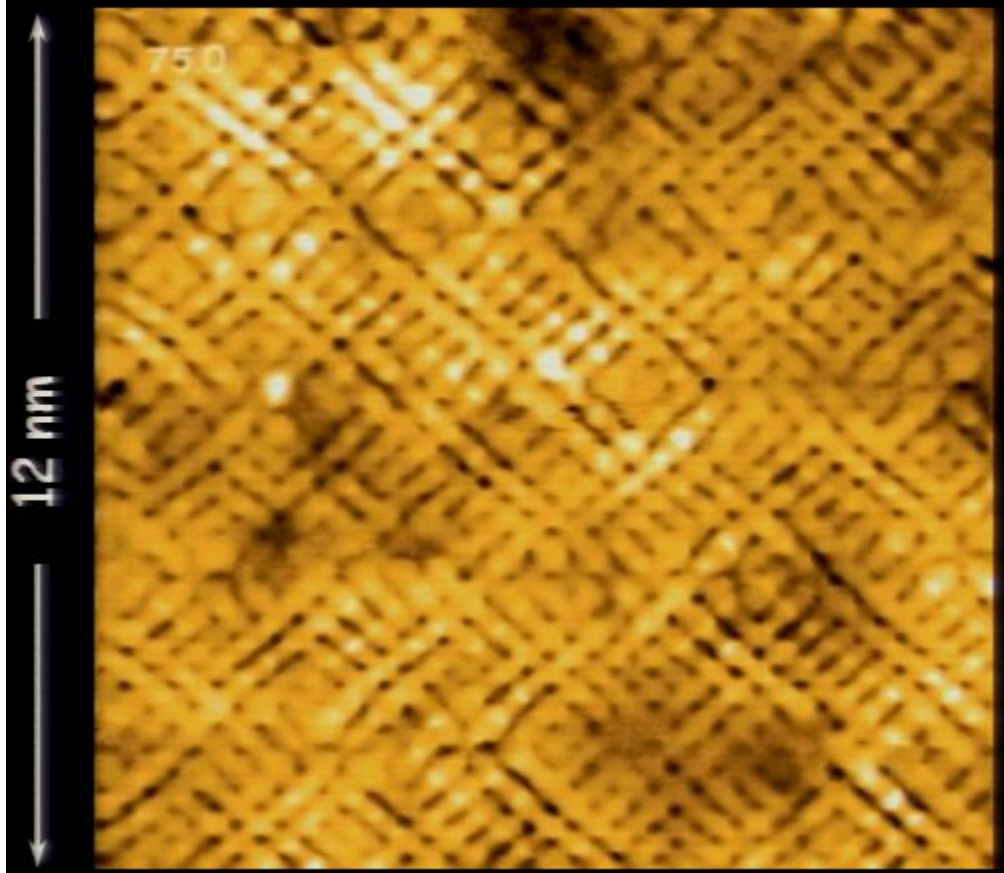

$Z(\vec{r},V)$

0.5 1.9

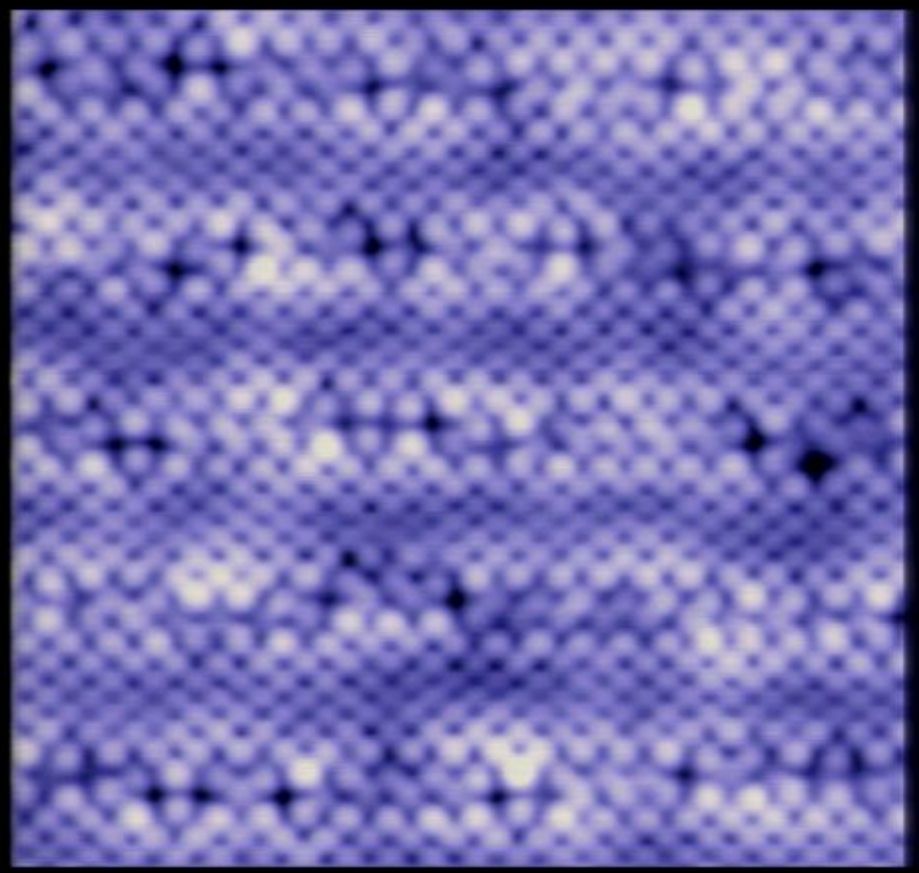

$Bi_{2.2}Sr_{1.8}(Ca,Dy)Cu_2O_y$

Cuprate electronic structure: two characteristic energy scales

Science 313, 1380 (2007); Nature 454, 1072, (2008), Nature 466, 374 (2010)

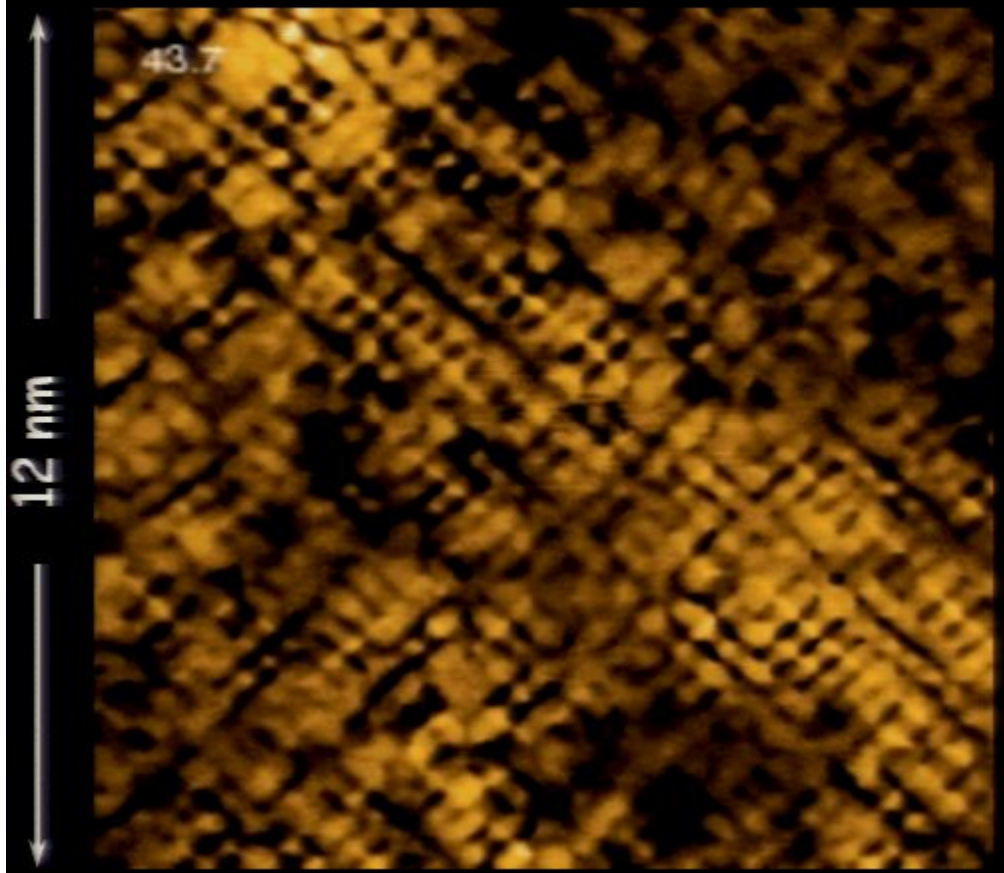

$Z(\vec{r},V)$

0.5 — 1.9

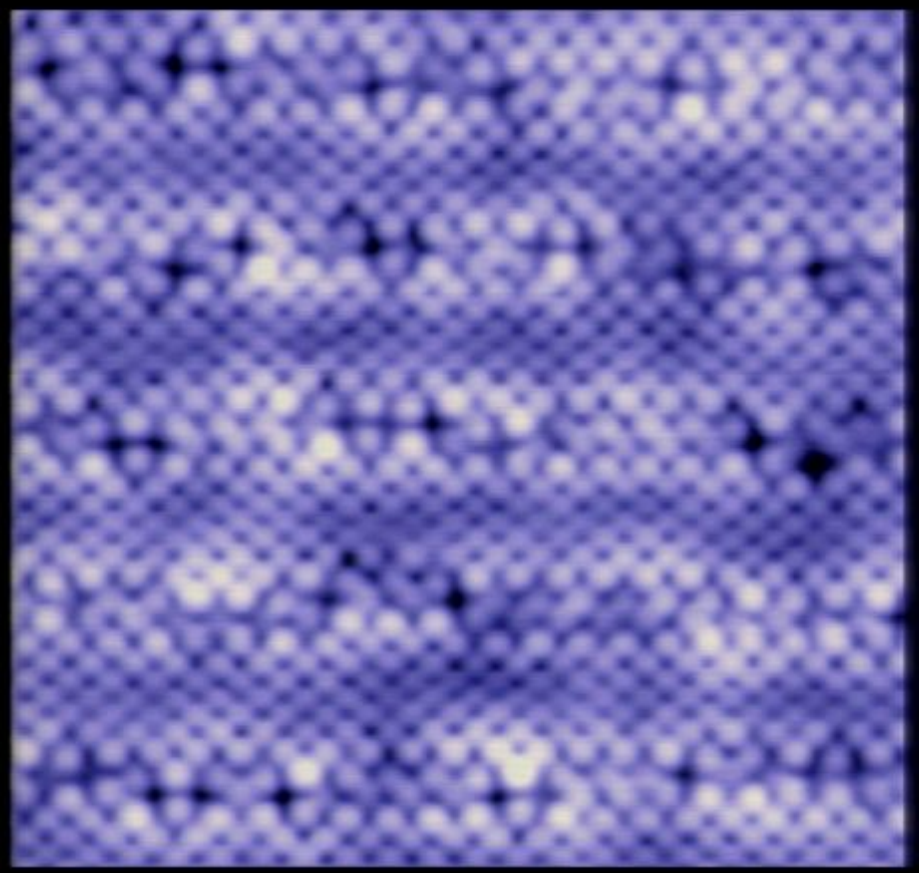

$Bi_{2.2}Sr_{1.8}(Ca,Dy)Cu_2O_y$

Cuprate electronic structure: two characteristic energy scales

Science 313, 1380 (2007); Nature 454, 1072, (2008), Nature 466, 374 (2010)

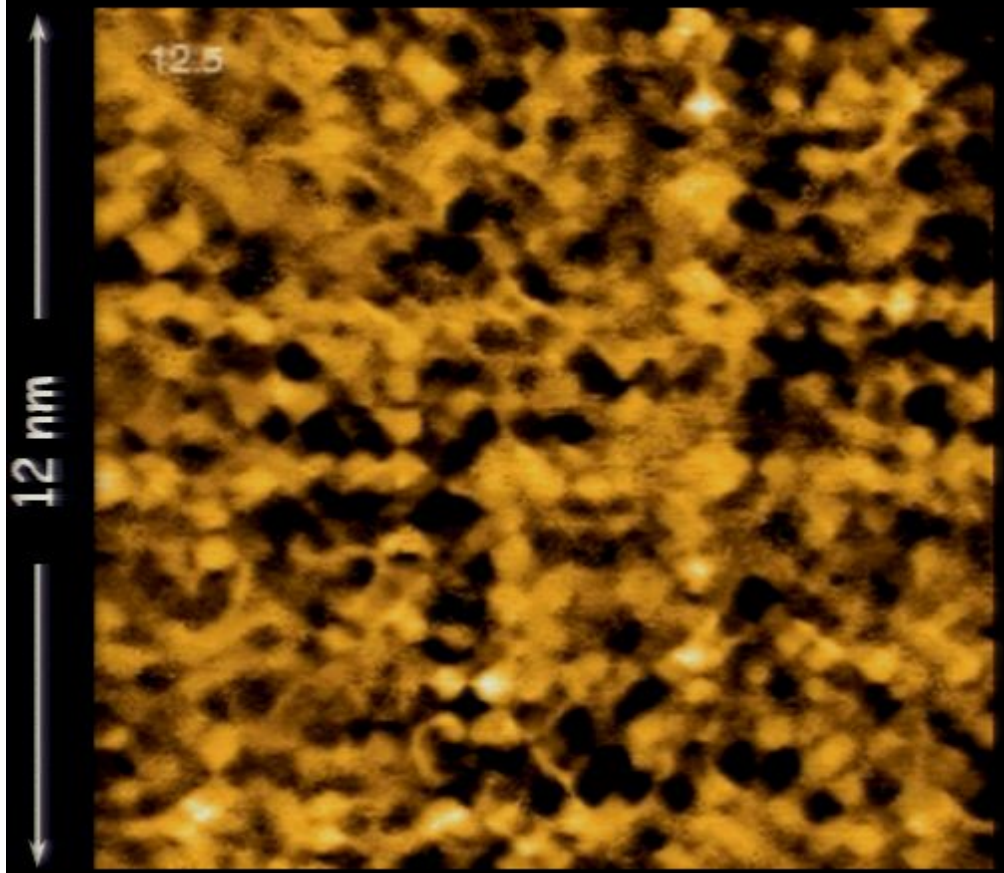

$Z(\vec{r},V)$

0.5 — 1.9

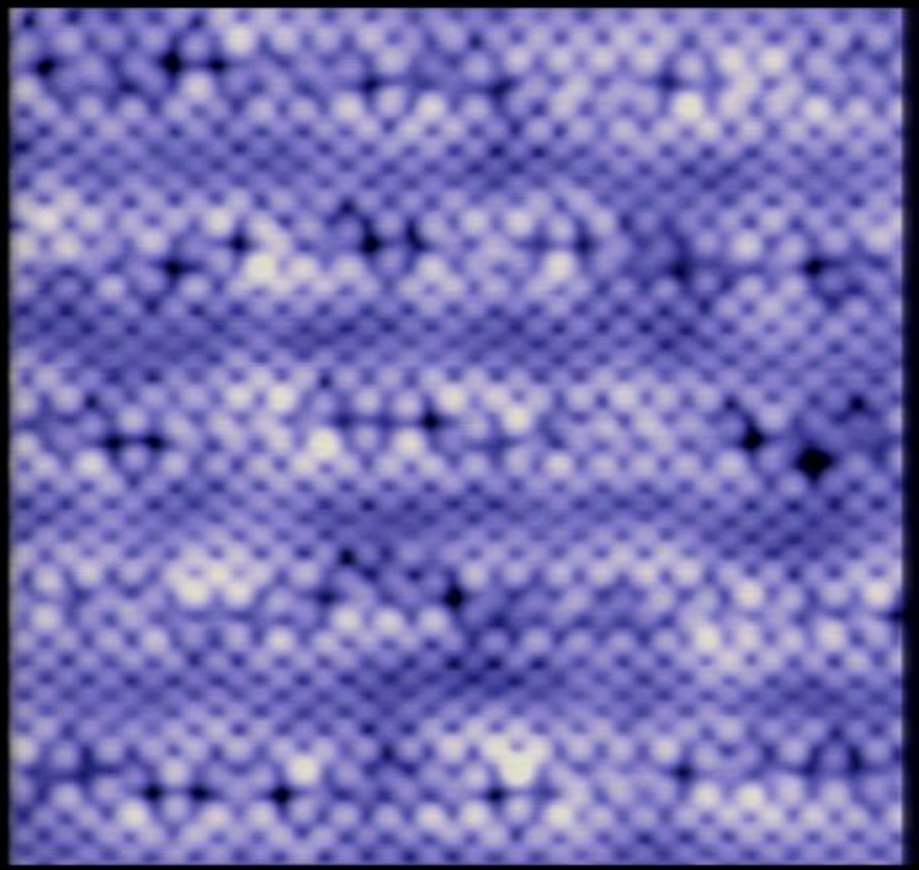

$Bi_{2.2}Sr_{1.8}(Ca,Dy)Cu_2O_y$

Cuprate electronic structure: two characteristic energy scales

Science 313, 1380 (2007); Nature 454, 1072, (2008), Nature 466, 374 (2010)

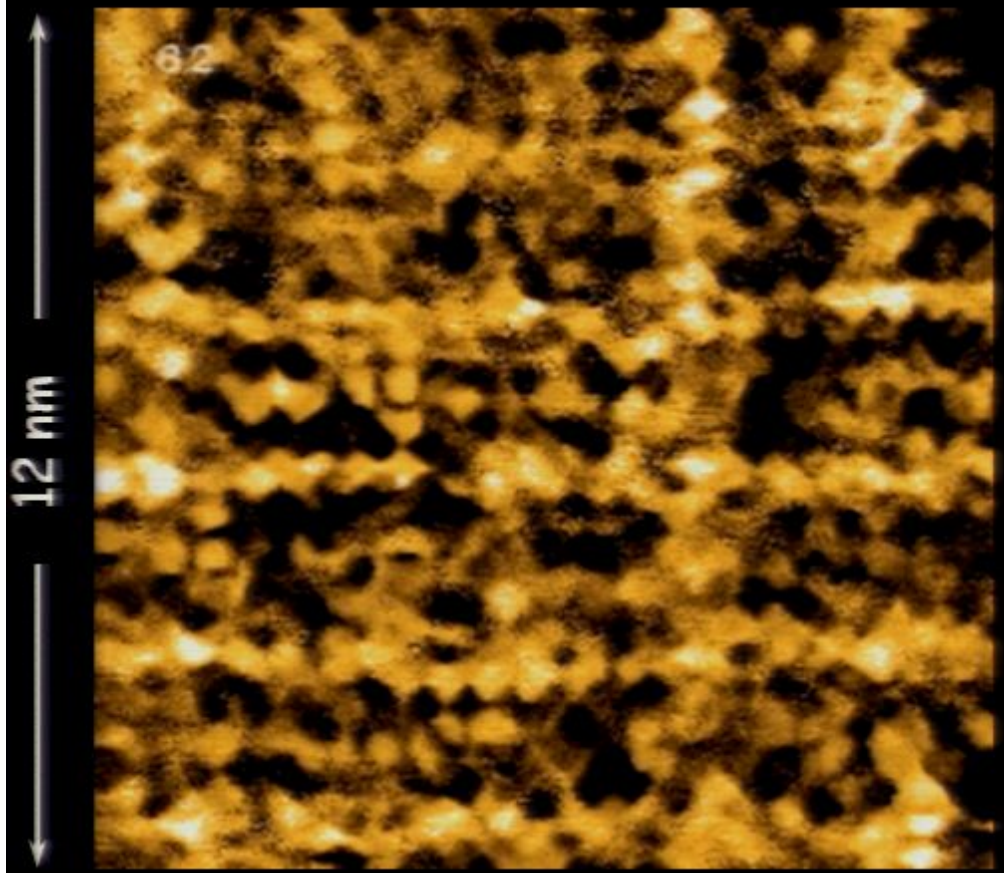

$Z(\vec{r},V)$

0.5 — 1.9

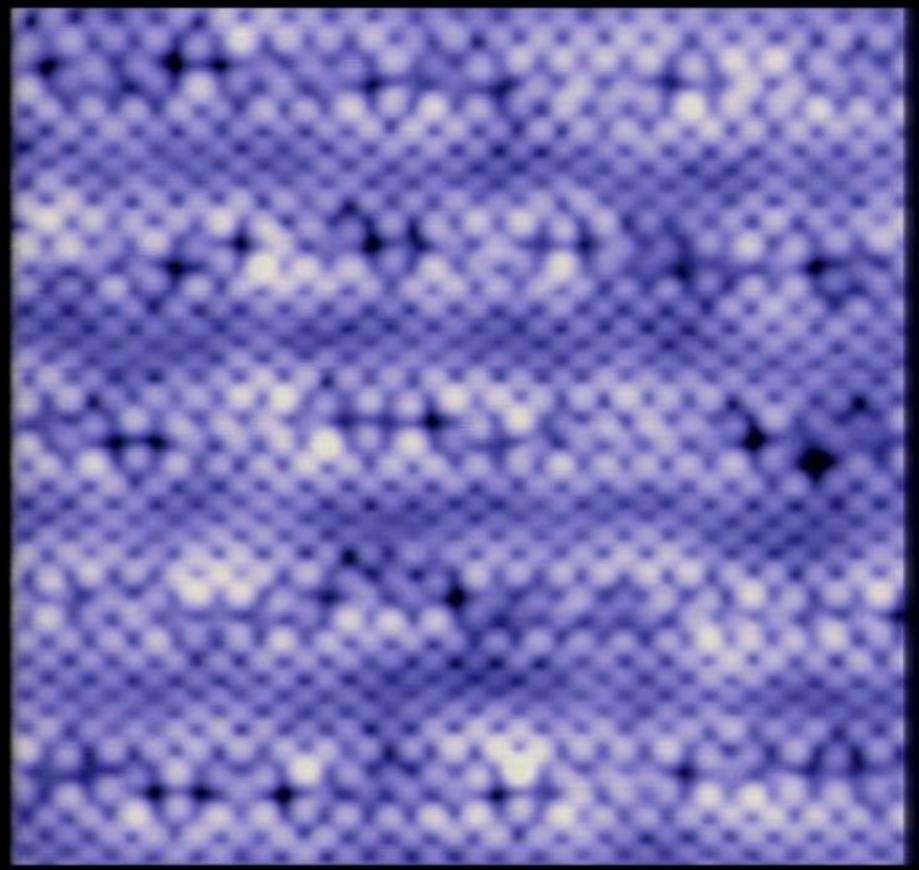

$Bi_{2.2}Sr_{1.8}(Ca,Dy)Cu_2O_y$

Cuprate electronic structure: two characteristic energy scales

Science 313, 1380 (2007); Nature 454, 1072, (2008), Nature 466, 374 (2010)

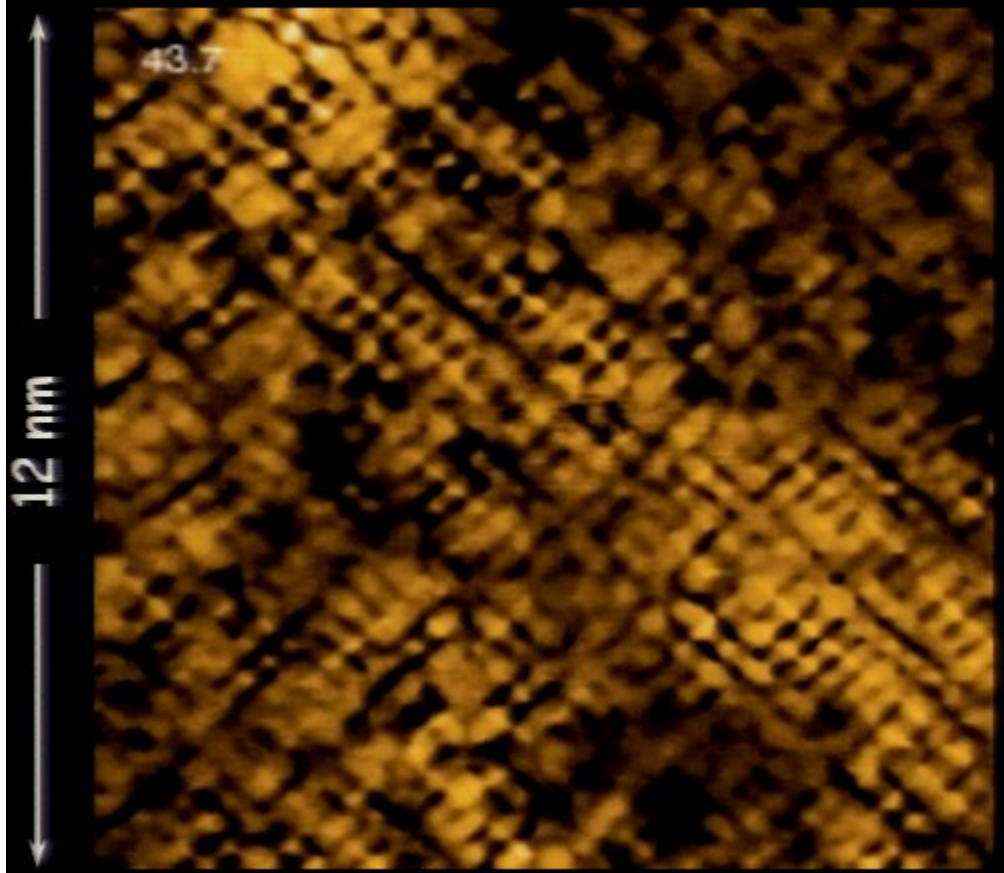

$Z(\vec{r},V)$

0.5 — 1.9

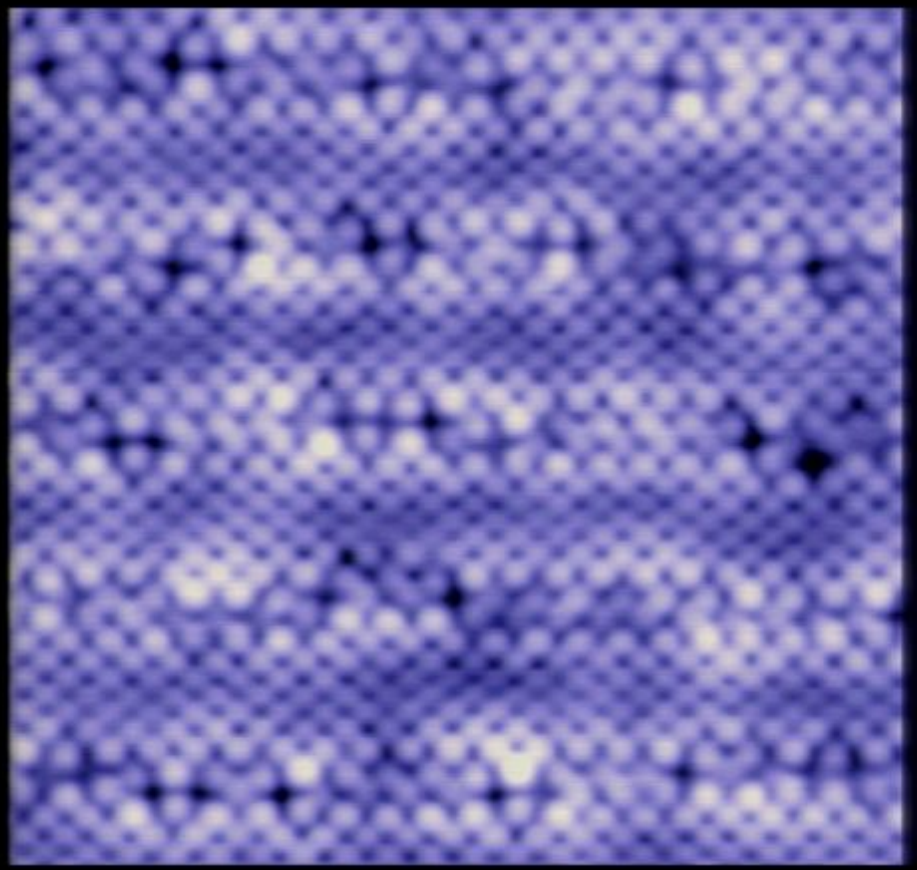

$Bi_{2.2}Sr_{1.8}(Ca,Dy)Cu_2O_y$

Cuprate electronic structure: two characteristic energy scales

Science 313, 1380 (2007); Nature 454, 1072, (2008), Nature 466, 374 (2010)

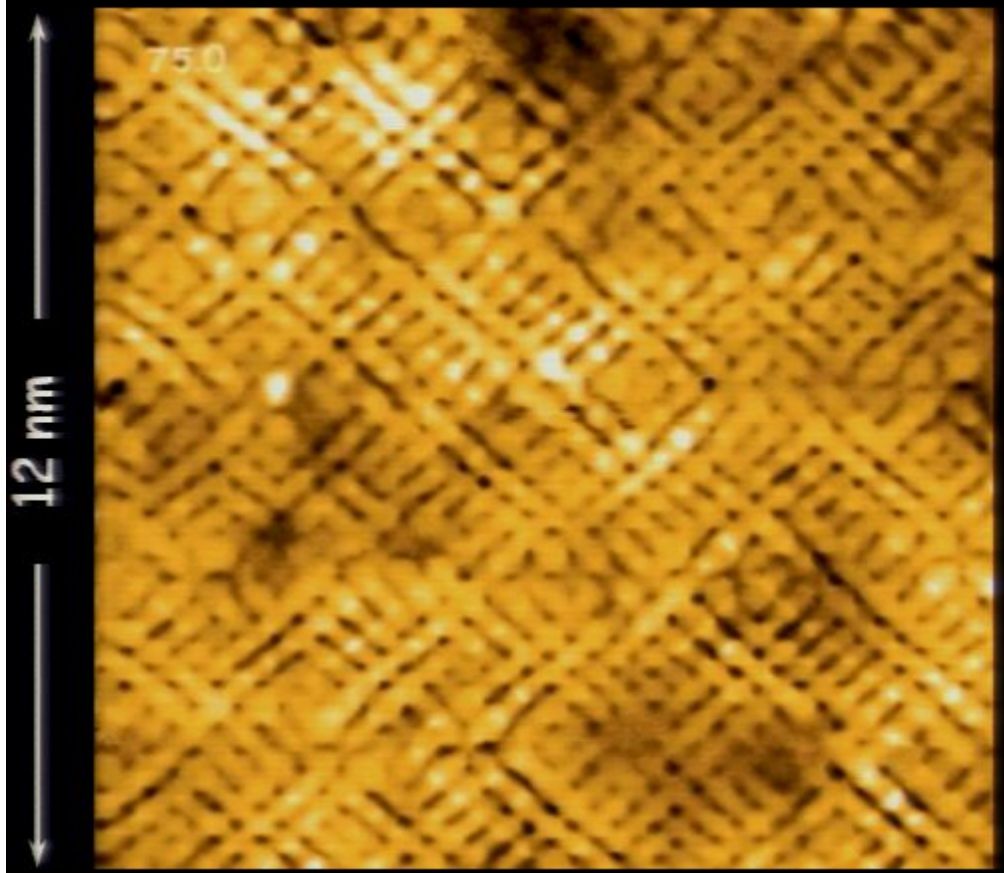

$Z(\vec{r},V)$

0.5 — 1.9

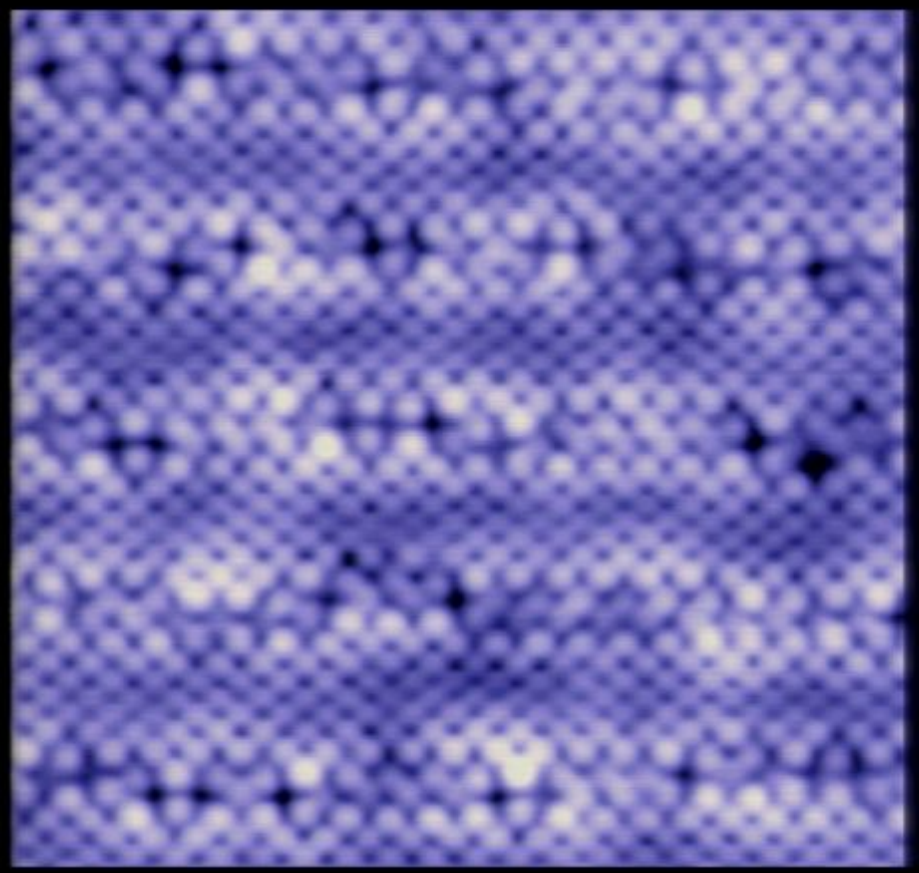

$Bi_{2.2}Sr_{1.8}(Ca,Dy)Cu_2O_y$

Cuprate electronic structure: two characteristic energy scales

Science 313, 1380 (2007); Nature 454, 1072, (2008), Nature 466, 374 (2010)

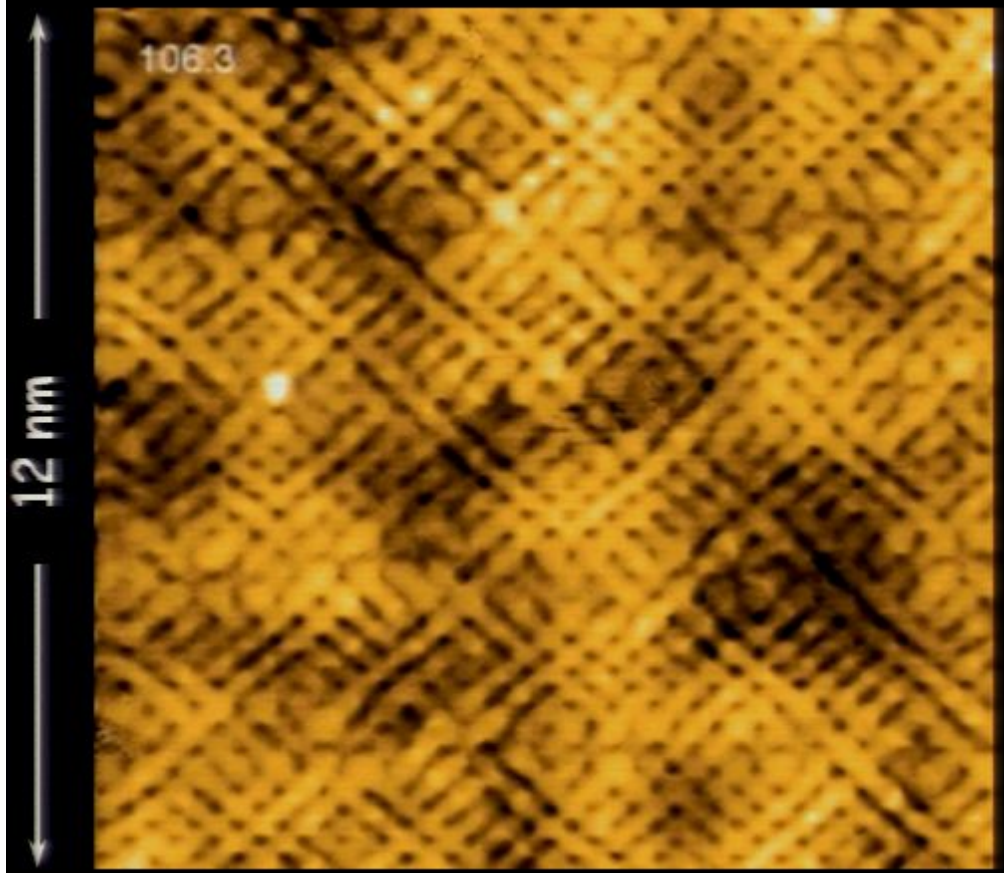

$Z(\vec{r},V)$

0.5 — 1.9

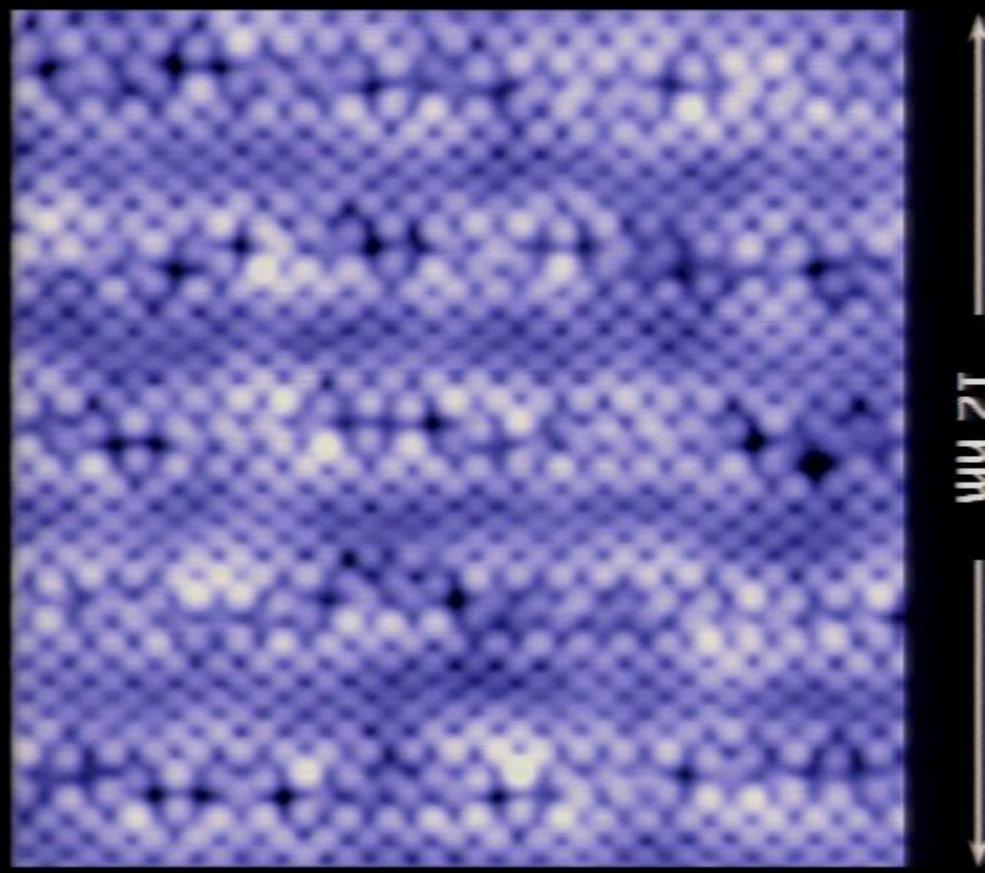

$Bi_{2.2}Sr_{1.8}(Ca,Dy)Cu_2O_y$

Cuprate electronic structure: two characteristic energy scales

Science 313, 1380 (2007); Nature 454, 1072, (2008), Nature 466, 374 (2010)

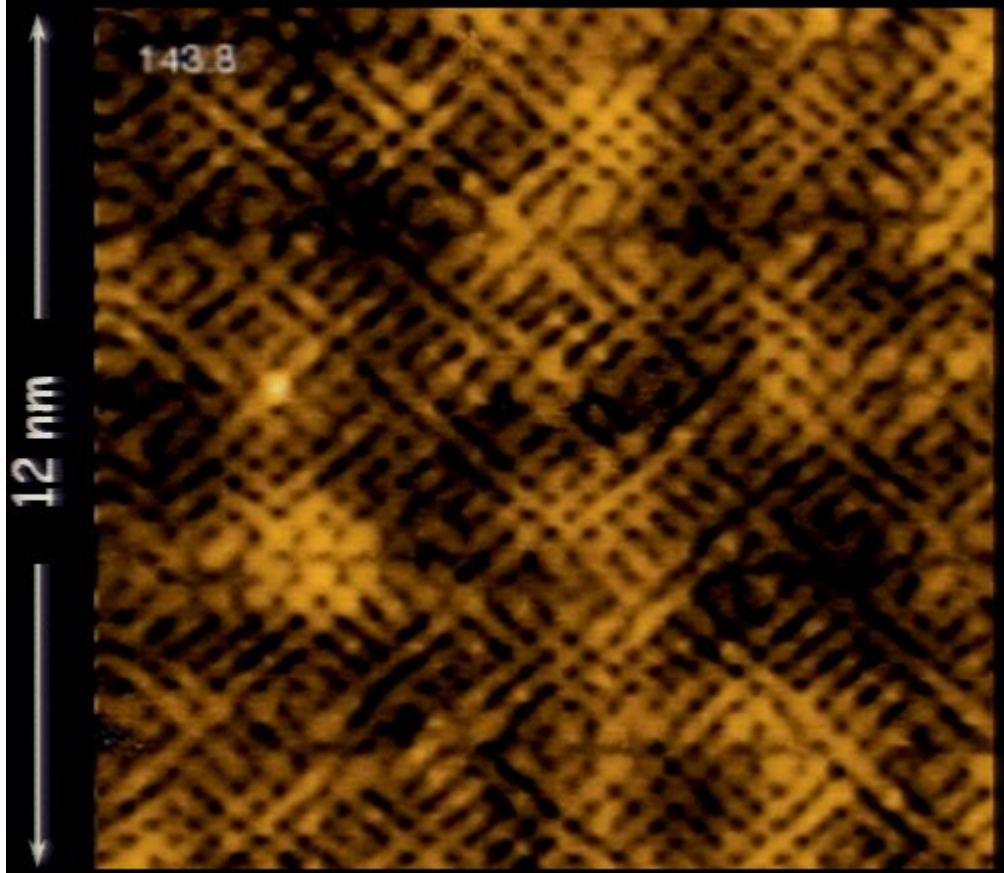

$Z(\vec{r},V)$

0.5 1.9

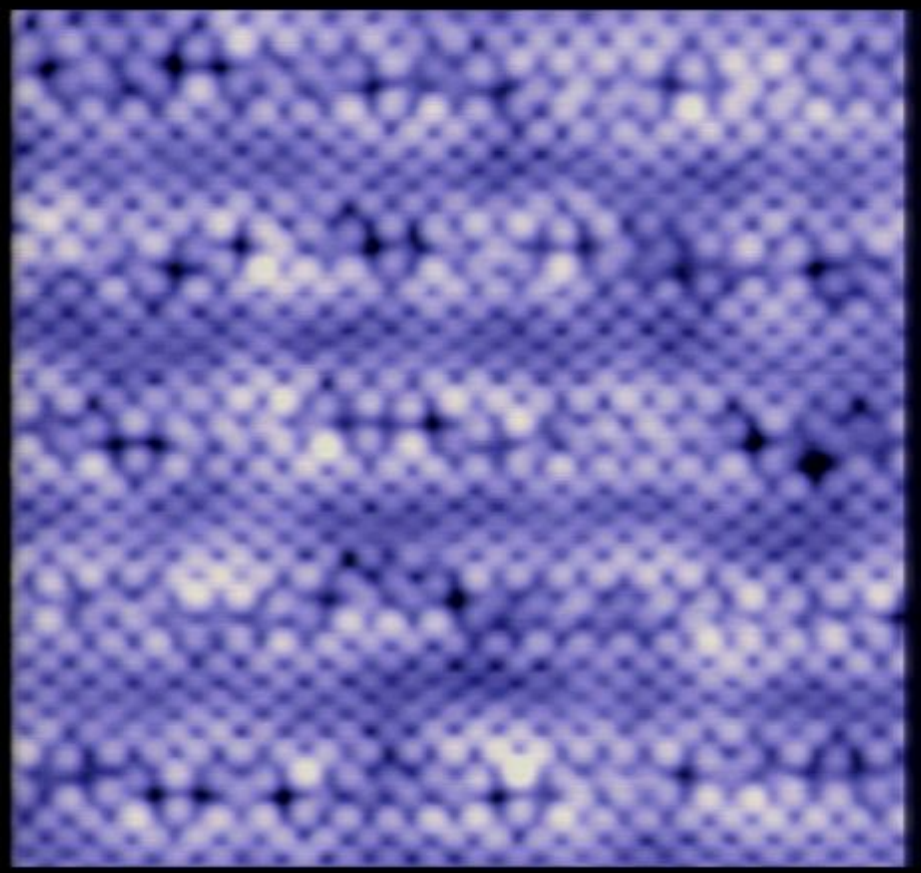

$Bi_{2.2}Sr_{1.8}(Ca,Dy)Cu_2O_y$

Cuprate electronic structure: two characteristic energy scales

Science 313, 1380 (2007); Nature 454, 1072, (2008), Nature 466, 374 (2010)

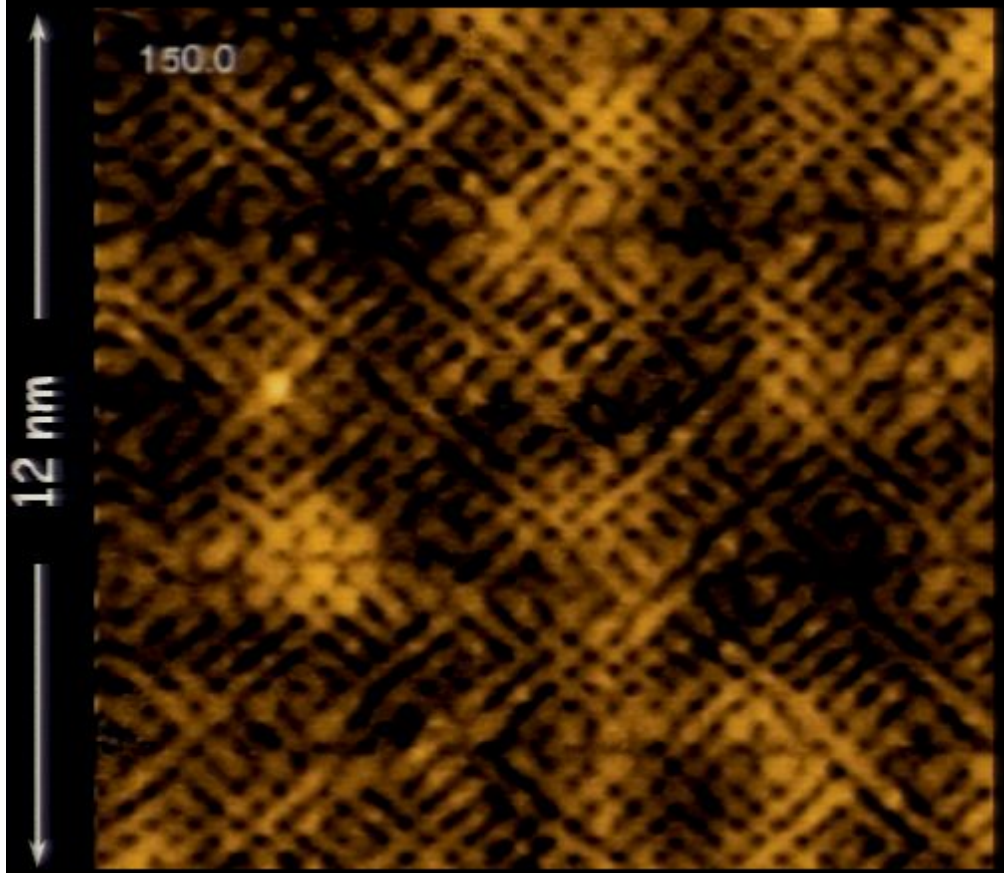

$Z(\vec{r},V)$

0.5 — 1.9

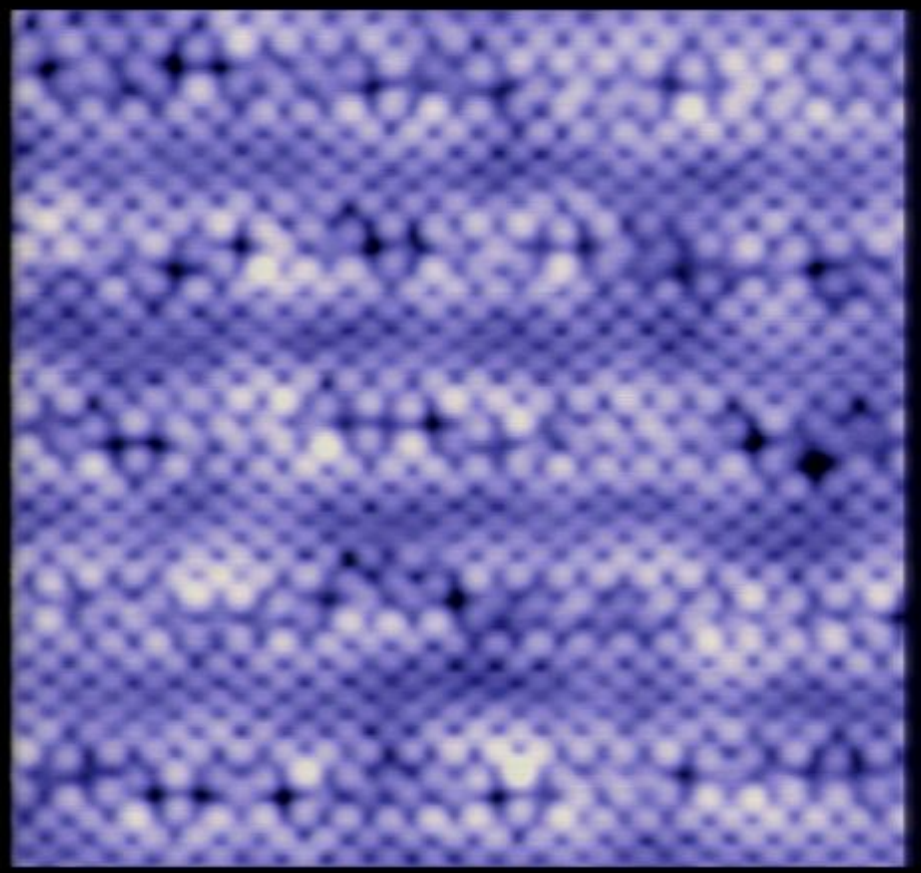

$Bi_{2.2}Sr_{1.8}(Ca,Dy)Cu_2O_y$

Cuprate electronic structure: two characteristic energy scales

Science 313, 1380 (2007); Nature 454, 1072, (2008), Nature 466, 374 (2010)

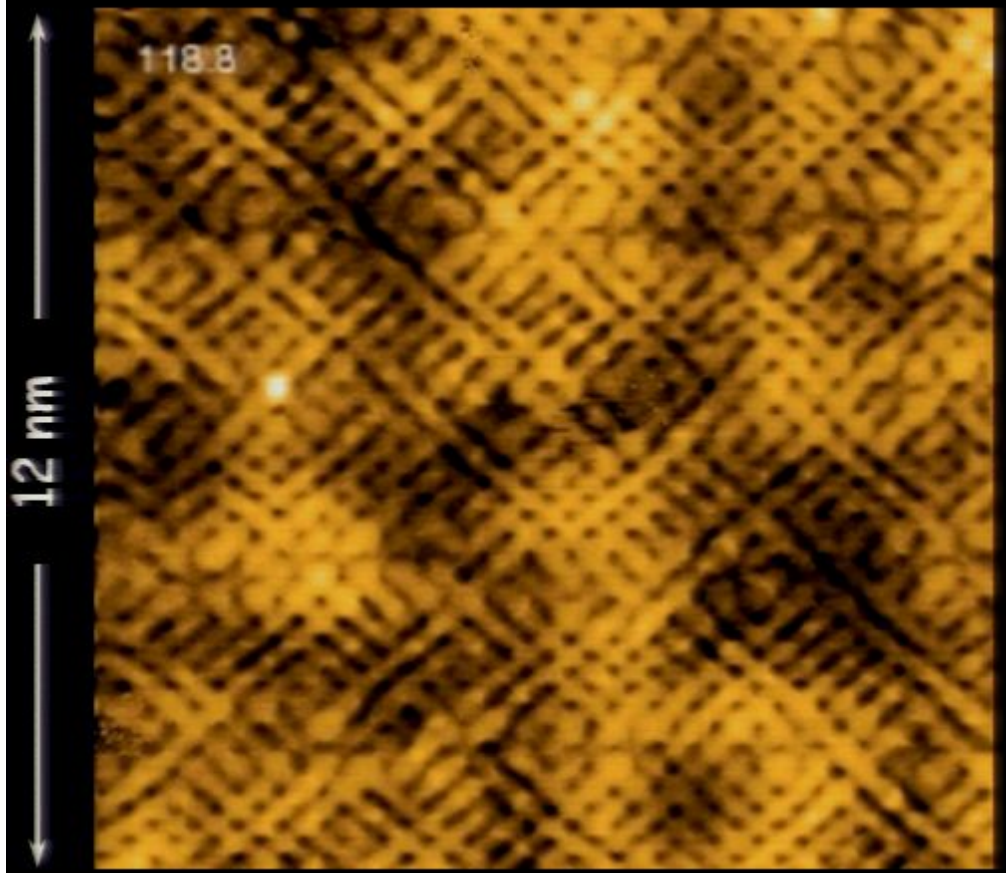

$Z(\vec{r},V)$

0.5 — 1.9

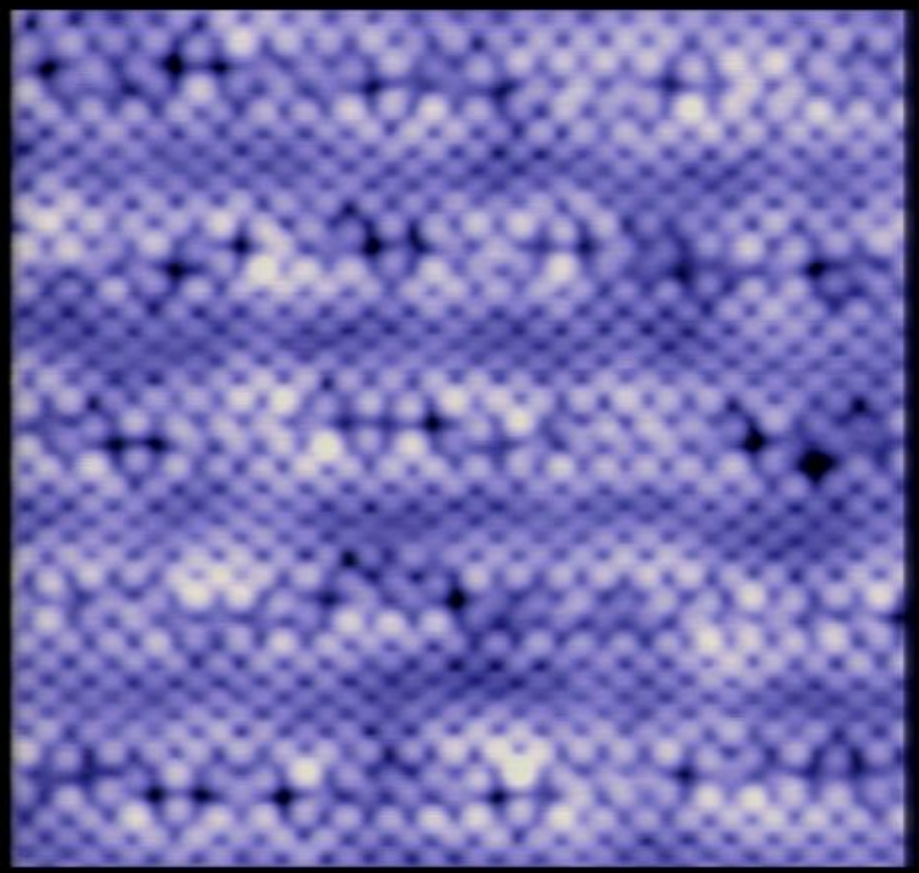

$Bi_{2.2}Sr_{1.8}(Ca,Dy)Cu_2O_y$

Cuprate electronic structure: two characteristic energy scales

Science 313, 1380 (2007); Nature 454, 1072, (2008), Nature 466, 374 (2010)

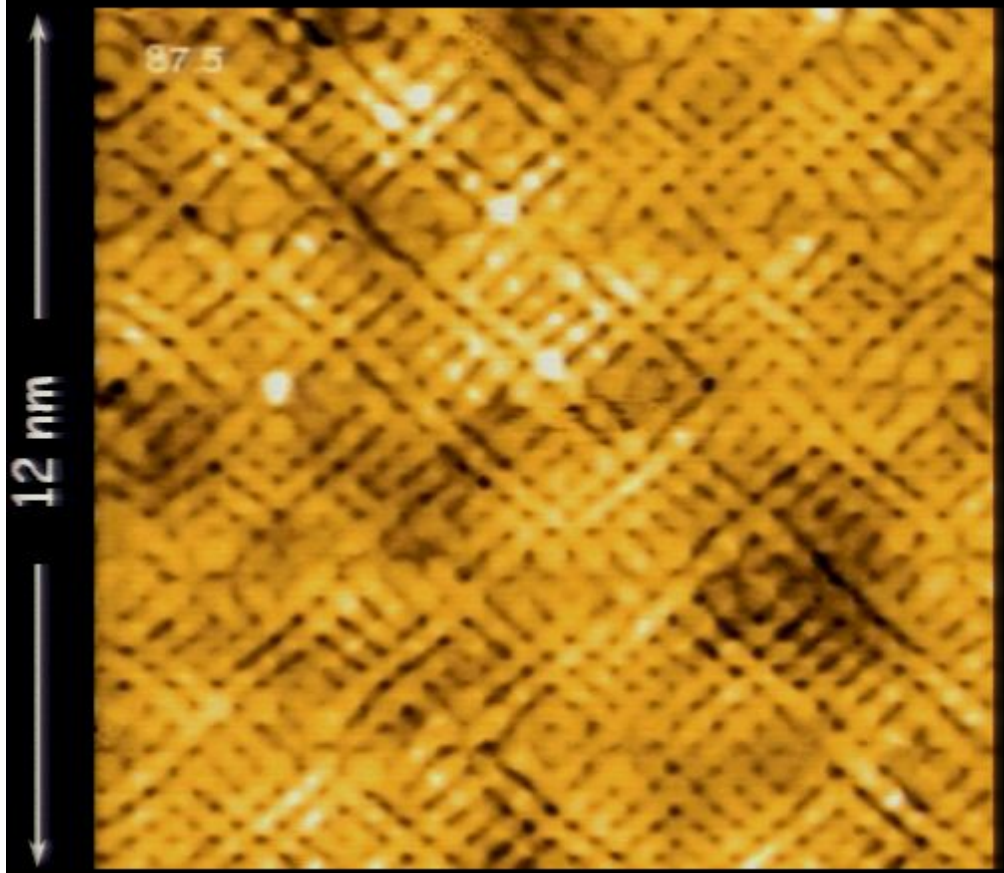

$Z(\vec{r},V)$

0.5 — 1.9

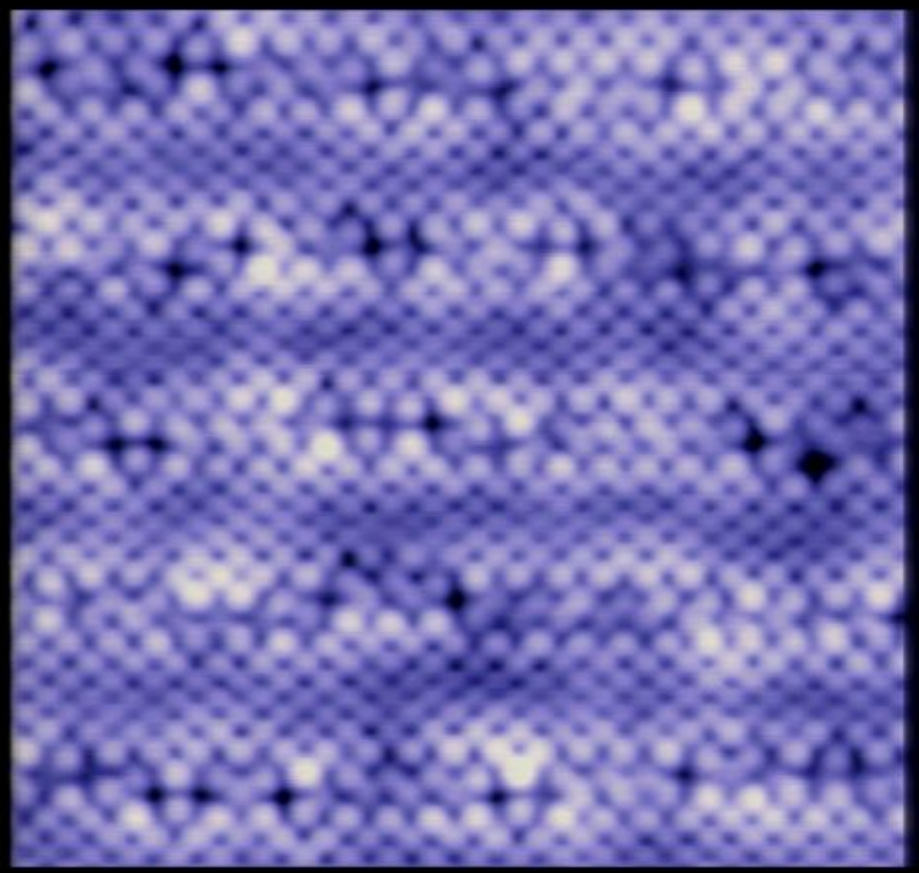

$Bi_{2.2}Sr_{1.8}(Ca,Dy)Cu_2O_y$

Cuprate electronic structure: two characteristic energy scales

Science 313, 1380 (2007); Nature 454, 1072, (2008), Nature 466, 374 (2010)

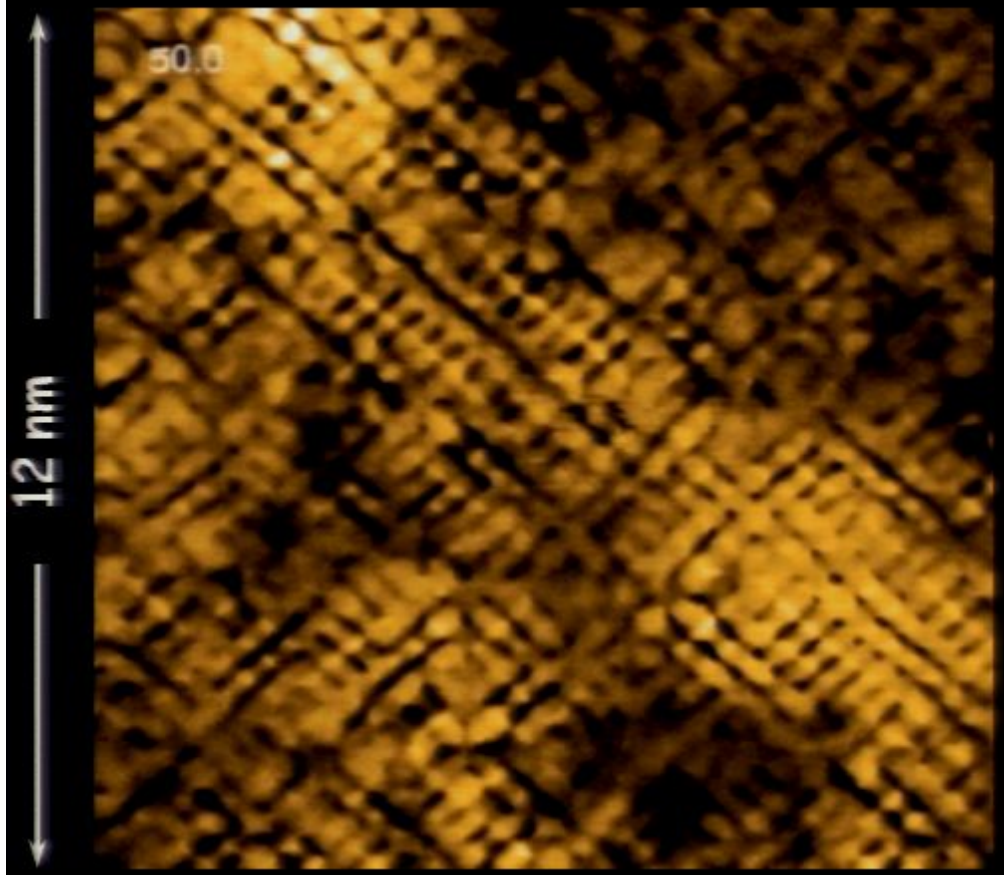

$Z(\vec{r},V)$

0.5 — 1.9

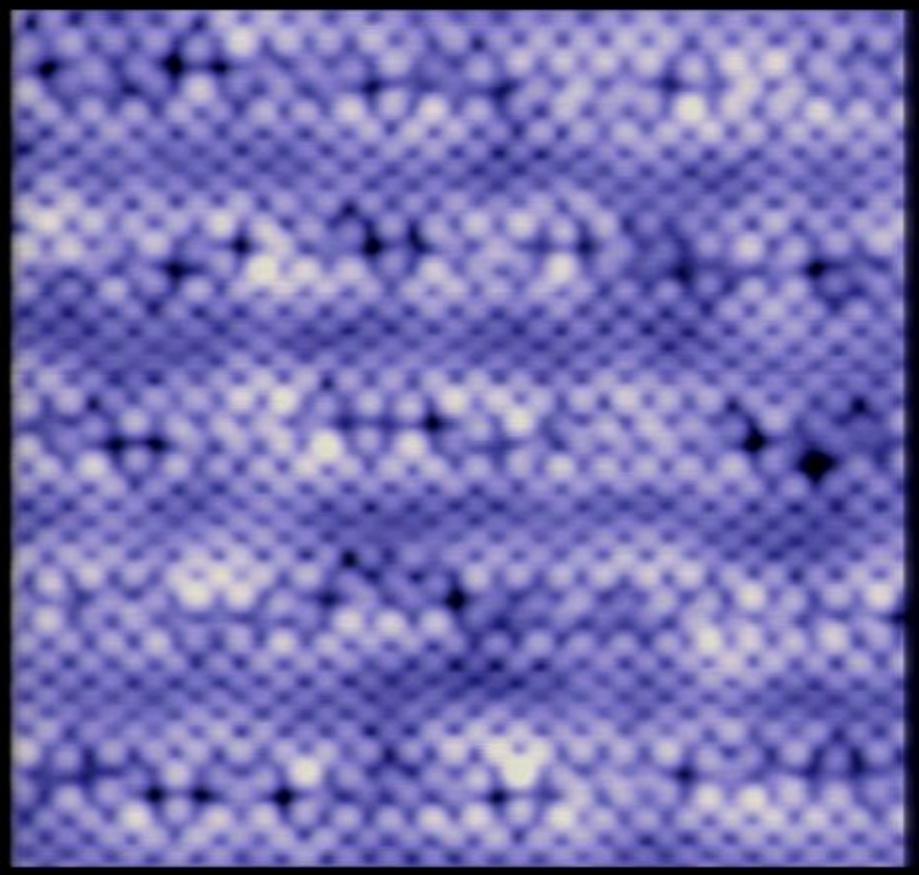

$Bi_{2.2}Sr_{1.8}(Ca,Dy)Cu_2O_y$

Cuprate electronic structure: two characteristic energy scales

Science 313, 1380 (2007); Nature 454, 1072, (2008), Nature 466, 374 (2010)

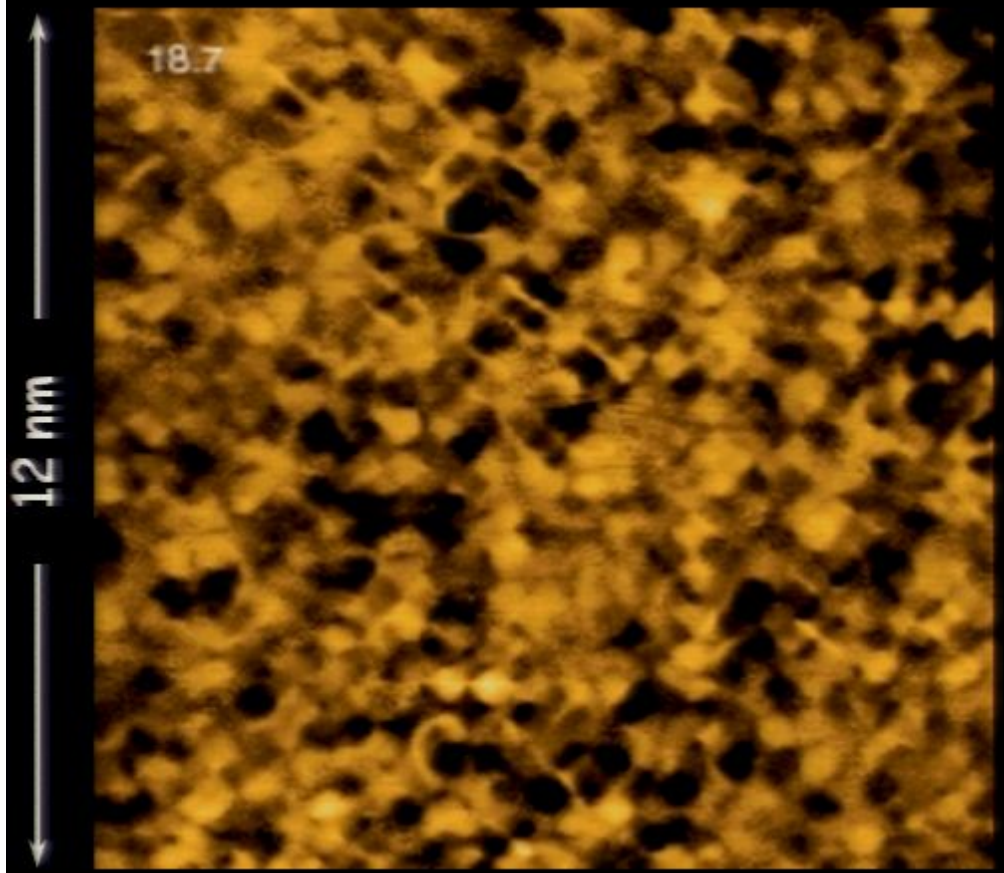

$Z(\vec{r},V)$

0.5 — 1.9

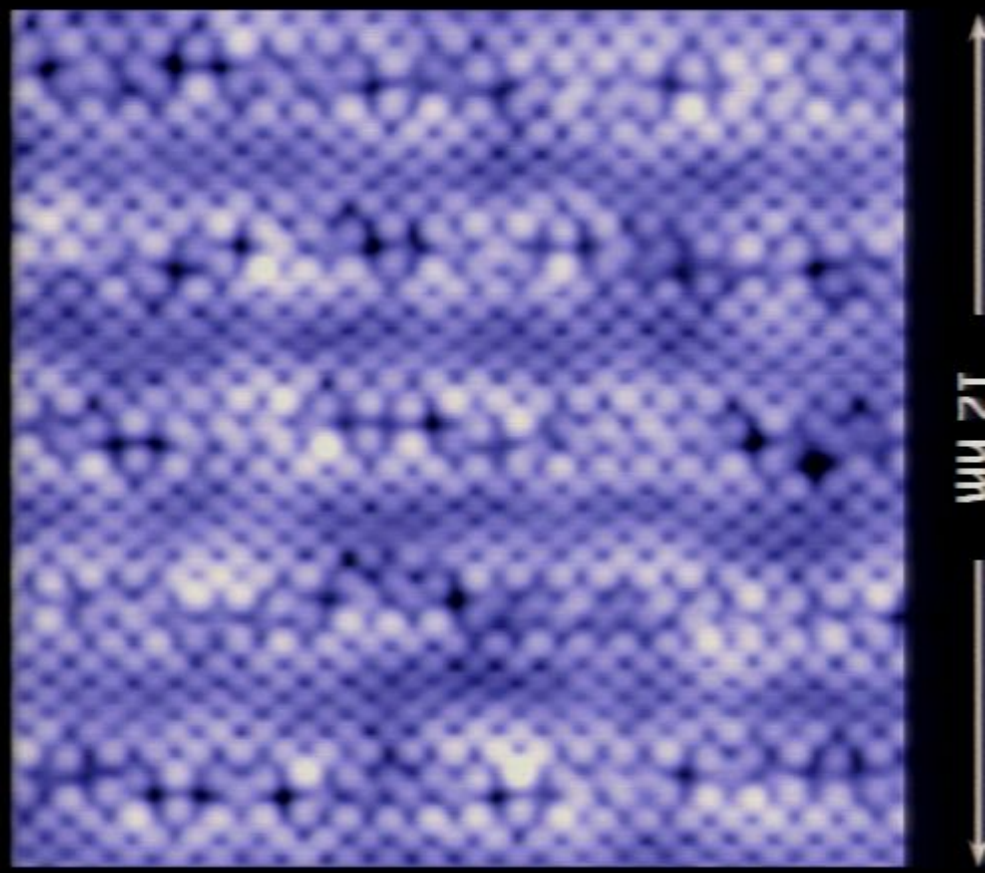

$Bi_{2.2}Sr_{1.8}(Ca,Dy)Cu_2O_y$

Cuprate electronic structure: two characteristic energy scales

Science 313, 1380 (2007); Nature 454, 1072, (2008), Nature 466, 374 (2010)

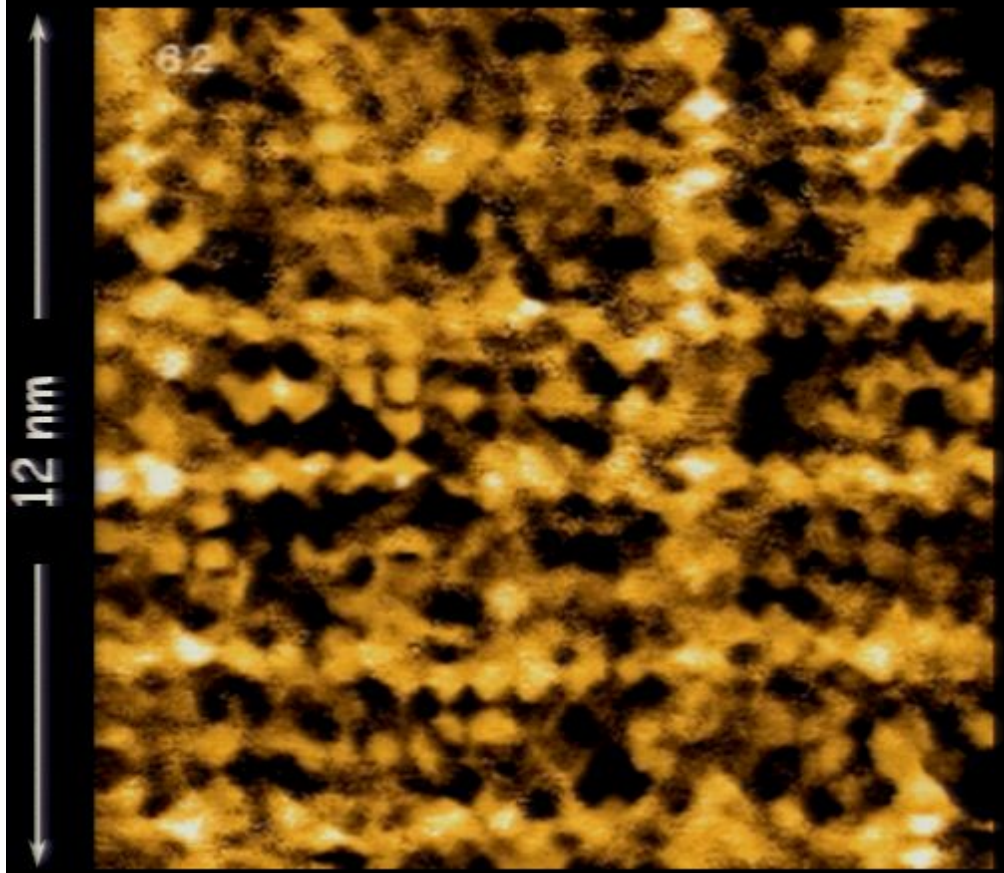

$Z(\vec{r},V)$

0.5 1.9

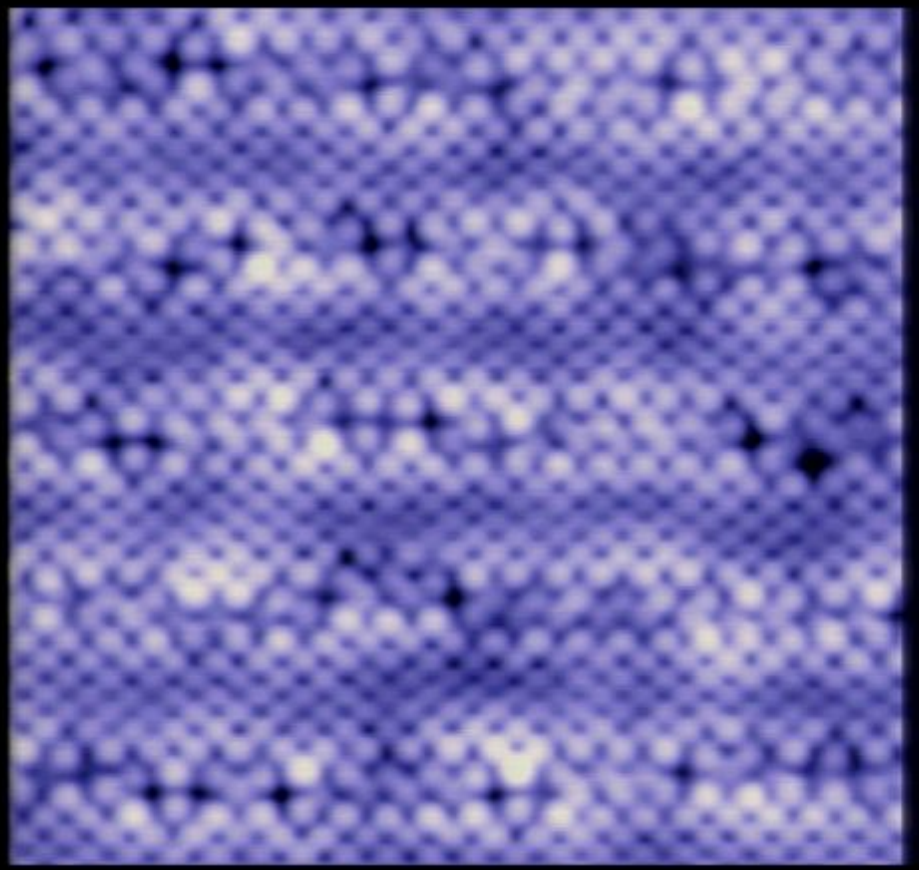

$Bi_{2.2}Sr_{1.8}(Ca,Dy)Cu_2O_y$

Cuprate electronic structure: two characteristic energy scales

Science 313, 1380 (2007); Nature 454, 1072, (2008), Nature 466, 374 (2010)

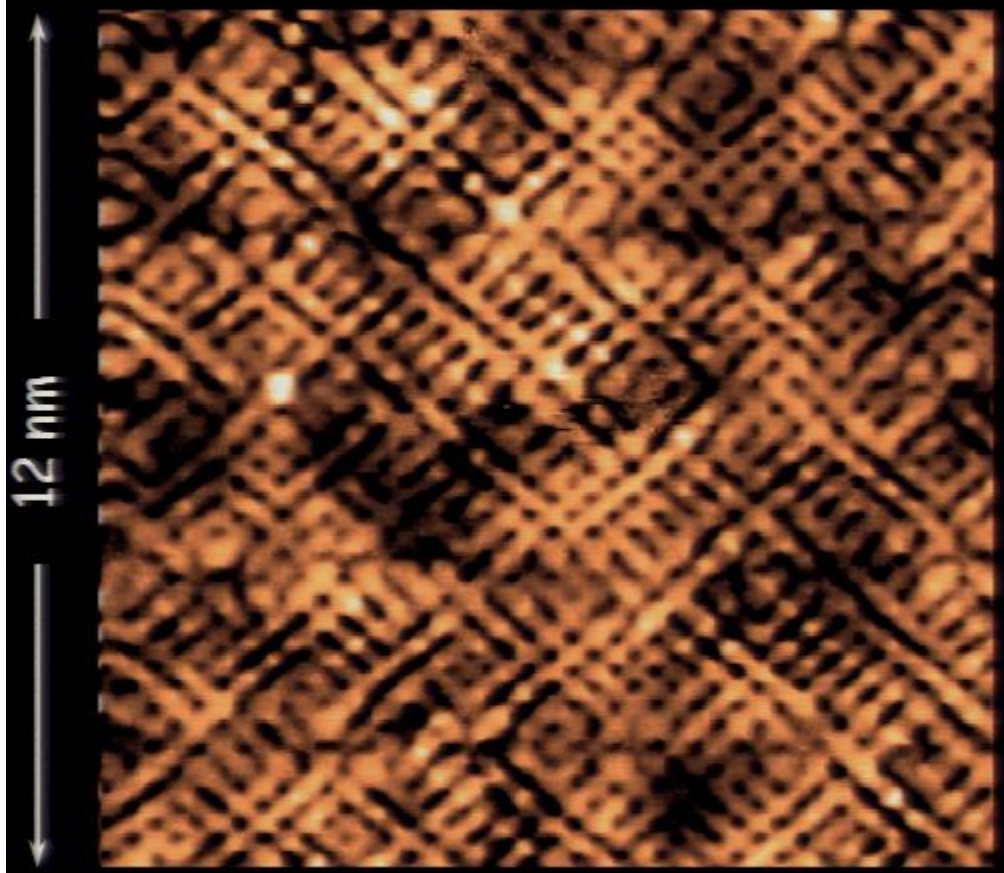

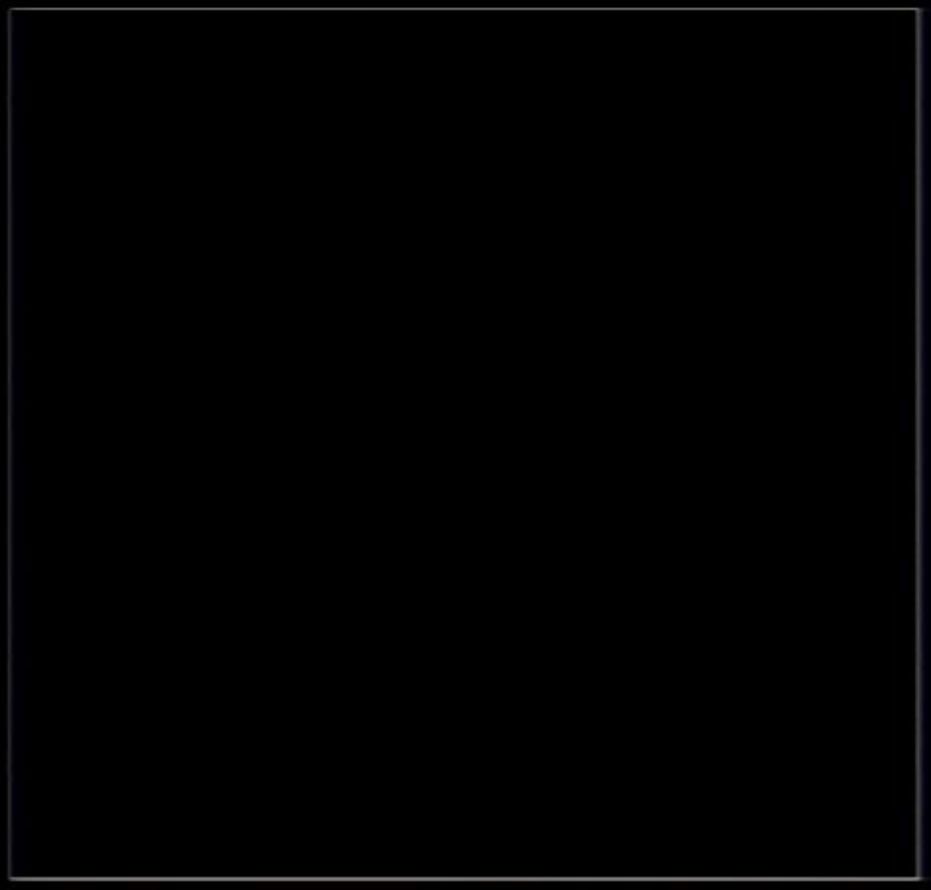

Cuprate electronic structure: two characteristic energy scales

Science 313, 1380 (2007); Nature 454, 1072, (2008), Nature 466, 374 (2010)

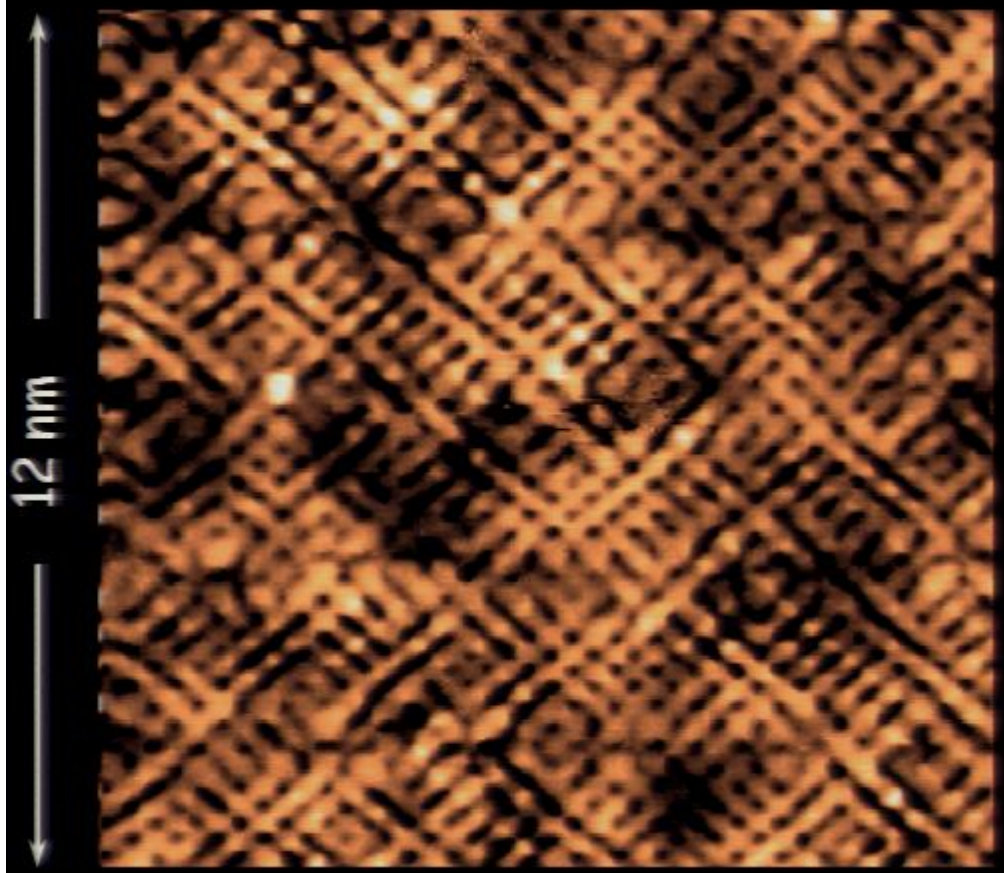

$Z(\vec{r},V)$

0.5 — 1.9

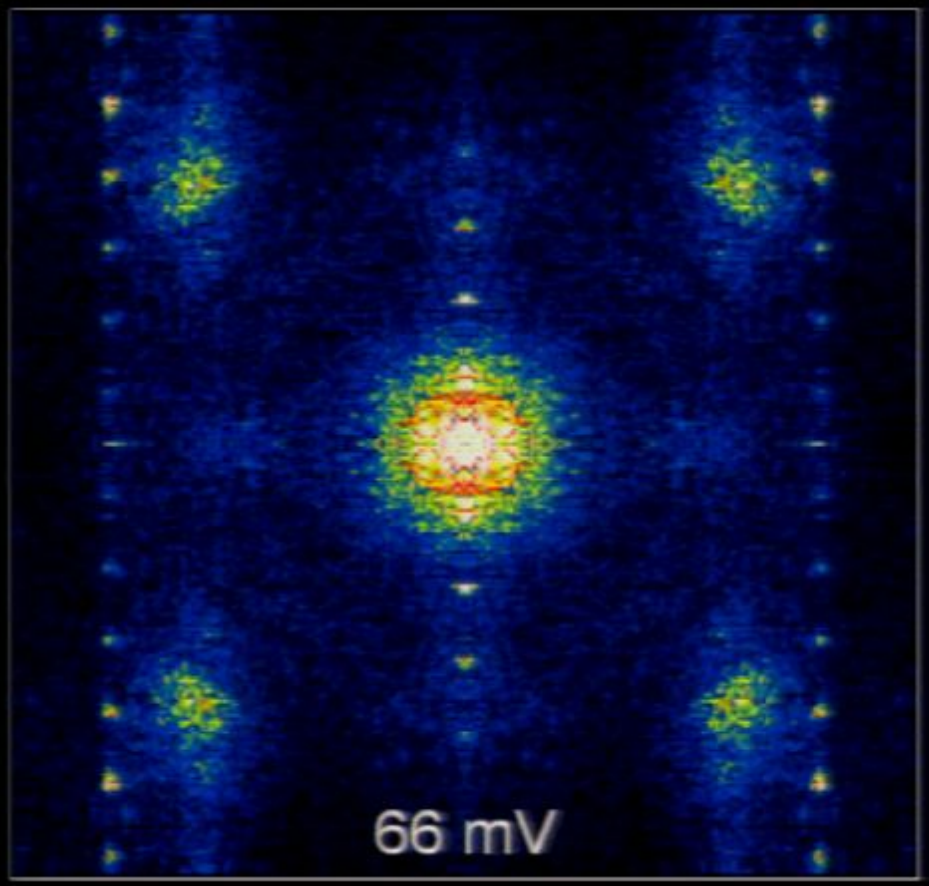

$Z(\vec{q},V)$

Which symmetries do $E<\Delta_0$ states exhibit?

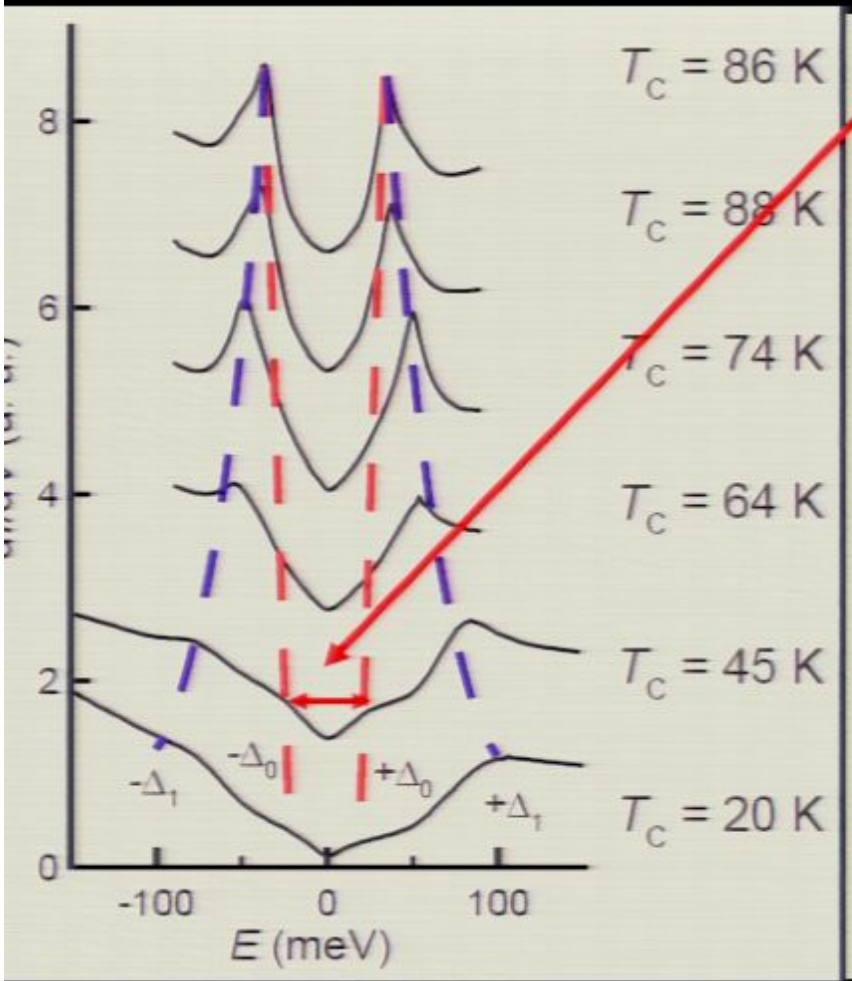

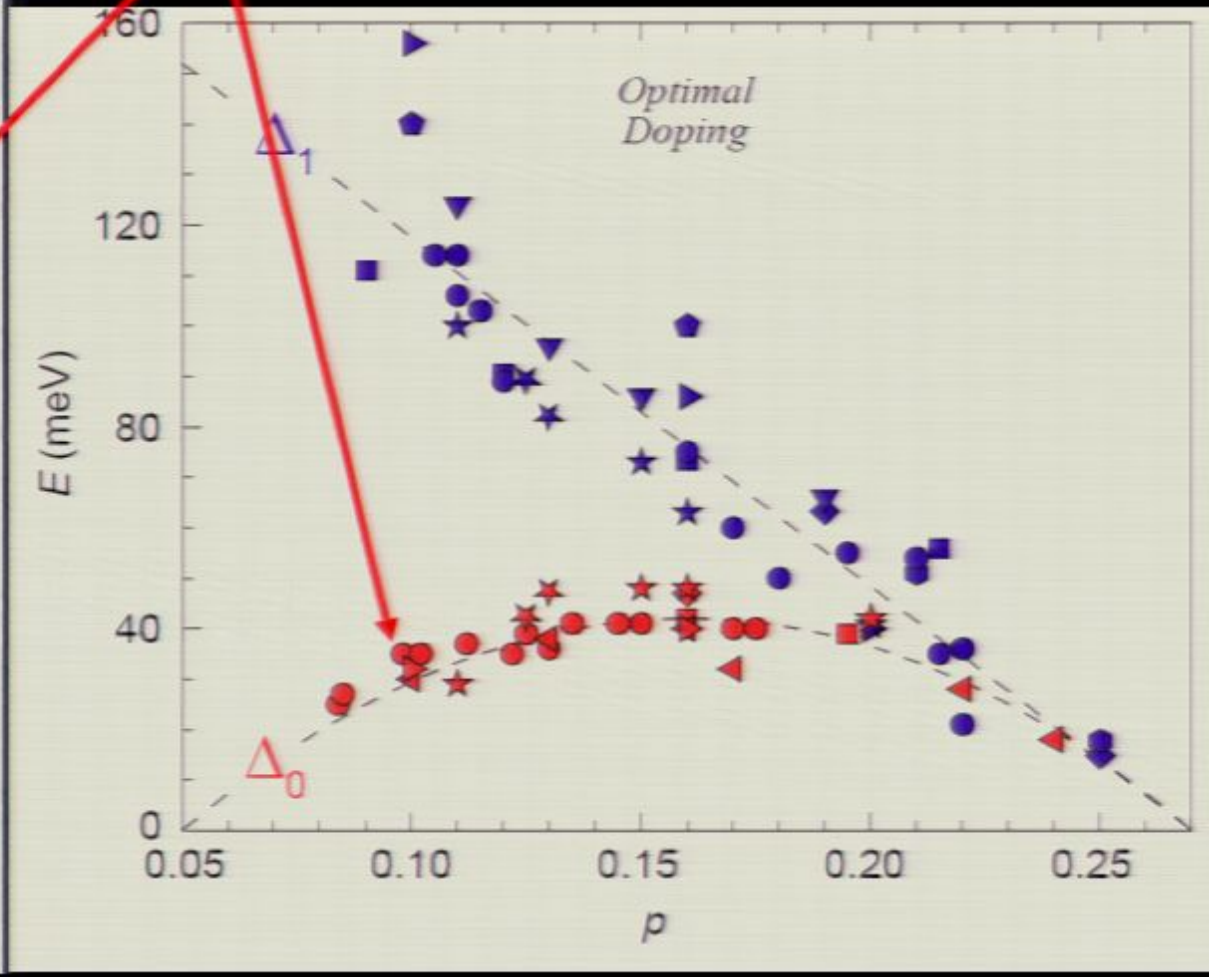

QPI Signature of dSC Cooper Pairing

$E_{node} = E_F$

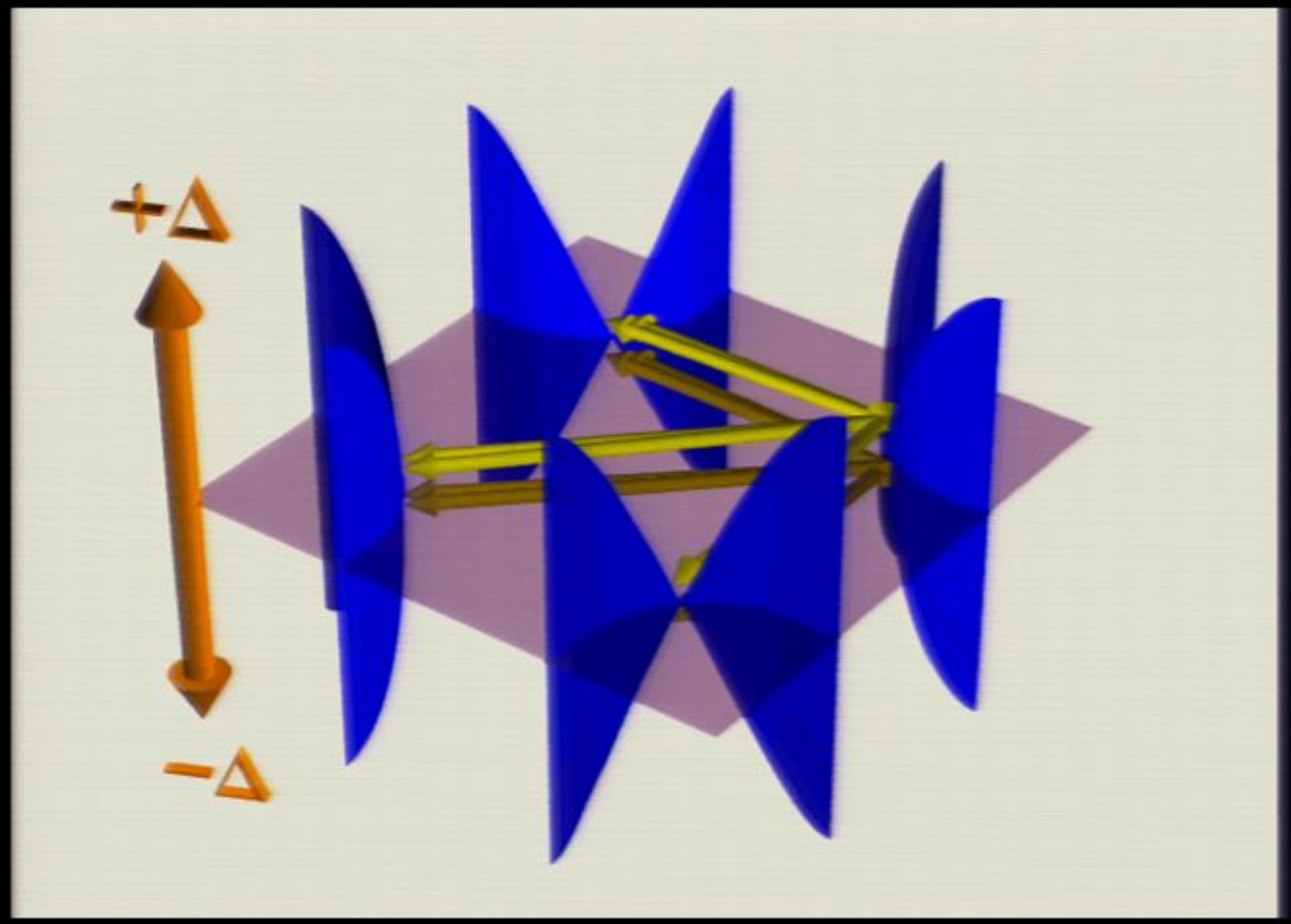

Scattering interference: particle-hole symmetric $q_i(\pm E)$ i=1,..7

Q. Wang & D.-H. Lee, ***Phys. Rev. B 67***, 020511 (2003).
L. Capriotti, D. J. Scalapino, R. D. Sedgewick, *Phys. Rev. B* **68**, 014508 (2003).

QPI Signature of dSC Cooper Pairing

$E_{node} = E_F$

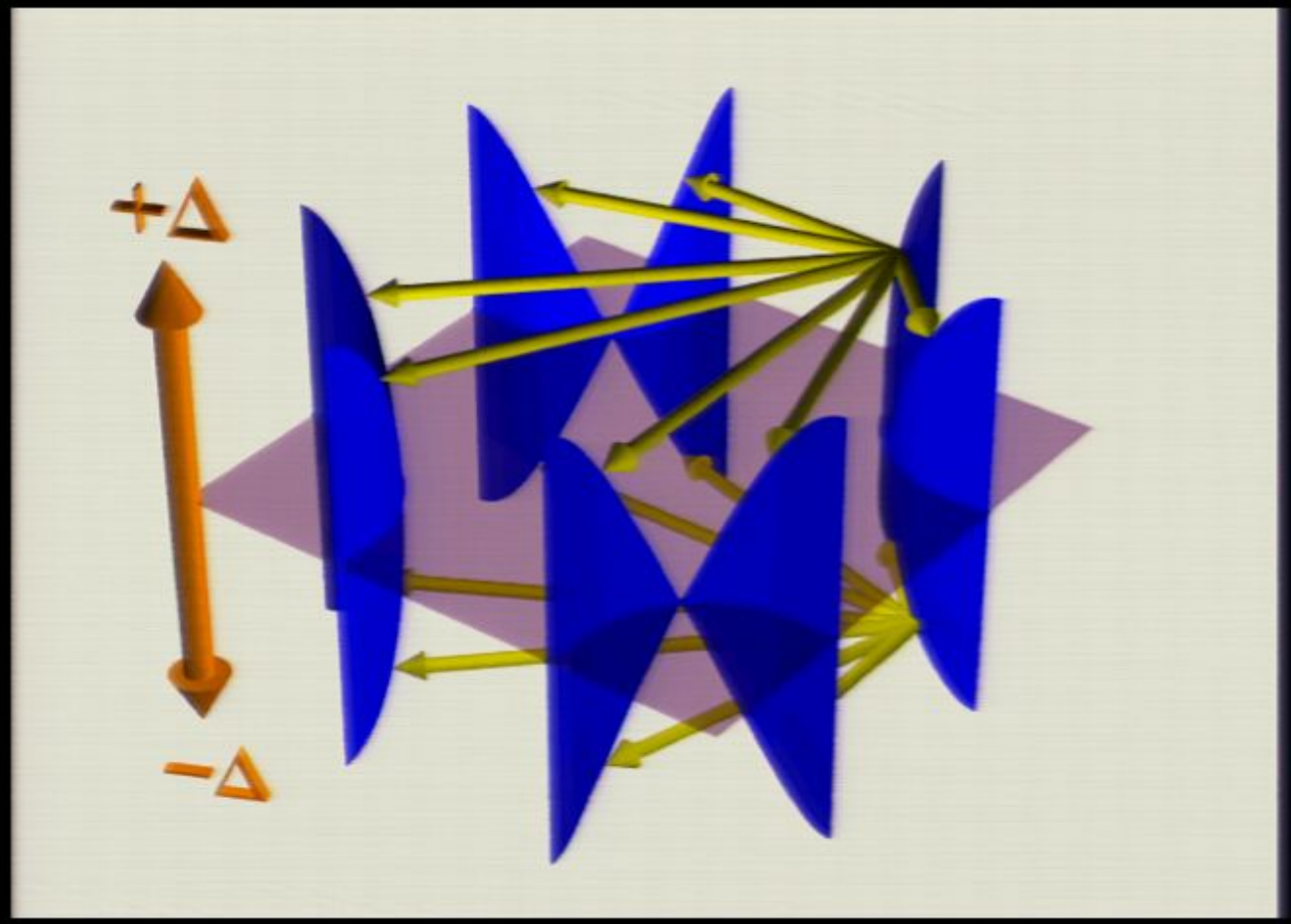

Scattering interference: particle-hole symmetric $q_i(\pm E)$ i=1,..7

Q. Wang & D.-H. Lee, ***Phys. Rev. B 67***, 020511 (2003).
L. Capriotti, D. J. Scalapino, R. D. Sedgewick, *Phys. Rev. B* **68**, 014508 (2003).

QPI Signature of dSC Cooper Pairing

$E_{node} = E_F$

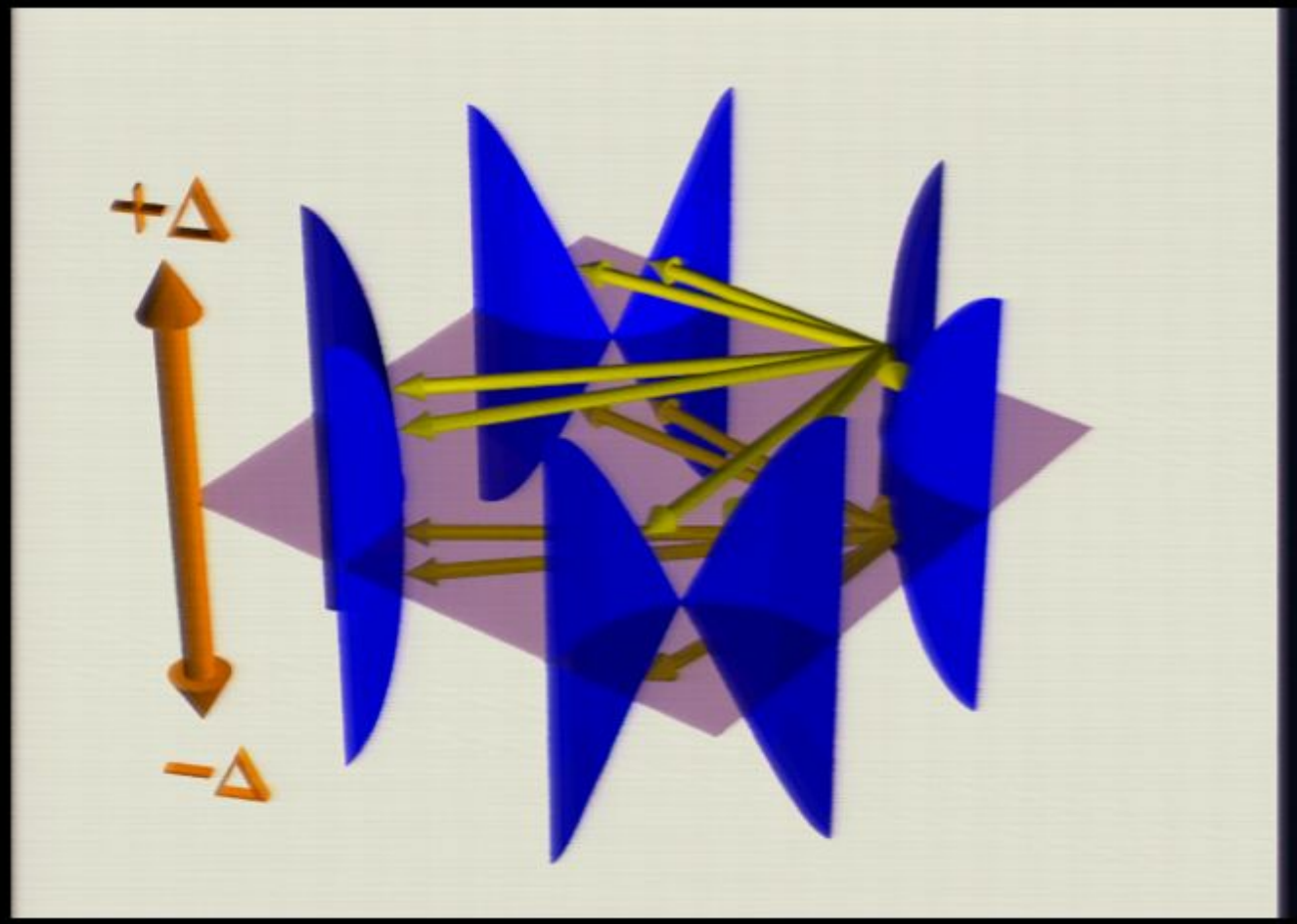

Scattering interference: particle-hole symmetric $q_i(\pm E)$ i=1,..7

Q. Wang & D.-H. Lee, ***Phys. Rev. B 67***, 020511 (2003).
L. Capriotti, D. J. Scalapino, R. D. Sedgewick, *Phys. Rev. B* **68**, 014508 (2003).

QPI Signature of dSC Cooper Pairing

$E_{node} = E_F$

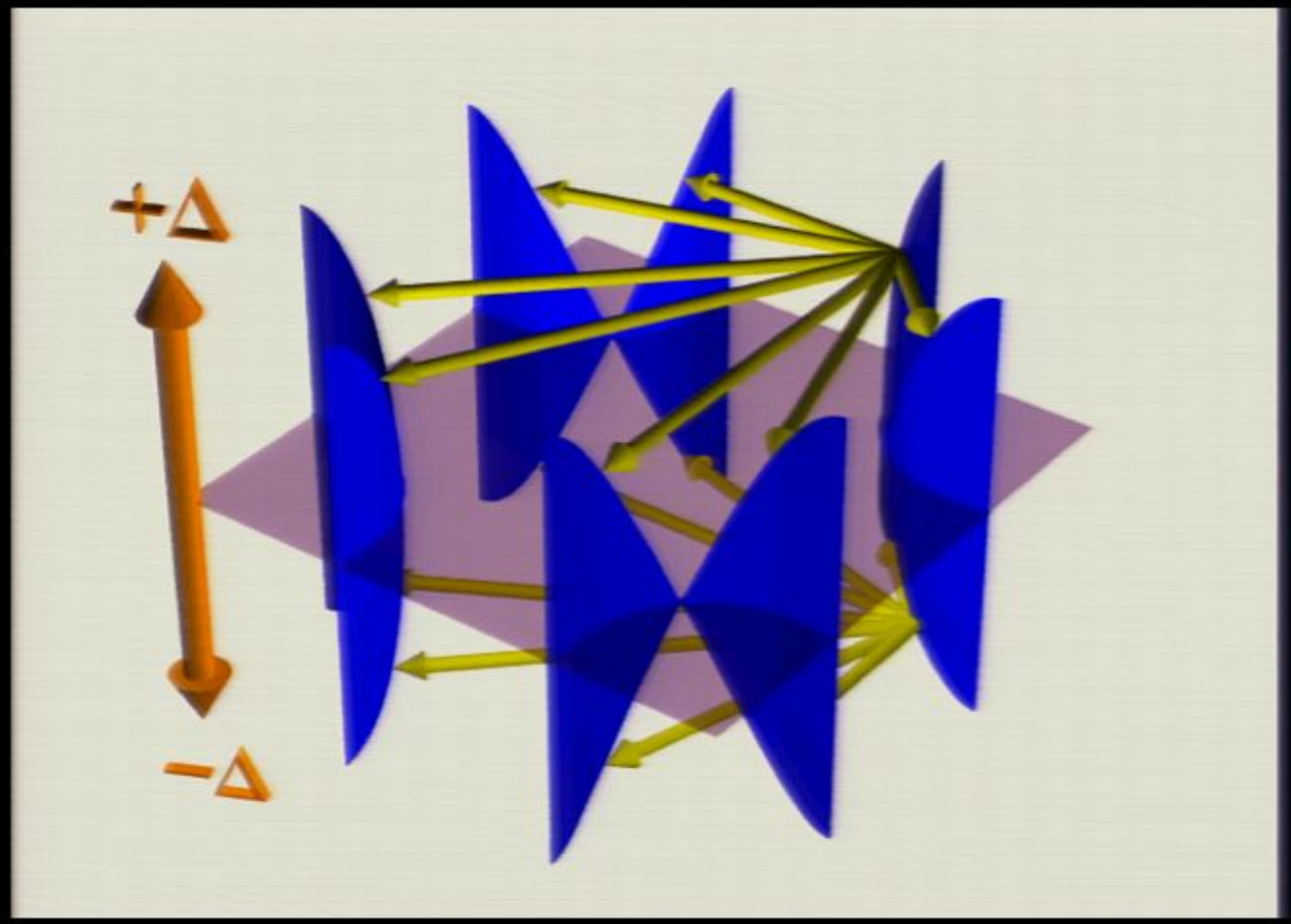

Scattering interference: particle-hole symmetric $q_i(\pm E)$ i=1,..7

Q. Wang & D.-H. Lee, ***Phys. Rev. B 67***, 020511 (2003).
L. Capriotti, D. J. Scalapino, R. D. Sedgewick, *Phys. Rev. B* **68**, 014508 (2003).

QPI Signature of dSC Cooper Pairing

$E_{node} = E_F$

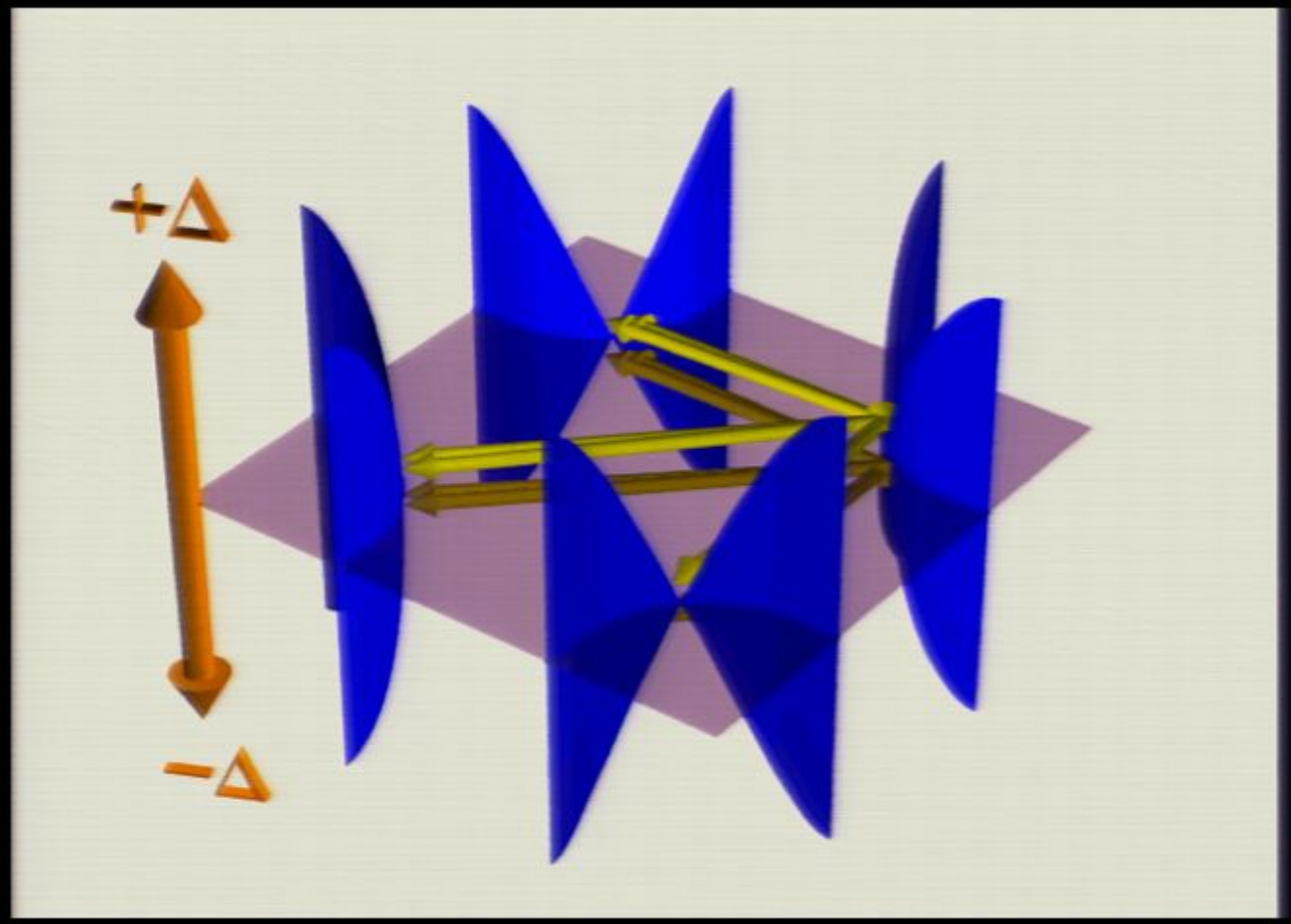

Scattering interference: particle-hole symmetric $q_i(\pm E)$ i=1,..7

Q. Wang & D.-H. Lee, ***Phys. Rev. B 67***, 020511 (2003).
L. Capriotti, D. J. Scalapino, R. D. Sedgewick, *Phys. Rev. B* **68**, 014508 (2003).

QPI Signature of dSC Cooper Pairing

$E_{node} = E_F$

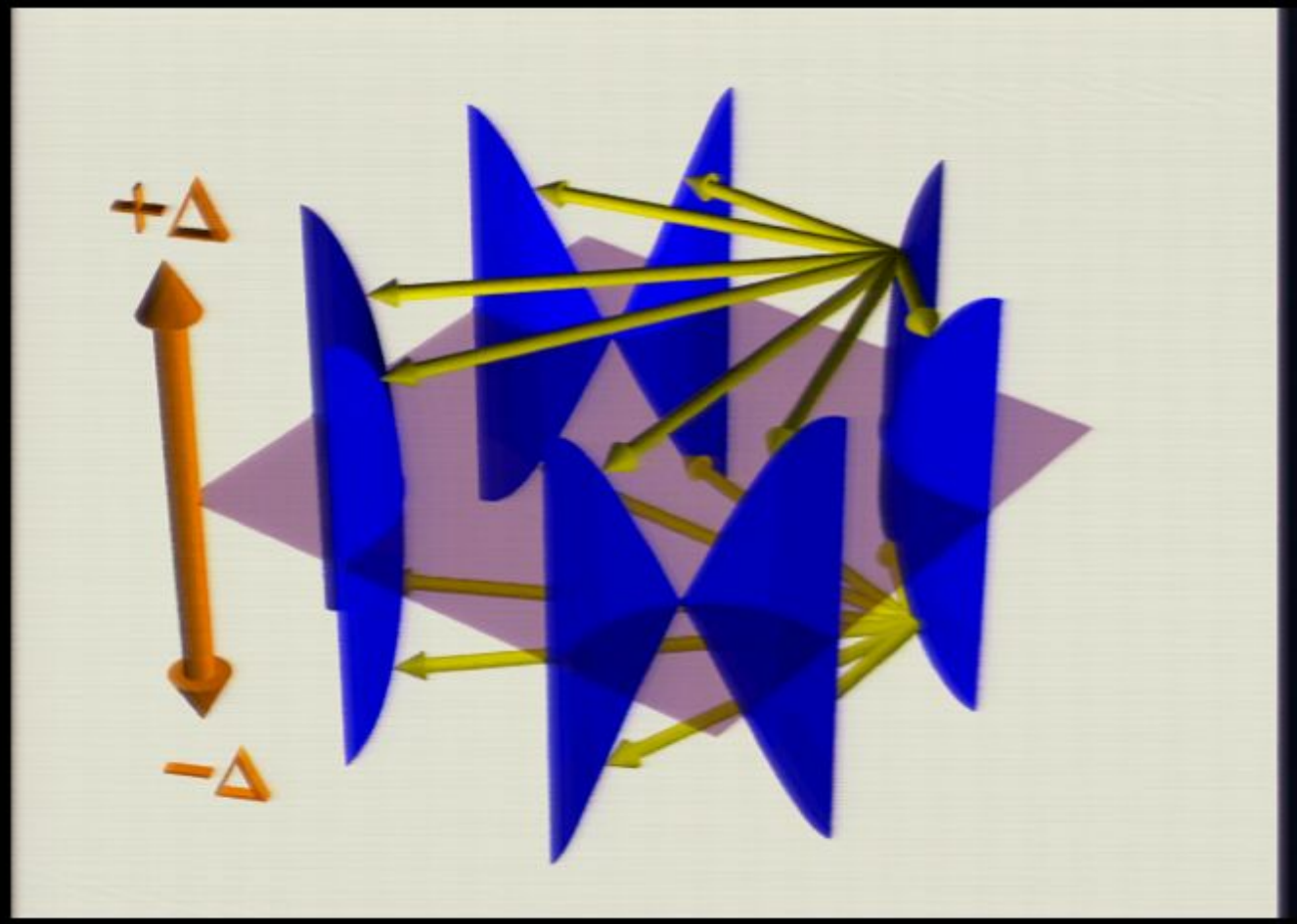

Scattering interference: particle-hole symmetric $q_i(\pm E)$ i=1,..7

Q. Wang & D.-H. Lee, ***Phys. Rev. B 67***, 020511 (2003).
L. Capriotti, D. J. Scalapino, R. D. Sedgewick, *Phys. Rev. B* **68**, 014508 (2003).

QPI Signature of dSC Cooper Pairing

$E_{node} = E_F$

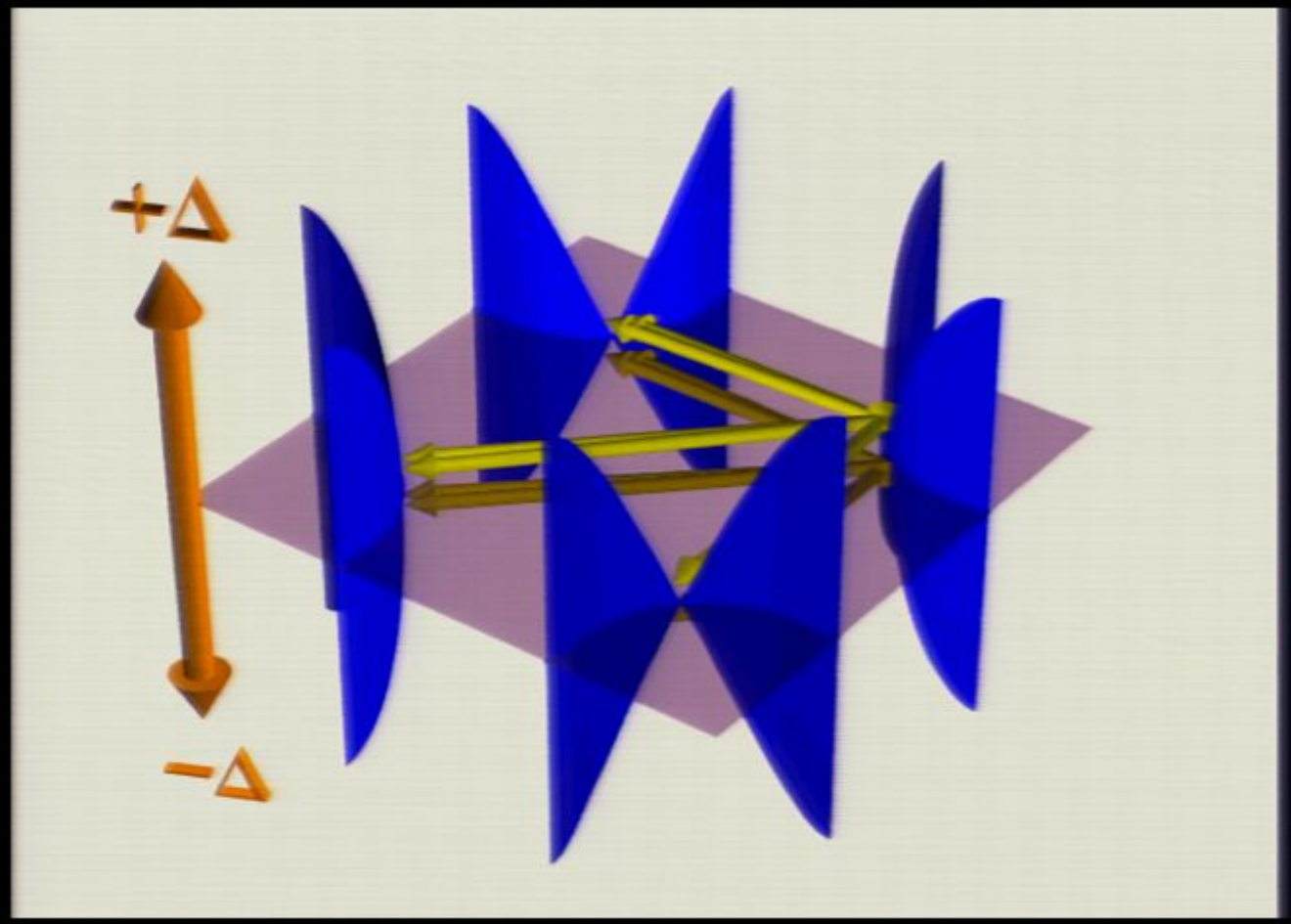

Scattering interference: particle-hole symmetric $q_i(\pm E)$ i=1,..7

Q. Wang & D.-H. Lee, ***Phys. Rev. B 67***, 020511 (2003).
L. Capriotti, D. J. Scalapino, R. D. Sedgewick, *Phys. Rev. B* **68**, 014508 (2003).

QPI Signature of dSC Cooper Pairing

$E_{node} = E_F$

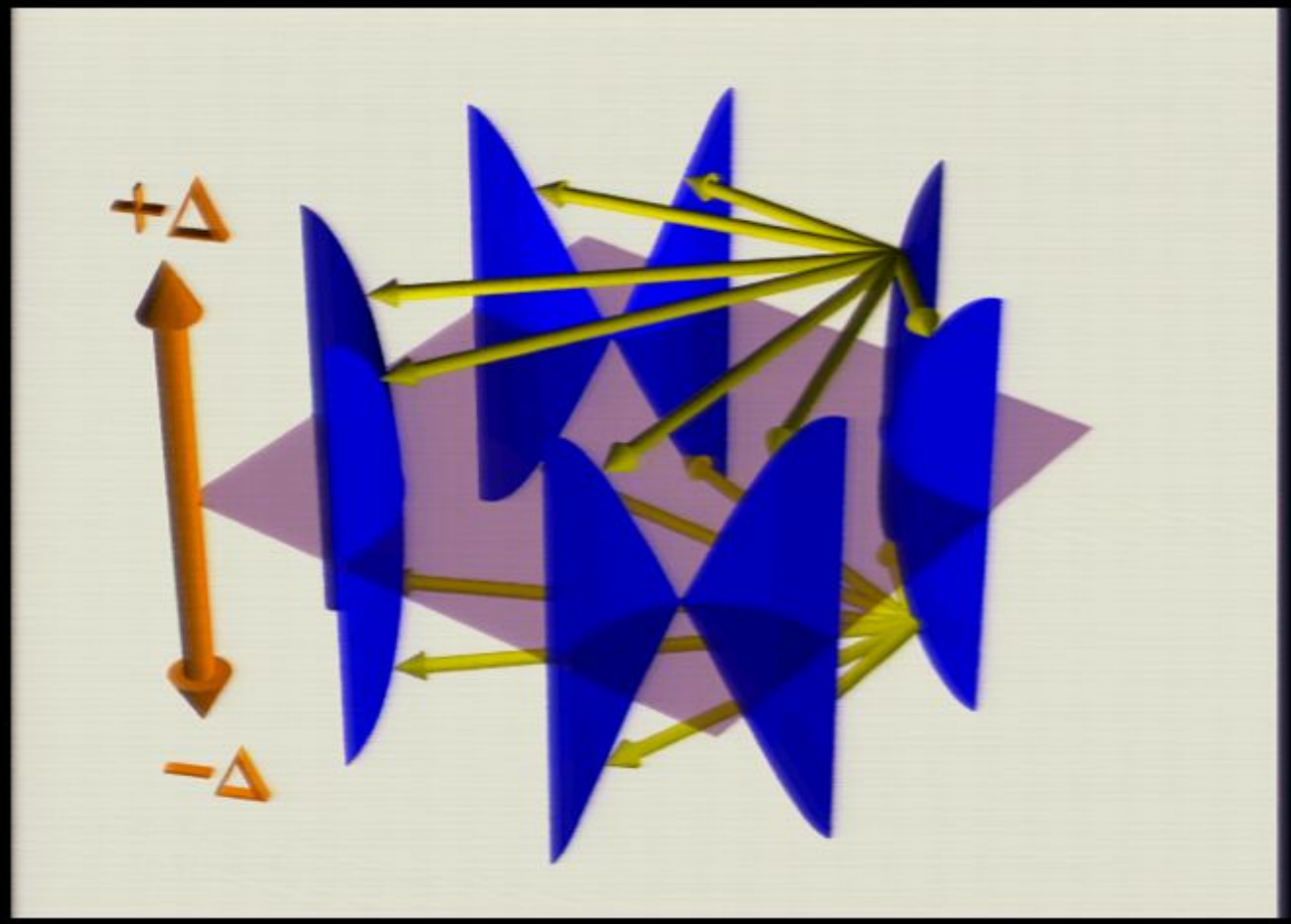

Scattering interference: particle-hole symmetric $q_i(\pm E)$ i=1,..7

Q. Wang & D.-H. Lee, ***Phys. Rev. B 67***, 020511 (2003).
L. Capriotti, D. J. Scalapino, R. D. Sedgewick, *Phys. Rev. B* **68**, 014508 (2003).

QPI Signature of dSC Cooper Pairing

$E_{node} = E_F$

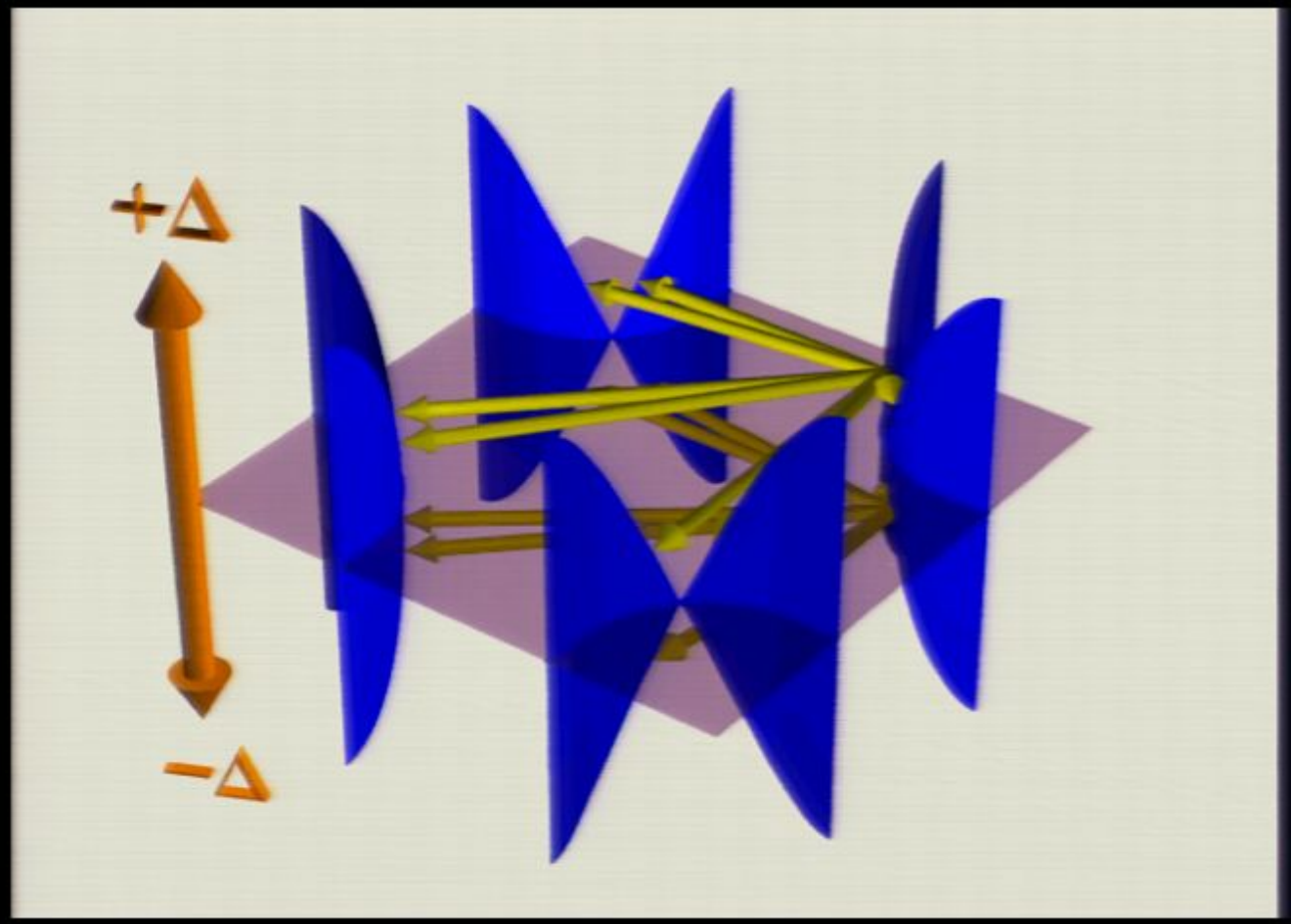

Scattering interference: particle-hole symmetric $q_i(\pm E)$ i=1,..7

Q. Wang & D.-H. Lee, ***Phys. Rev. B 67***, 020511 (2003).
L. Capriotti, D. J. Scalapino, R. D. Sedgewick, *Phys. Rev. B* **68**, 014508 (2003).

QPI Signature of dSC Cooper Pairing

$E_{node} = E_F$

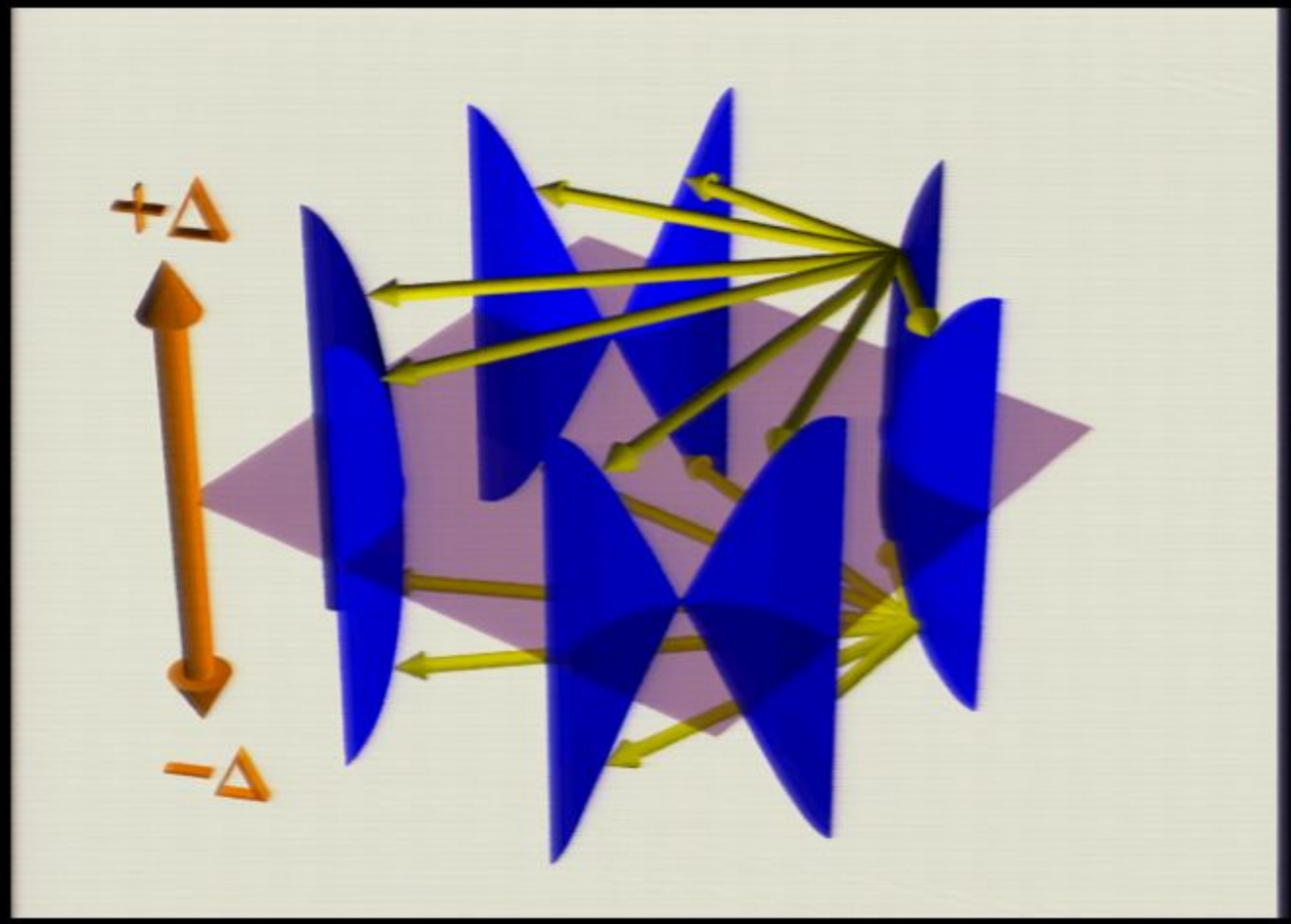

Scattering interference: particle-hole symmetric $q_i(\pm E)$ i=1,..7

Q. Wang & D.-H. Lee, ***Phys. Rev. B 67***, 020511 (2003).
L. Capriotti, D. J. Scalapino, R. D. Sedgewick, *Phys. Rev. B* **68**, 014508 (2003).

QPI Signature of dSC Cooper Pairing

$E_{node} = E_F$

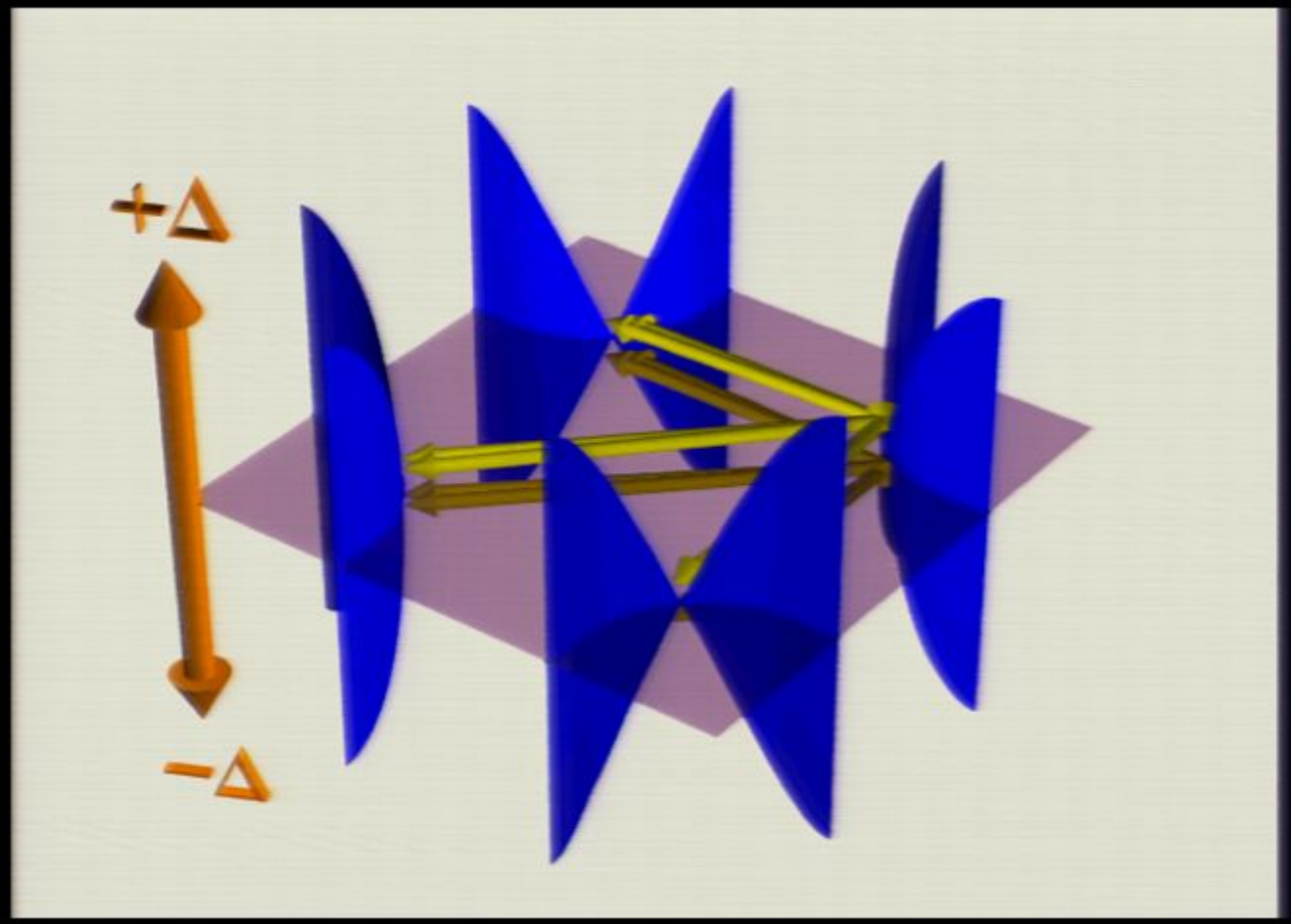

Scattering interference: particle-hole symmetric $q_i(\pm E)$ i=1,..7

Q. Wang & D.-H. Lee, ***Phys. Rev. B 67***, 020511 (2003).
L. Capriotti, D. J. Scalapino, R. D. Sedgewick, *Phys. Rev. B* **68**, 014508 (2003).

QPI Signature of dSC Cooper Pairing

$E_{node} = E_F$

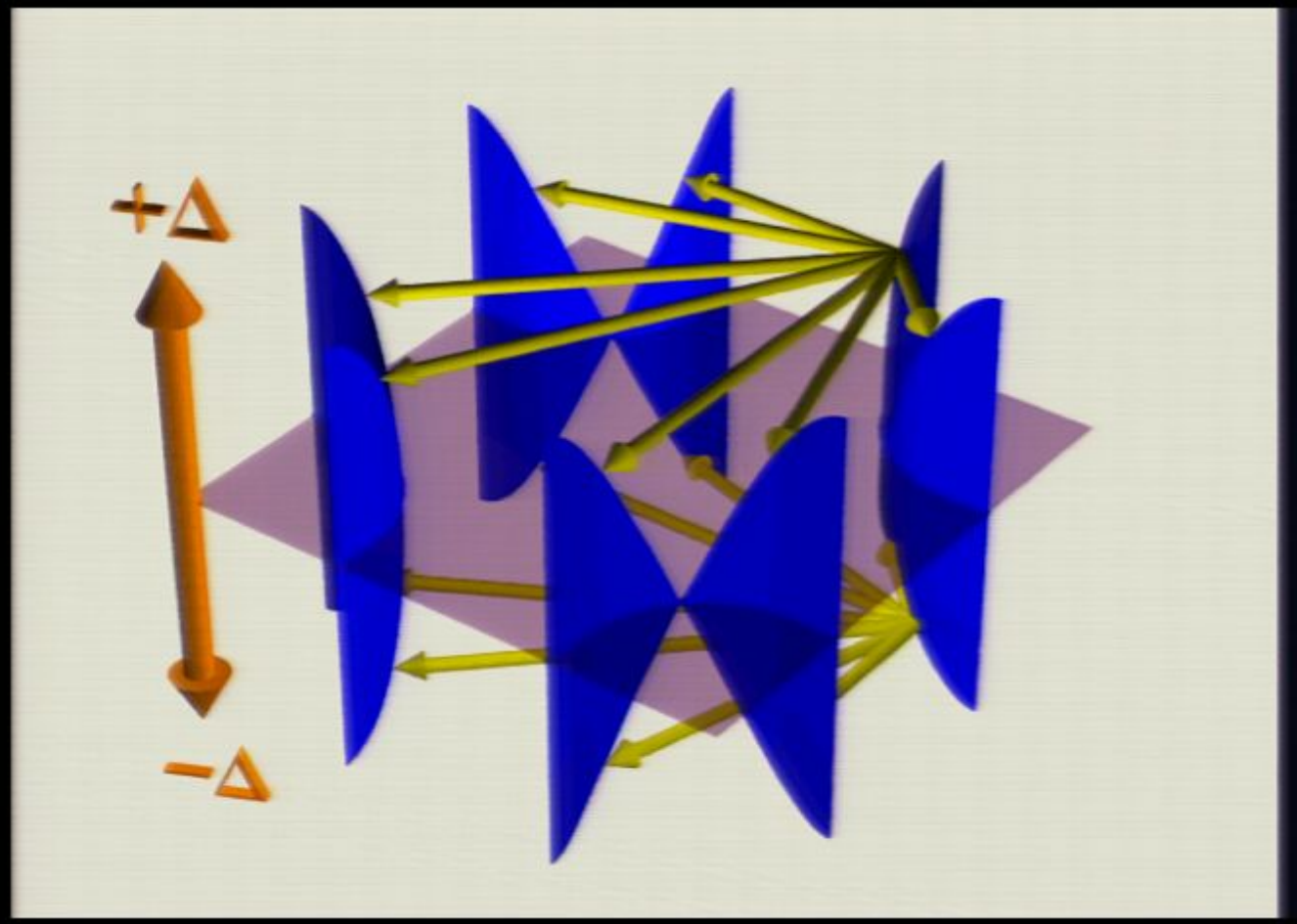

Scattering interference: particle-hole symmetric $q_i(\pm E)$ i=1,..7

Q. Wang & D.-H. Lee, ***Phys. Rev. B 67***, 020511 (2003).
L. Capriotti, D. J. Scalapino, R. D. Sedgewick, *Phys. Rev. B* **68**, 014508 (2003).

QPI signature of dSC Cooper pairing

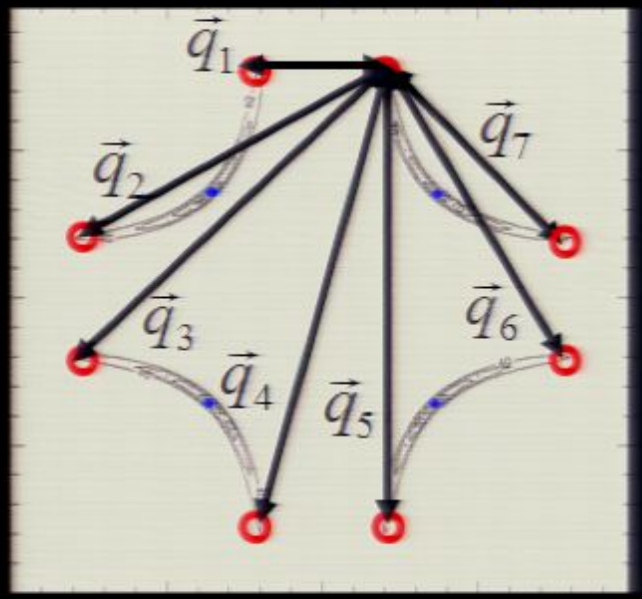

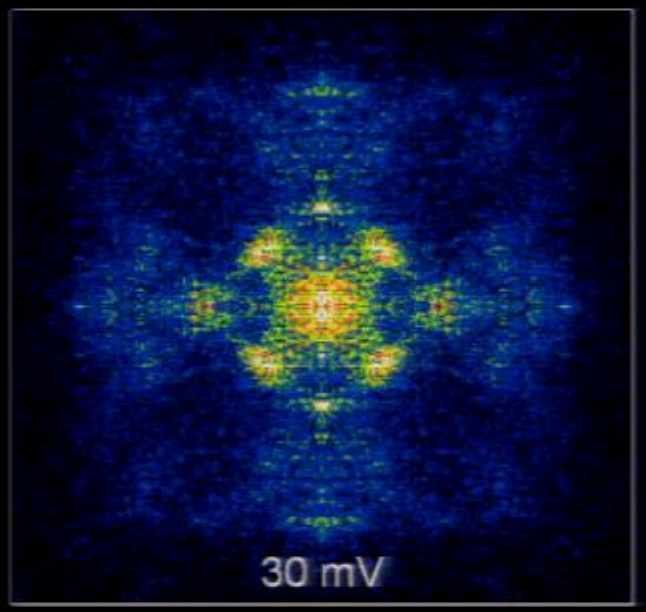

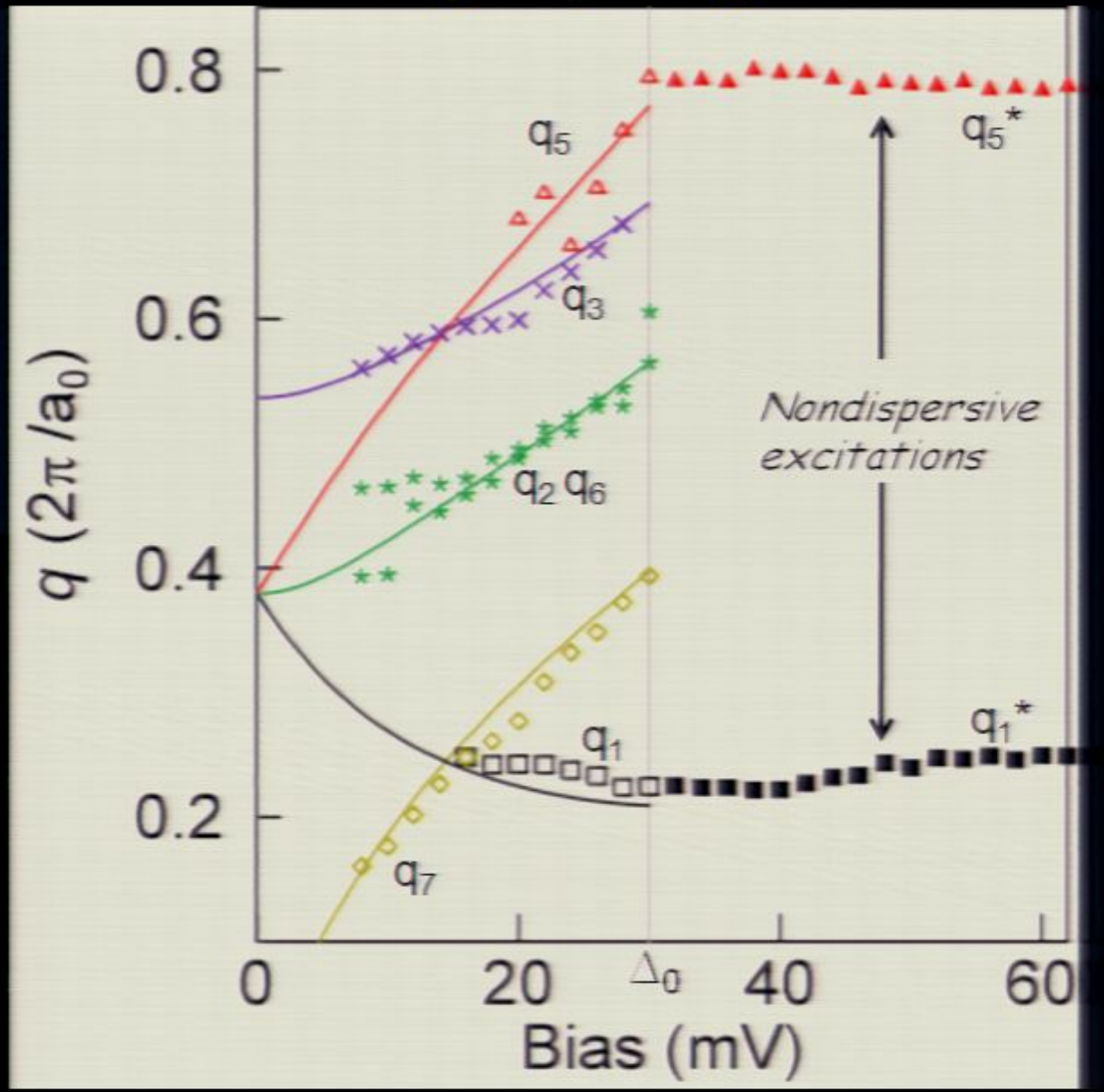

Shrinking arc of homogeneous dSC Cooper pairing as $p \to 0$

Nature 454, 1072, (2008)

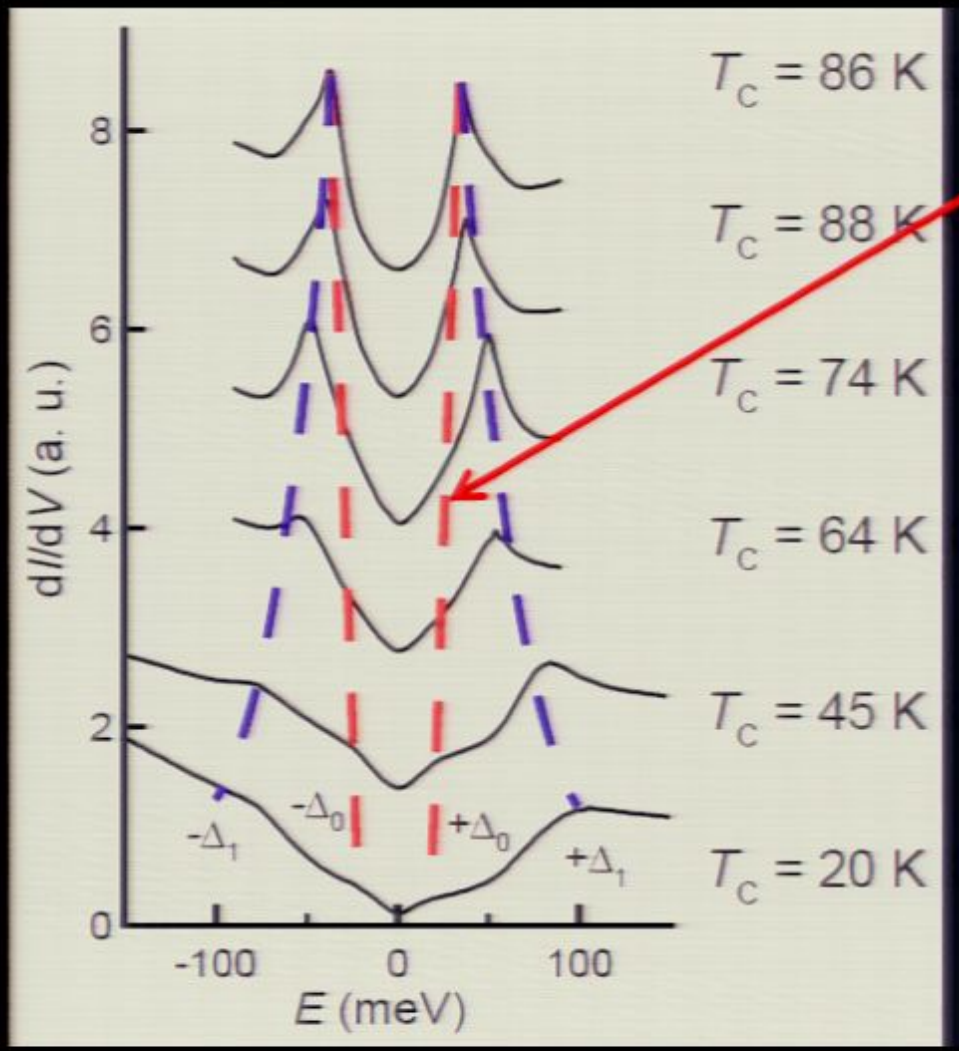

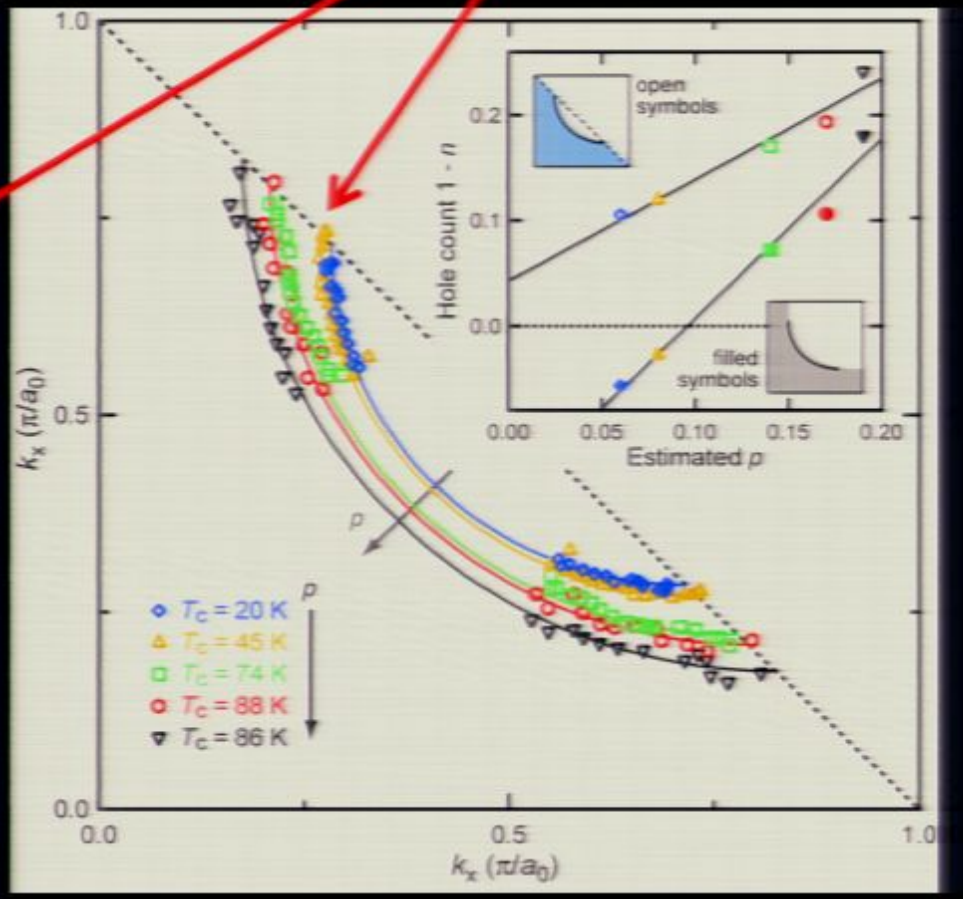

QPI signature of dSC Cooper pairing

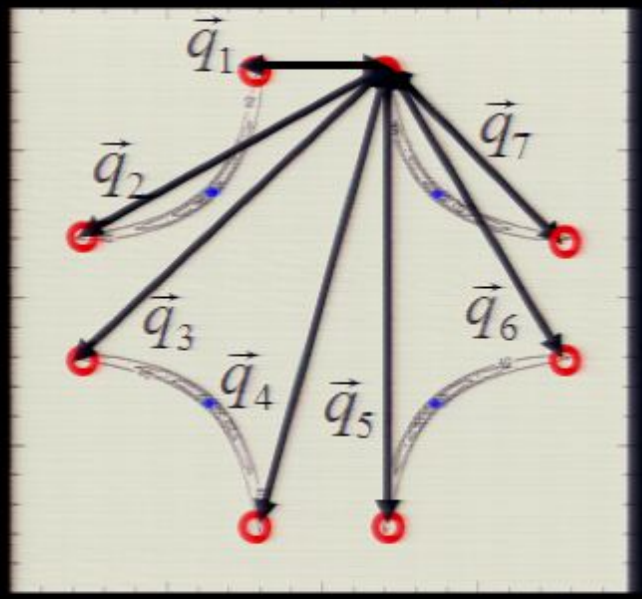

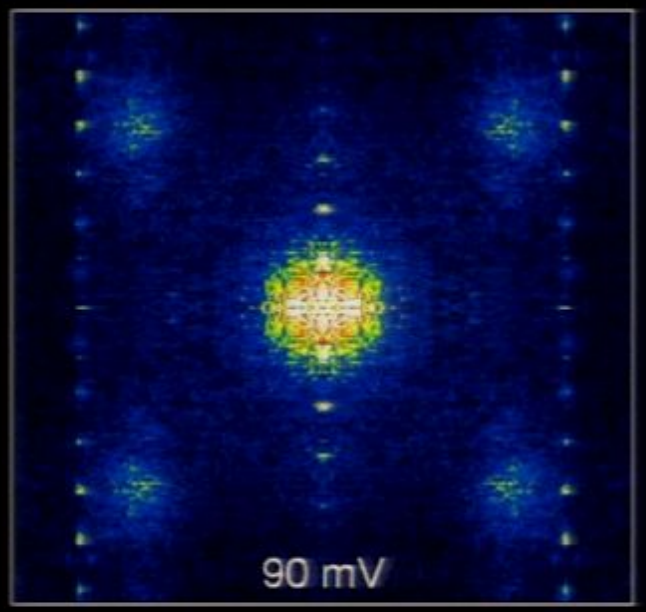

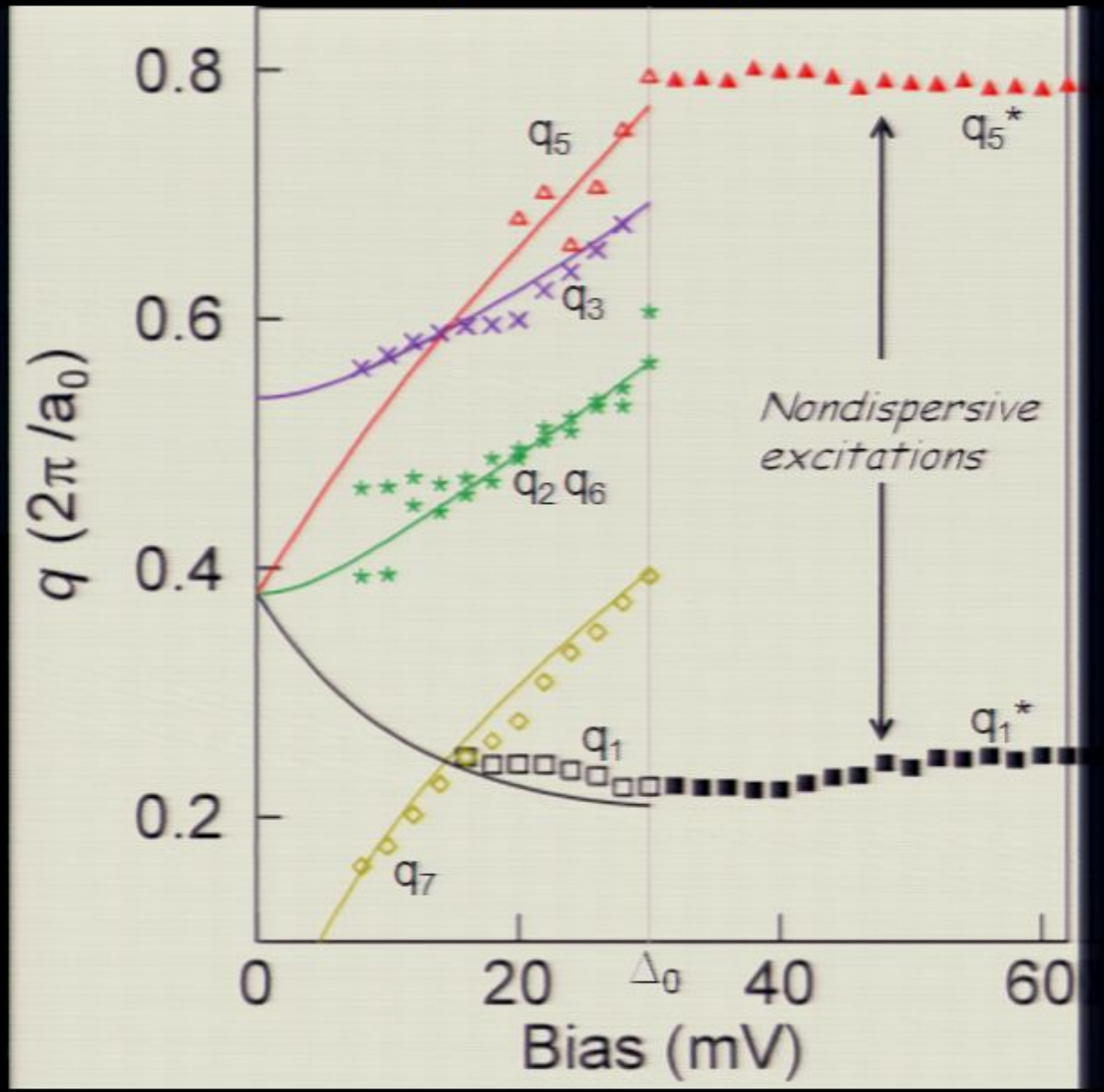

Shrinking arc of homogeneous dSC Cooper pairing as $p \to 0$

Nature 454, 1072, (2008)

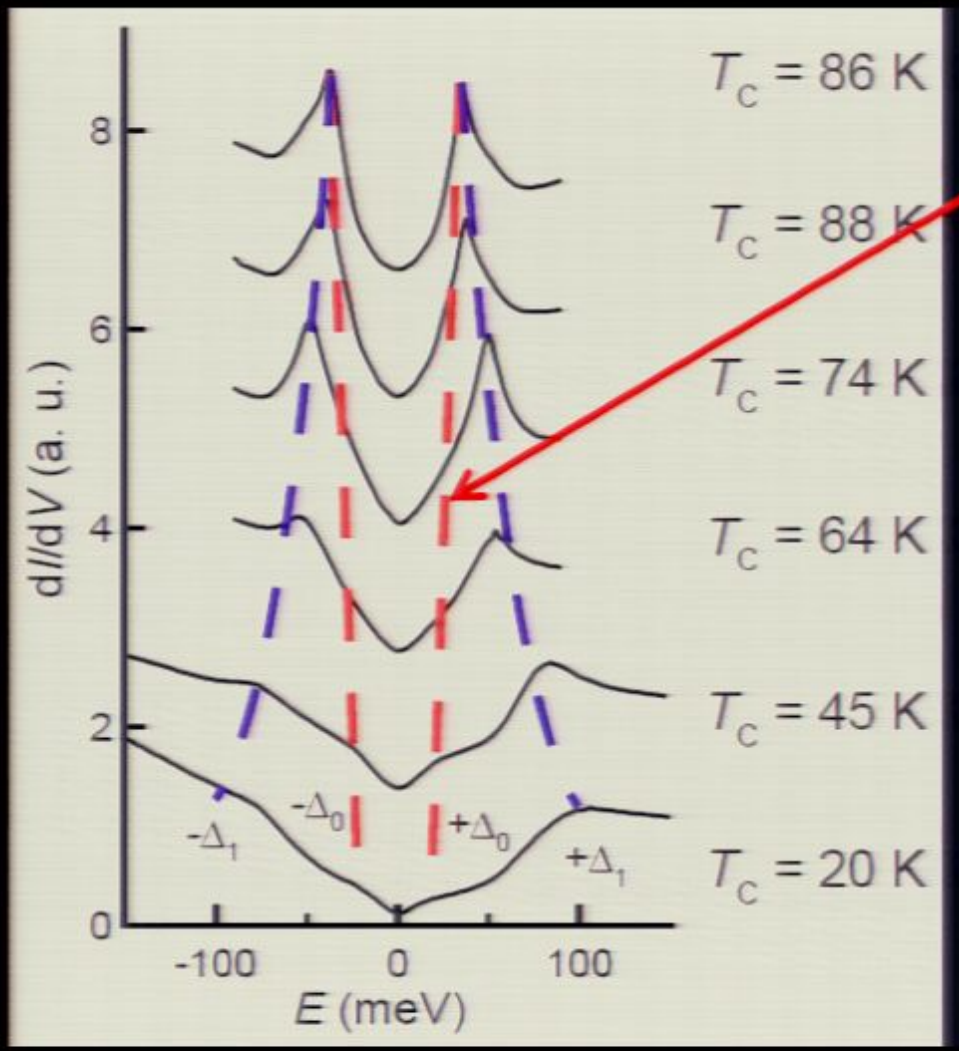

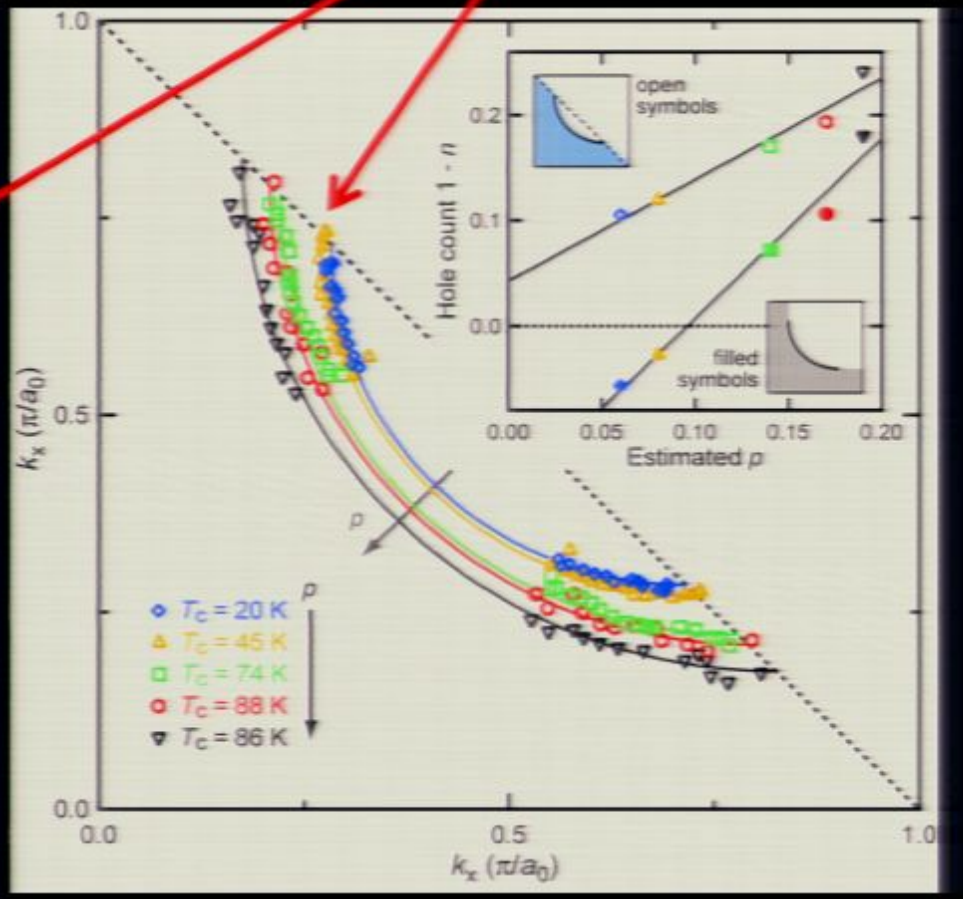

Shrinking arc of homogeneous dSC Cooper pairing as $p \rightarrow 0$

Nature **454**, 1072, (2008)

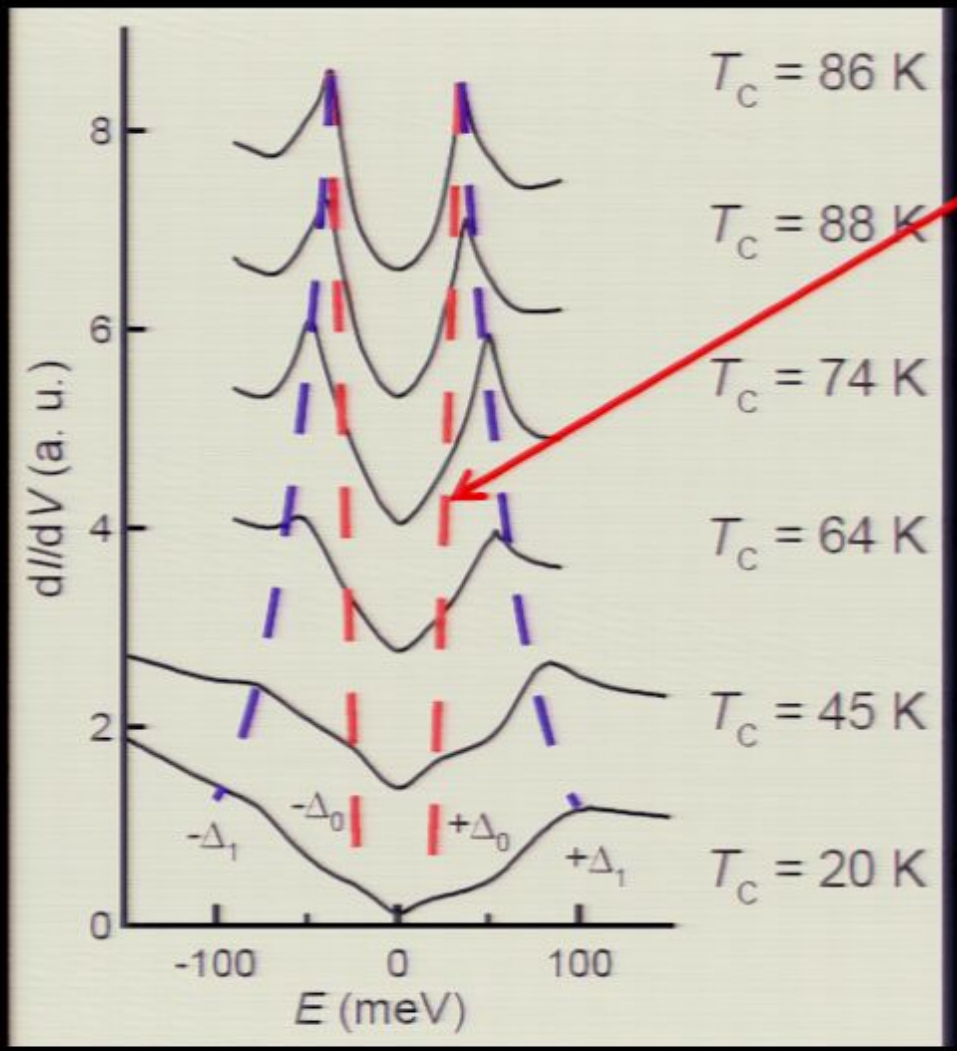

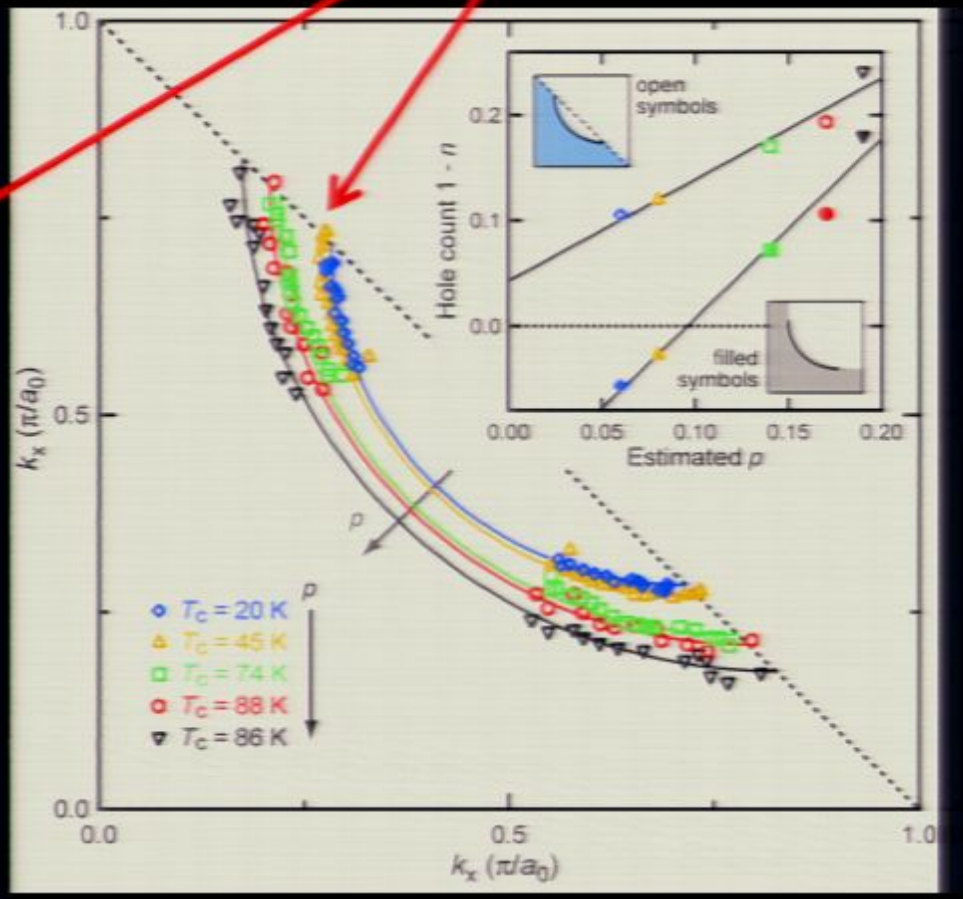

Shrinking arc of homogeneous dSC Cooper pairing as $p \to 0$

Nature **454**, 1072, (2008)

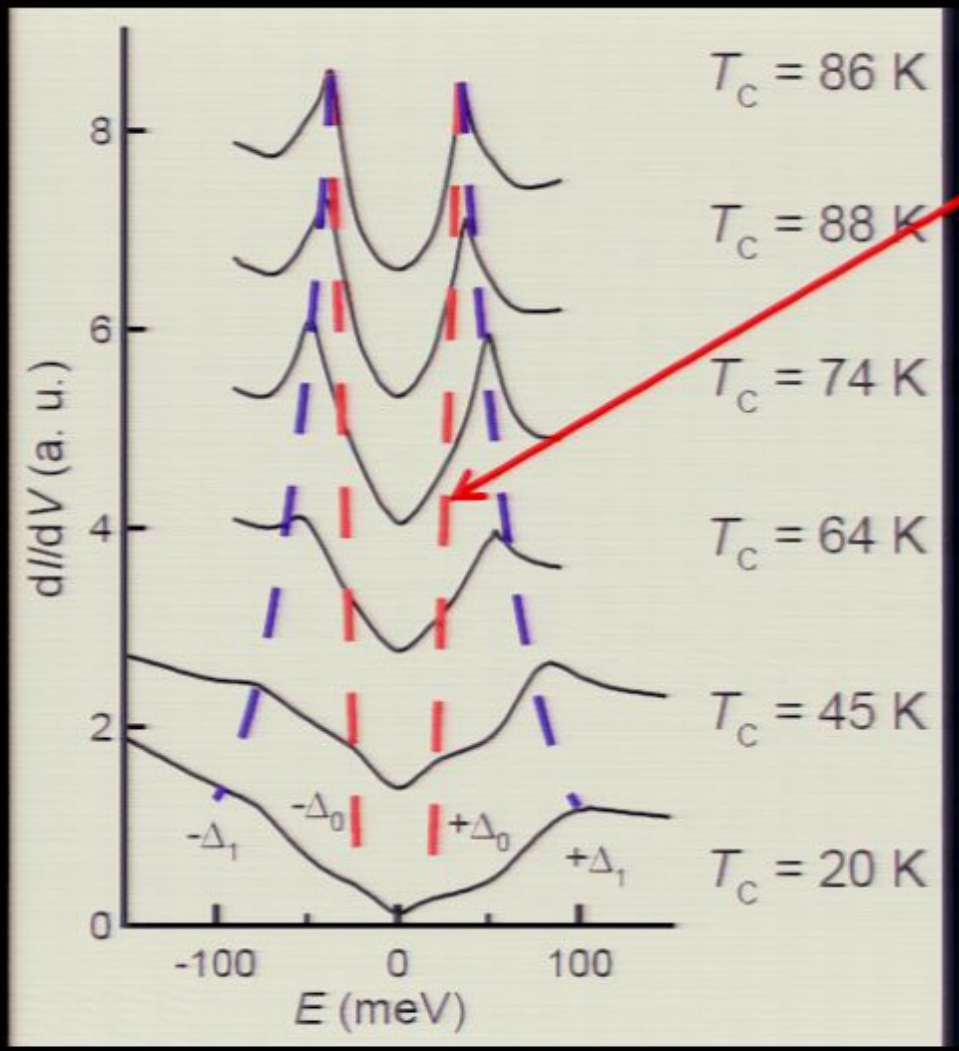

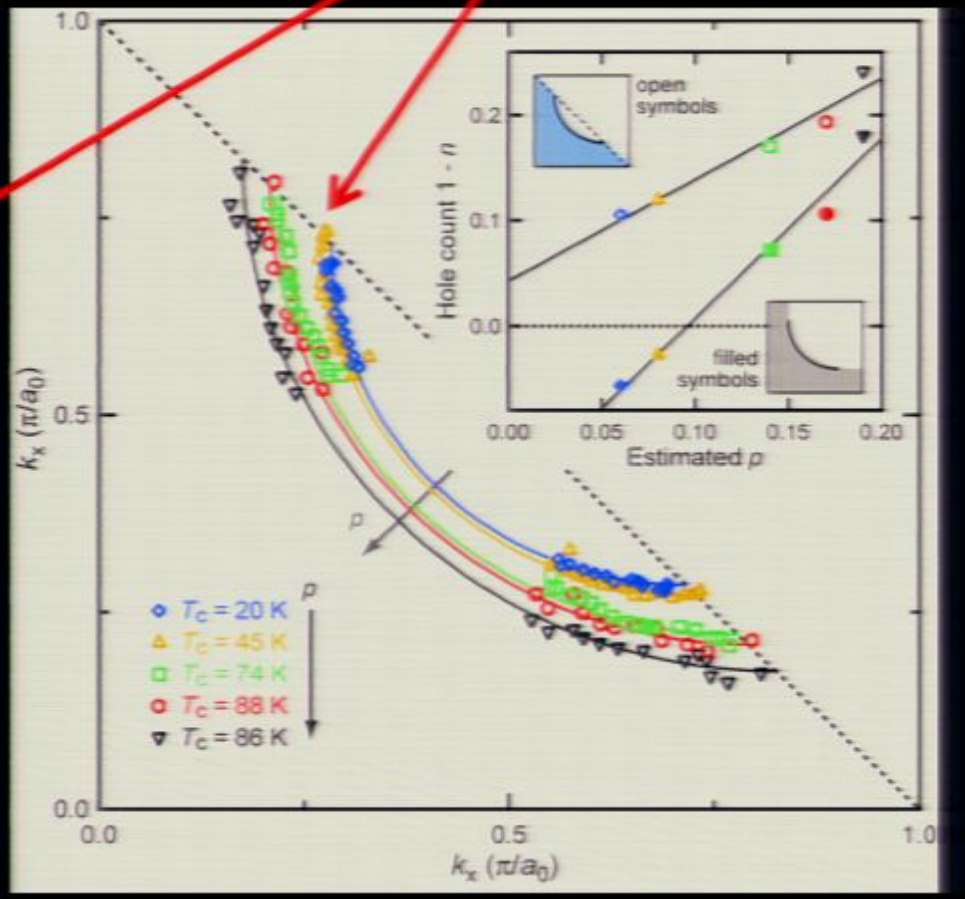

Shrinking arc of homogeneous dSC Cooper pairing as $p \to 0$

Nature 454, 1072, (2008)

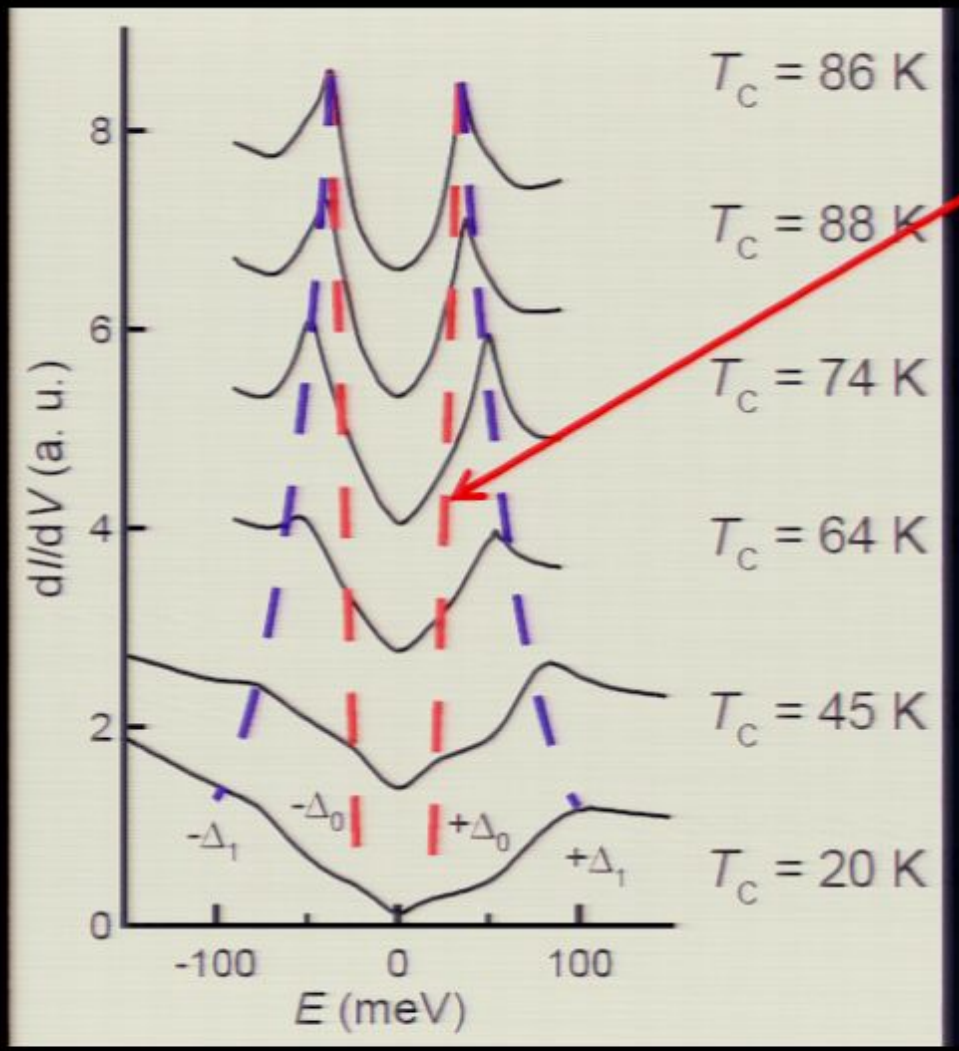

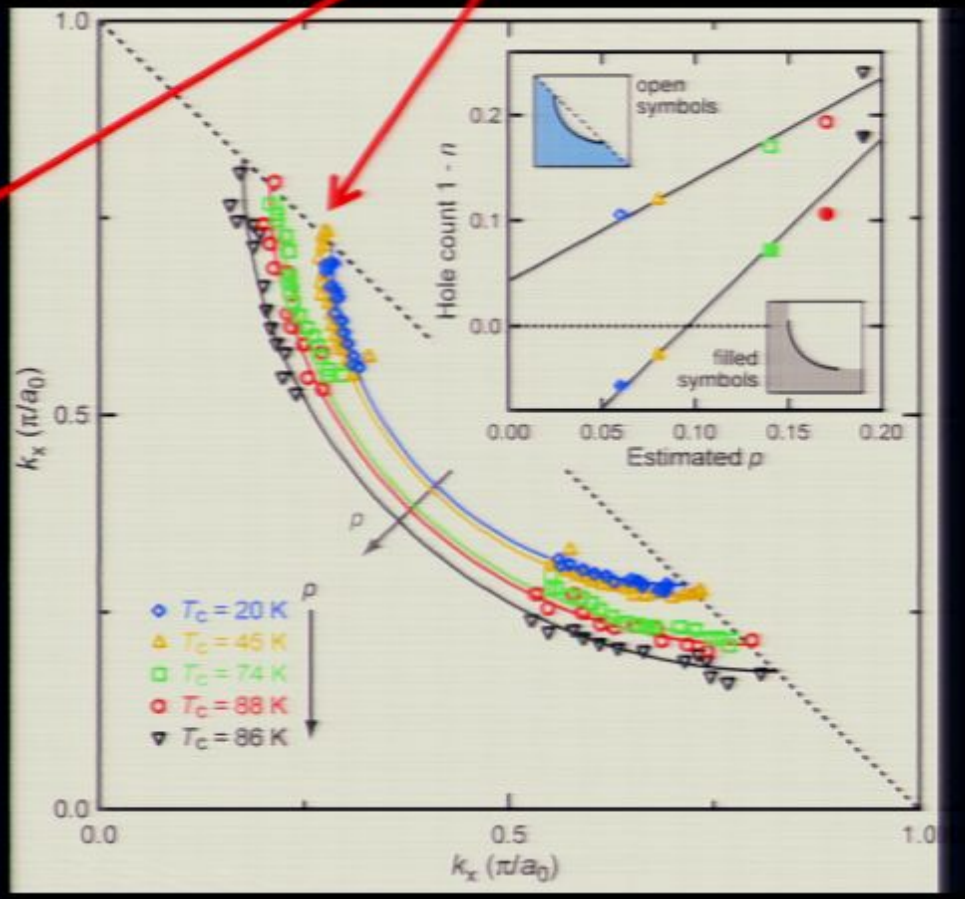

QPI signature of dSC Cooper pairing in PG phase?

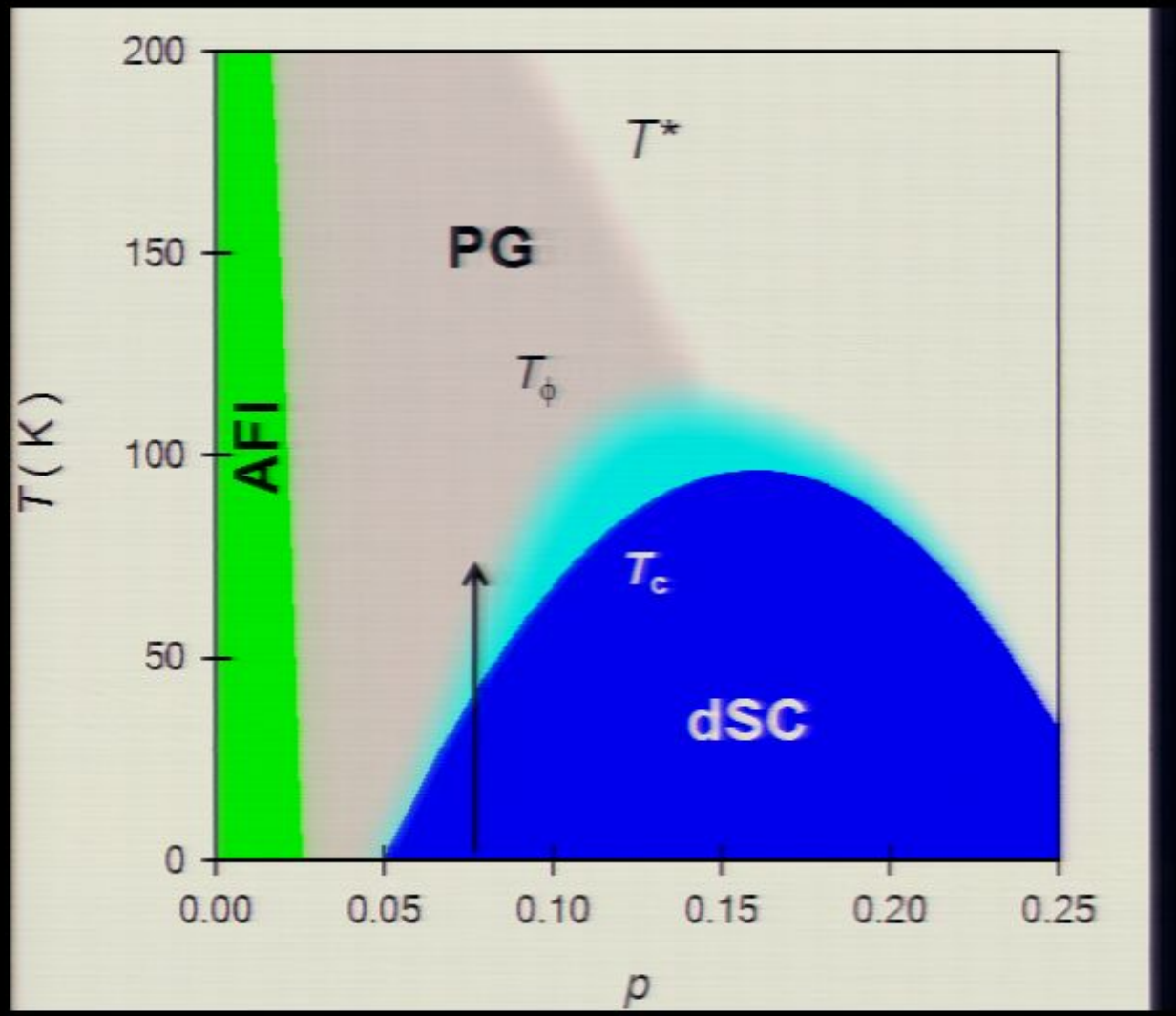

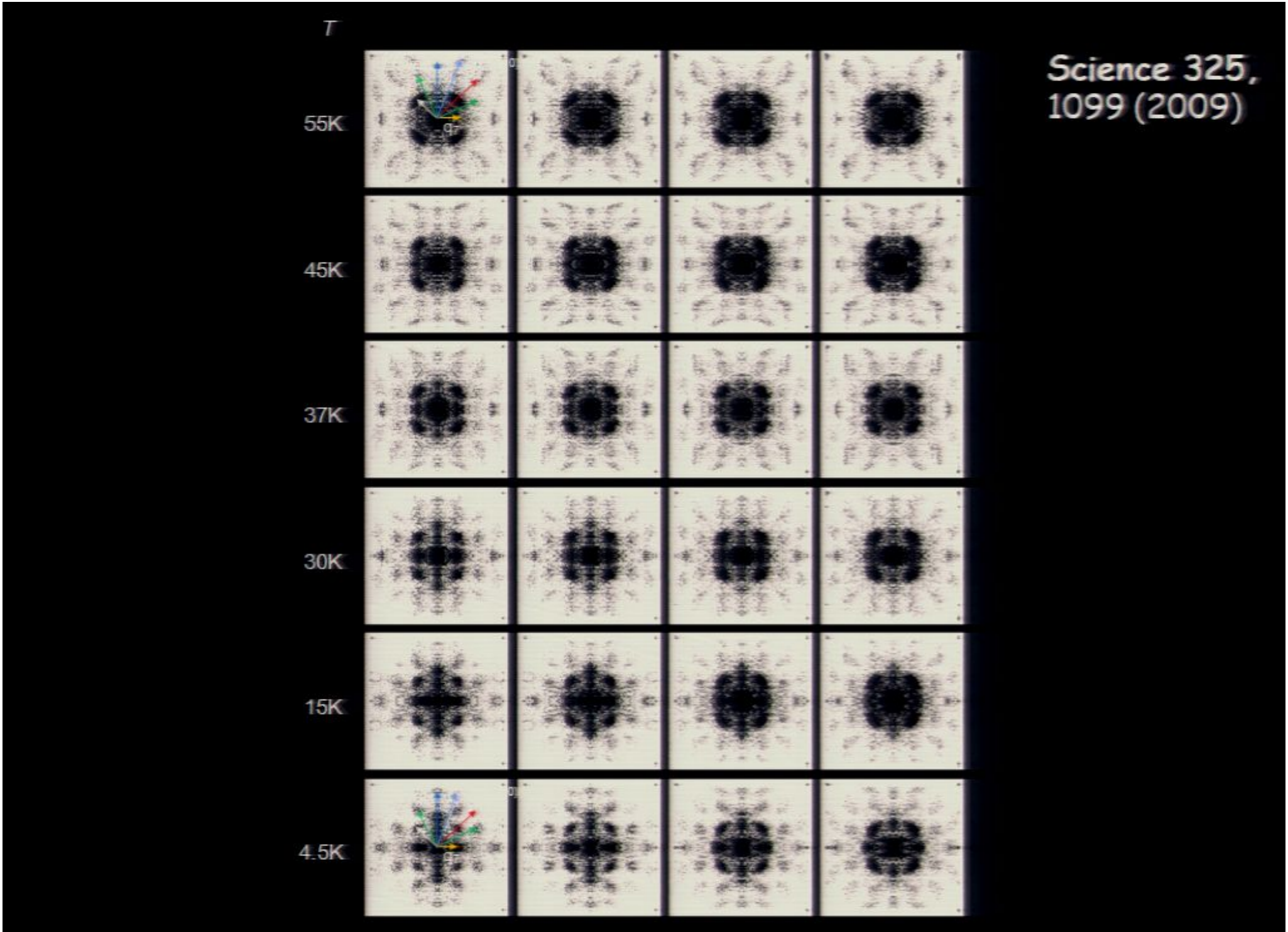
T
55K
45K
37K
30K
15K
4.5K
Science 325, 1099 (2009)

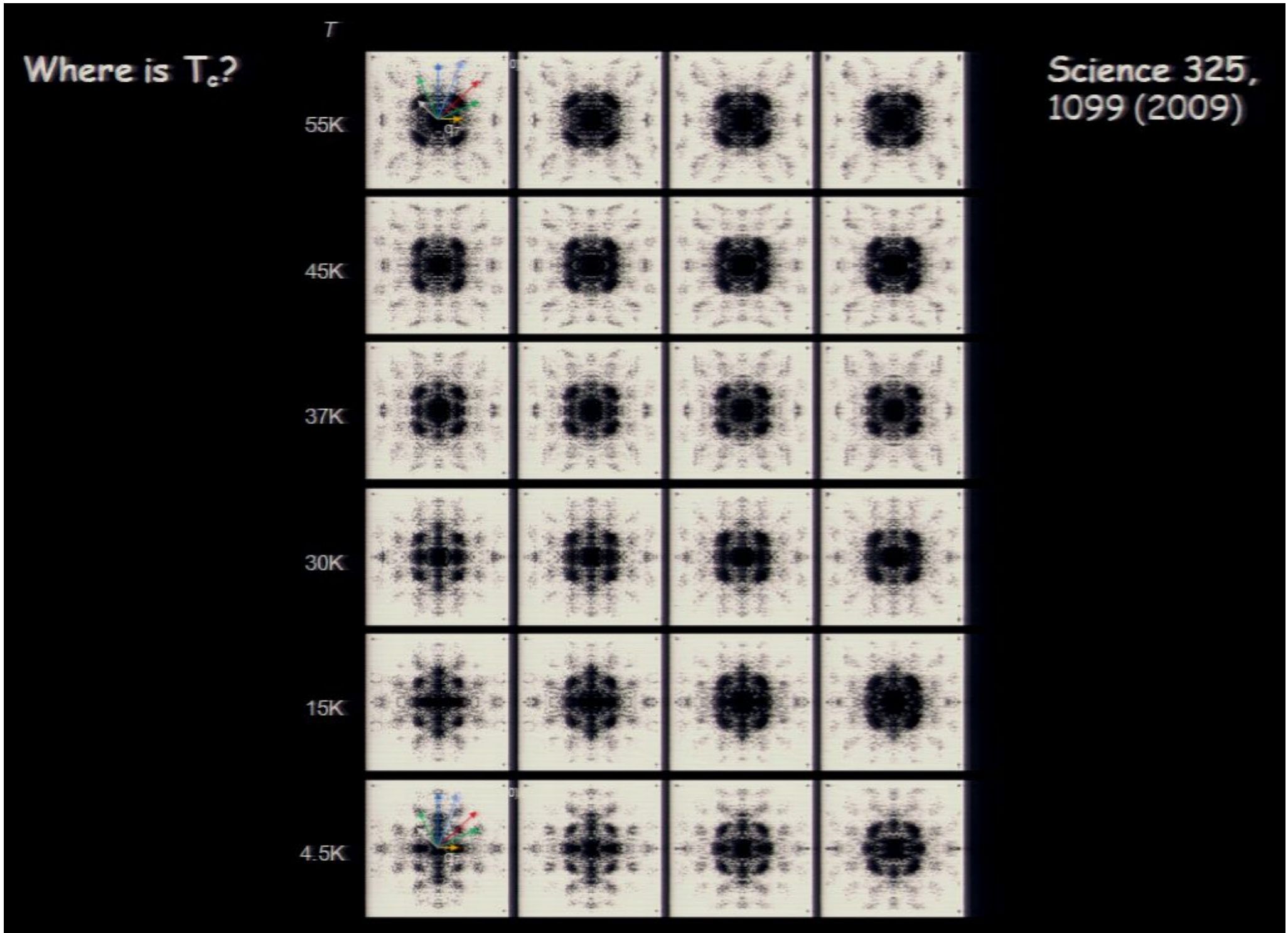
Where is T_c?
T
55K
45K
37K
30K
15K
4.5K
Science 325, 1099 (2009)

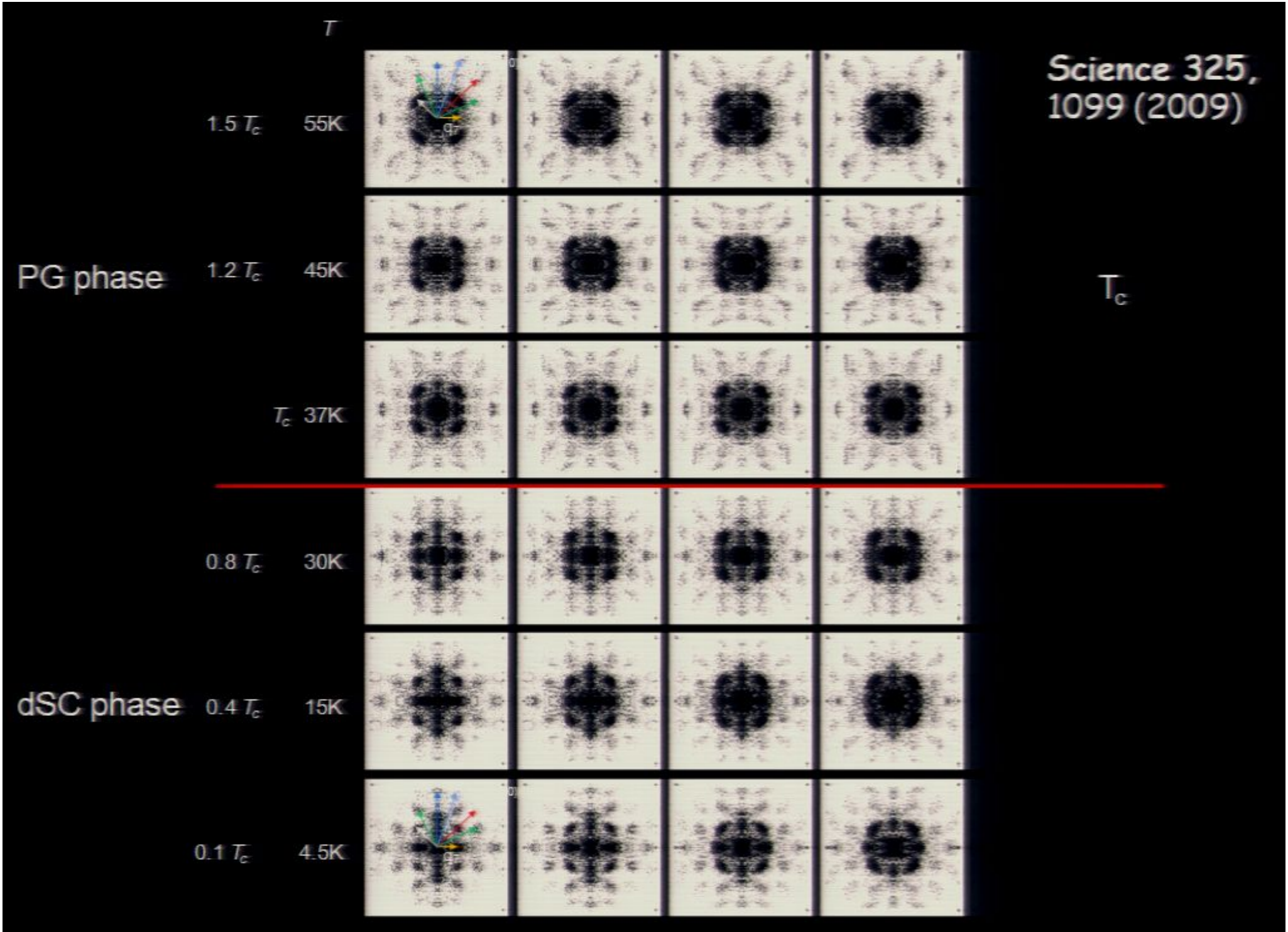
T
1.5 T_c
55K
1.2 T_c
45K
T_c
37K
0.8 T_c
30K
0.4 T_c
15K
0.1 T_c
4.5K
PG phase
dSC phase
T_c
Science 325, 1099 (2009)

Comparison of d-wave QPI in SC and PG Phases

Science 325, 1099 (2009)

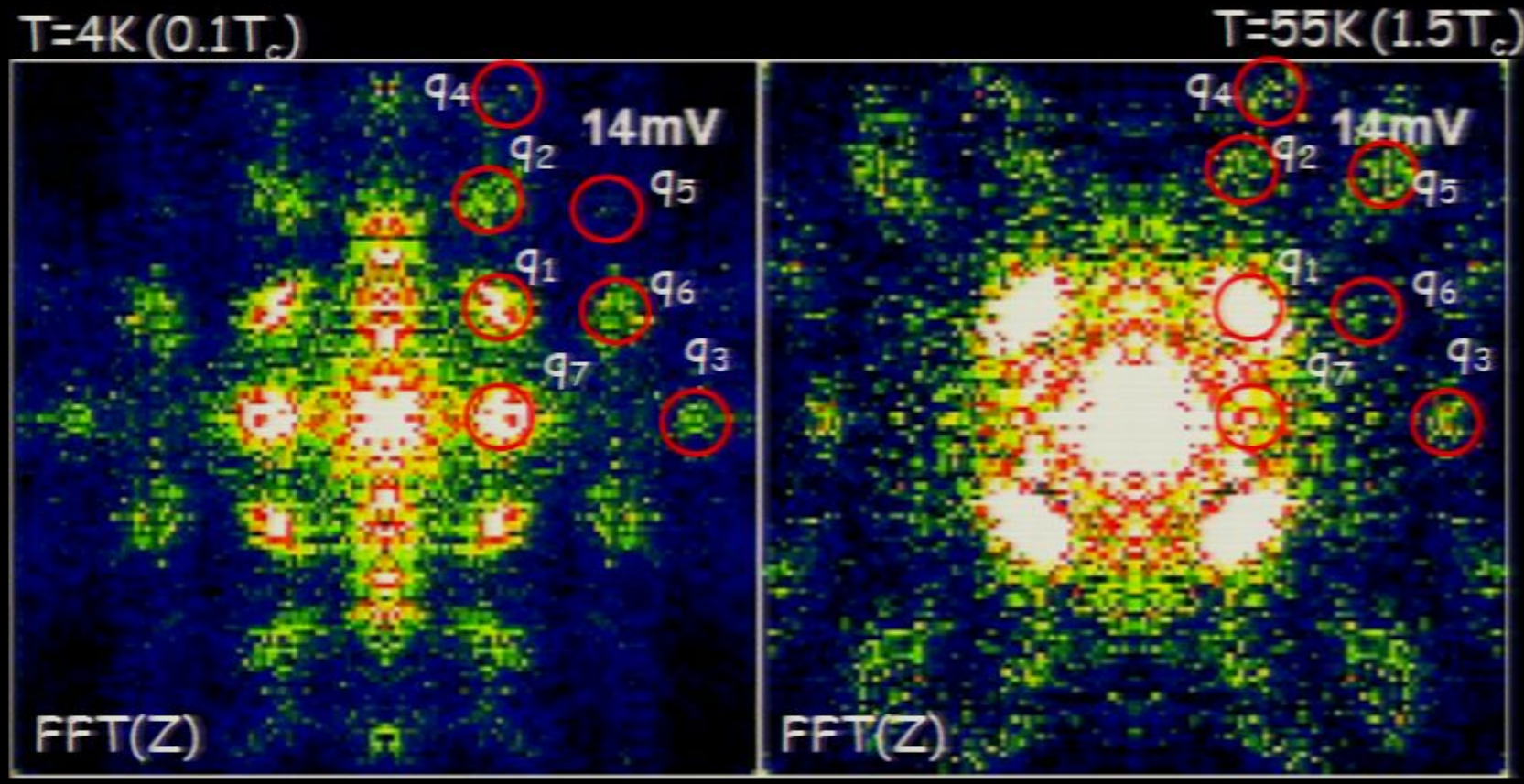

Complete set of particle-hole symmetric dispersive wavevectors of octet model survives even at T=55K (T~1.5Tc)

Octet $q_i(E)$ modulations are all dispersive ($E<\Delta_0$) in PG phase

Science 325, 1099 (2009)

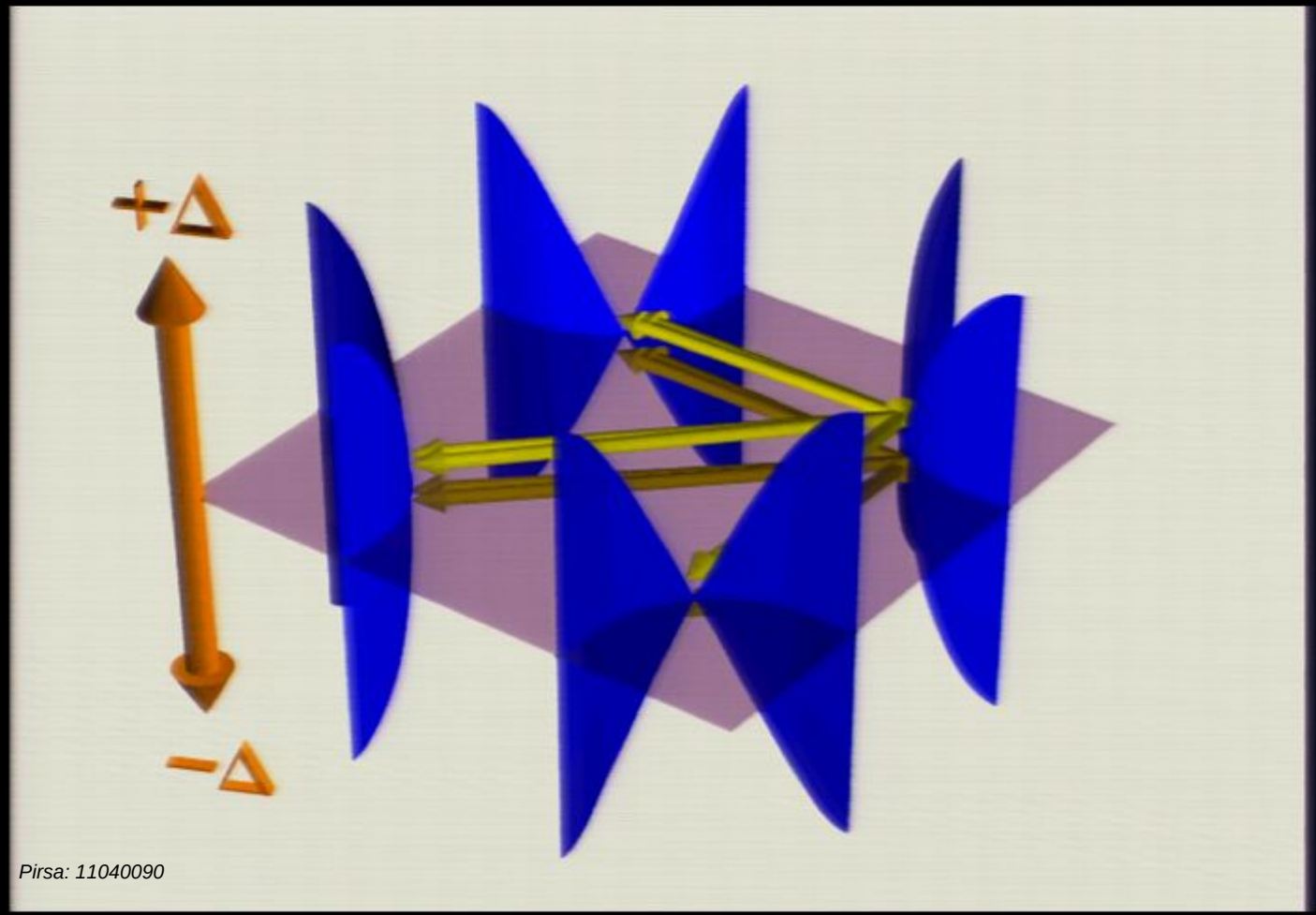

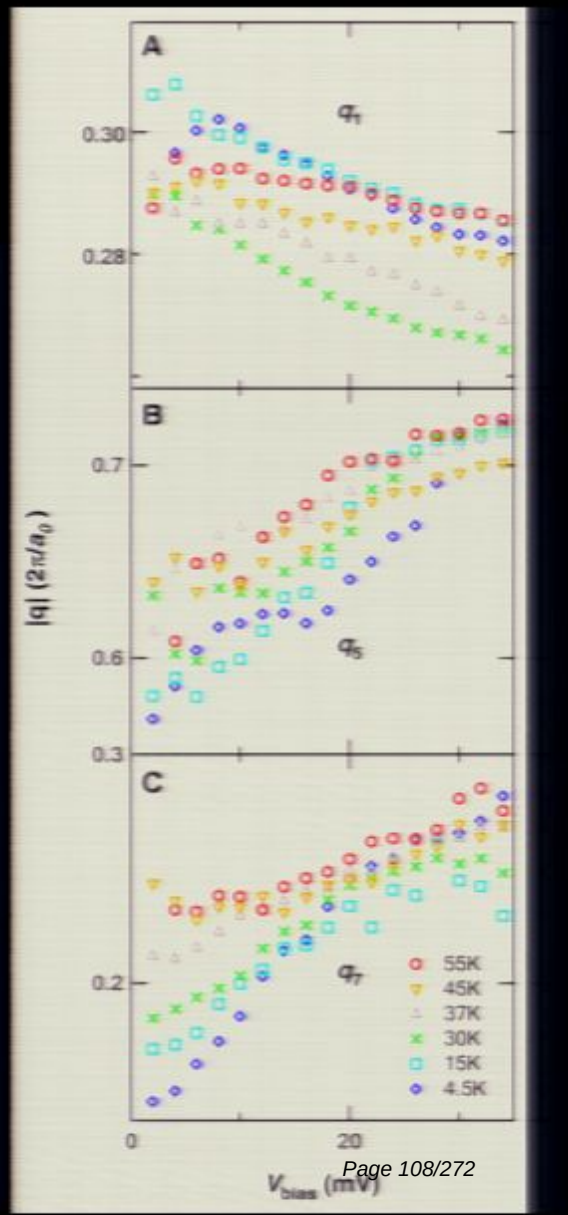

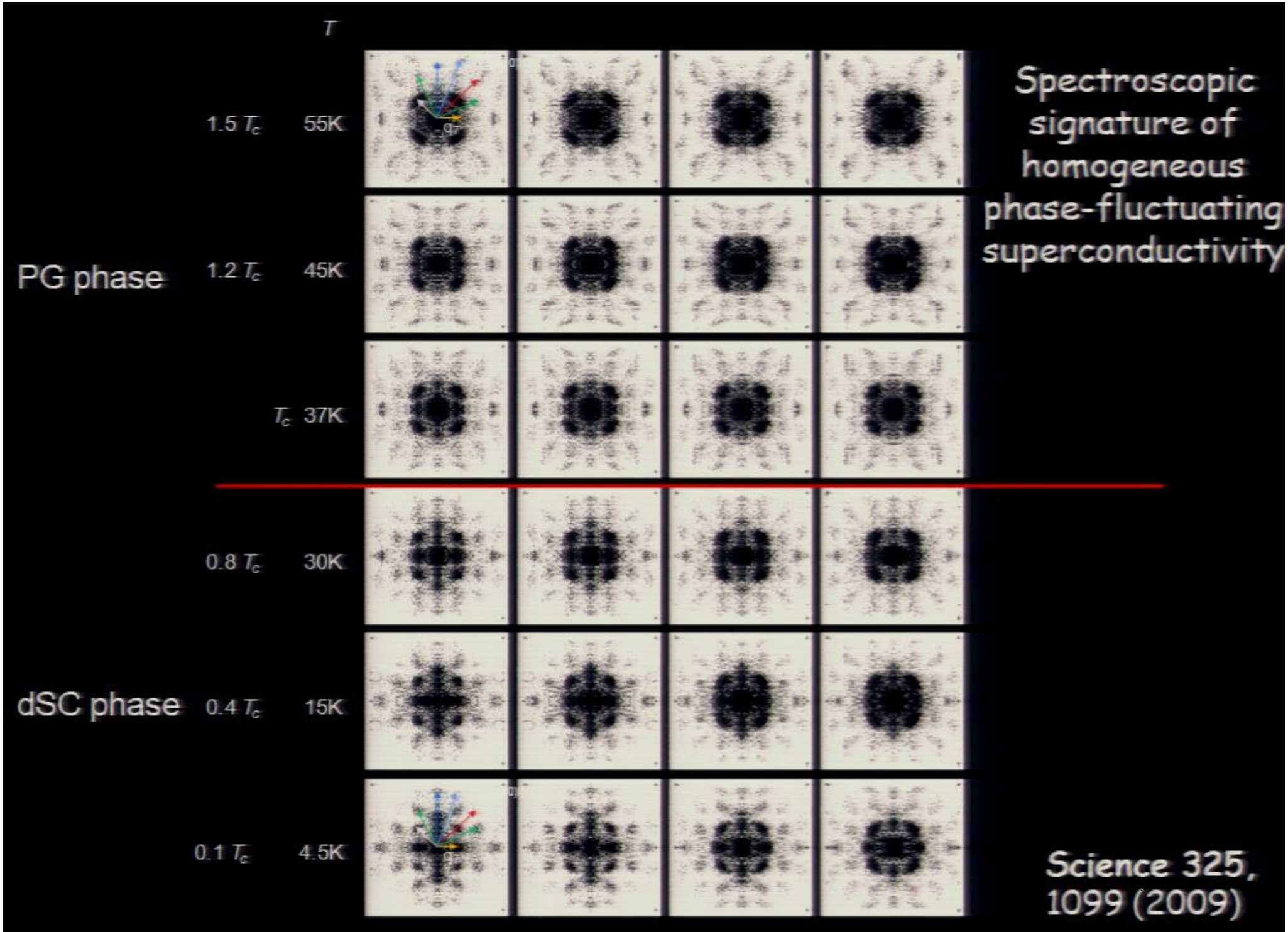
T
1.5 T_c
55K
PG phase
1.2 T_c
45K
T_c
37K
0.8 T_c
30K
dSC phase
0.4 T_c
15K
0.1 T_c
4.5K
Spectroscopic signature of homogeneous phase-fluctuating superconductivity
Science 325, 1099 (2009)

d-wave Cooper pairing signature $E<\Delta_0$ - both phases

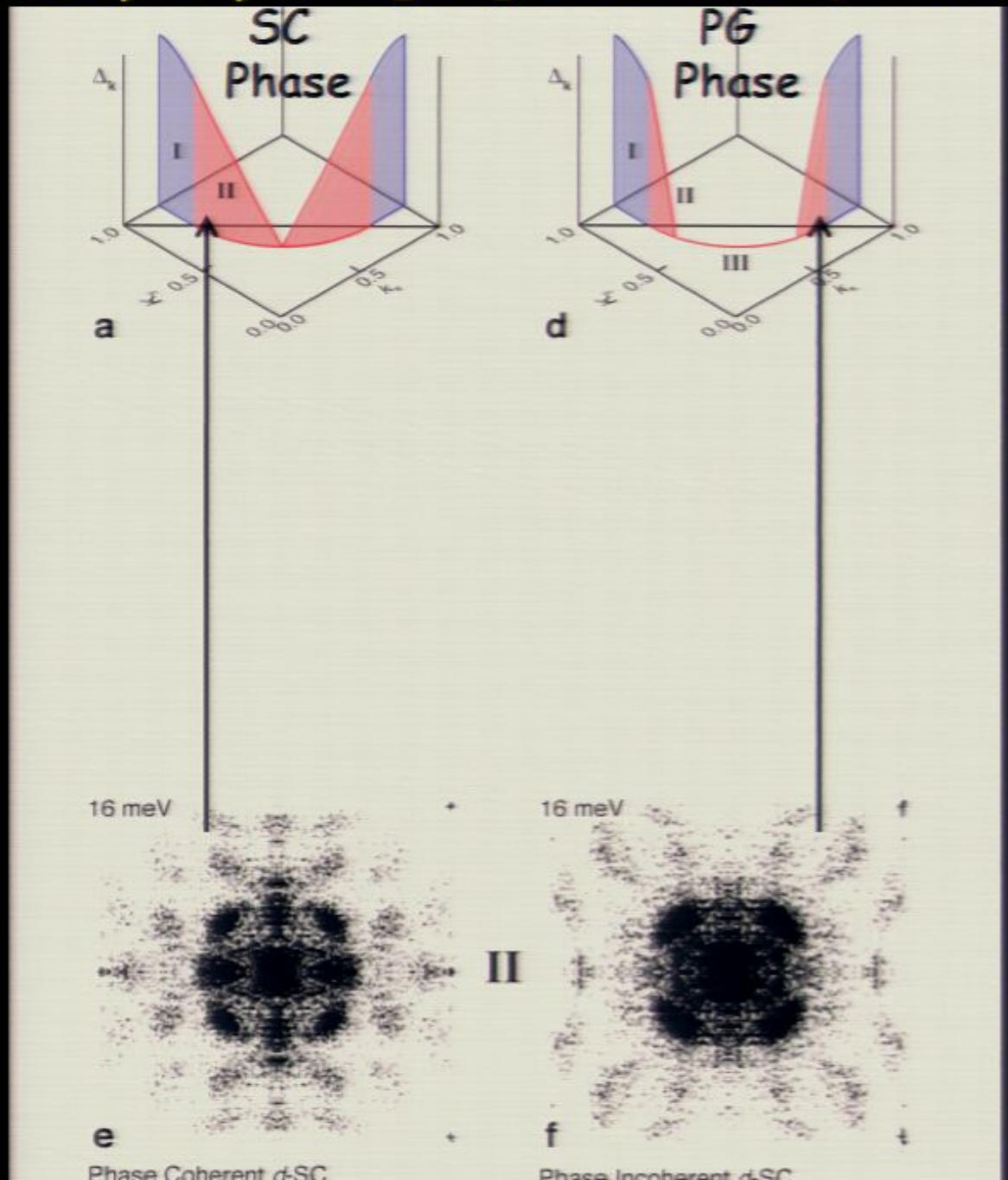

Nature 454, 1072 (2008)

Science 325, 1099 (2009)

Schmidt *et al* (2011)

What about E~Δ_1 pseudogap states ?

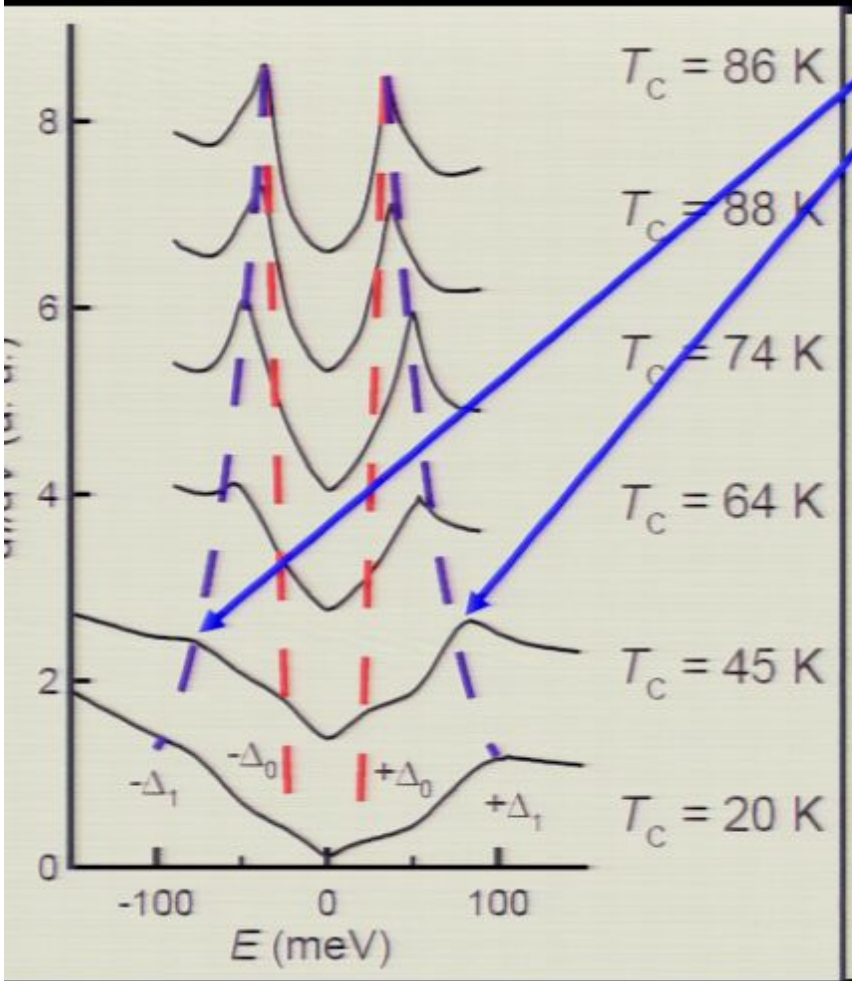

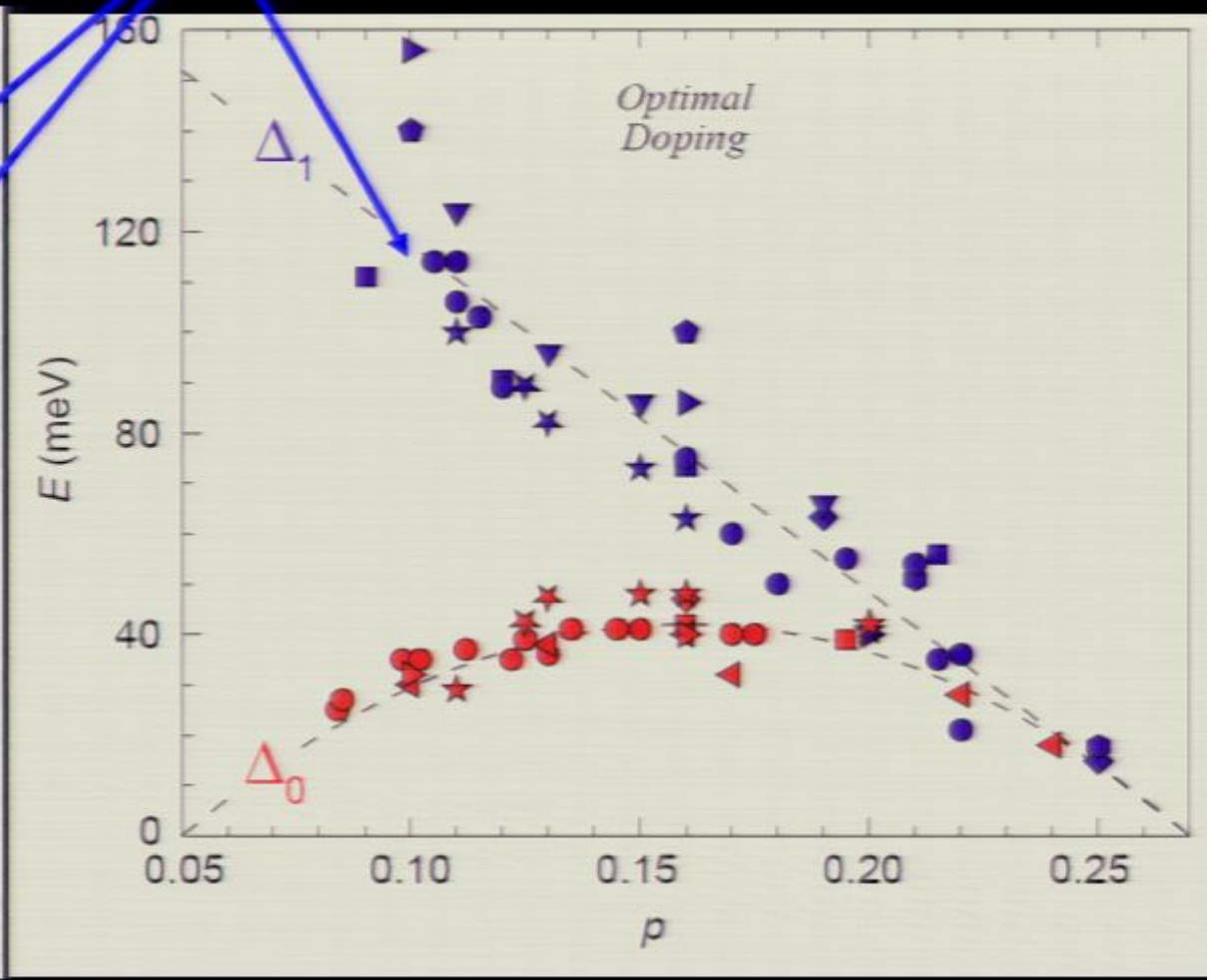

$E > \Delta_0$: Pairing Signature Disappears $\Rightarrow \vec{q} = \vec{Q}_{Bragg}$ and $\vec{q} = \vec{S}$

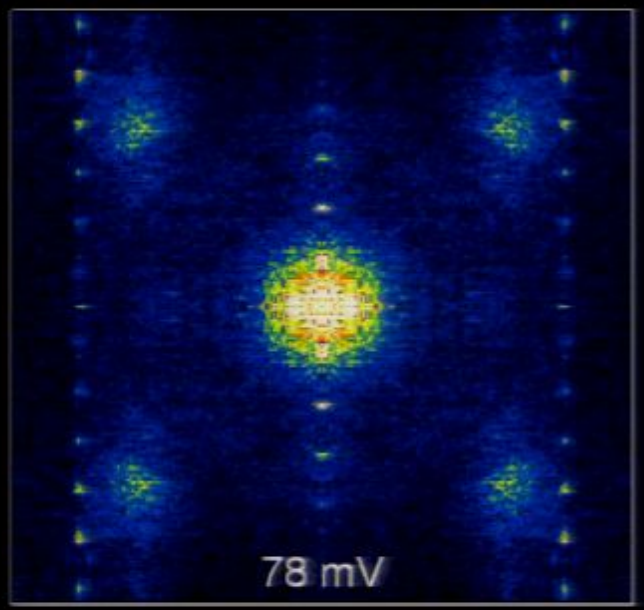

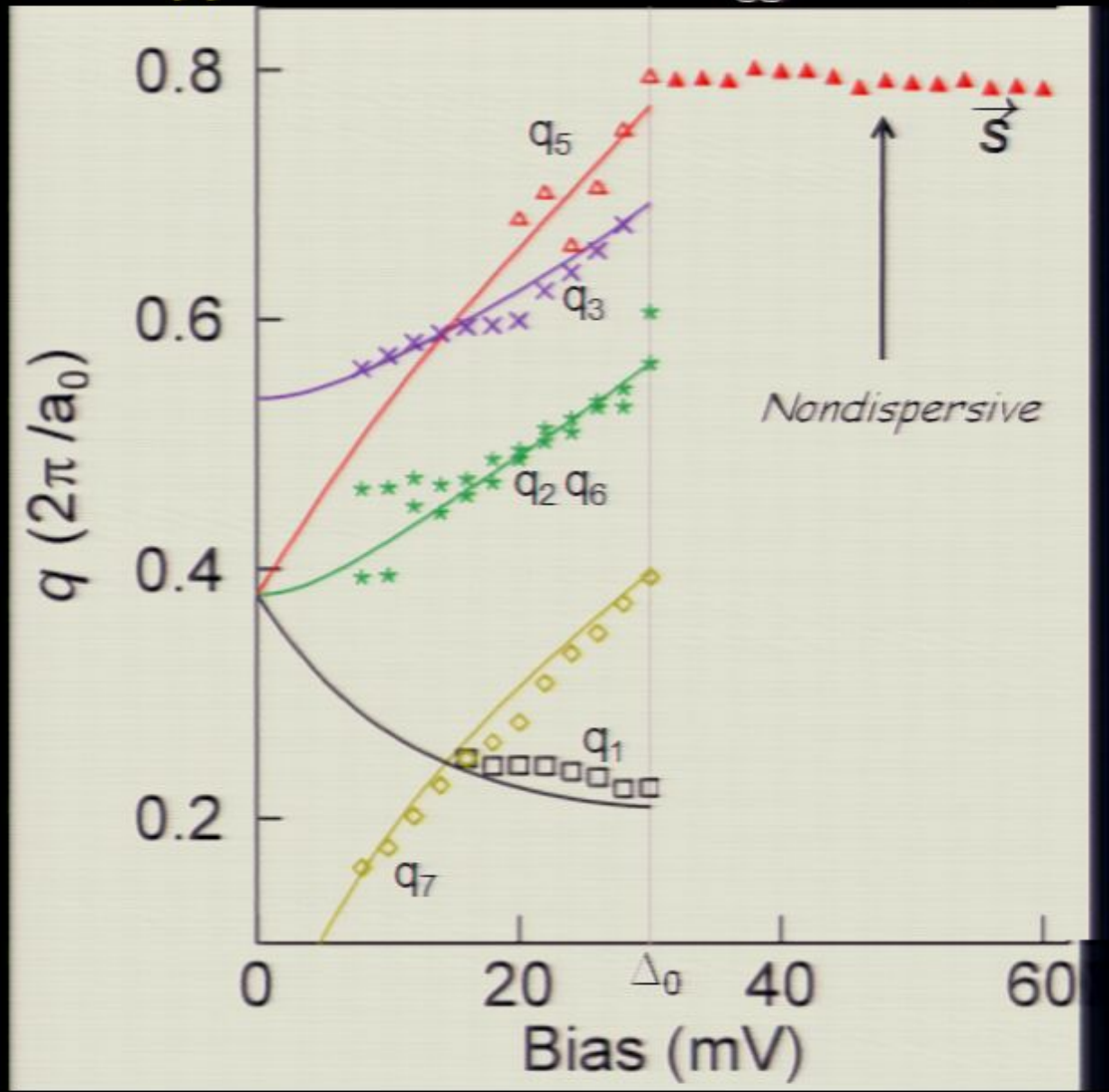

$E > \Delta_0$: Pairing Signature Disappears $\Rightarrow \vec{q} = \vec{Q}_{Bragg}$ and $\vec{q} = \vec{S}$

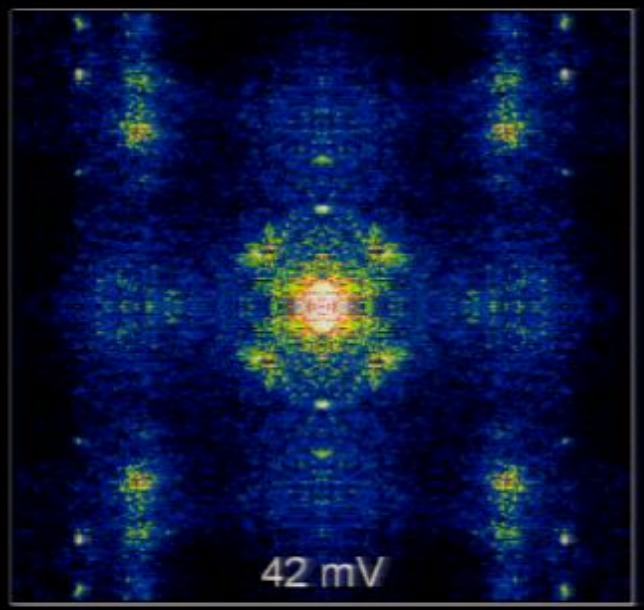

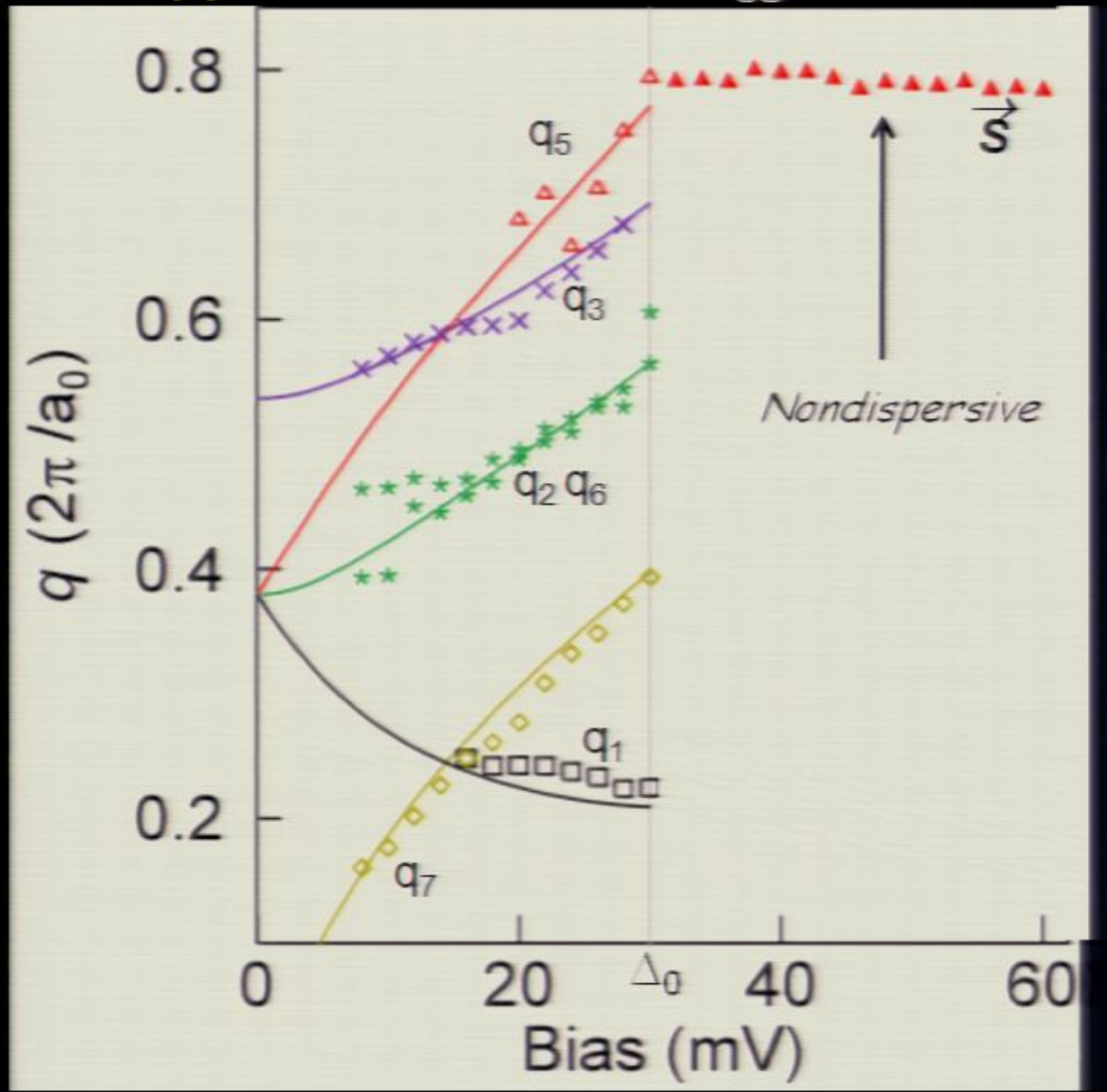

$E > \Delta_0$: Pairing Signature Disappears $\Rightarrow$ $\vec{q} = \vec{Q}_{Bragg}$ and $\vec{q} = \vec{S}$

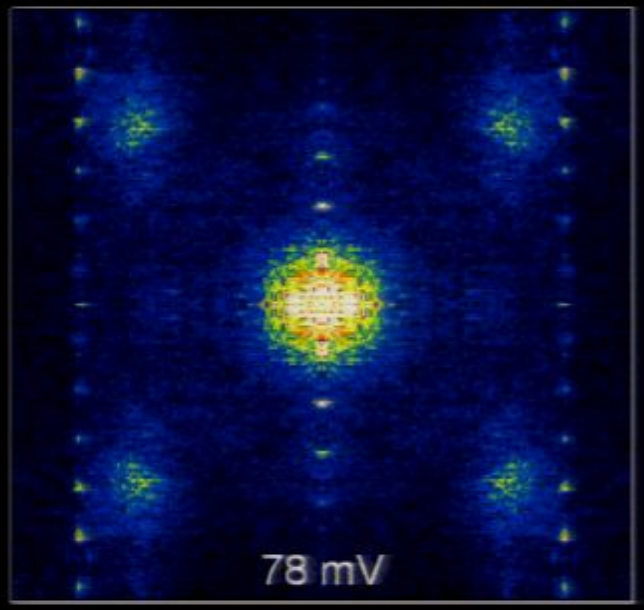

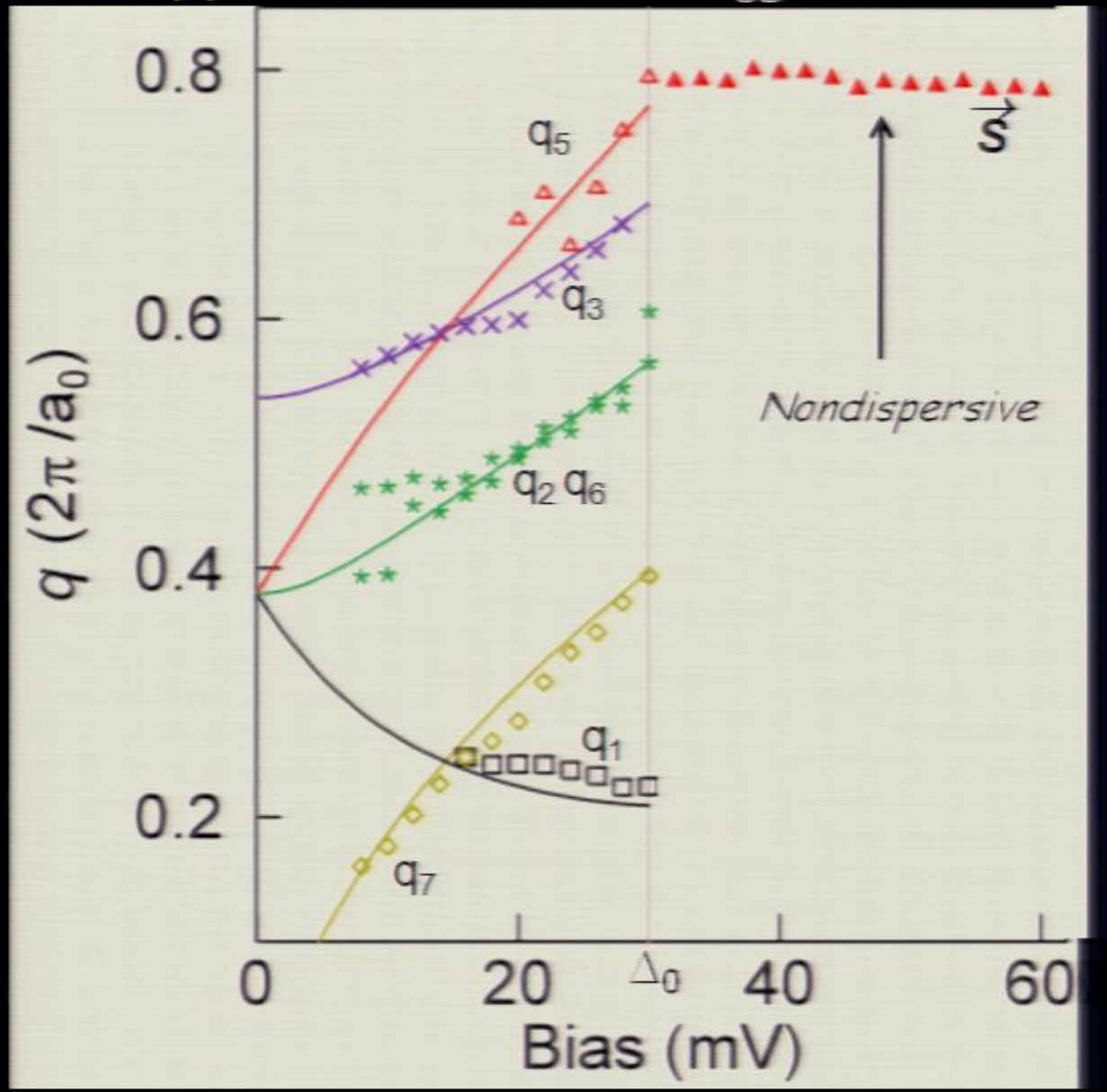

$E > \Delta_0$: Pairing Signature Disappears $\Rightarrow \vec{q} = \vec{Q}_{Bragg}$ and $\vec{q} = \vec{S}$

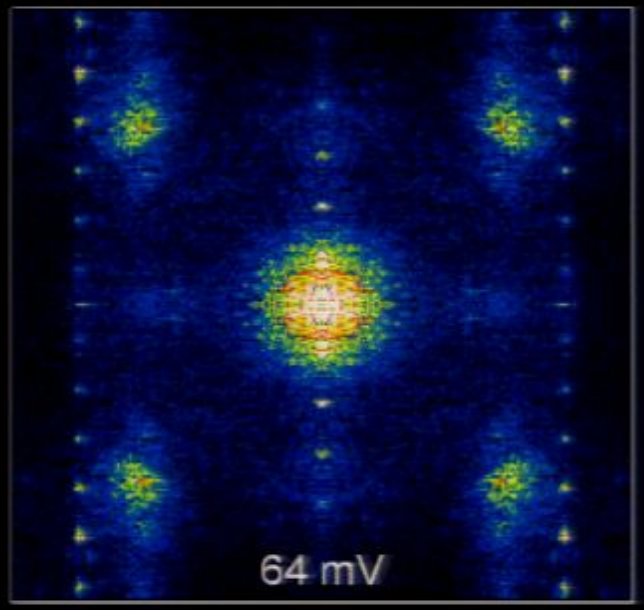

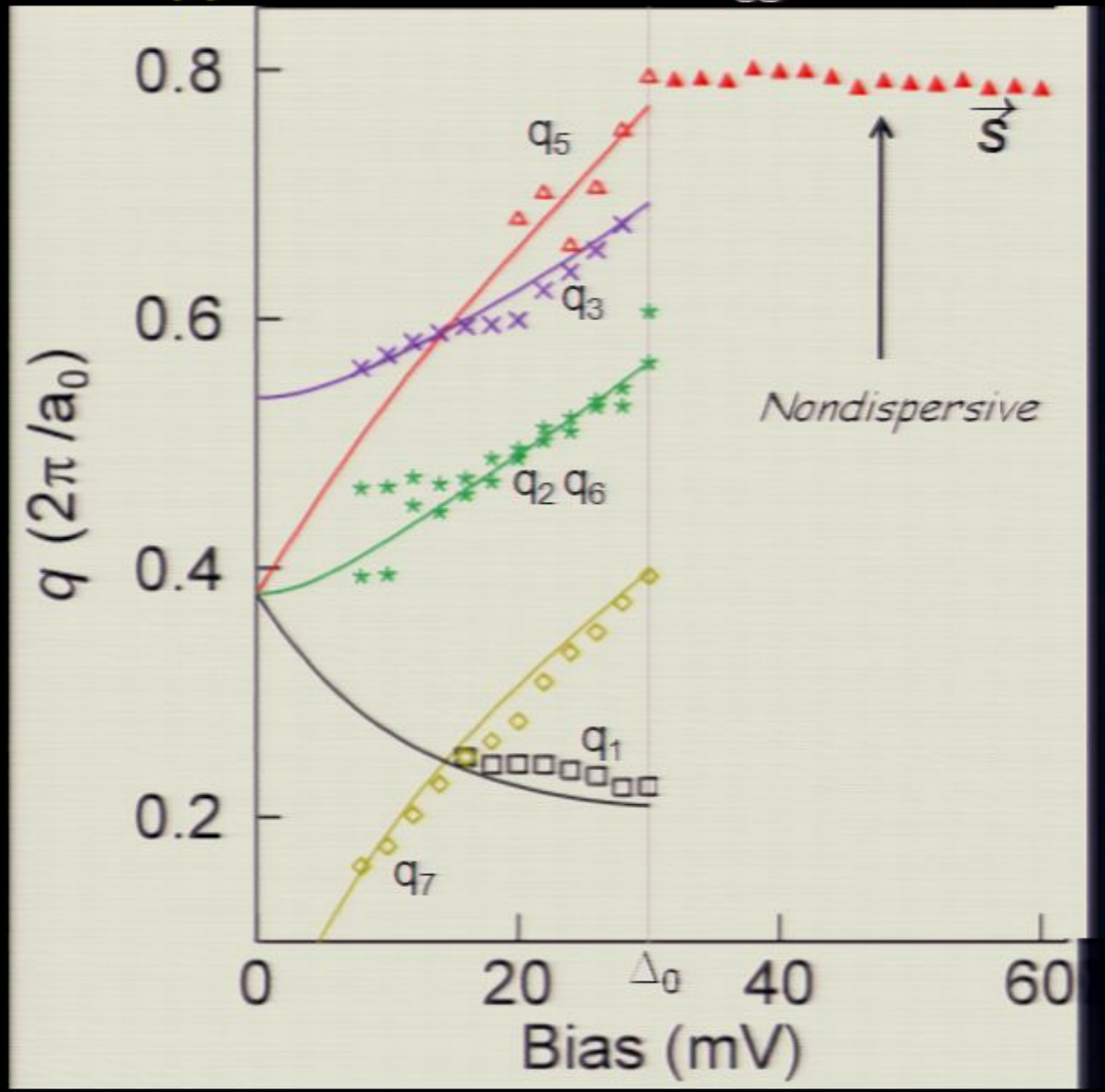

E~ Δ_1: Static electronic structure breaks spatial symmetries

Science 315, 1389 (2007); Science 325, 1099 (2009), Nature 466, 374 (2010)

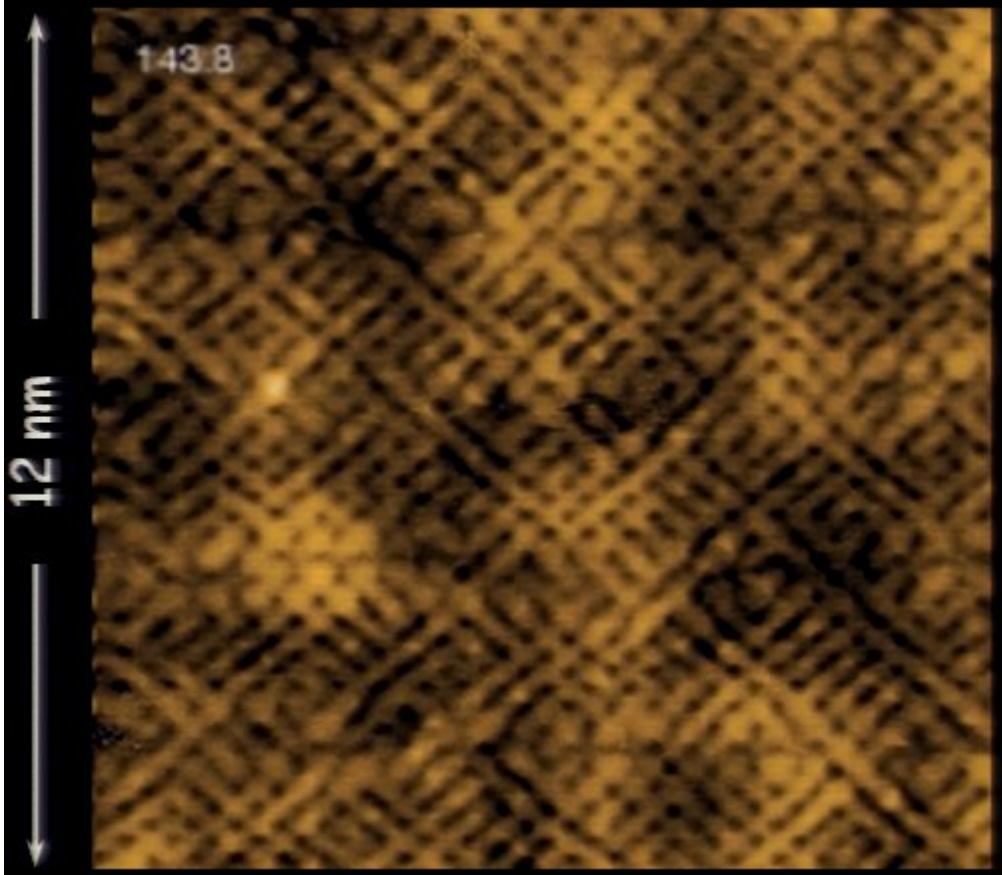

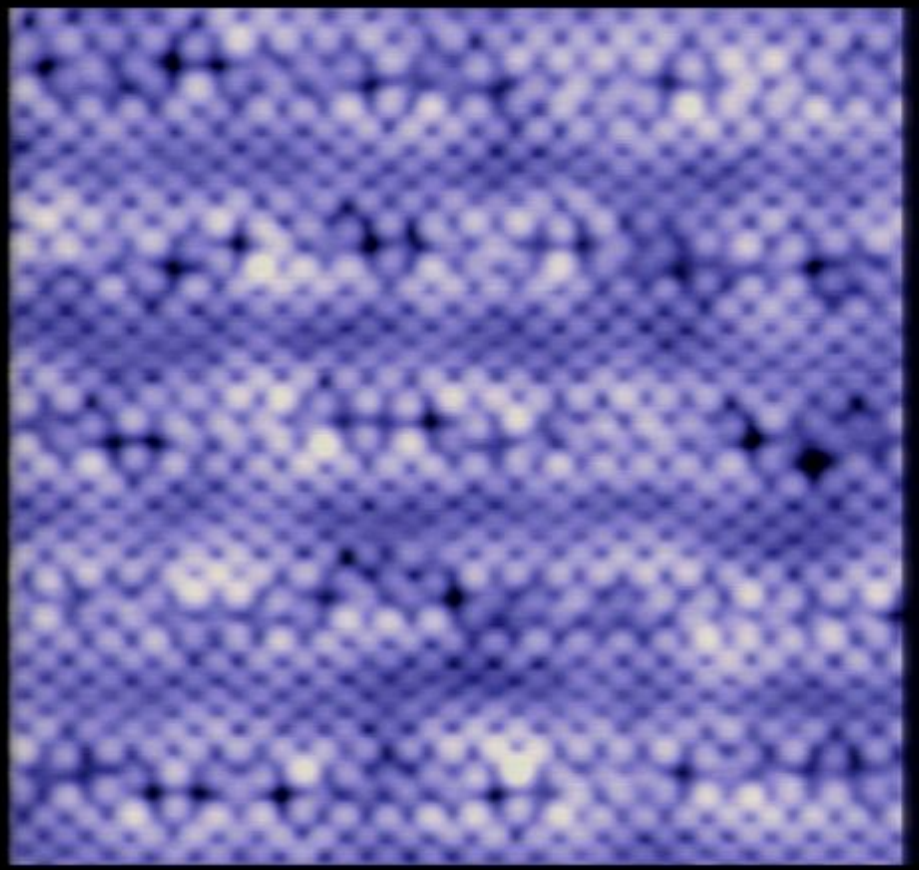

E~ Δ_1: Static electronic structure breaks spatial symmetries

Science 315, 1389 (2007); Science 325, 1099 (2009), Nature 466, 374 (2010)

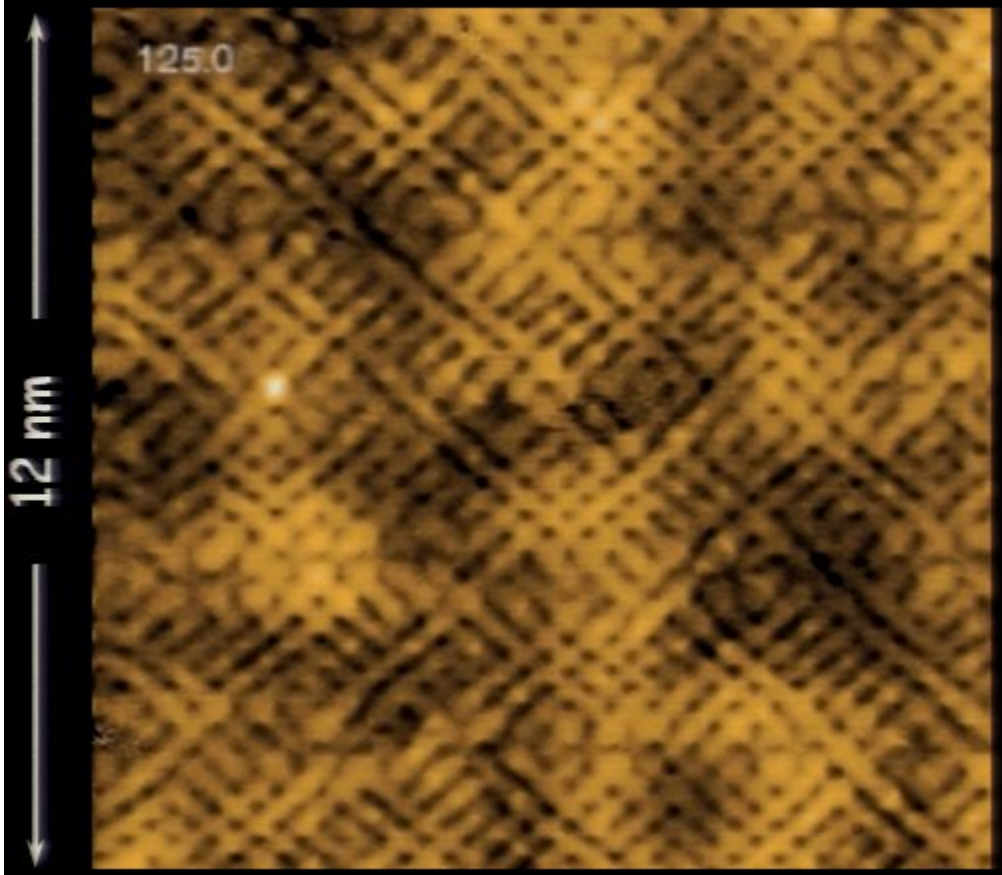

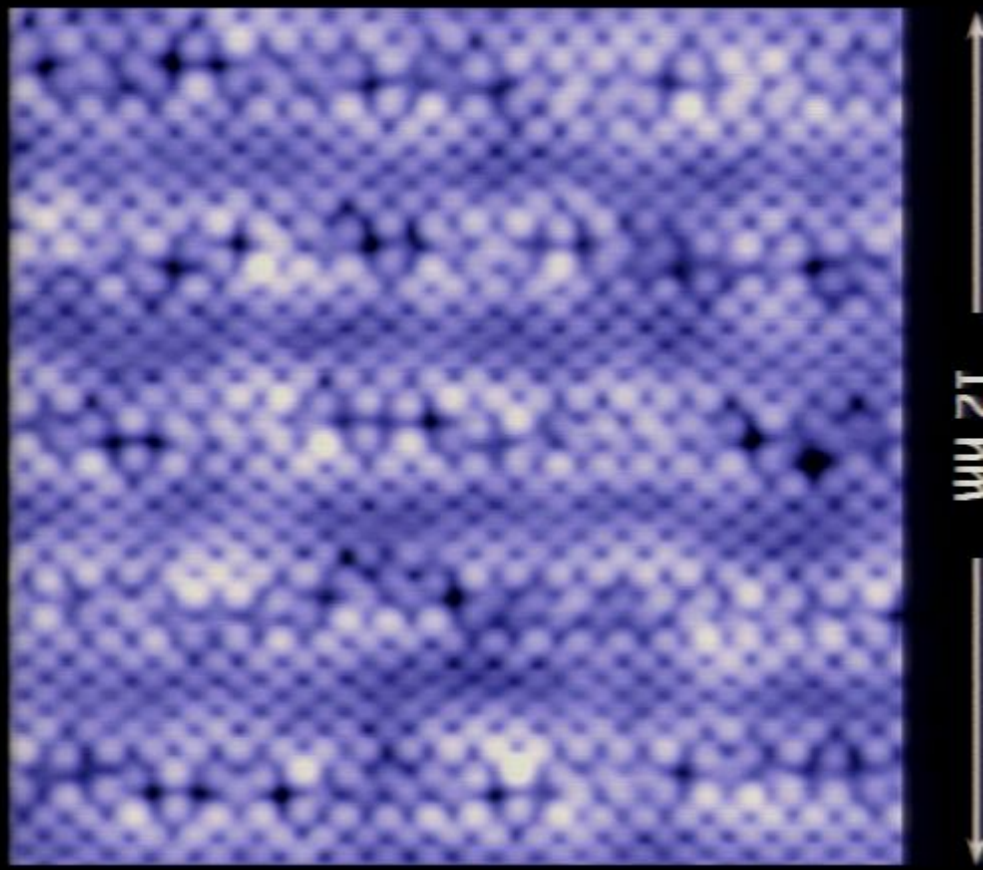

E~ Δ_1: Static electronic structure breaks spatial symmetries

Science 315, 1389 (2007); Science 325, 1099 (2009), Nature 466, 374 (2010)

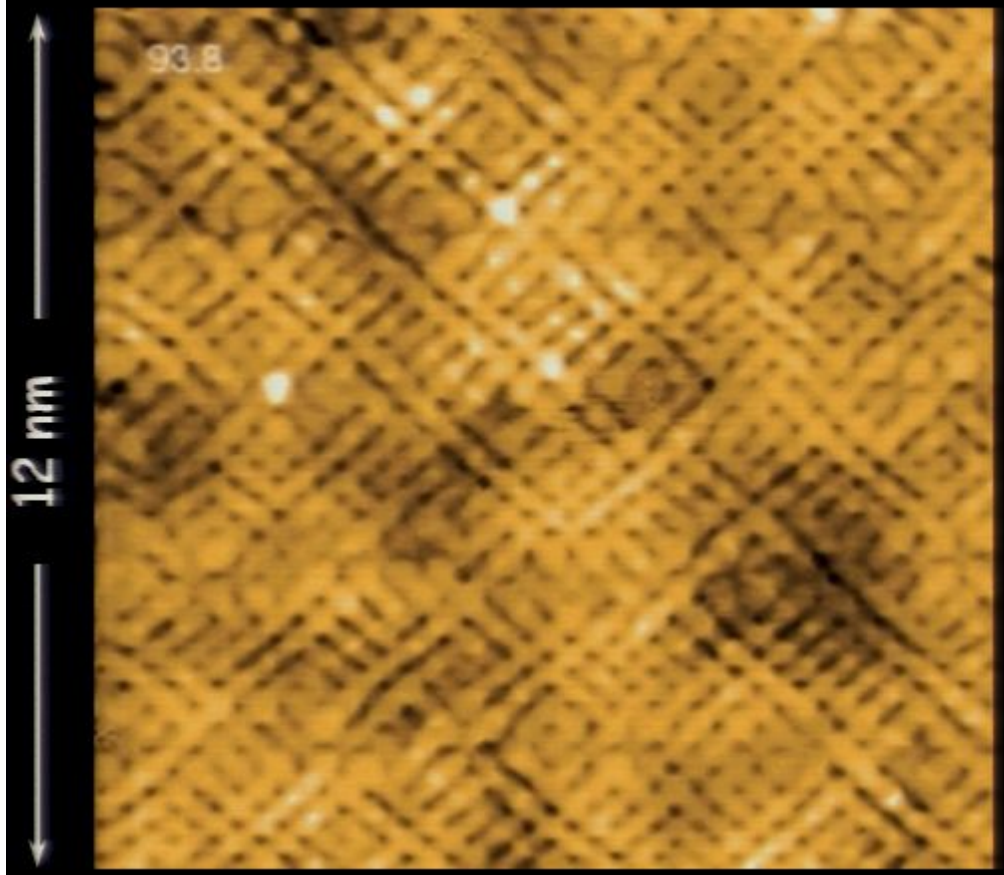

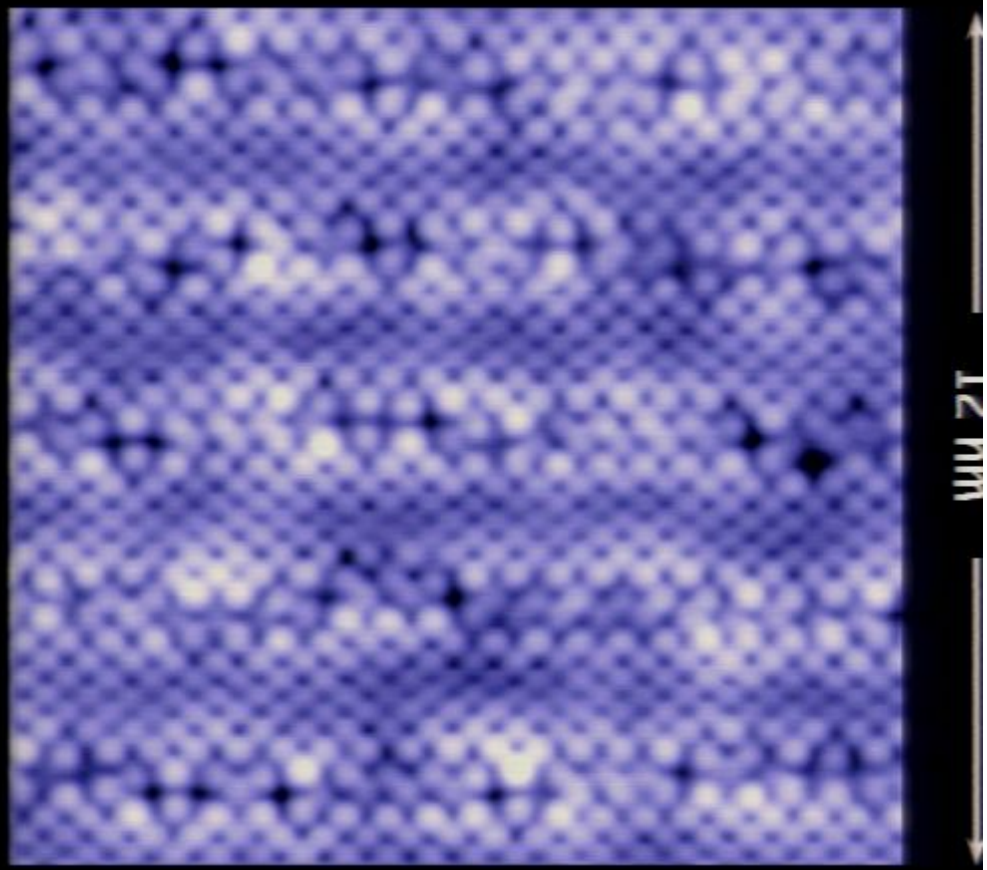

Symmetry breaking is concentrated on pseudogap states $E \sim \Delta_1$

Nature 466, 374 (2010)

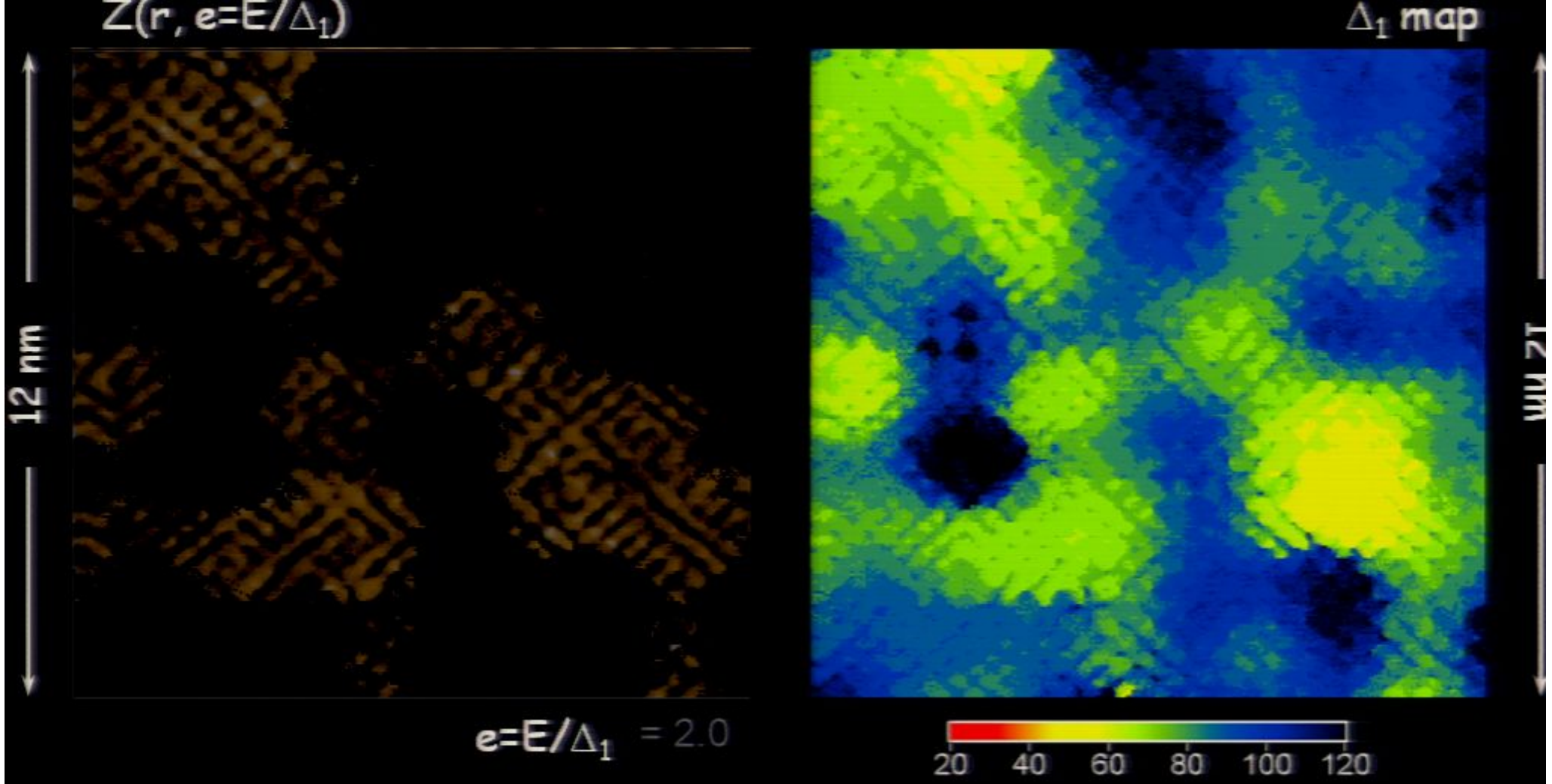

Symmetry breaking is concentrated on pseudogap states $E \sim \Delta_1$

Nature 466, 374 (2010)

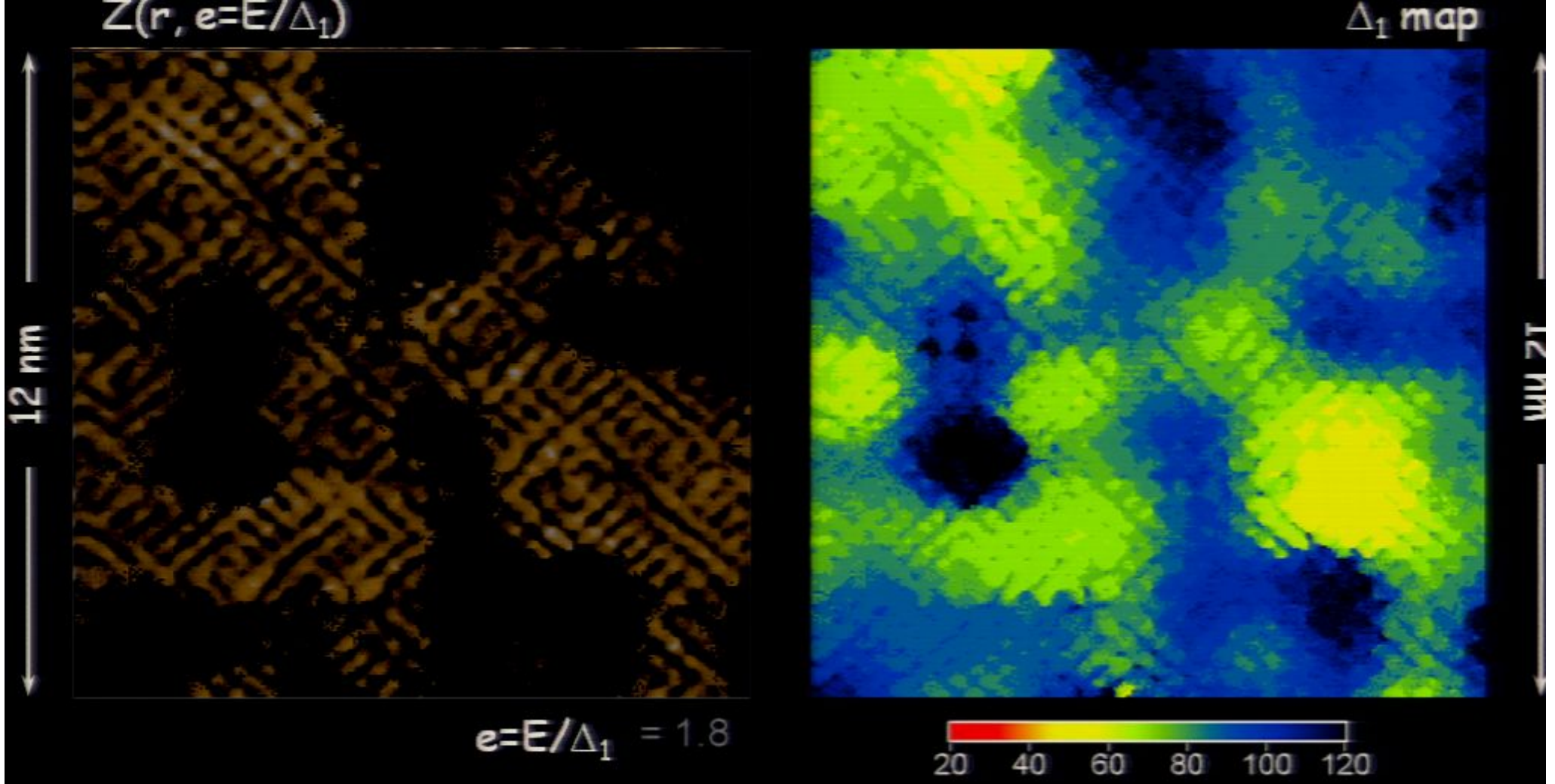

Symmetry breaking is concentrated on pseudogap states $E \sim \Delta_1$

Nature 466, 374 (2010)

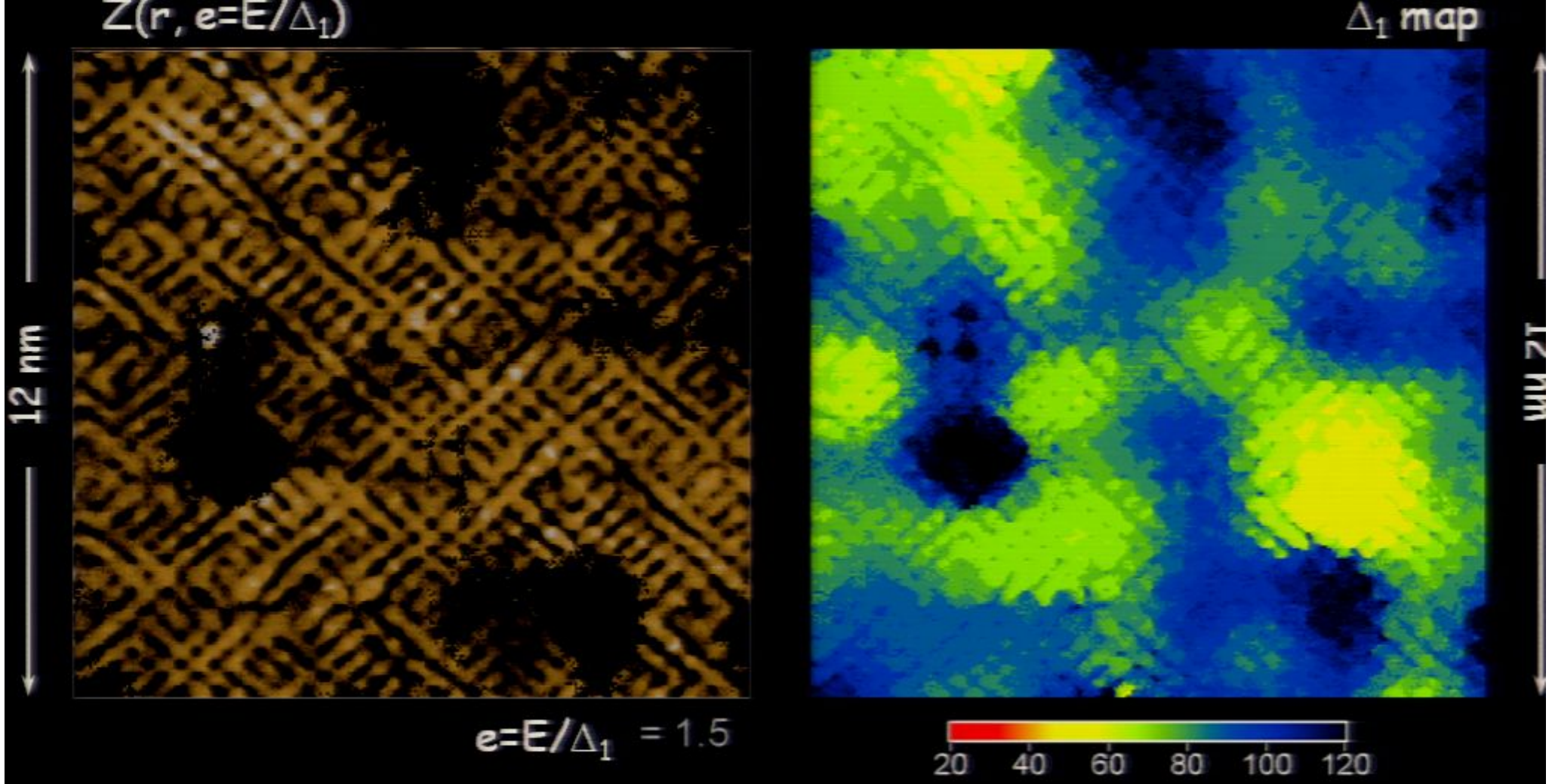

Symmetry breaking is concentrated on pseudogap states $E \sim \Delta_1$

Nature 466, 374 (2010)

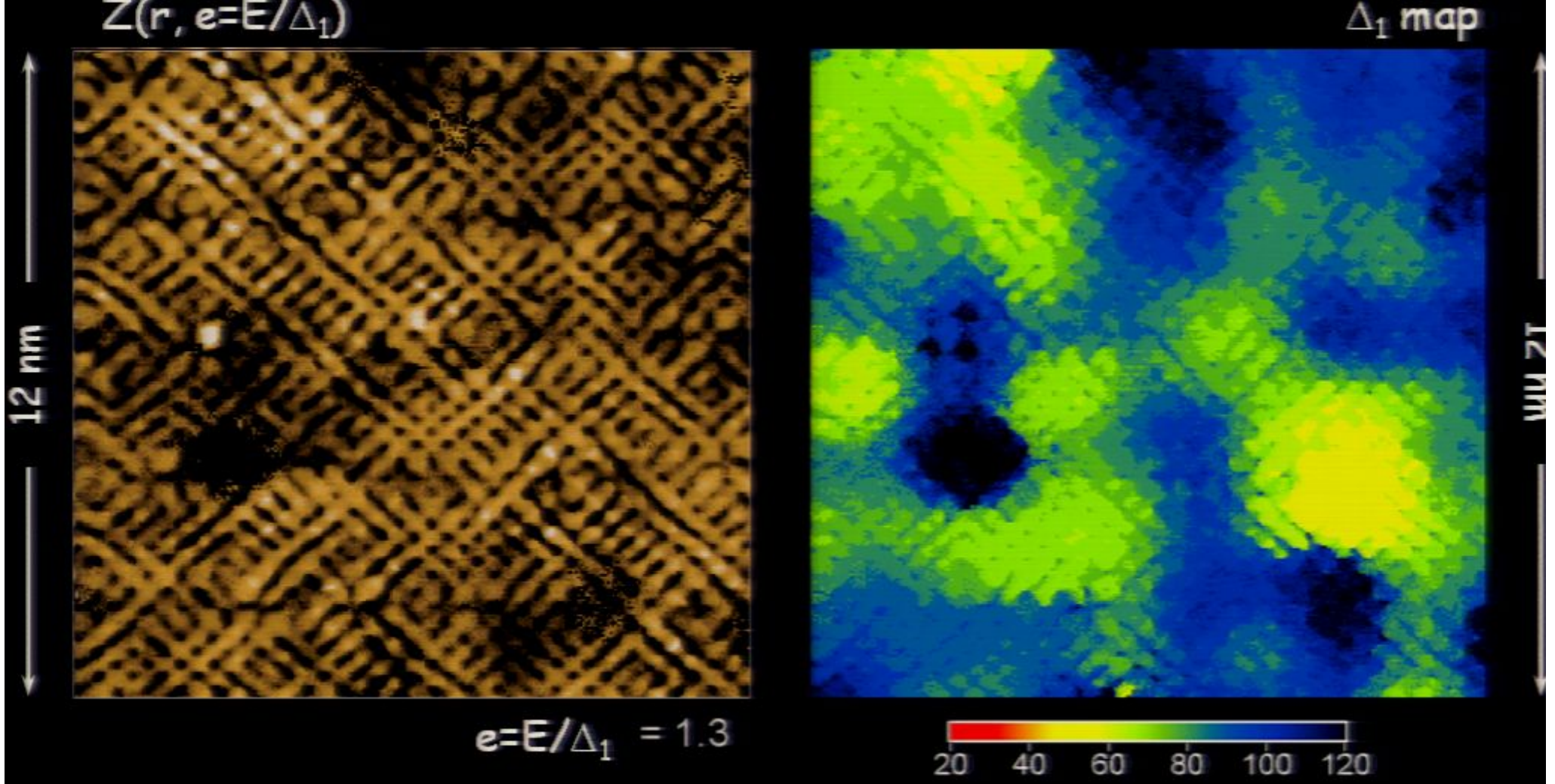

Symmetry breaking is concentrated on pseudogap states $E \sim \Delta_1$

Nature 466, 374 (2010)

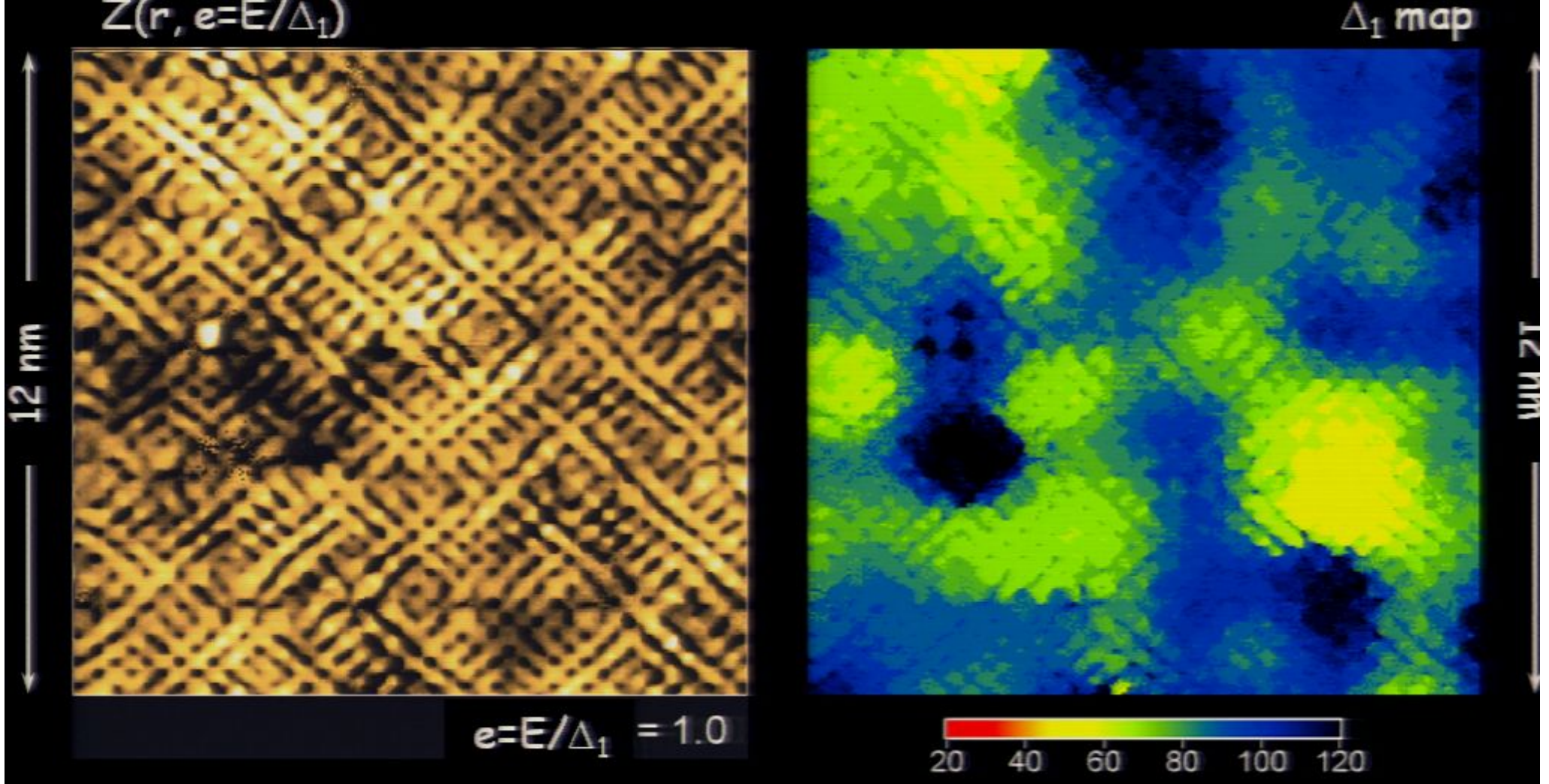

Symmetries of $E \sim \Delta_1$ states identical in SC and PG phase

Science 325, 1099 (2009)

T ~ 0 K

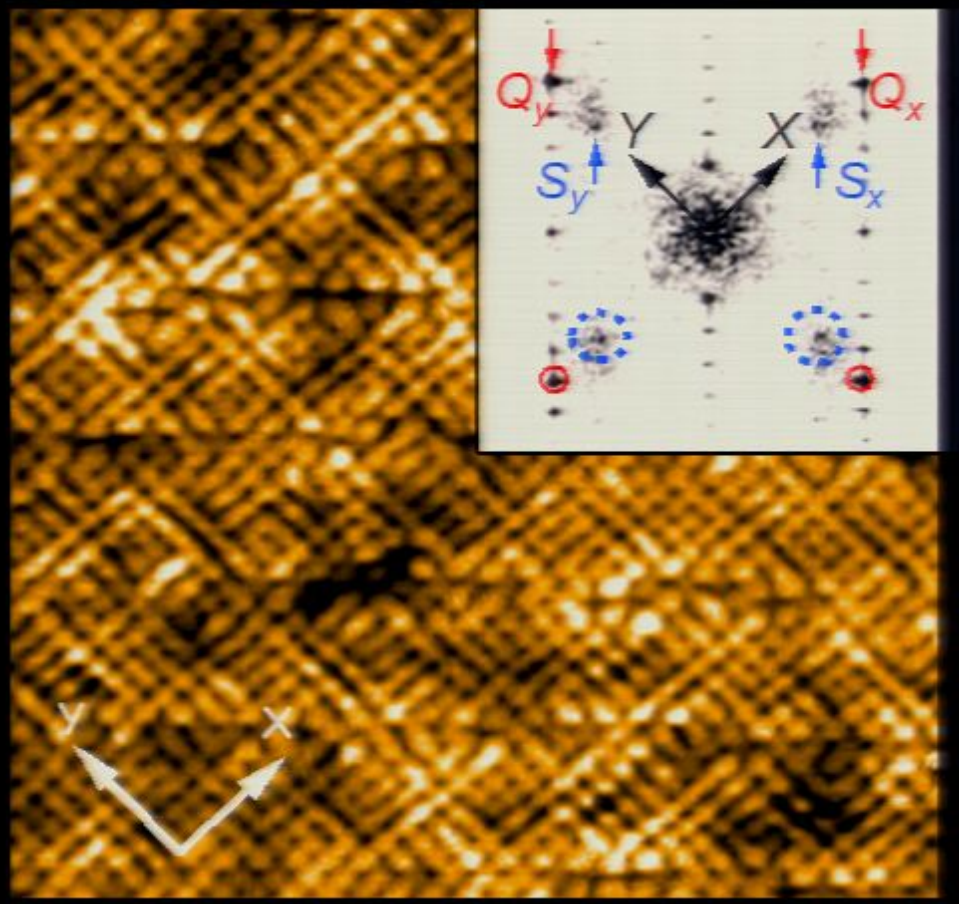

e~1

$T > T_c$

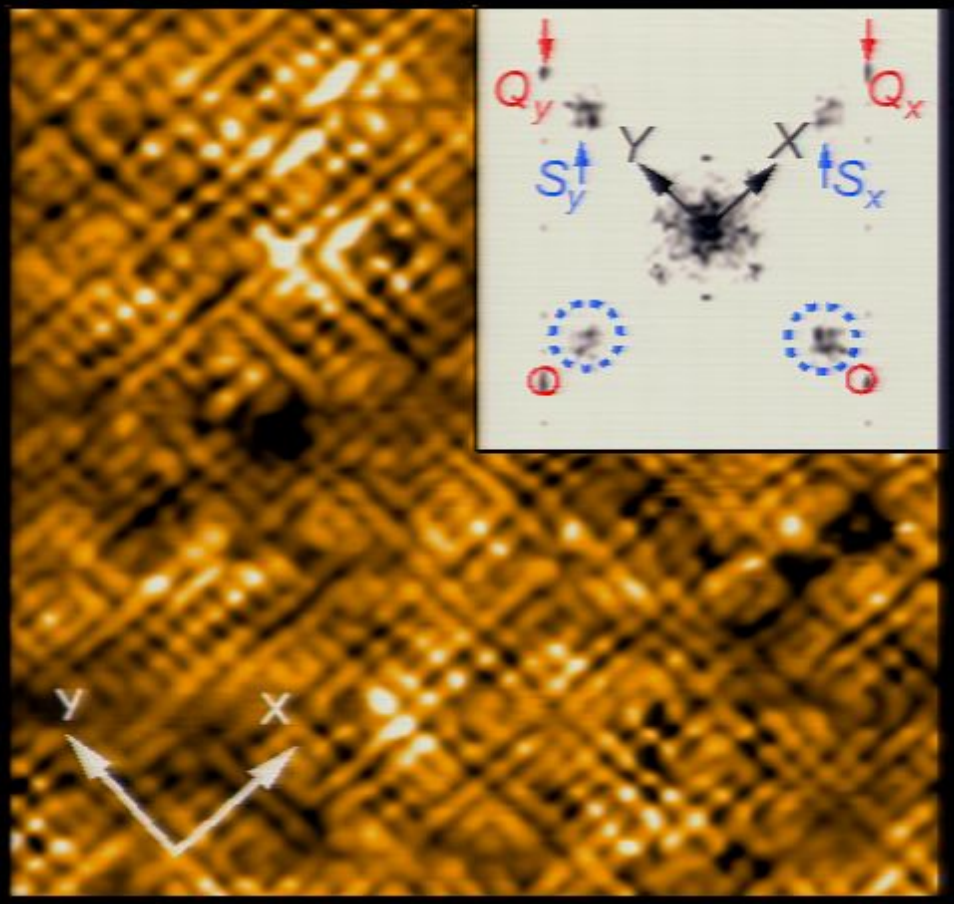

e~1

Electronic Structure of UD Cuprates

Heterogeneous, non-dispersive, broken-symmetry PG states

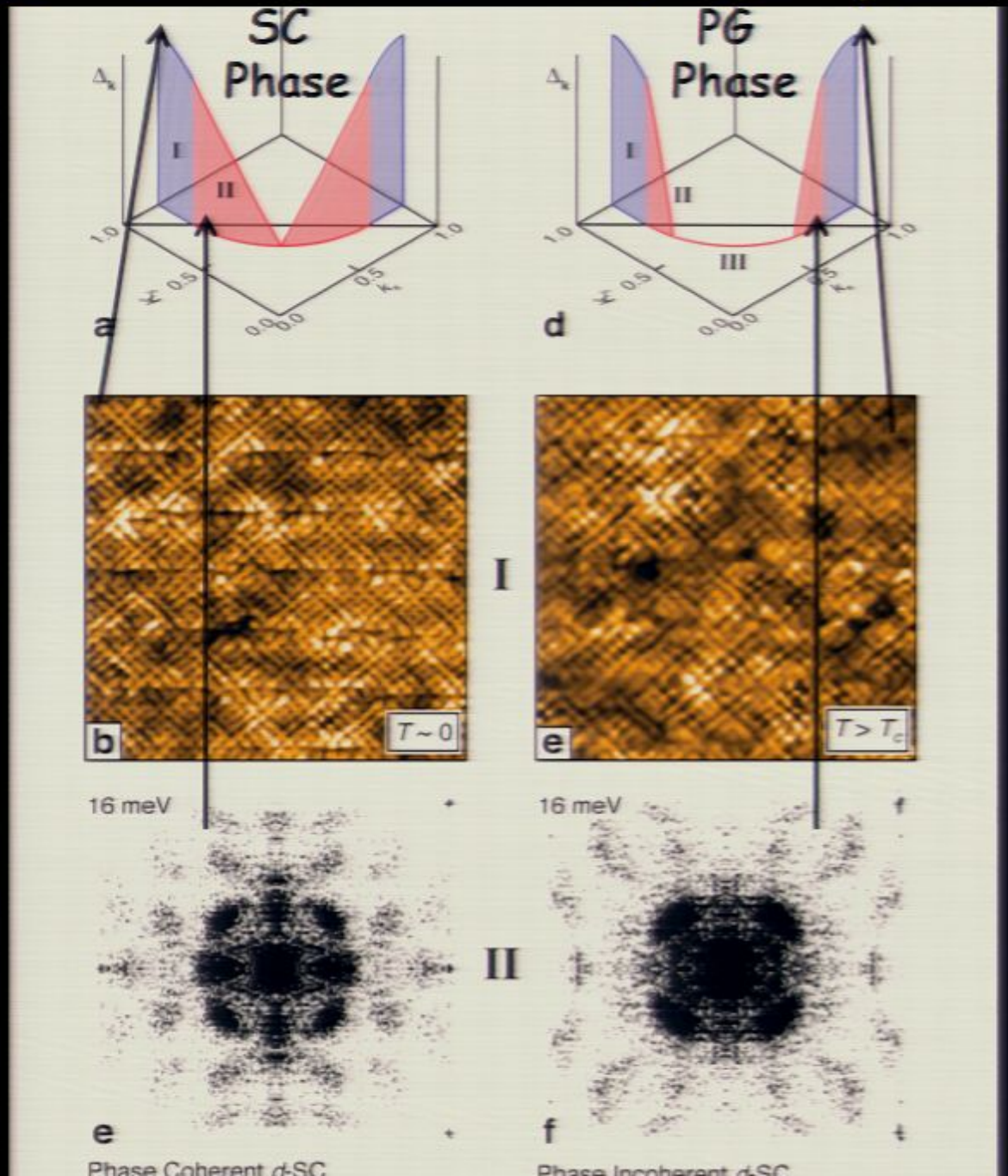

Heterogeneous, non-dispersive broken-symmetry PG states

Homogeneous, phase coherent d-wave Cooper pairs

Homogeneous, phase incoherent d-wave Cooper pairs

A. R. Schmidt

Intra-unit-cell Symmetry Breaking of Cuprate Pseudogap States

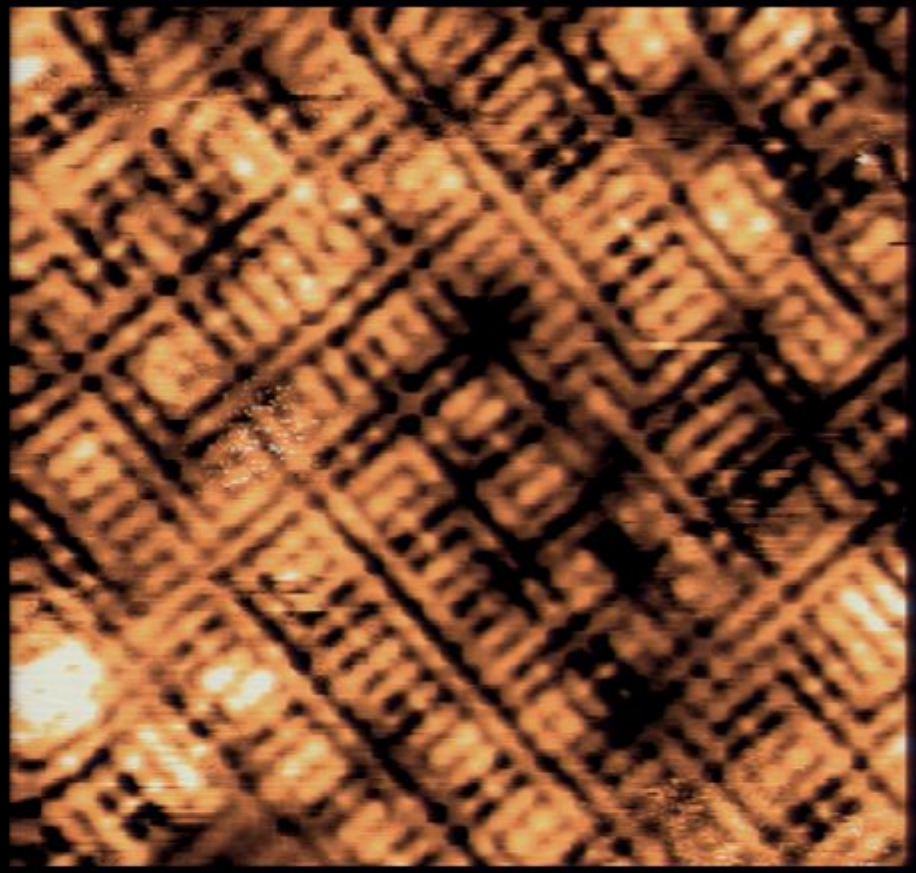

Dr. K. Fujita
Cornell
BNL

Dr. A. R. Schmidt
Cornell
Berkeley

Chung Koo Kim
Cornell
BNL

Dr. H. Eisaki
AIST

Prof. S. Uchida
U. Of Tokyo

Prof. M. J. Lawler
Cornell U.
Binghamton U.

Prof. Eun-Ah Kim
Cornell U.

Prof. J. P. Sethna
Cornell U.

Dr. Y. Kohsaka
RIKEN

Prof. H. Takagi
RIKEN

$E \sim \Delta_1$: Static electronic structure breaks spatial symmetries

Science 315, 1389 (2007); Science 325, 1099 (2009), Nature 466, 374 (2010)

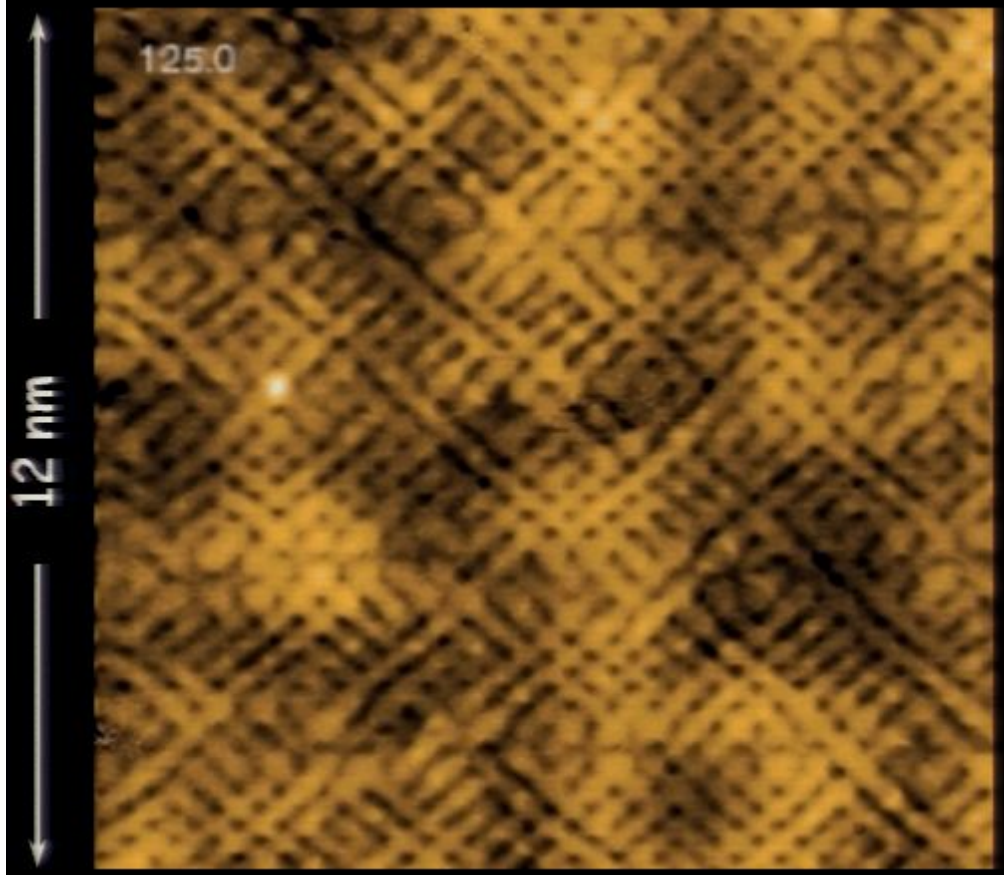

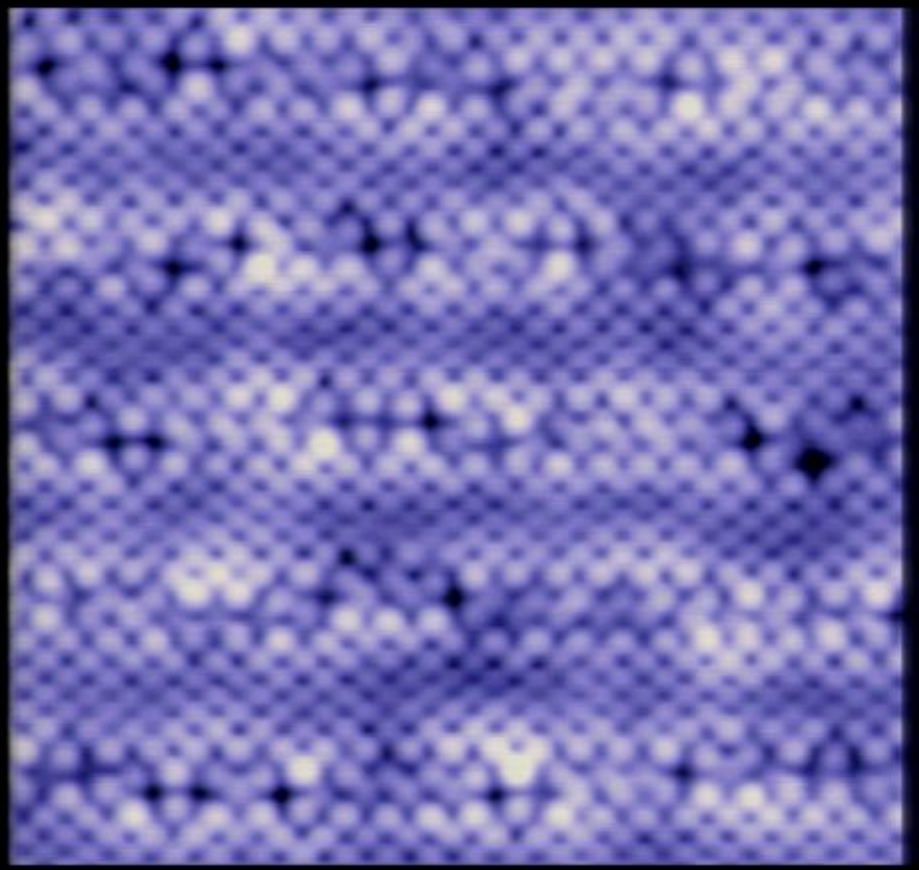

E~ Δ_1: Static electronic structure breaks spatial symmetries

Science 315, 1389 (2007); Science 325, 1099 (2009), Nature 466, 374 (2010)

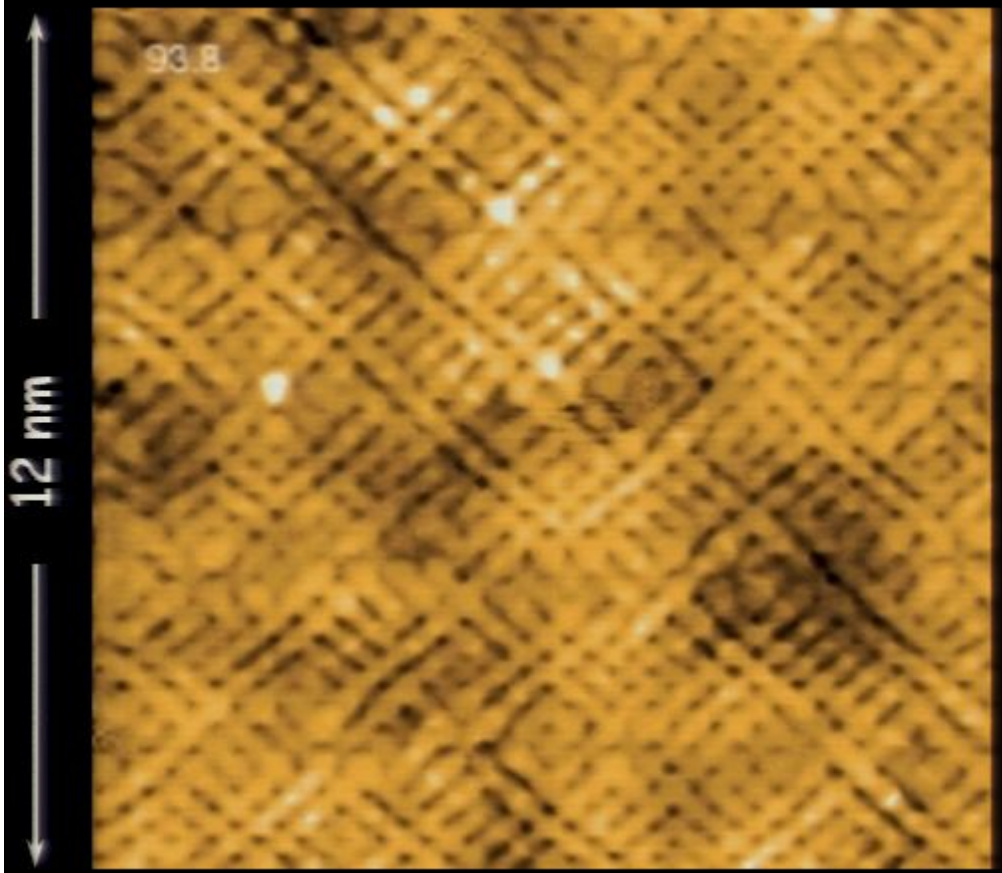

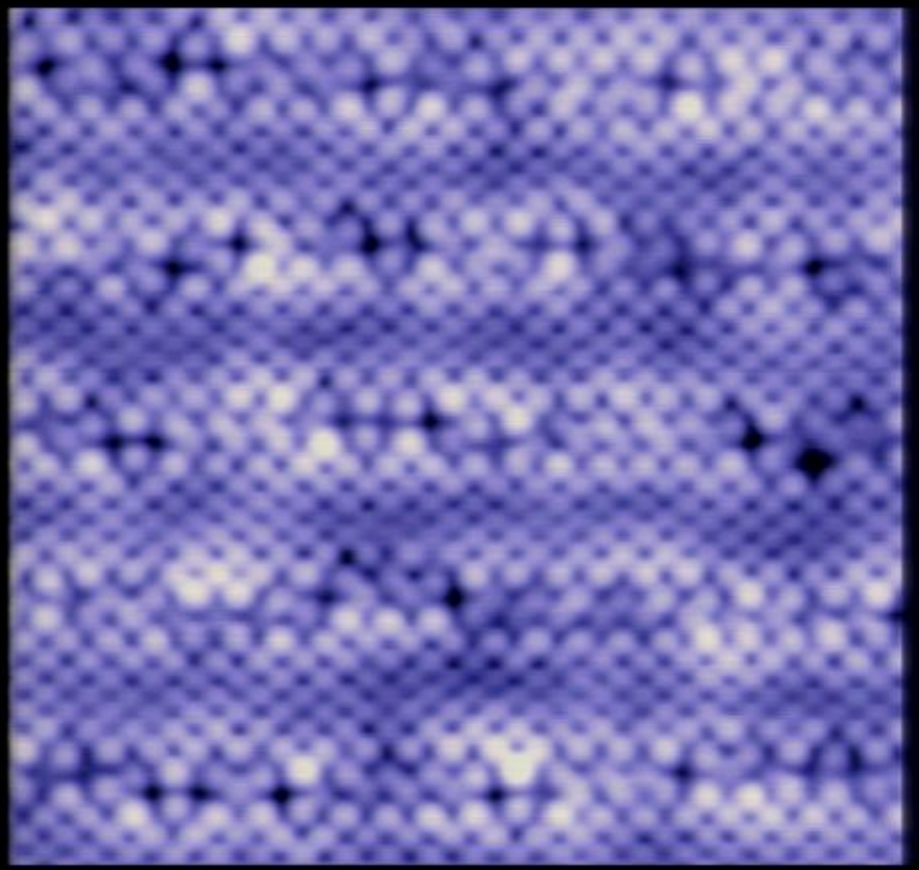

E~ Δ_1: Static electronic structure breaks spatial symmetries

Science 315, 1389 (2007)

$Ca_{1.90}Na_{0.10}CuO_2Cl_2$

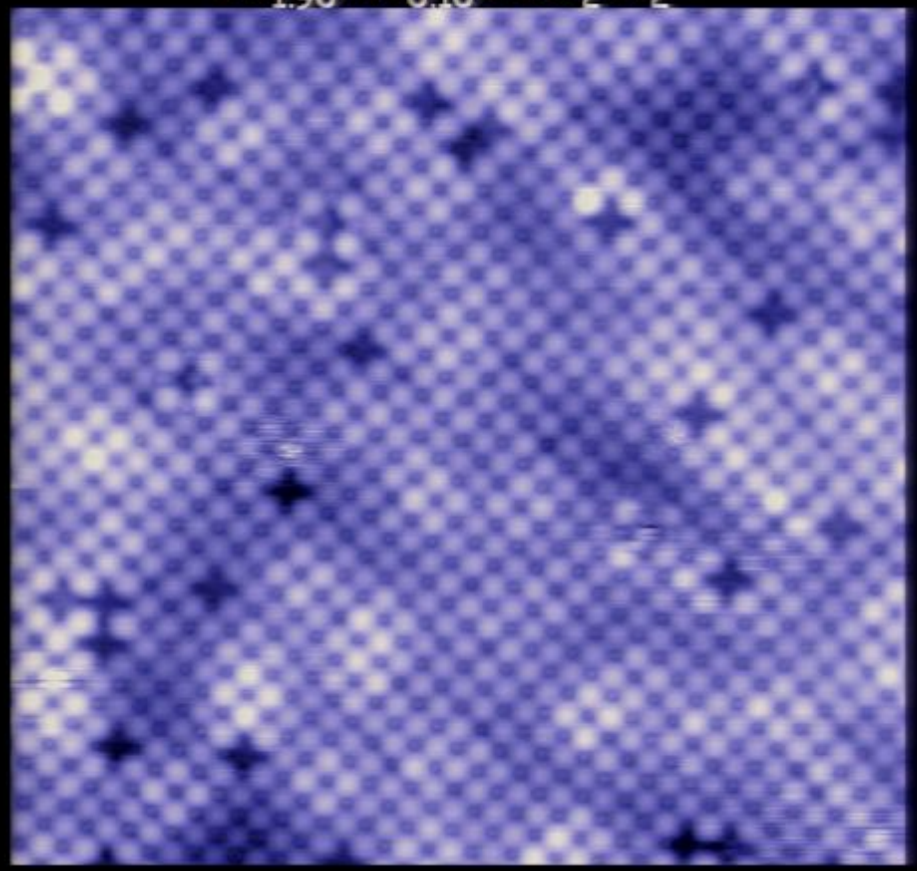

$Bi_{2.2}Sr_{1.8}Ca_{0.8}Dy_{0.2}Cu_2O_y$

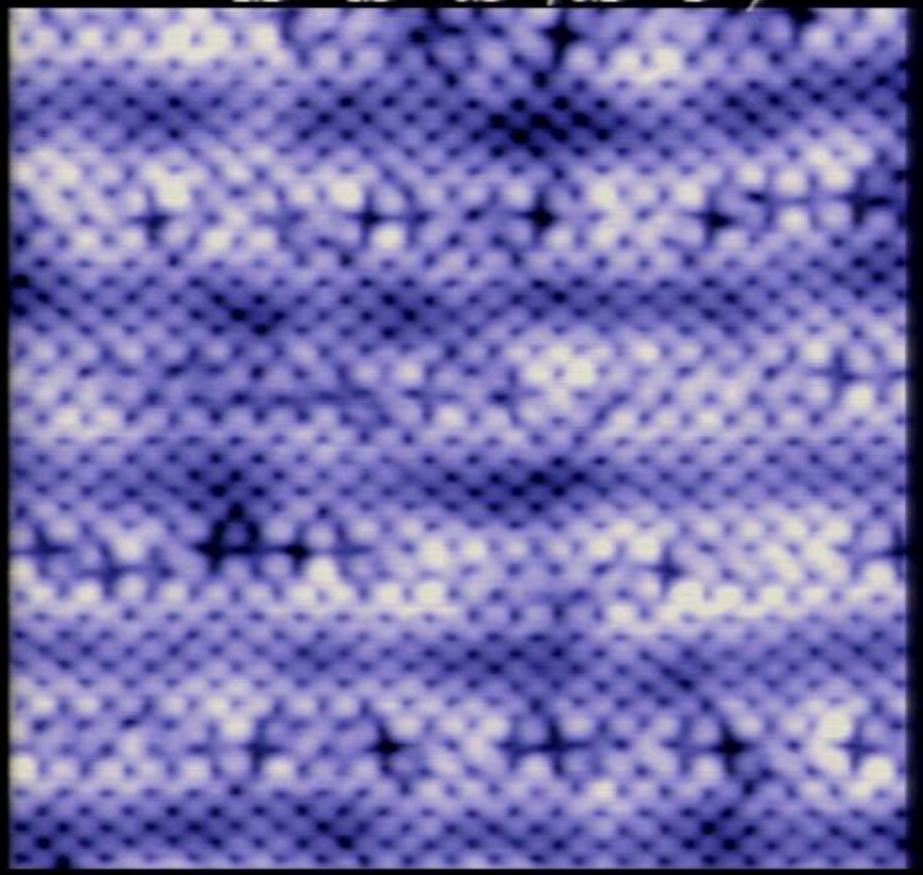

E~ Δ_1: Static electronic structure breaks spatial symmetries

Science 315, 1389 (2007); Science 325, 1099 (2009), Nature 466, 374 (2010)

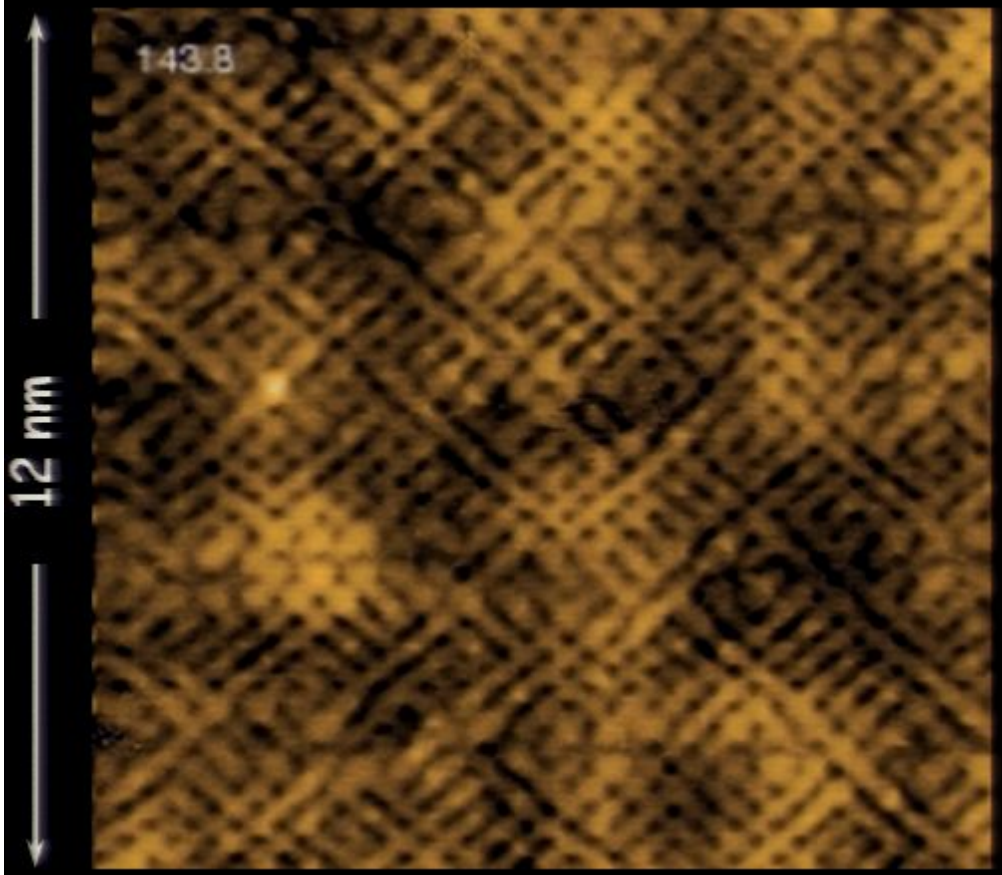

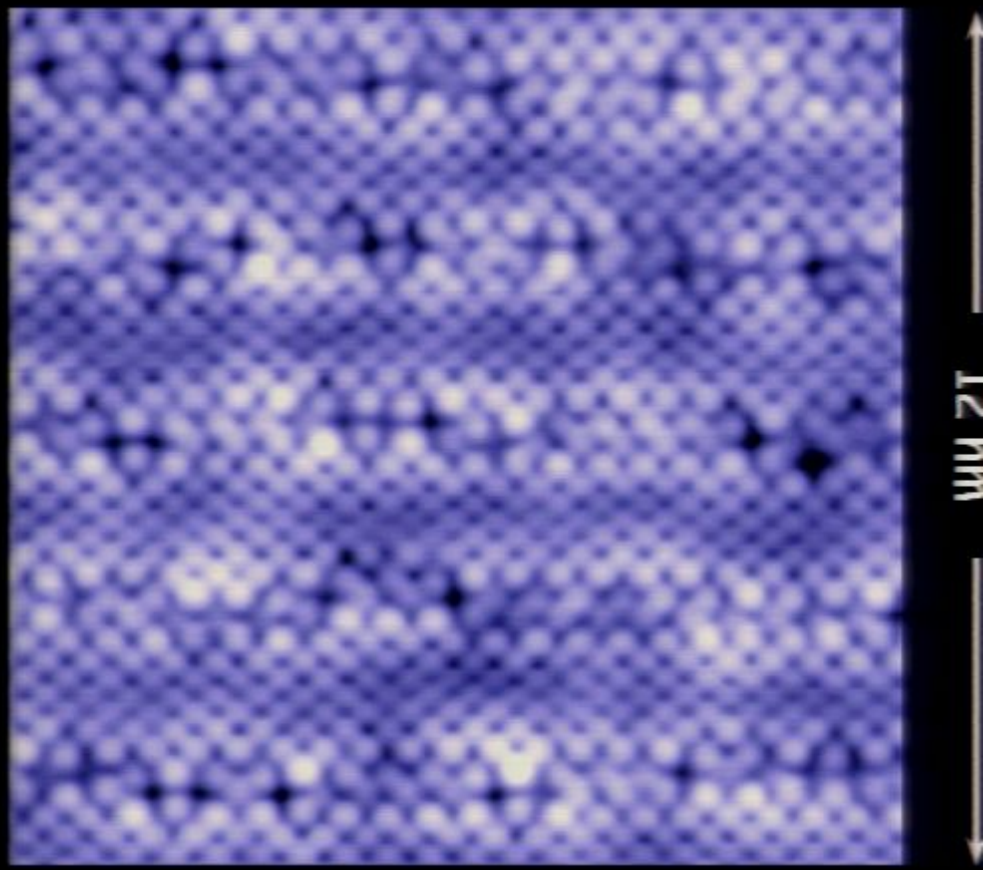

E~ Δ_1: Static electronic structure breaks spatial symmetries

Science 315, 1389 (2007); Science 325, 1099 (2009), Nature 466, 374 (2010)

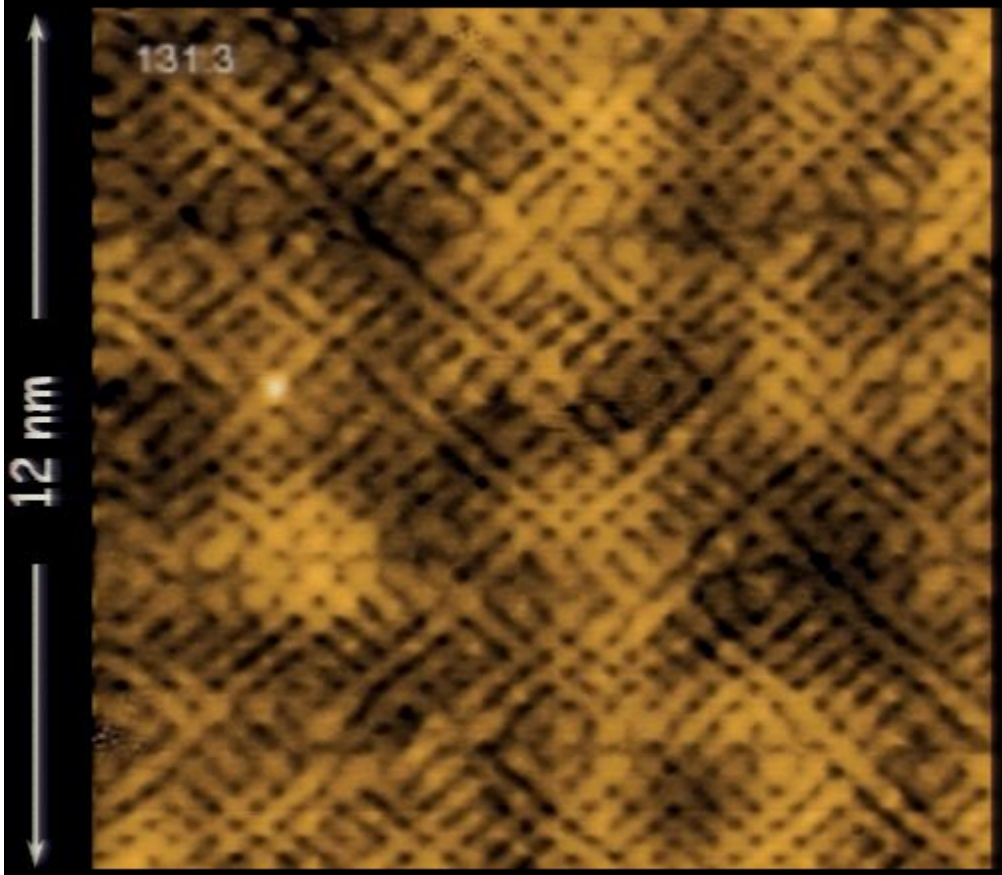

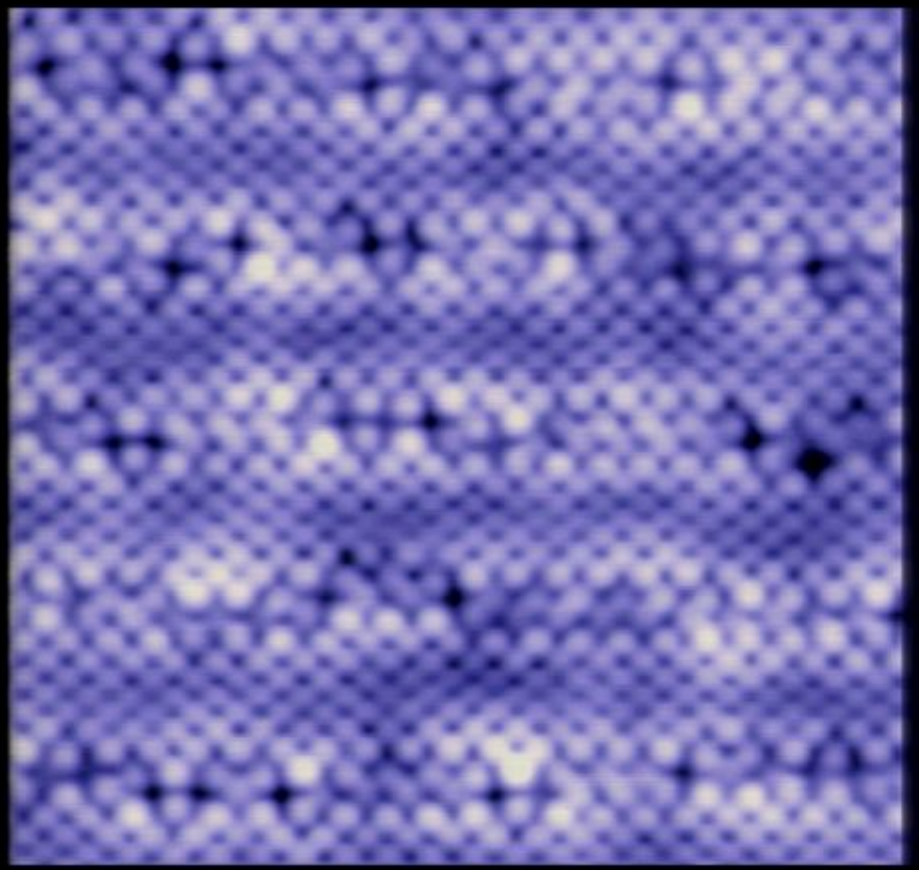

E~ Δ_1: Static electronic structure breaks spatial symmetries

Science 315, 1389 (2007); Science 325, 1099 (2009), Nature 466, 374 (2010)

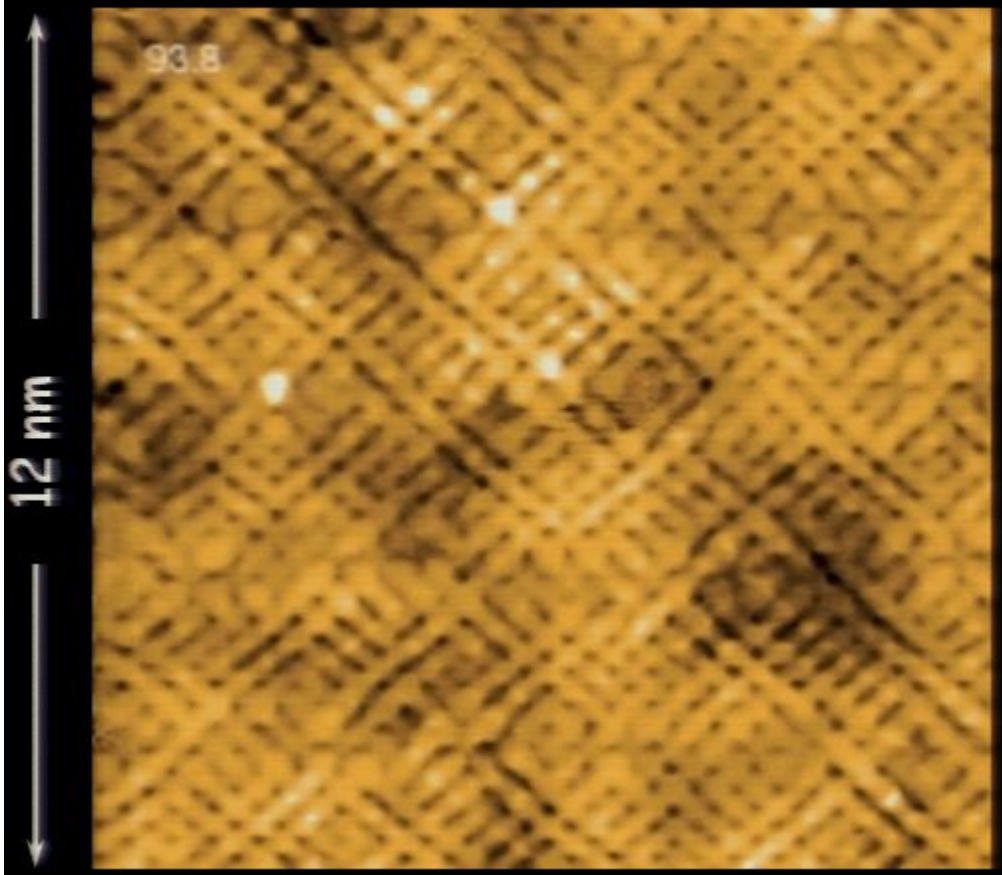

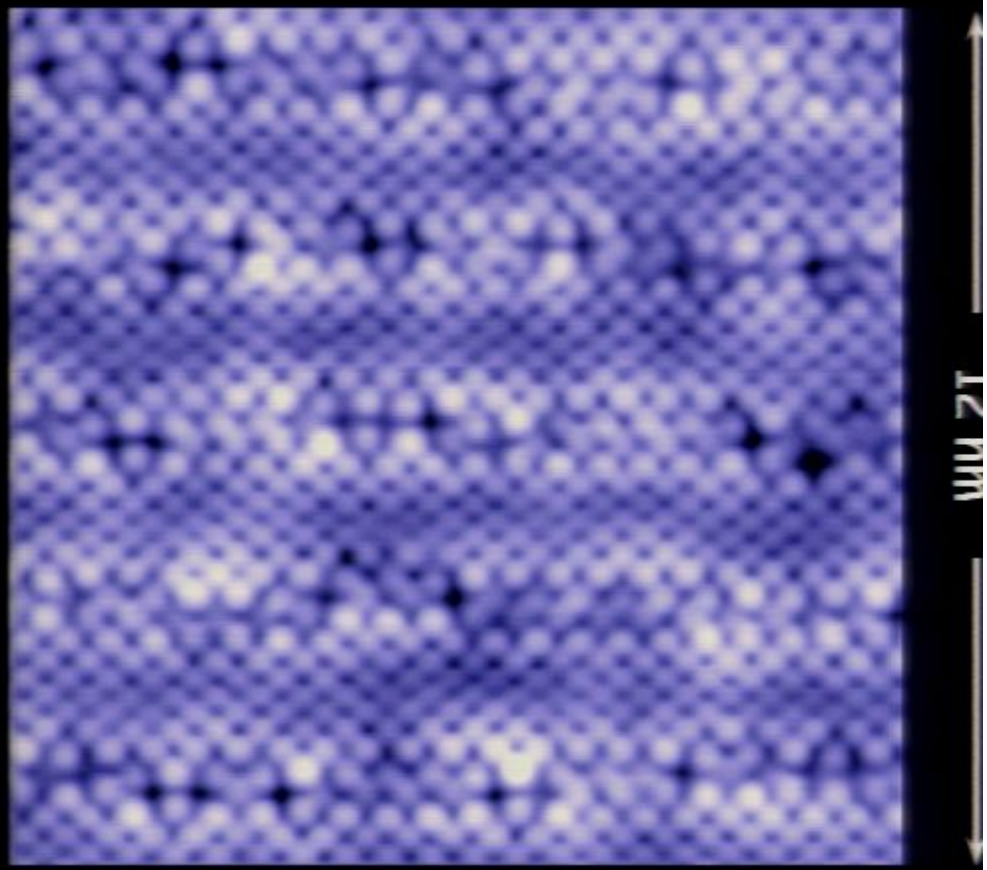

E~ Δ_1: Static electronic structure breaks spatial symmetries

Science 315, 1389 (2007); Science 325, 1099 (2009), Nature 466, 374 (2010)

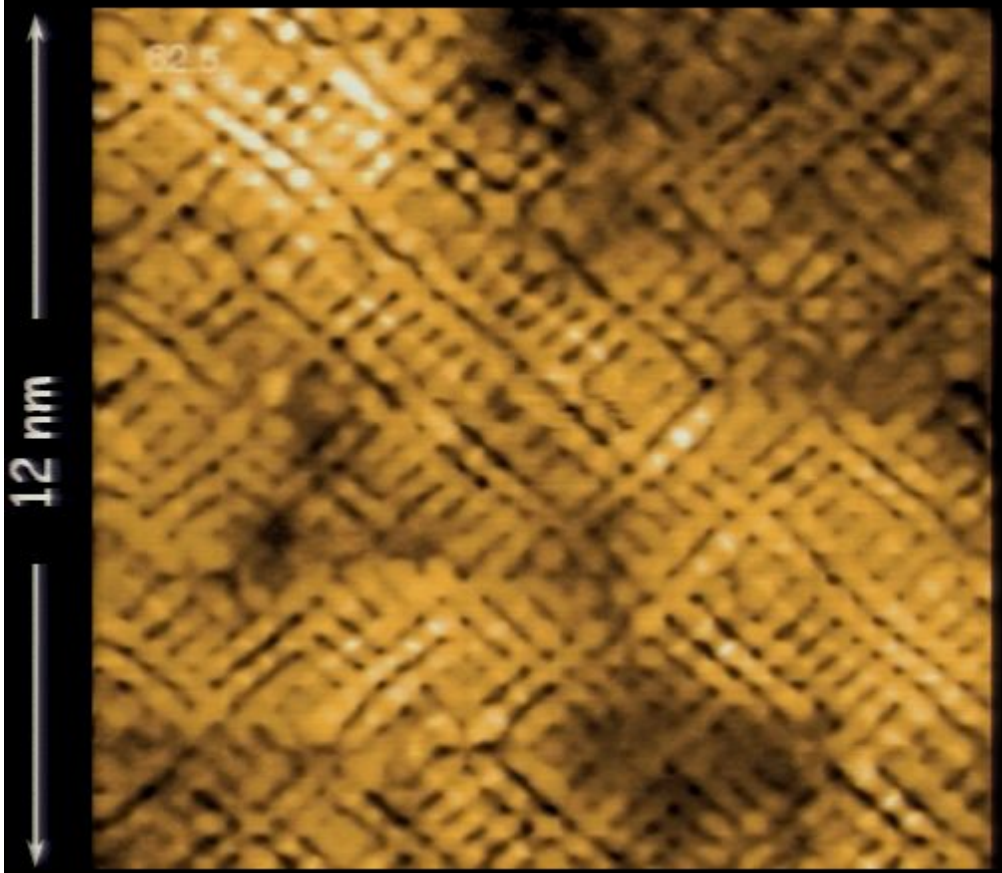

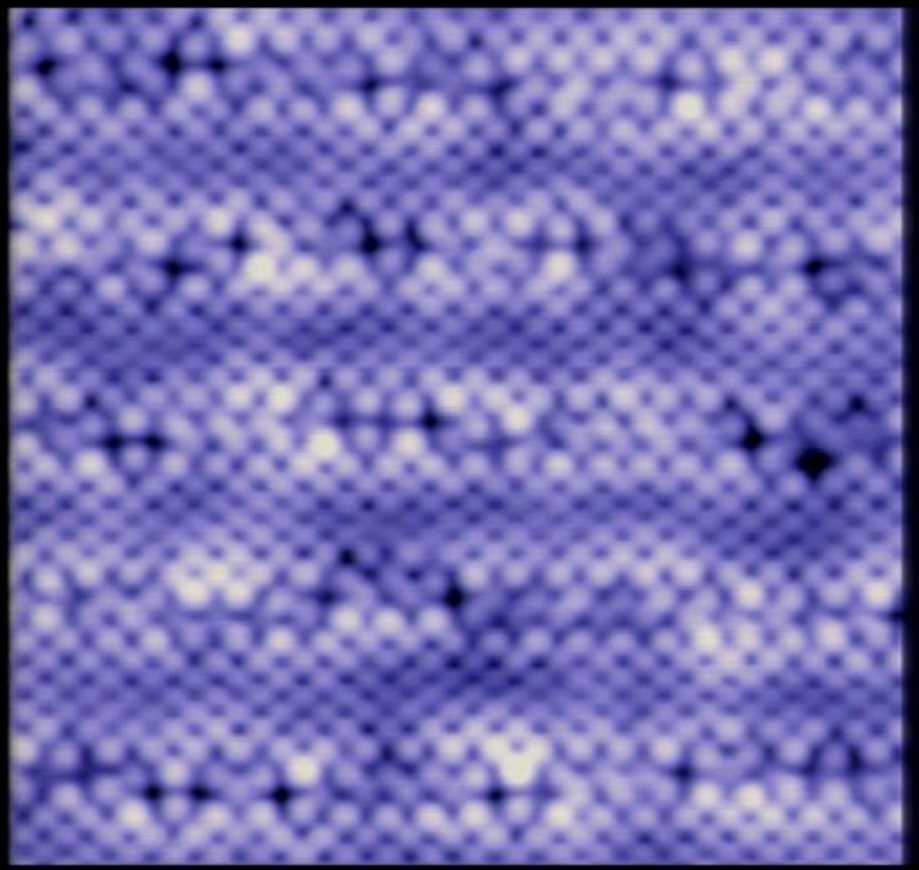

E~ Δ_1: Static electronic structure breaks spatial symmetries

Science 315, 1389 (2007); Science 325, 1099 (2009), Nature 466, 374 (2010)

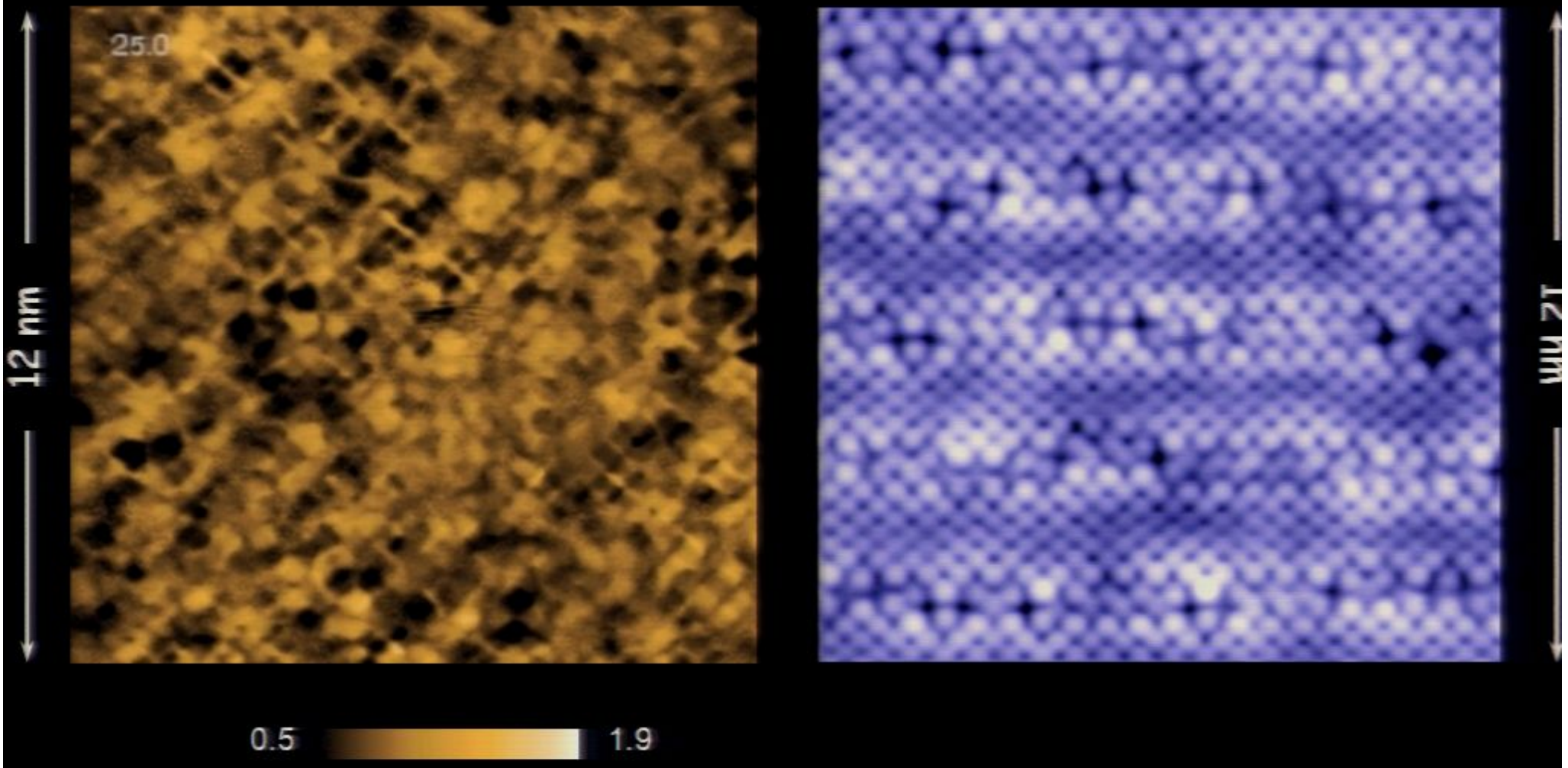

E~ Δ_1: Static electronic structure breaks spatial symmetries

Science 315, 1389 (2007)

$Ca_{1.90}Na_{0.10}CuO_2Cl_2$

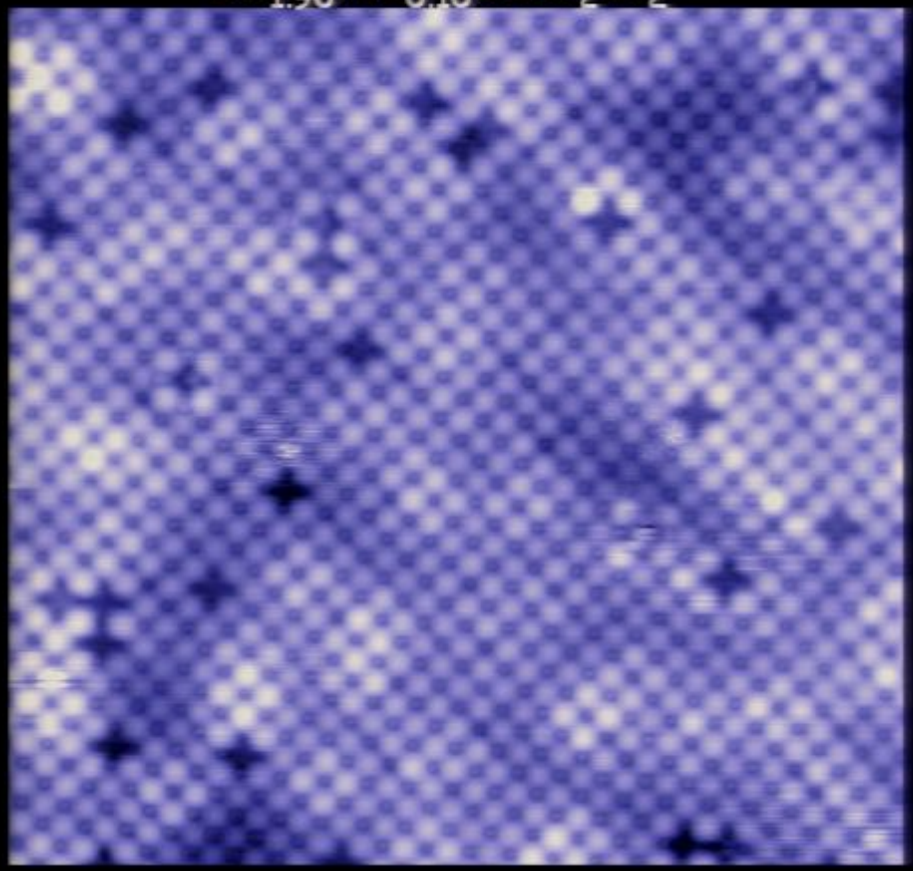

$Bi_{2.2}Sr_{1.8}Ca_{0.8}Dy_{0.2}Cu_2O_y$

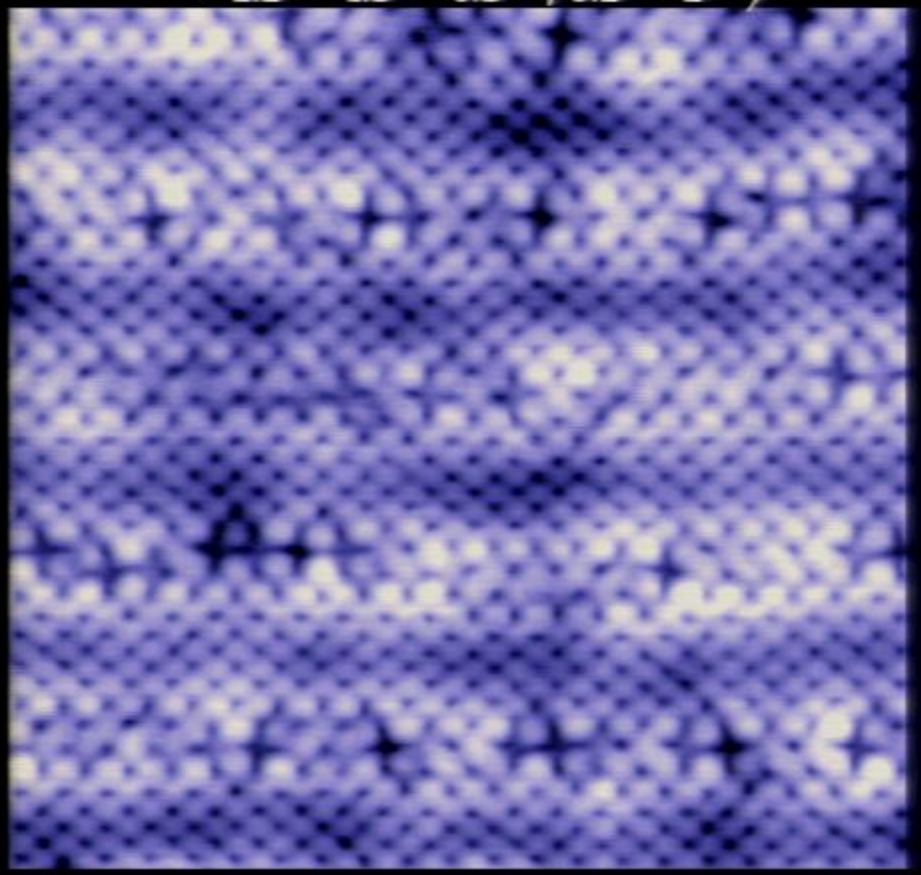

E~ Δ_1: Static electronic structure breaks spatial symmetries

Science 315, 1389 (2007)

$Ca_{1.90}Na_{0.10}CuO_2Cl_2$

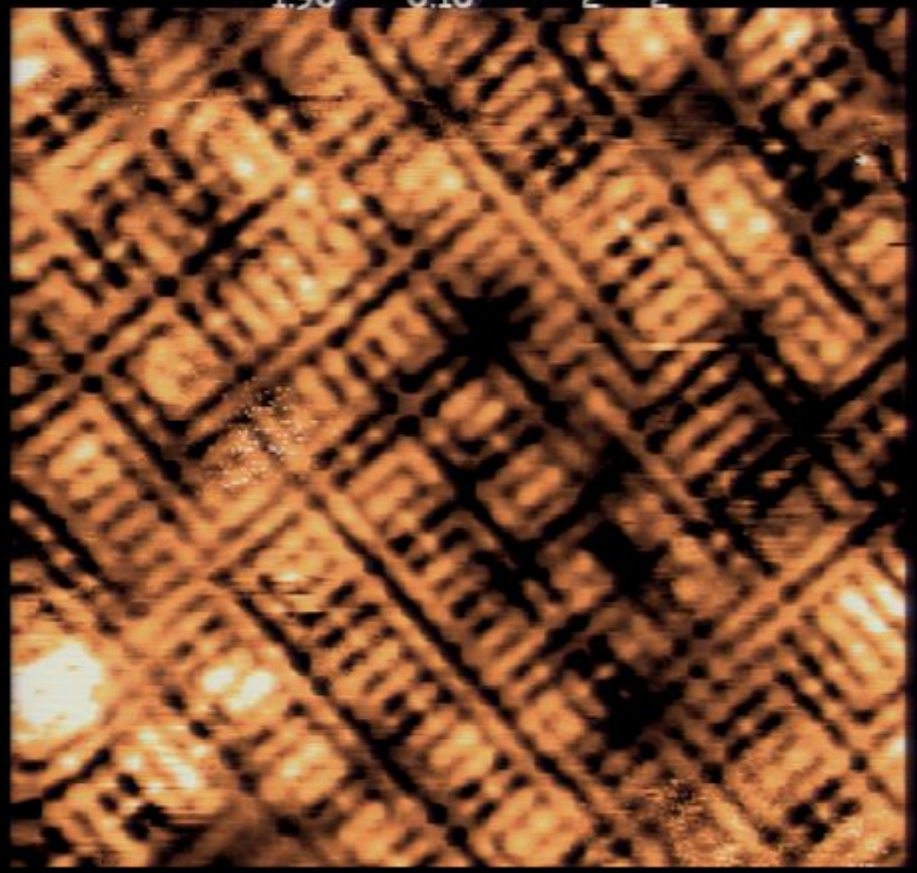

$Bi_{2.2}Sr_{1.8}Ca_{0.8}Dy_{0.2}Cu_2O_y$

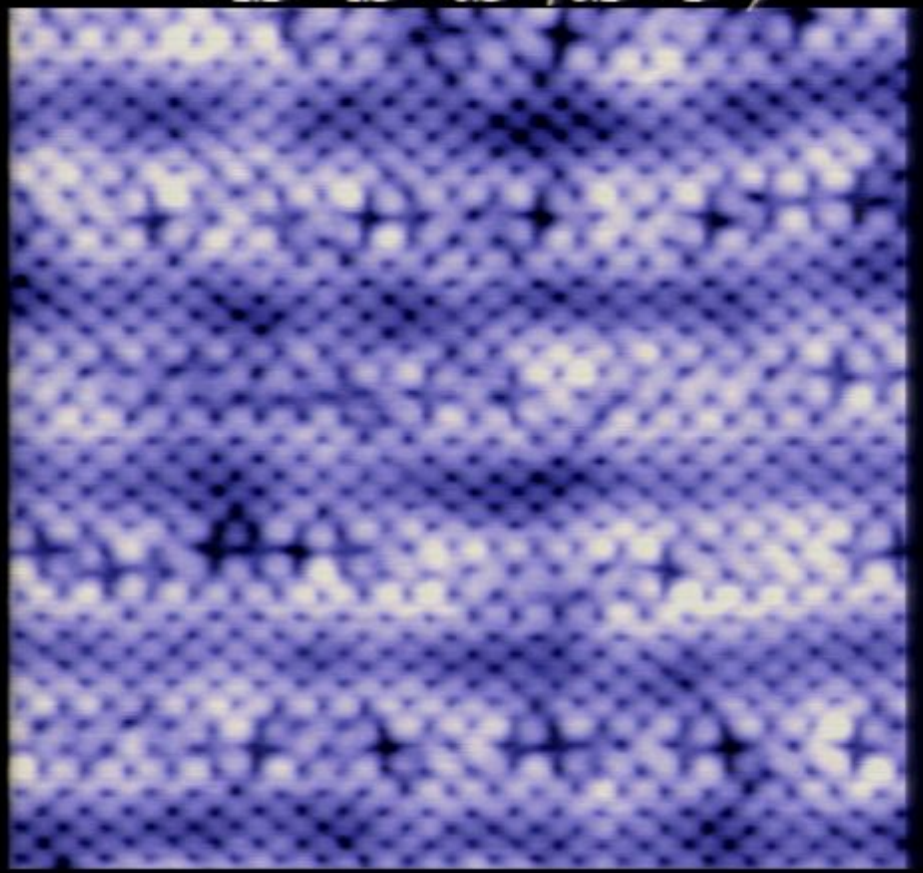

4 nm

E~ Δ_1: Static electronic structure breaks spatial symmetries

Science 315, 1389 (2007)

$Ca_{1.90}Na_{0.10}CuO_2Cl_2$

$Bi_{2.2}Sr_{1.8}Ca_{0.8}Dy_{0.2}Cu_2O_y$

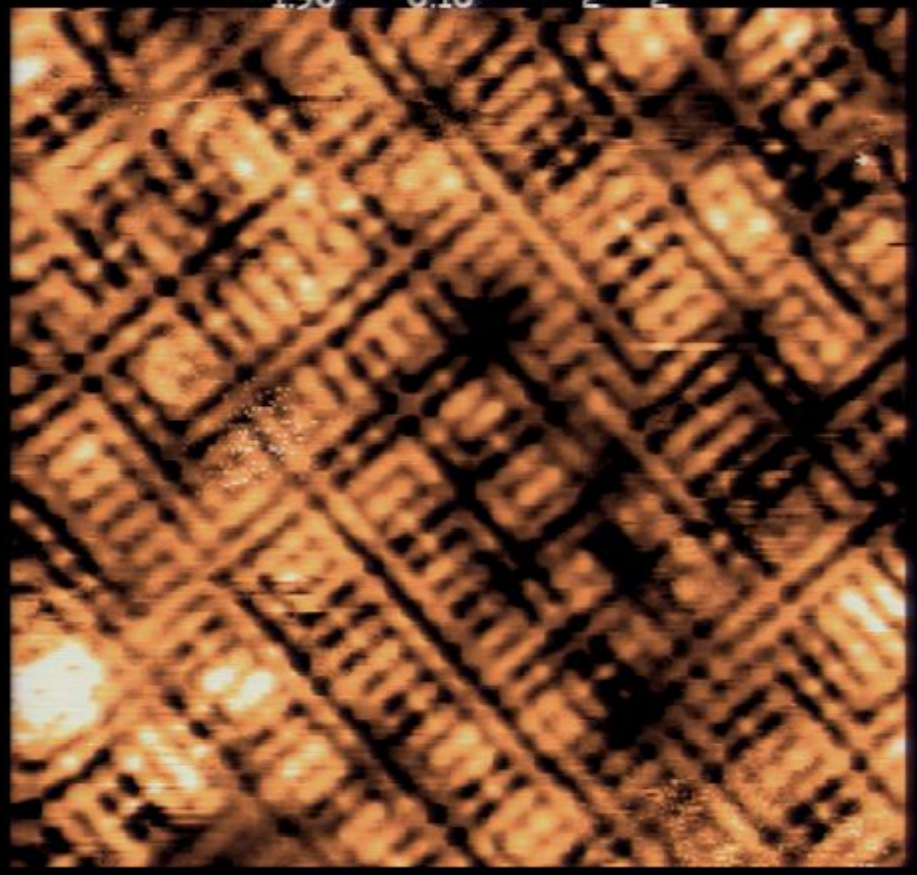

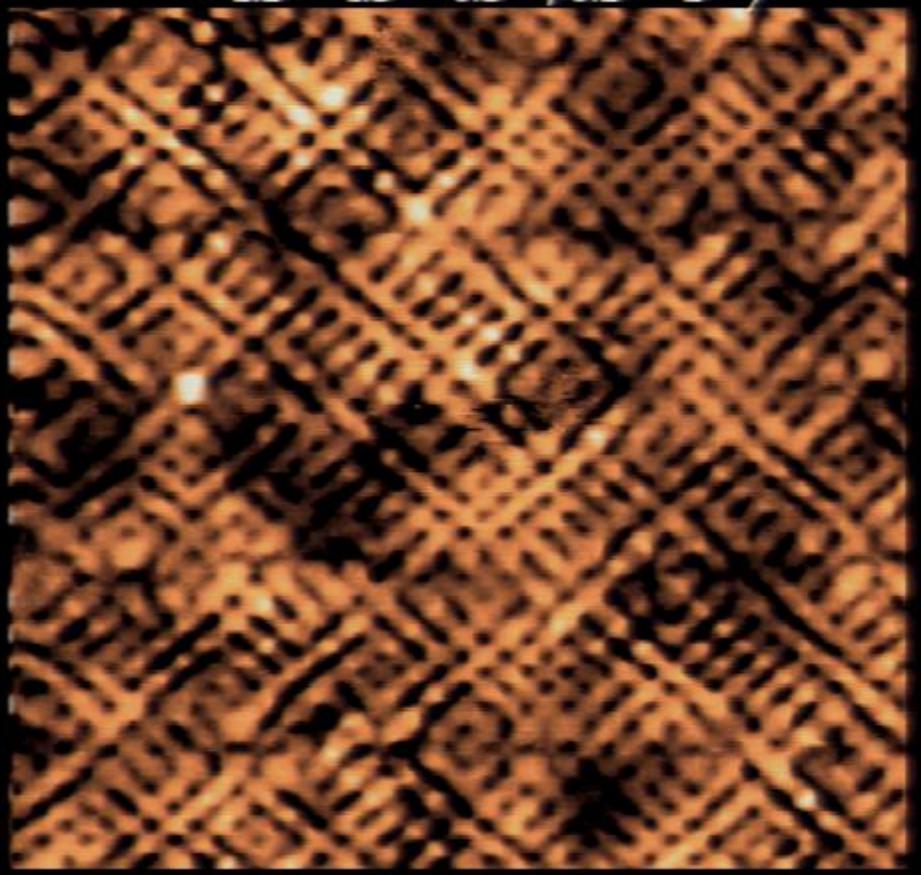

$E \sim \Delta_1$: Static electronic structure breaks spatial symmetries

Science 315, 1389 (2007)

$Ca_{1.90}Na_{0.10}CuO_2Cl_2$

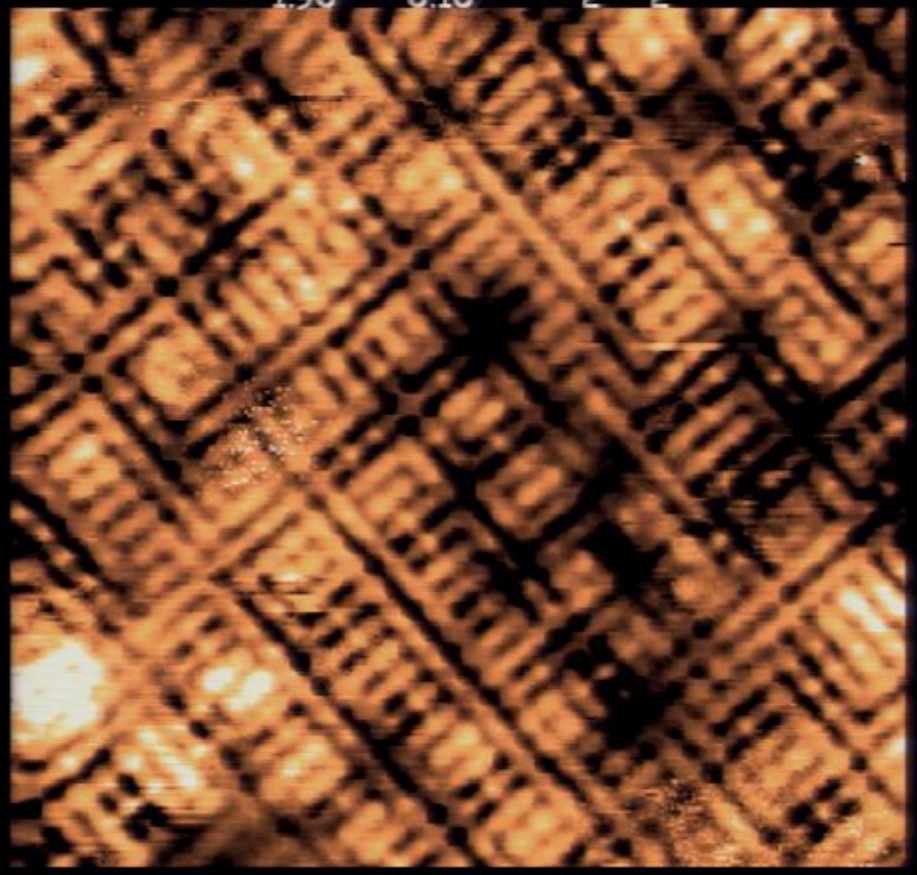

$Bi_{2.2}Sr_{1.8}Ca_{0.8}Dy_{0.2}Cu_2O_y$

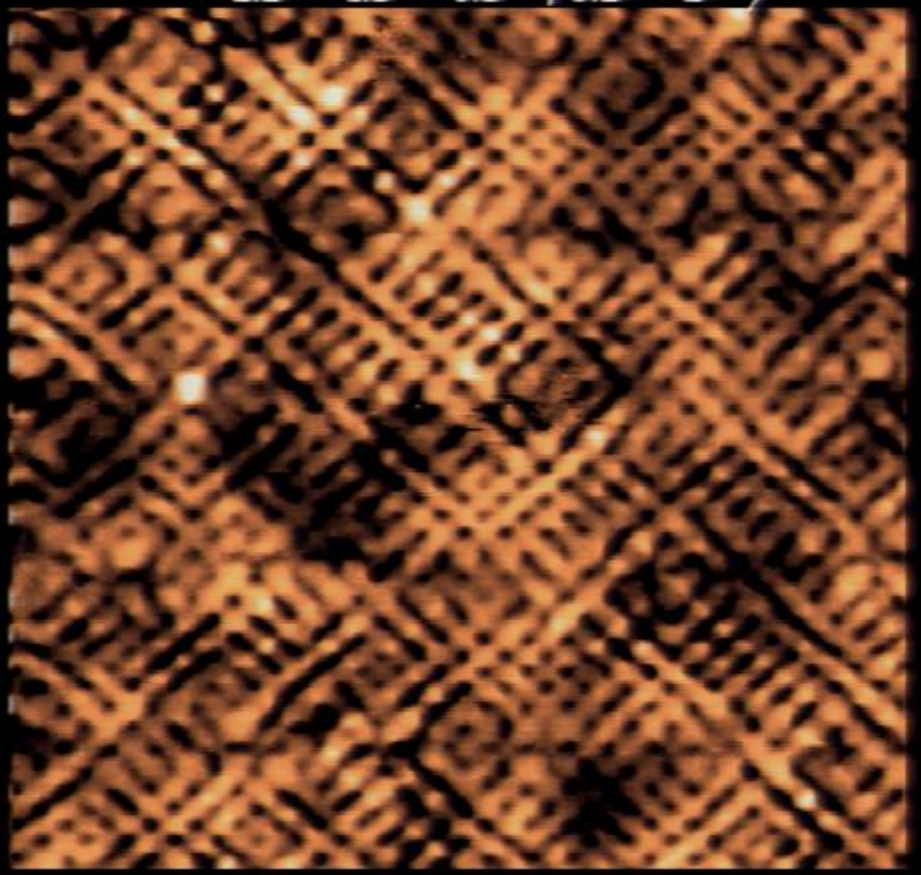

12 nm

Independent of crystal surface, cleave layer, matrix element, dopant=>

broken spatial symmetries are property of CuO_2 plane electronic structure only

Intra-unit-cell C_4-breaking at $E \sim \Delta_1$

Science 315, 1389 (2007); Science 325, 1099 (2009), Nature 466, 374 (2010)

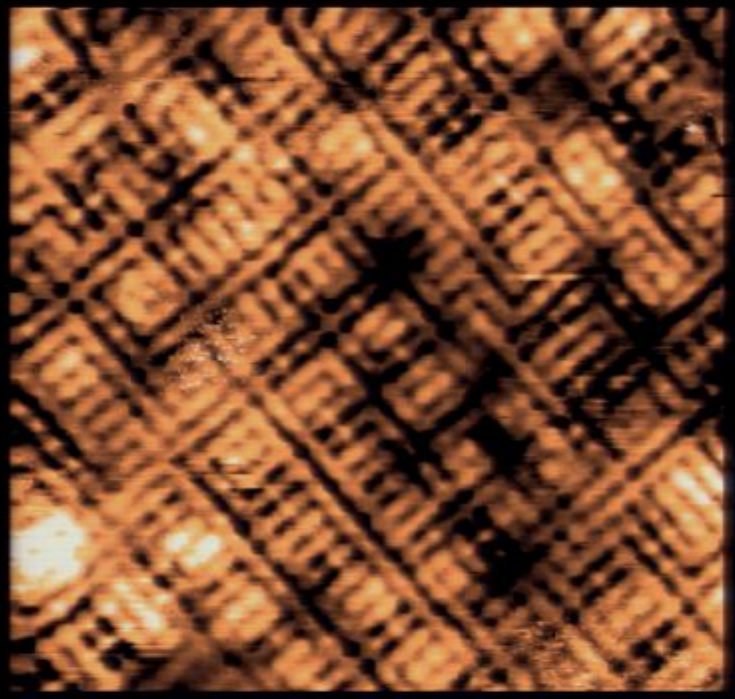

12 nm

Intra-unit-cell C_4-breaking at $E \sim \Delta_1$

Science 315, 1389 (2007); Science 325, 1099 (2009), Nature 466, 374 (2010)

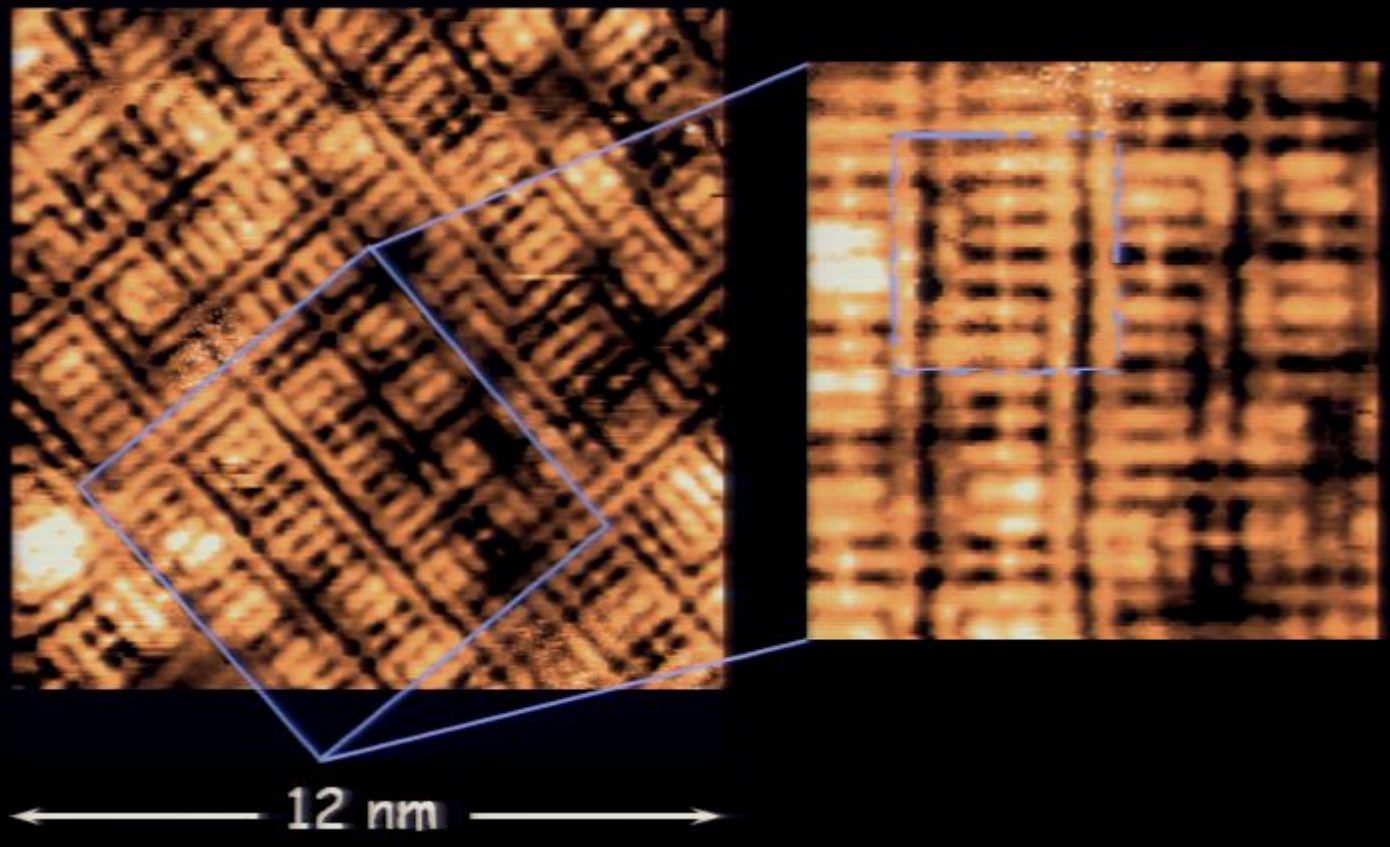

Intra-unit-cell C_4-breaking at $E \sim \Delta_1$

Science 315, 1389 (2007); Science 325, 1099 (2009), Nature 466, 374 (2010)

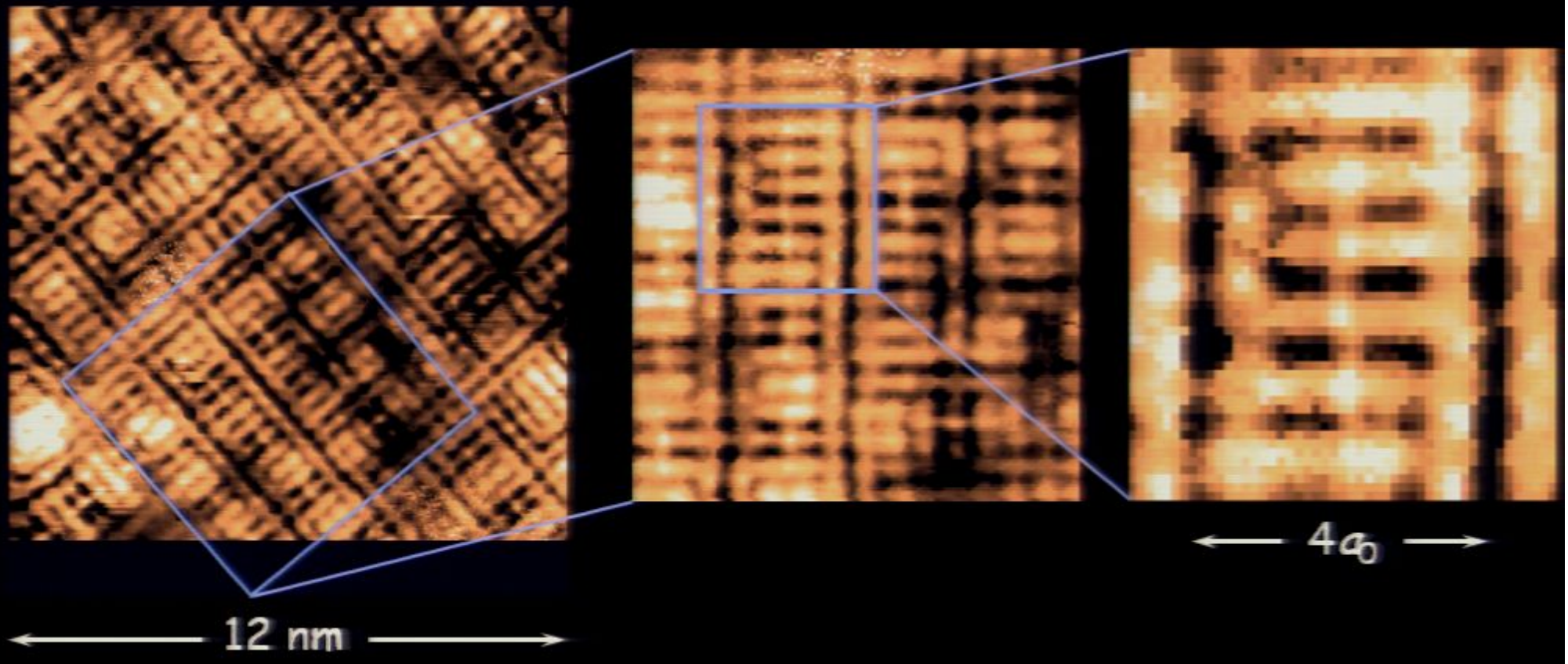

Intra-unit-cell C_4-breaking at $E \sim \Delta_1$

Science 315, 1389 (2007); Science 325, 1099 (2009), Nature 466, 374 (2010)

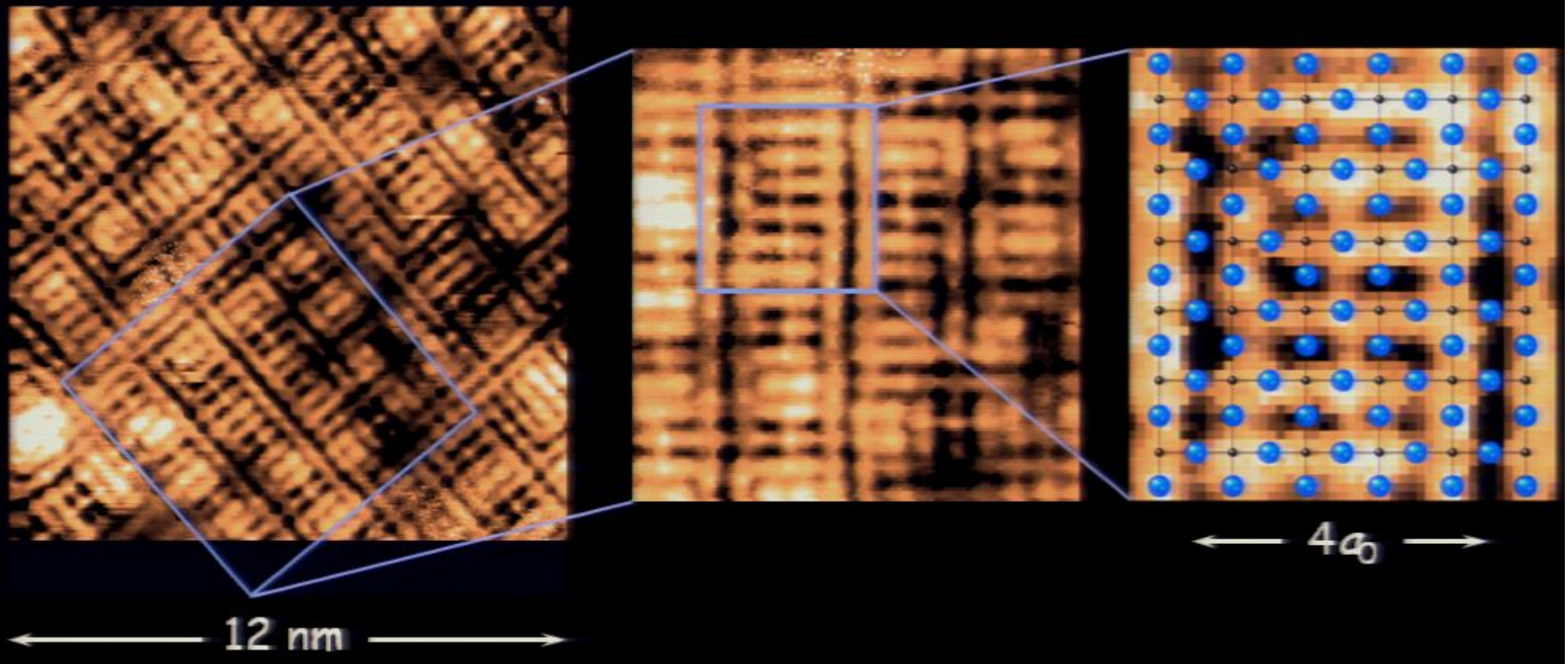

Intra-unit-cell C_4-breaking at $E \sim \Delta_1$

Science 315, 1389 (2007); Science 325, 1099 (2009), Nature 466, 374 (2010)

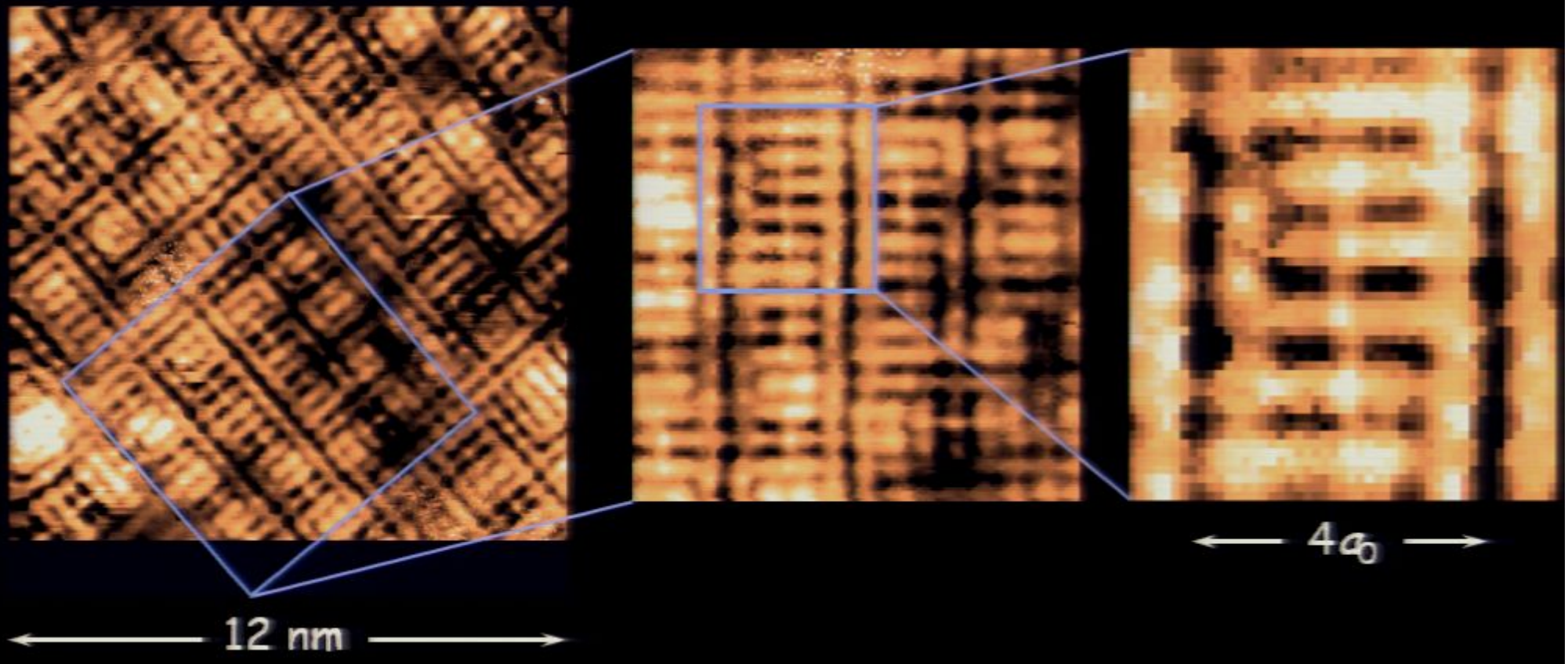

Intra-unit-cell C_4-breaking at $E \sim \Delta_1$

Science 315, 1389 (2007); Science 325, 1099 (2009), Nature 466, 374 (2010)

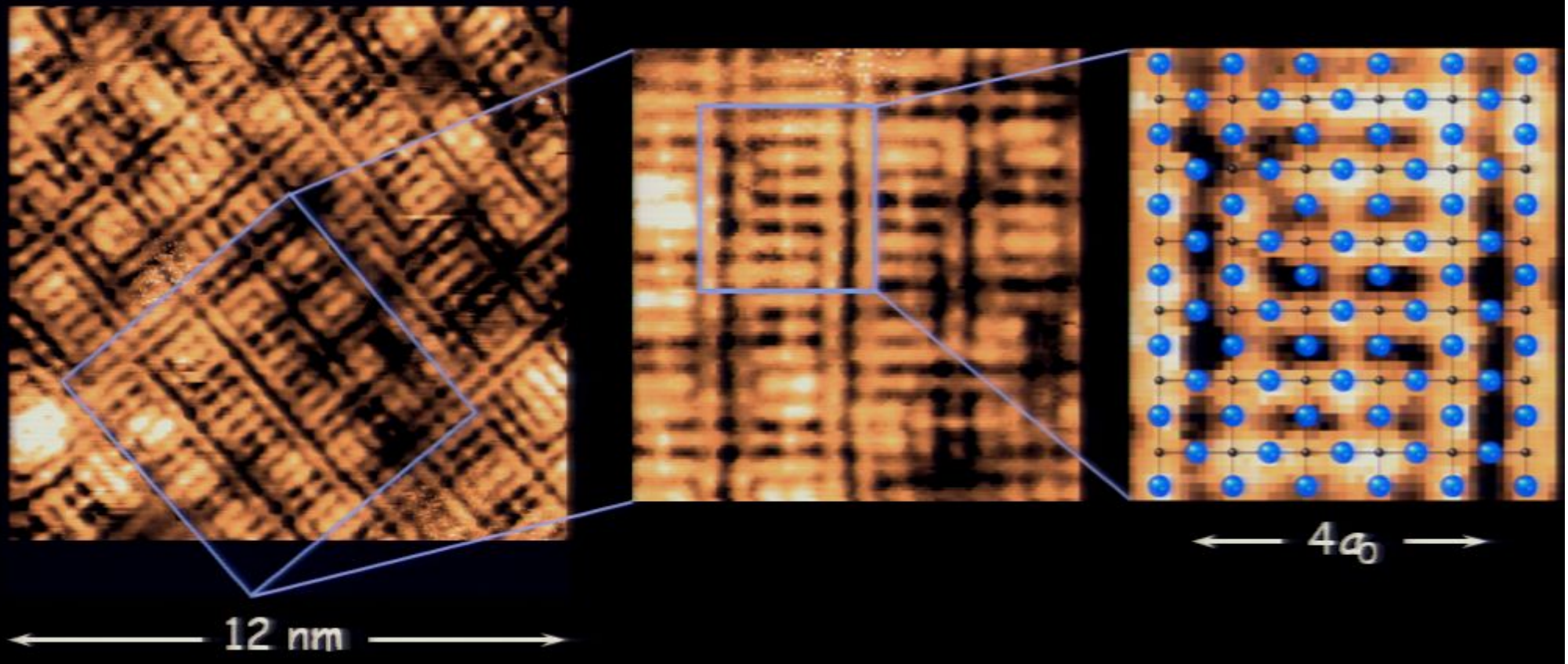

Intra-unit-cell C_4-breaking at $E \sim \Delta_1$

Science 315, 1389 (2007); Science 325, 1099 (2009), Nature 466, 374 (2010)

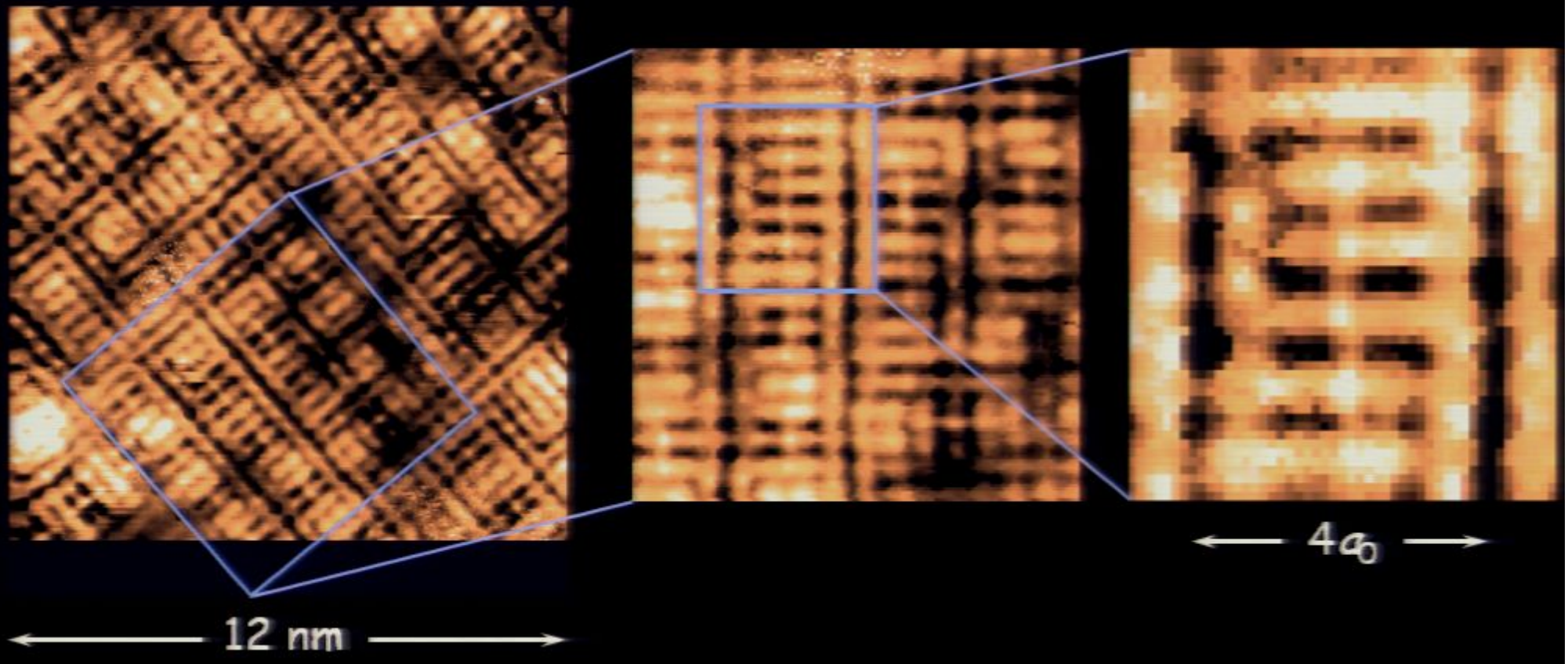

Intra-unit-cell C_4-breaking at $E \sim \Delta_1$

Science 315, 1389 (2007); Science 325, 1099 (2009), Nature 466, 374 (2010)

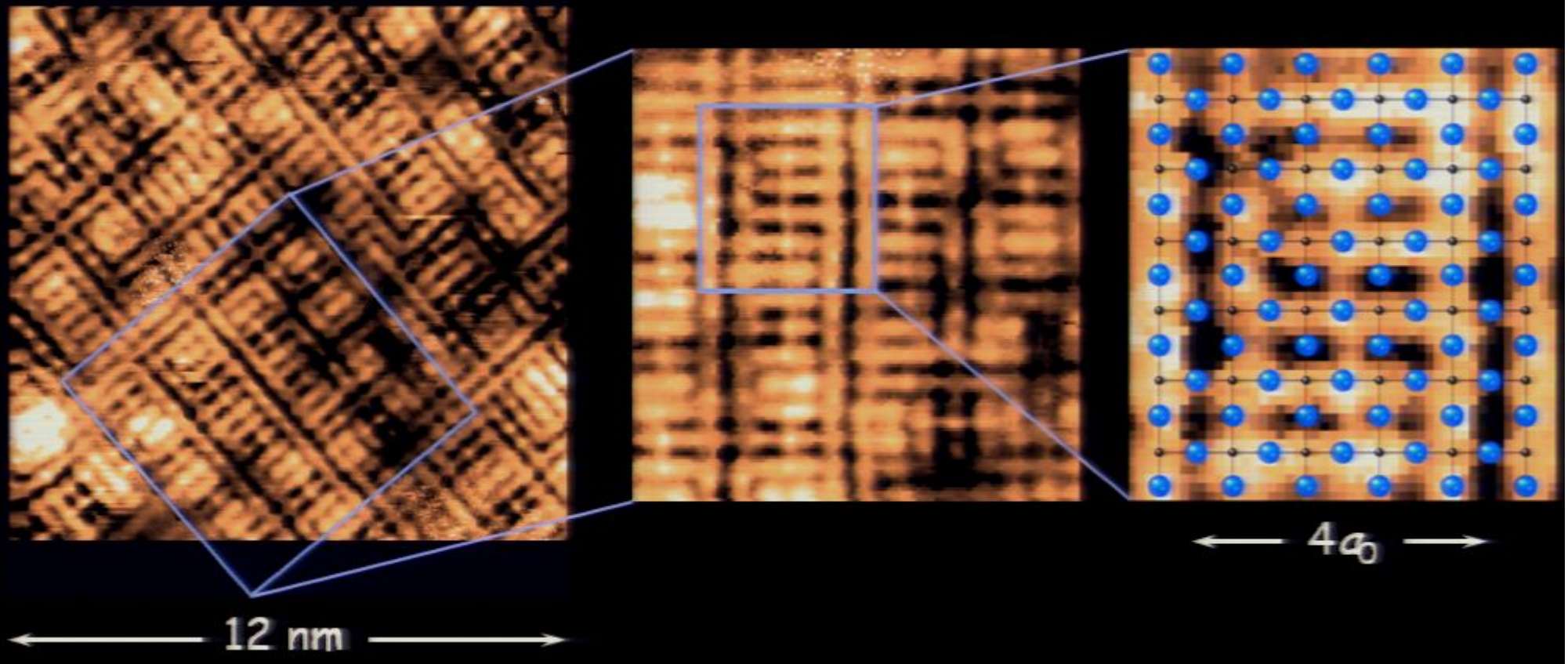

Intra-unit-cell C_4-breaking at $E \sim \Delta_1$

Science 315, 1389 (2007); Science 325, 1099 (2009), Nature 466, 374 (2010)

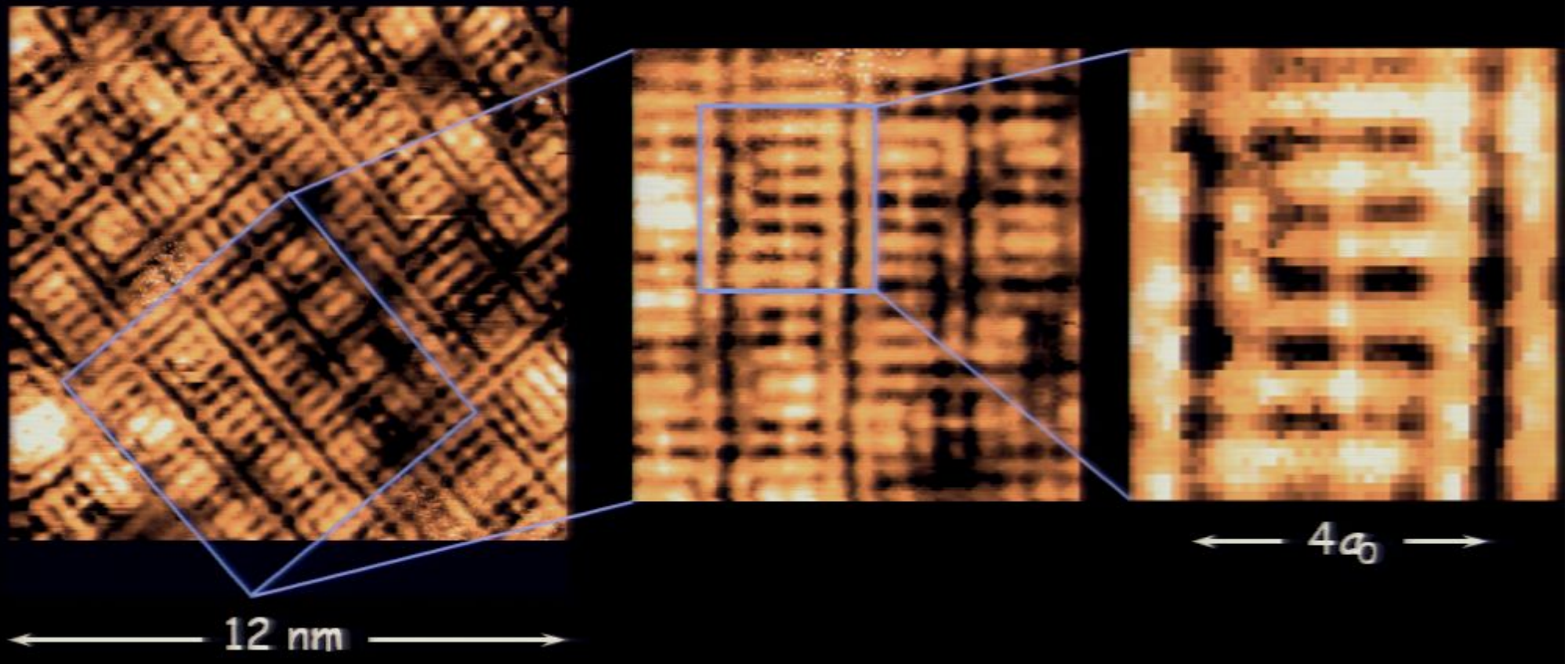

Study Bragg Peaks of FT images of PG States E~Δ_1

Nature 466, 374 (2010)

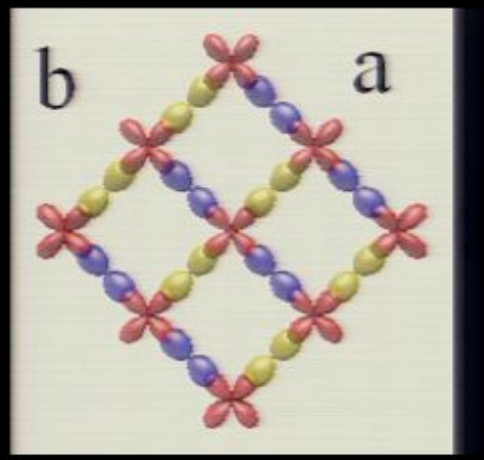

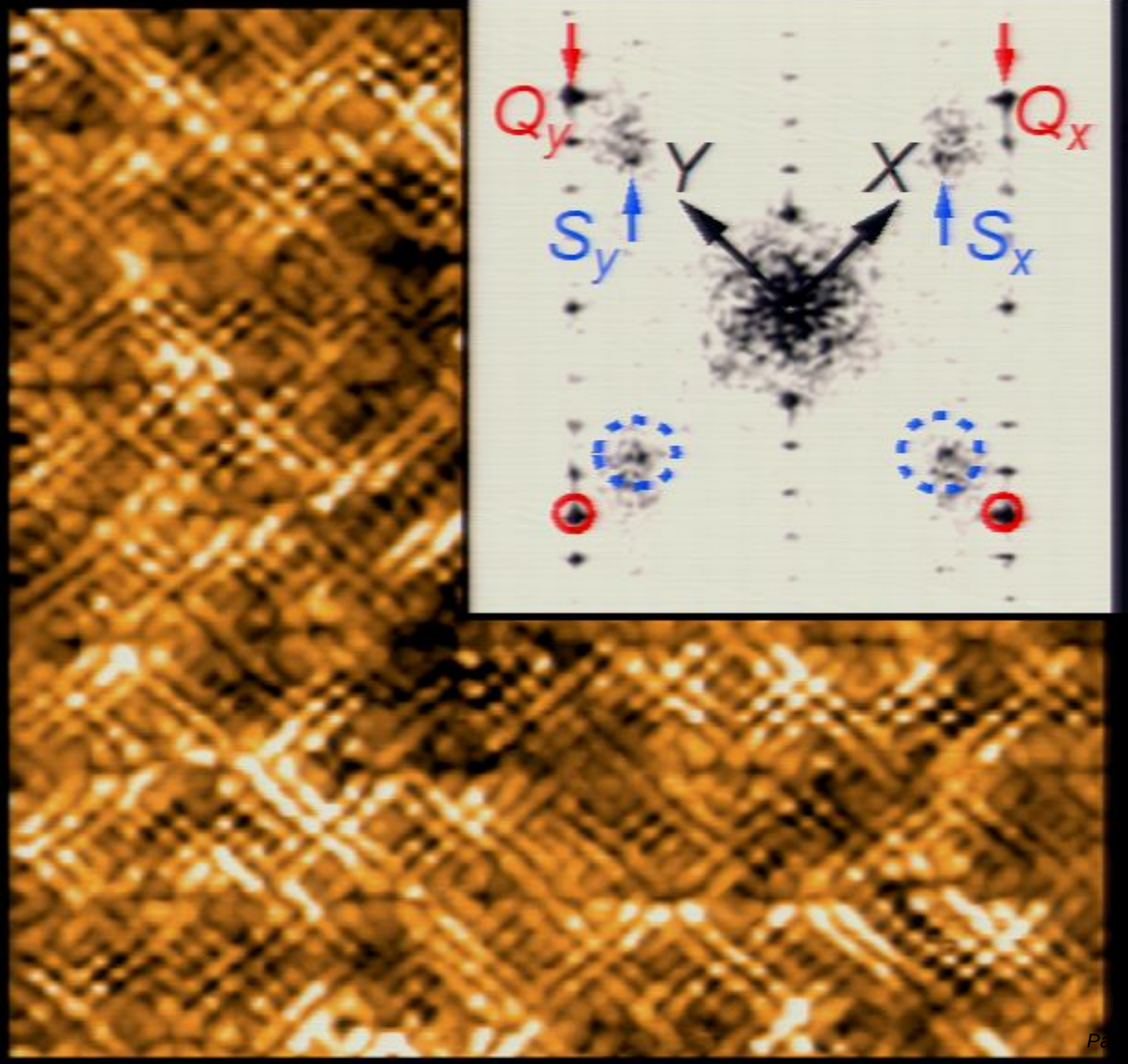

Intra-unit-cell C_4-breaking at $E \sim \Delta_1$

Science 315, 1389 (2007); Science 325, 1099 (2009), Nature 466, 374 (2010)

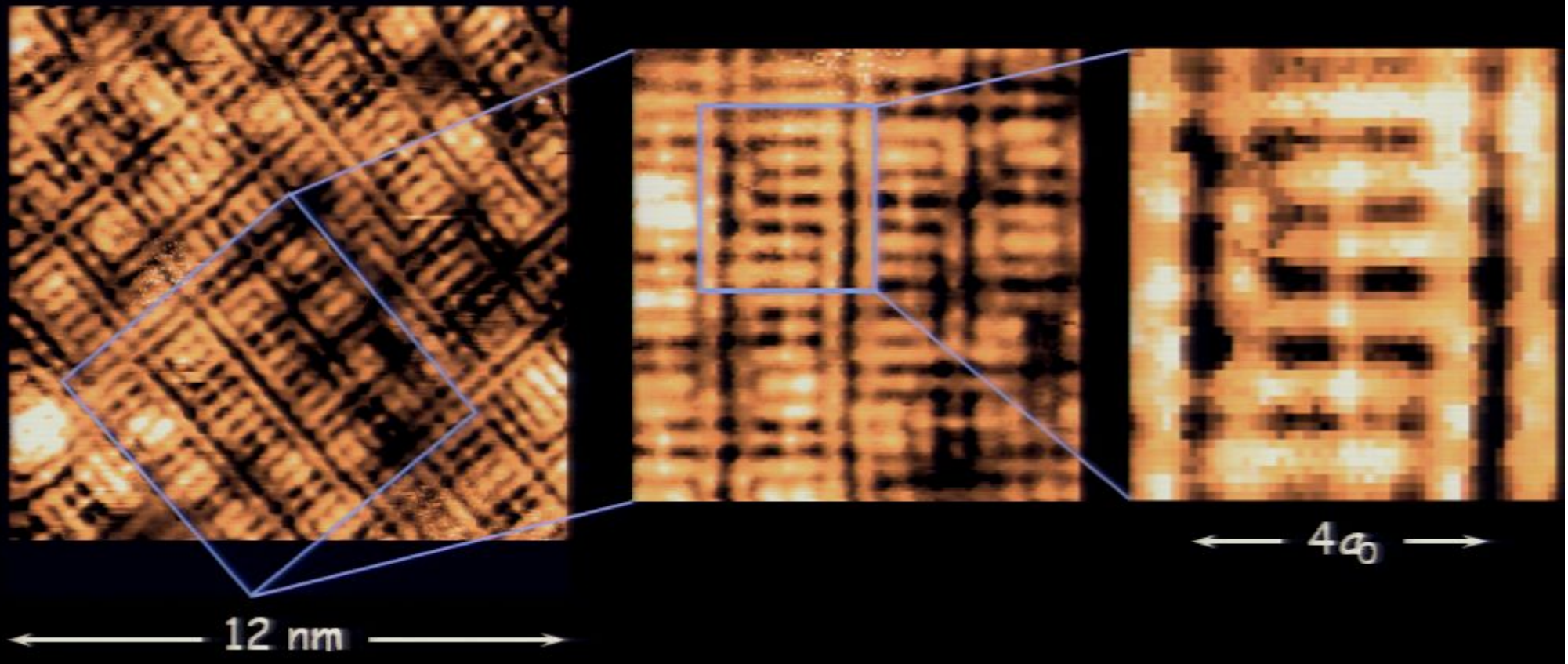

Intra-unit-cell C_4-breaking at $E \sim \Delta_1$

Science 315, 1389 (2007); Science 325, 1099 (2009), Nature 466, 374 (2010)

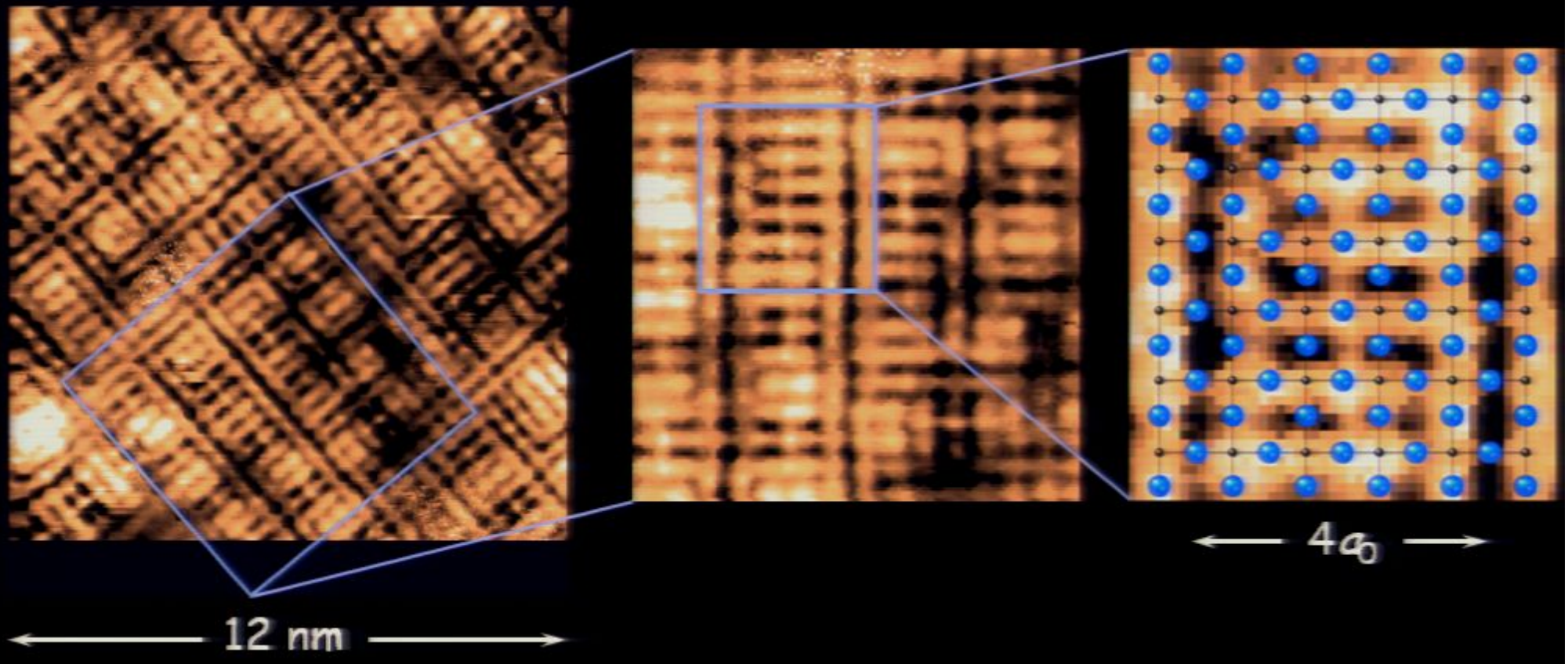

Study Bragg Peaks of FT images of PG States E~Δ_1

Nature 466, 374 (2010)

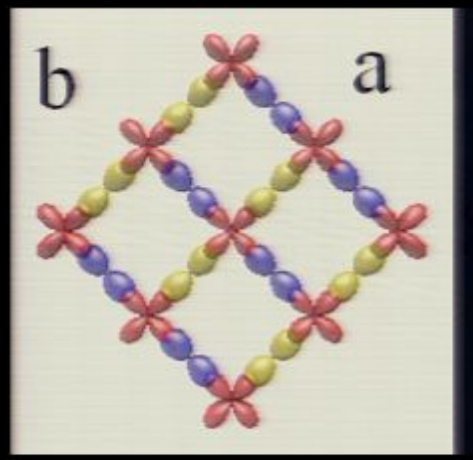

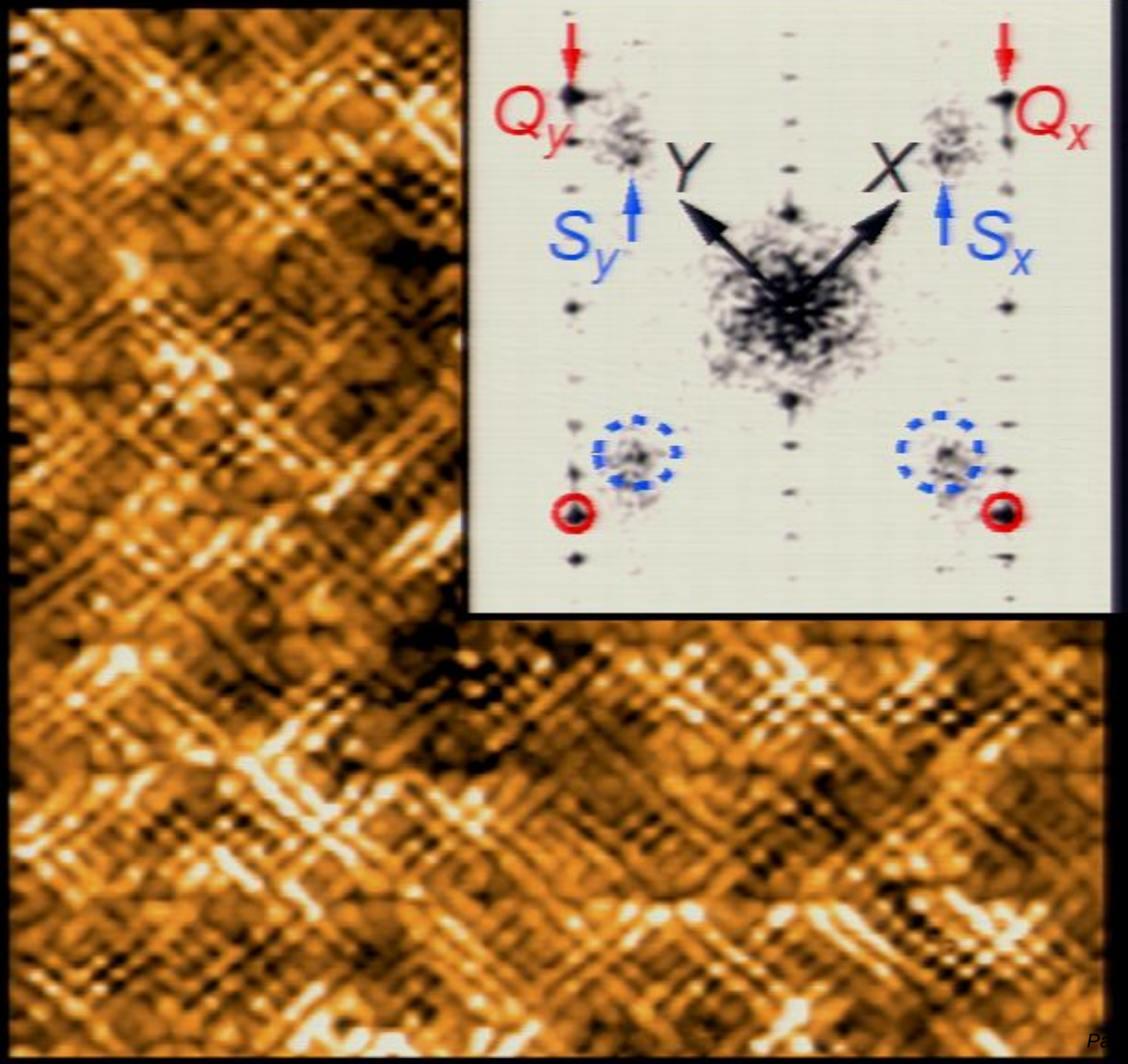

Sub-Atomic Phase Correction

Nature 466, 374 (2010)

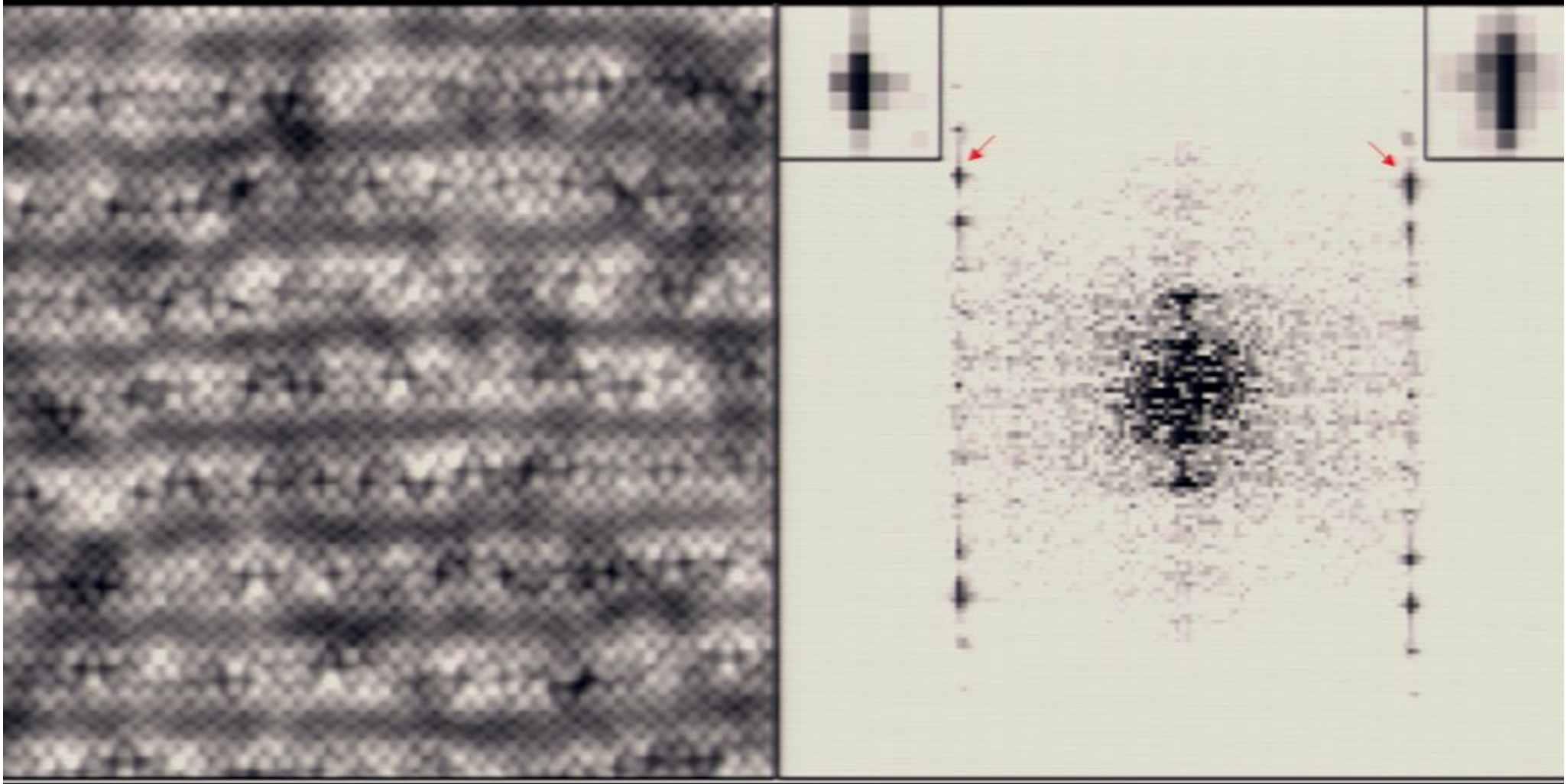

Sub-Atomic Phase Correction
:Bragg peaks become single pixel within resolution

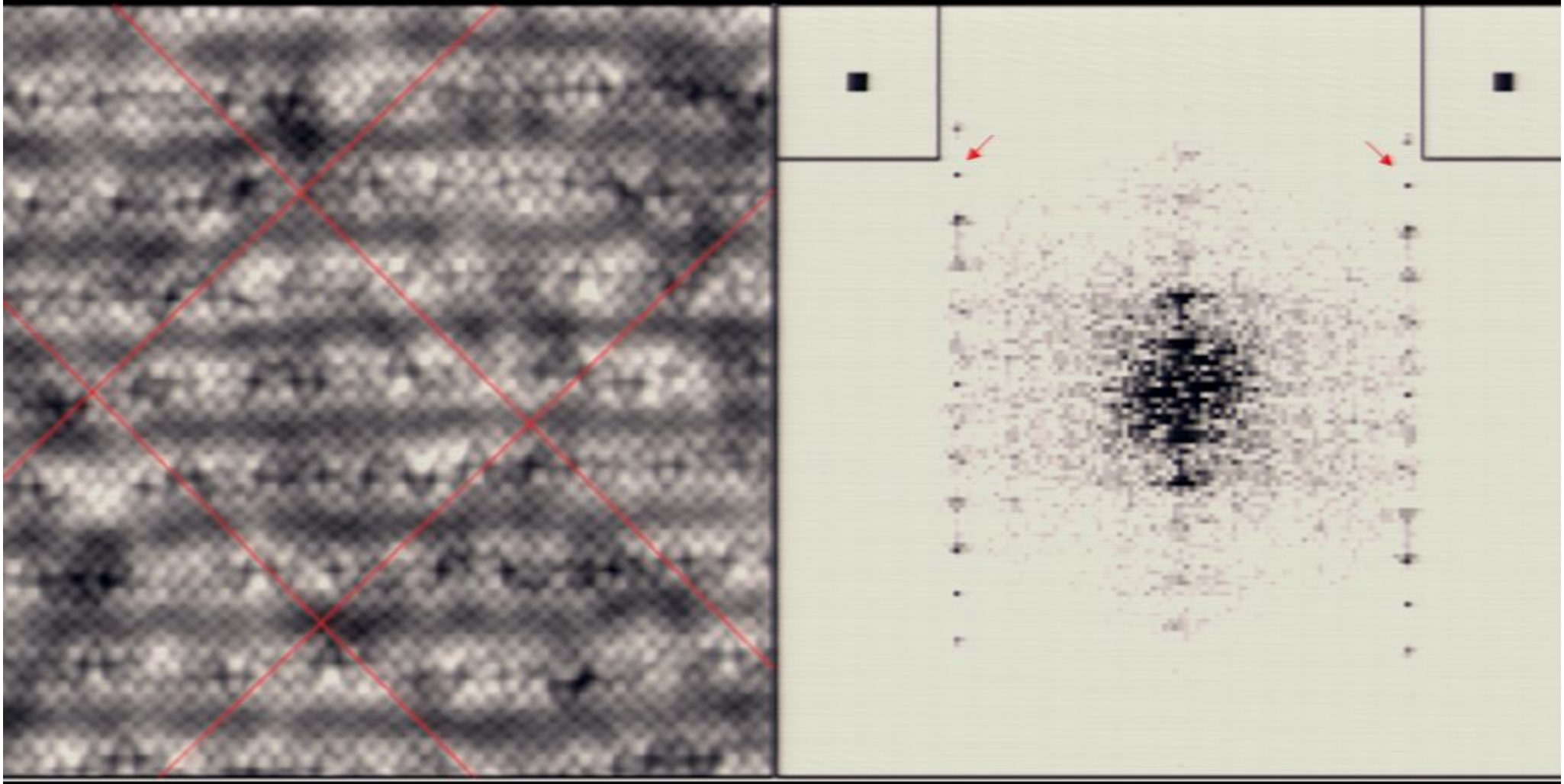

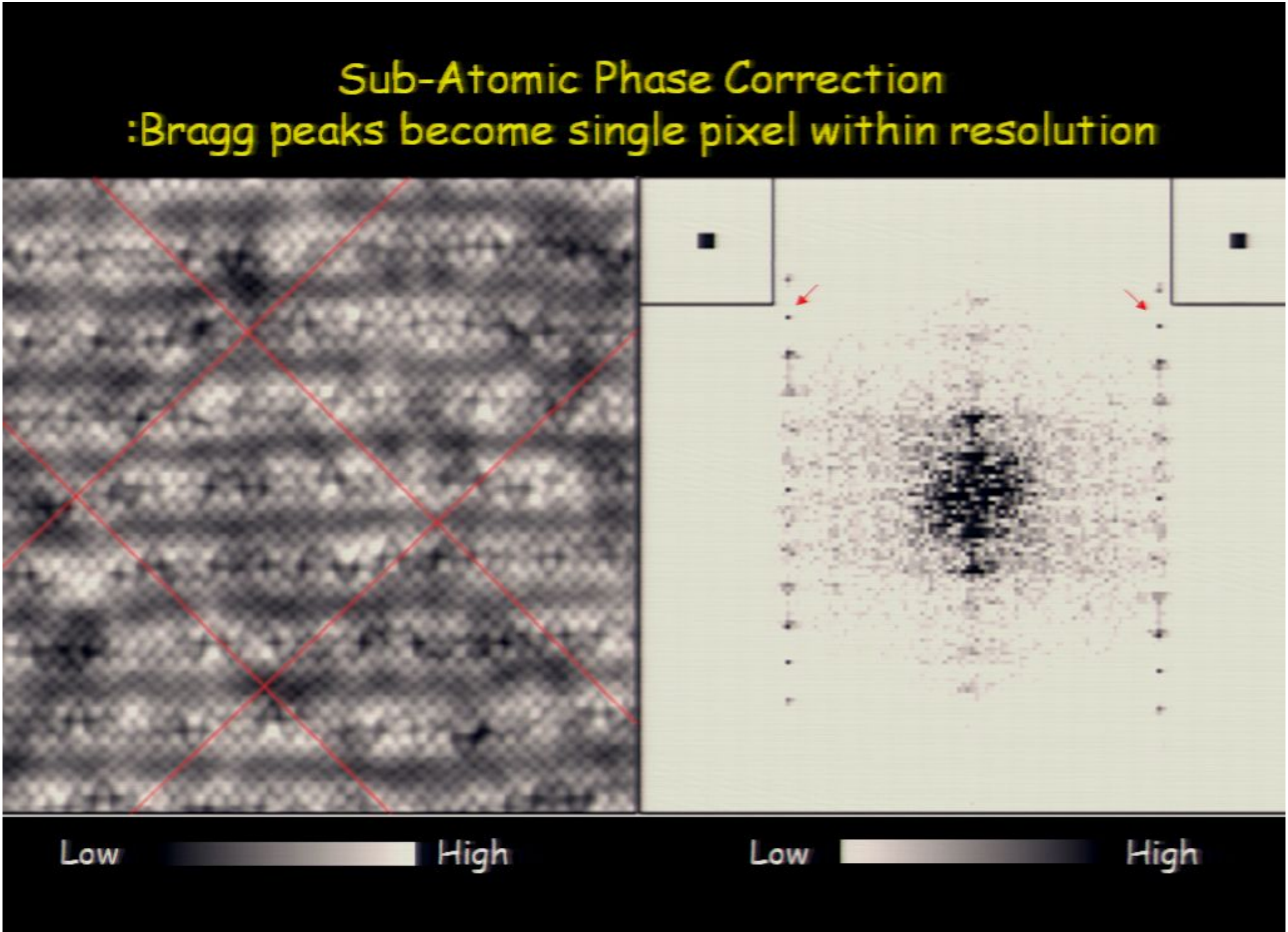
Sub-Atomic Phase Correction
:Bragg peaks become single pixel within resolution
Low
High
Low
High

Sub-Atomic Phase Correction
:Bragg peaks become single pixel within resolution

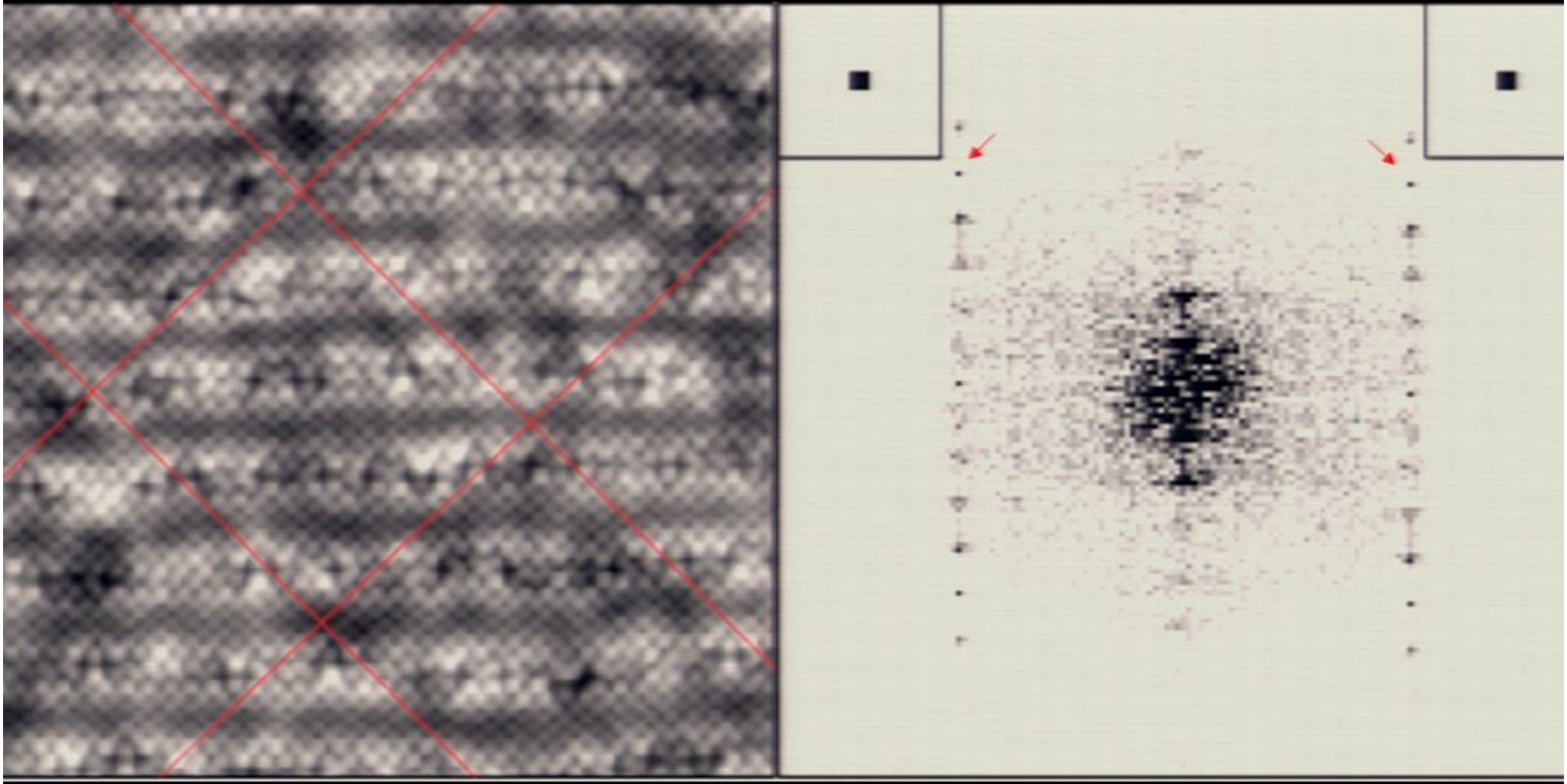

Measure of C_4-breaking O_N^Q

Nature 466, 374 (2010)

$$O_N^Q(e) = \frac{\mathrm{Re}\,\tilde{Z}(Q_y,e) - \mathrm{Re}\,\tilde{Z}(Q_x,e)}{\bar{Z}(r,e)}$$

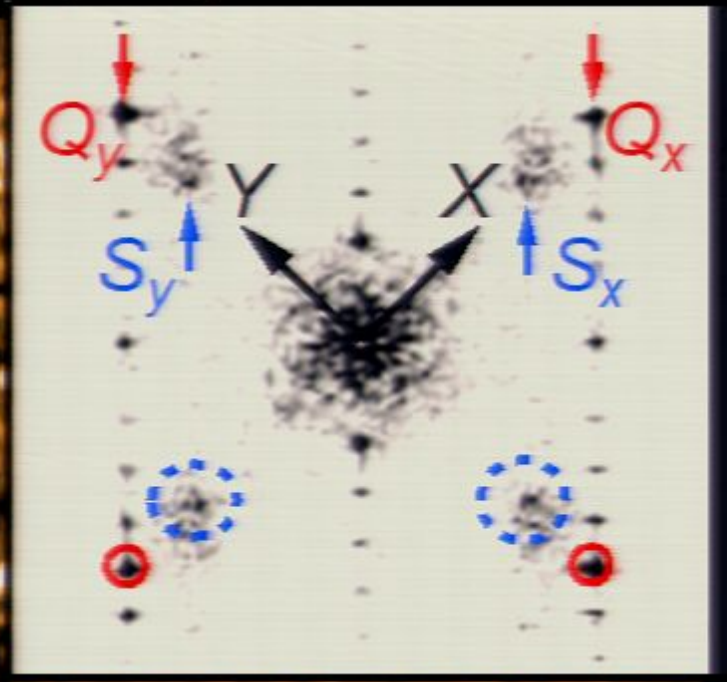

Z(q,e=1)

Z(r,e=1)

Topograph T(r) maintains C_4 Symmetry

Nature 466, 374 (2010)

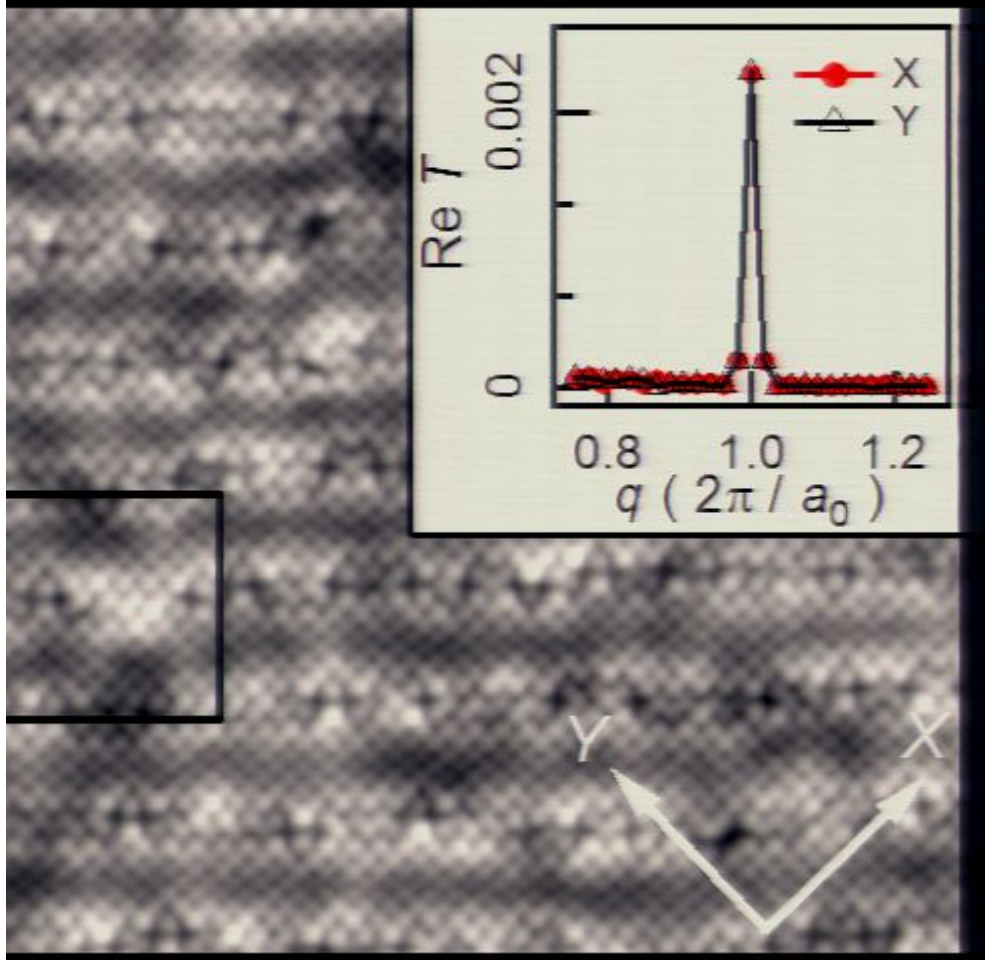

Pseudogap states (simultaneous) strongly break C_4 symmetry

T(r) Nature 466, 374 (2010) Z(r,e=1)

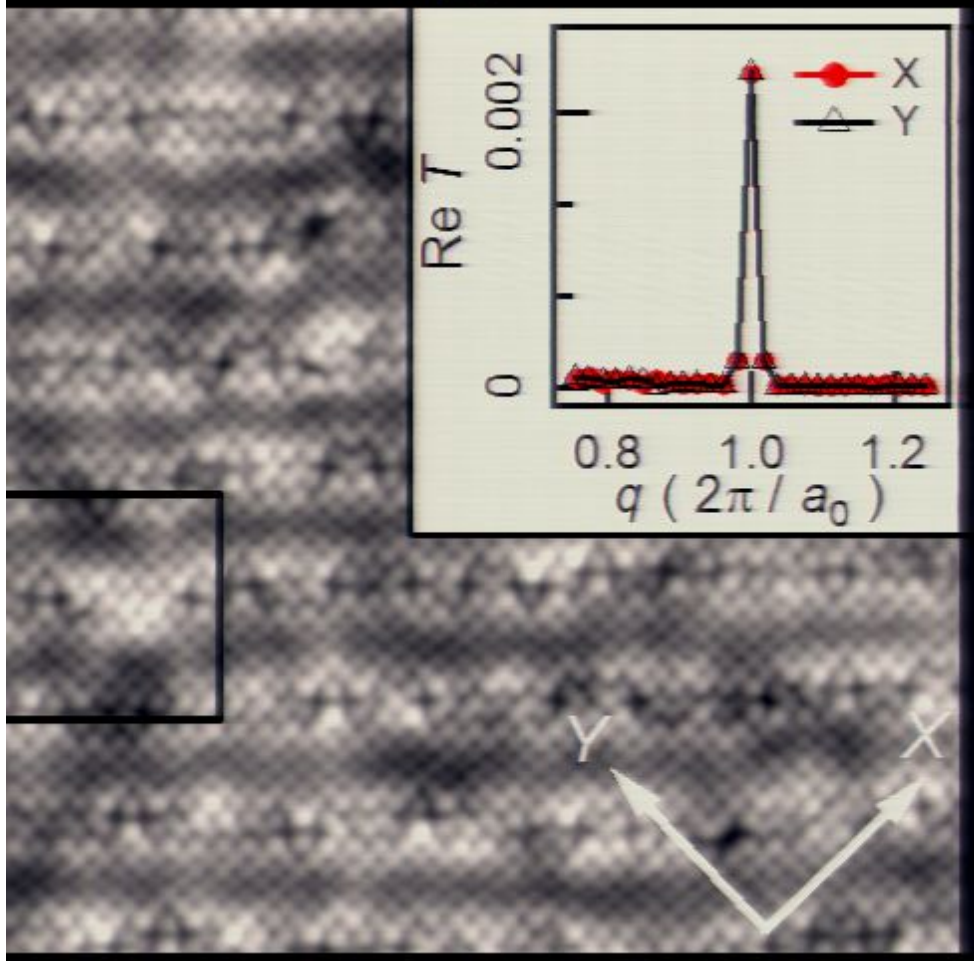

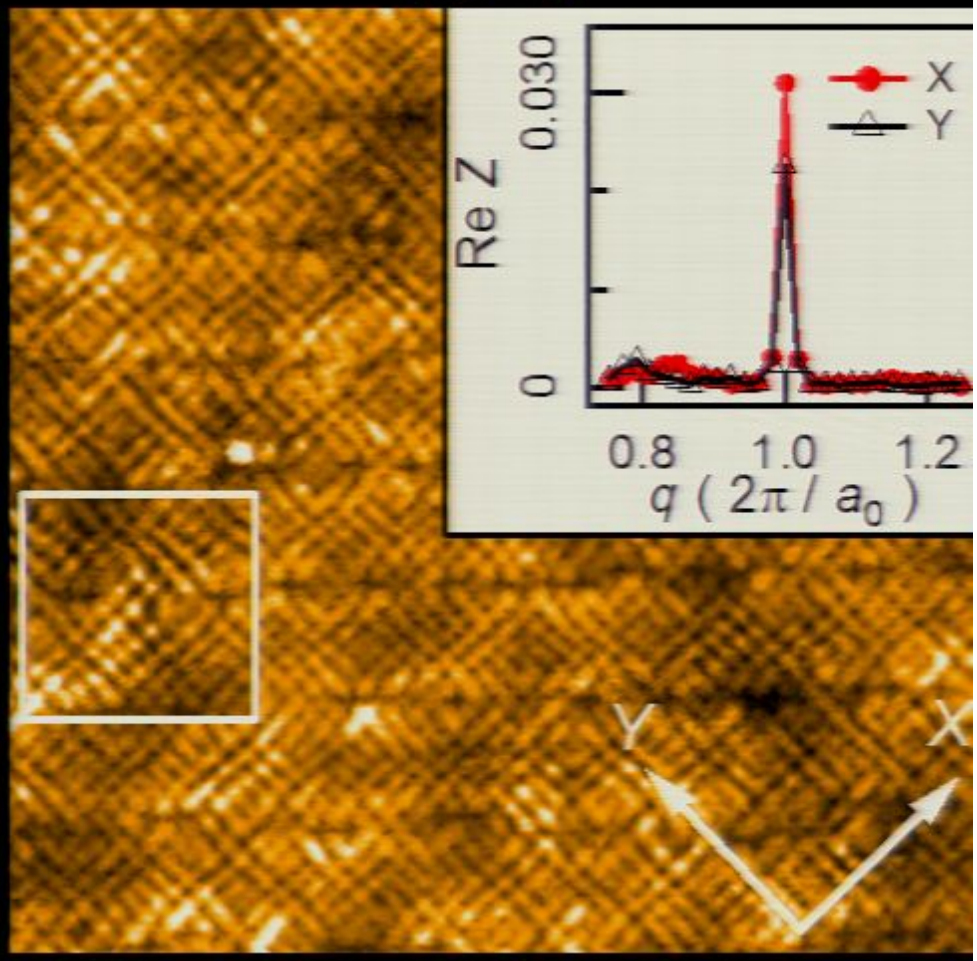

20nm x 20nm Low High 20nm x 20nm 0.5 1.5

$$O_N^Q(e) = \frac{\mathrm{Re}\,\tilde{Z}(\mathrm{Q}_y, e) - \mathrm{Re}\,\tilde{Z}(\mathrm{Q}_x, e)}{\overline{Z}(r, e)}$$

C_4-breaking in O_N^Q is specific to pseudogap states

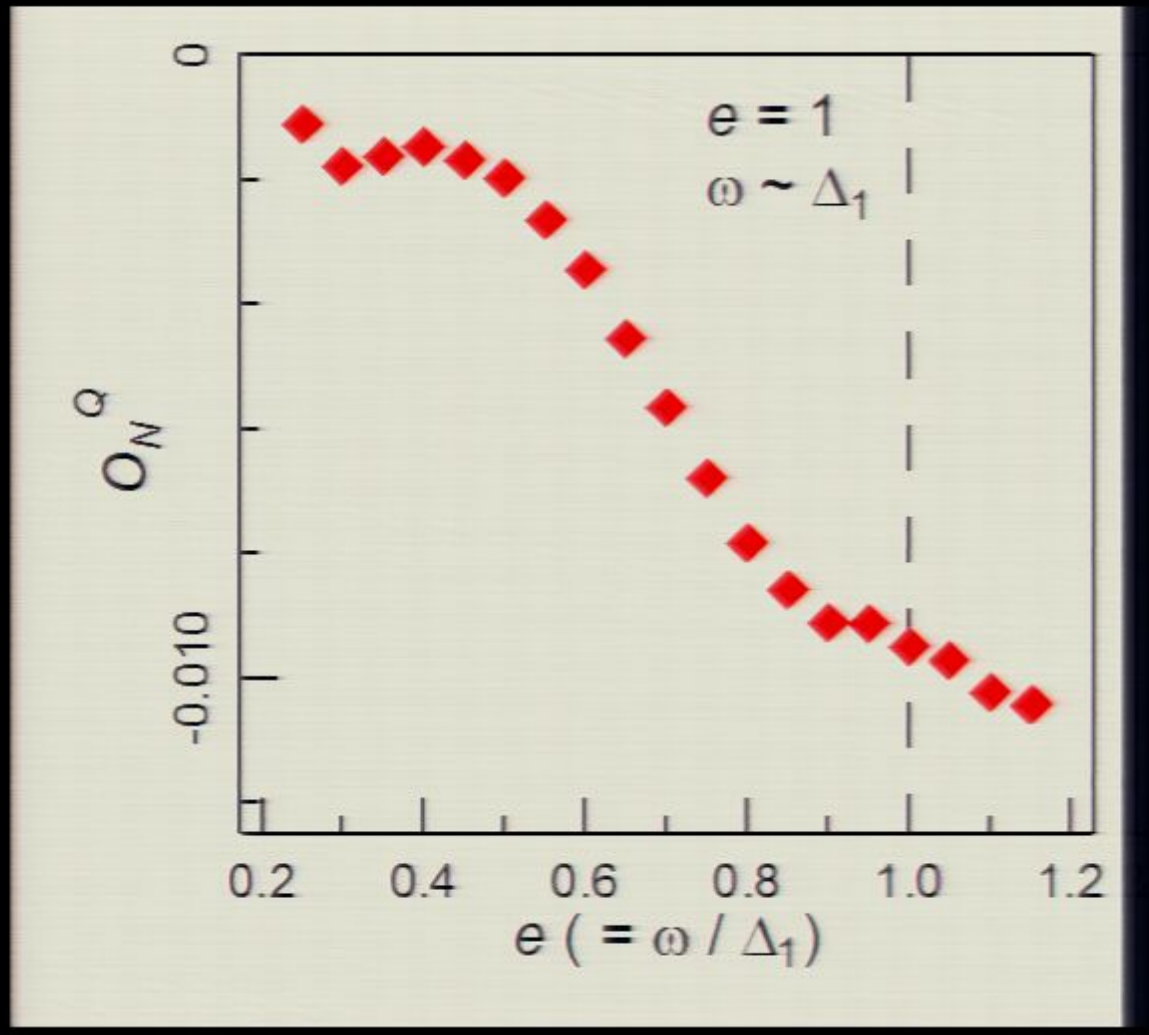

$$O_N^Q(e) = \frac{\mathrm{Re}\,\tilde{Z}(\mathrm{Q}_y, e) - \mathrm{Re}\,\tilde{Z}(\mathrm{Q}_x, e)}{\bar{Z}(\mathrm{Q}, e)}$$

Intra-unit-cell C_4-breaking at $E \sim \Delta_1$ in underdoped BI2212

Nature 466, 374 (2010)

$$\rho_N(e) \equiv \frac{\mathrm{Re}\tilde{Z}(\mathbf{Q}_y,e) - \mathrm{Re}\tilde{Z}(\mathbf{Q}_x,e)}{\bar{Z}(e)}$$

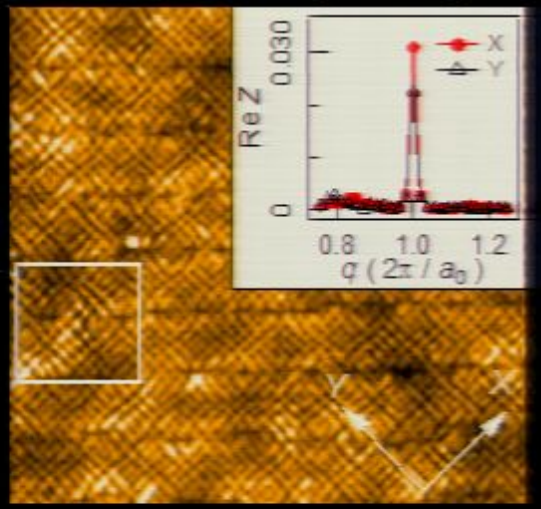

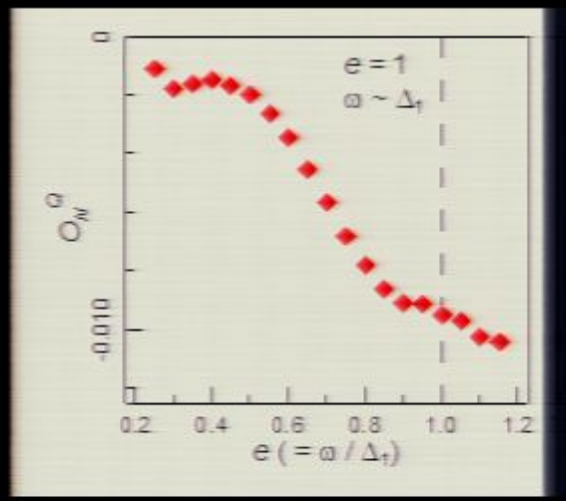

$$O_N^R(e) \equiv \sum_{\mathbf{R}} \frac{Z_x(\mathbf{R},e) - Z_y(\mathbf{R},e)}{\bar{Z}(e)N}$$

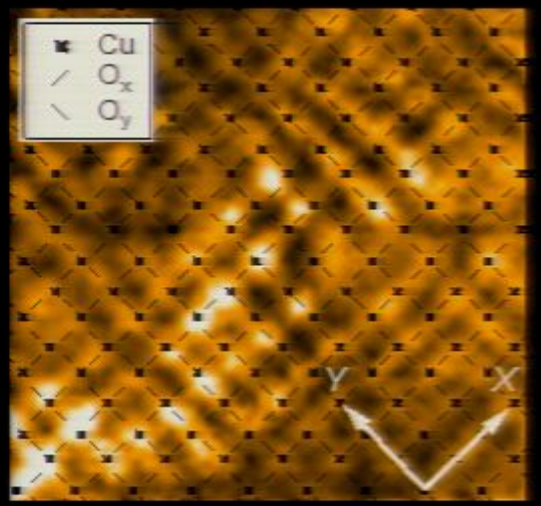

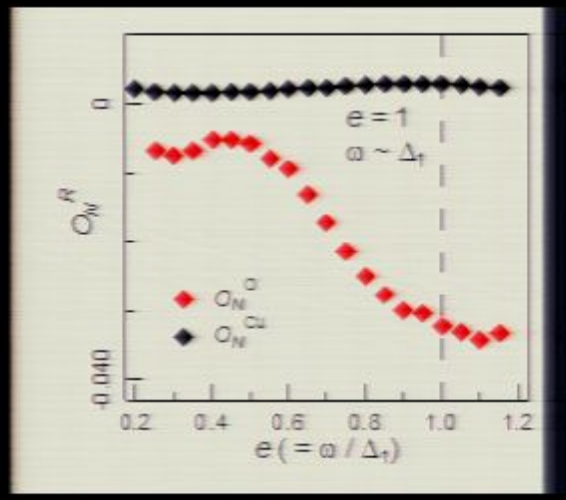

Intra-unit-cell C_4-breaking at $E \sim \Delta_1$

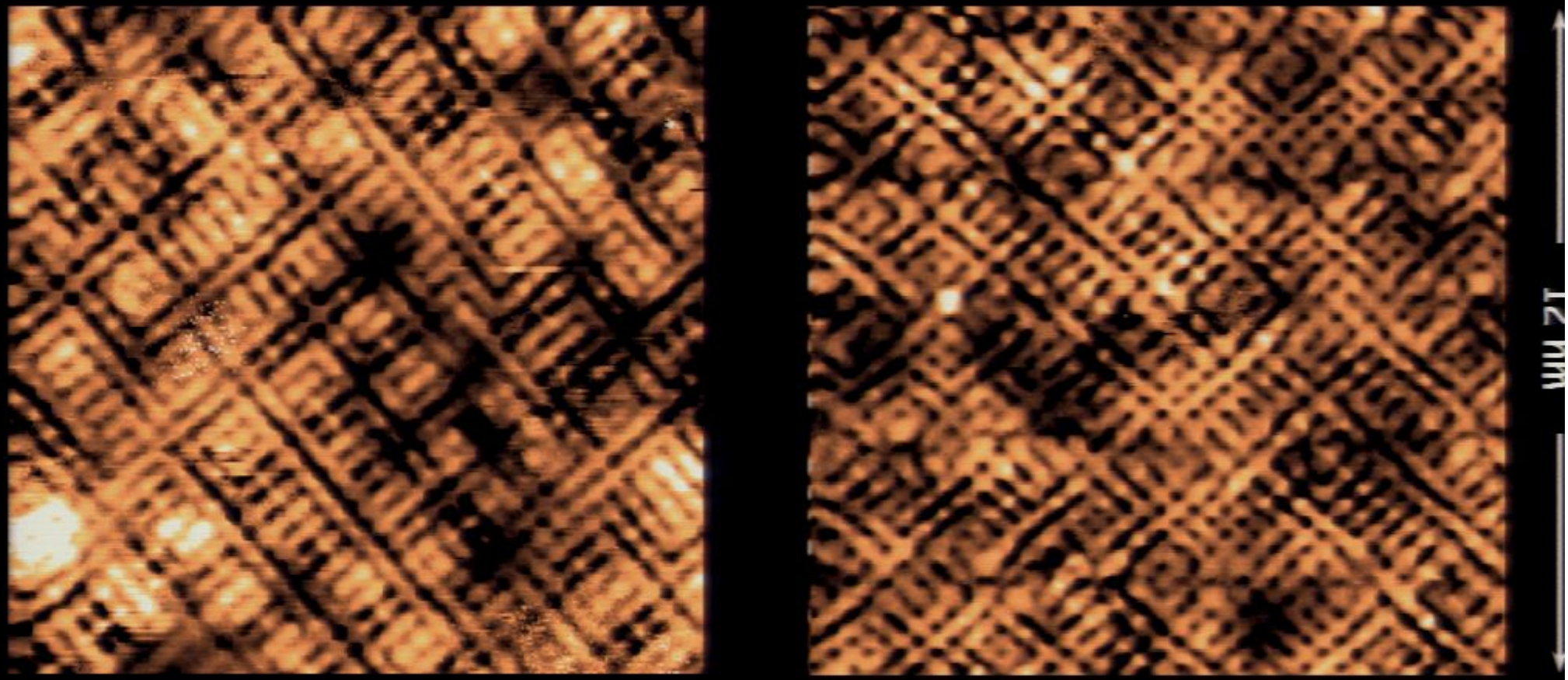

Science 313, 1380 (2007); Nature 454, 1072, (2008), Nature 466, 374 (2010)

PG Broken Symmetries: ARPES

Time-reversal (T) and 90-degree rotation (C_4) breaking @ k=π/a

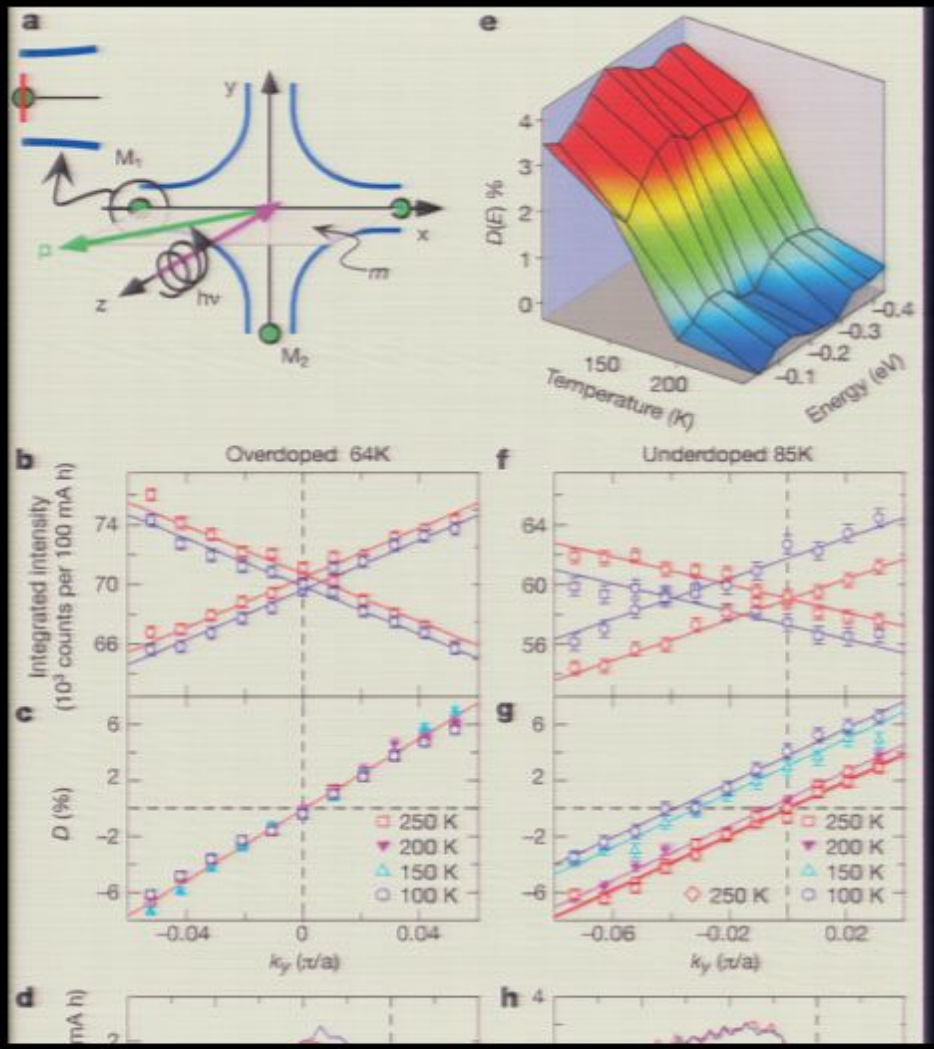

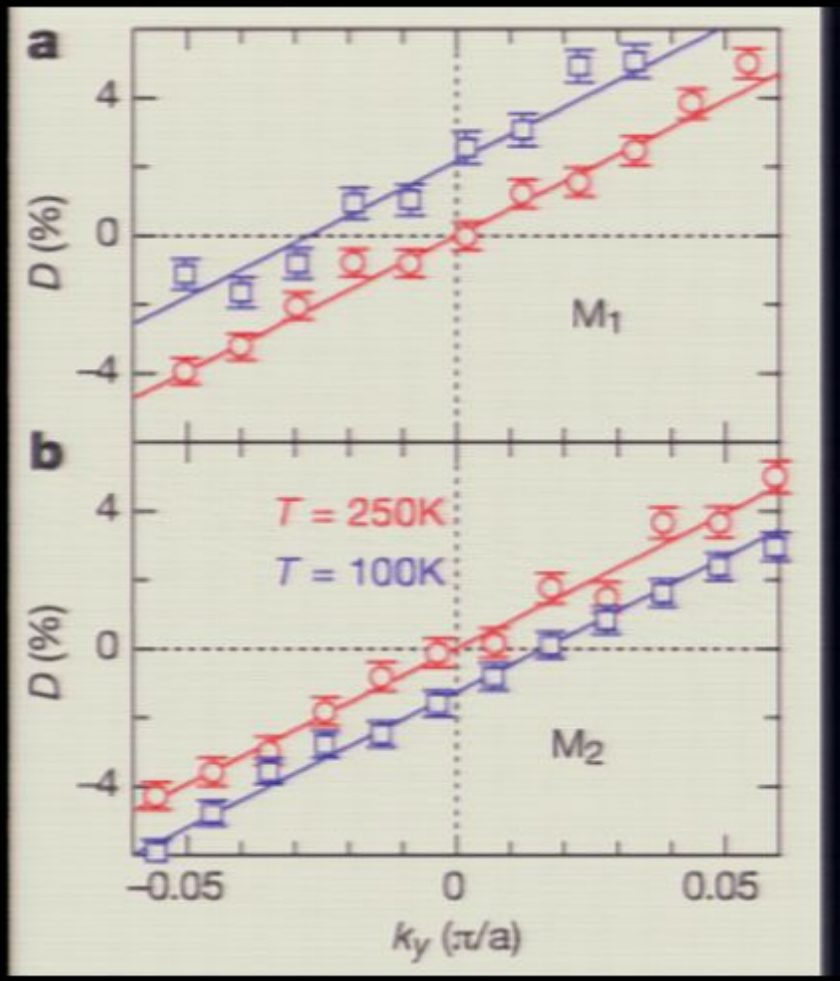

Kaminski, A. *et al.* Spontaneous breaking of time-reversal symmetry in the pseudogap state of a high-T_c superconductor. *Nature* **416**, 610-613 (2002).

PG Broken Symmetries: Elastic NS

Time-reversal (T) and 90-degree rotation (C_4) breaking @ $q=Q_{Bragg}$

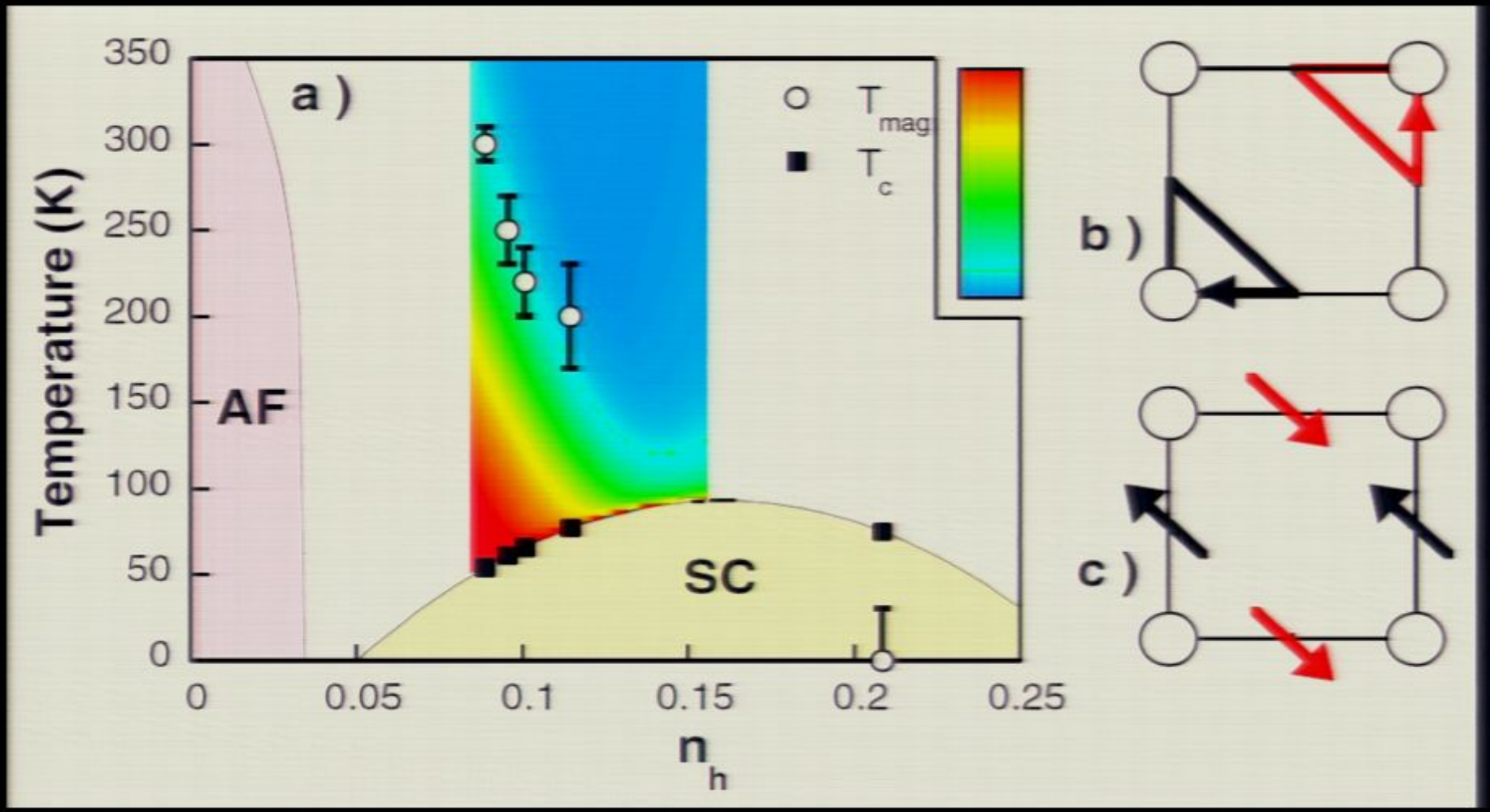

B. Fauqué, *et al*, *Phys. Rev. Lett.* 96, 197001 (2006)
H. Mook *et al*, *Phys. Rev. B* 78, 205006 (2008)
Y. Li *et al* , Nature 455, 372 (2008)

PG Broken Symmetries: SI-STM

Intra-unit-cell Inversion Symmetry Breaking
(C_4breaking @ $q=Q_{Bragg}$)

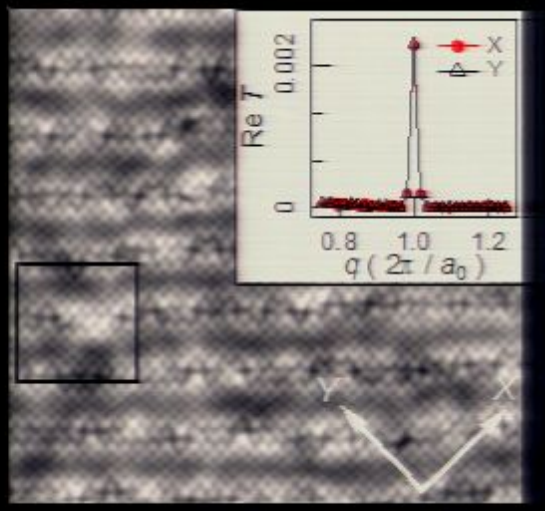

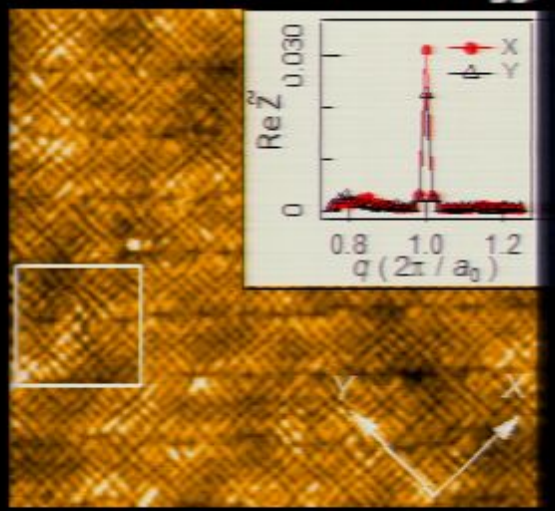

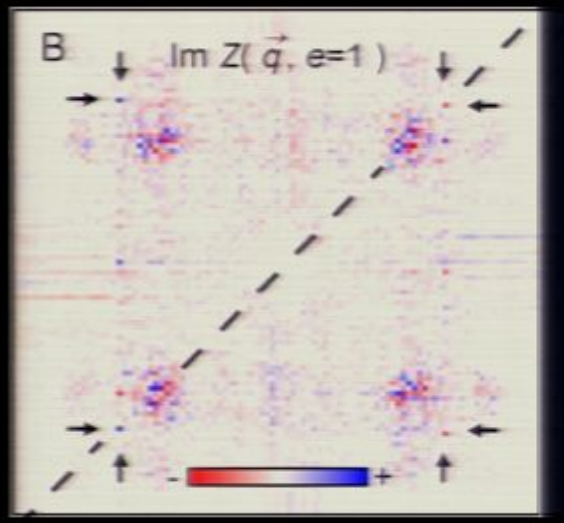

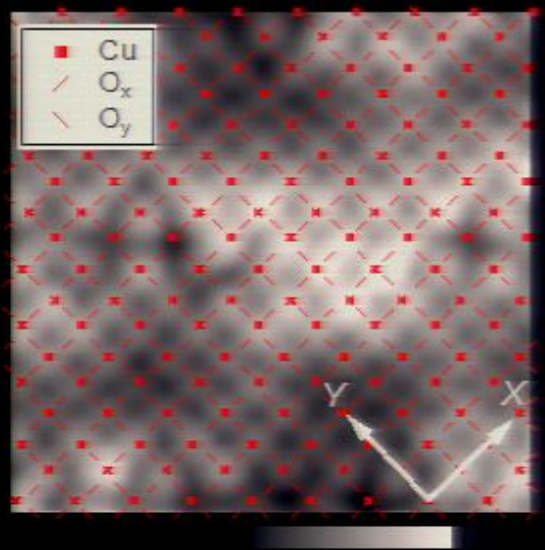

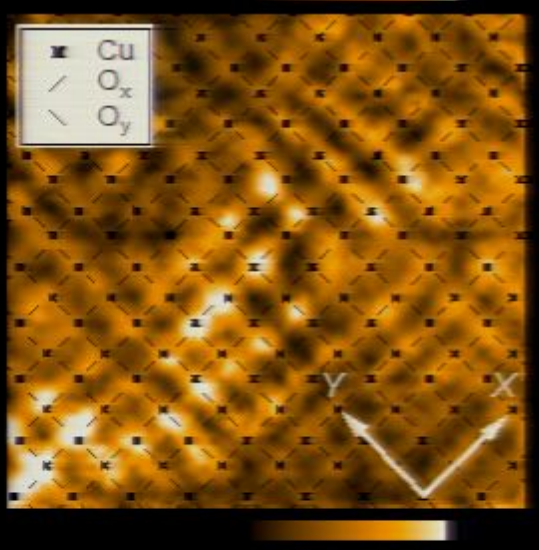

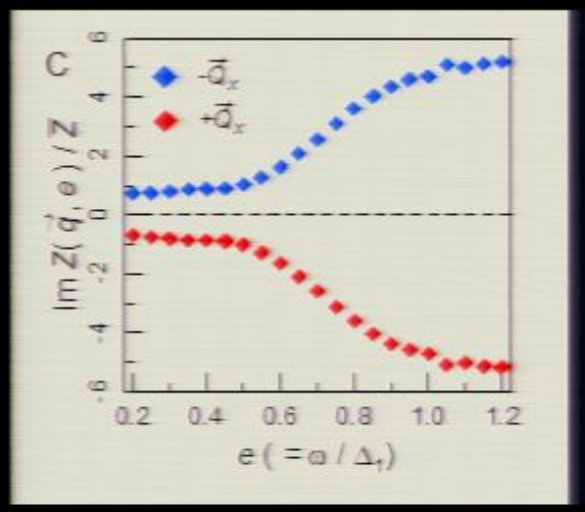

PG Broken Symmetries: Intra-unit-cell breaking of T, I

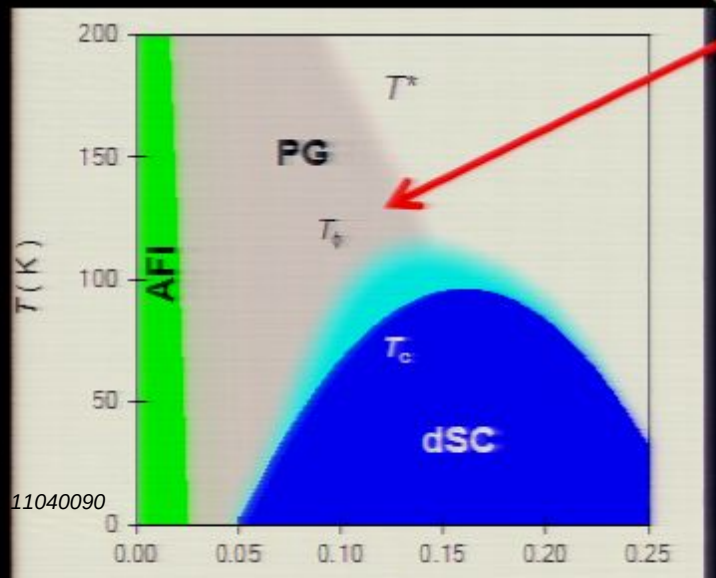

11040090

ARPES

$k=\pi/a_0$

T*
Specific

T

I-U-C

C_4

INS

T*
Specific

I-U-C

C_4

C_4

I-U-C

C_4

I-U-C

Pseudogap Energy

IUC Inversion

SI-STM

PG Broken Symmetries: Intra-unit-cell breaking of T, I

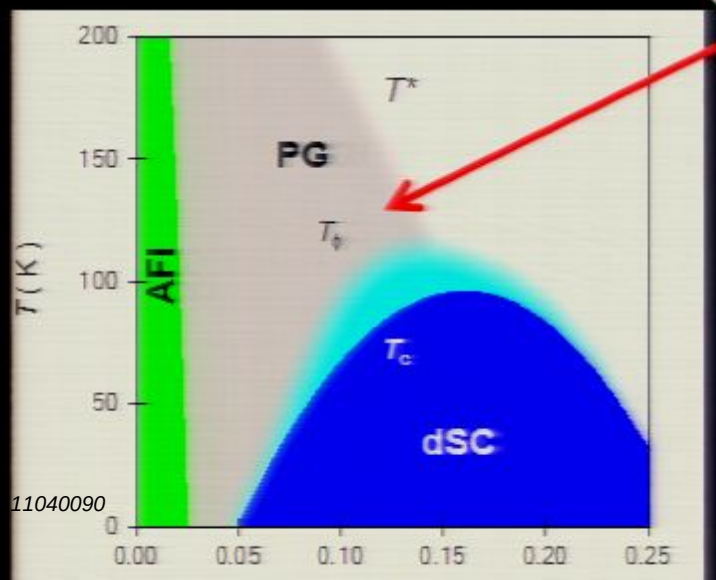

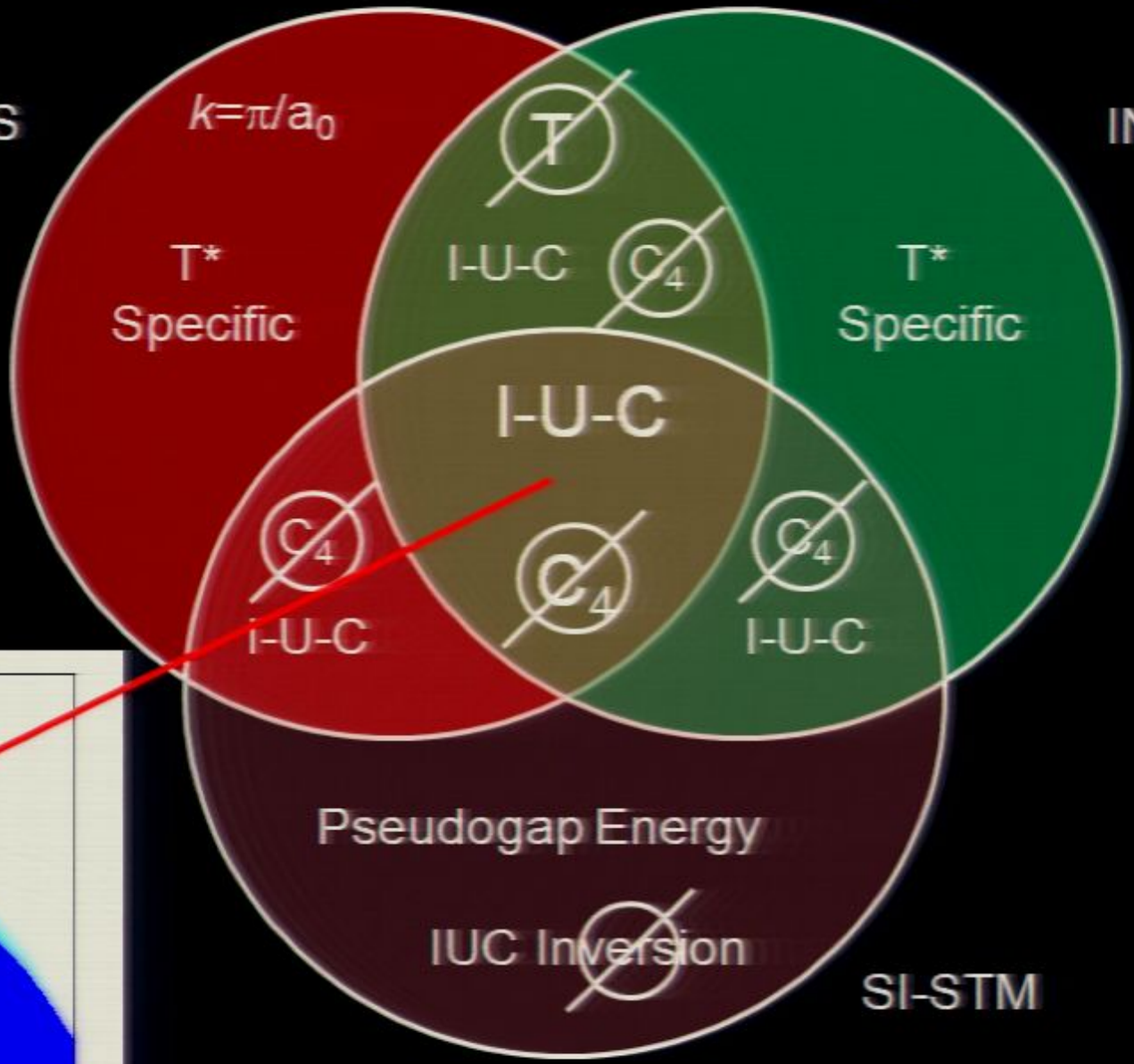

Coupling between $\vec{q} = \vec{Q}_{Bragg}$ and $\vec{q} = \vec{S}$ broken electronic symmetries

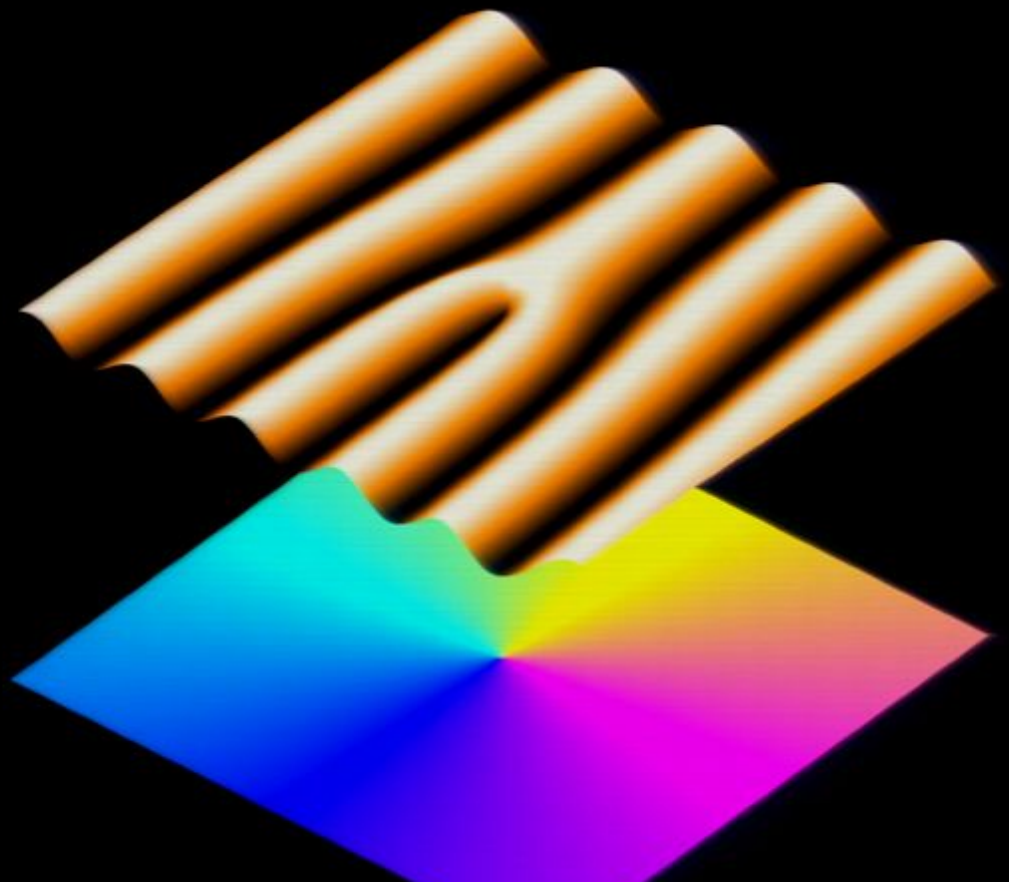

PG Broken Symmetries: Elastic NS

Time-reversal (T) and 90-degree rotation (C_4) breaking @ $q=Q_{Bragg}$

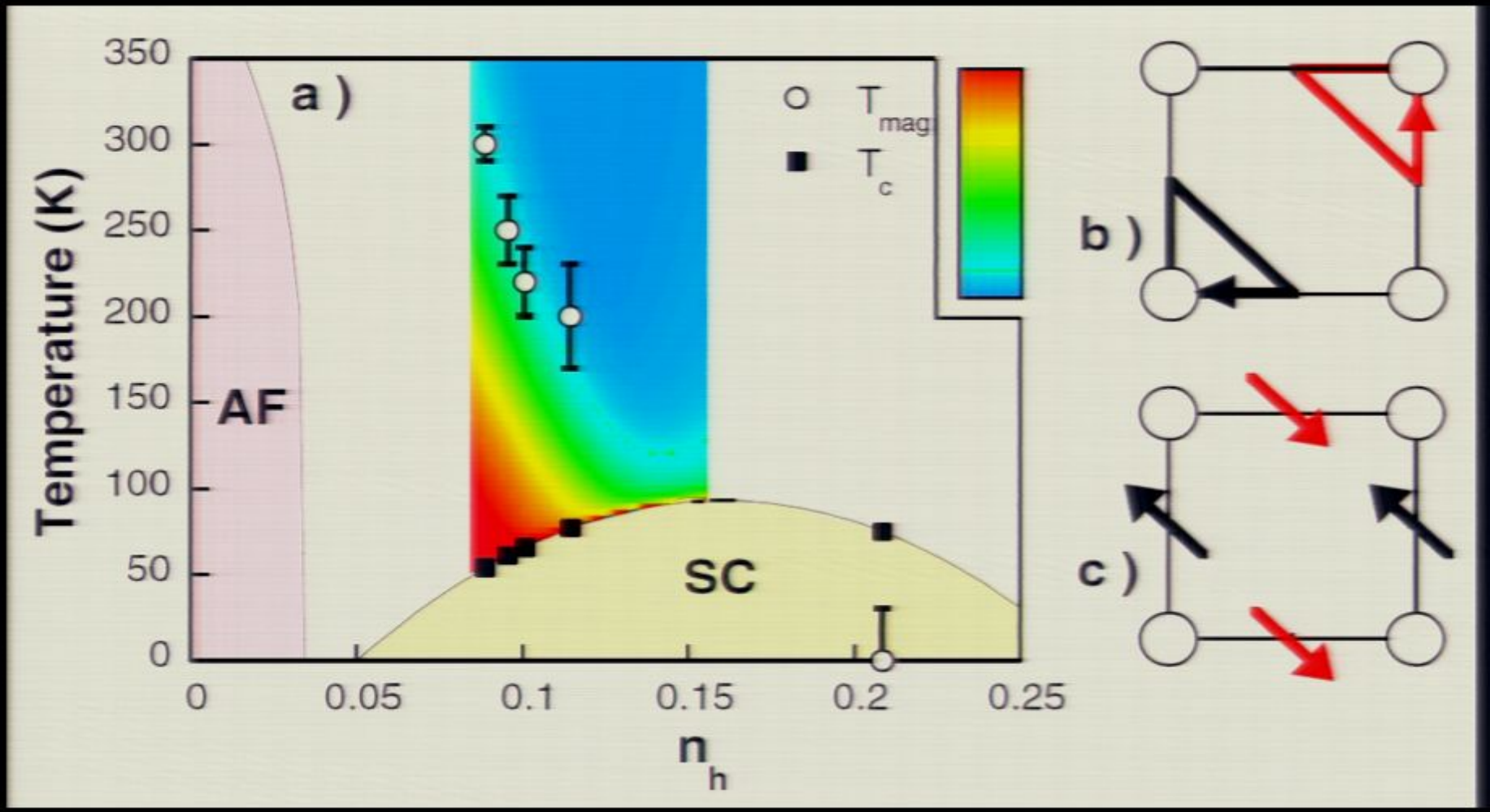

B. Fauqué, *et al*, *Phys. Rev. Lett.* 96, 197001 (2006)
H. Mook *et al*, *Phys. Rev. B* 78, 205006 (2008)
Y. Li *et al*, Nature 455, 372 (2008)

Pseudogap Broken Symmetries: NS & INS

Incommensurate Translational & Rotational Symmetry Breaking

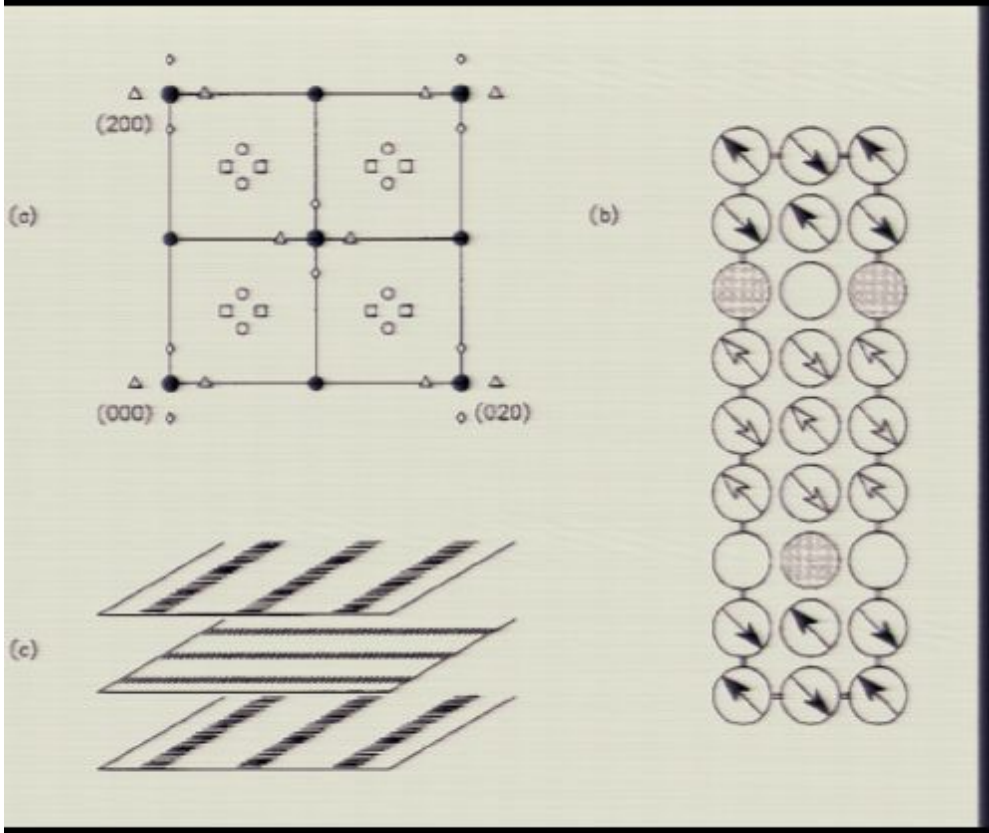

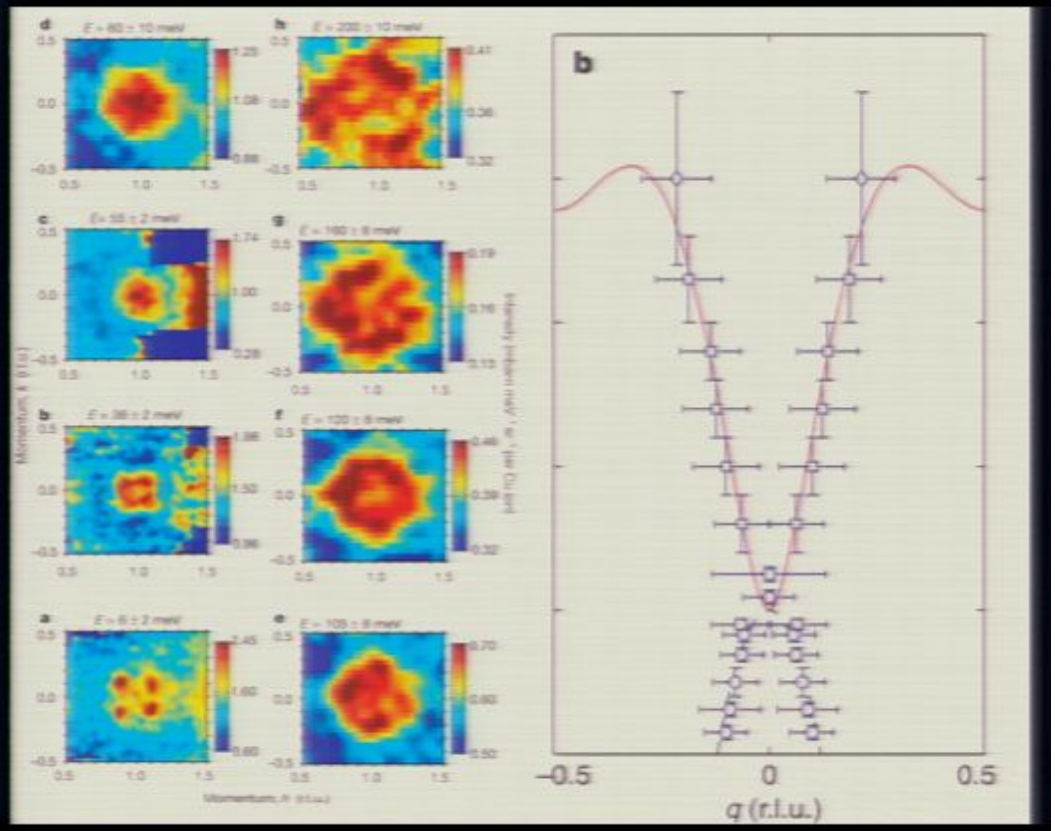

anquada *et al*, Nature 375, 561 (1995) Abbamonte *et al*, Nat. Phys. 1, 155 (2005)
Nature 429, 534 (2004)

PG Broken Symmetries: Elastic NS

Time-reversal (T) and 90-degree rotation (C_4) breaking @ $q=Q_{Bragg}$

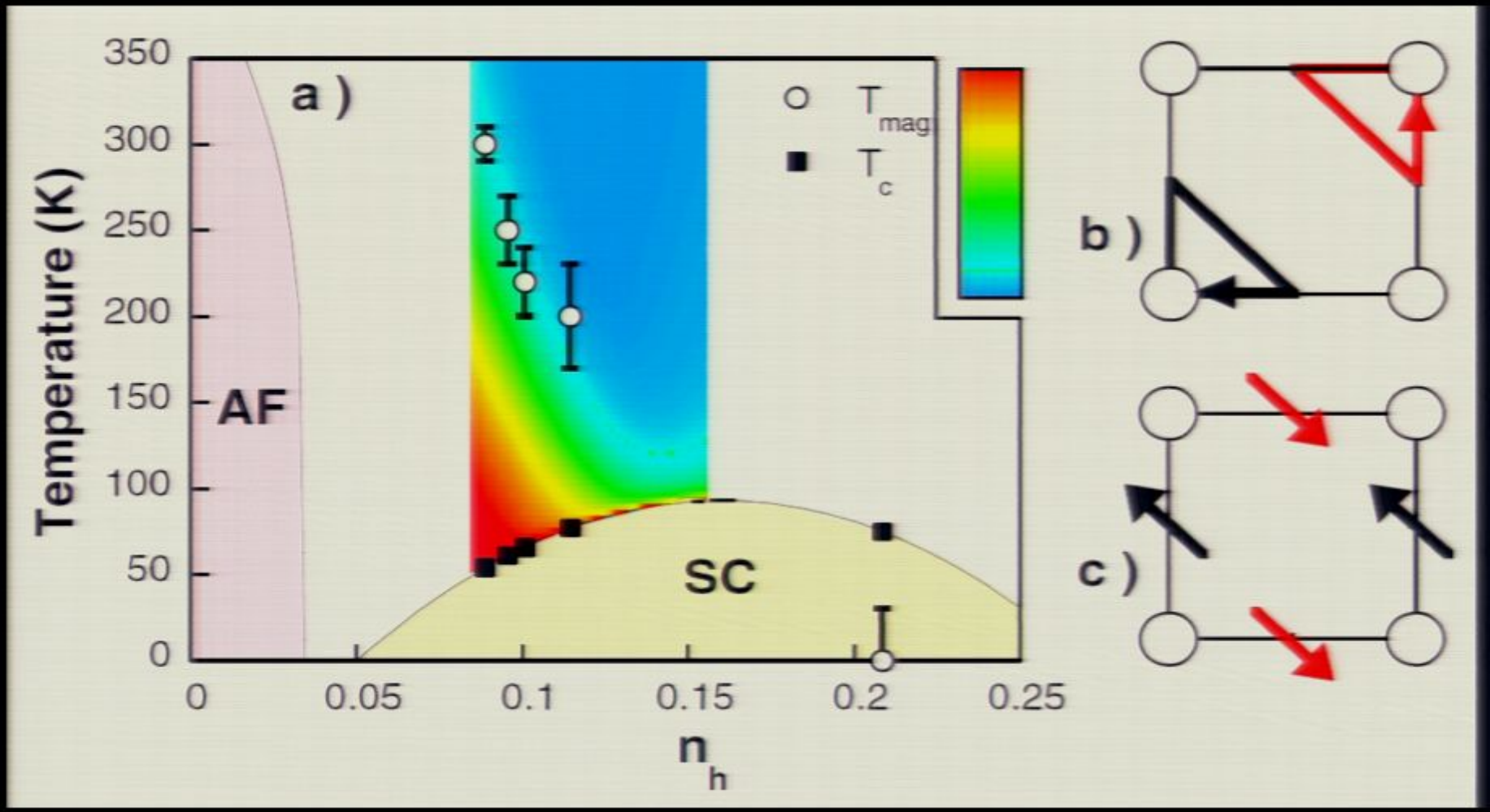

B. Fauqué, *et al*, *Phys. Rev. Lett.* 96, 197001 (2006)
H. Mook *et al*, *Phys. Rev. B* 78, 205006 (2008)
Y. Li *et al*, Nature 455, 372 (2008)

Pseudogap Broken Symmetries: NS & INS

Incommensurate Translational & Rotational Symmetry Breaking

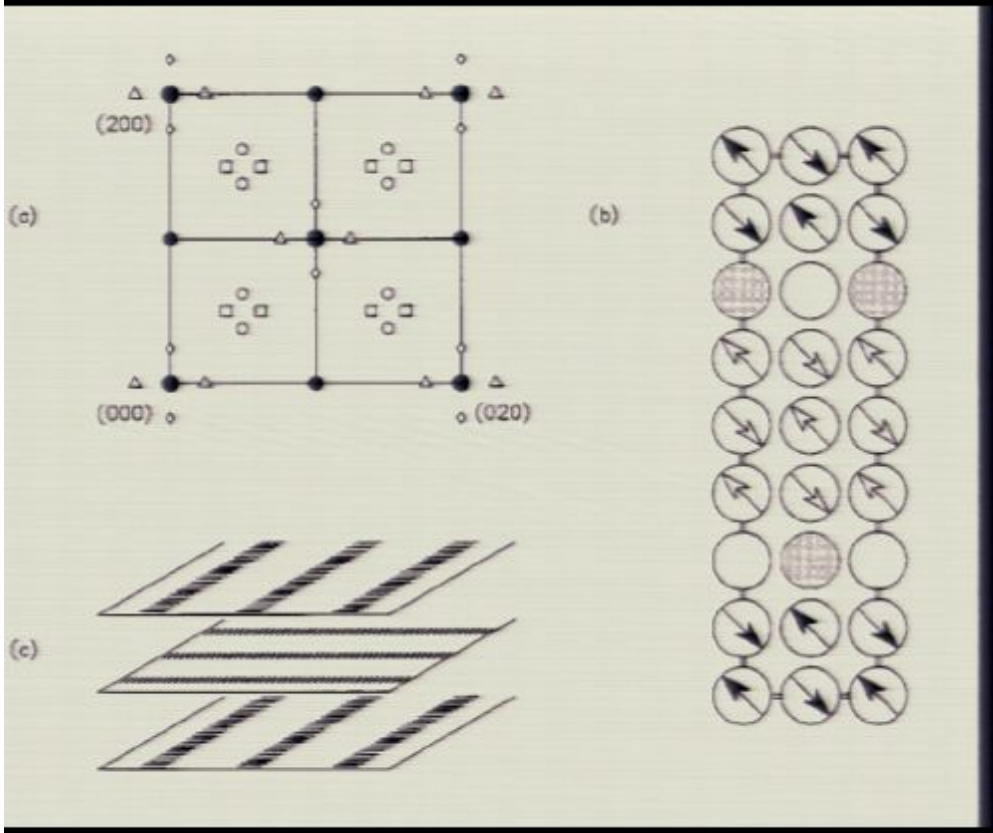

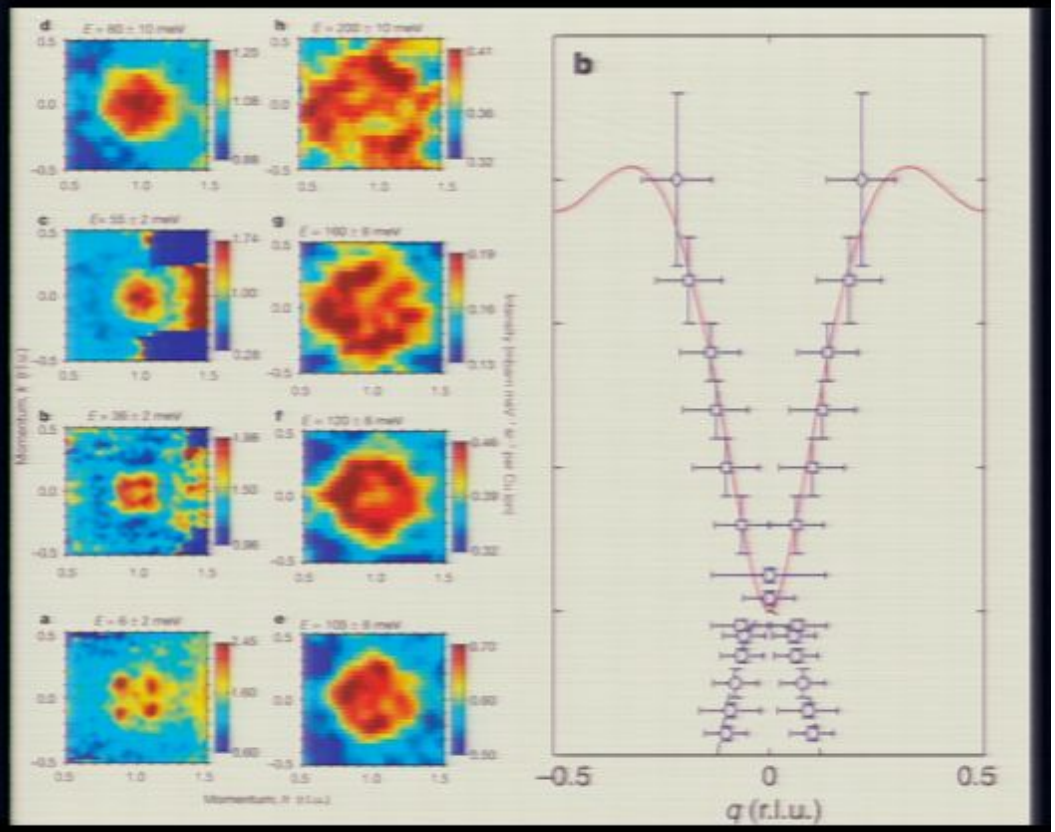

anquada *et al*, Nature 375, 561 (1995) Abbamonte *et al*, Nat. Phys. 1, 155 (2005)
Nature 429, 534 (2004)

SI-STM Images contain BOTH Intra-unit-cell and Incommensurate Components

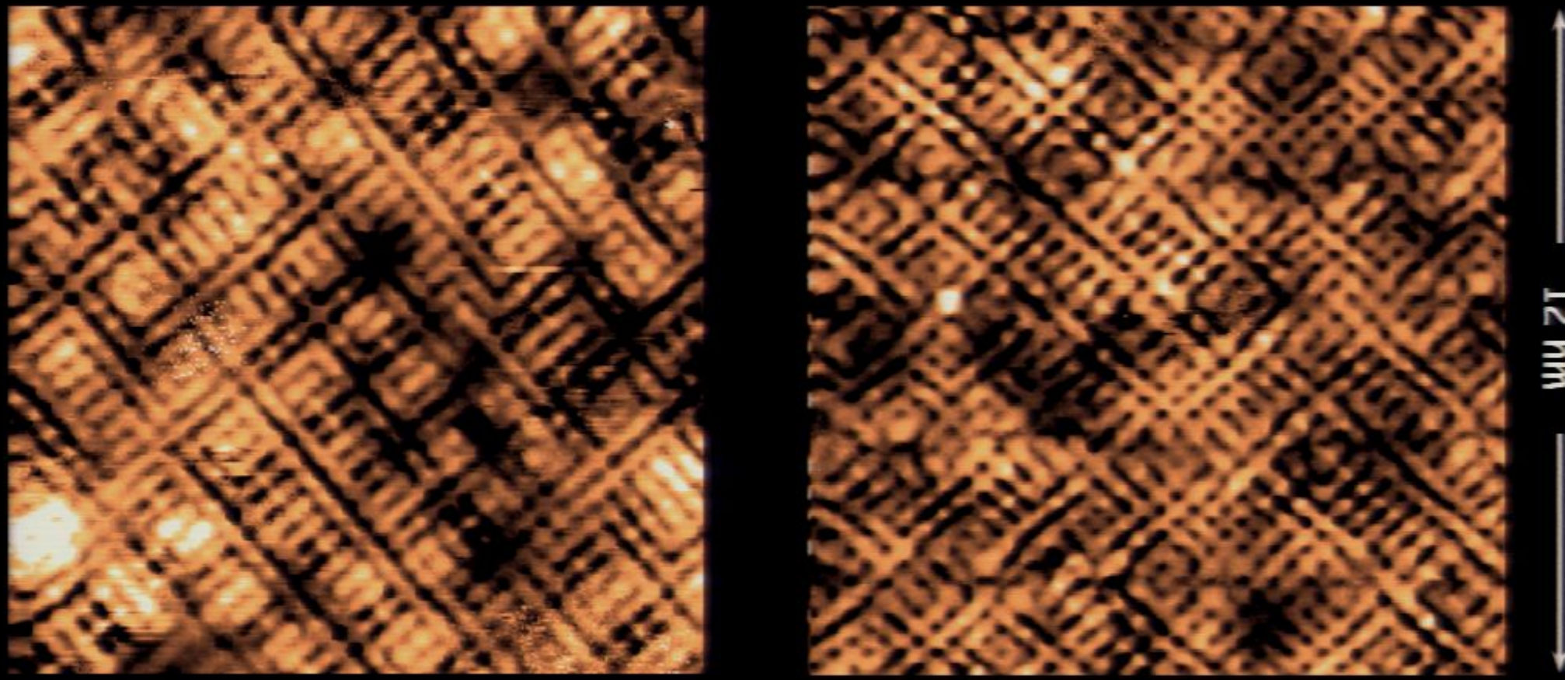

Electronic Smectic: Broken Translational & Rotational Symmetries

Science 313, 1380 (2007); Nature 454, 1072, (2008), Nature 466, 374 (2010)

Link Intra-unit-cell ⇔ Incommensurate Symmetry Breaking ?

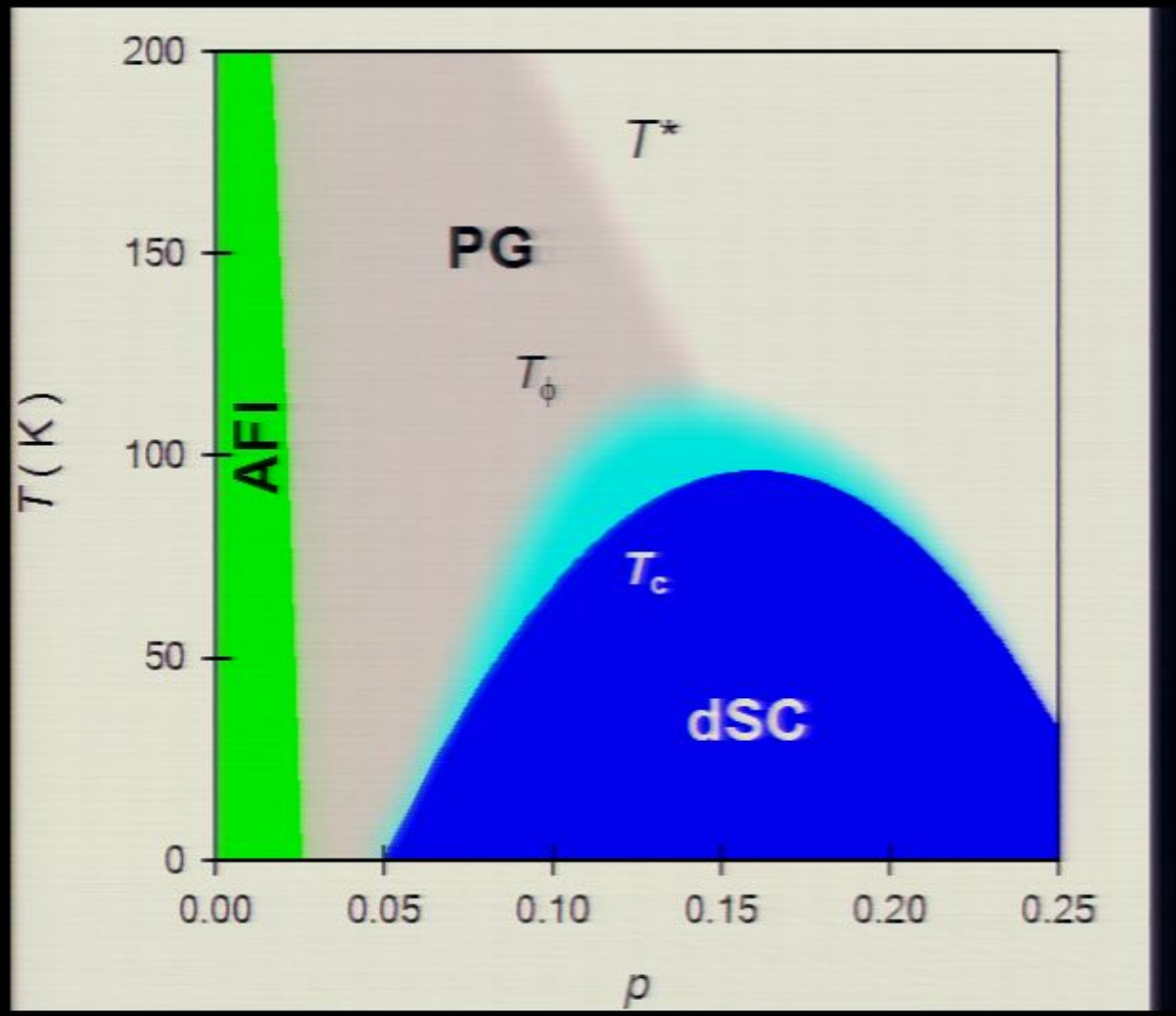

Collaborators

Prof. J. Zaanen
Universiteit Leiden

Prof. S. Sachdev
Harvard U.

Prof. M. J. Lawler
Binghamton U.
Cornell U.

Prof. Eun-Ah Kim
Cornell U.

A. Mesaros
Universiteit Leiden

Dr. K. Fujita
Cornell
BNL

Dr. H. Eisaki
AIST

Prof. S. Uchida
U. Of Tokyo

Long range at $\vec{q} = \vec{Q}_{Bragg}$ but $\vec{q} = \vec{S}$ very short range

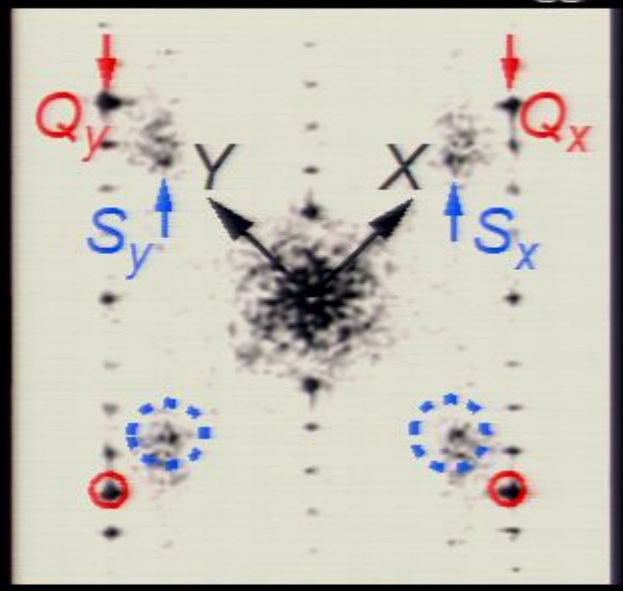

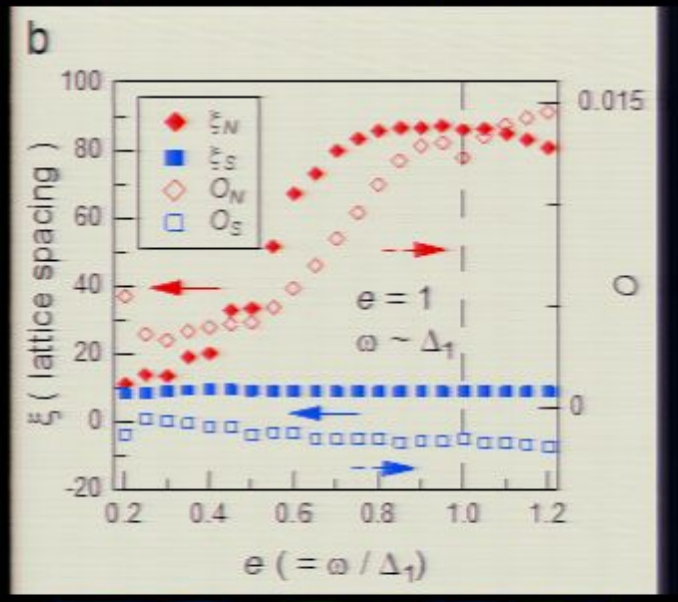

lature 466,
74 (2010)

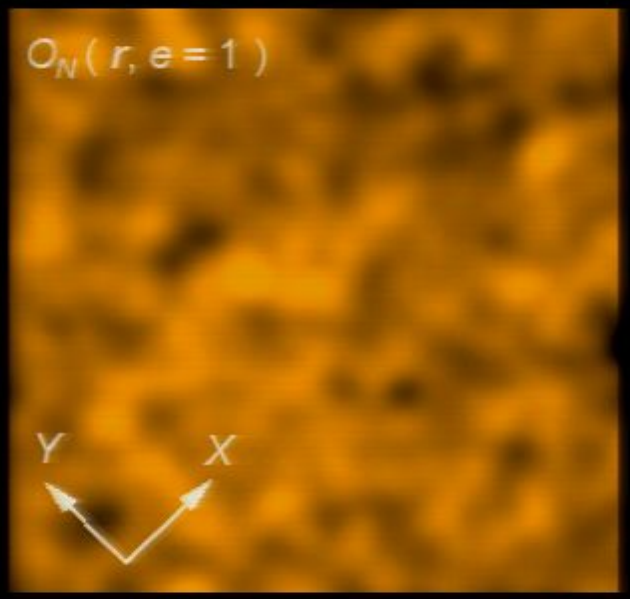

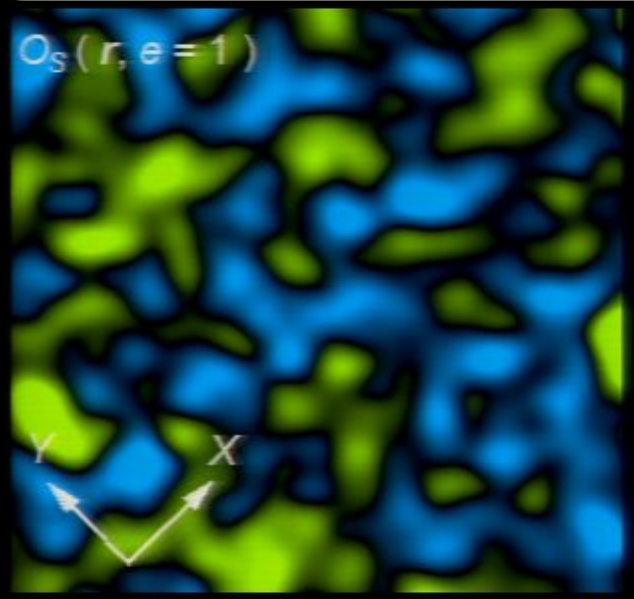

-0.020 +0.020 -0.035 +0.035

Bi2212

Interaction between these states?

Visualize C_4-breaking component PG electronic structure

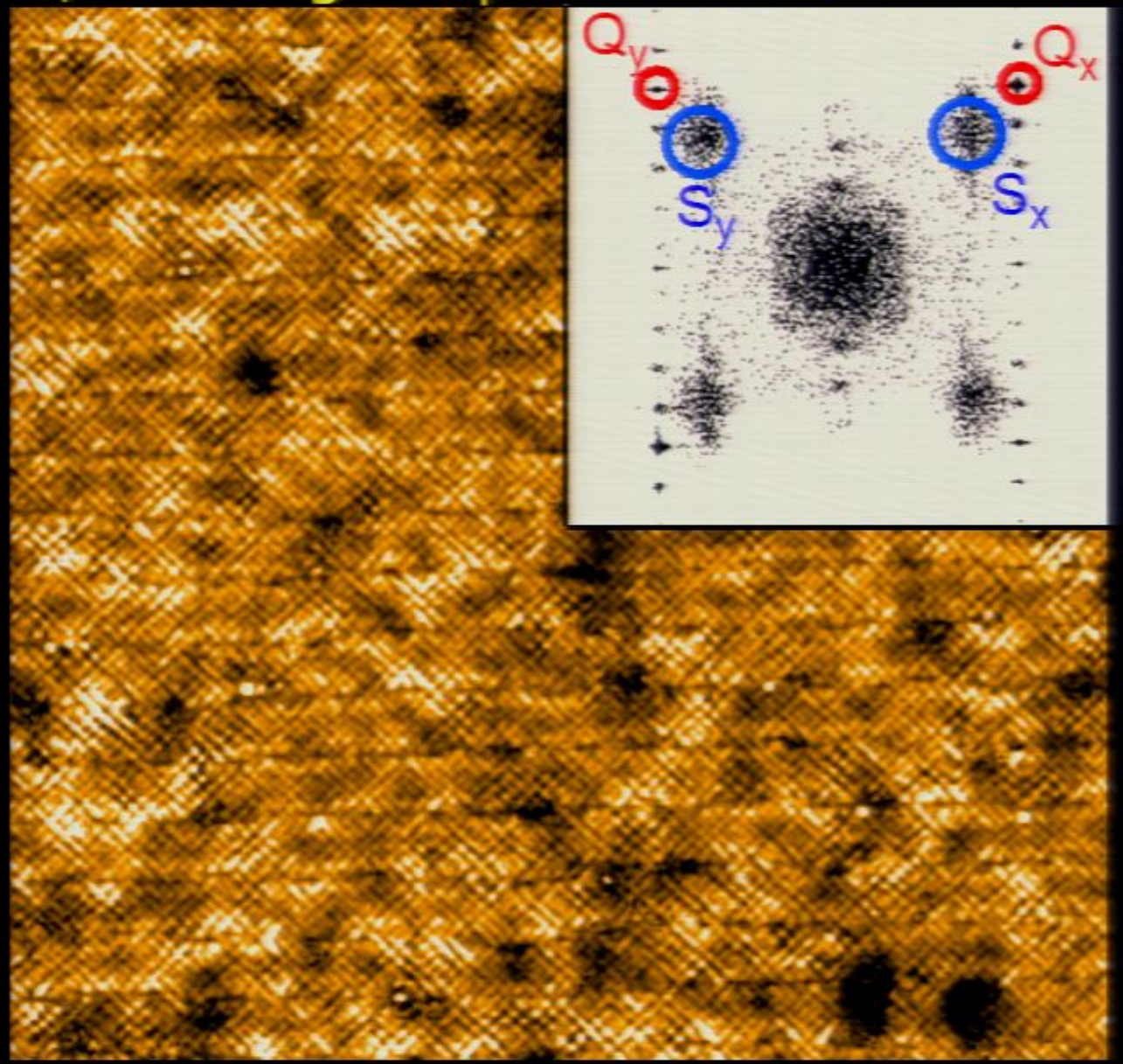

Visualize C_4-breaking component PG electronic structure

$O_n(\mathbf{r})$

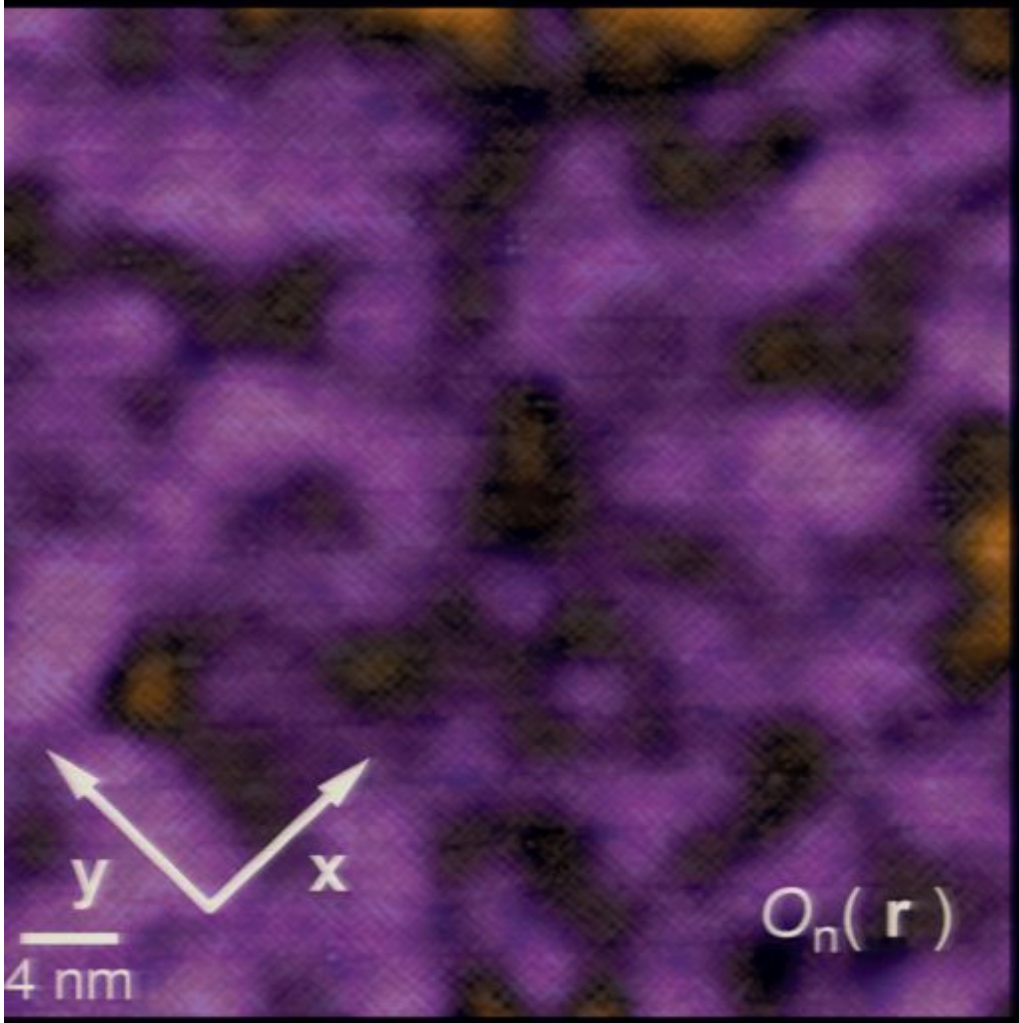

-0.16 0

$$Q^R(r,e=1) \equiv \frac{Z_x(r,e) - Z_y(r,e)}{}$$

Visualize C_4-breaking component PG electronic structure

$O_n(\mathbf{r})$

$\delta O_n(\mathbf{r})$

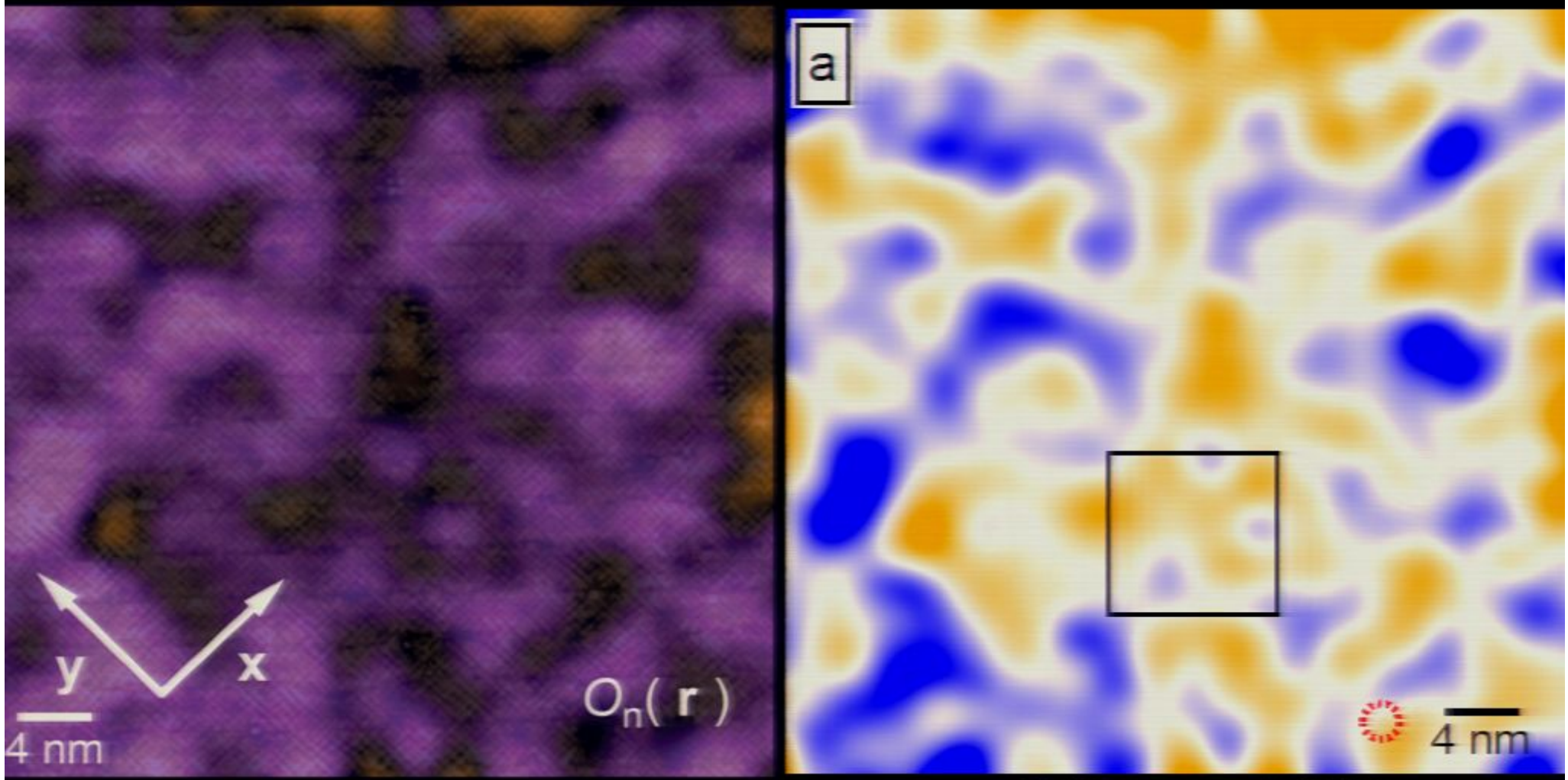

Finite $\langle O_n(\mathbf{r}) \rangle$

$\delta O_n(\mathbf{r}) = O_n(\mathbf{r}) - \langle O_n(\mathbf{r}) \rangle$

Visualize $\vec{q} = \vec{S}$ component PG electronic structure

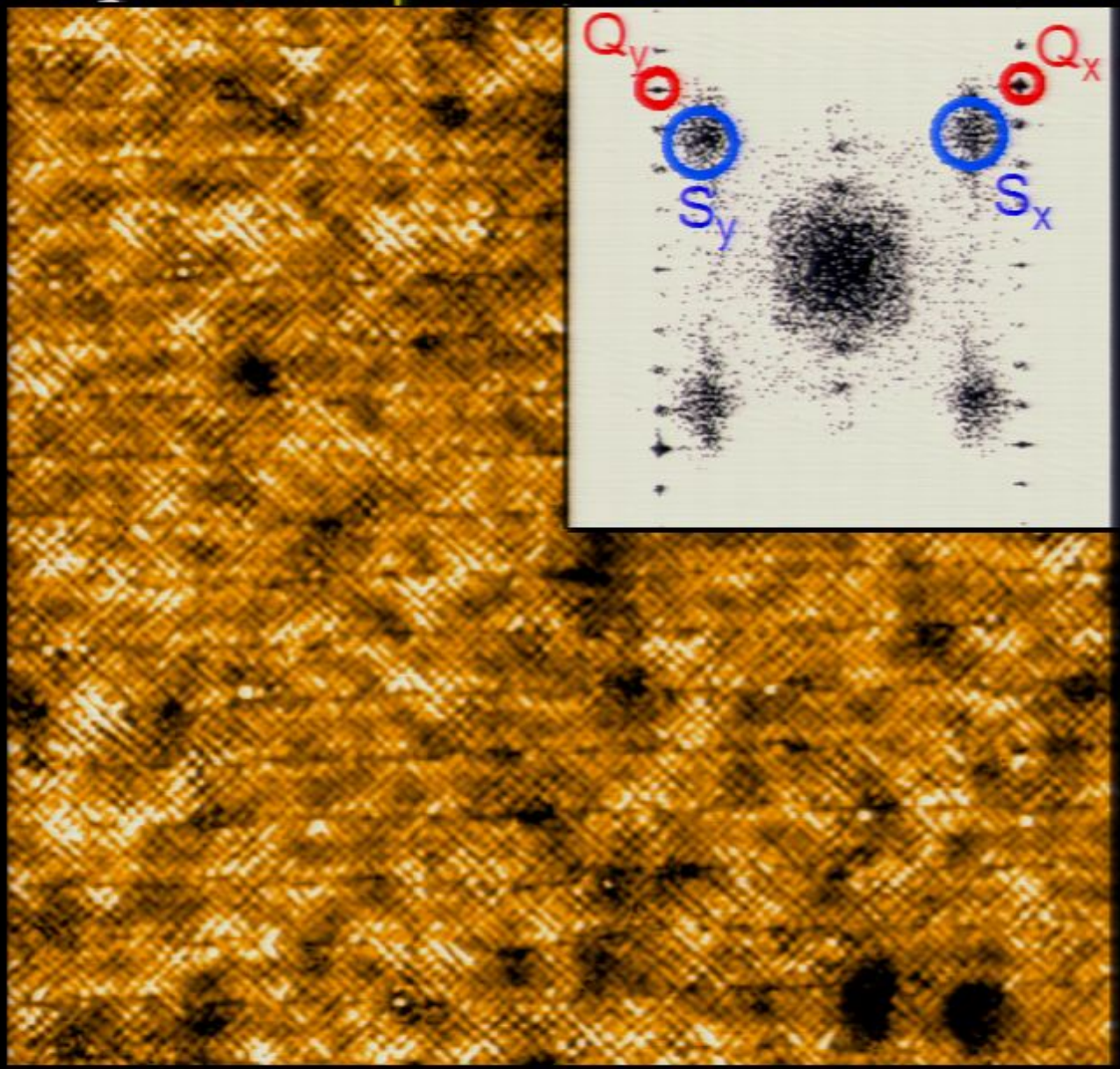

Bi2212

Visualize C_4-breaking component PG electronic structure

$O_n(\mathbf{r})$

$\delta O_n(\mathbf{r})$

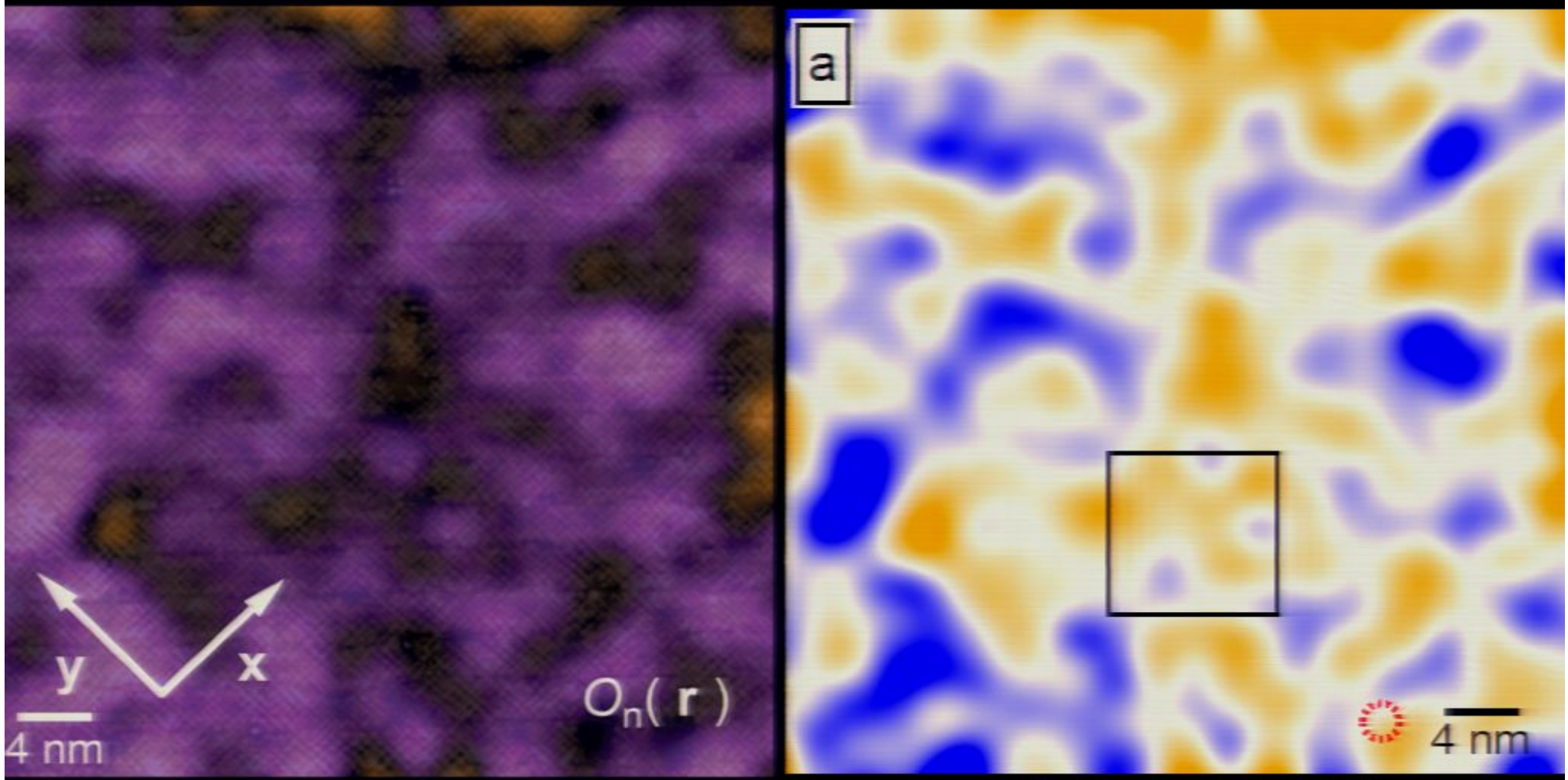

Finite $\langle O_n(\mathbf{r}) \rangle$

$\delta O_n(\mathbf{r}) = O_n(\mathbf{r}) - \langle O_n(\mathbf{r}) \rangle$

Visualize $\vec{q} = \vec{S}$ component PG electronic structure

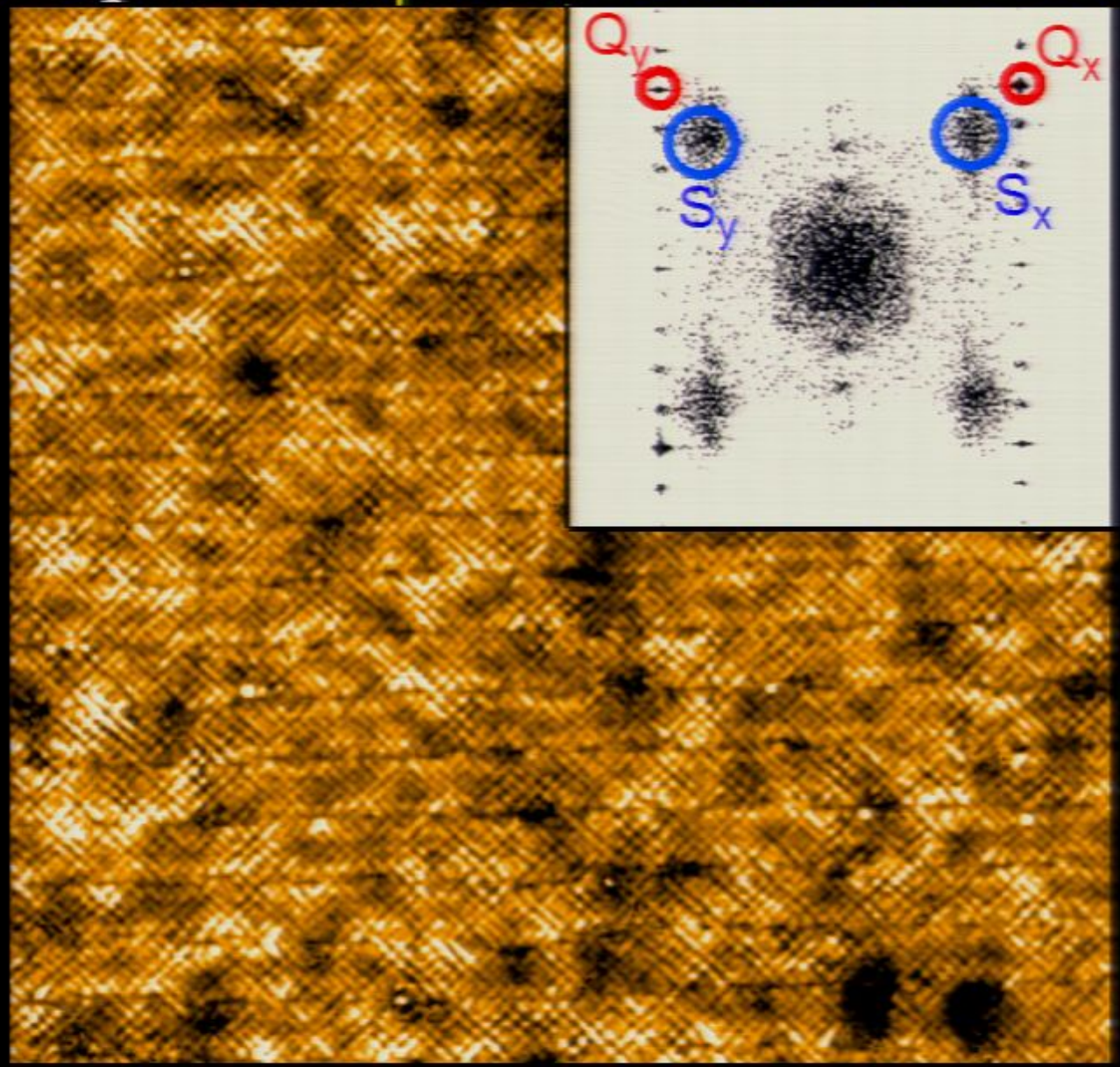

Bi2212

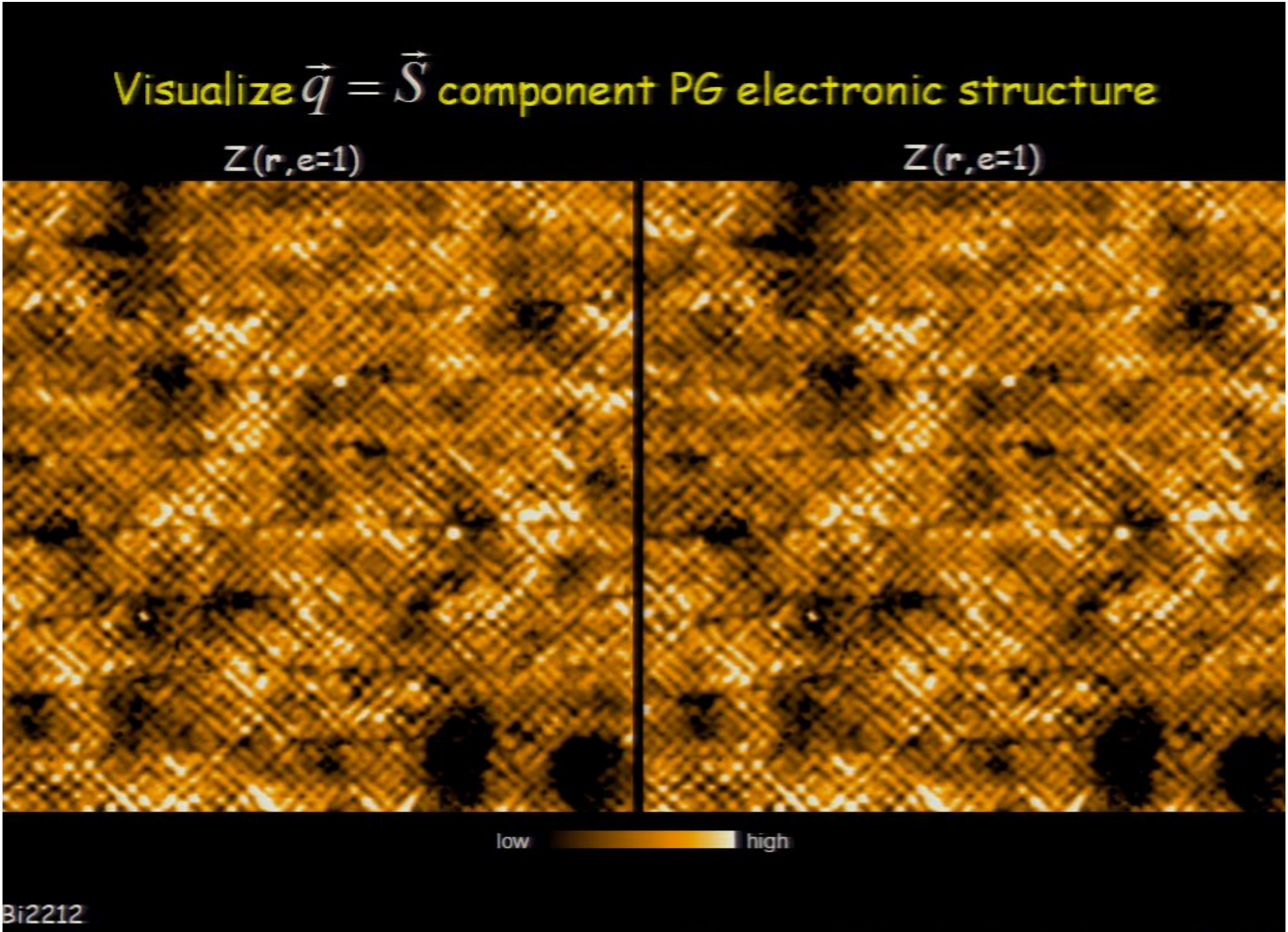
Visualize $\vec{q} = \vec{S}$ component PG electronic structure
Z(r,e=1)
Z(r,e=1)
low
high
Bi2212

Visualize $\vec{q} = \vec{S}$ component PG electronic structure

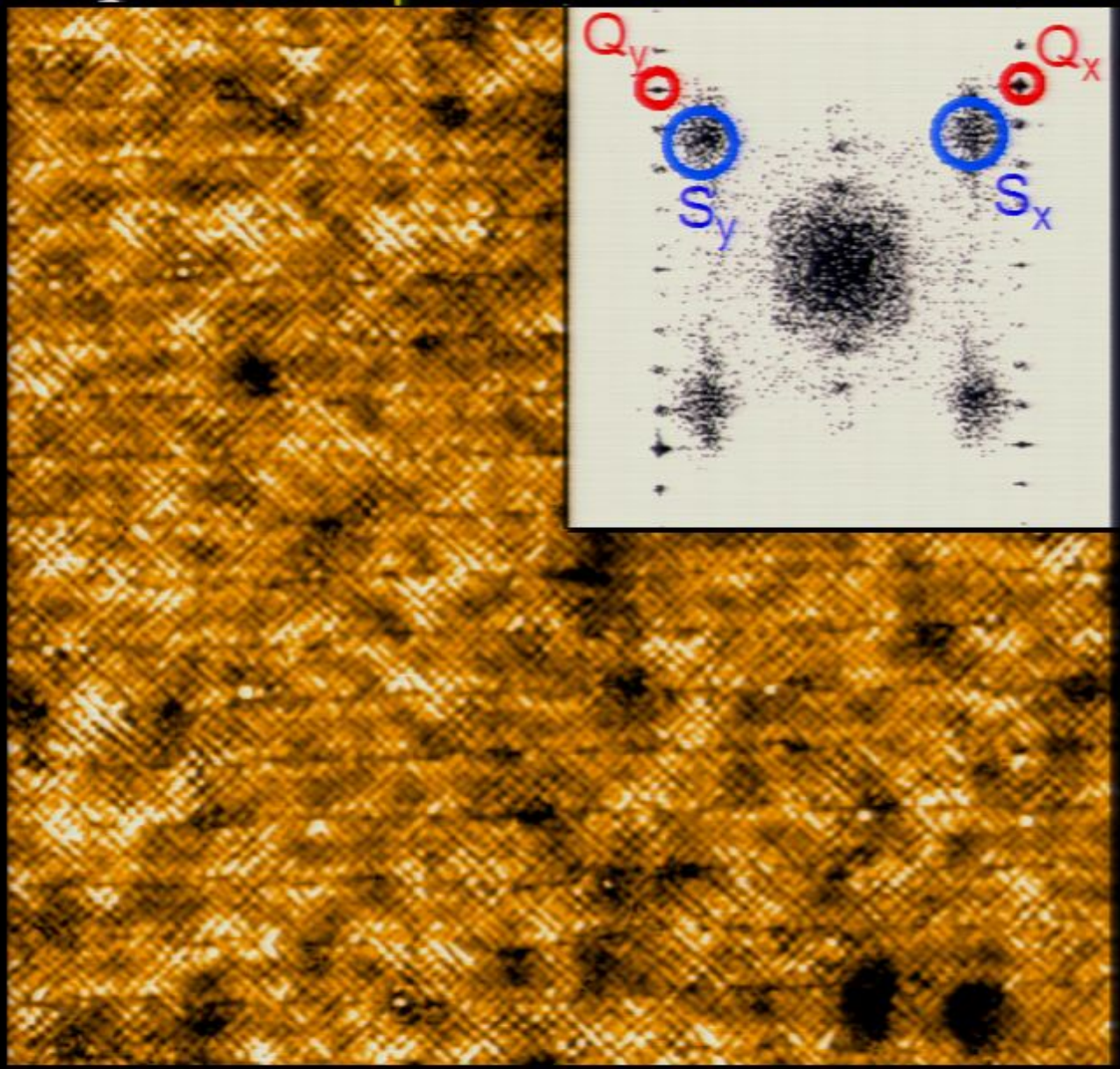

Bi2212

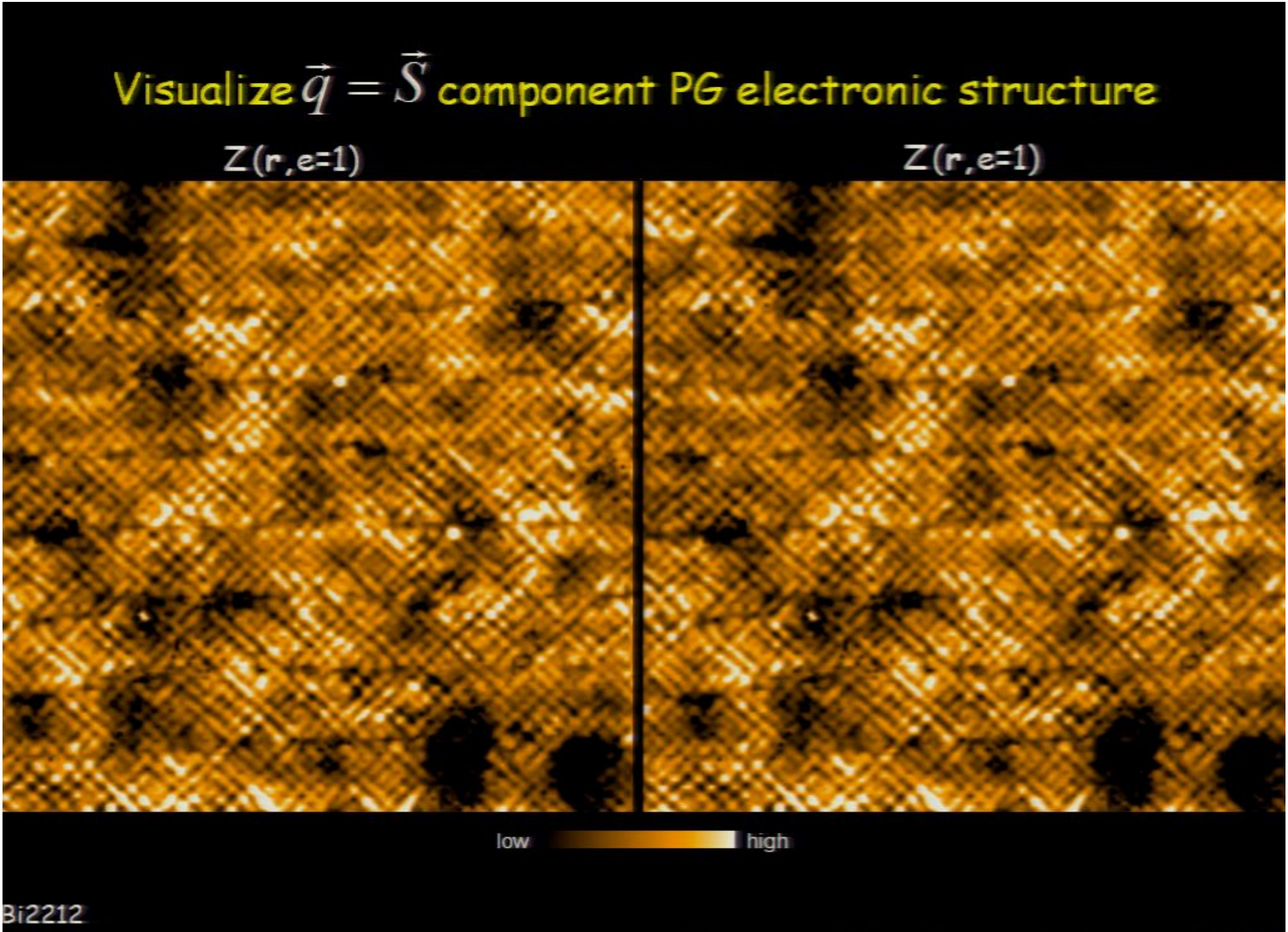
Visualize $\vec{q} = \vec{S}$ component PG electronic structure
Z(r,e=1)
Z(r,e=1)
low
high
Bi2212

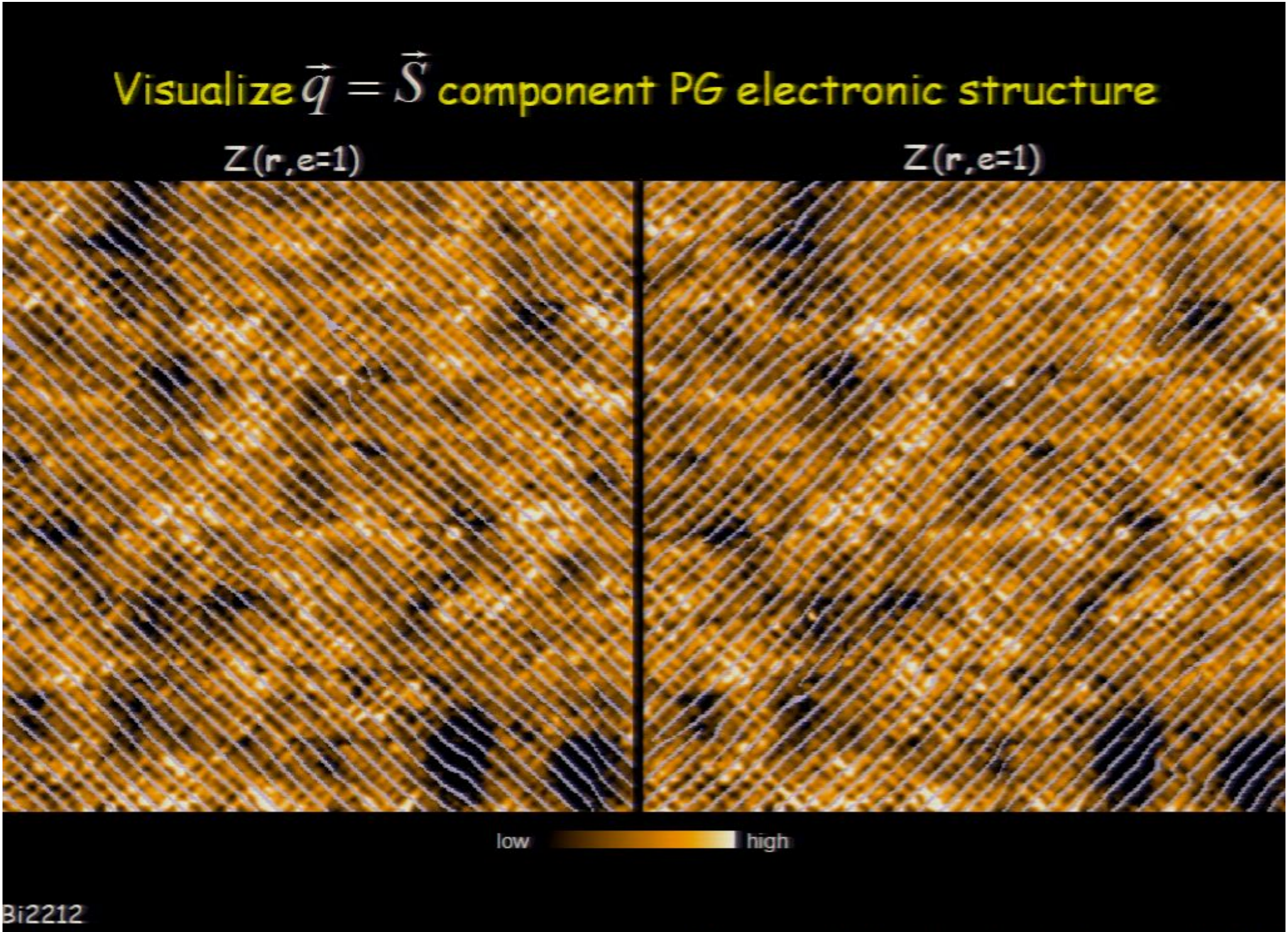
Visualize $\vec{q} = \vec{S}$ component PG electronic structure
Z(r,e=1)
Z(r,e=1)
low
high
Bi2212

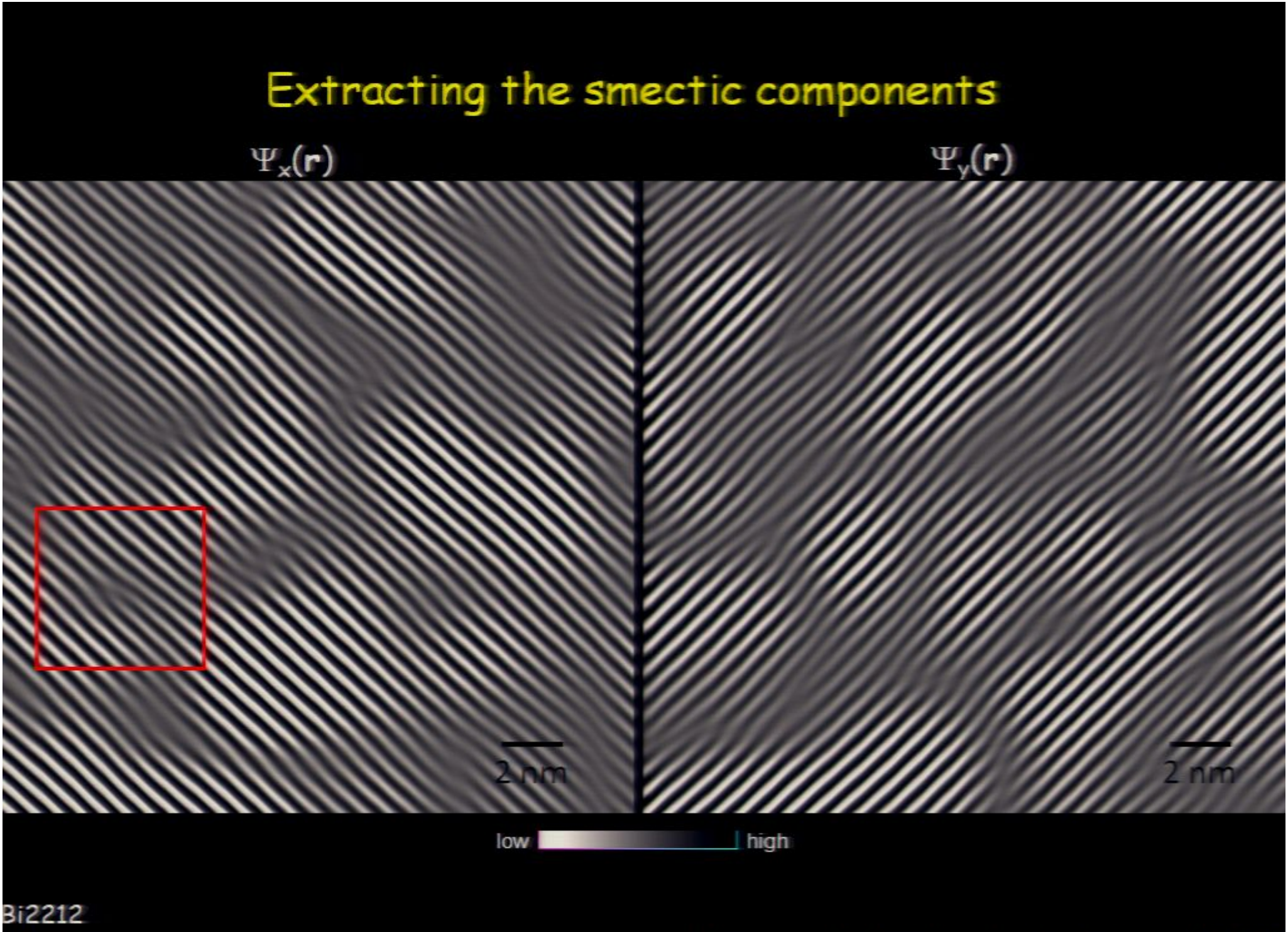
Extracting the smectic components
$\Psi_x(\mathbf{r})$
$\Psi_y(\mathbf{r})$
2 nm
2 nm
low
high
Bi2212

Measuring phase of smectic components

$$\Psi_x(\mathbf{S}_x;\mathbf{r}) = \left|\Psi_x(\mathbf{S}_x;\mathbf{r})\right| e^{i\phi_x(\mathbf{r})}$$

$$\Psi_y(\mathbf{S}_y;\mathbf{r}) = \left|\Psi_y(\mathbf{S}_y;\mathbf{r})\right| e^{i\phi_y(\mathbf{r})}$$

$$\phi_x(\mathbf{r}) = \tan^{-1}\left(\mathrm{Im}\,\Psi_x(\mathbf{S}_x;\mathbf{r}) / \mathrm{Re}\,\Psi_x(\mathbf{S}_x;\mathbf{r})\right)$$

$$\phi_y(\mathbf{r}) = \tan^{-1}\left(\mathrm{Im}\,\Psi_y(\mathbf{S}_y;\mathbf{r}) / \mathrm{Re}\,\Psi_y(\mathbf{S}_y;\mathbf{r})\right)$$

Measuring phase of smectic components

$$\Psi_x(\mathbf{S}_x;\mathbf{r}) = \left|\Psi_x(\mathbf{S}_x;\mathbf{r})\right| e^{i\phi_x(\mathbf{r})}$$

$$\Psi_y(\mathbf{S}_y;\mathbf{r}) = \left|\Psi_y(\mathbf{S}_y;\mathbf{r})\right| e^{i\phi_y(\mathbf{r})}$$

$$\phi_x(\mathbf{r}) = \tan^{-1}\left(\mathrm{Im}\,\Psi_x(\mathbf{S}_x;\mathbf{r}) / \mathrm{Re}\,\Psi_x(\mathbf{S}_x;\mathbf{r})\right)$$

$$\phi_y(\mathbf{r}) = \tan^{-1}\left(\mathrm{Im}\,\Psi_y(\mathbf{S}_y;\mathbf{r}) / \mathrm{Re}\,\Psi_y(\mathbf{S}_y;\mathbf{r})\right)$$

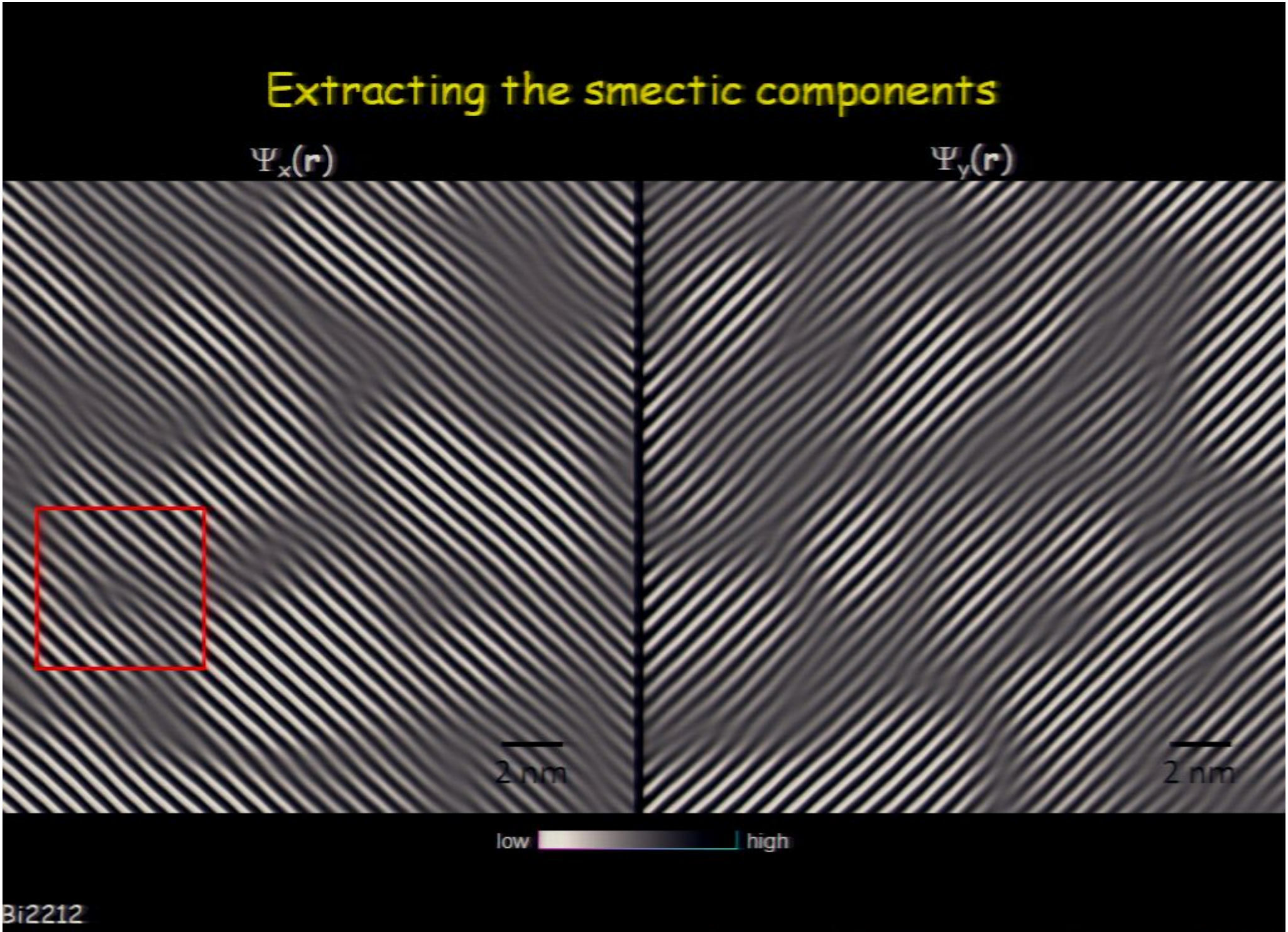
Extracting the smectic components
$\Psi_x(\mathbf{r})$
$\Psi_y(\mathbf{r})$
2 nm
2 nm
low
high
Bi2212

Measuring phase of smectic components

$$\Psi_x(\mathbf{S}_x;\mathbf{r}) = \left|\Psi_x(\mathbf{S}_x;\mathbf{r})\right| e^{i\phi_x(\mathbf{r})}$$

$$\Psi_y(\mathbf{S}_y;\mathbf{r}) = \left|\Psi_y(\mathbf{S}_y;\mathbf{r})\right| e^{i\phi_y(\mathbf{r})}$$

$$\phi_x(\mathbf{r}) = \tan^{-1}\left(\mathrm{Im}\,\Psi_x(\mathbf{S}_x;\mathbf{r}) / \mathrm{Re}\,\Psi_x(\mathbf{S}_x;\mathbf{r})\right)$$

$$\phi_y(\mathbf{r}) = \tan^{-1}\left(\mathrm{Im}\,\Psi_y(\mathbf{S}_y;\mathbf{r}) / \mathrm{Re}\,\Psi_y(\mathbf{S}_y;\mathbf{r})\right)$$

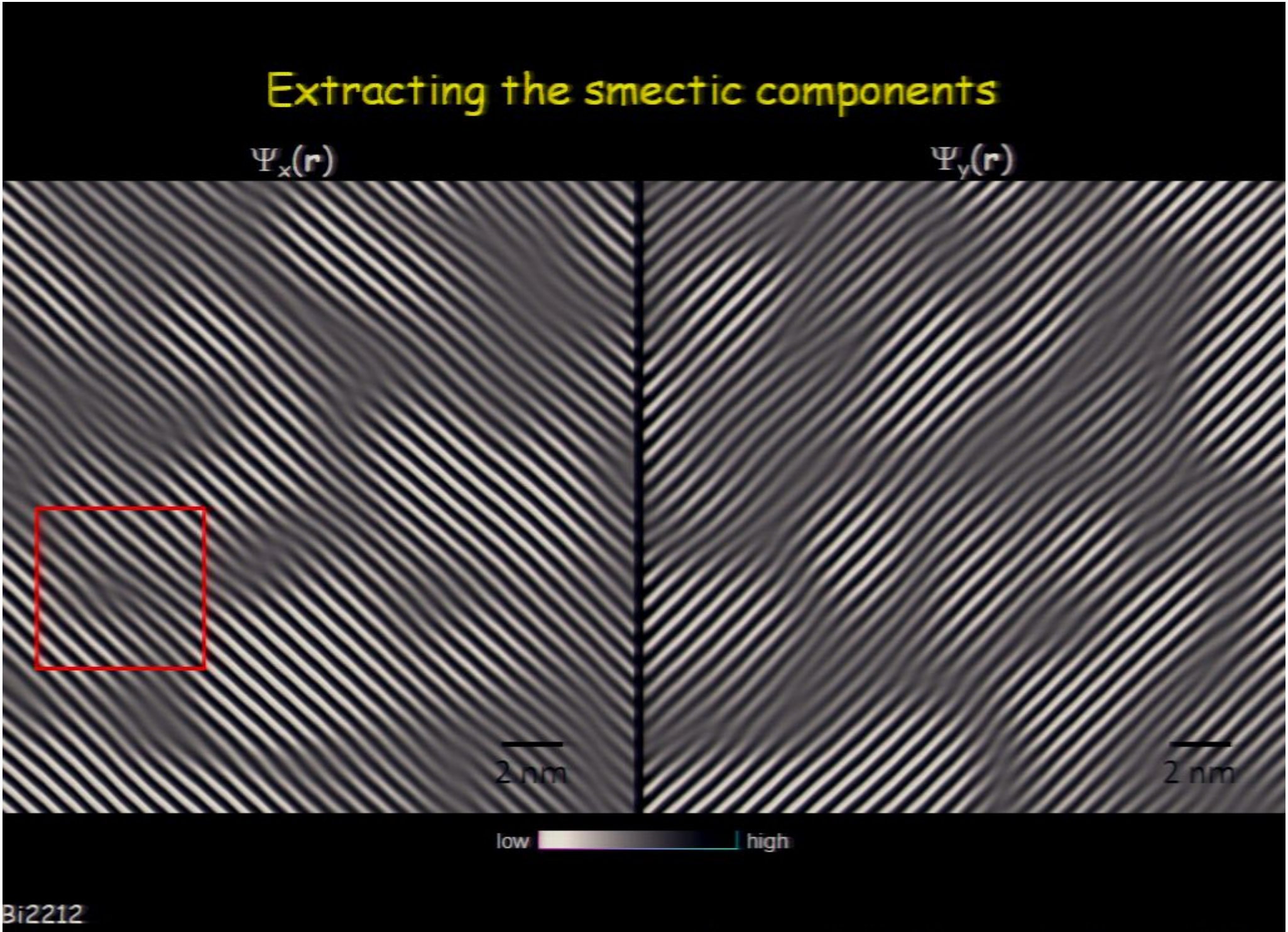
Extracting the smectic components
$\Psi_x(\mathbf{r})$
$\Psi_y(\mathbf{r})$
2 nm
2 nm
low
high
Bi2212

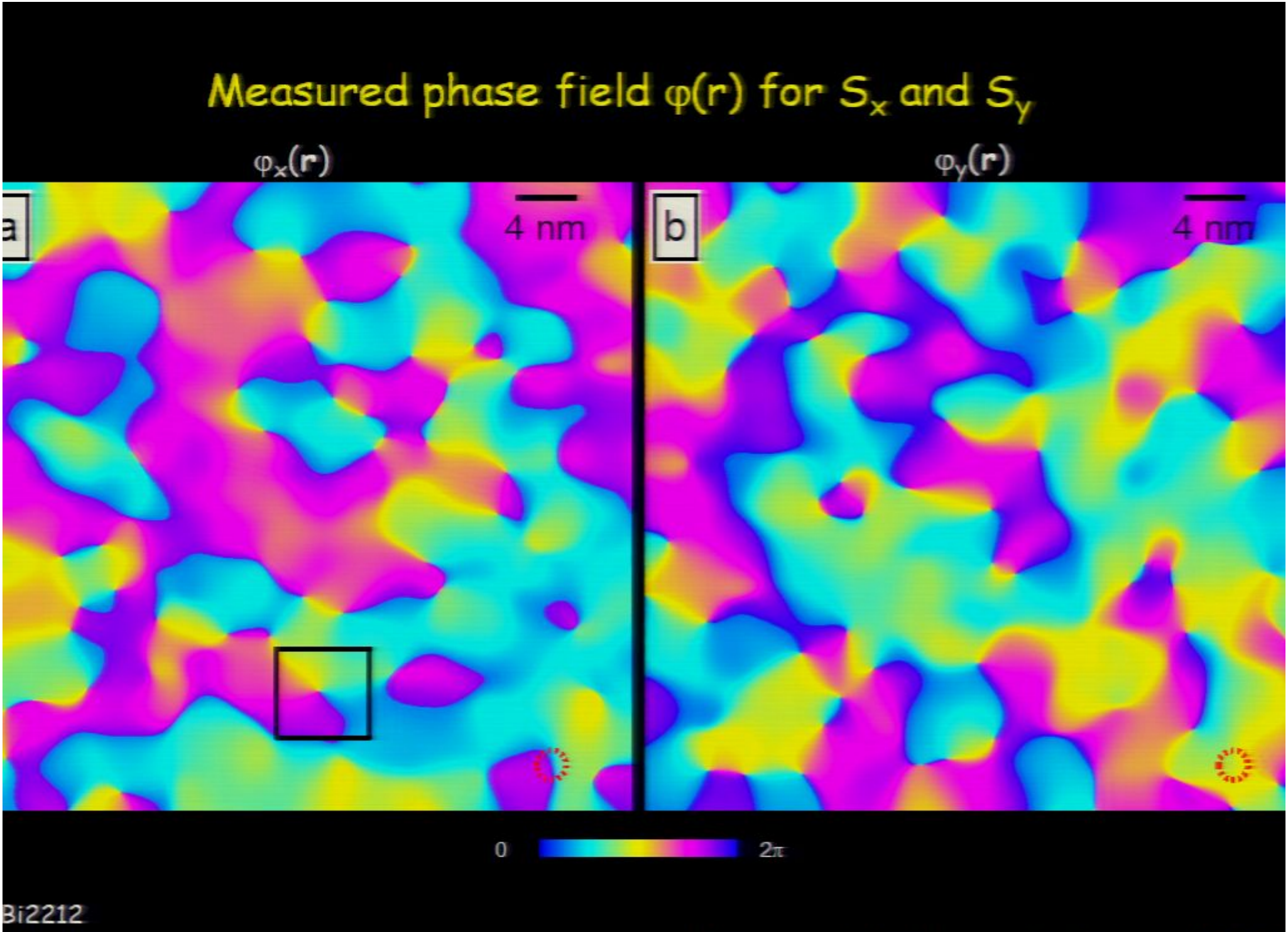
Measured phase field φ(r) for S_x and S_y
$\varphi_x(\mathbf{r})$
$\varphi_y(\mathbf{r})$
a
b
4 nm
4 nm
0
2π
Bi2212

Fluctuations of C_4-breaking $\delta O_n(\mathbf{r})$ + locations of smectic 2π topological defects

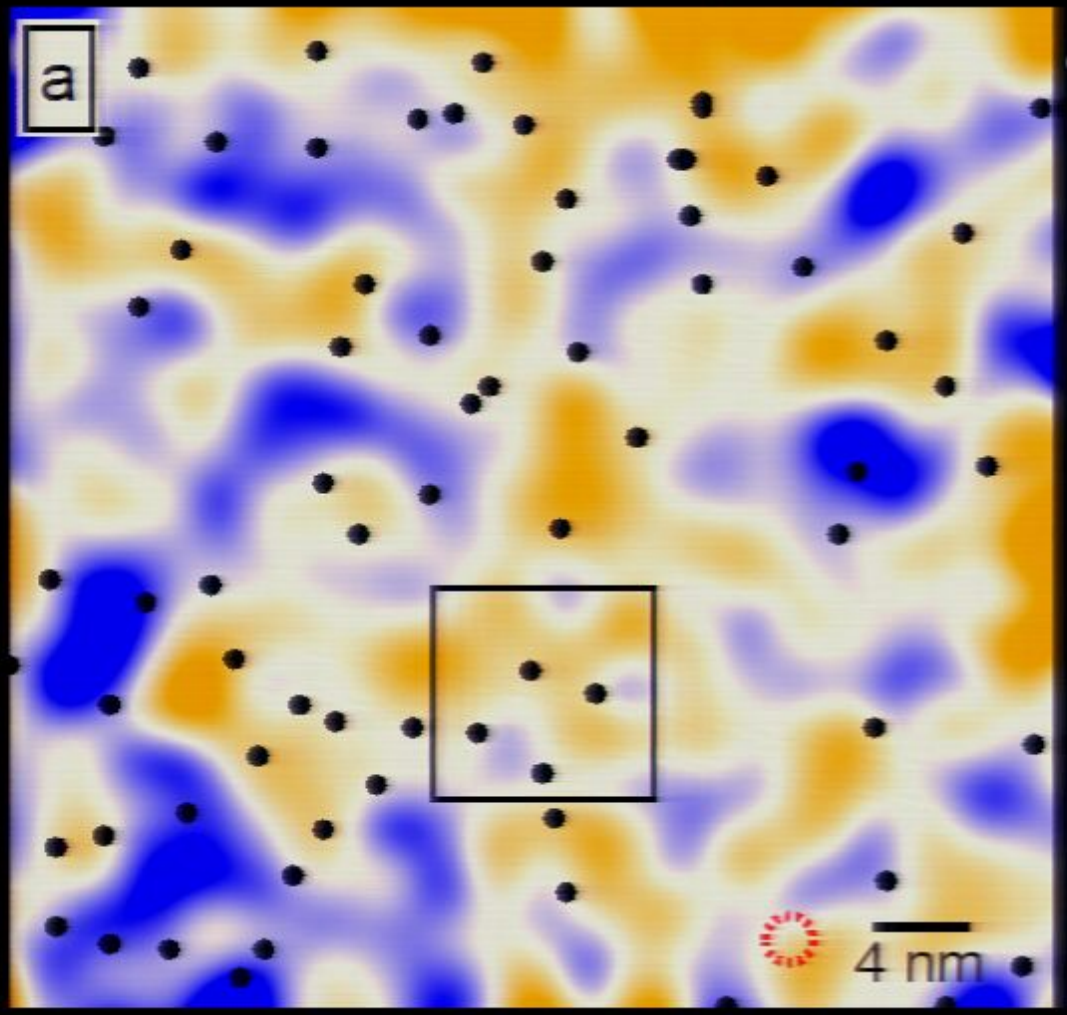

Bi2212

Can we find a Ginzburg-Landau functional linking q=Q to q=S states using the 2π defects?

$O_n(\mathbf{r})$

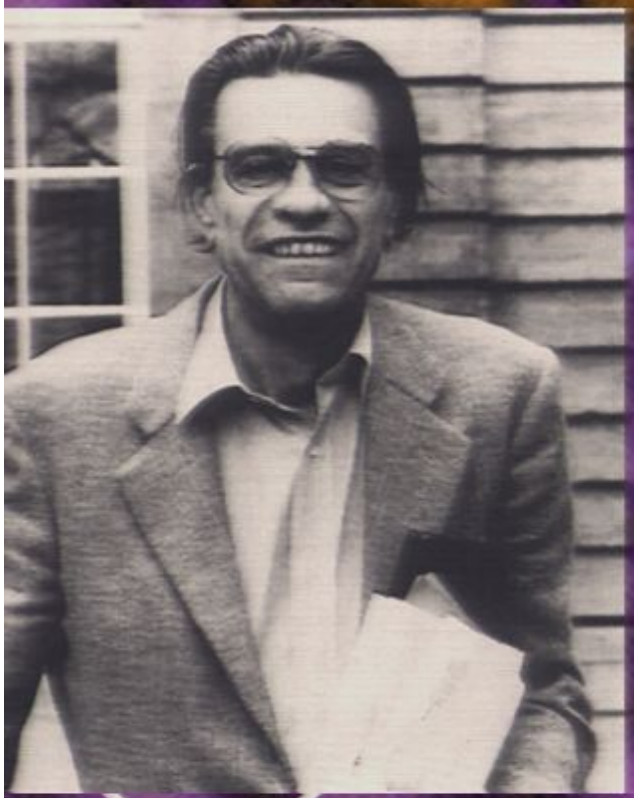

y x

4 nm

$O_n(\mathbf{r})$

$\delta O_n(\mathbf{r})$

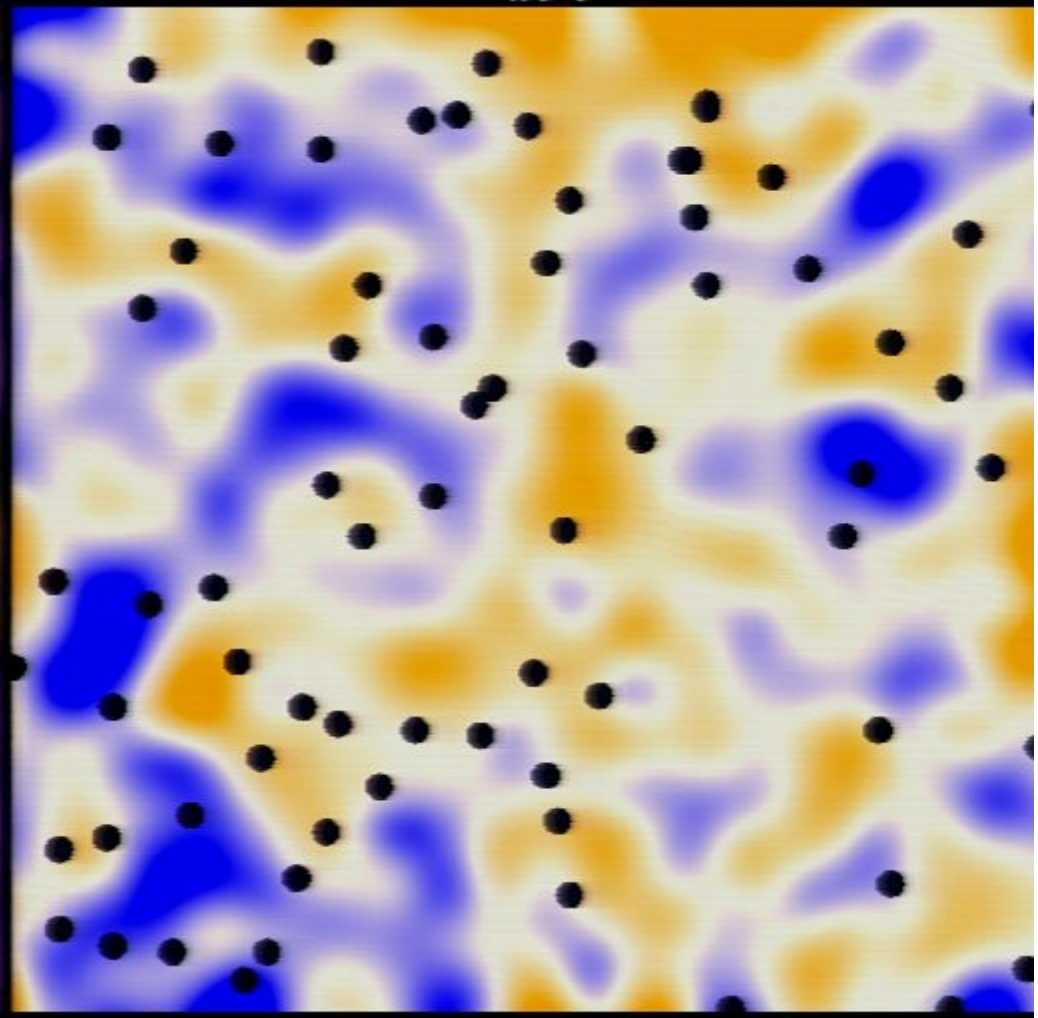

-0.0043 +0.0043

P. G. de Gennes, *Solid State*

Reminder: Ginzburg-Landau free energy at 2π topological defect in superconductor

$$F_{GL}[\psi,\mathbf{A}] = \int d\mathbf{r}^3 \left[a|\psi|^2 + C\left|(\nabla + i\frac{2e}{\hbar}\mathbf{A})\psi\right|^2 + \frac{1}{2}g|\psi|^4 \right]$$

$$+\frac{1}{8\pi\mu_0}\int d\mathbf{r}^3(\nabla\times\mathbf{A})^2 - \frac{1}{4\pi}\int d\mathbf{r}^3 H\cdot(\nabla\times\mathbf{A})$$

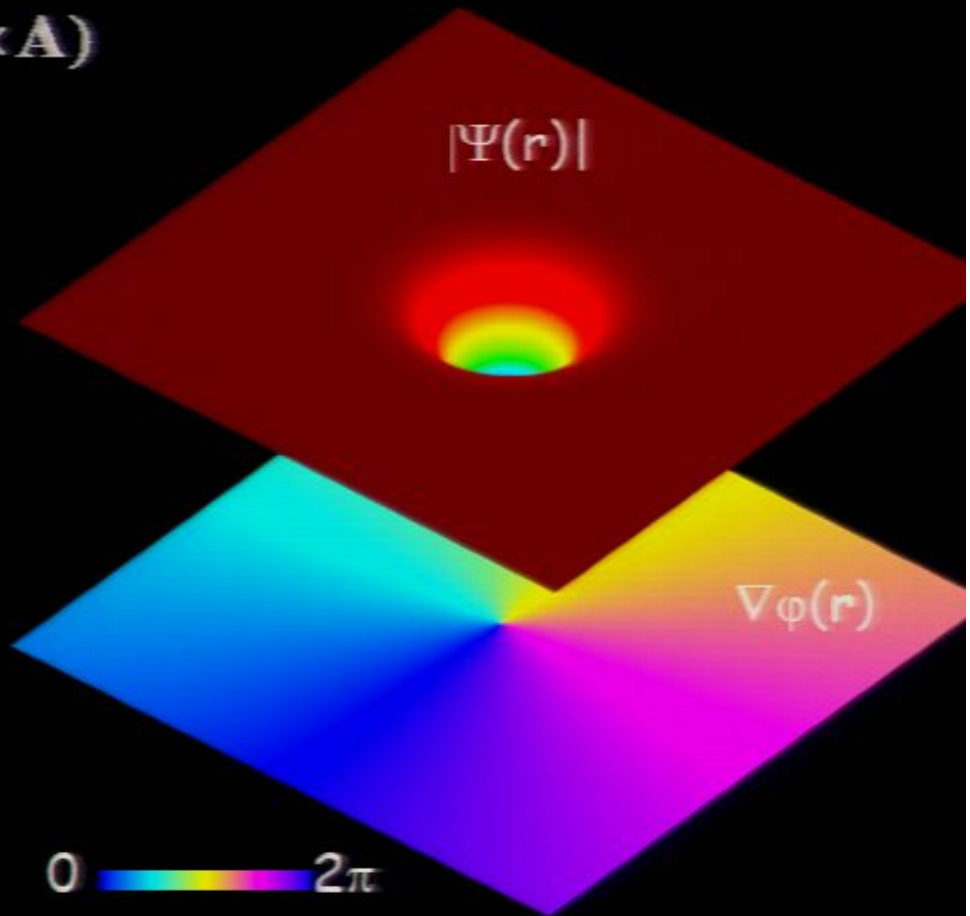

G-L functional leads to a particular type of C_4-breaking fluctuation linked to the smectic 2π defect

$$F_{GL}[\delta O_n, \psi_1, \psi_2] = F_n[\delta O_n]$$
$$+\int d\mathbf{r}^2 \sum_{s=1,2}\left[a_{x,s}\left|(\nabla_x + ic_x\delta O_n)\psi_s\right|^2 + a_{y,s}\left|(\nabla_y + ic_y\delta O_n)\psi_s\right|^2 + m_s\left|\psi_s\right|^2 + \beta_s\delta O_n\left|\psi_s\right|^2\right.$$

C_4-breaking fluctuation

$$\delta O_n(\mathbf{r}) \propto \vec{l} \bullet \nabla_i \varphi_s(\mathbf{r})$$

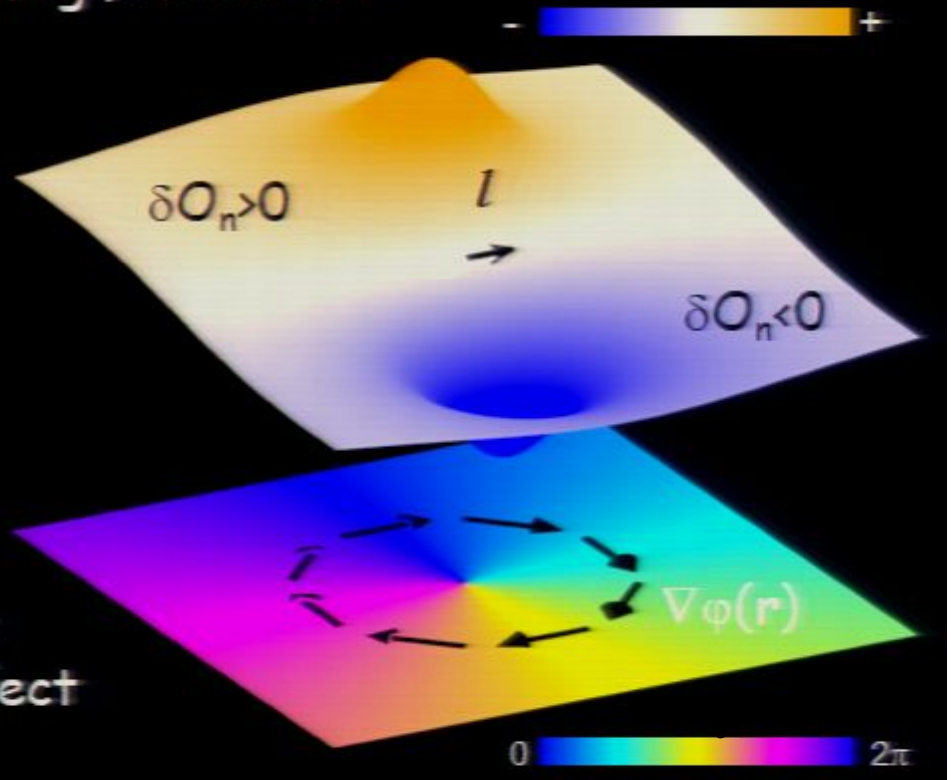

Smectic 2π topological defect

G-L functional leads to a particular type of C_4-breaking fluctuation linked to the smectic 2π defect

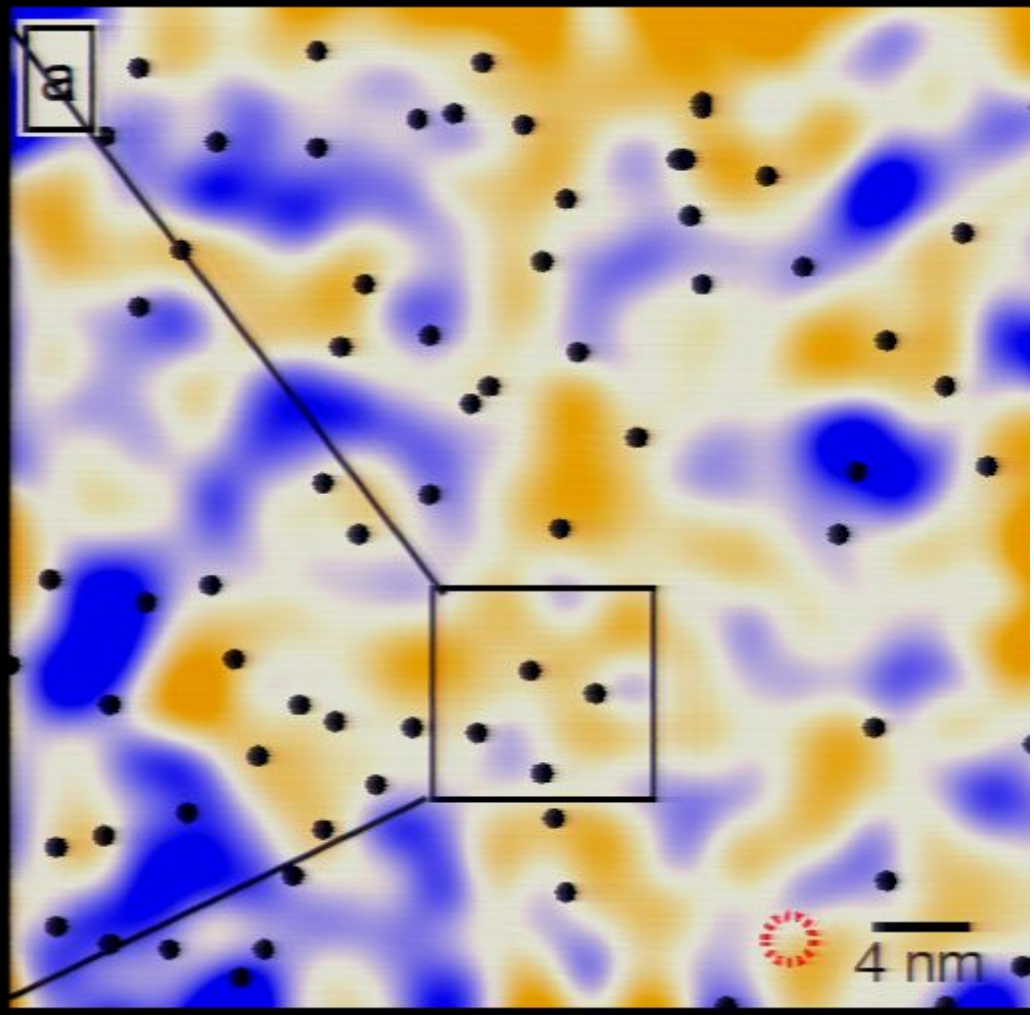

-0.0043 +0.0043

Bi2212

G-L functional leads to a particular type of C_4-breaking fluctuation linked to the smectic 2π defect

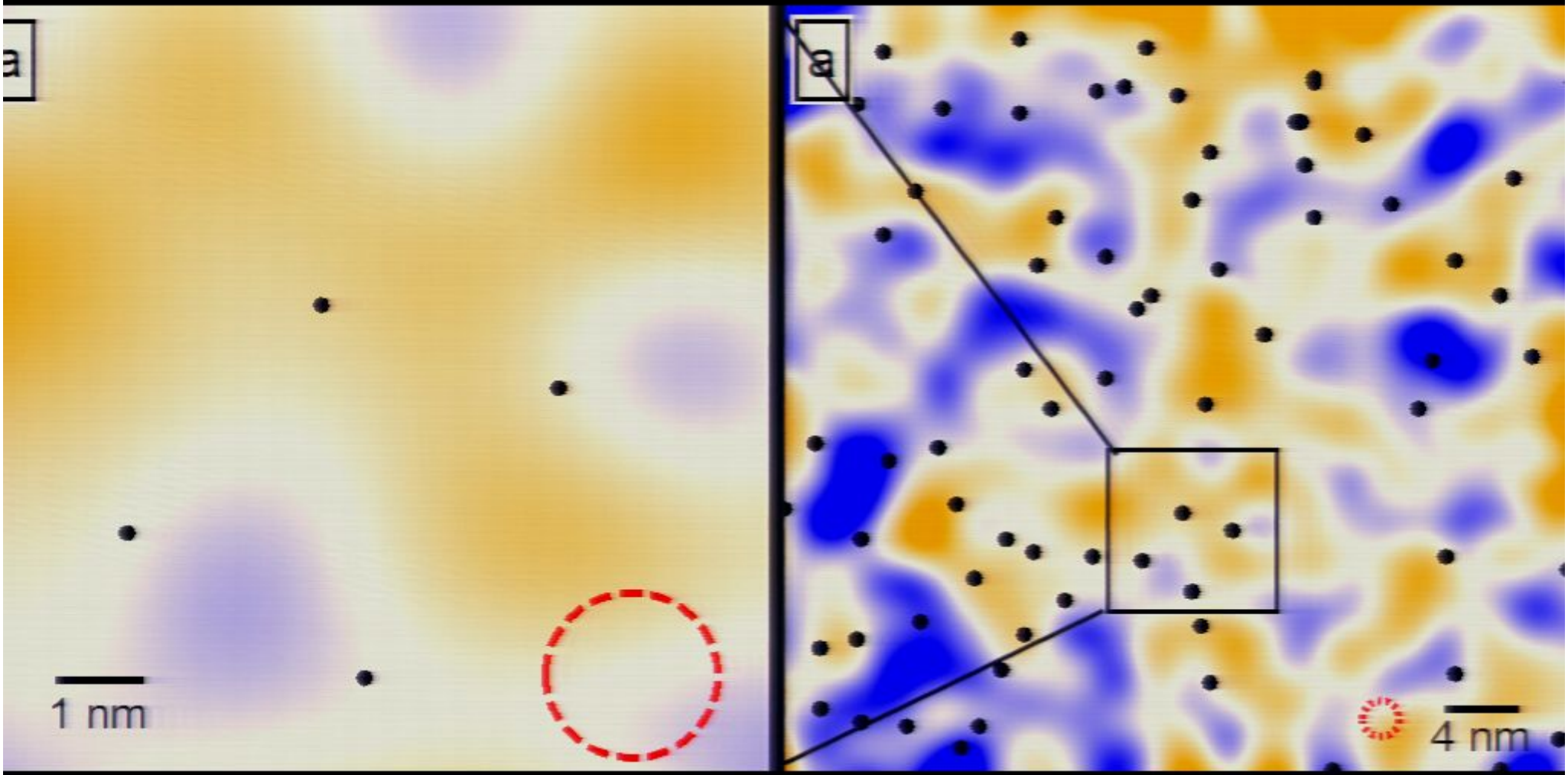

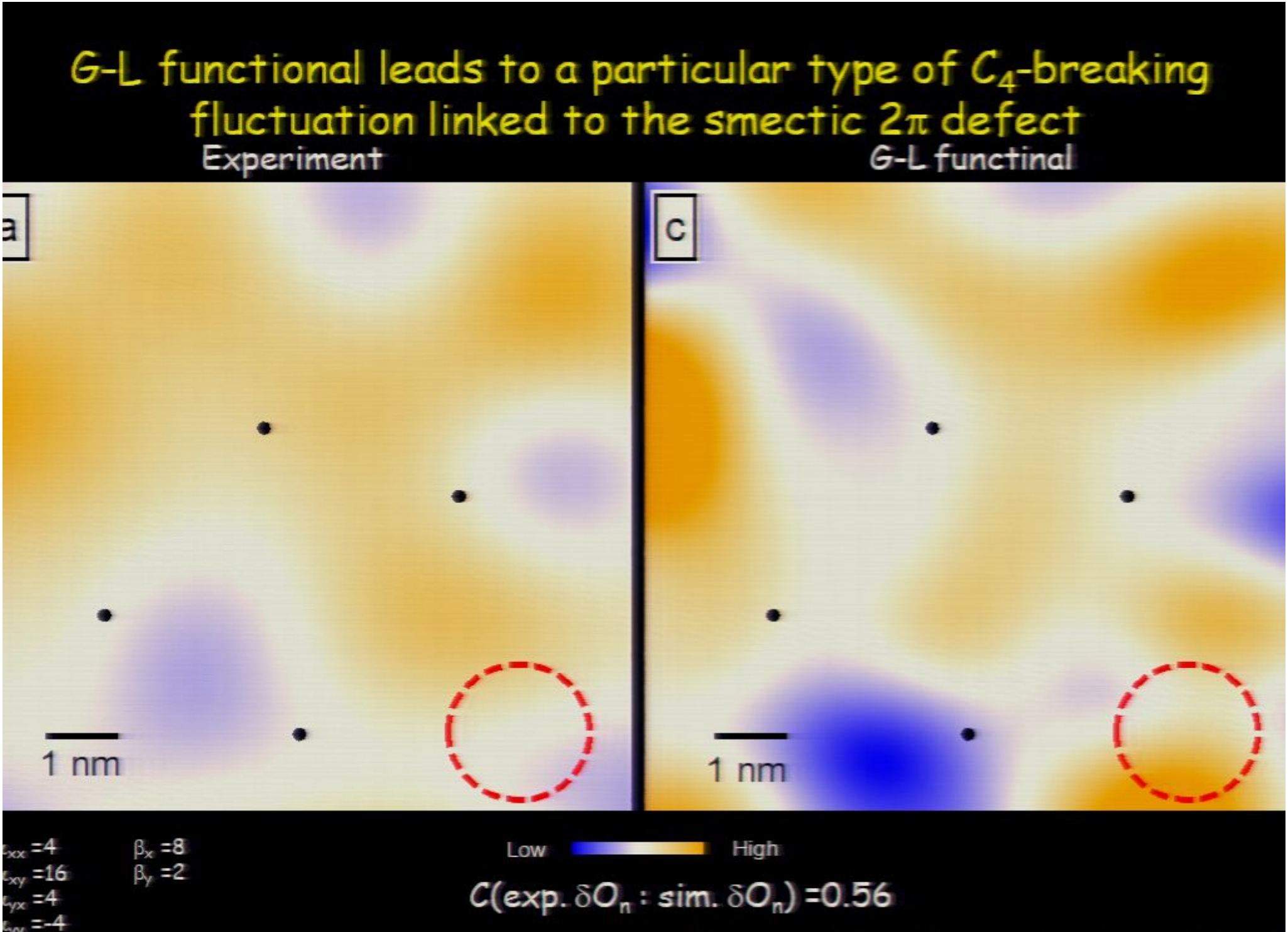
G-L functional leads to a particular type of C_4-breaking fluctuation linked to the smectic 2π defect
Experiment
G-L functinal
a
c
1 nm
1 nm
ζ_{xx} =4
ζ_{xy} =16
ζ_{yx} =4
ζ_{yy} =-4
β_x =8
β_y =2
Low
High
$C(\text{exp. } \delta O_n : \text{sim. } \delta O_n)$ =0.56

G-L functional leads to a particular type of C_4-breaking fluctuation linked to the smectic 2π defect

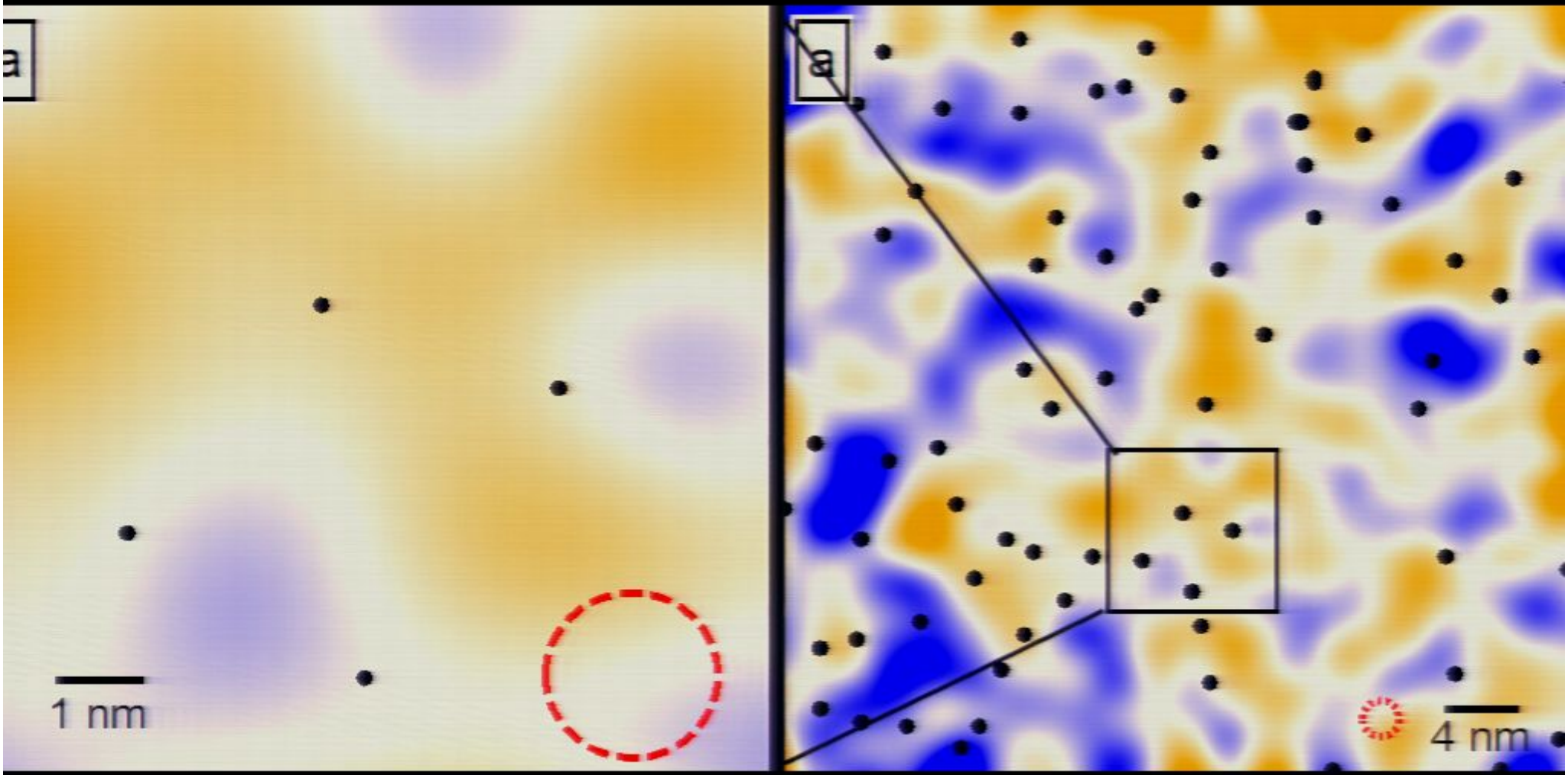

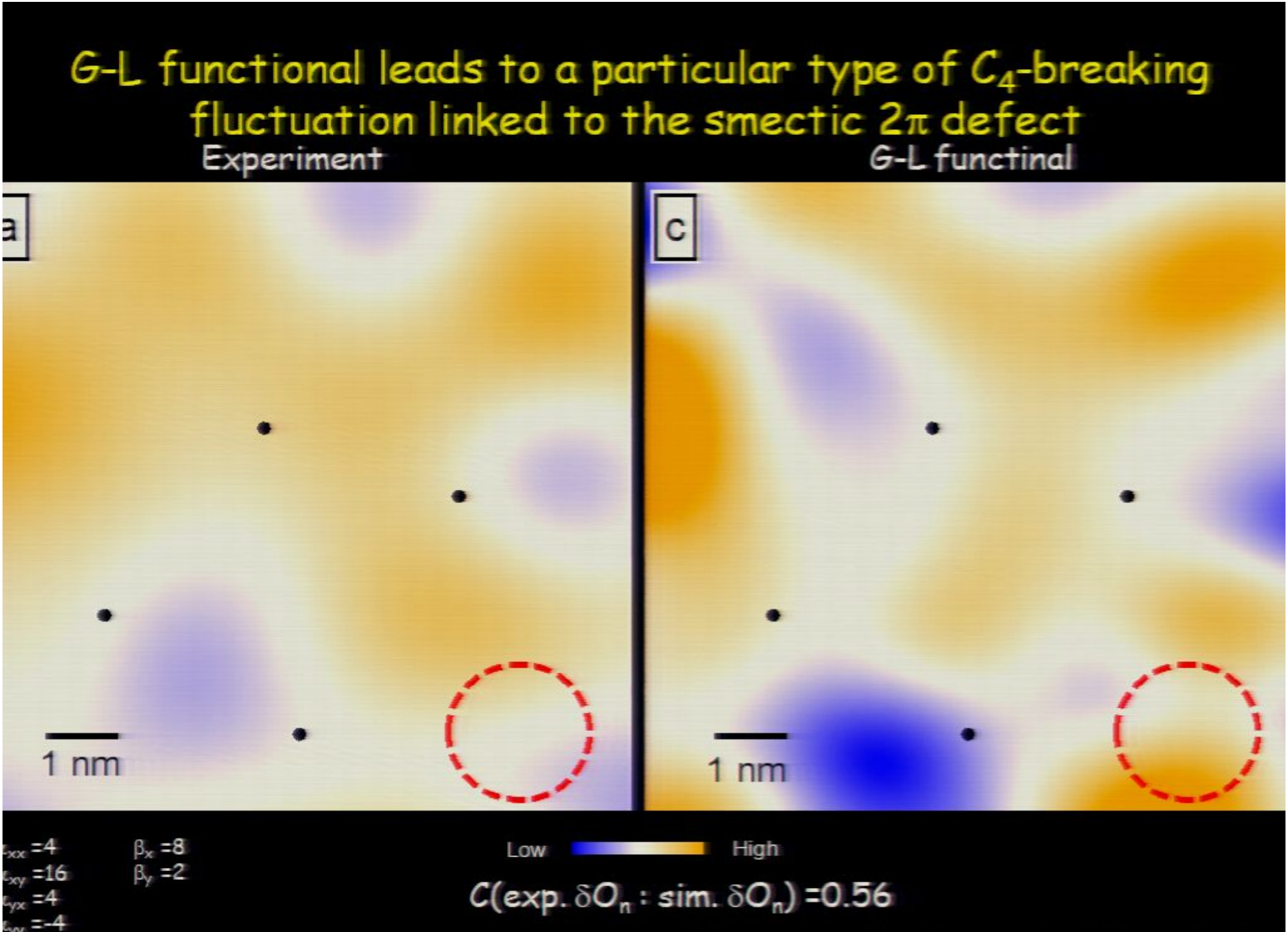
G-L functional leads to a particular type of C_4-breaking fluctuation linked to the smectic 2π defect
Experiment
G-L functinal
a
c
1 nm
1 nm
ζ_{xx} =4
ζ_{xy} =16
ζ_{yx} =4
ζ_{yy} =-4
β_x =8
β_y =2
Low
High
$C(\text{exp. } \delta O_n : \text{sim. } \delta O_n)$ =0.56

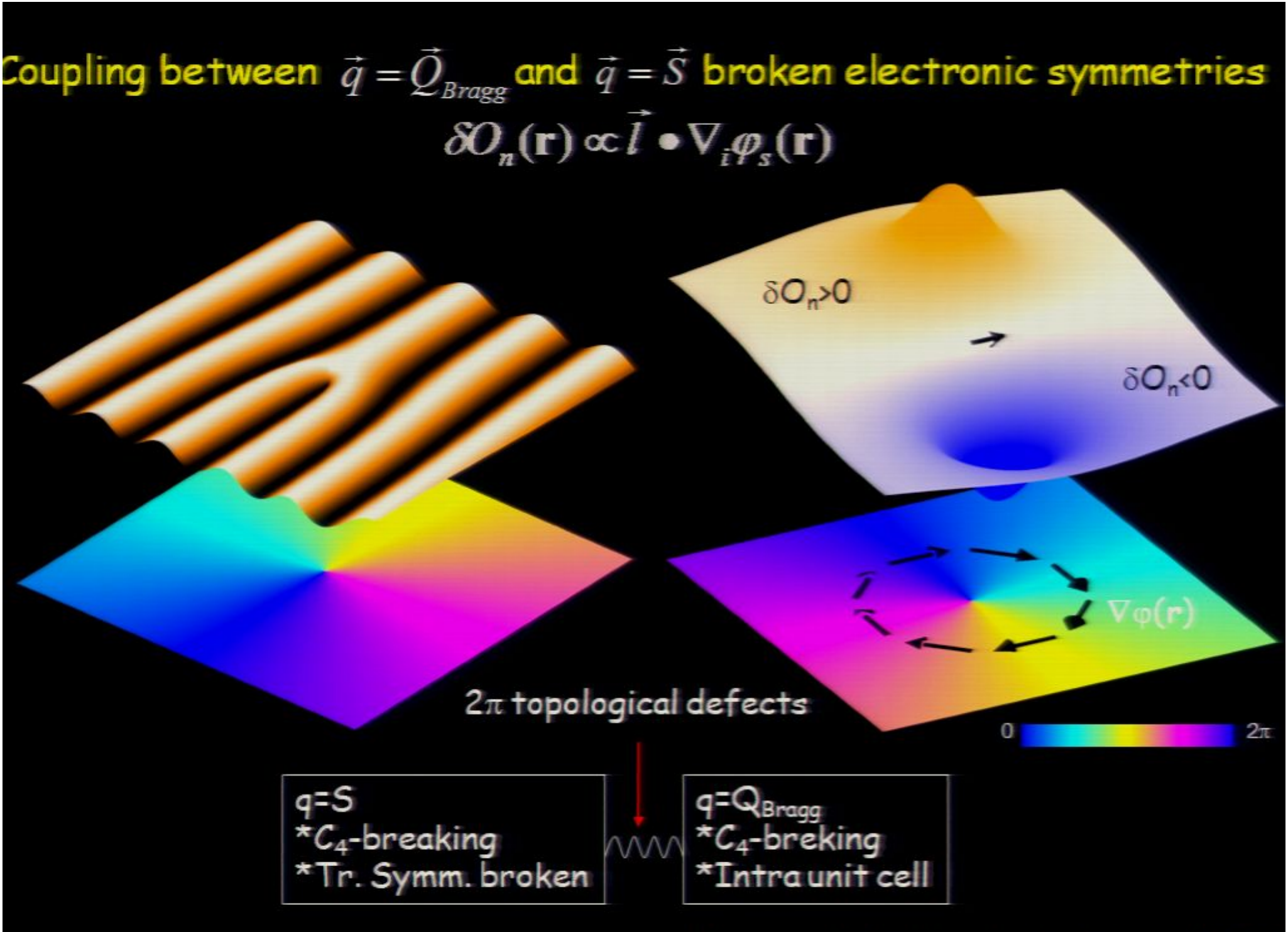
Coupling between $\vec{q}=\vec{Q}_{Bragg}$ and $\vec{q}=\vec{S}$ broken electronic symmetries
$\delta O_n(\mathbf{r}) \propto \vec{l} \bullet \nabla_i \varphi_S(\mathbf{r})$
$\delta O_n>0$
$\delta O_n<0$
$\nabla\varphi(\mathbf{r})$
2π topological defects
0
2π
q=S
*C_4-breaking
*Tr. Symm. broken
q=Q_{Bragg}
*C_4-breking
*Intra unit cell

SUMMARY

Coupling between $\vec{q} = \vec{Q}_{Bragg}$ and $\vec{q} = \vec{S}$ broken electronic symmetries

$$\delta O_n(\mathbf{r}) \propto \vec{l} \bullet \nabla_i \varphi_s(\mathbf{r})$$

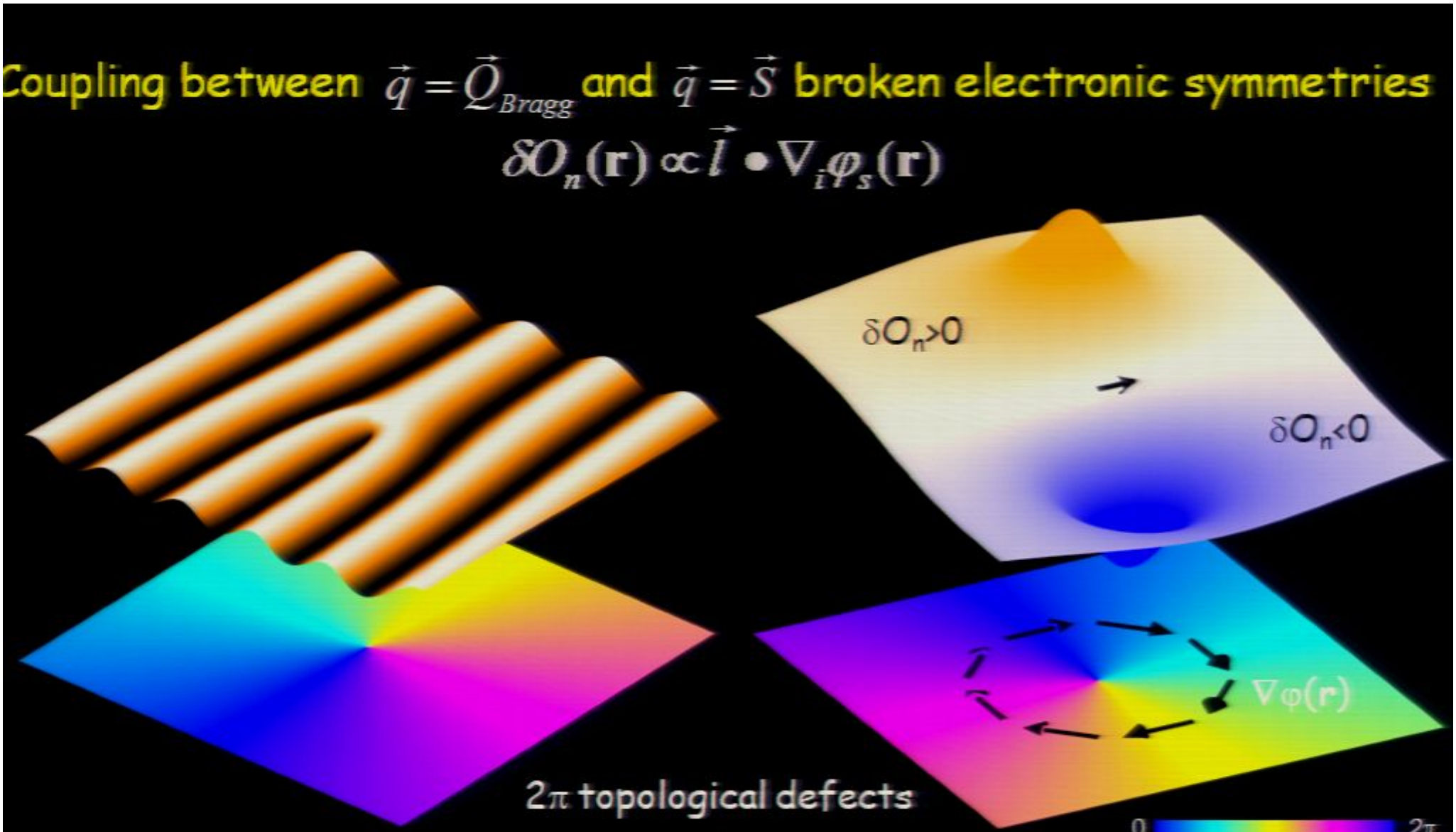

2π topological defects

q=S *C_4-breaking *Tr. Symm. broken	q=Q_{Bragg} *C_4-breking *Intra unit cell

SUMMARY

Electronic Structure of UD Cuprates

Heterogeneous, non-dispersive, broken-symmetry PG states

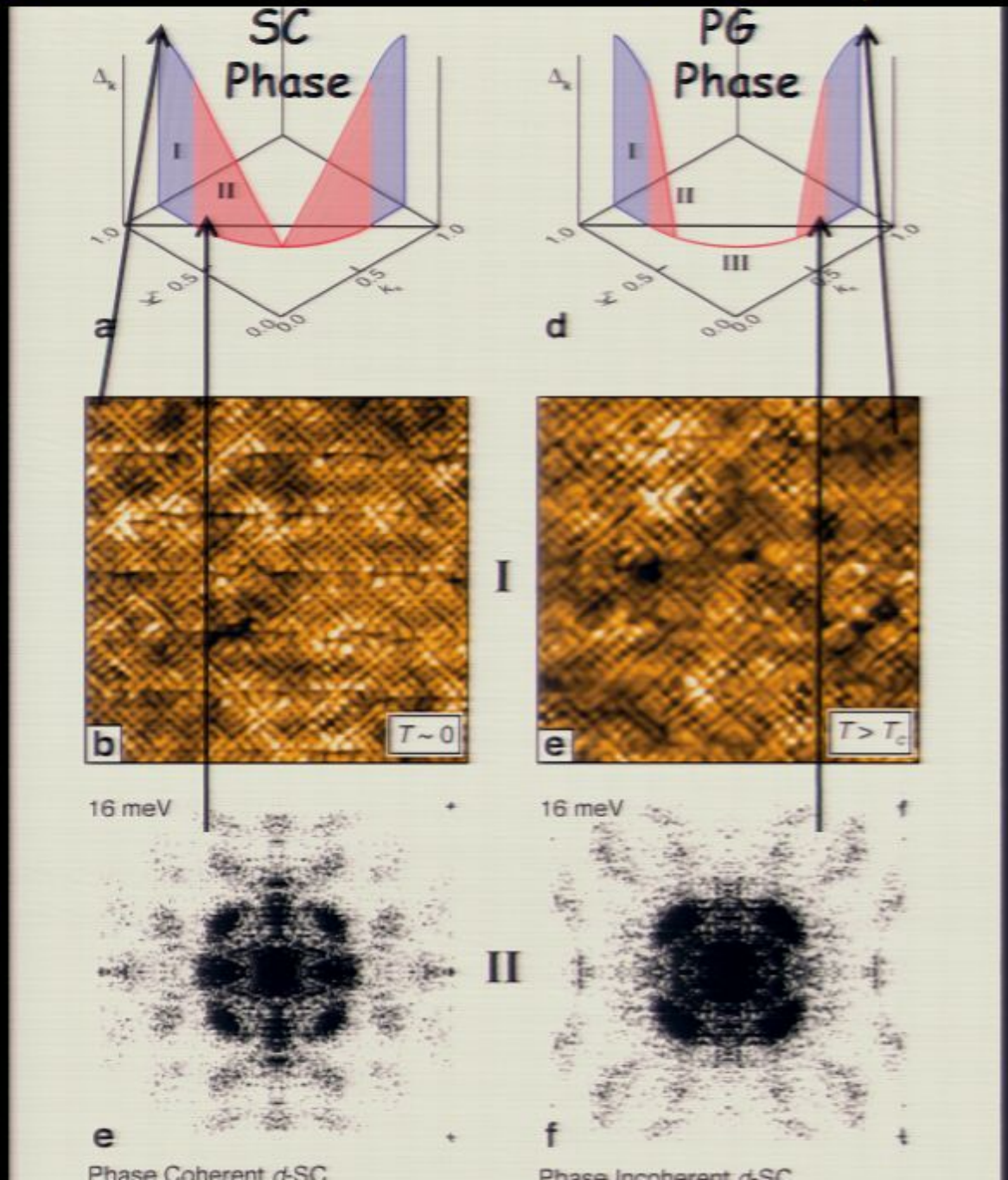

Heterogeneous, non-dispersive broken-symmetry PG states

Homogeneous, phase coherent d-wave Cooper pairs

Homogeneous, phase incoherent d-wave Cooper pairs

A. R. Schmidt

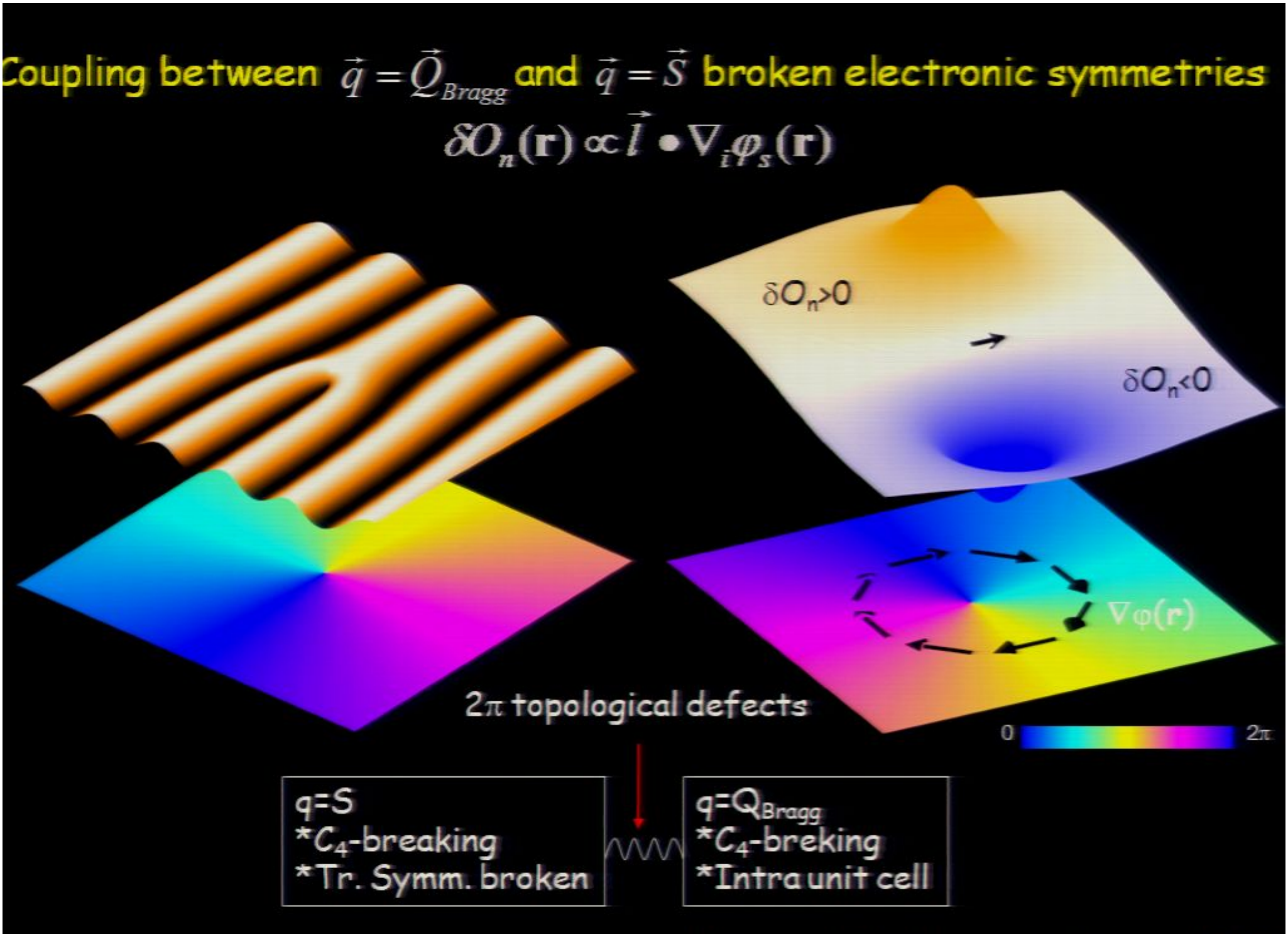
Coupling between $\vec{q} = \vec{Q}_{Bragg}$ and $\vec{q} = \vec{S}$ broken electronic symmetries
$\delta O_n(\mathbf{r}) \propto \vec{l} \bullet \nabla_i \varphi_S(\mathbf{r})$
δO_n>0
δO_n<0
$\nabla\varphi(\mathbf{r})$
2π topological defects
0
2π
q=S
*C_4-breaking
*Tr. Symm. broken
q=Q_{Bragg}
*C_4-breking
*Intra unit cell

Iron-based HTS

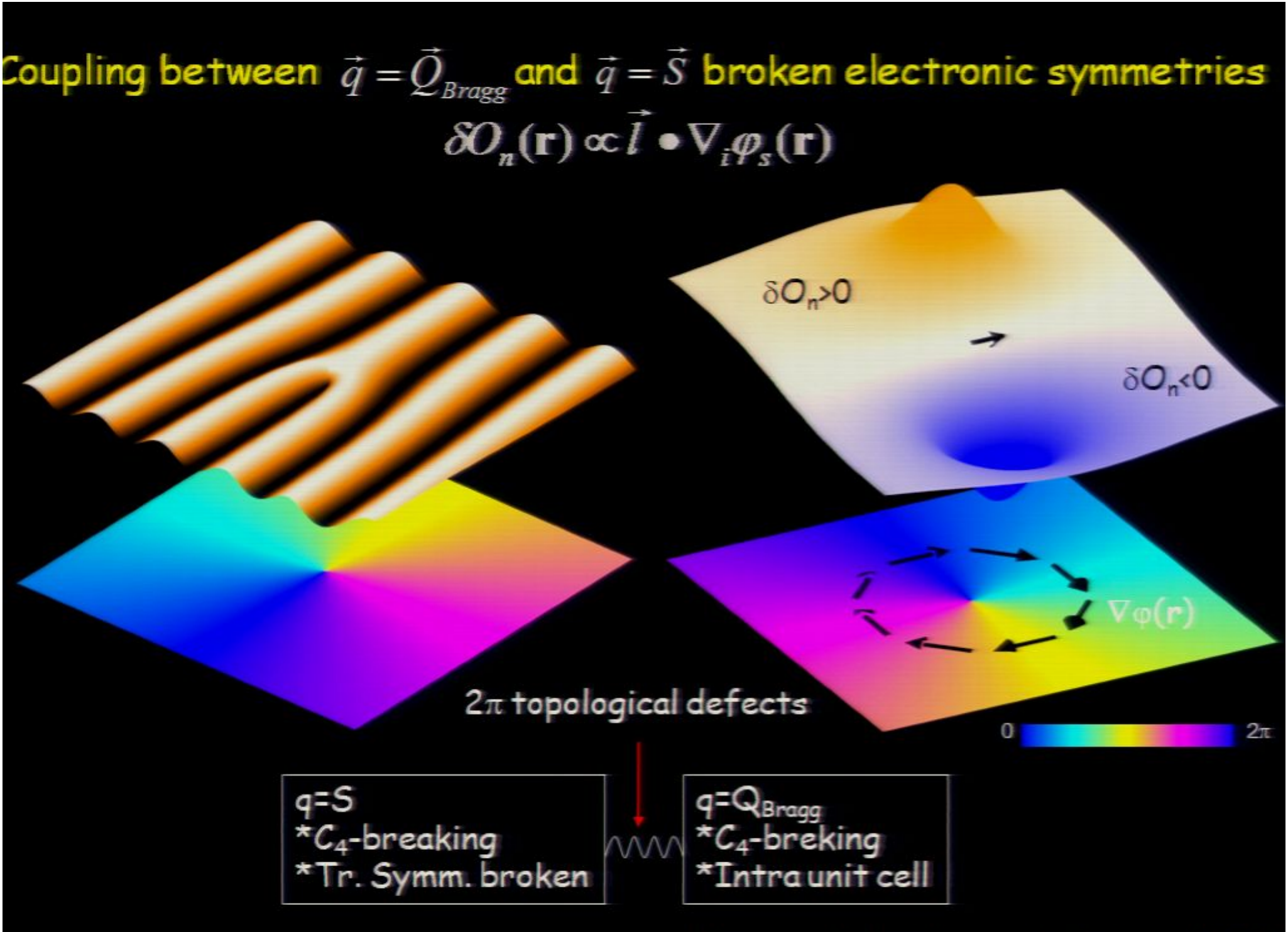
Coupling between $\vec{q} = \vec{Q}_{Bragg}$ and $\vec{q} = \vec{S}$ broken electronic symmetries
$\delta O_n(\mathbf{r}) \propto \vec{l} \bullet \nabla_i \varphi_S(\mathbf{r})$
δO_n>0
δO_n<0
$\nabla\varphi(\mathbf{r})$
2π topological defects
0
2π
q=S
*C_4-breaking
*Tr. Symm. broken
q=Q_{Bragg}
*C_4-breking
*Intra unit cell

Electronic Structure of UD Cuprates

Heterogeneous, non-dispersive, broken-symmetry PG states

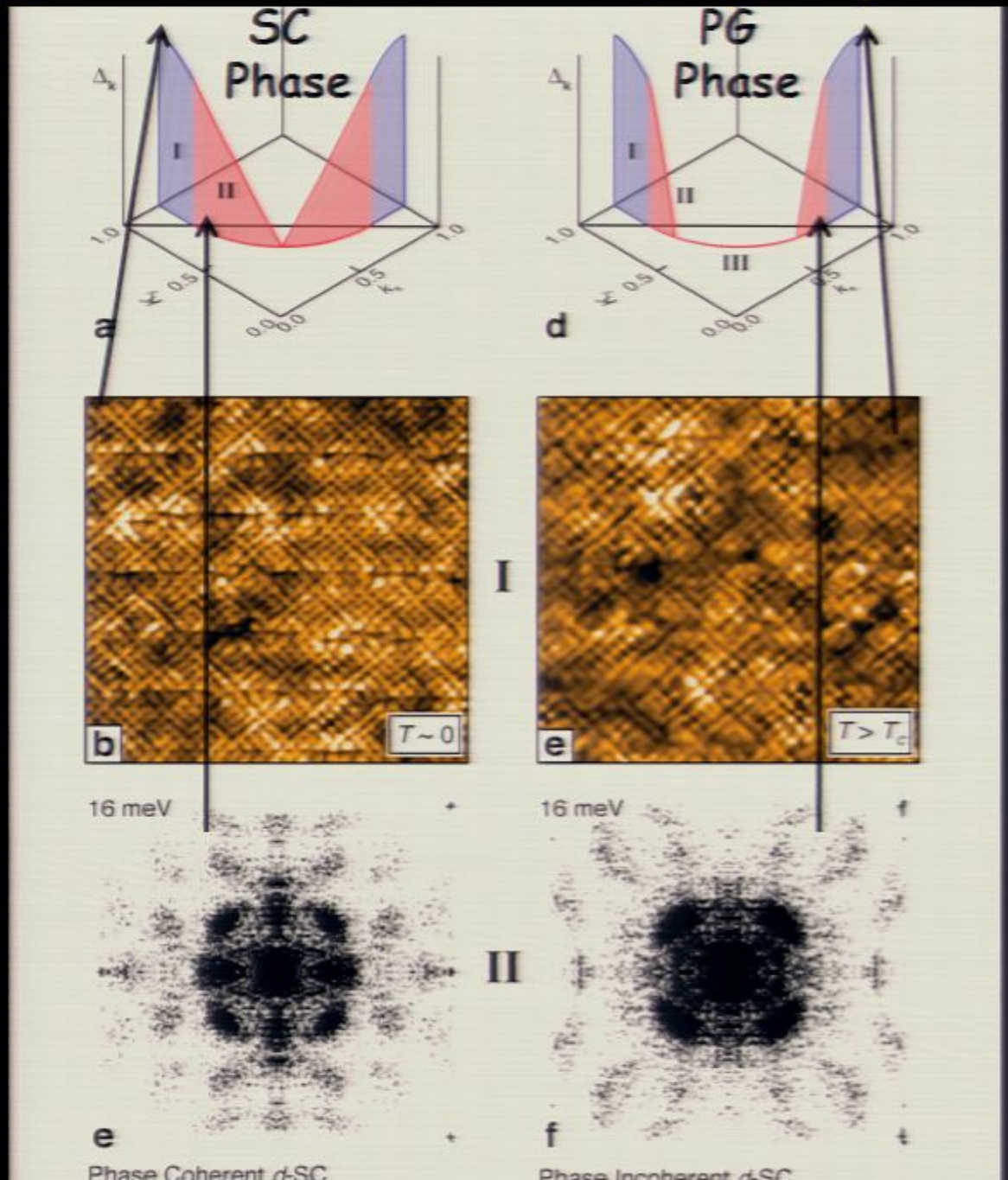

Heterogeneous, non-dispersive broken-symmetry PG states

Homogeneous, phase coherent d-wave Cooper pairs

Homogeneous, phase incoherent d-wave Cooper pairs

A. R. Schmidt

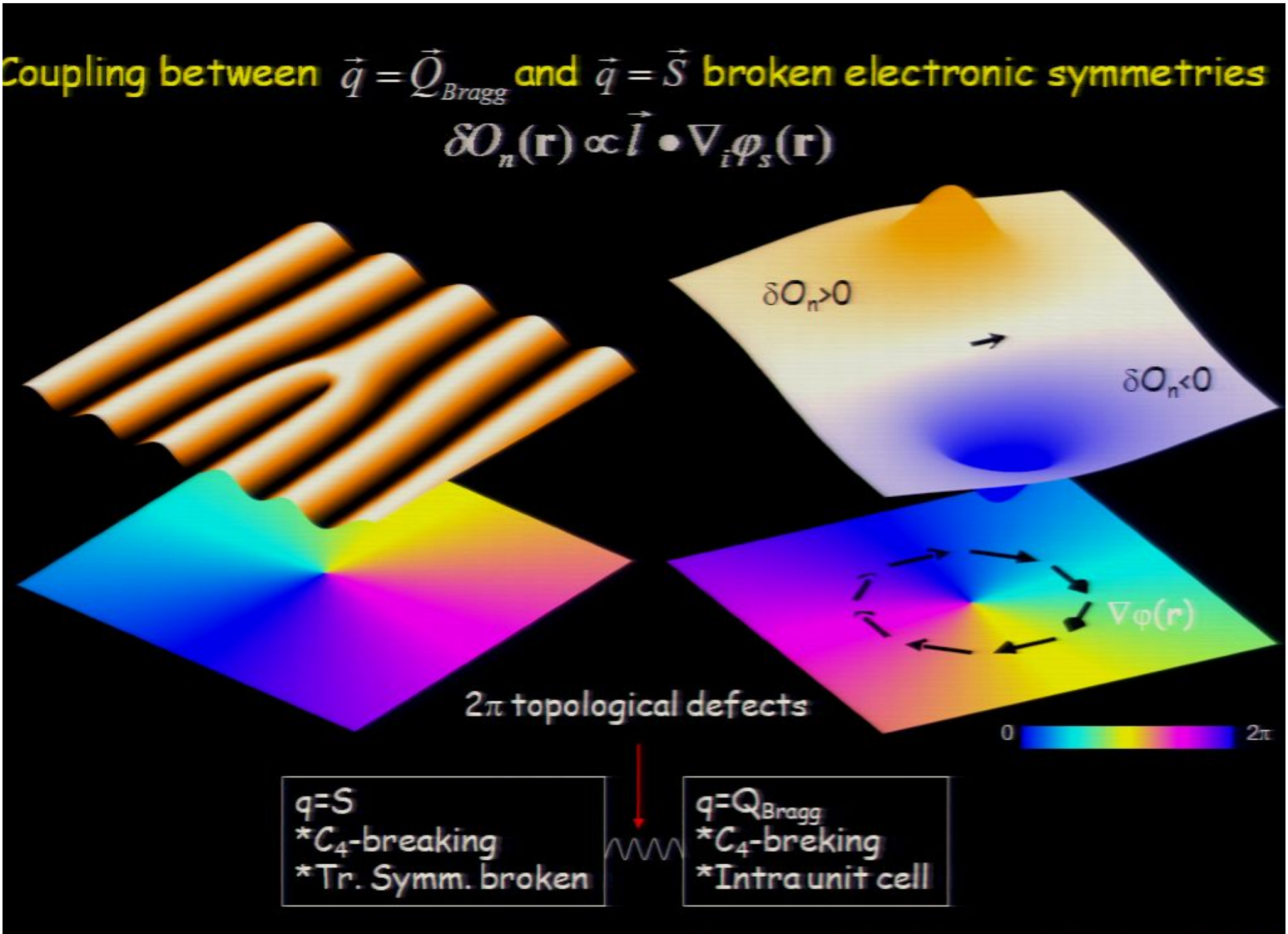
Coupling between $\vec{q} = \vec{Q}_{Bragg}$ and $\vec{q} = \vec{S}$ broken electronic symmetries
$\delta O_n(\mathbf{r}) \propto \vec{l} \bullet \nabla_i \varphi_S(\mathbf{r})$
δO_n>0
δO_n<0
$\nabla\varphi(\mathbf{r})$
2π topological defects
0
2π
q=S
*C_4-breaking
*Tr. Symm. broken
q=Q_{Bragg}
*C_4-breking
*Intra unit cell

Electronic Structure of UD Cuprates

Heterogeneous, non-dispersive, broken-symmetry PG states

Homogeneous, phase coherent d-wave Cooper pairs

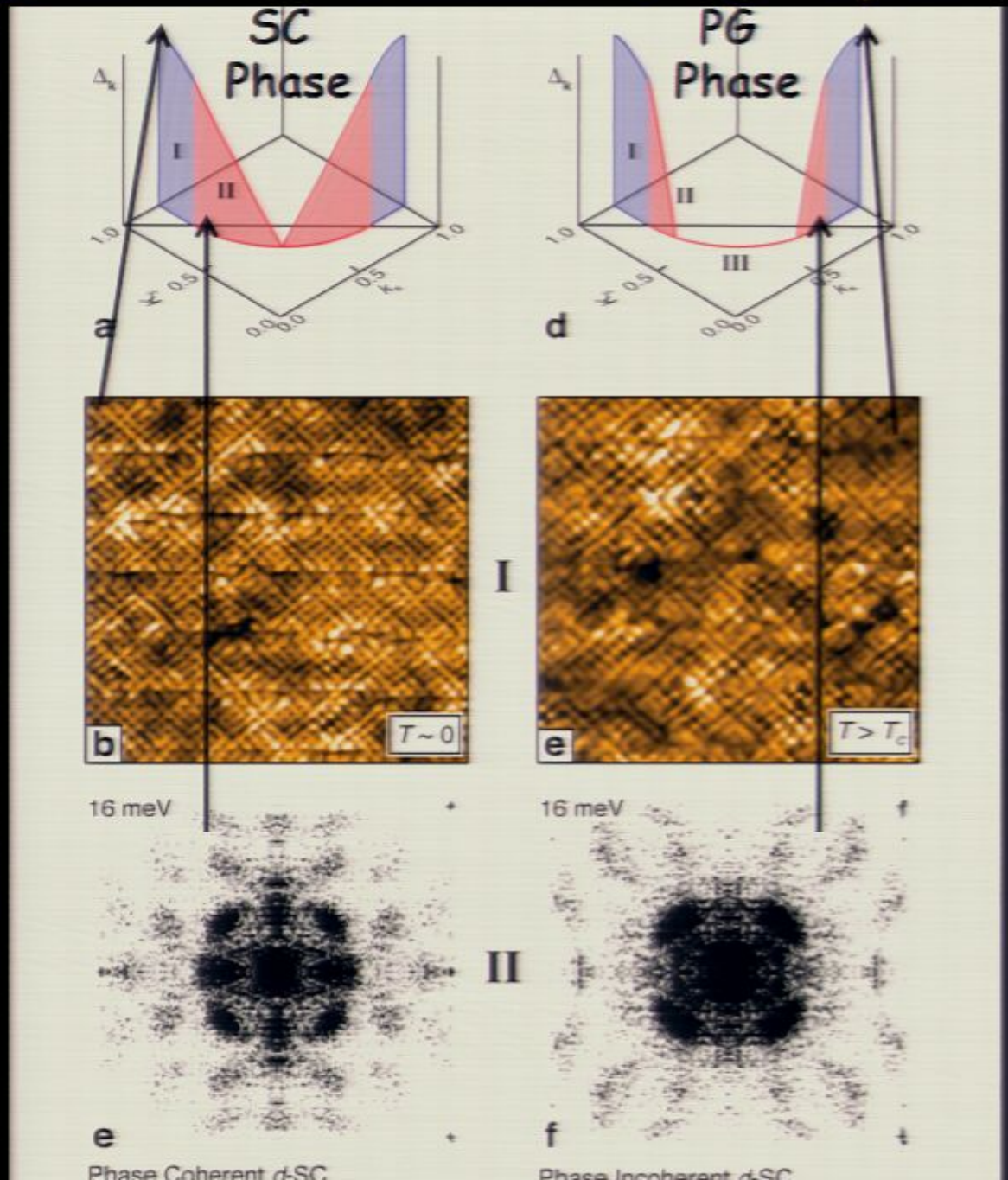

Heterogeneous, non-dispersive broken-symmetry PG states

Homogeneous, phase incoherent d-wave Cooper pairs

A. R. Schmidt

Iron-based HTS

$Ca(Fe_{1-x}Co_x)_2As_2$

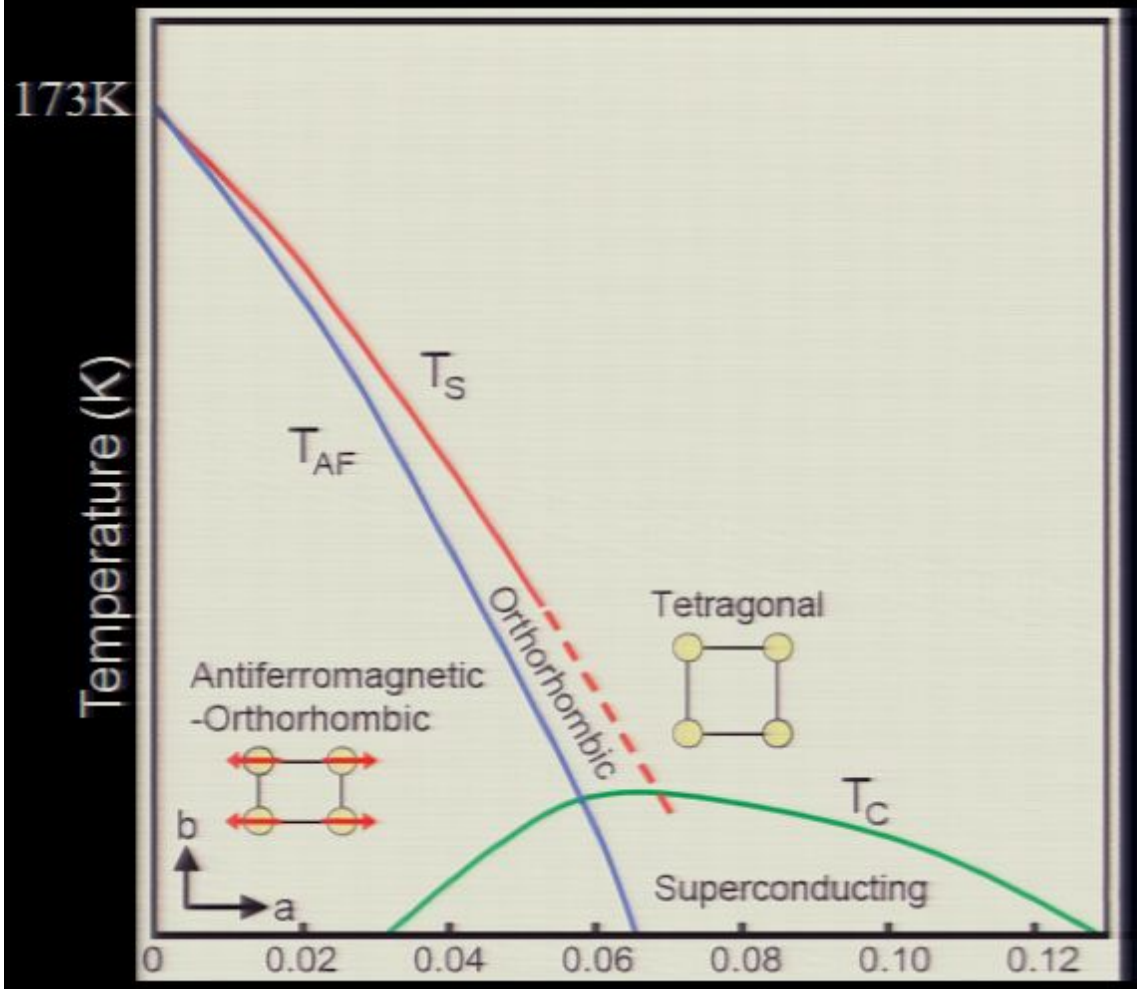

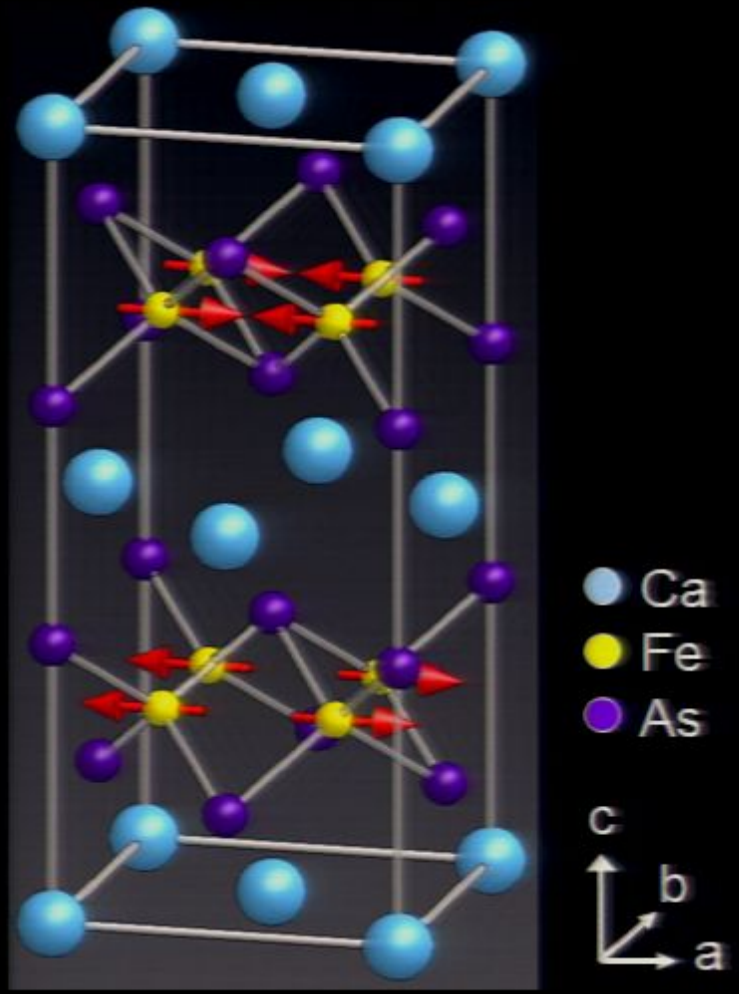

$Ca(Fe_{1-x}Co_x)_2As_2$ -- Excellent cryo-cleave surface

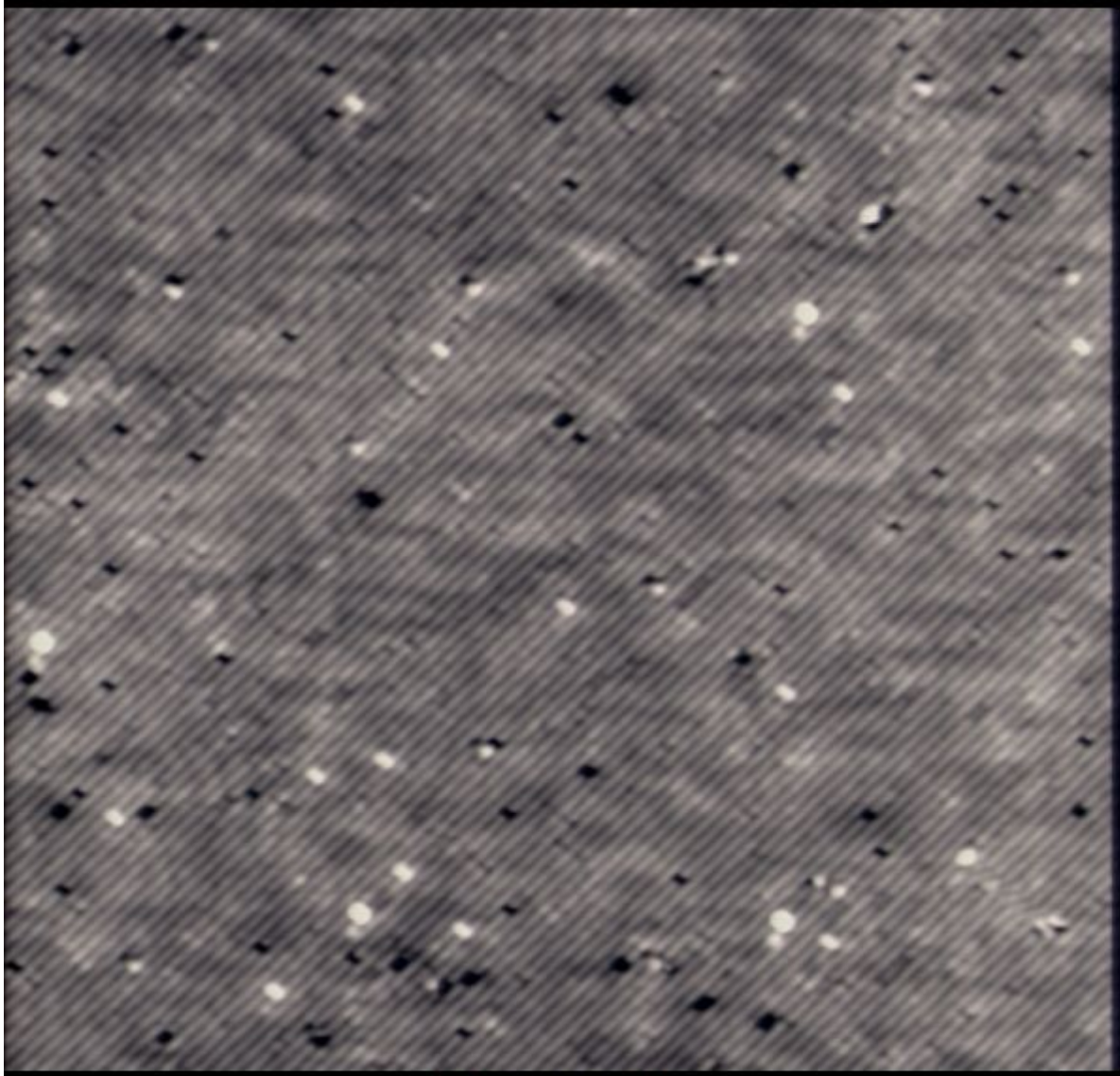

1.2

0Å

Topograph,

710Å

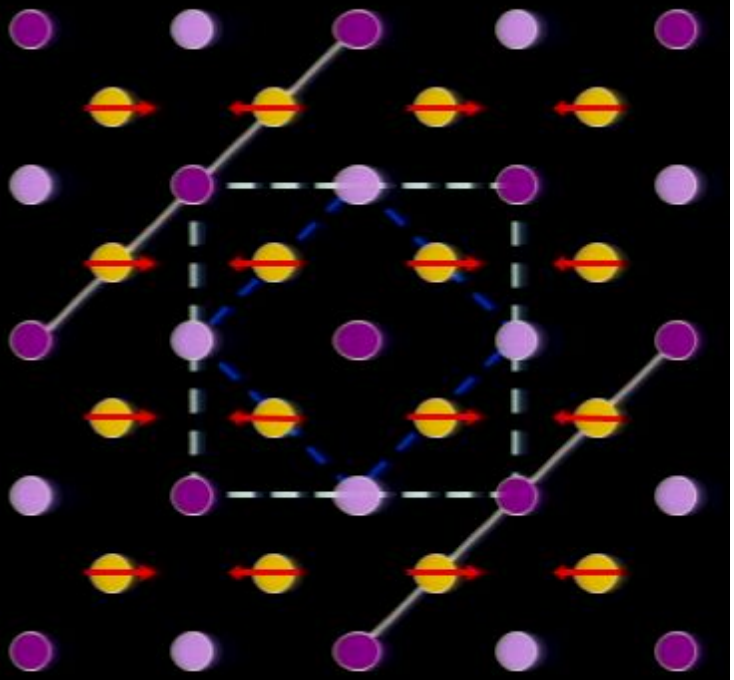

Fe or Co

As (Top)

As (Bottom)

Ferropnictide Spectroscopic Imaging

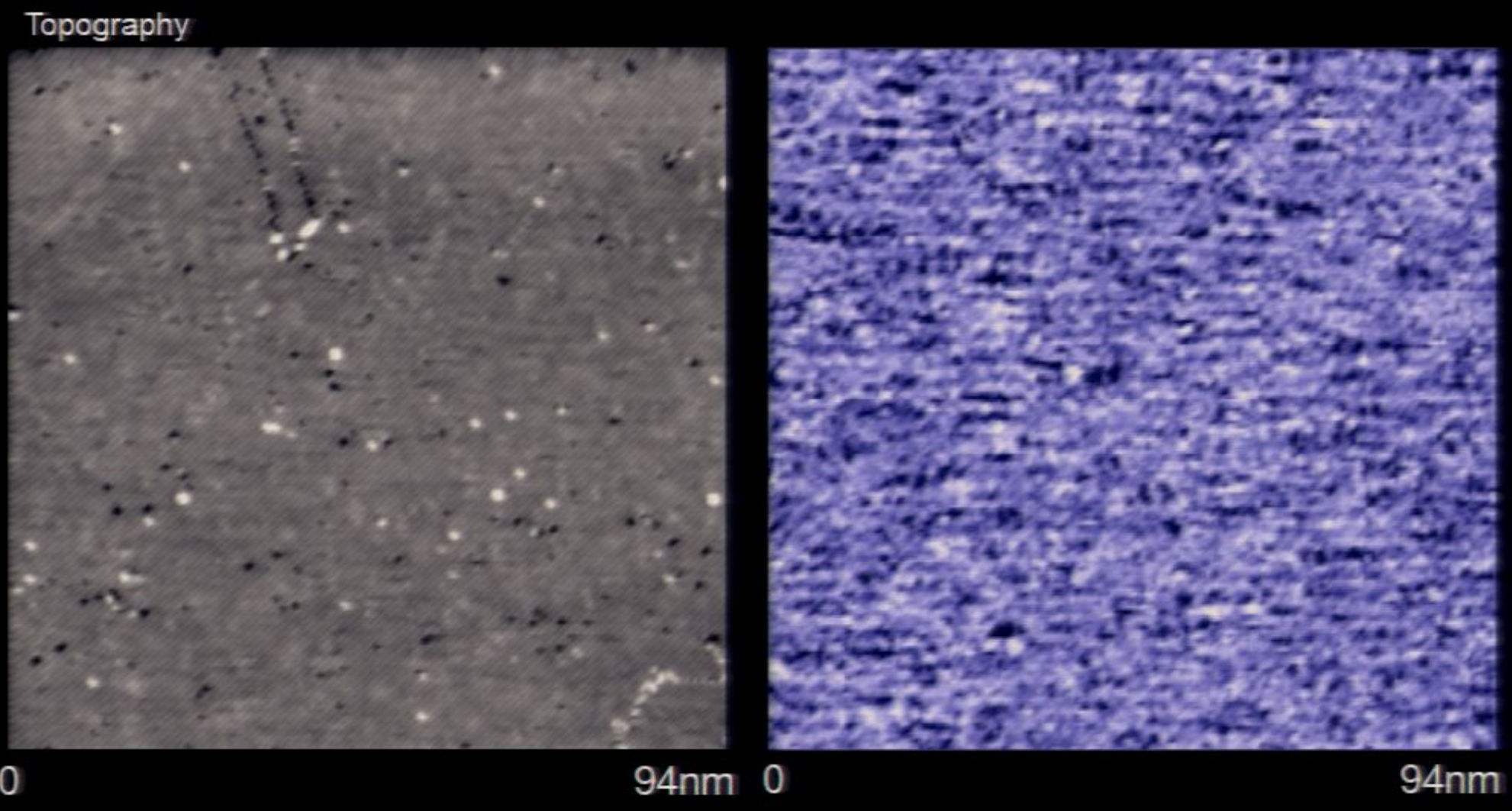

Ferropnictide Spectroscopic Imaging

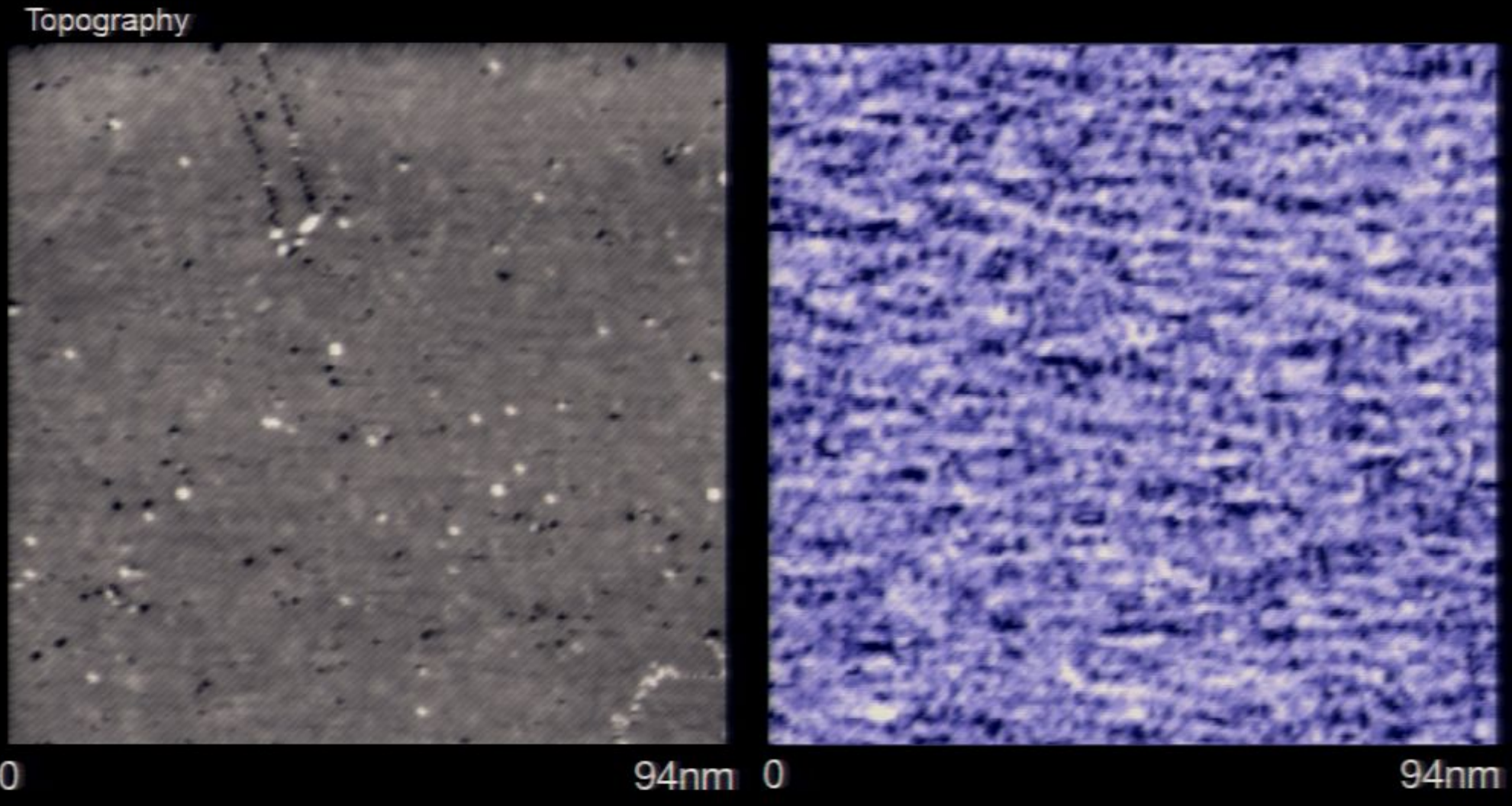

Ferropnictide Spectroscopic Imaging

Topography

0 94nm

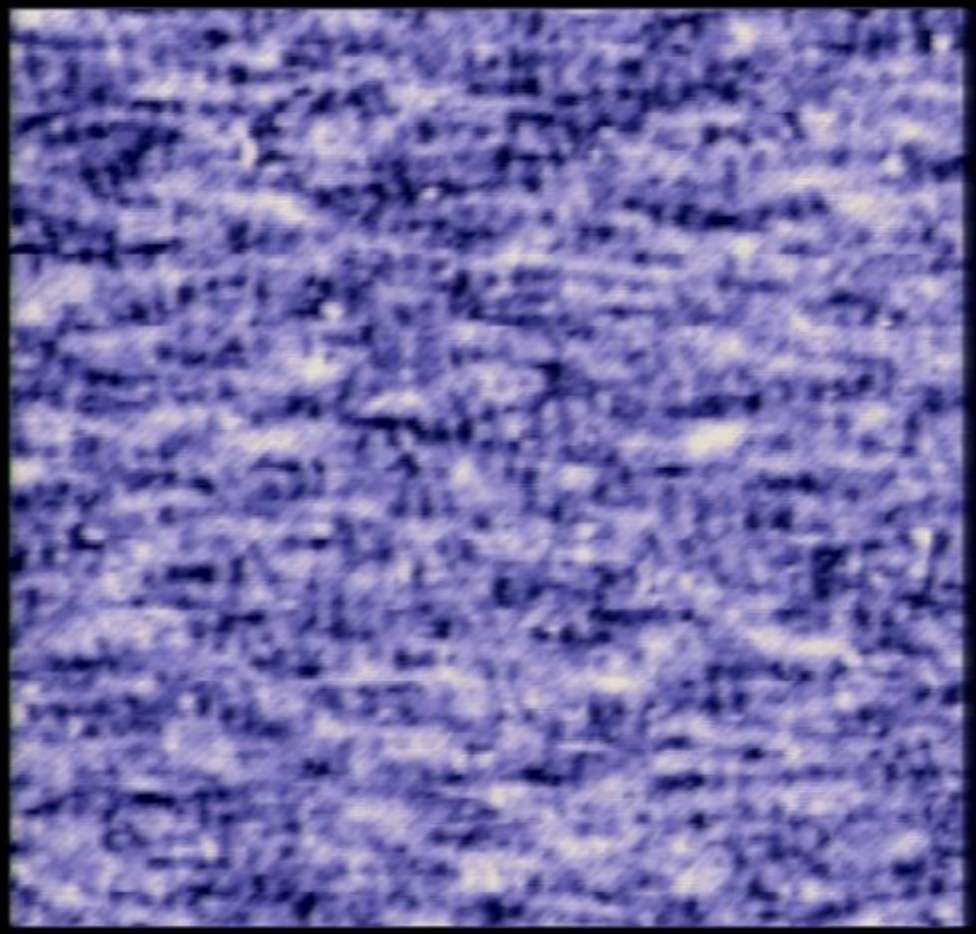

0 94nm

Ferropnictide Spectroscopic Imaging

Topography

0 94nm

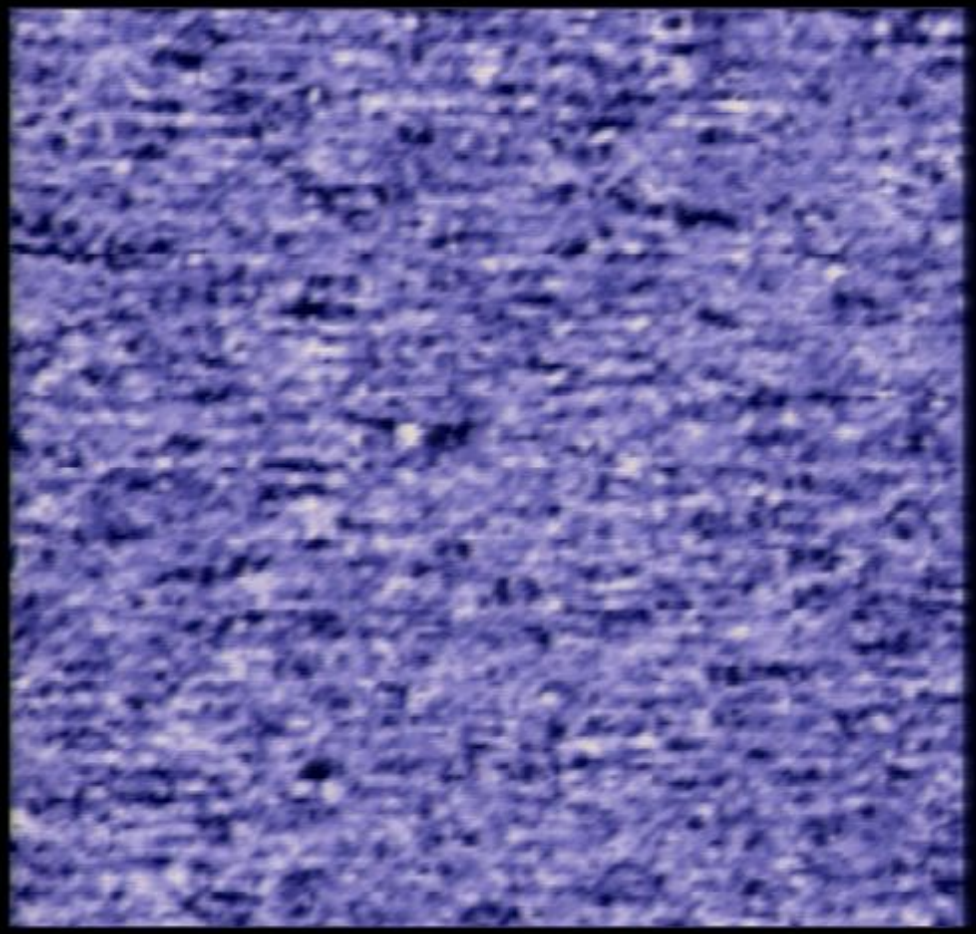

0 94nm

Ferropnictide Spectroscopic Imaging

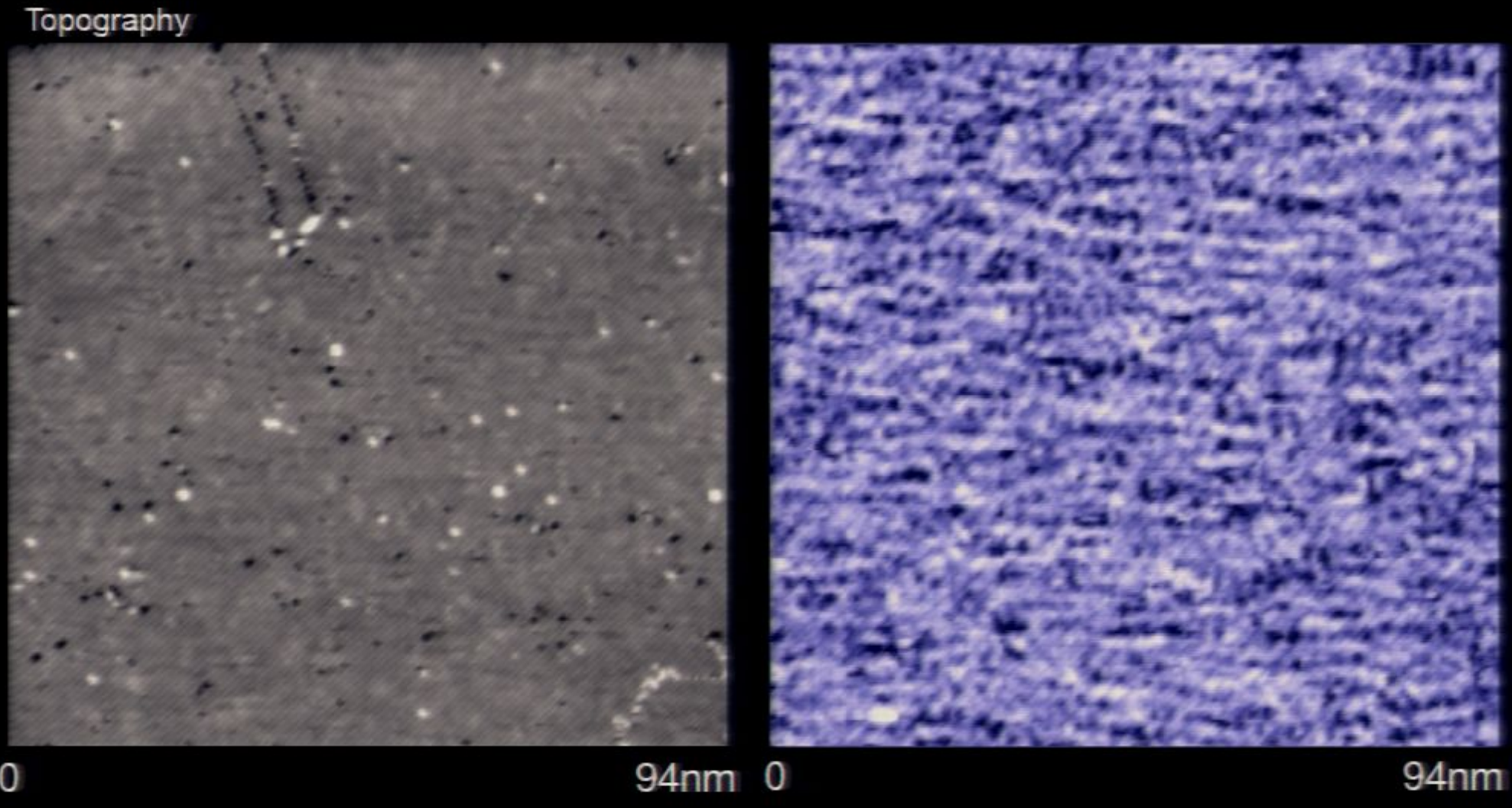

Ferropnictide Spectroscopic Imaging

Topography

0 94nm

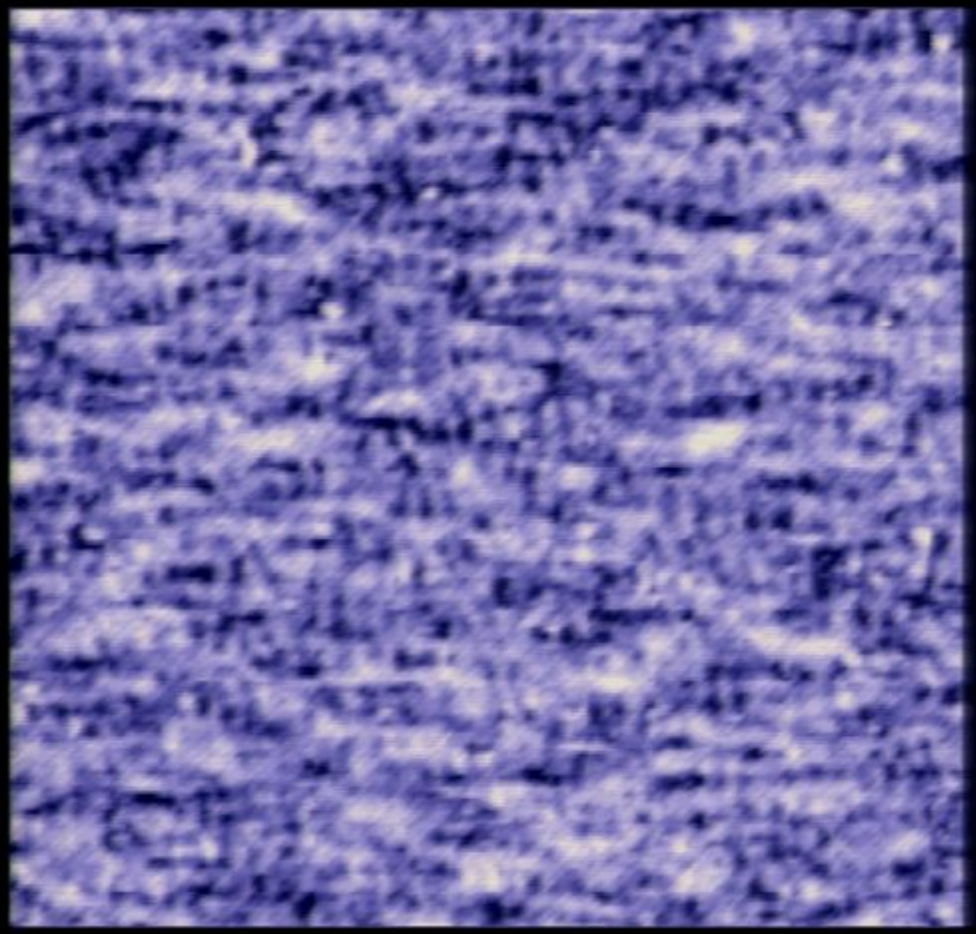

0 94nm

Static electronic structures size ~8a_{FeFe} along one axis

$$I(\vec{r}, V = 50mV) = Ce^{-\frac{z(V)}{z_0}} \int_0^{eV} LDOS(\vec{r}, E)\,dE$$

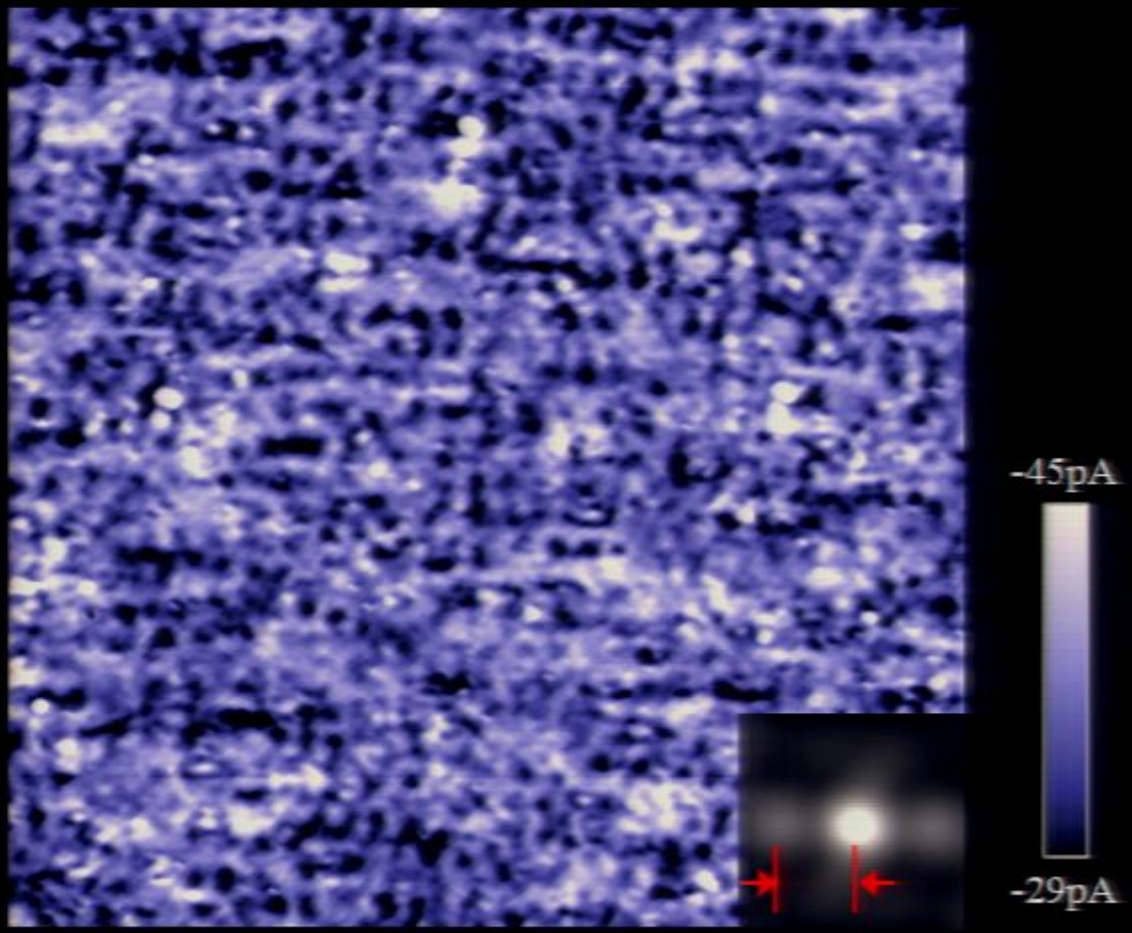

QPI of delocalized states UD Ca-122

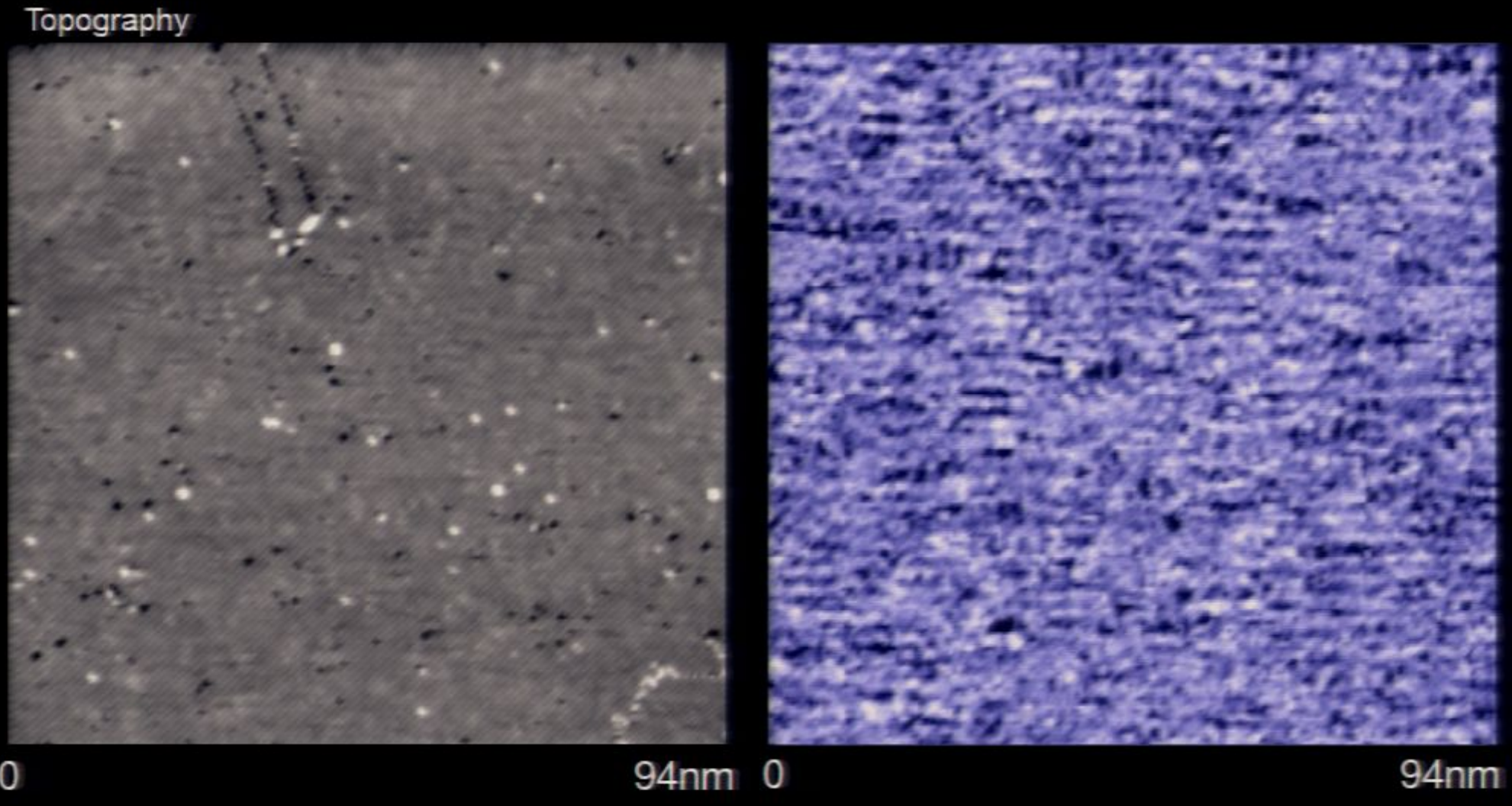

QPI of delocalized states UD Ca-122

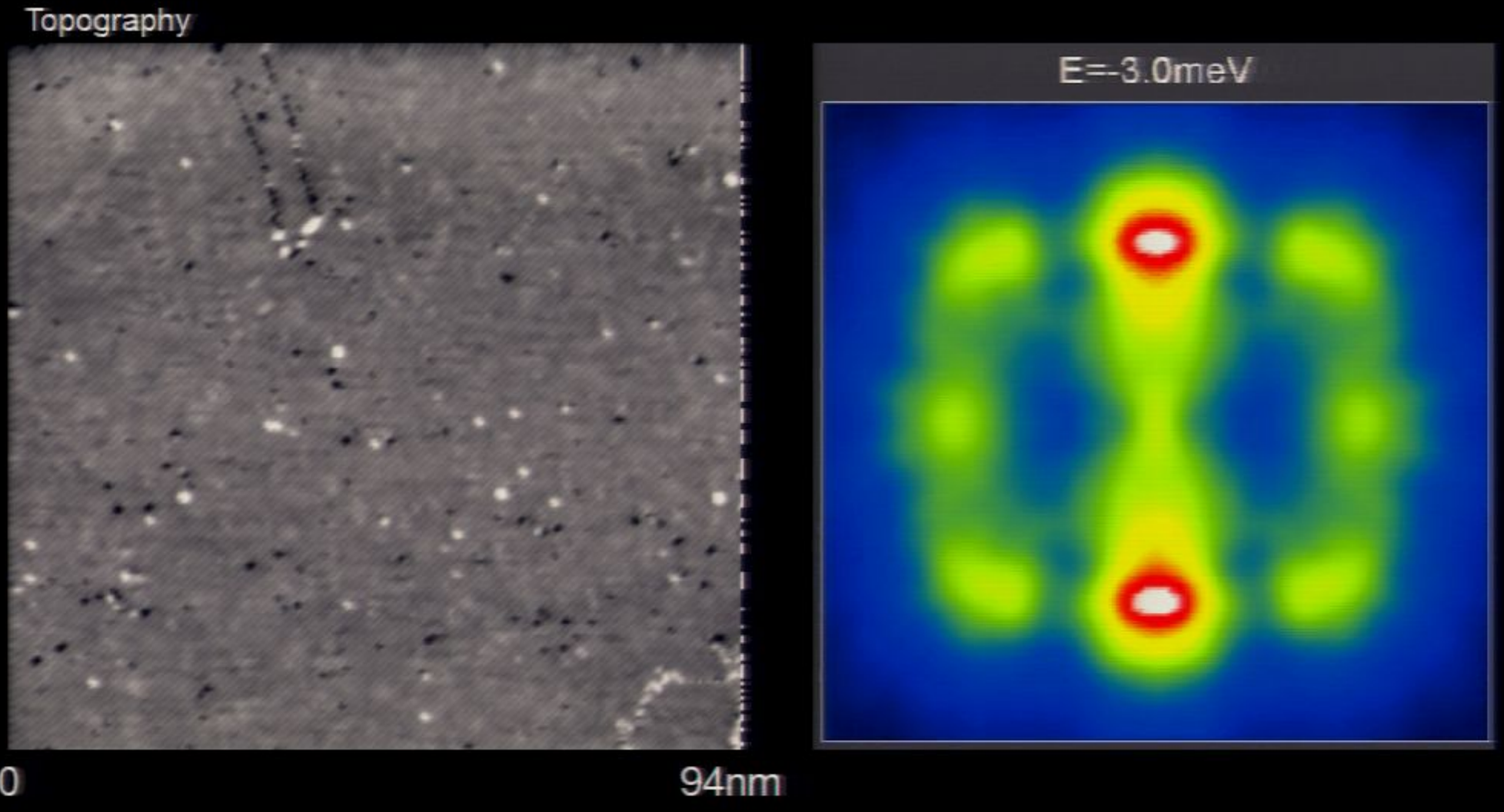

QPI of delocalized states UD Ca-122

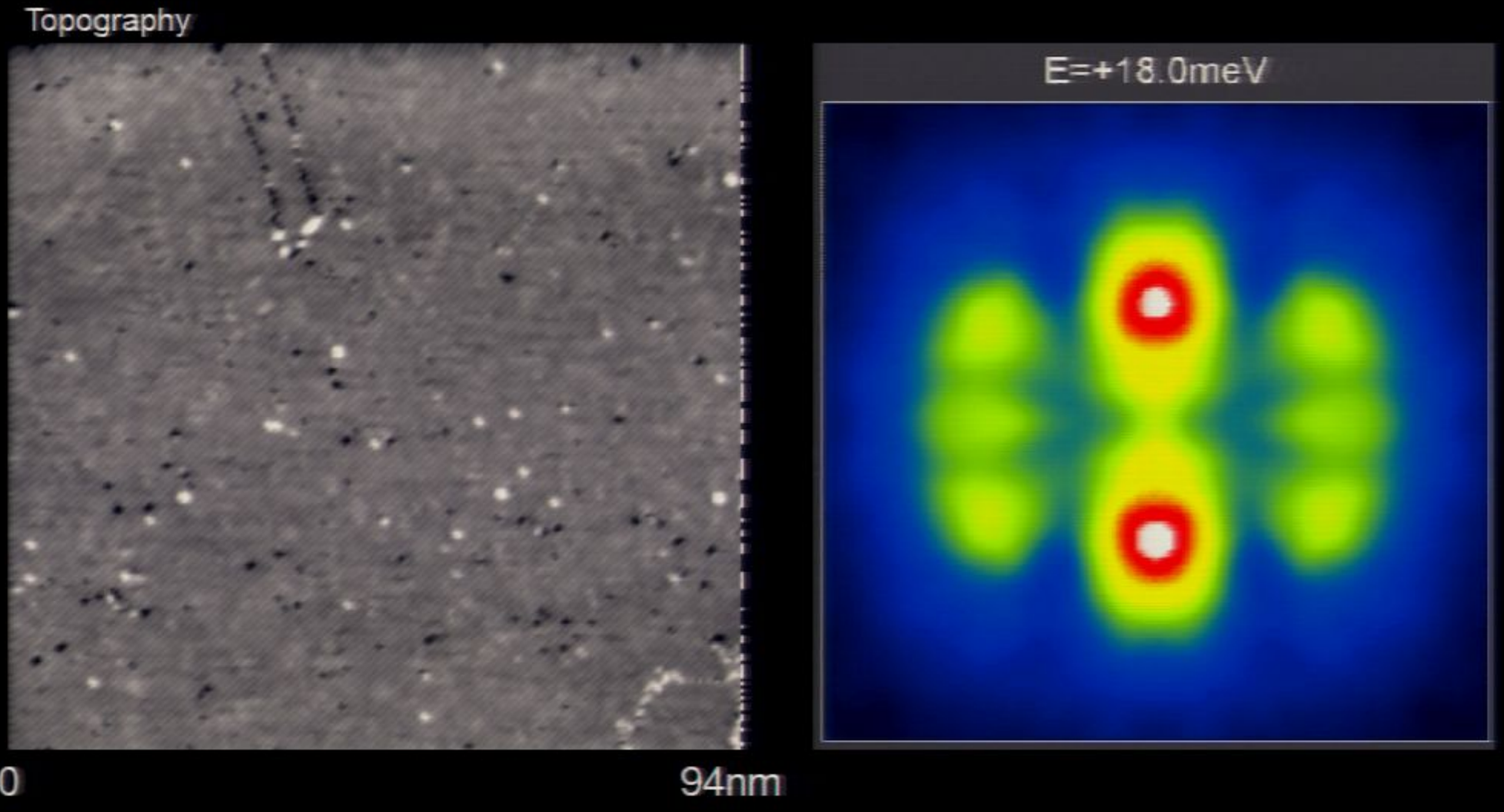

QPI of delocalized states UD Ca-122

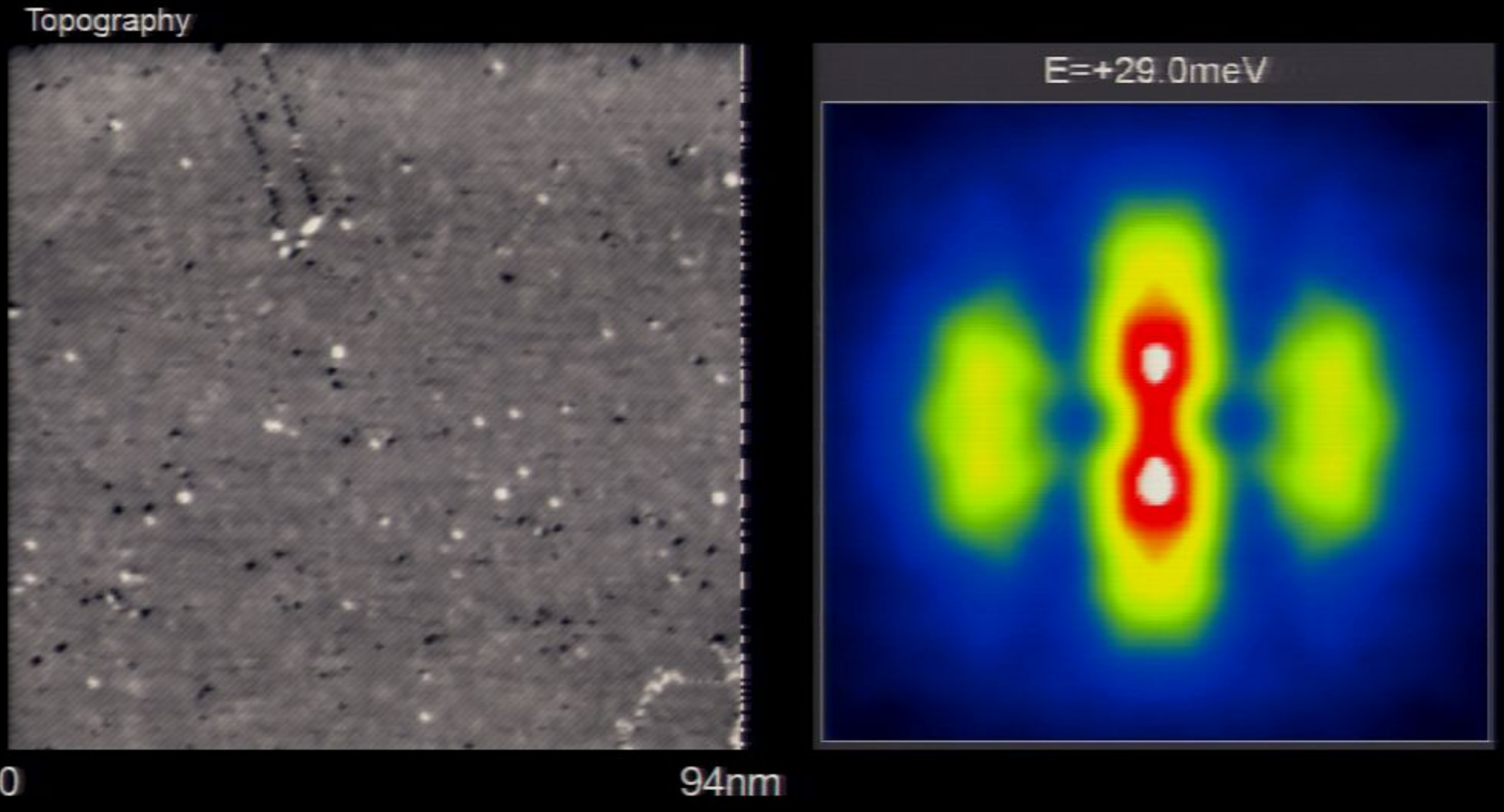

QPI of delocalized states UD Ca-122

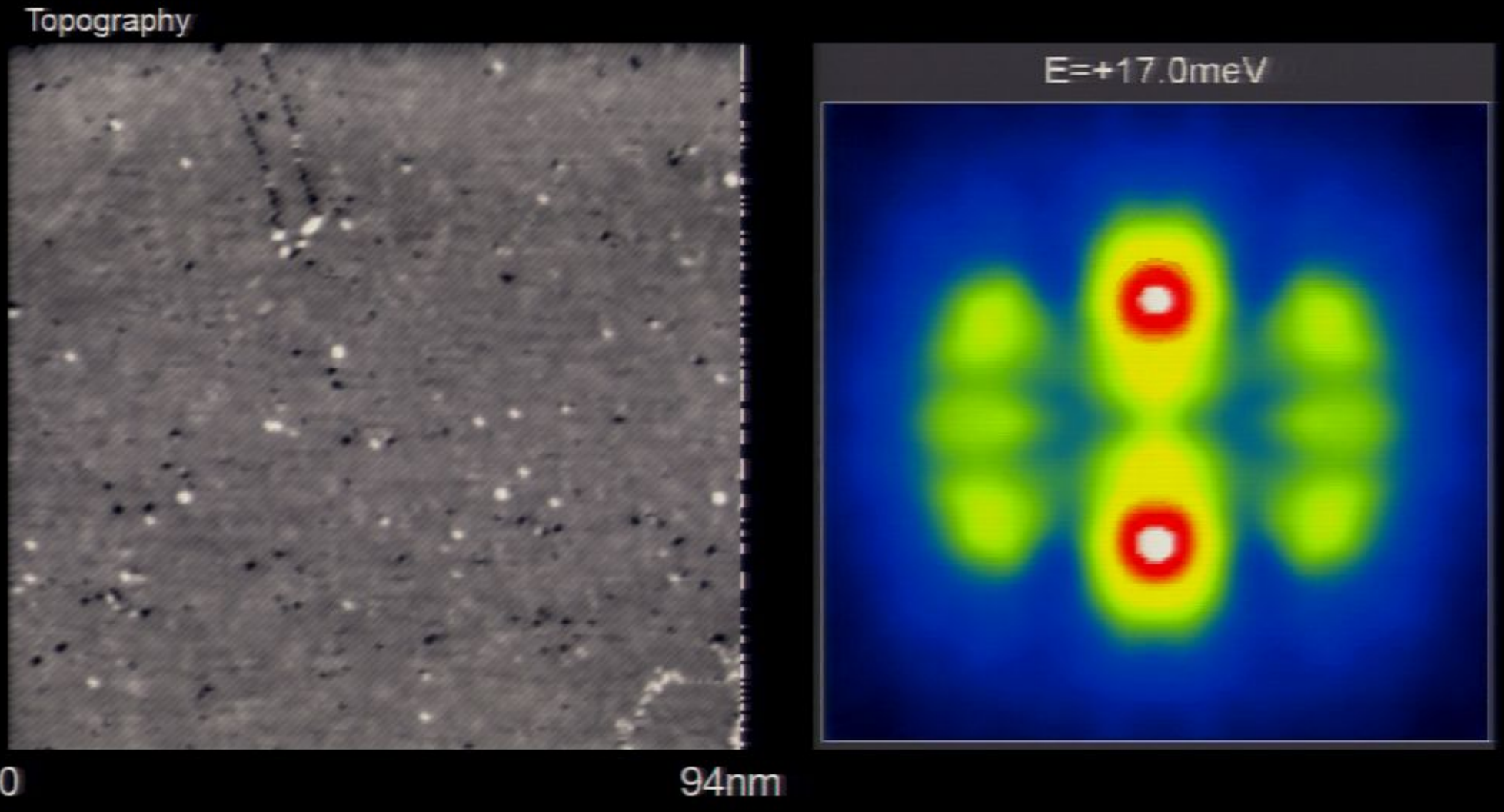

QPI of delocalized states UD Ca-122

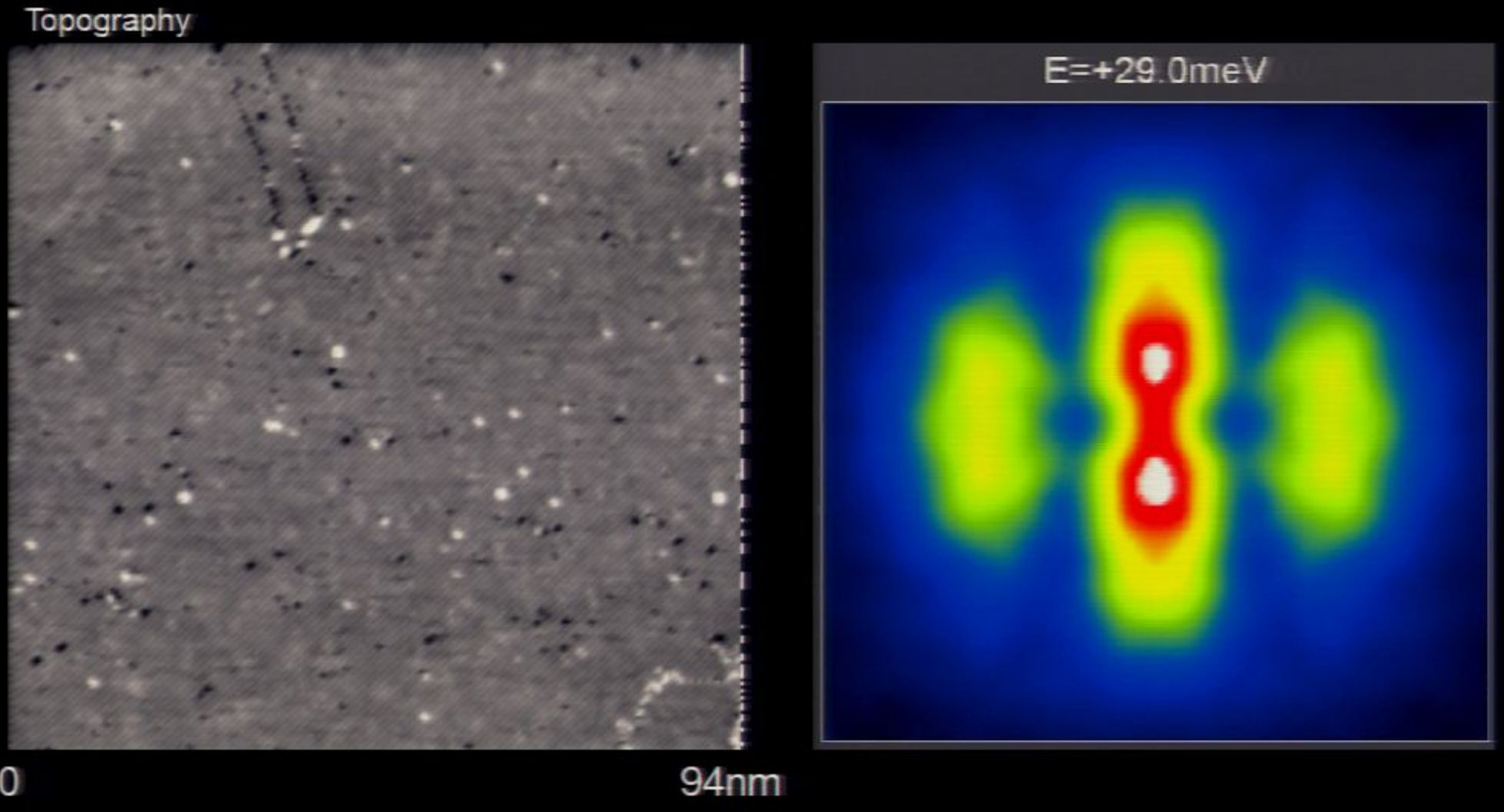

Mere orthorhombicity of crystal will NOT produce this effect!

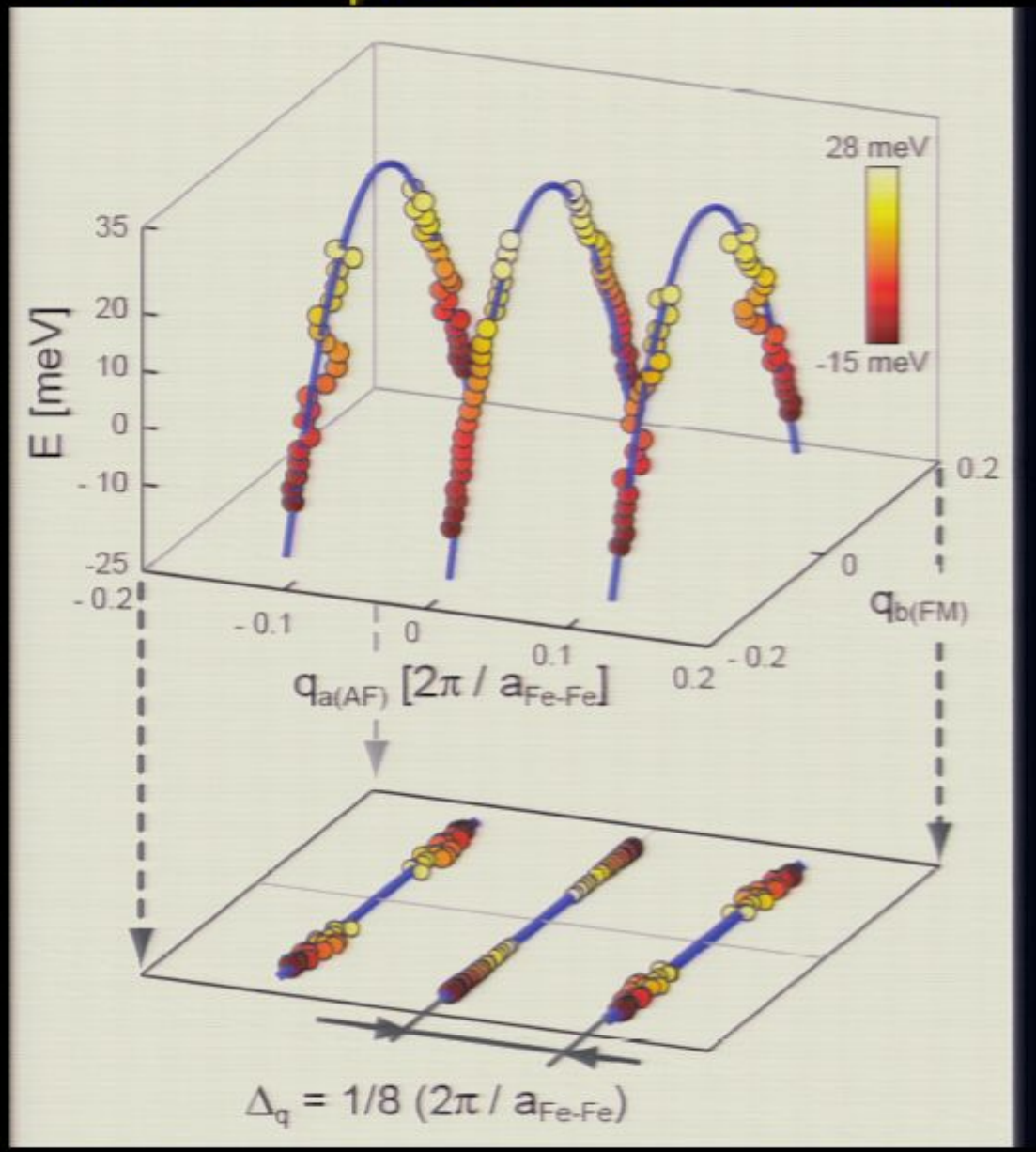

Nematic electronic structure is a bulk property of underdoped $CaFe_{1-x}Co_xAs_2$ near critical point

Science **327**, 181 (2010)

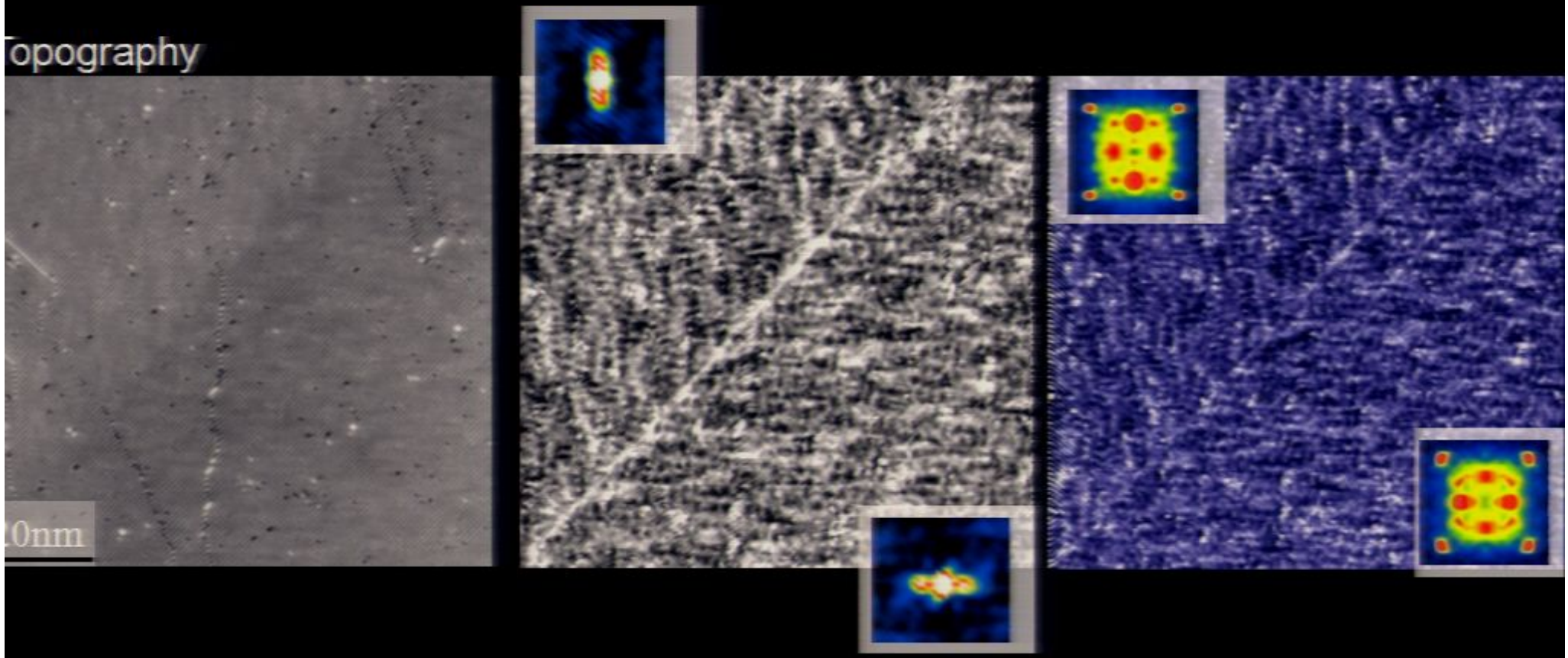

Mere orthorhombicity of crystal will NOT produce this effect!

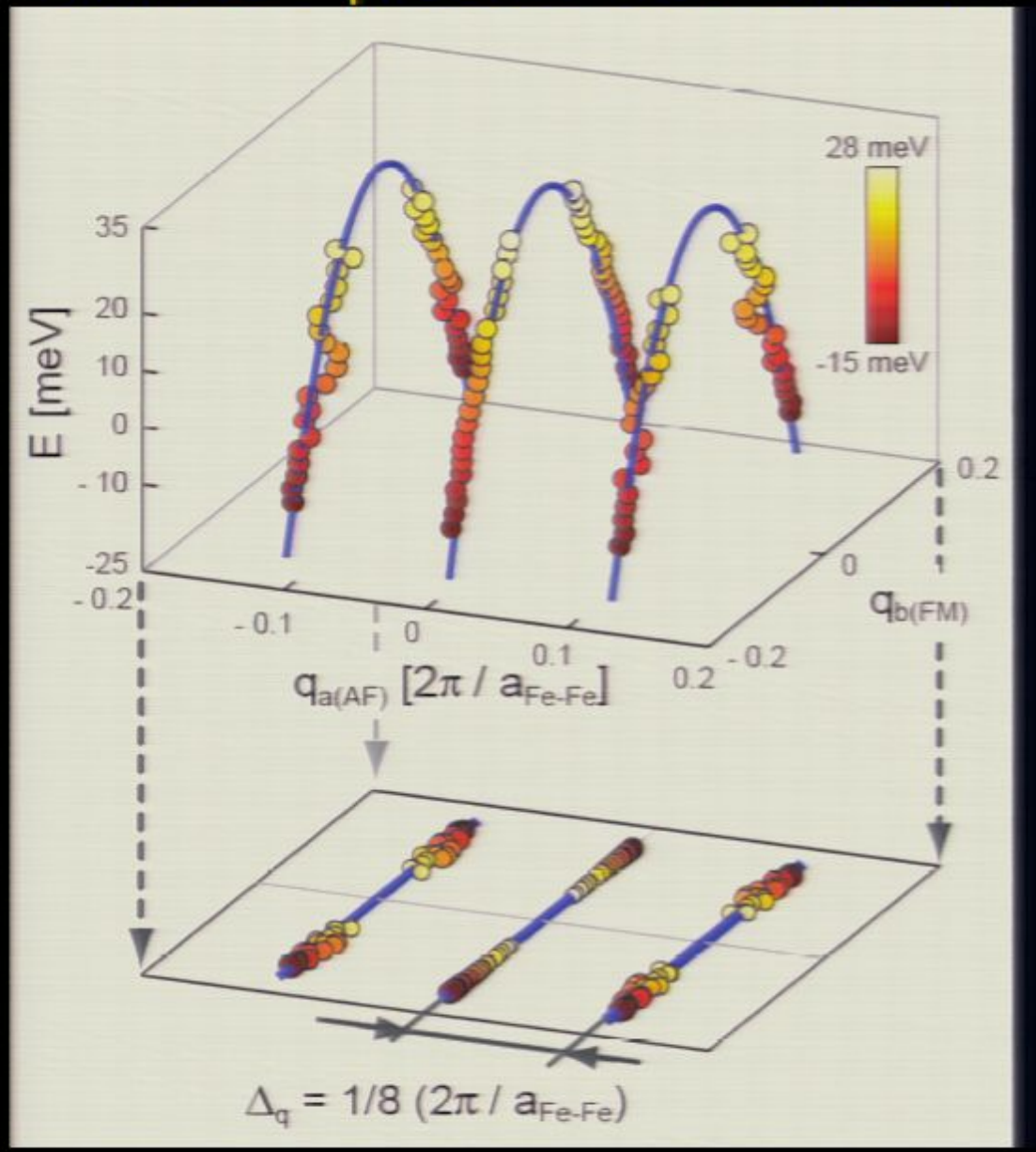

Nematic electronic structure is a bulk property of underdoped $CaFe_{1-x}Co_xAs_2$ near critical point

Science **327**, 181 (2010)

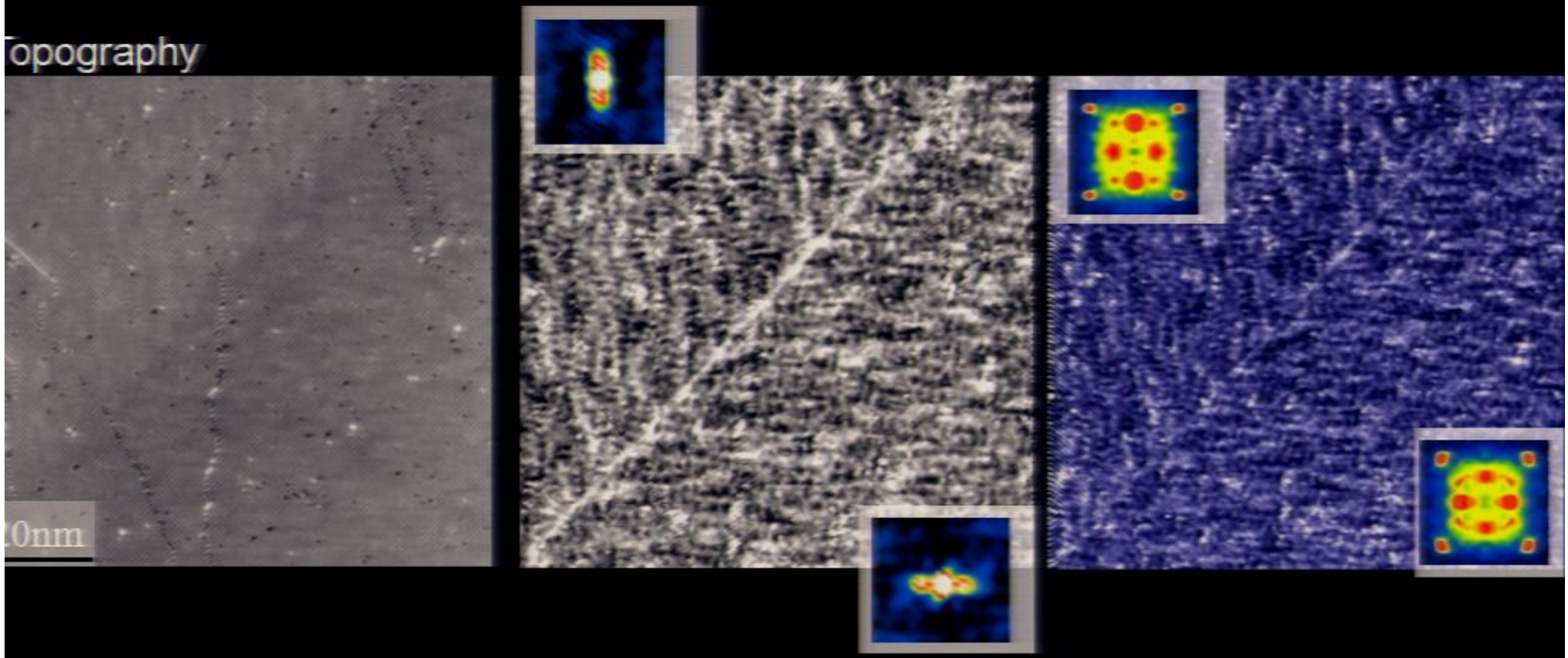

Nematic electronic structure in underdoped iron-based superconductors below critical point

Science 327, 181 (2010)

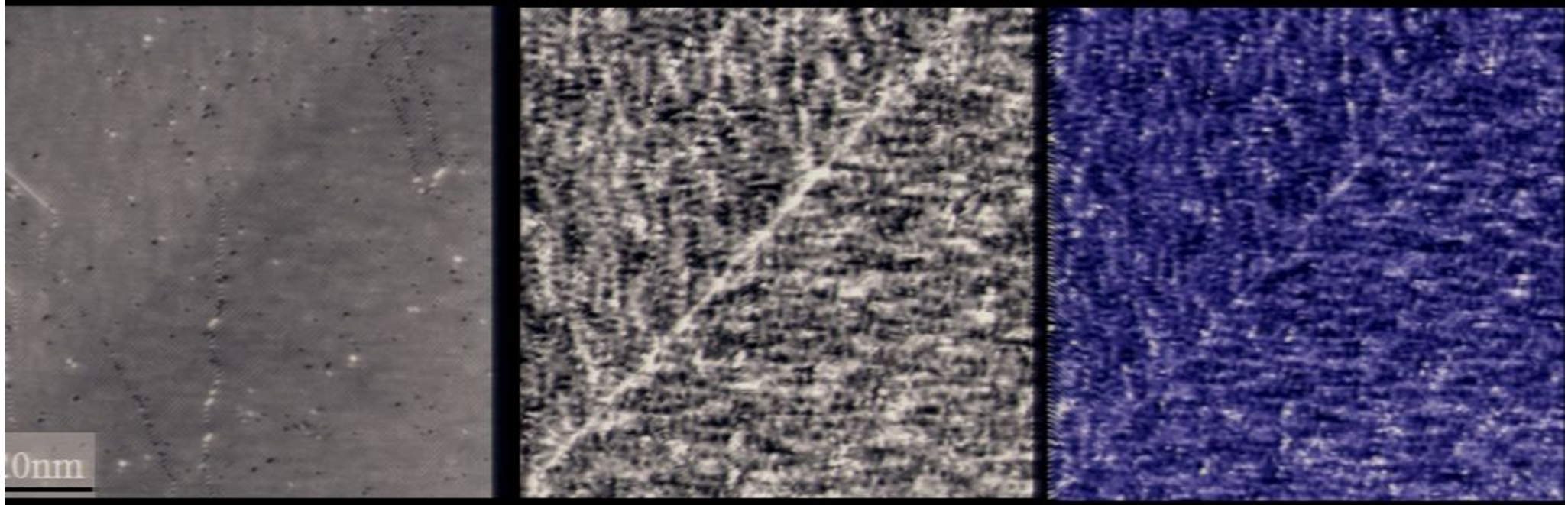

Transport

J.-H. Chu *et al.*, Science 329, 824 (2010)

M. Tanatar *et al.*, PRB 81, 184508 (2010)

ARPES

Wang et al., arXiv:1009.0271 (2010)

M. Yi et al., arXiv:1011.0050 (2010)

Optical Conductivity

A. Dusza *et al.* arXiv:1007.2543 (2010)

M. Nakajima, *et al.*, Abstr. Meet. PSJ 3, 453 (2010)

Magnetic torque measurements

Matsuda Group, Kyoto *unpublished*

Transport anisotropy NOT due to crystal orthorhombicity

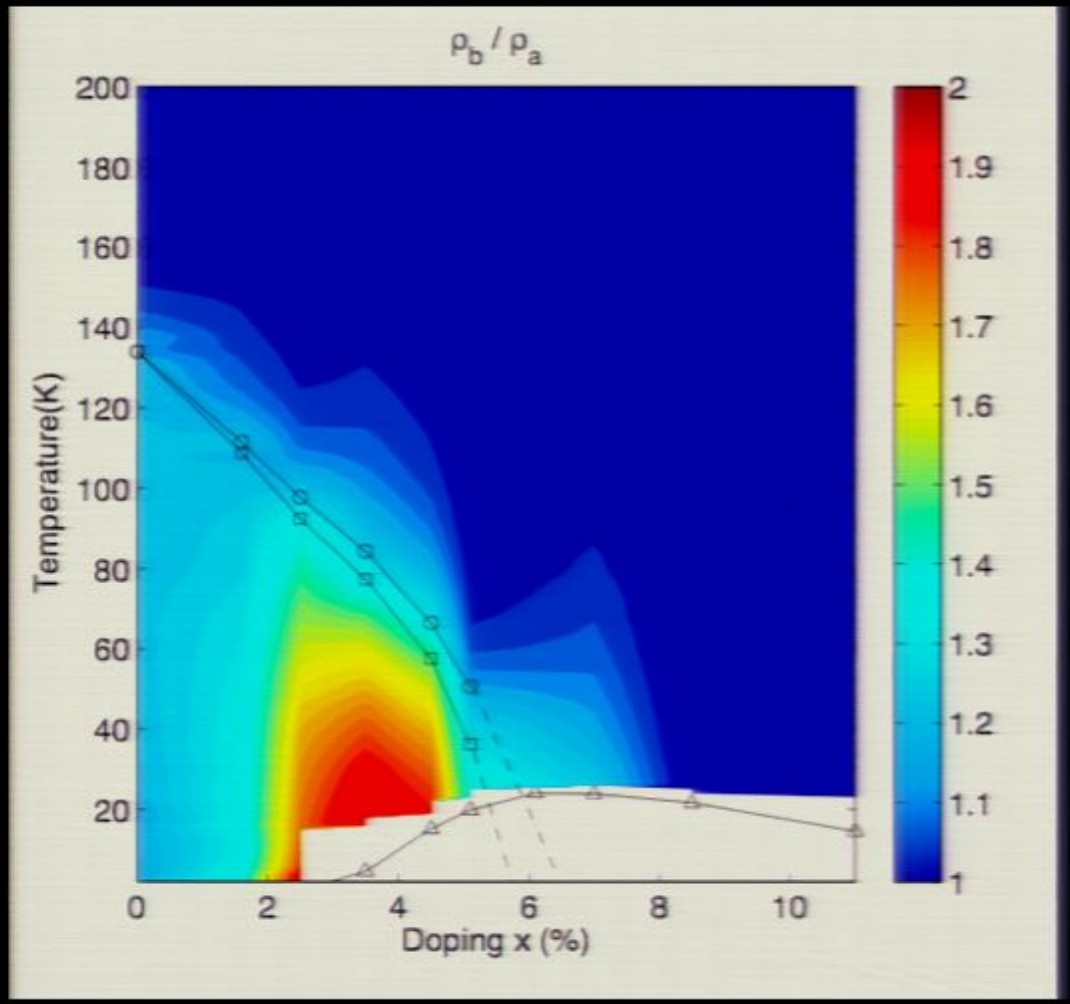

Nematic electronic transport in 122 (highest signal at ~4%)

J.-H. Chu *et al.*, Science **329**, 824 (2010)
M. Tanatar *et al.*, PRB **81**, 184508 (2010)

$8a_0$ Unidirectional Electronic Structures

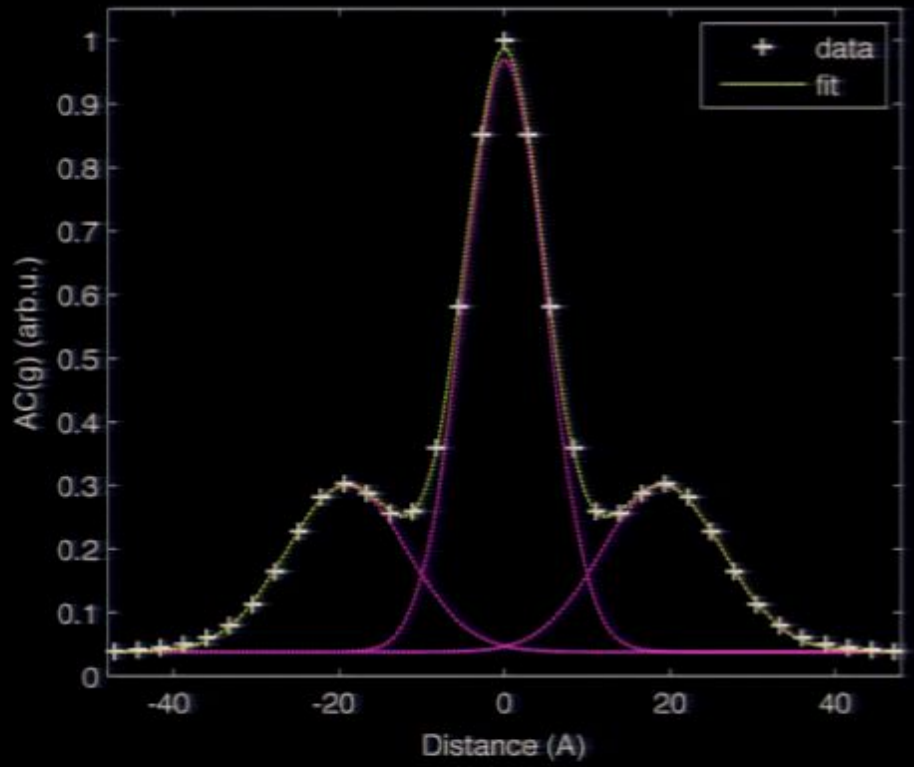

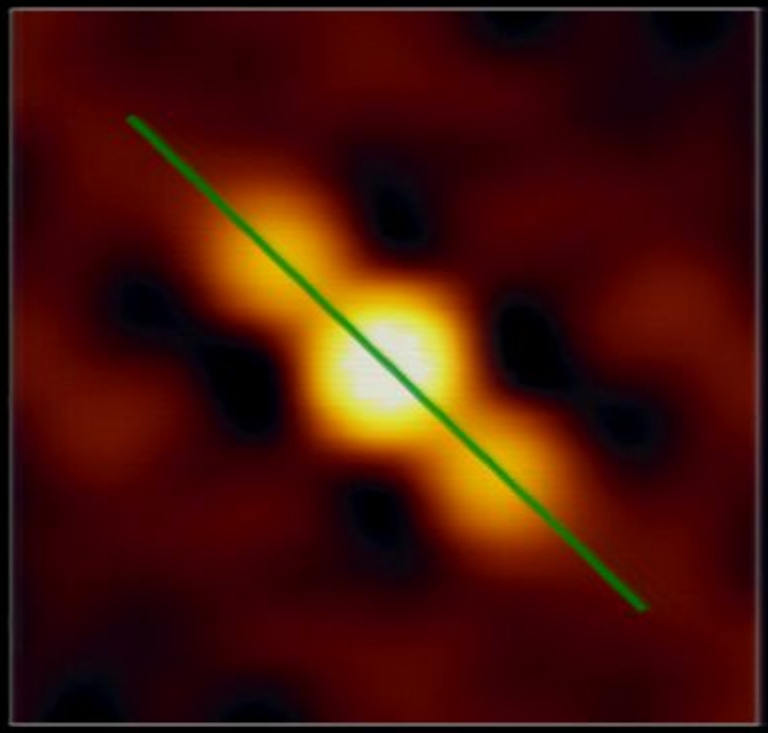

- Triple-peak autocorrelation indicates a self-similarity of ~$8a_{FeF}$ all aligned along same axis

$8a_0$ Unidirectional Electronic Structures

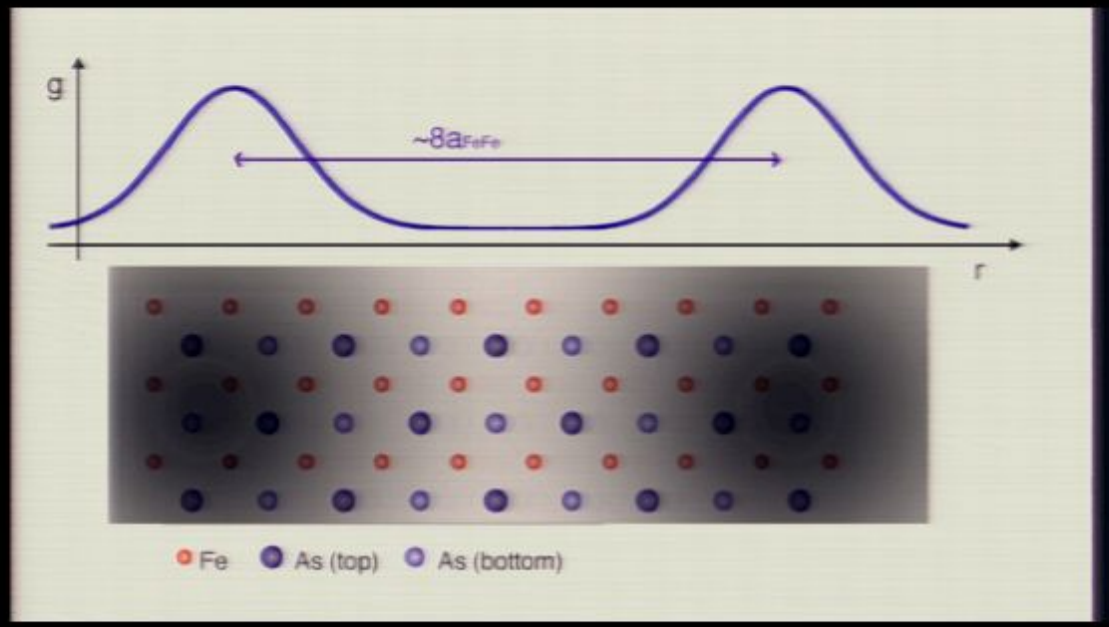

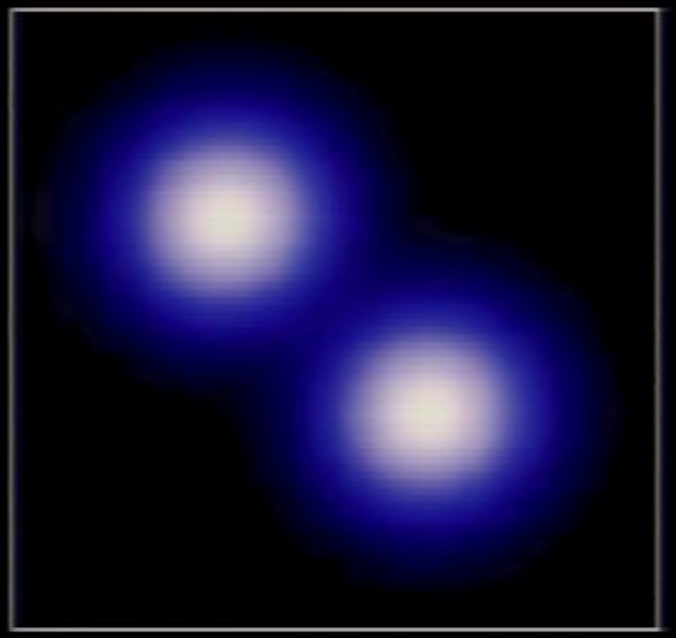

$$g(\mathbf{r}) = \sum_{\mathbf{R_j} \in \mathscr{R}} \mathcal{N}(\mathbf{r} - \mathbf{R_j}), \quad \mathcal{N}(\mathbf{r}) = \mathcal{G}_\sigma(\mathbf{r}) + \mathcal{G}_\sigma(\mathbf{r} + \mathbf{d}),$$

$$\mathcal{G}_\sigma(\mathbf{r}) = \left[a \cdot e^{-\frac{|\mathbf{r}|^2}{\sigma^2}} \right] \mathrm{mS},$$

$8a_0$ Unidirectional Electronic Structures

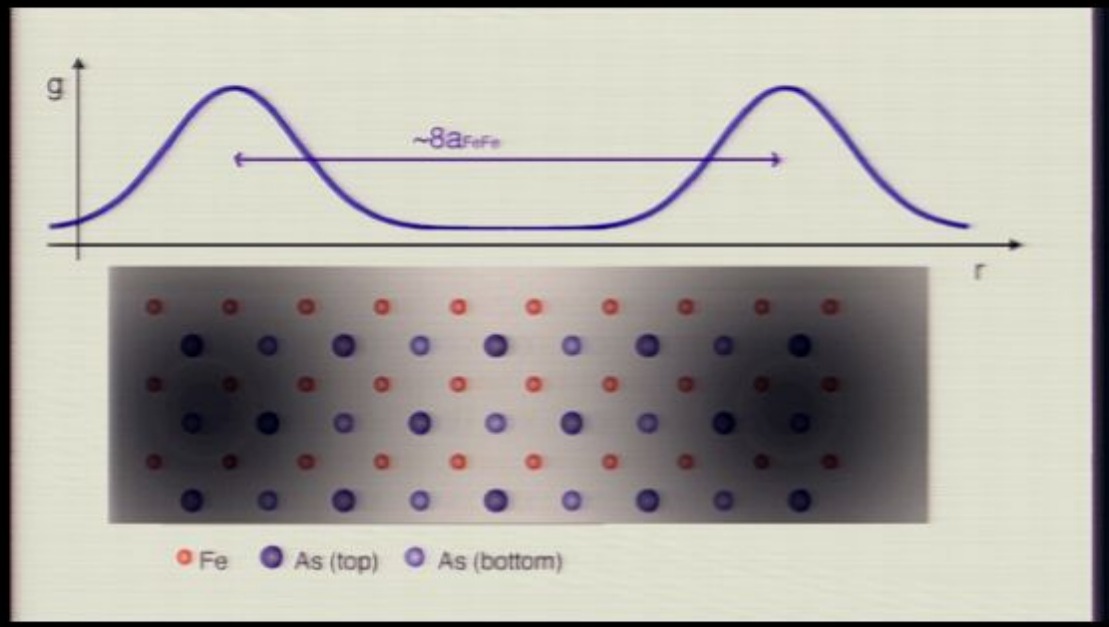

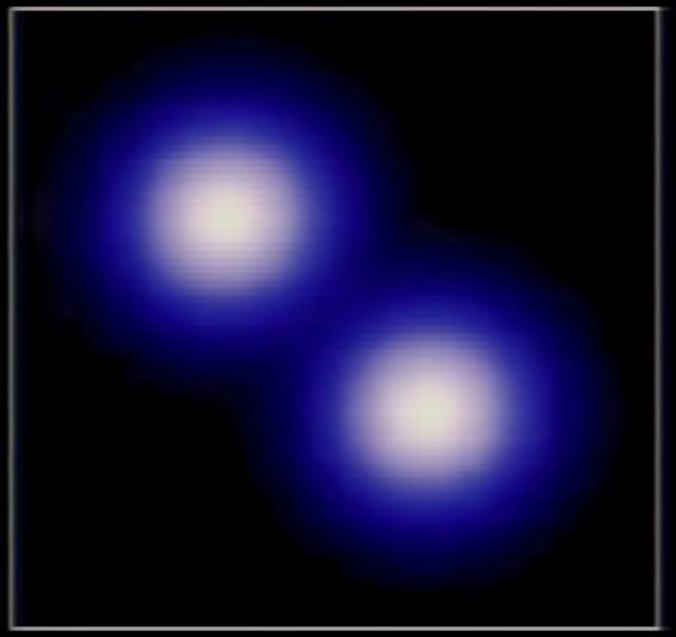

$$g(\mathbf{r}) = \sum_{\mathbf{R_j} \in \mathscr{R}} \mathcal{N}(\mathbf{r} - \mathbf{R_j}), \quad \mathcal{N}(\mathbf{r}) = \mathcal{G}_\sigma(\mathbf{r}) + \mathcal{G}_\sigma(\mathbf{r} + \mathbf{d}),$$

$$\mathcal{G}_\sigma(\mathbf{r}) = \left[a \cdot e^{-\frac{|\mathbf{r}|^2}{\sigma^2}} \right] \mathrm{mS},$$

$8a_0$ Unidirectional Electronic Structures

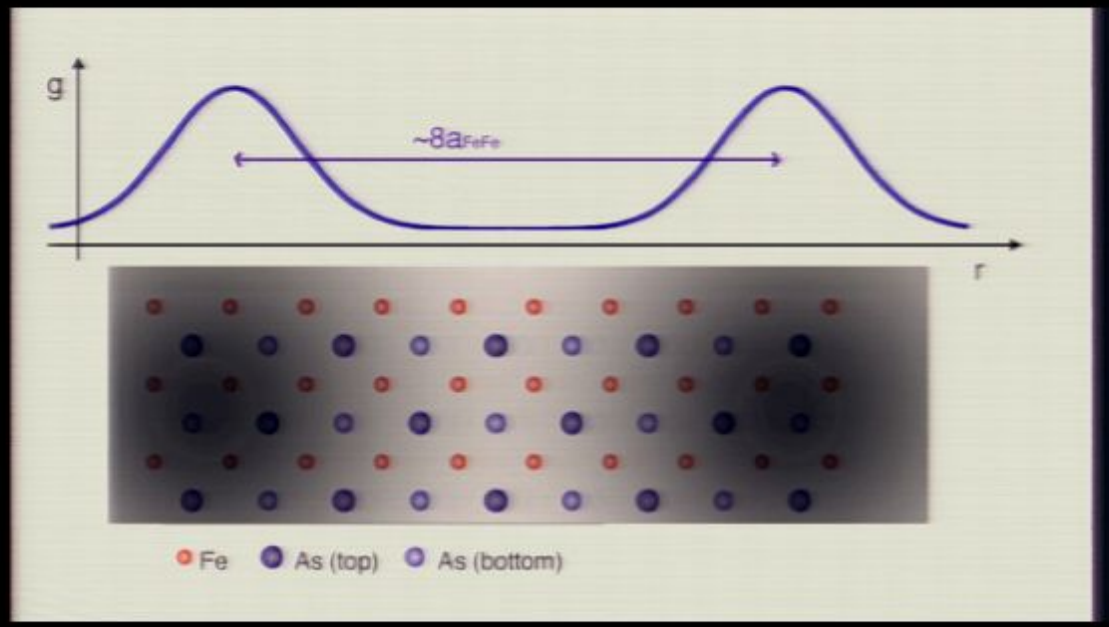

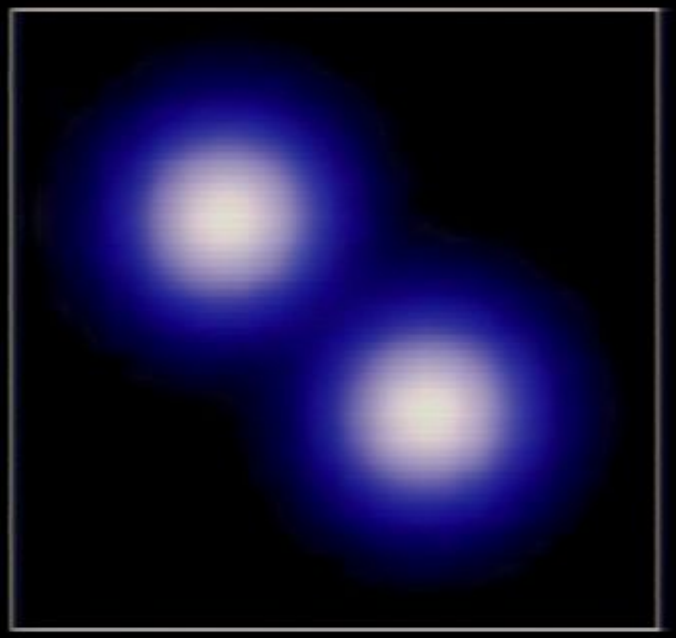

$$g(\mathbf{r}) = \sum_{\mathbf{R_j} \in \mathscr{R}} \mathcal{N}(\mathbf{r} - \mathbf{R_j}), \quad \mathcal{N}(\mathbf{r}) = \mathcal{G}_\sigma(\mathbf{r}) + \mathcal{G}_\sigma(\mathbf{r} + \mathbf{d}),$$

$$\mathcal{G}_\sigma(\mathbf{r}) = \left[a \cdot e^{-\frac{|\mathbf{r}|^2}{\sigma^2}} \right] \mathrm{mS},$$

$8a_0$ Unidirectional Electronic Structures

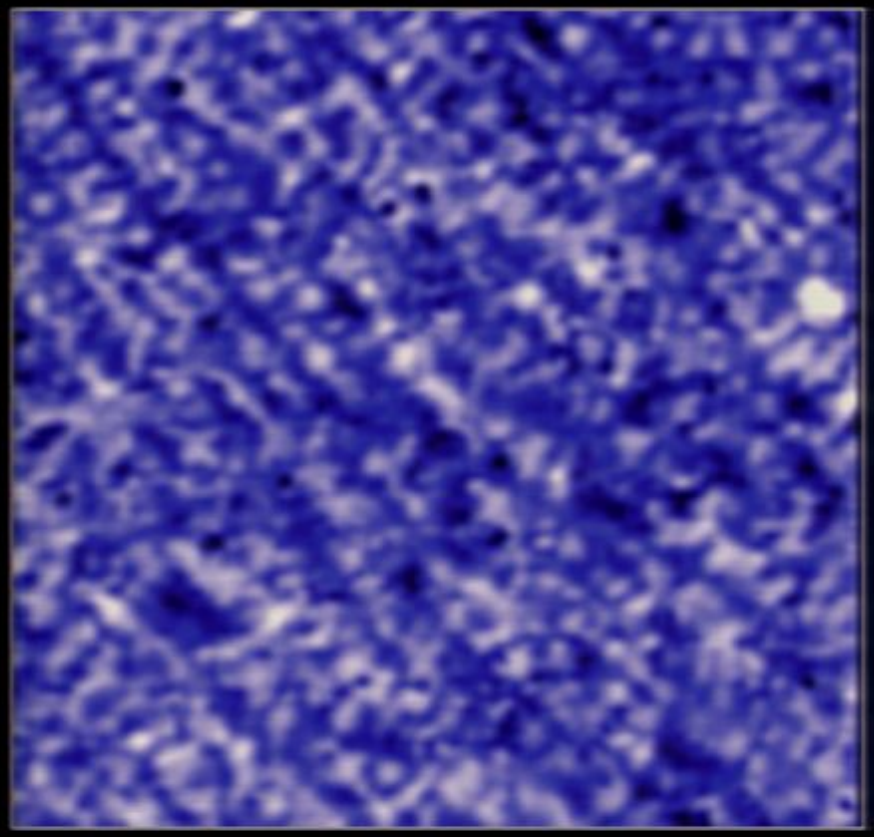

Data : *g(r,E=–37meV)*(48x48nm^2)

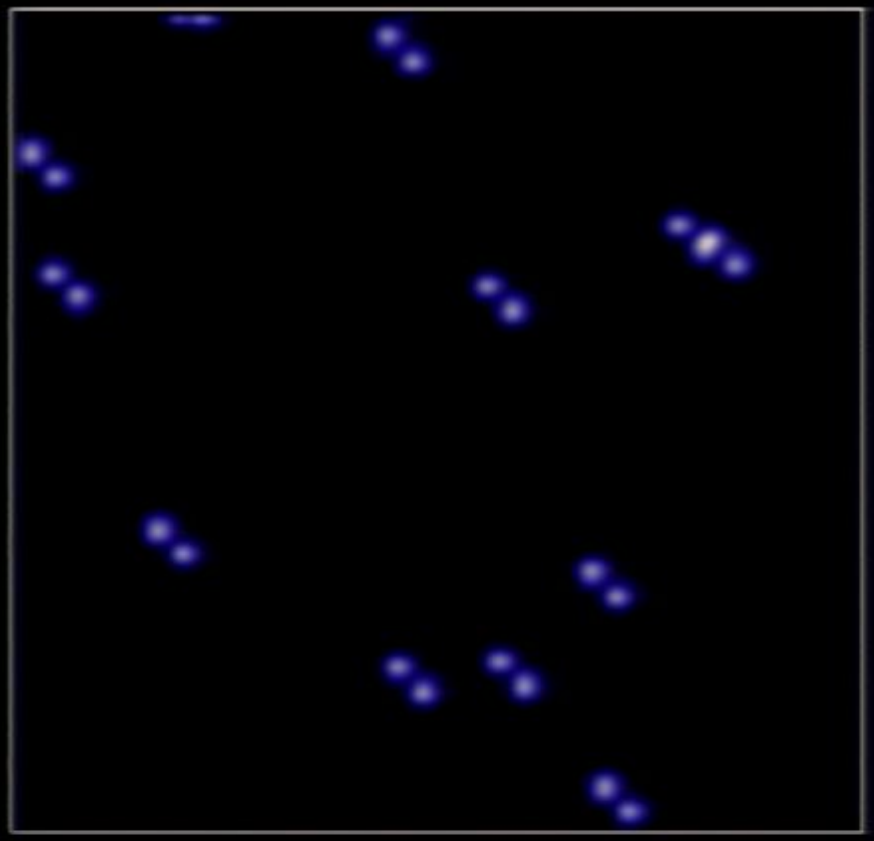

Simulation : *N = 12*

$$g(\mathbf{r}) = \sum_{\mathbf{R_j} \in \mathscr{R}} \mathcal{N}(\mathbf{r} - \mathbf{R_j}), \quad \mathcal{N}(\mathbf{r}) = \mathcal{G}_\sigma(\mathbf{r}) + \mathcal{G}_\sigma(\mathbf{r} + \mathbf{d}),$$

$$\mathcal{G}_\sigma(\mathbf{r}) = \left[a \cdot e^{-\frac{|\mathbf{r}|^2}{\sigma^2}}\right] \mathrm{mS},$$

$8a_{FeFe}$ Electronic 'Dimers'

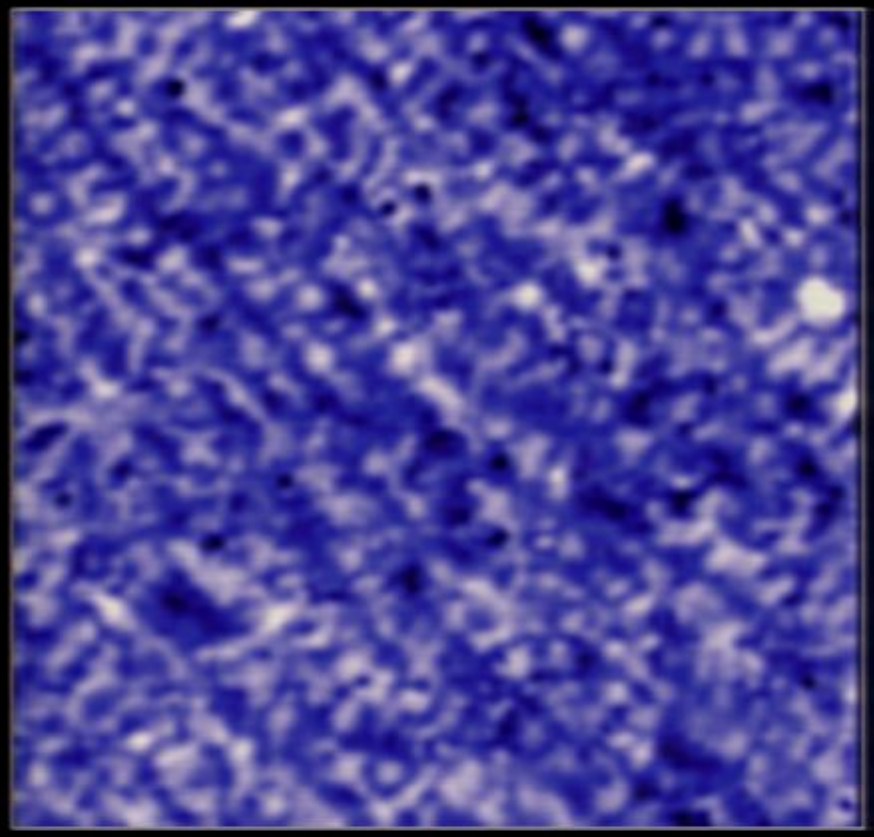

Data : $g(r,E=-37meV)$(48x48nm^2)

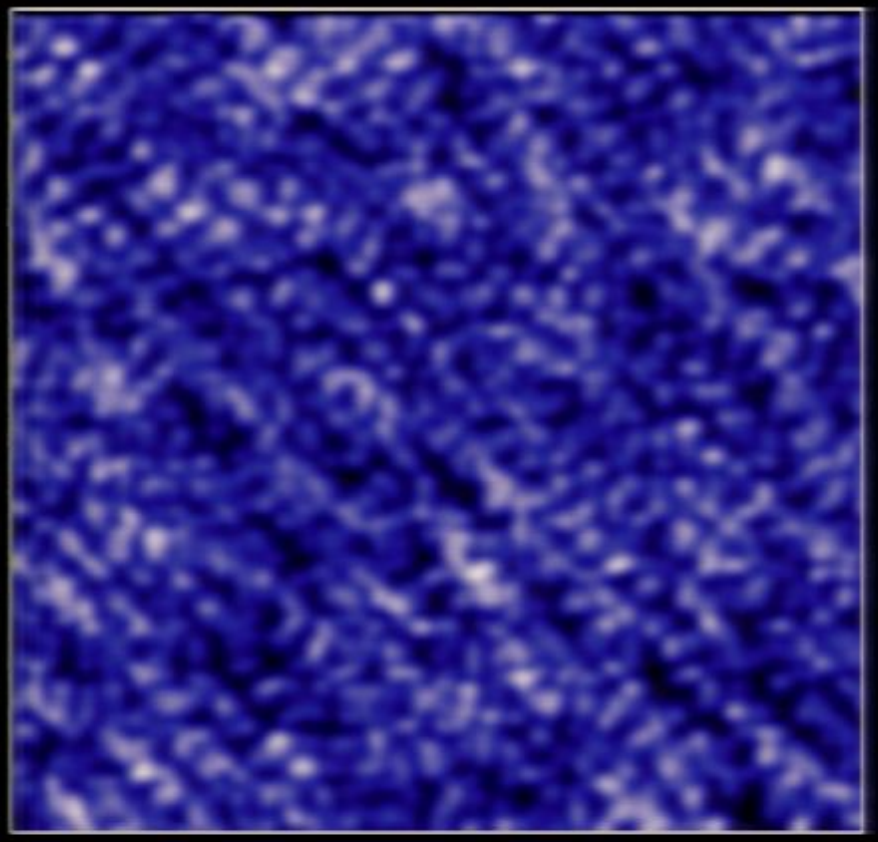

Simulation : $N = 2200$

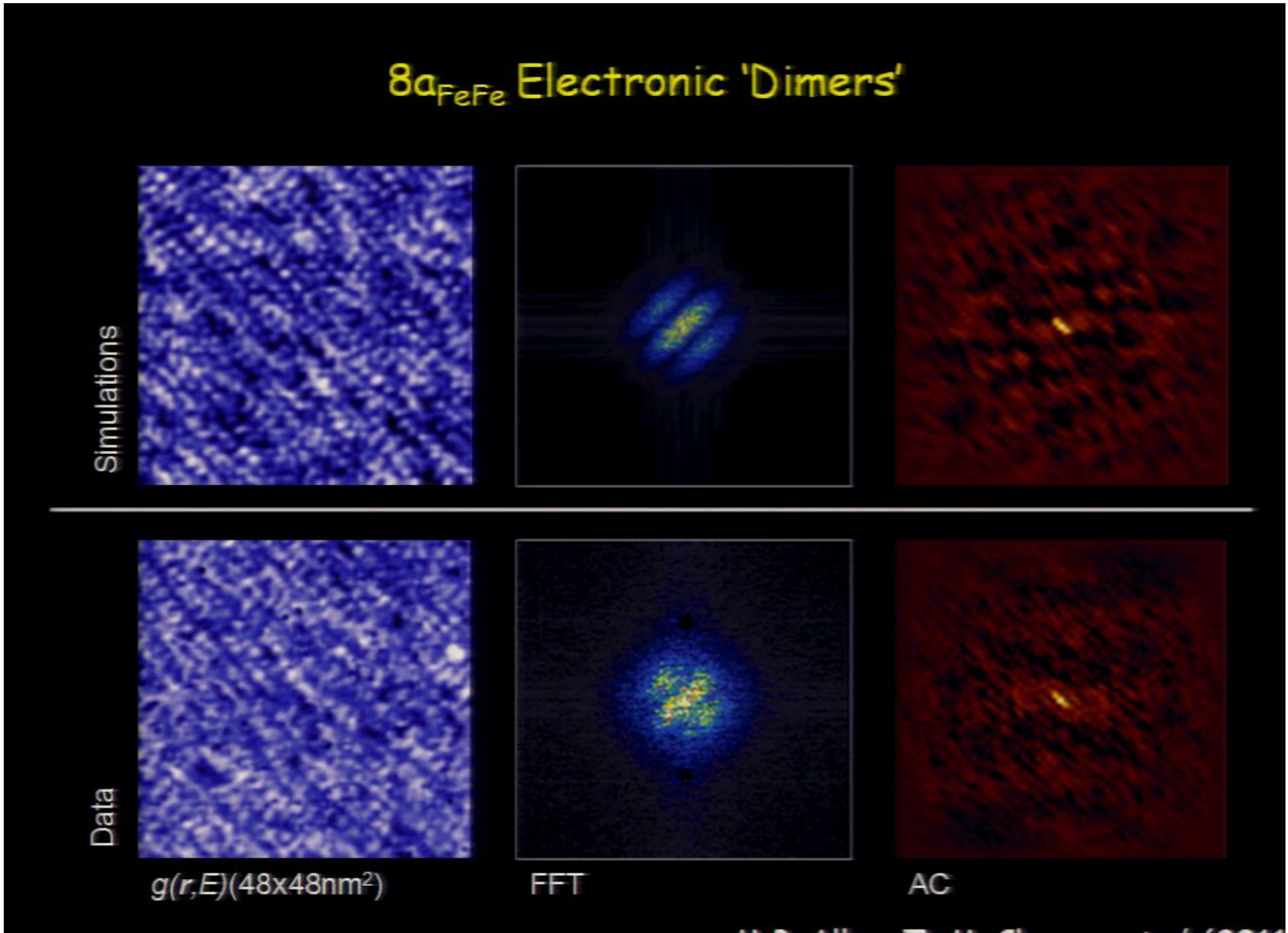
8a$_{FeFe}$ Electronic 'Dimers'
Simulations
Data
$g(r,E)$(48x48nm^2)
FFT
AC

$8a_{FeFe}$ Electronic 'Dimers'

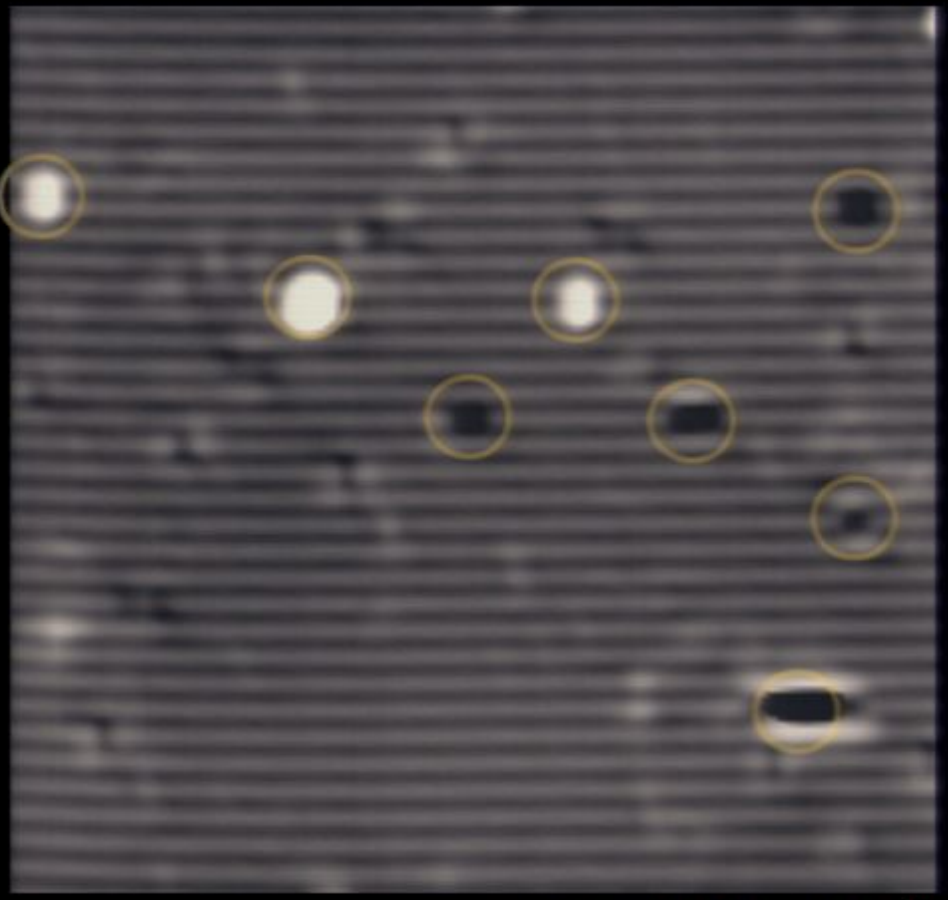

Topograph ($24x24nm^2$)

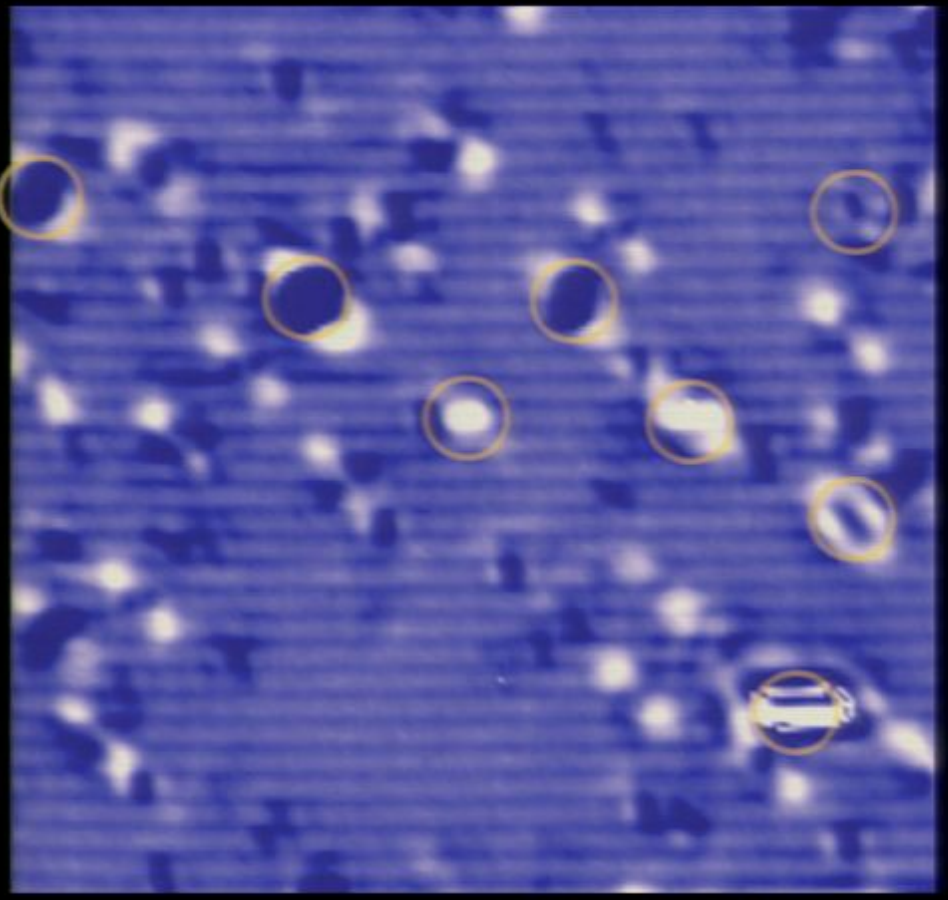

~LDOS ($24x24nm^2$)

$8a_{FeFe}$ Electronic 'Dimers'

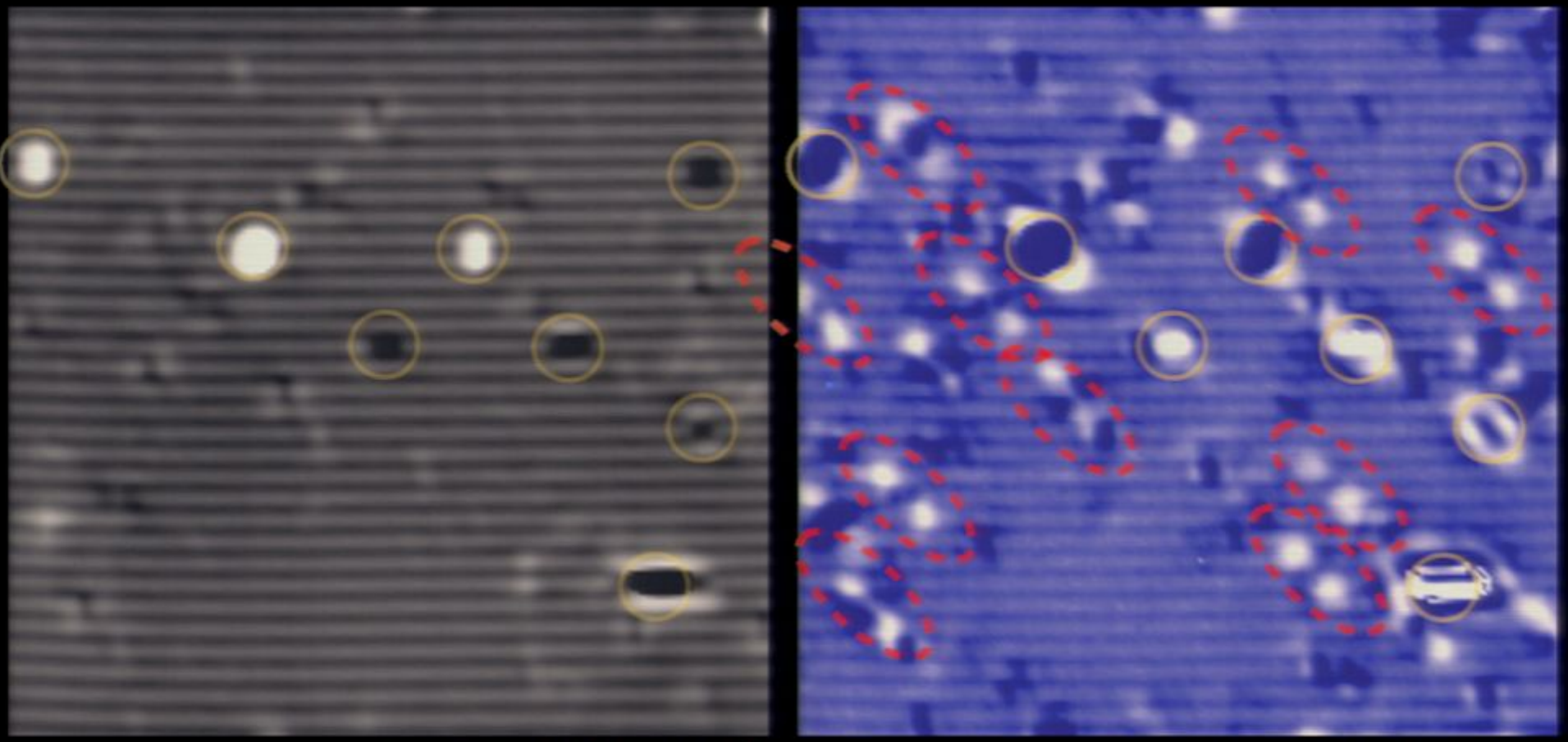

Topograph (24x24nm^2)

~LDOS (24x24nm^2)

Individual dimers are sometimes observed.

$8a_0$ dimer source: Co-dopant atoms ?

$I(\vec{r},+50mV)$

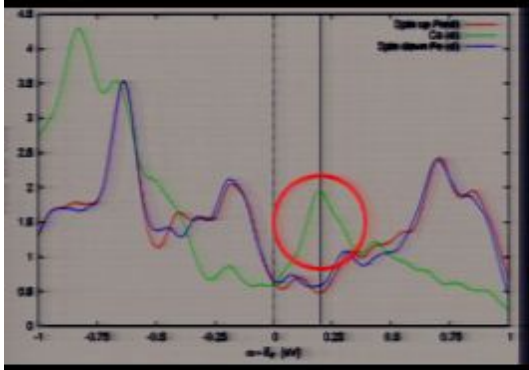

F. Kemper *et. al.*, PRB 2009

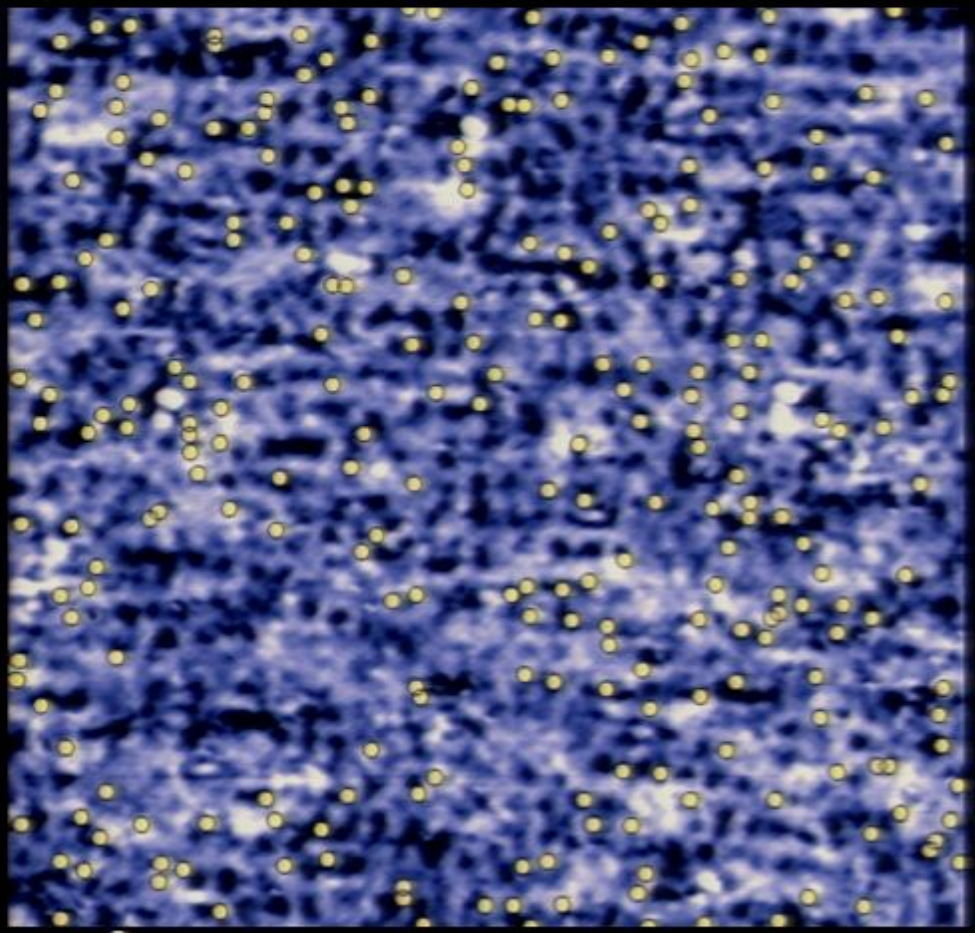

550Å

-45pA

-29pA

$8a_0$ dimer source: Co-dopant atoms ?

$I(\vec{r},+50mV)$

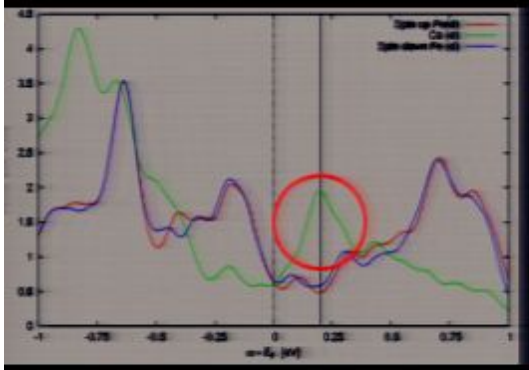

F. Kemper *et. al.*, PRB 2009

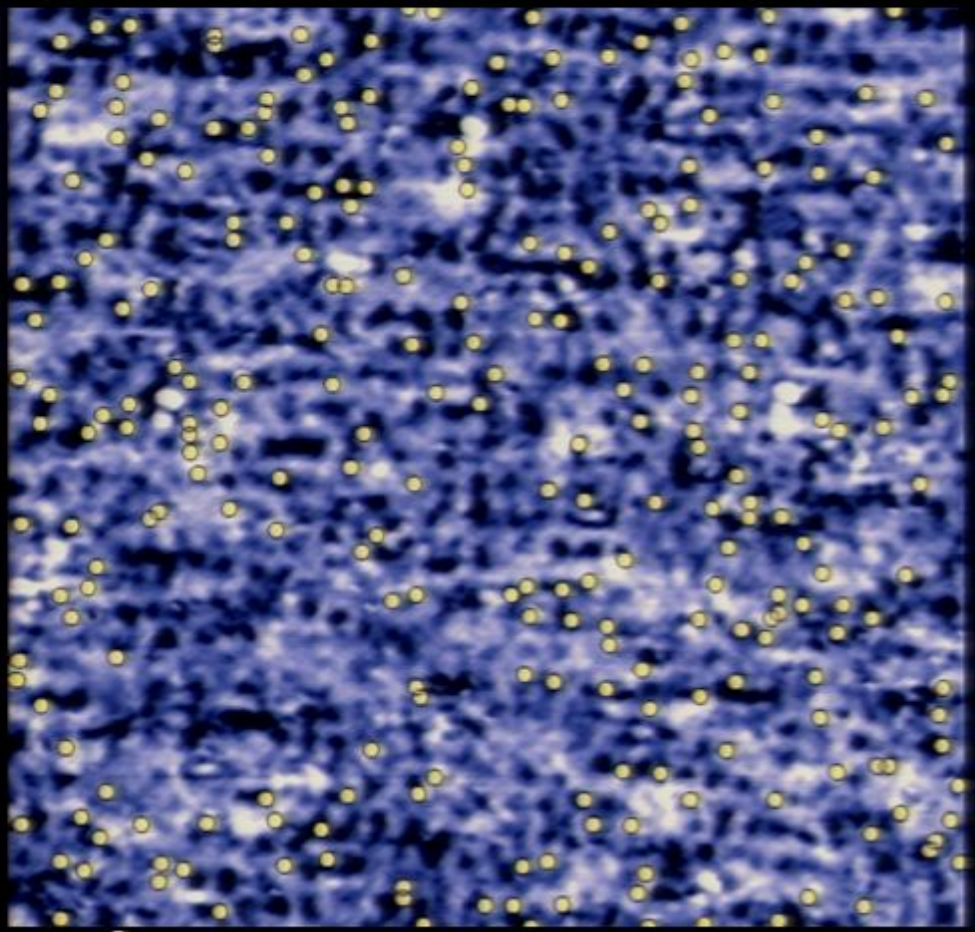

550Å

-45pA

-29pA

$8a_0$ dimers correlated with Co-dopant atoms

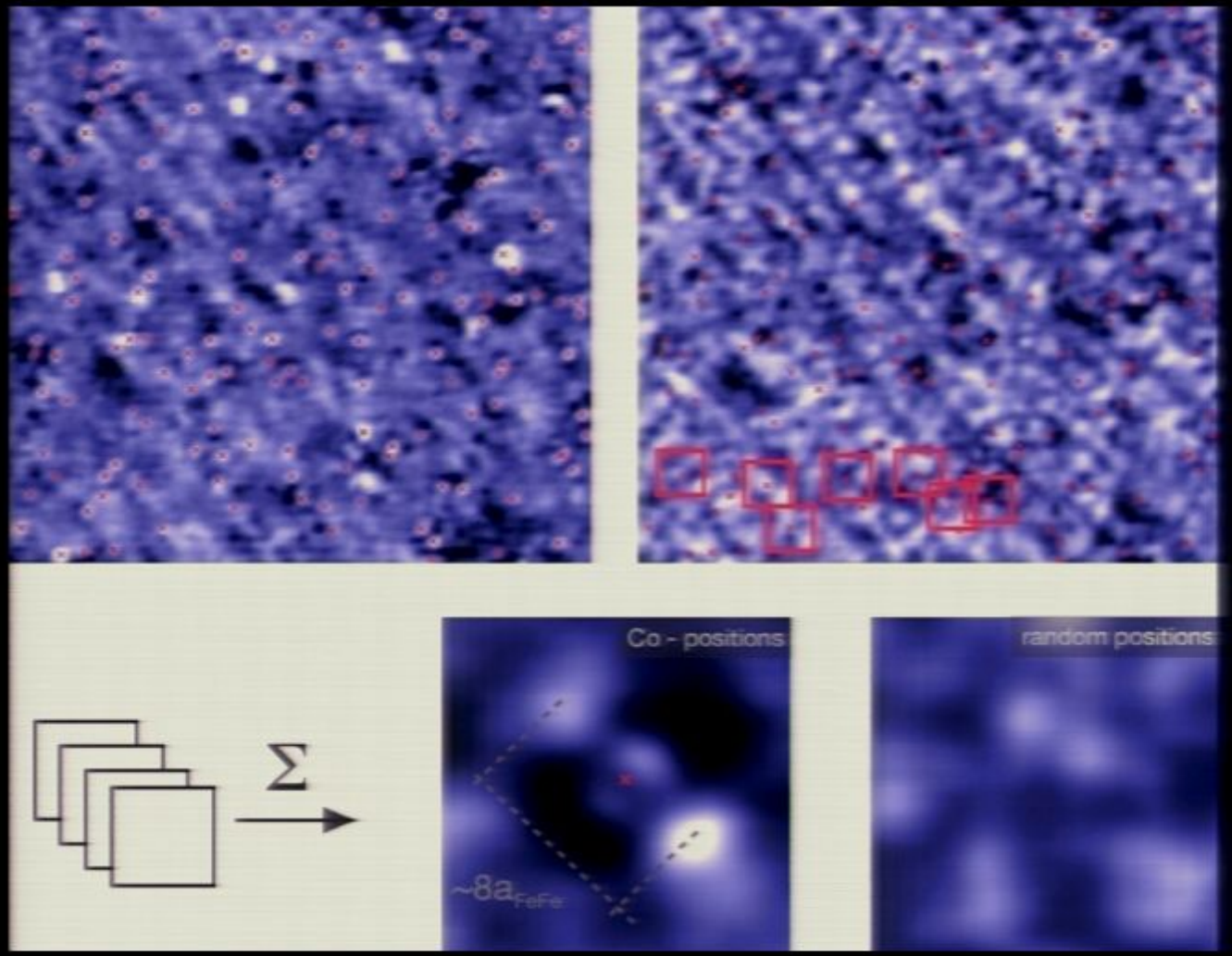

Electronic anisotropy produced by Nematicity + $8a_0$ Electronic Dimers ?

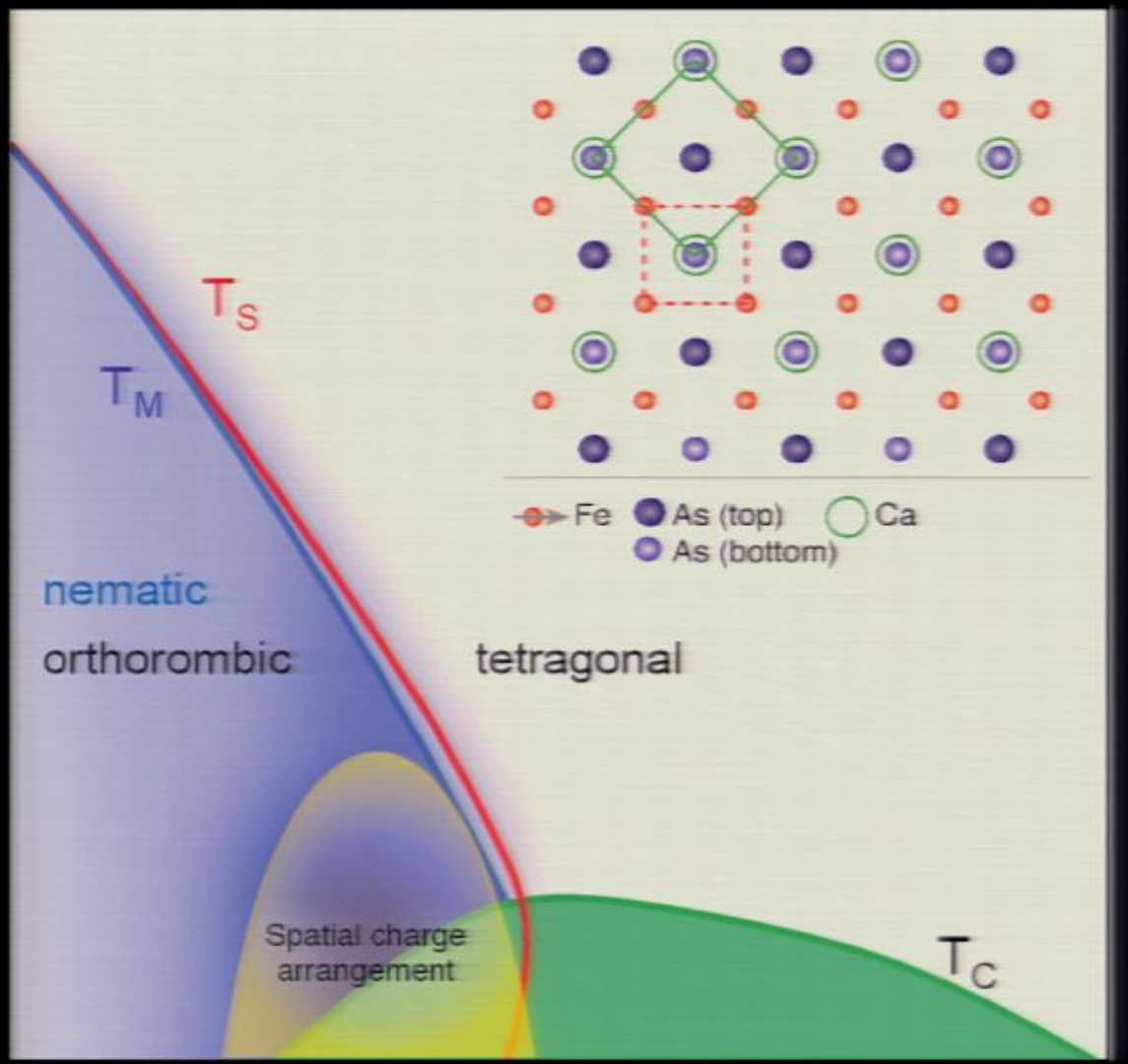

$8a_0$ dimers correlated with Co-dopant atoms

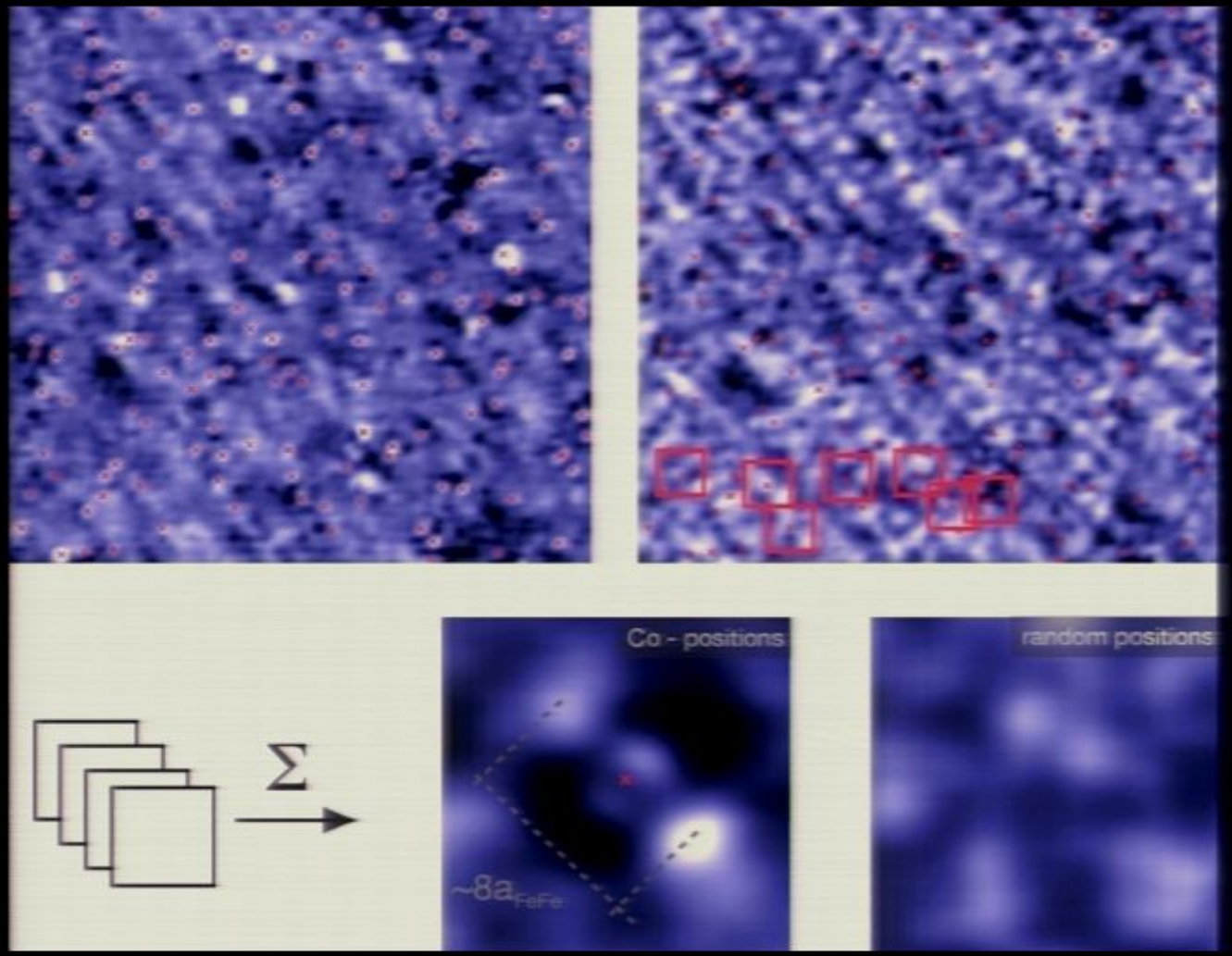

Electronic anisotropy produced by Nematicity + $8a_0$ Electronic Dimers ?

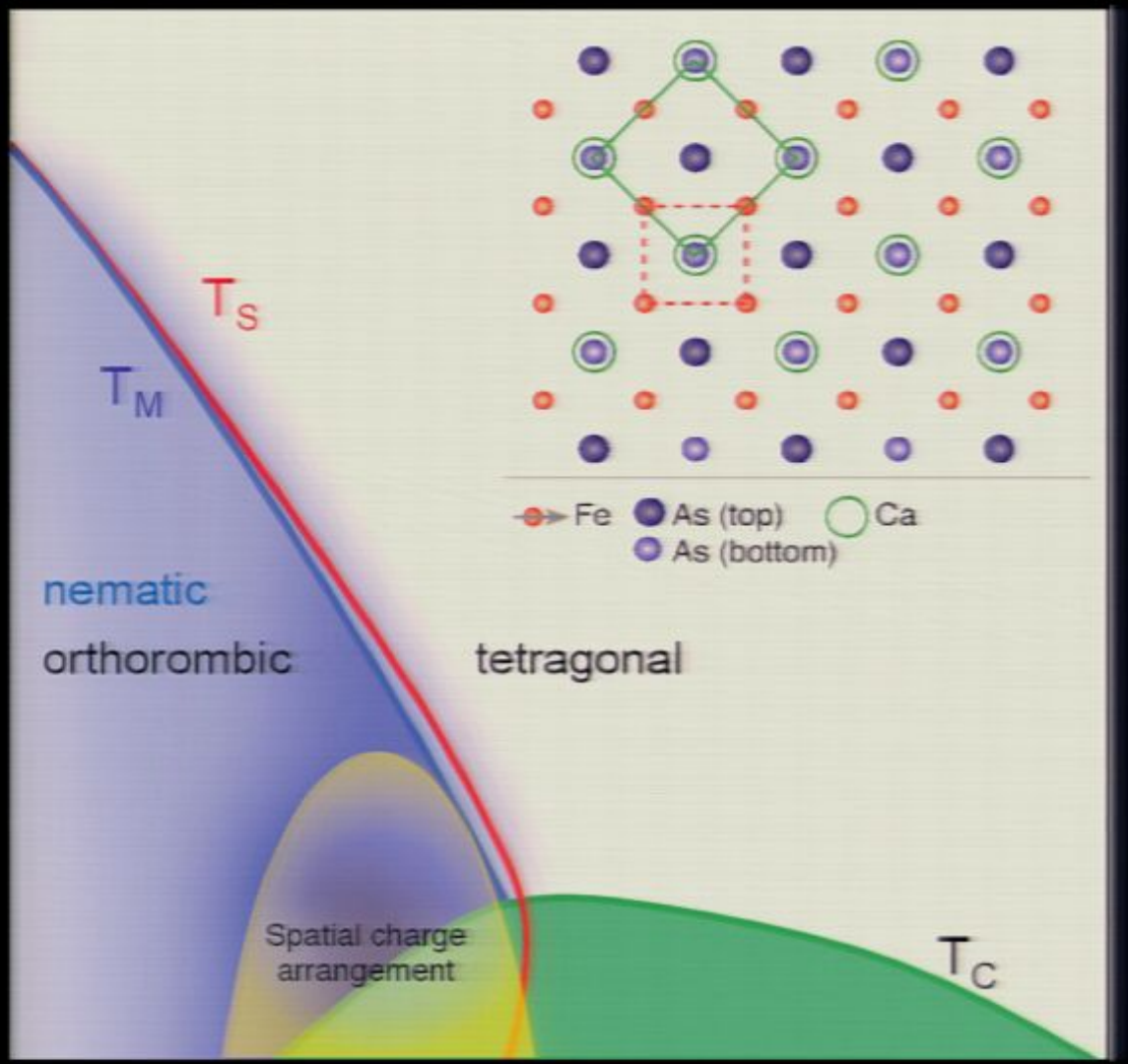

Cause of anisotropic QP Scattering Interference ?

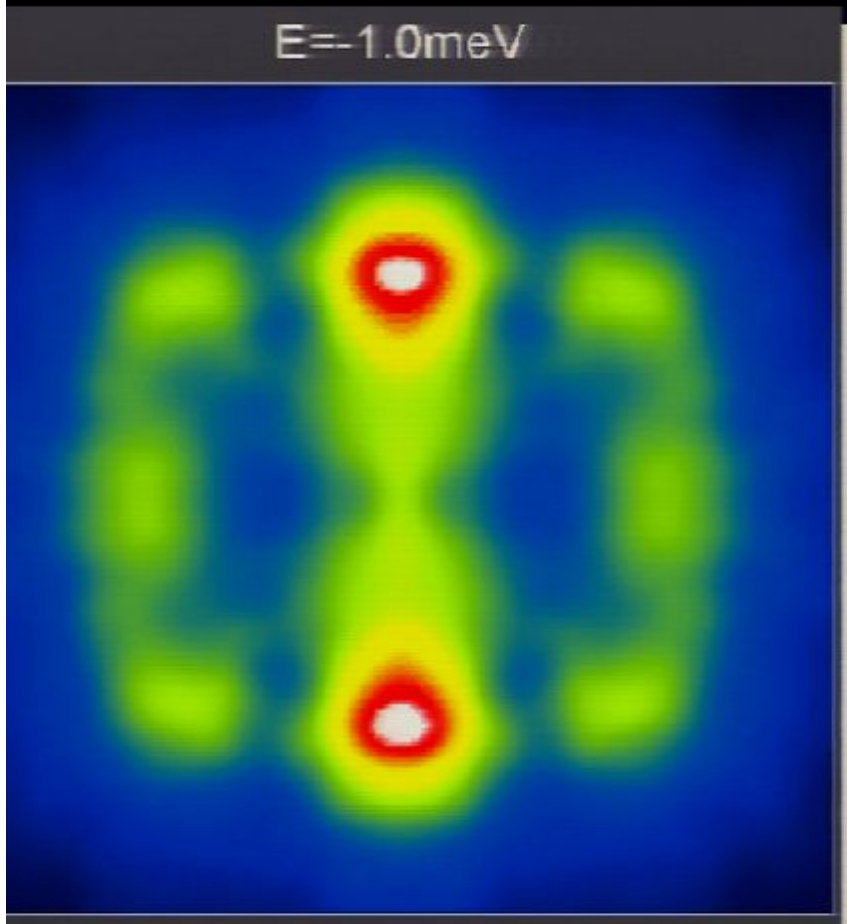

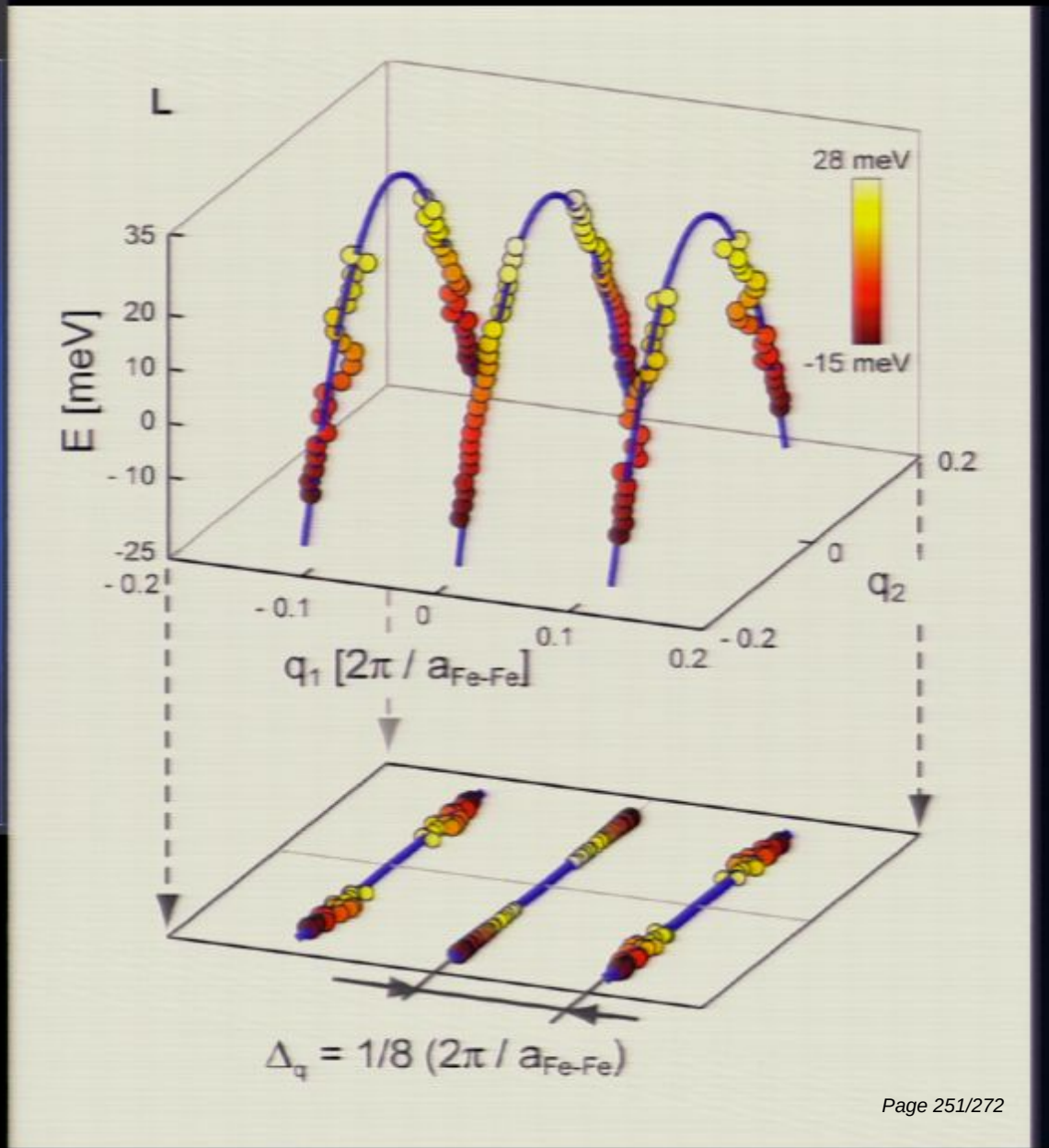

Cause of anisotropic QP Scattering Interference ?

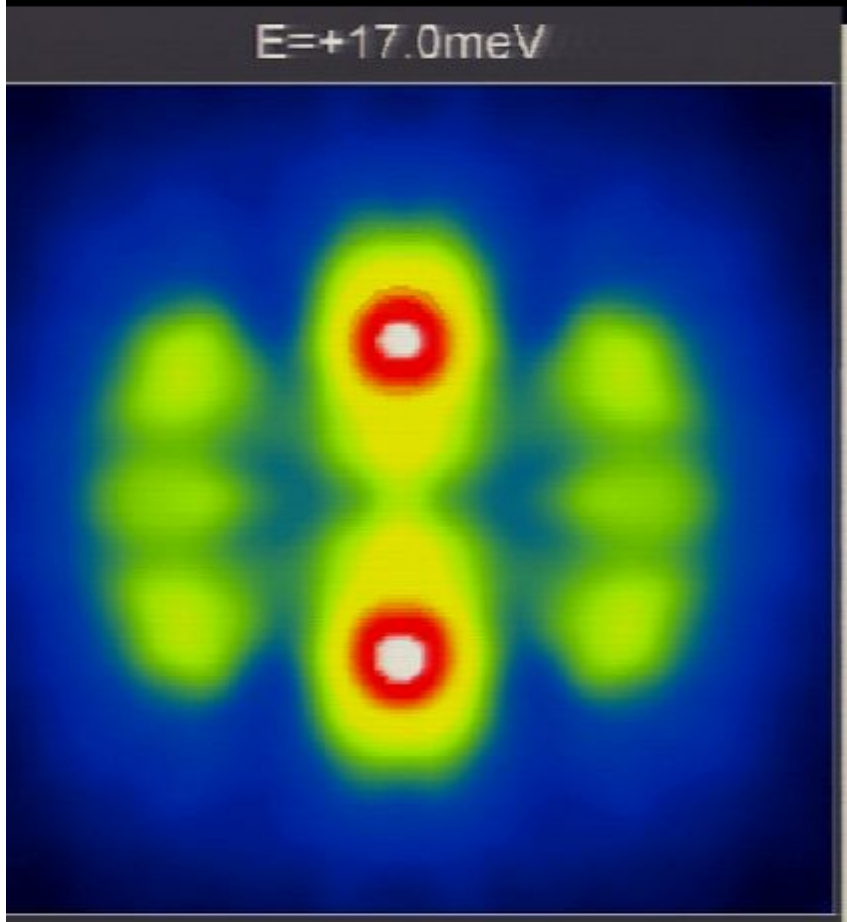

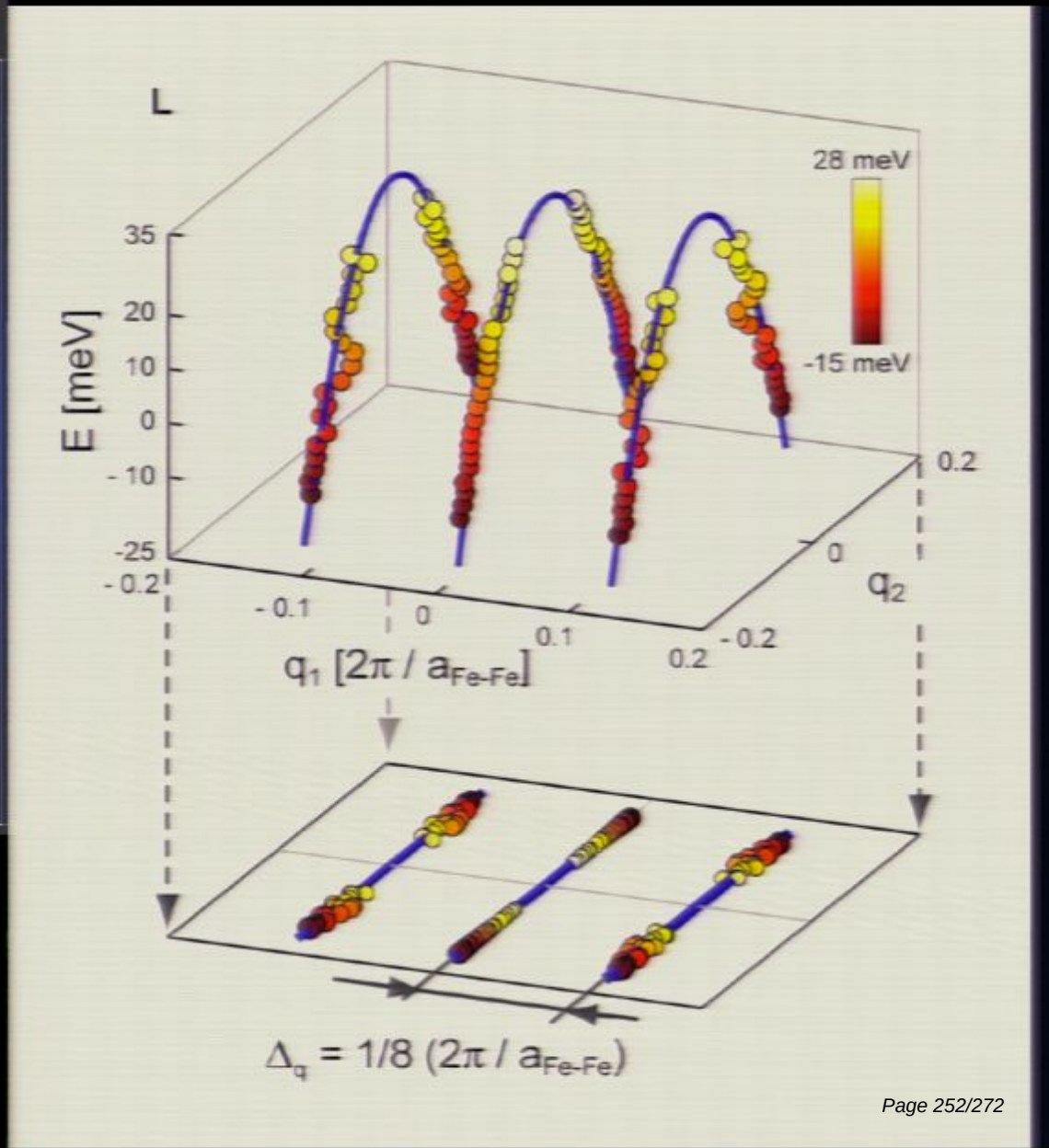

Cause of anisotropic QP Scattering Interference ?

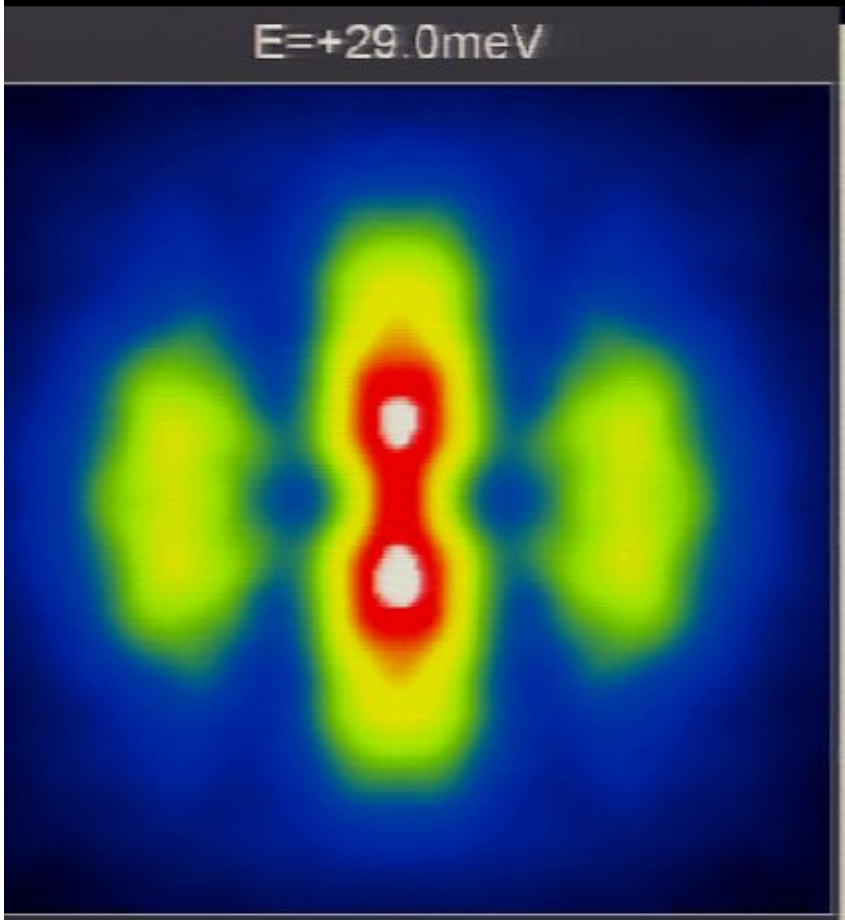

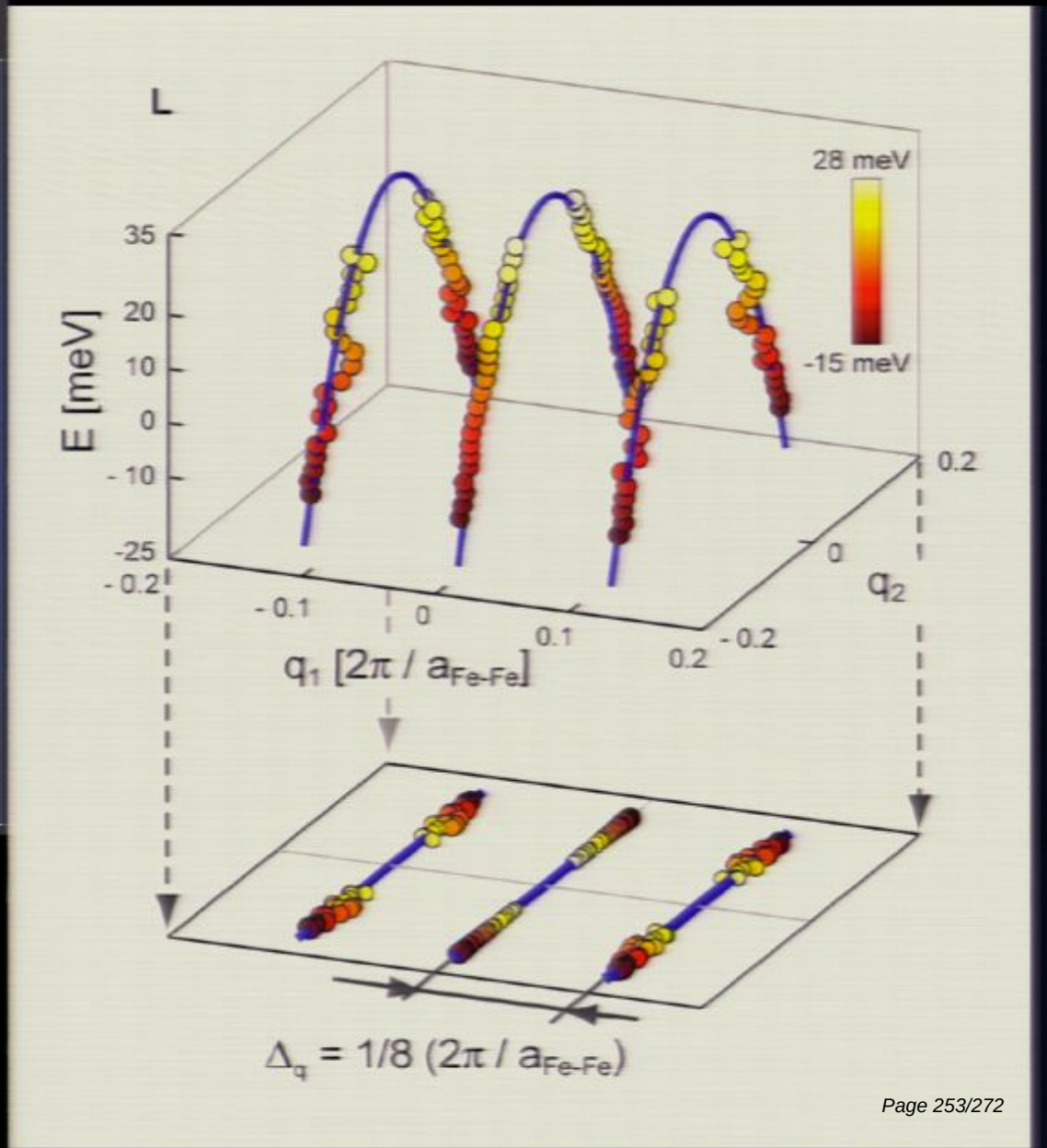

Cause of anisotropic QP Scattering Interference ?

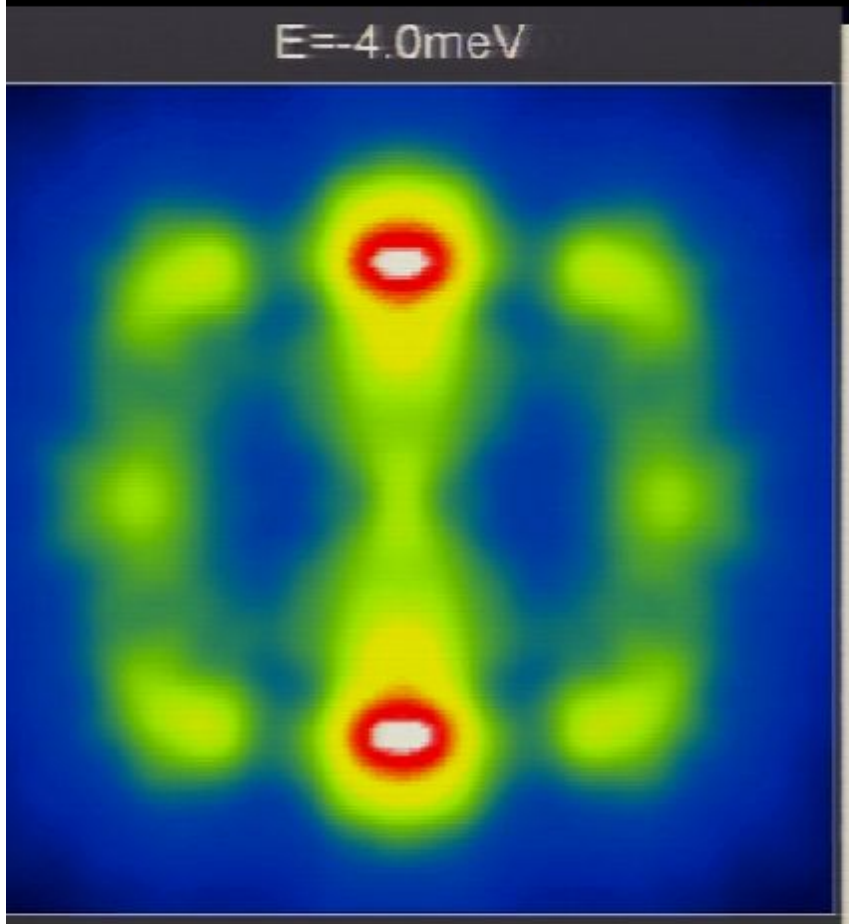

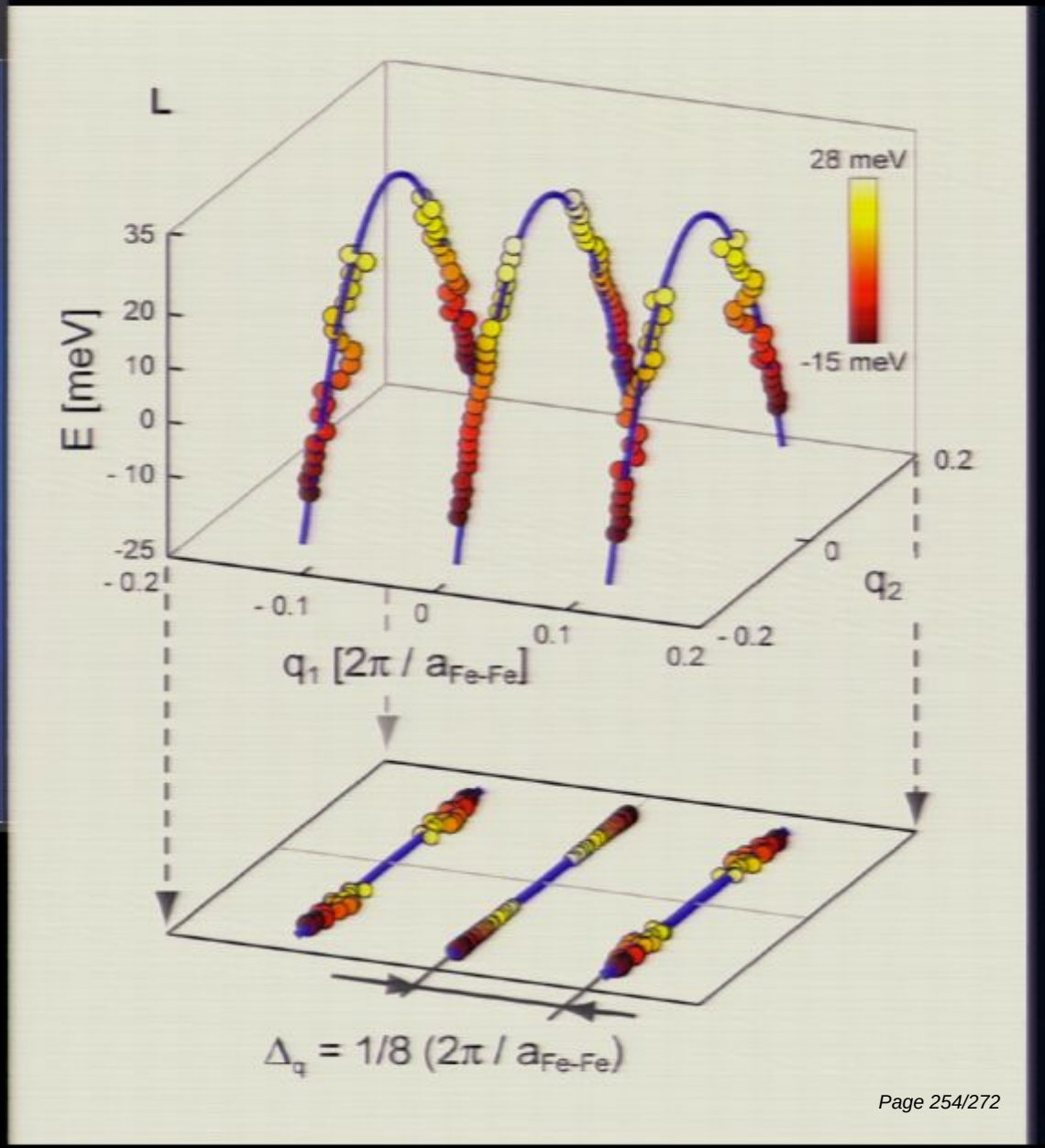

Cause of anisotropic QP Scattering Interference ?

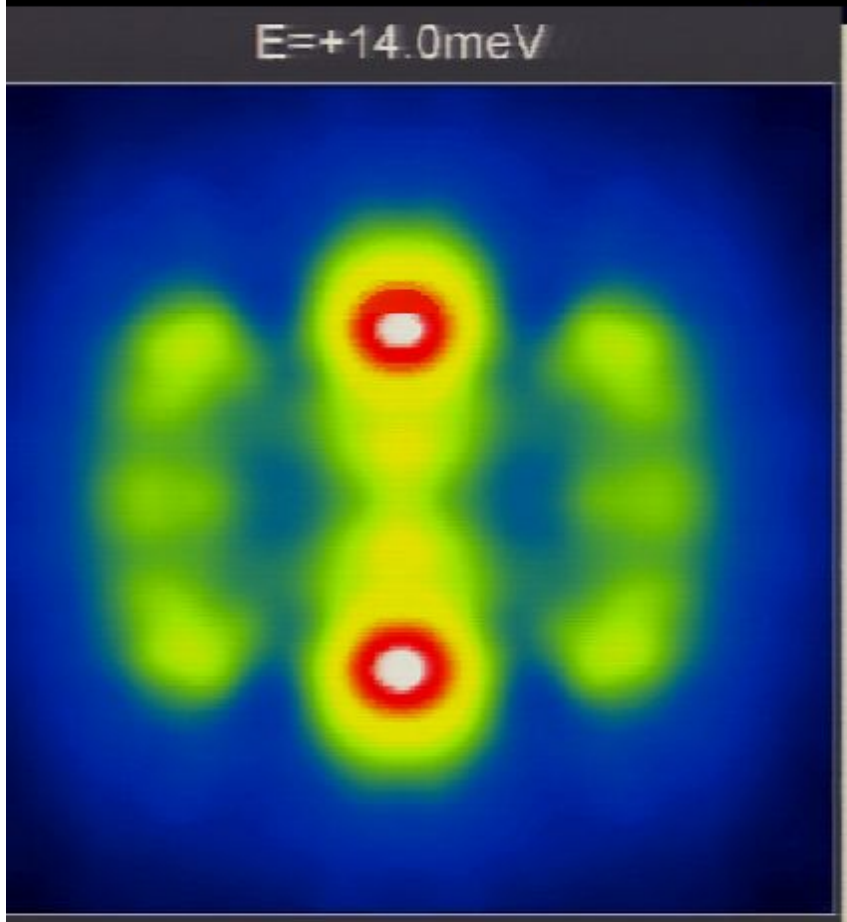

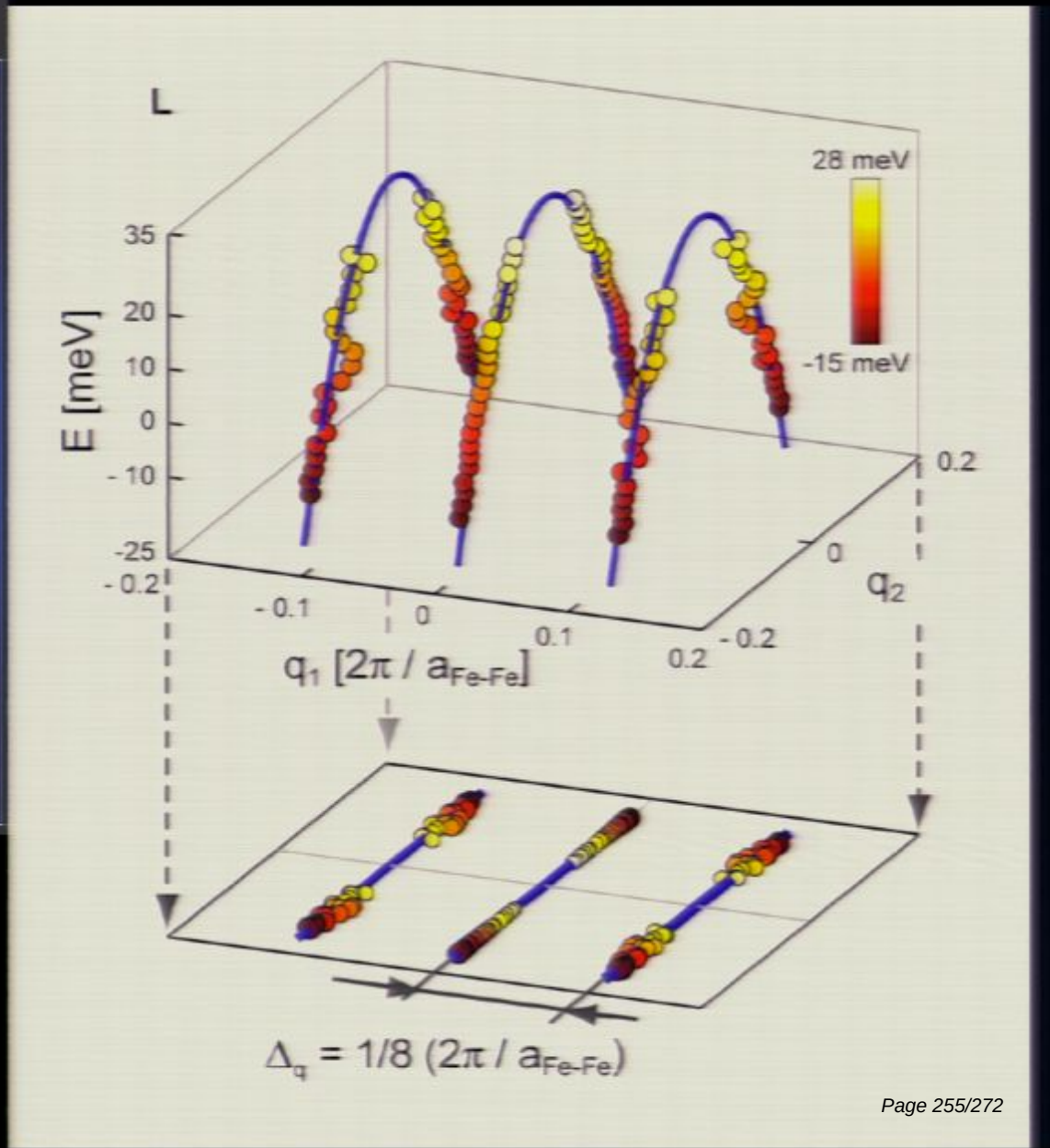

Cause of anisotropic QP Scattering Interference ?

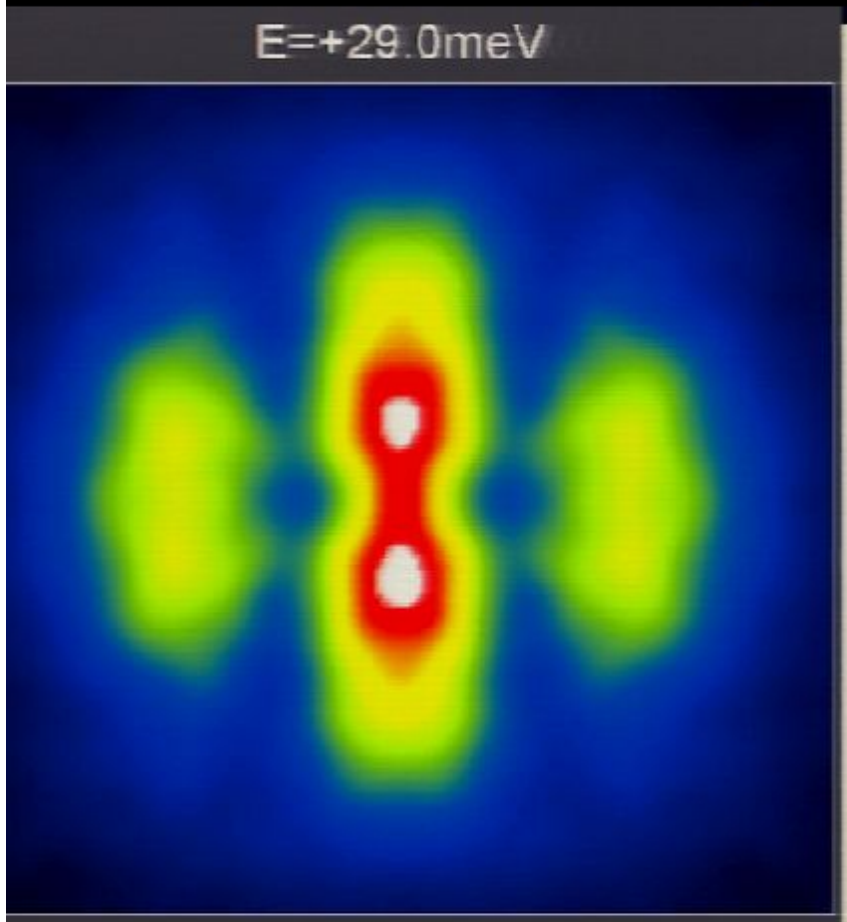

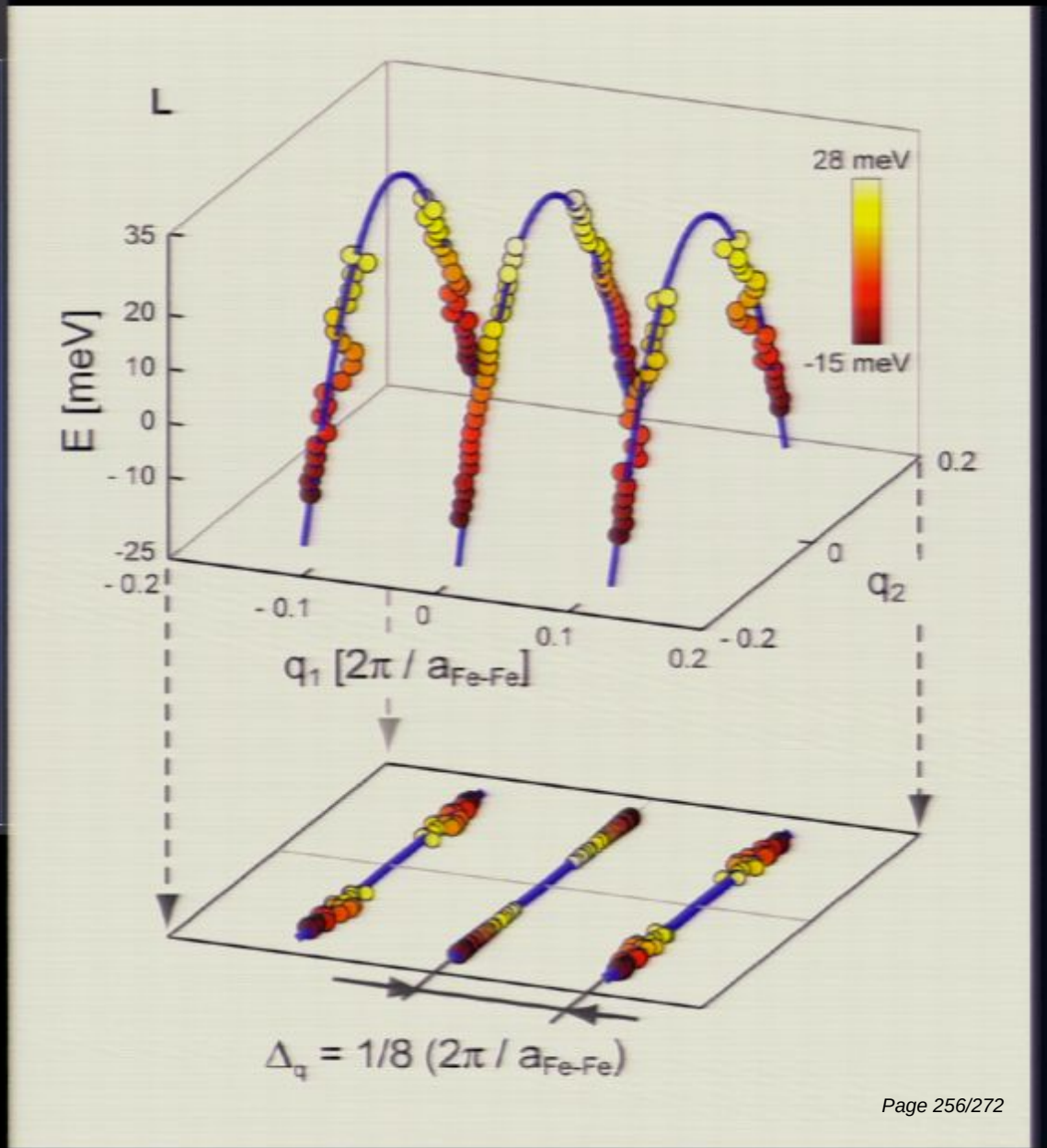

Consider realistic scattering interference model

(all data from *detwinned* Ca122 crystals)

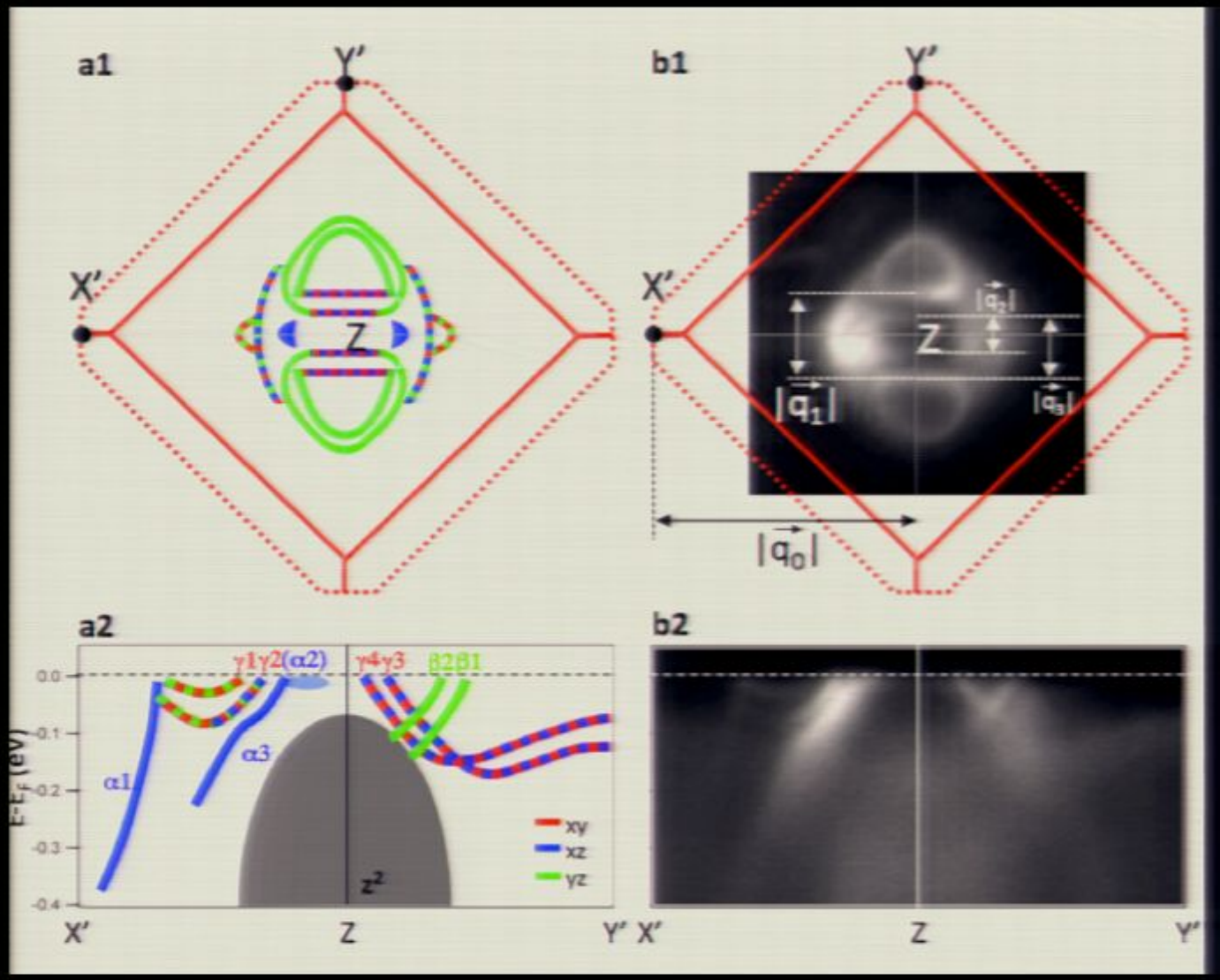

QPI vs. ARPES : Autocorrelation($A(k,w)$)

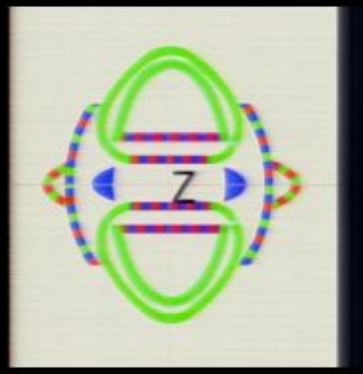

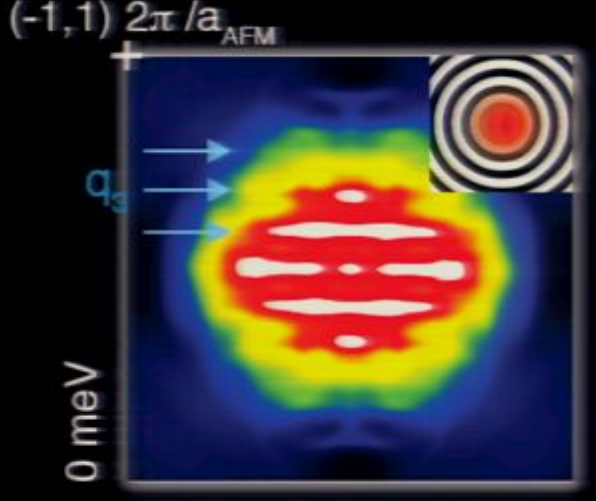

Autocorrelation of
$A(k,\omega)$(Pointscatterer)

M.P.Allan, T. M. Chuang *et al*, 2011

QPI vs. ARPES : Autocorrelation($A(k,w)$)

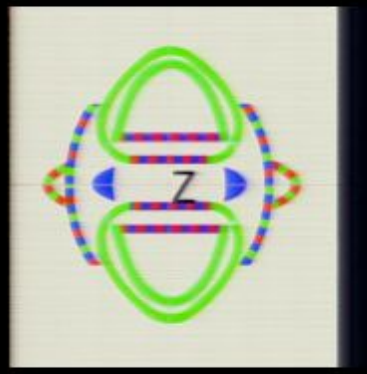

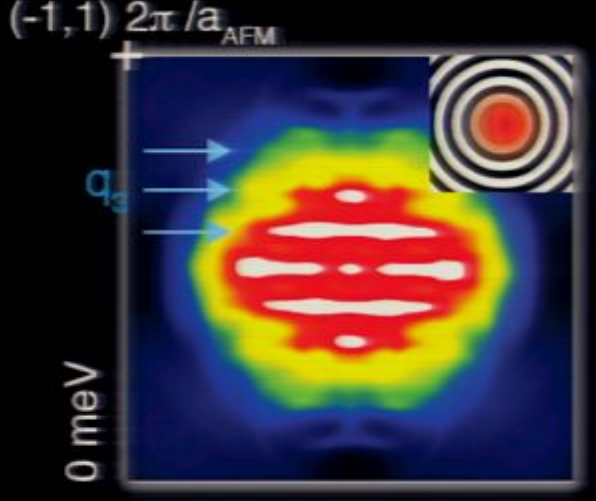

Autocorrelation of
$A(k,\omega)$(Pointscatterer)

Inconsistent

↔

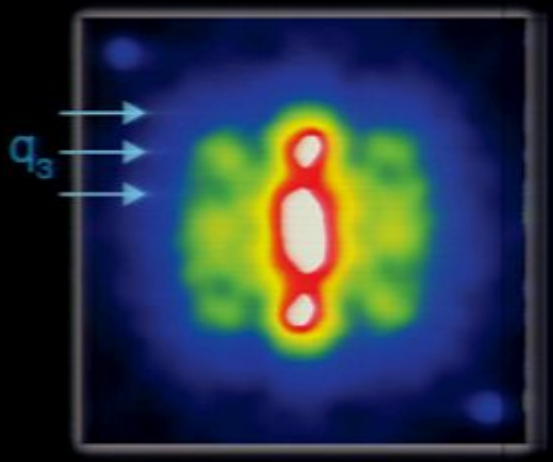

QPI Data

M.P.Allan, T.-M. Chuang *et al.* 2011

QPI vs. ARPES : Autocorrelation($A(k,w)$)

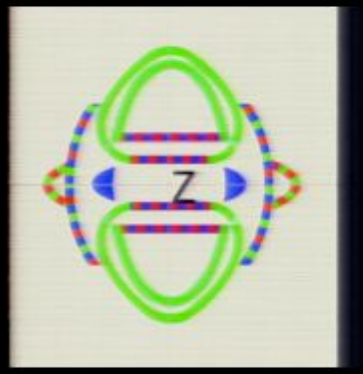

Suppressed intensity

(-1,1) $2\pi/a_{AFM}$

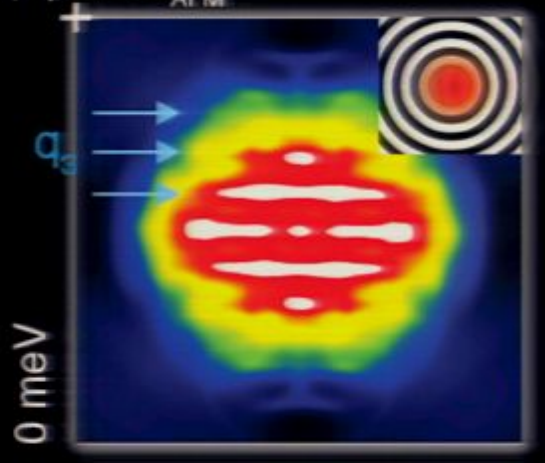

Autocorrelation of
$A(k,\omega)$(Pointscatterer)

Inconsistent

↔

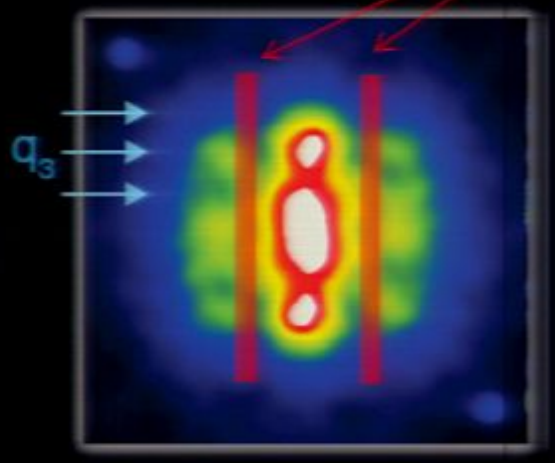

QPI Data

M.P.Allan, T.-M. Chuang *et al.* 2011

Structure Factor in QPI

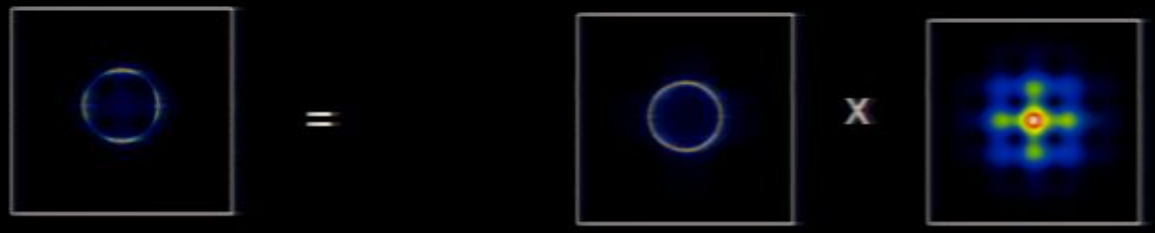

$$P(q,\omega) = \frac{1}{N}\left|\frac{1}{\pi}\mathrm{Im}\,\Lambda(q,\omega)\right|^2 |\delta\epsilon(q)|^2$$

$$\delta\epsilon(q) = \int \frac{d^2x}{a^2}\,\delta\epsilon(x)e^{-iq\cdot x}$$

Resulting QPI

'bare' QPI

Structure factor =
FFT(scattering potential)

from: Capriotti*et al.*, PRB 68, 014508 2003

M.P.Allan, T.-M. Chuang *et al.*, 2011

QPI vs. ARPES : Point Scatterer

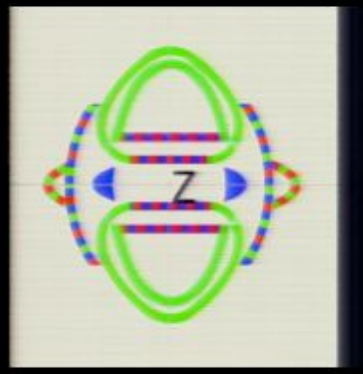

$$P(q,\omega) = \frac{1}{N}\left|\frac{1}{\pi}\mathrm{Im}\,\Lambda(q,\omega)\right|^2 \overline{|\delta\epsilon(q)|^2}$$

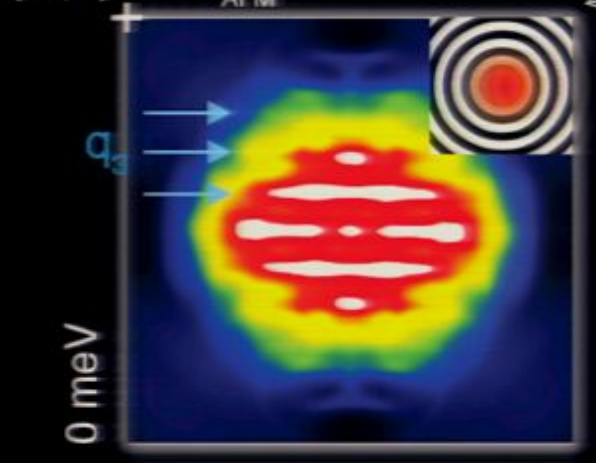

Autocorrelation of
$A(k,\omega)$
(Point scatterer)

Inconsistent

↔

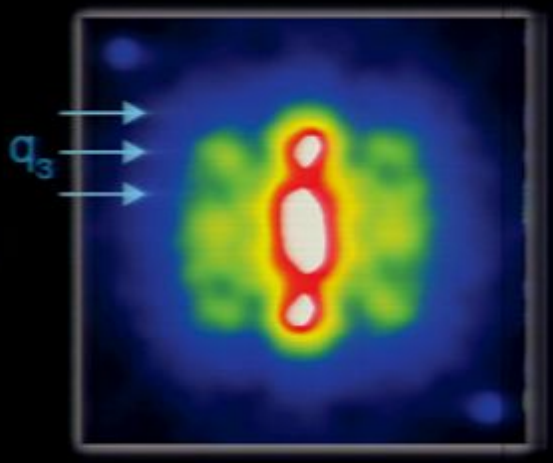

QPI Data

M.P.Allan, T.-M. Chuang *et al.* 2011

QPI vs. ARPES : Dimer Scatterer

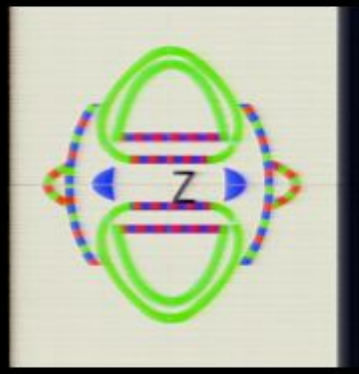

$$P(q,\omega) = \frac{1}{N}\left|\frac{1}{\pi}\mathrm{Im}\,\Lambda(q,\omega)\right|^2 \left|\delta\epsilon(q)\right|^2$$

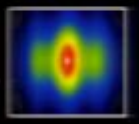

(-1,1) $2\pi/a_{AFM}$

q_3

0 meV

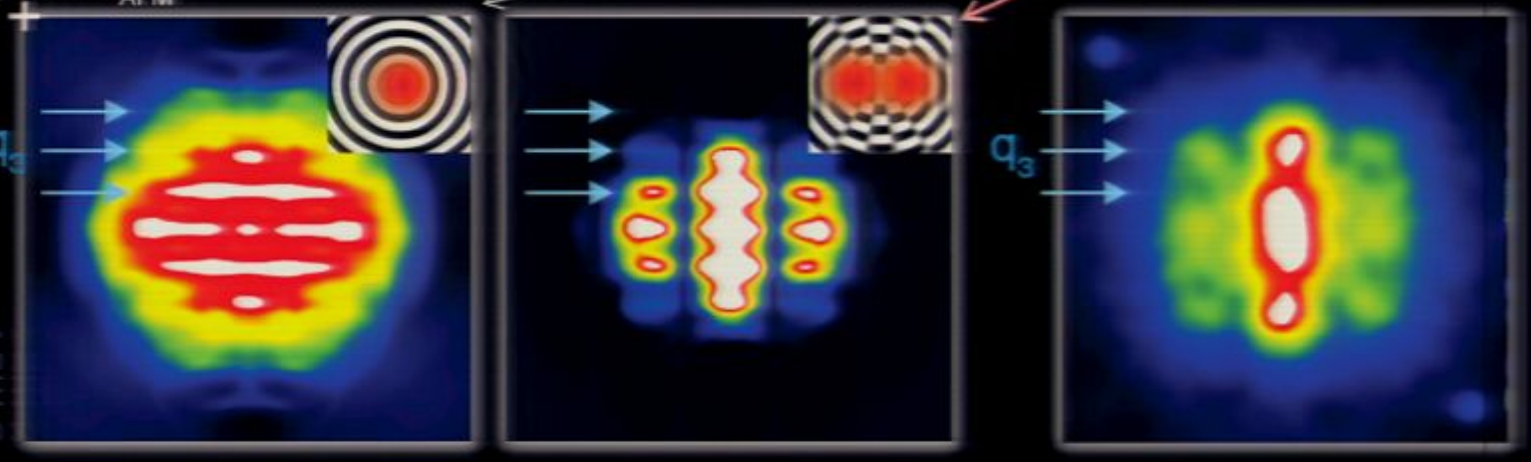

Autocorrelation of $A(k,\omega)$ (Point scatterer)

Autocorrelation of $A(k,\omega)$ ($8a_0$dimer scatterer)

QPI Data

Consistent!

M.P.Allan, T.-M. Chuang *et al.* 2011

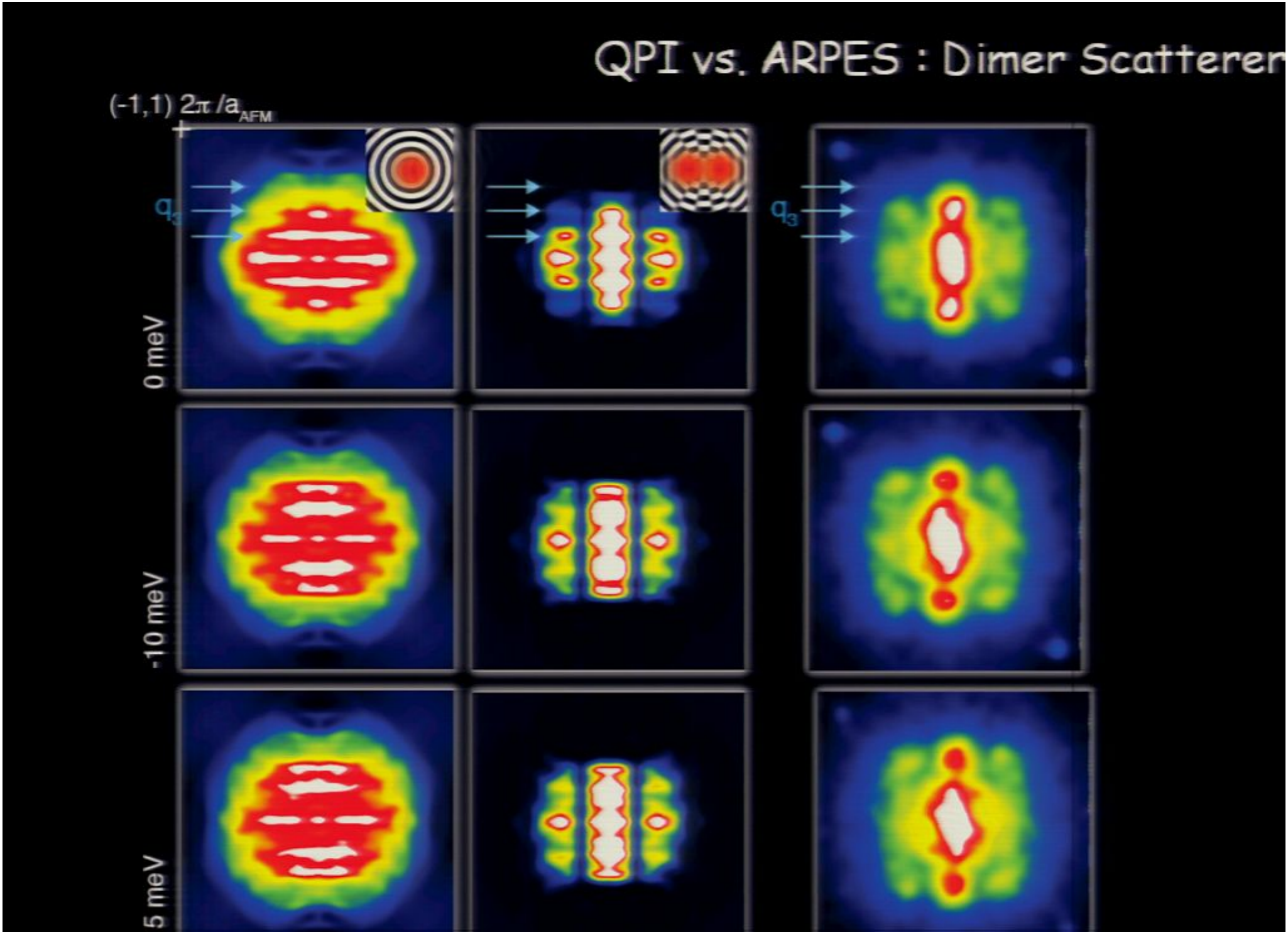
QPI vs. ARPES : Dimer Scatterer
(-1,1) 2π /a AFM
q3
q3
0 meV
-10 meV
5 meV

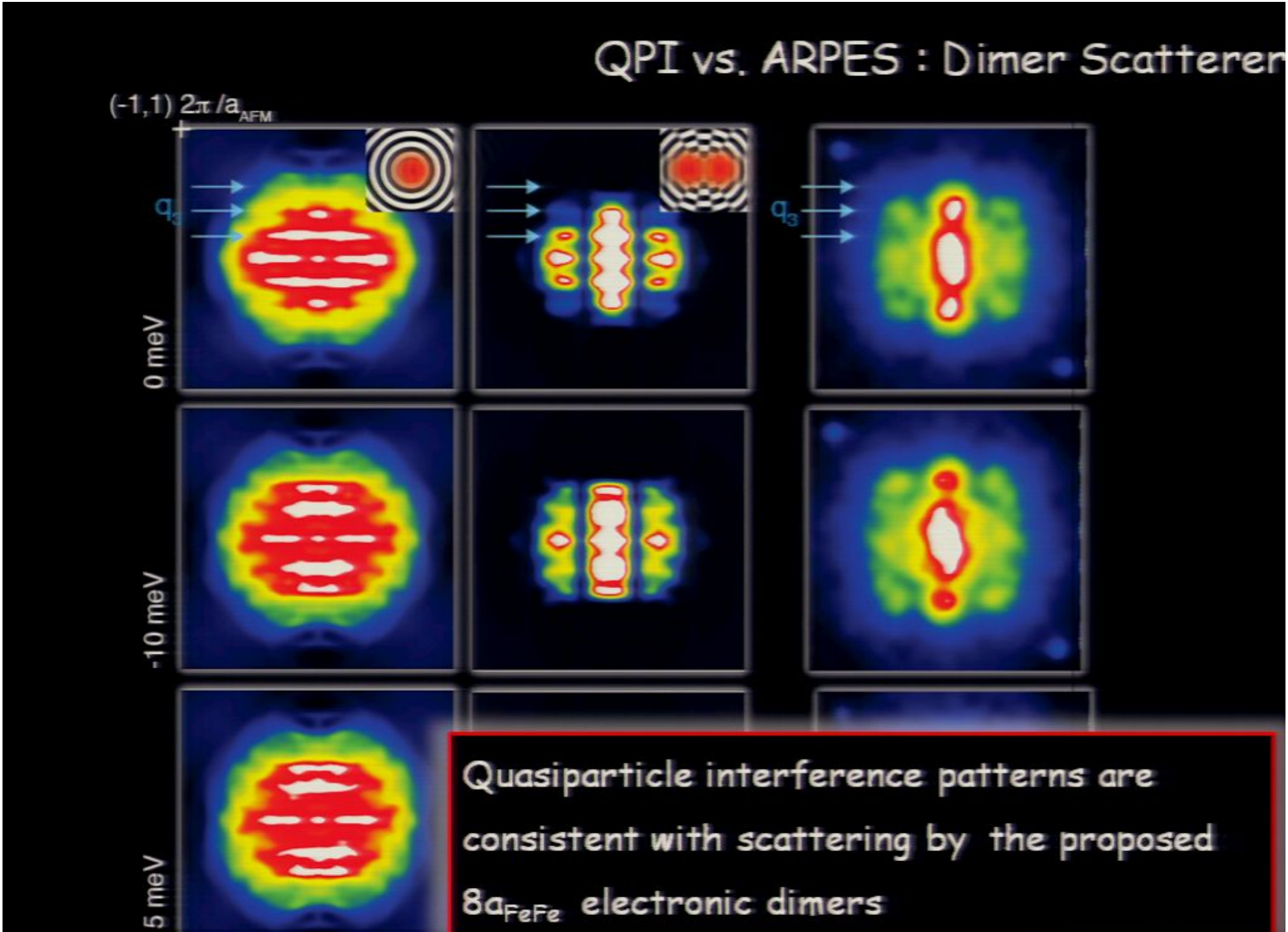
QPI vs. ARPES : Dimer Scatterer
(-1,1) 2π /a_AFM
q3
q3
0 meV
-10 meV
-15 meV
Quasiparticle interference patterns are consistent with scattering by the proposed 8a_FeFe electronic dimers

Anisotropy: Nematicity + Dimer-induced Scattering

Science 327, 181 (2010): M P Allan & T-M Chuang *et al* (2011)

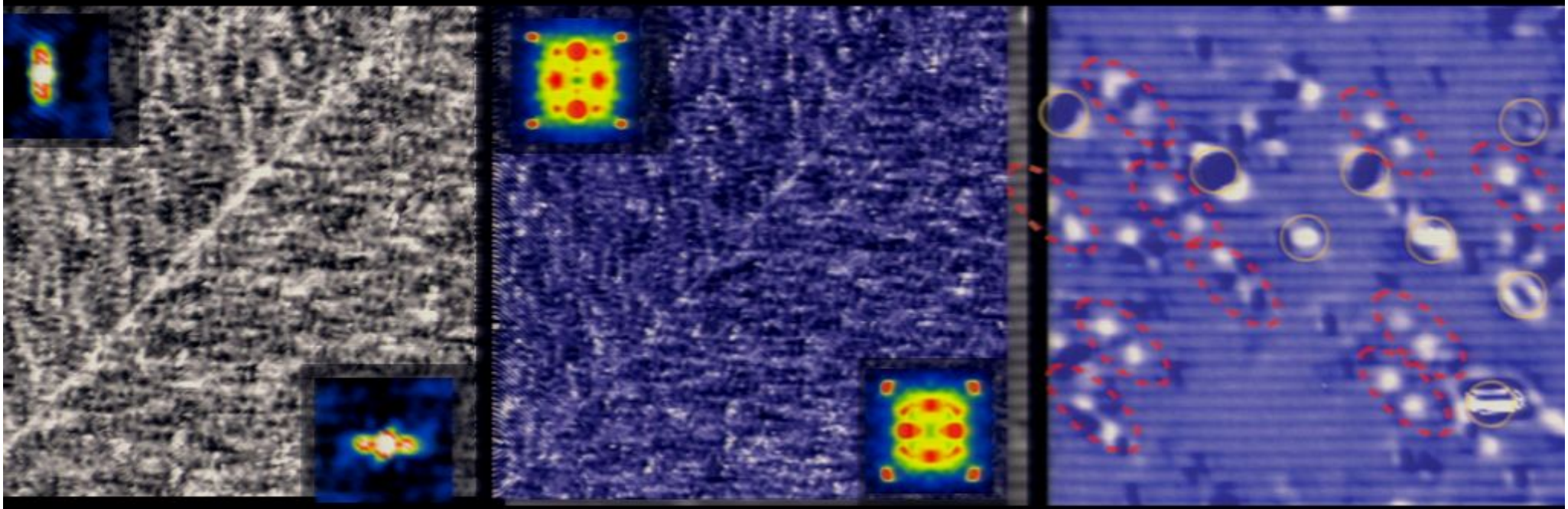

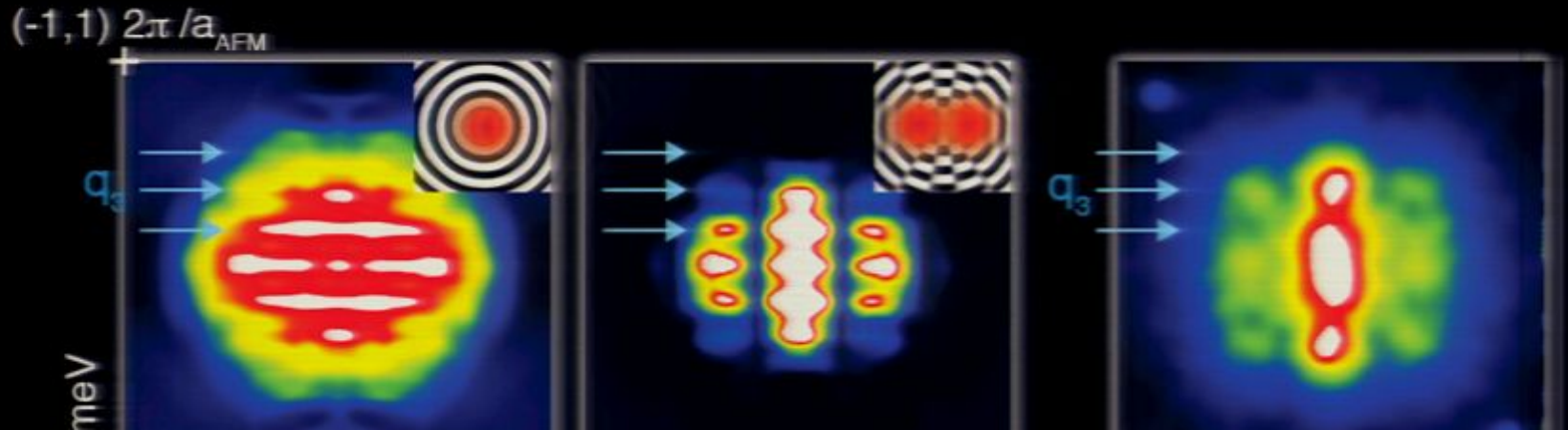

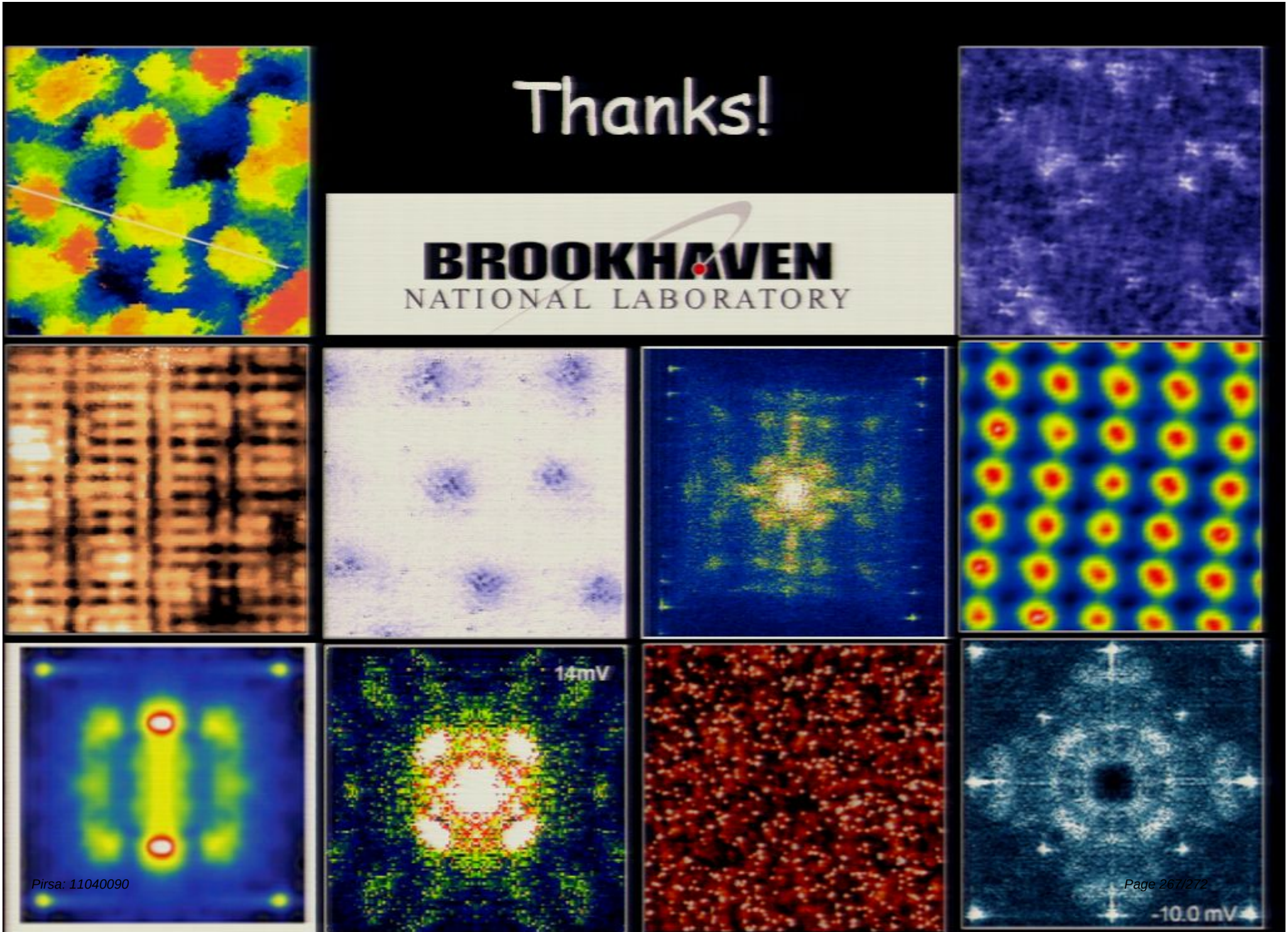

Anisotropy: Nematicity + Dimer-induced Scattering

Science 327, 181 (2010): M P Allan & T-M Chuang *et al* (2011)

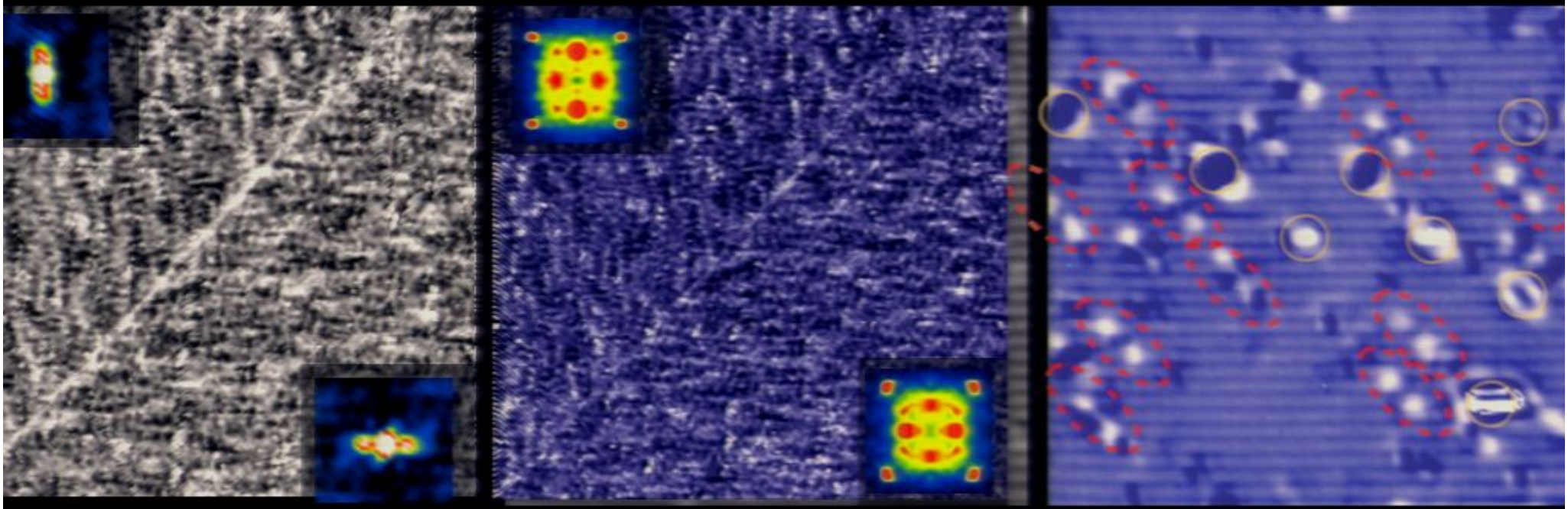

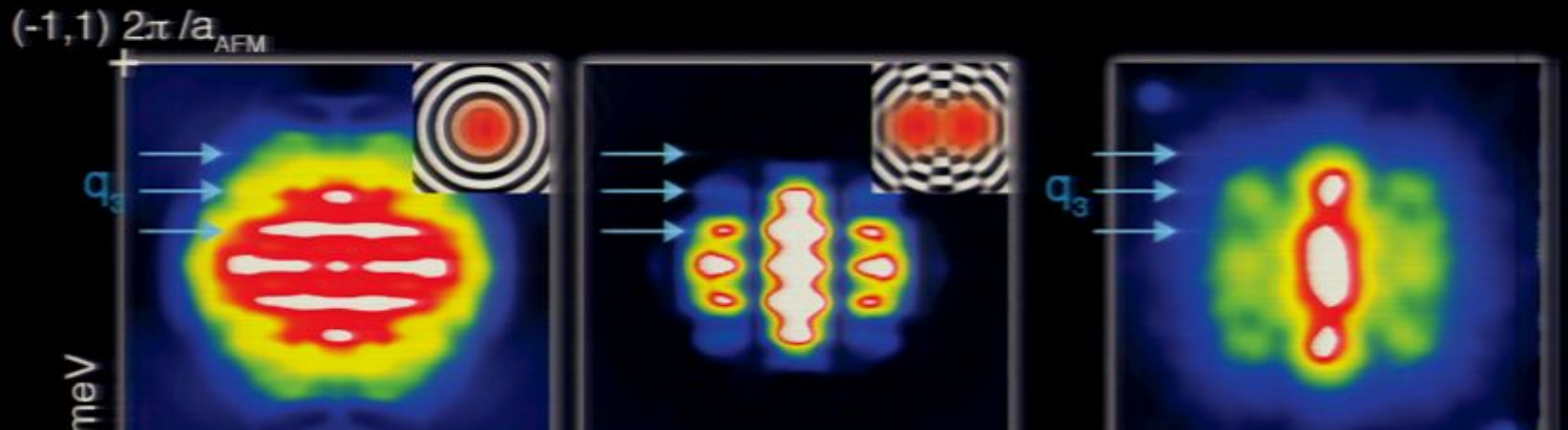

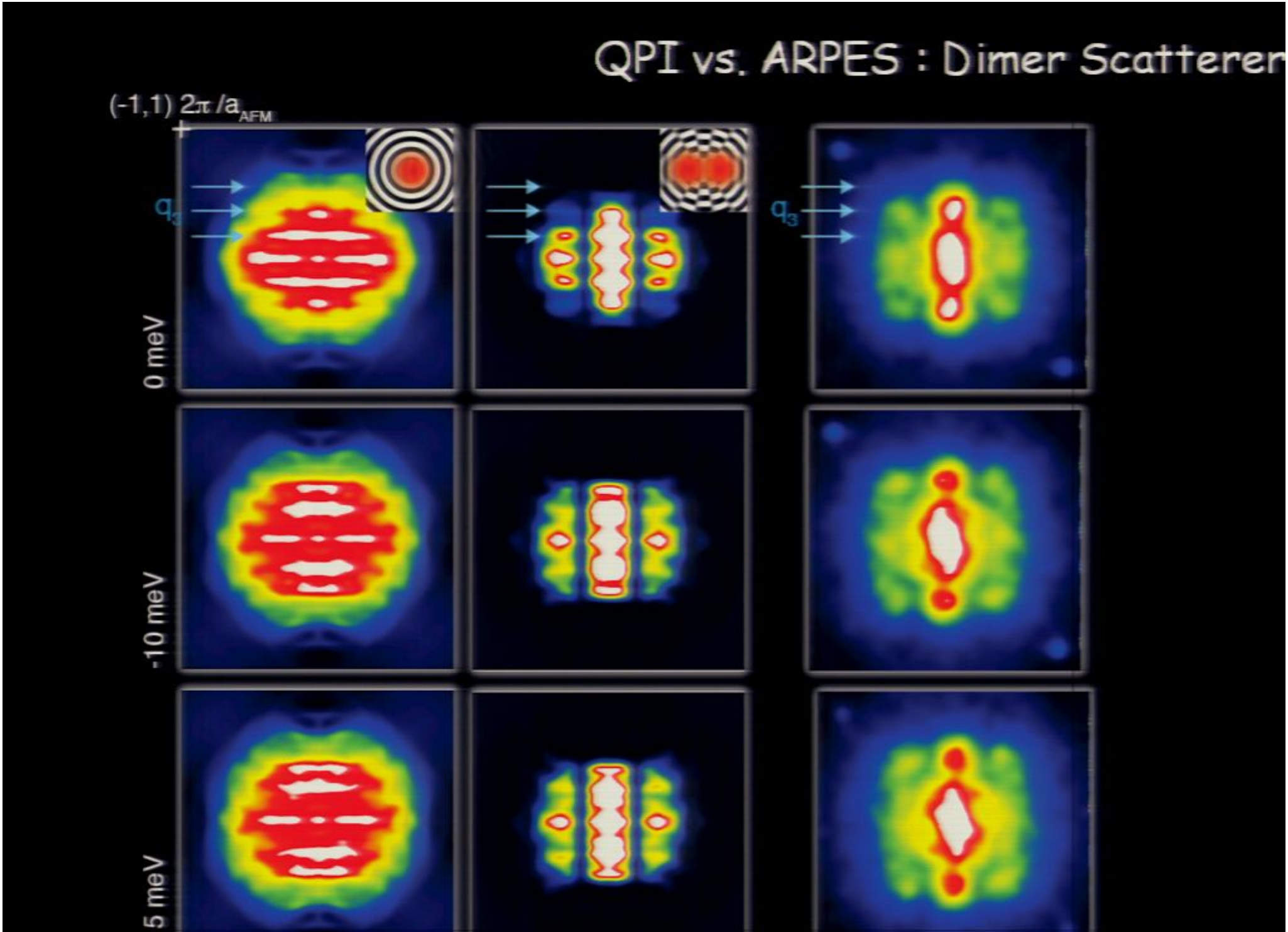
QPI vs. ARPES : Dimer Scatterer
(-1,1) 2π /a_AFM
q3
q3
0 meV
-10 meV
5 meV

QPI vs. ARPES : Autocorrelation($A(k,w)$)

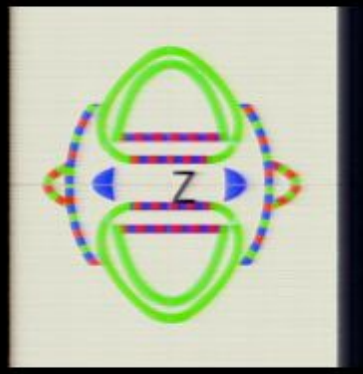

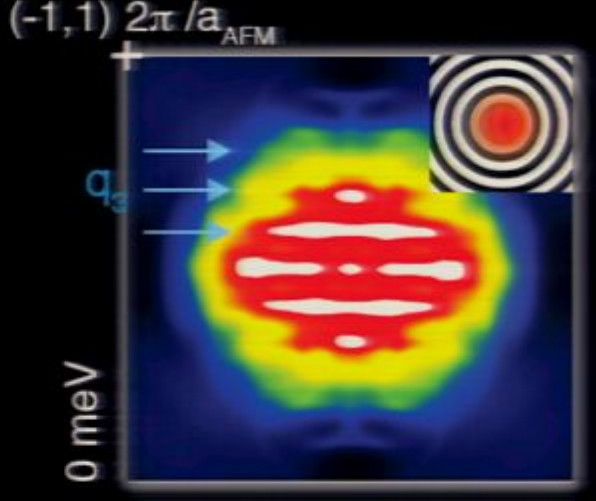

Autocorrelation of
$A(k,\omega)$(Pointscatterer)

M.P.Allan, T.-M. Chuang *et al.* 2011

Electronic anisotropy produced by Nematicity + $8a_0$ Electronic Dimers ?

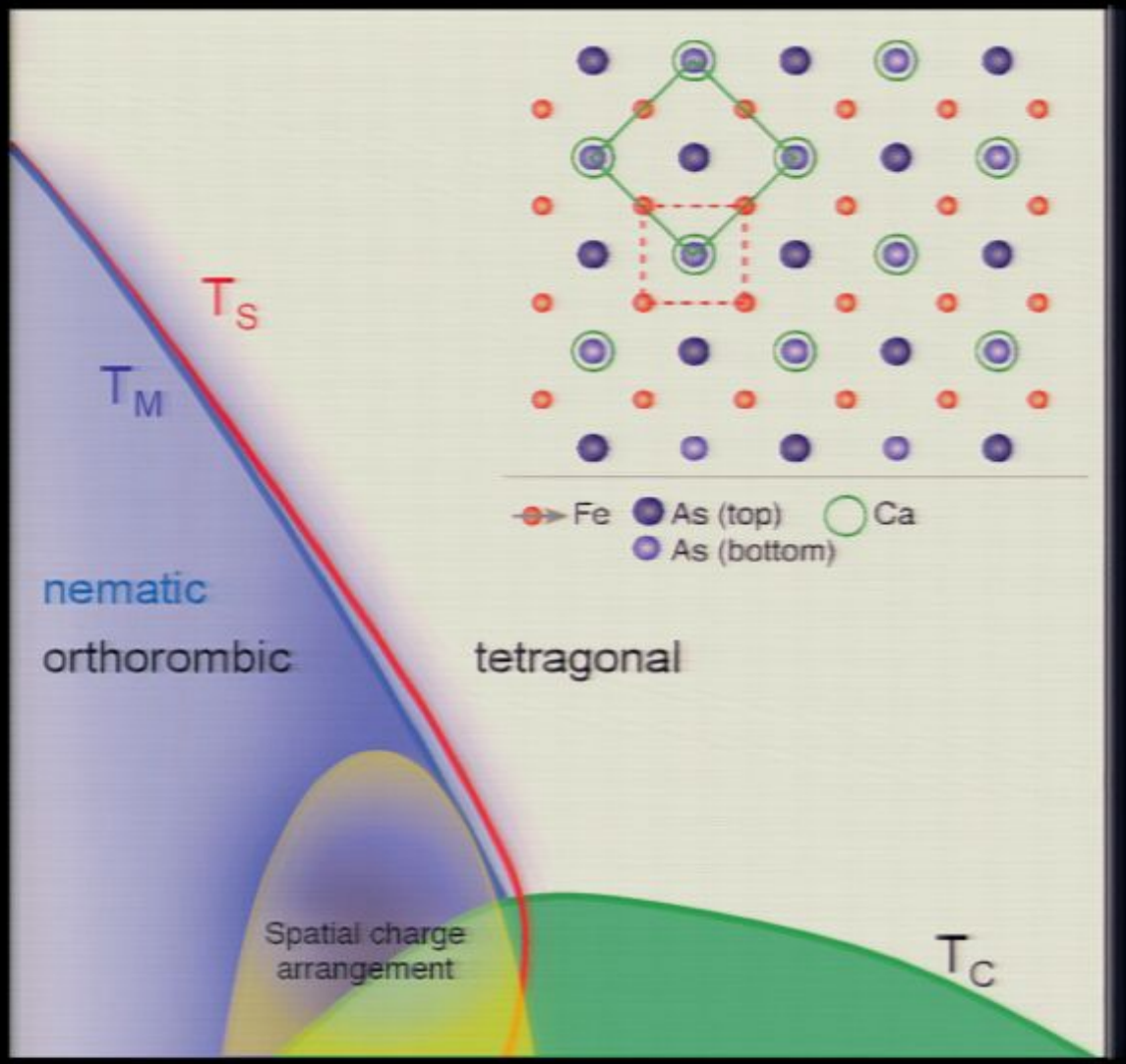

$8a_{FeFe}$ Electronic 'Dimers'

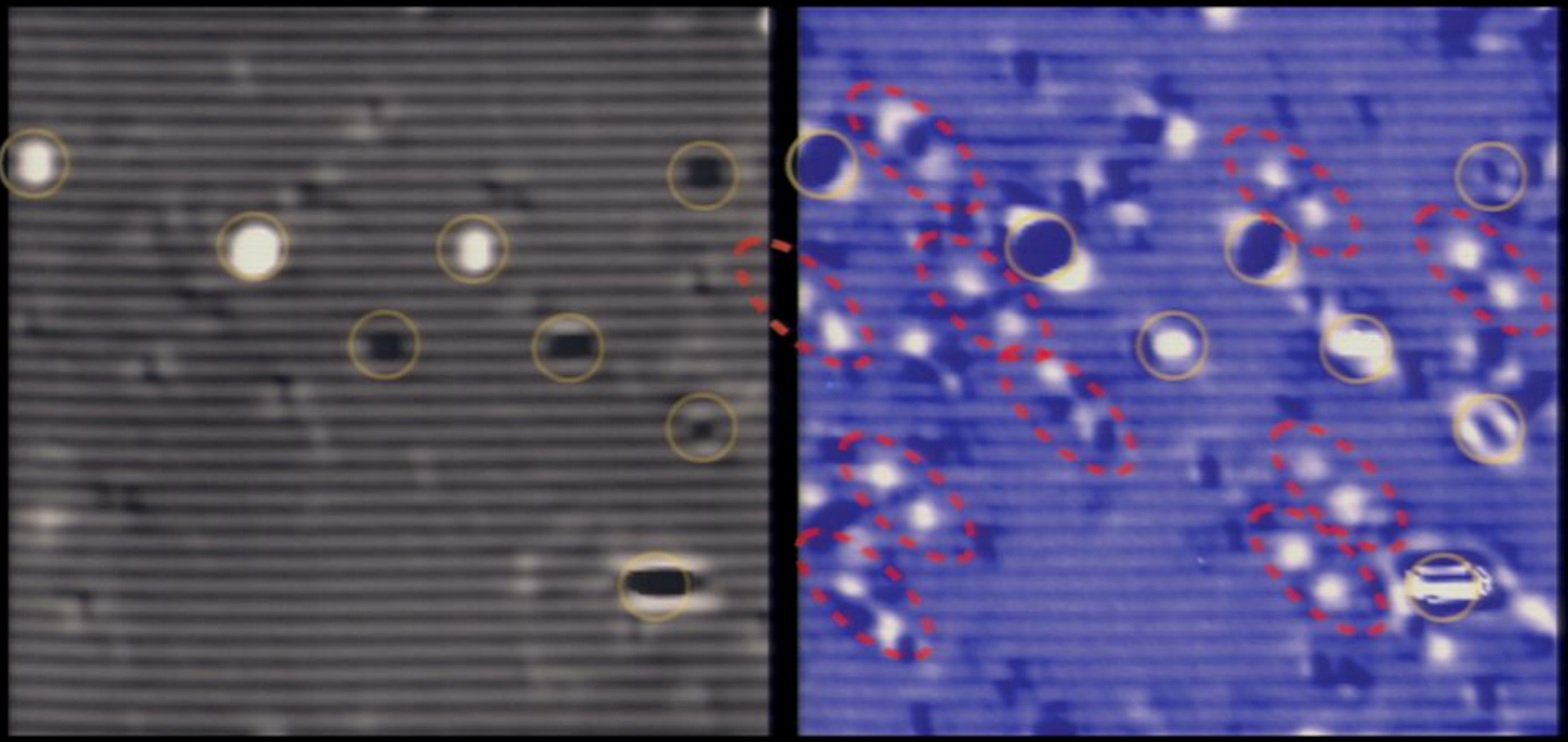

Topograph (24x24nm^2)

~LDOS (24x24nm^2)

Individual dimers are sometimes observed.